

Dissertation zur Erlangung des Doktorgrades
der Fakultät für Chemie und Pharmazie
der Ludwig-Maximilians-Universität München

**Phosphorus Ylides, Sulfur Ylides, and Related Carbanions as
Reference Nucleophiles for the Quantification of the
Electrophilic Reactivities of Aldehydes, Imines, and Enones**



Roland Joachim Appel

aus München

2011

Erklärung

Diese Dissertation wurde im Sinne von §13 Abs. 3 bzw. 4 der Promotionsordnung vom 29. Januar 1998 (in der Fassung der vierten Änderungssatzung vom 26. November 2004) von Herrn Professor Dr. Herbert Mayr betreut.

Ehrenwörtliche Versicherung

Diese Dissertation wurde selbständig, ohne unerlaubte Hilfe erarbeitet.

München, 10.02.2011

Roland Appel

Dissertation eingereicht am: 10.02.2011

1. Gutachter: Prof. Dr. Herbert Mayr

2. Gutachter: Prof. Dr. Manfred Heuschmann

Mündliche Prüfung am: 05.04.2011

FÜR MEINE ELTERN

Acknowledgment

First, I would like to express my deepest gratitude to Professor Dr. Mayr for giving me the opportunity to perform this thesis in his group. I have always appreciated the valuable discussions with him, his endless support, his expert knowledge in any field of chemistry, his inspiring confidence, and the possibility for a self-contained planning and presenting of projects. I really enjoyed working under these excellent conditions and I cannot overemphasize my gratitude for all the things I learned during this time.

Furthermore, I want to thank Professor Dr. Heuschmann for reviewing this thesis and the board of examiners for their participation in my defense examination.

The financial support by the Fonds der Chemischen Industrie (scholarship for PhD students) is gratefully acknowledged. Besides the funding for two years of my time during the PhD, this scholarship gave me the possibility to attend several international conferences.

Furthermore, I would like to thank all my colleagues within the group of Professor Dr. Mayr (and the group of Dr. Konrad Koszinowski) for the great and pleasant working atmosphere, especially Dr. Tanja Kanzian, Dr. Sami Lakhdar, Dr. Martin Breugst, Christoph Nolte (The famous "Olah-Lab-Crew"), and Dr. Nicolas Streidl. I will never forget the great time with you, our professional and private conversations, and I hope that these friendships will continue in the future. Special thanks go to Dr. Sami Lakhdar for fantastic advices to plan my projects and for giving me the opportunity to see the most beautiful places of Tunisia on the occasion of the International Symposium of Modern Organic Chemistry (ISMOC) in Monastir 2009. I would also like to thank Nicolai Hartmann and Vasily Mezhnev for their great collaboration during their undergraduate research laboratories. Sincere thanks are given to Nathalie Hampel for synthesizing our reference electrophiles and for her original Bavarian charm, Brigitte Janker for solving any emerging problem, and Hildegard Lipfert for her never-ending help in organizational tasks. The excellent advices for improvement of manuscripts as well as the critical and valuable suggestions by Dr. Armin R. Ofial are gratefully acknowledged.

Acknowledgment

Additionally, I want to thank my colleagues from the group of Professor Dr. Paul Knochel. I really have profited from their expertise in organometallic chemistry and I will never forget the great parties where I was always welcome.

I am also very grateful for the support of all my friends and I want to thank particularly Sebastian Bernhardt and Garwin Pichler, who accompanied me throughout my chemistry studies. Your illustrious companionship always kept my spirits high during the sometimes exhausting daily routine of chemistry.

For the efficient and fast proofreading of this thesis, I am very grateful to Dr. Martin Breugst, Dr. Tanja Kanzian, Dominik Allgäuer, Tobias Nigst, and Francisco Corral.

Last but not least, I want to thank my family for the unique and fantastic support. I cannot overemphasize my gratitude for your help and encouragement. In particular, I am deeply indebted to my parents, who were backing me all the way. This thesis is dedicated to you! Thank you very much!

Publications

Nucleophilicities of the Anions of Arylacetonitriles and Arylpropionitriles in Dimethyl Sulfoxide

O. Kaumanns, R. Appel, T. Lemek, F. Seeliger, H. Mayr, *J. Org. Chem.* **2009**, *74*, 75-81.

Nucleophilicity Parameters for Phosphoryl-Stabilized Carbanions and Phosphorus Ylides: Implications for Wittig and Related Olefination Reactions

R. Appel, R. Loos, H. Mayr, *J. Am. Chem. Soc.* **2009**, *131*, 704-714.

How Does Electrostatic Activation Control Iminium Catalyzed Cyclopropanations?

[Wie werden Iminium-katalysierte Cyclopropanierungen durch elektrostatische Aktivierung gesteuert?]

S. Lakhdar, R. Appel, H. Mayr, *Angew. Chem.* **2009**, *121*, 5134-5137; *Angew. Chem. Int. Ed.* **2009**, *48*, 5034-5037.

Nucleophilic Reactivities of Sulfur Ylides and Related Carbanions: Comparison with Structurally Related Organophosphorus Compounds

R. Appel, H. Mayr, *Chem. Eur. J.* **2010**, *16*, 8610-8614.

Scope and Limitations of Cyclopropanations with Sulfur Ylides

R. Appel, N. Hartmann, H. Mayr, *J. Am. Chem. Soc.* **2010**, *132*, 17894-17900.

Quantification of the Electrophilic Reactivities of Aldehydes, Imines, and Enones

R. Appel, H. Mayr, *J. Am. Chem. Soc.* **2011**, submitted.

Conference Contributions

- 03/2008 1st workshop of the Sonderforschungsbereich 749, Wildbad Kreuth, Germany, oral presentation: “Ambident Reactivity of α,β -Unsaturated Carbonyl Compounds; From the Free Carbanion to the Organometallic Species”
- 09/2008 2nd EuCheMS Chemistry Congress, Torino, Italy, poster presentation: “Nucleophilic Reactivities of Wittig Ylides and Phosphoryl-Stabilized Carbanions”
- 02/2009 International Symposium on Modern Organic Chemistry, Monastir, Tunisia, oral- and poster presentation: “Nucleophilicity Parameters for Phosphoryl-Stabilized Carbanions and Phosphorus Ylides: Implications for Wittig and Related Olefination Reactions”
- 03/2009 Synthesefest, Munich, Germany, poster presentation: “Nucleophilicity Parameters for Phosphoryl-Stabilized Carbanions and Phosphorus Ylides: Implications for Wittig and Related Olefination Reactions”
- 03/2010 International Meeting of the Sonderforschungsbereich 749, Kloster Irsee, Germany, oral- and poster presentation: “Nucleophilicity Parameters for Sulfur Ylides: Reference Compounds for Elucidating the Ambident Reactivities of α,β -Unsaturated Carbonyl Compounds and Imines”
- 07/2010 9th International Symposium on Carbanion Chemistry, Florence, Italy, oral presentation: “Nucleophilic Reactivities of Sulfur Ylides and Related Carbanions: Comparison with Structurally Related Organophosphorus Compounds”

Table of Contents

Chapter 1:	Summary	1
Chapter 2:	Introduction	19
Chapter 3:	Nucleophilicity Parameters for Phosphoryl-Stabilized Carbanions and Phosphorus Ylides: Implications for Wittig and Related Olefination Reactions	27
Chapter 4:	Nucleophilic Reactivities of Sulfur Ylides and Related Carbanions: Comparison with Structurally Related Organophosphorus Compounds	93
Chapter 5:	Scope and Limitations of Cyclopropanations with Sulfur Ylides	129
Chapter 6:	How Does Electrostatic Activation Control Iminium Catalyzed Cyclopropanations?	187
Chapter 7:	Quantification of the Electrophilic Reactivities of Aldehydes, Imines, and Enones	201
Chapter 8:	Ambident Electrophilicity of a Cinnamaldehyde-Derived Imine	271
Chapter 9:	Nucleophilicities of the Anions of Arylacetonitriles and Arylpropionitriles in Dimethyl Sulfoxide	311
Chapter 10:	Nucleophilic Reactivities of Alkali Cyclopentadienides (CpK, CpNa, CpLi)	347

Chapter 1: Summary

1 General

Many organic reactions can be classified as nucleophile-electrophile combinations, the rates of which can be described by eq 1, where $k_{20^{\circ}\text{C}}$ is the second-order rate constant in $\text{M}^{-1} \text{s}^{-1}$, s is a nucleophile-specific slope parameter, N is a nucleophilicity parameter, and E is an electrophilicity parameter.

$$\log k_{20^{\circ}\text{C}} = s(N + E) \quad (1)$$

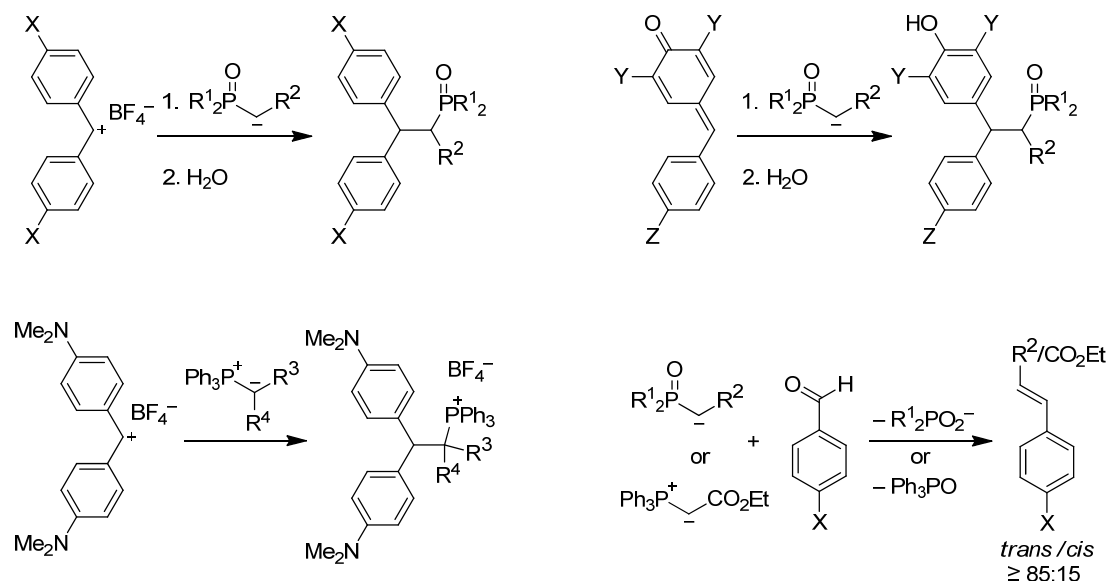
Based on this correlation equation, the reactivities of many different classes of nucleophiles have already been quantified and compared. On the contrary, only a rather limited amount of electrophiles including carbocations, benzhydrylium ions, cationic metal π -complexes, and electron-deficient Michael acceptors have so far been characterized according to their electrophilicity E . In spite of their general importance in organic synthesis, E parameters have neither been reported for imines nor for ordinary carbonyl compounds or enones.

This thesis was designed to derive the nucleophilic reactivities of phosphorus- and sulfur ylides as well as those of related carbanions in order to systematically investigate their reactions with carbonyl compounds, imines, and Michael acceptors. In this way, the quantification of the reactivity of these important electrophilic species should be achieved. Furthermore, the nucleophilic reactivities of stabilized carbanions and their dependence on the alkali counterion should be investigated in order to elucidate the dependence of the nucleophilicity on the corresponding counterion.

2 Nucleophilicity Parameters for Phosphoryl-Stabilized Carbanions and Phosphorus Ylides: Implications for Wittig and Related Olefination Reactions

Kinetics for the reactions of four phosphoryl-stabilized carbanions and of four phosphorus ylides with benzhydrylium ions and structurally related quinone methides as well as with various substituted benzaldehydes have been determined by UV-Vis spectroscopy. While the reactions with carbocations and Michael acceptors yielded simple addition products, the well-known Wittig-type olefination products were obtained in the reactions with benzaldehydes (Scheme 1).

Scheme 1: Reactions of Phosphoryl-Stabilized Carbanions and Phosphorus Ylides with Benzhydrylium Ions, Quinone Methides, and Benzaldehydes.



The obtained second-order rate constants ($\log k_2$) correlated linearly with the electrophilicity parameters E of the employed benzhydrylium ions and Michael acceptors as required by eq 1, which allowed us to calculate the nucleophile-specific parameters N and s for phosphoryl-substituted carbanions and phosphorus ylides (Figure 1).

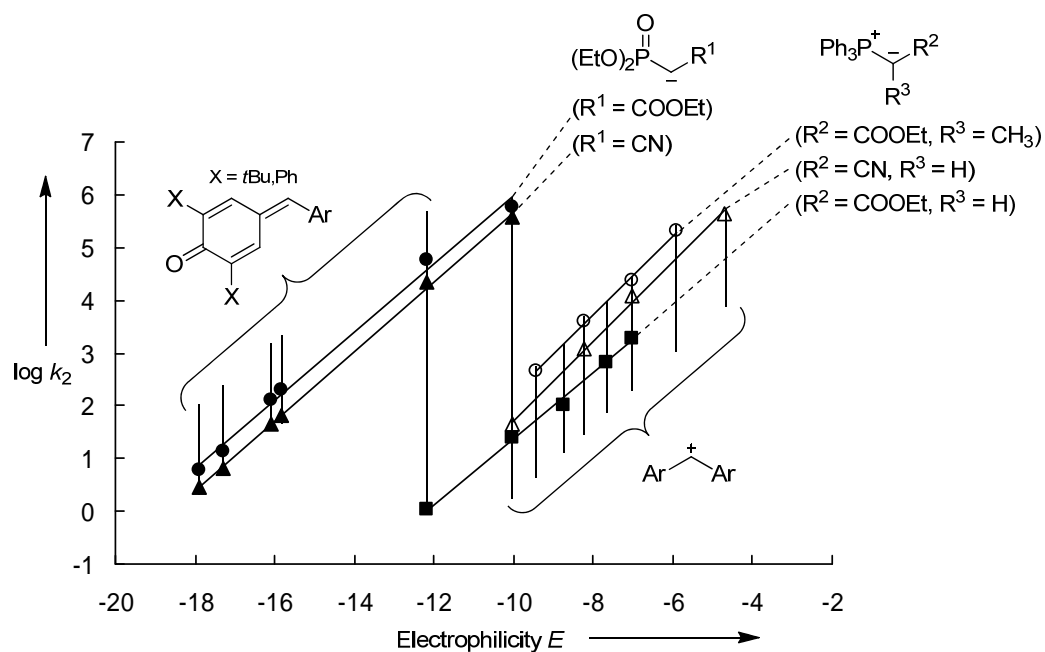


Figure 1: Plots of $\log k_2$ for the reactions of phosphonate-stabilized carbanions and phosphorus ylides with benzhydrylium ions and quinone methides at 20°C versus their electrophilicity parameters E (filled symbols denote reactions in DMSO, open symbols reactions in CH_2Cl_2).

From these correlations, a direct comparison between the nucleophilic reactivities of Horner-Wadsworth-Emmons carbanions and Wittig ylides becomes possible (Figure 2). Ph_2PO and $(\text{EtO})_2\text{PO}$ substituted carbanions are found to show similar reactivities towards Michael acceptors and are 10^4 - 10^5 times more reactive than analogously substituted phosphorus ylides. Counterion studies (K^+ , Na^+ and Li^+) on the nucleophilicities of phosphonate-stabilized carbanions in DMSO revealed that the effects of K^+ and Na^+ are almost negligible for all types of carbanions investigated. However, Li^+ coordination reduces the reactivities of phosphonate-substituted acetic ester anions by 10^2 while the reactivities of phosphonate-substituted acetonitrile anions remain almost unaffected.

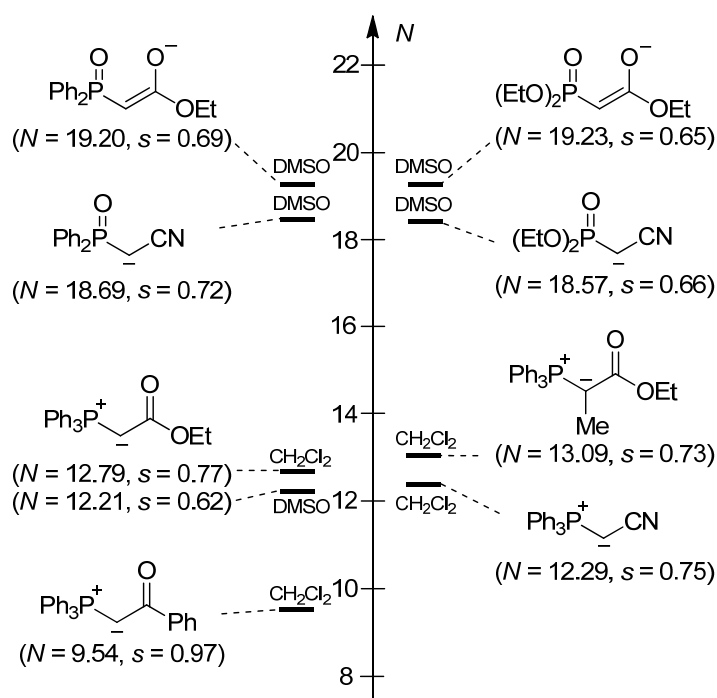


Figure 2: Comparison of the nucleophilicity parameters N (in DMSO or CH_2Cl_2) of phosphorus ylides, phosphonate-stabilized carbanions, and phosphine oxide-stabilized carbanions.

Significant differences between the relative reactivities of phosphorus-substituted nucleophiles towards carbocations and Michael acceptors on one side and benzaldehydes on the other side (Figure 3) are in line with a concerted asynchronous oxaphosphetane formation in the rate-determining step of Wittig-type olefination reactions.

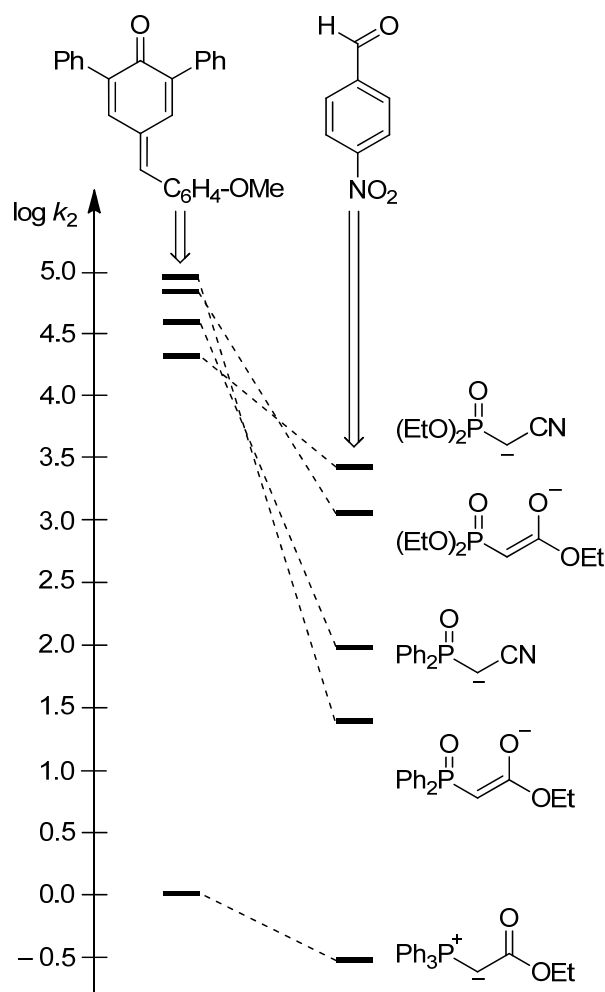
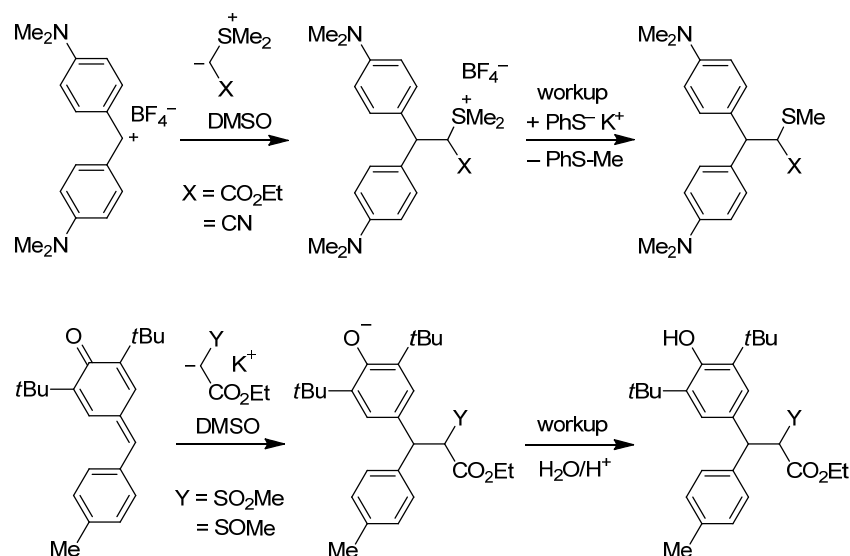


Figure 3: Comparison of the second-order rate constants k_2 for the reactions of different phosphorus-stabilized nucleophiles with a quinone methide (on the left) and *p*-nitrobenzaldehyde (on the right) in DMSO at 20°C.

3 Nucleophilic Reactivities of Sulfur Ylides and Related Carbanions: Comparison with Structurally Related Organophosphorus Compounds

The rates of the reactions of stabilized sulfur ylides as well as sulfonyl- and sulfinyl-stabilized carbanions with benzhydrylium ions and quinone methides have been determined photometrically. Representative product analyses revealed the reaction course illustrated in Scheme 2.

Scheme 2: Reactions of Stabilized Sulfur Ylides and Related Carbanions with Benzhydrylium Ions and Quinone Methides.



The good correlations between the obtained second-order rate constants and the electrophilicity parameters of the employed benzhydrylium ions and quinone methides showed the applicability of eq 1 also for these reactions (Figure 4).

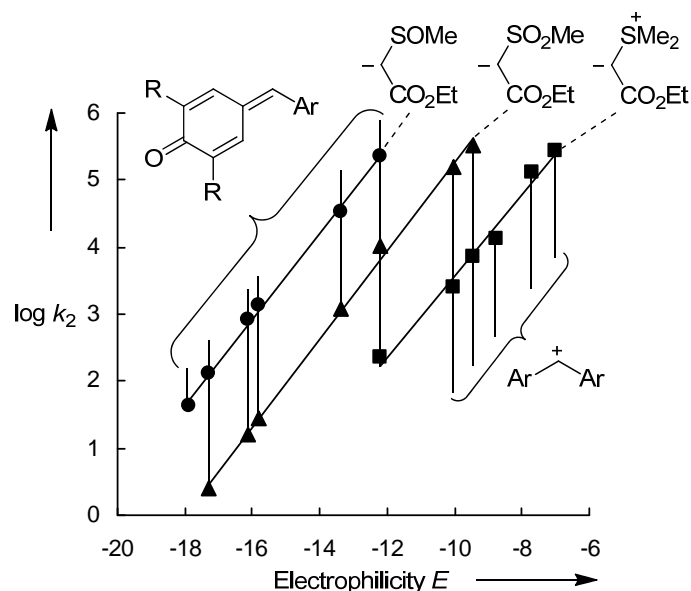


Figure 4: Plots of $\log k_2$ for the reactions of ethoxycarbonyl-stabilized sulfur ylides and sulfur-stabilized carbanions with the reference electrophiles at 20°C in DMSO versus their electrophilicity parameters E .

Accordingly, the nucleophilie-specific parameters N and s for stabilized sulfur ylides, a methylsulfonyl-stabilized and a methylsulfinyl-stabilized carbanion have been determined and

compared with those of analogously substituted phosphoryl-stabilized carbanions and phosphorus ylides (Figure 5).

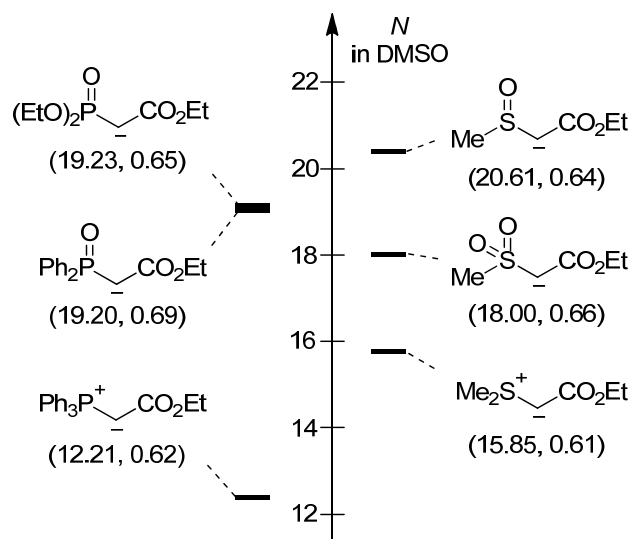


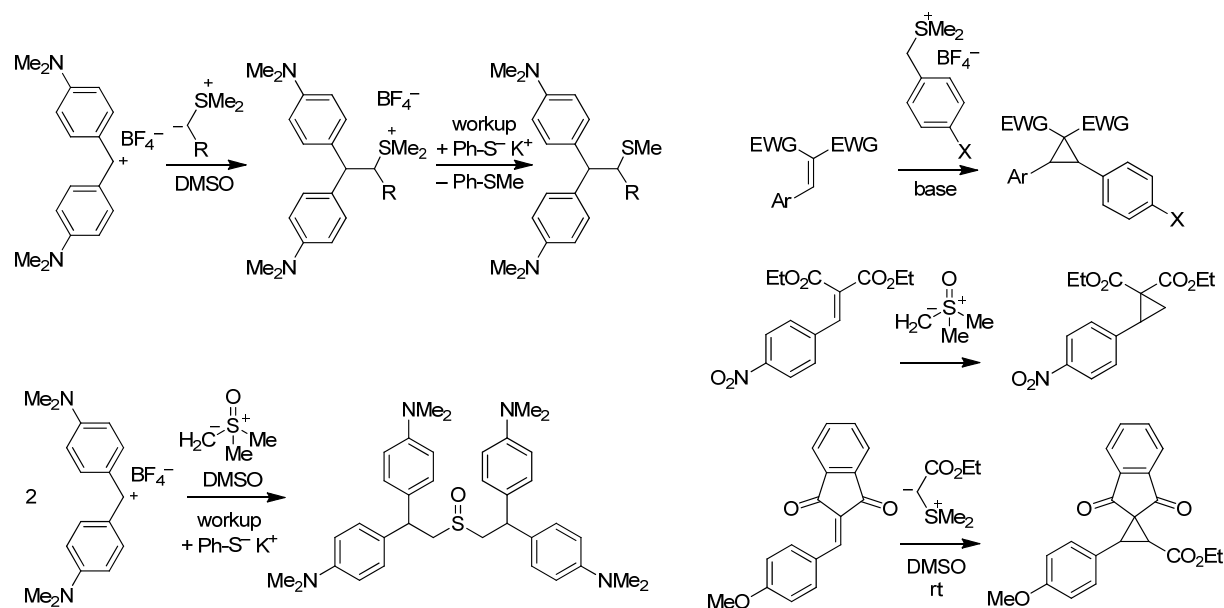
Figure 5: Comparison of the nucleophilicity parameters (N , s) in DMSO of sulfur-stabilized nucleophiles with those of a phosphorus ylide and of phosphoryl-stabilized carbanions.

While the nucleophilic reactivities of phosphoryl-stabilized carbanions are in between those of sulfinyl- and sulfonyl-stabilized carbanions, an ethoxycarbonyl-stabilized dimethylsulfonium ylide is approximately 170 times more nucleophilic than an analogously substituted triphenylphosphonium ylide. Moreover, it has been shown that the obtained nucleophile-specific parameters N and s can efficiently predict the rates of the reactions of sulfur ylides and sulfur-stabilized carbanions with nitrostyrenes.

4 Scope and Limitations of Cyclopropanations with Sulfur Ylides

The rates of the reactions of five stabilized and three semistabilized sulfur ylides with benzhydrylium ions and Michael acceptors have been determined by UV-Vis spectroscopy in DMSO at 20°C. While the reactions of the investigated sulfur ylides with benzhydrylium ions yielded simple addition products, cyclopropane derivatives were predominantly formed in their reactions with Michael acceptors (Scheme 3).

Scheme 3: Reactions of Different Sulfur Ylides with a Benzhydrylium Tetrafluoroborate and Several Michael Acceptors.



The second-order rate constants ($\log k_2$) of the investigated reactions correlated linearly with the electrophilicity parameters E of the employed electrophiles (Figure 6) as required by eq 1, which allowed us to calculate the nucleophile-specific parameters N and s for various stabilized and semistabilized sulfur ylides.

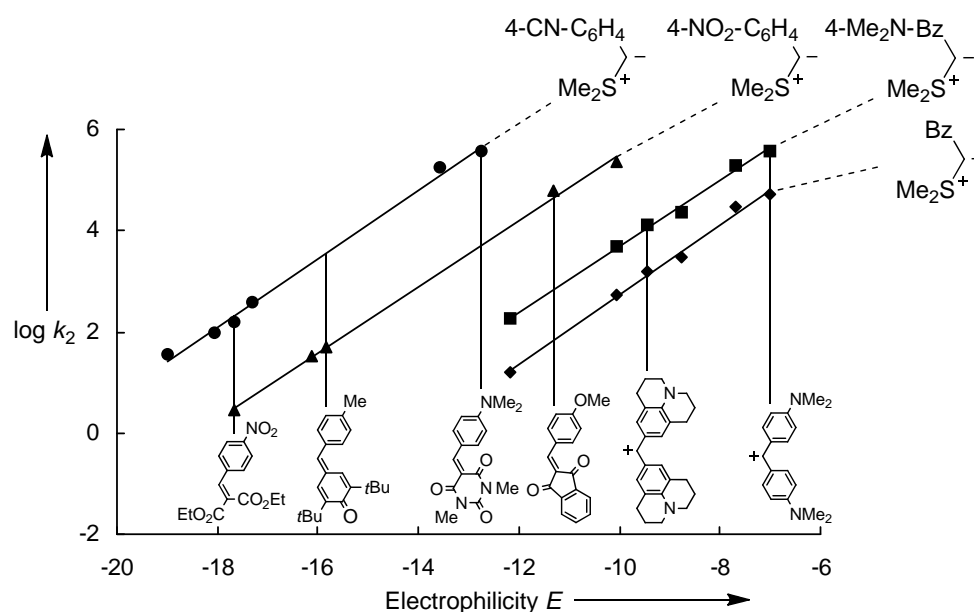


Figure 6: Plots of $\log k_2$ for the reactions of stabilized and semistabilized sulfur ylides with benzhydrylium ions and Michael acceptors (in DMSO at 20°C) versus their electrophilicity parameters E .

As shown in Figure 6, the rate constants for the cyclopropanation reactions of sulfur ylides with Michael acceptors lie on the same correlation line as the rate constants for the reactions of sulfur ylides with carbocations. These findings are in line with a stepwise or highly asynchronous mechanism for the cyclopropanation of Michael acceptors with sulfur ylides, in which the formation of the first CC bond is rate-determining. As previous mechanistic investigations have shown that cyclopropanation reactions with sulfur ylides usually proceed with rate-determining formation of zwitterions, followed by fast cyclizations, the rule of thumb that nucleophile-electrophile combinations at room temperature only occur when $E + N > -5$ can be employed to predict whether a certain cyclopropanation reaction is likely to take place.

The nucleophilicity parameters N (and s) can now be used to directly compare the nucleophilic reactivities of a large variety of synthetically important sulfur ylides (Figure 7).

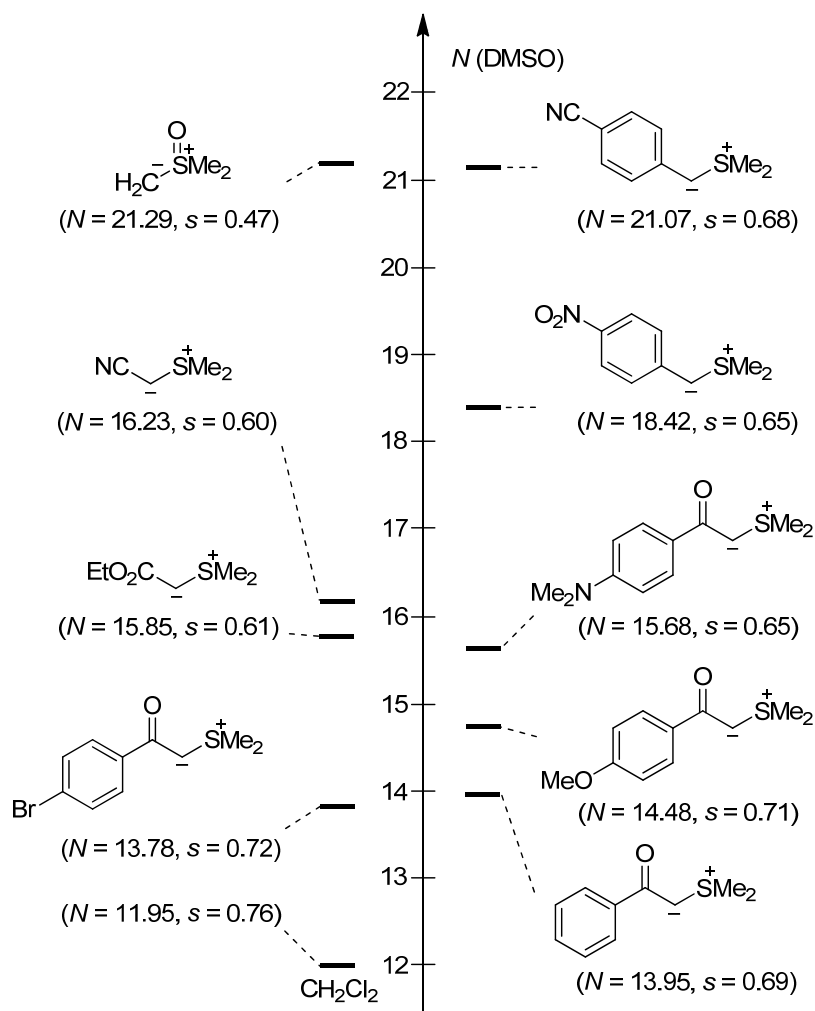


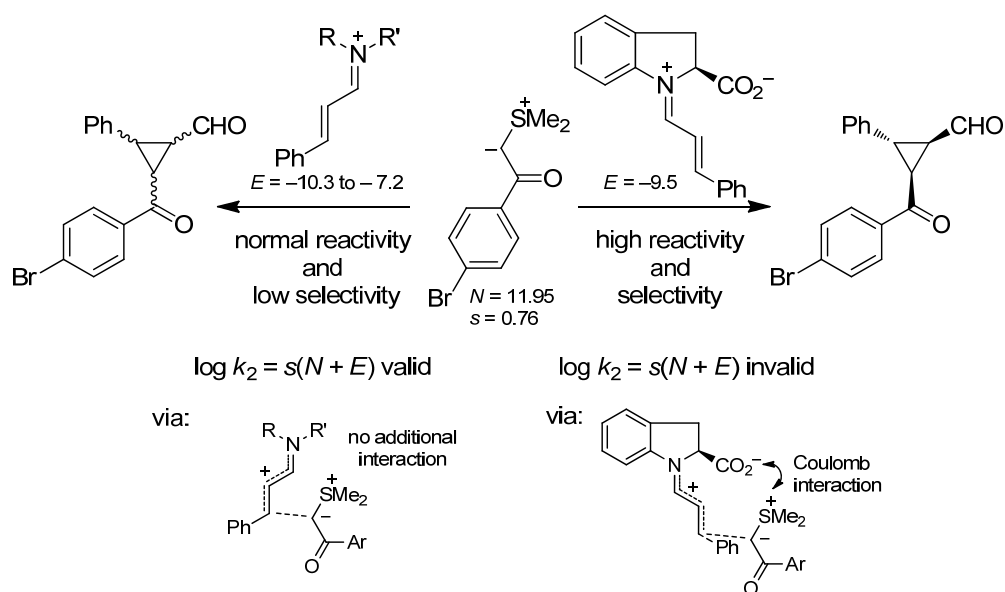
Figure 7: Comparison of the nucleophilicity parameters N (in DMSO at 20°C) of stabilized and semistabilized sulfur ylides.

5 How Does Electrostatic Activation Control Iminium Catalyzed Cyclopropanations?

From the rates of the reactions of a *p*-bromobenzoyl-substituted dimethylsulfonium ylide with benzhydrylium ions, the nucleophile-specific parameters N and s of this stabilized sulfur ylide has been determined in CH_2Cl_2 solution according to eq 1. Complementary to previously investigated imidazolidinone- and amine-derived iminium ions of cinnamaldehyde, the electrophilic reactivity E of a indoline-2-carboxylic acid-derived iminium ion of cinnamaldehyde was derived from the rates of its reactions with ketene acetals.

The rates of the cyclopropanation reactions of the *p*-bromobenzoyl-substituted dimethylsulfonium ylide with various cinnamaldehyde-derived iminium ions were generally predicted by eq 1 with deviations of factors of 3 to 32 from the nucleophilicity parameters N and s of the sulfur ylide and the electrophilicity parameters E of the iminium ions. In contrast, the reaction of the iminium ion derived from indoline-2-carboxylic acid and cinnamaldehyde proceeds more than 10^5 times faster than calculated by eq 1. Electrostatic activation, i.e., Coulomb interaction between the negatively charged carboxylate group of the iminium ion and the positively charged sulfonium group of the sulfur ylide, was accounted for this tremendous acceleration as well as for the high stereoselectivity in this cyclopropanation reaction (Scheme 4).

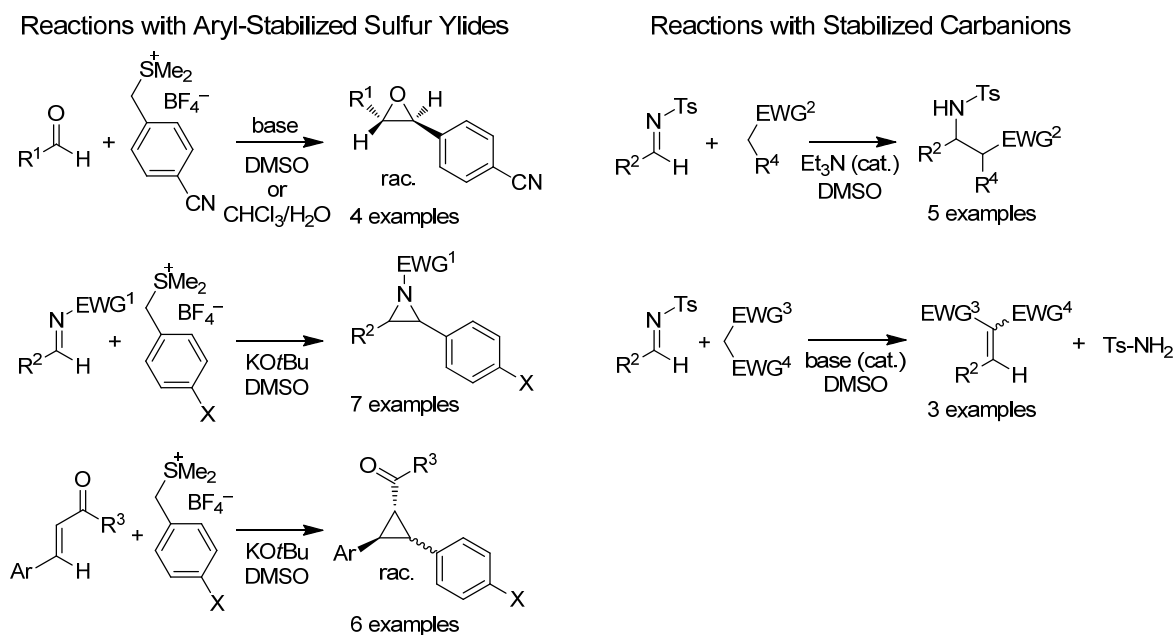
Scheme 4: Cyclopropanation Reactions of a *p*-Bromobenzoyl-Substituted Sulfur Ylide with Different Cinnamaldehyde Derived Iminium Ions in CH_2Cl_2 .



6 Quantification of the Electrophilic Reactivities of Aldehydes, Imines, and Enones

The rates of the epoxidation reactions of aldehydes, of the aziridination reactions of aldimines and of the cyclopropanation reactions of α,β -unsaturated ketones with aryl-stabilized dimethylsulfonium ylides have been determined photometrically. All of these sulfur ylide-mediated cyclization reactions as well as the addition reactions of stabilized carbanions to *N*-tosyl-activated aldimines have been found to follow a second-order rate law, where the rate constants reflect the (initial) CC bond formation between nucleophile and electrophile. While the reactions of aryl-stabilized sulfur ylides with aldehydes, *N*-activated imines, and enones yielded the expected epoxides, aziridines, and cyclopropanes, respectively, simple addition products as well as Knoevenagel-type condensation products were isolated from the reactions of carbanions with *N*-tosyl-activated imines (Scheme 5).

Scheme 5: Reactions of Aryl-Stabilized Sulfur Ylides with Aldehydes, Imines, and Michael Acceptors and Reactions of Stabilized Carbanions with *N*-Tosyl-Activated Imines.



The obtained second-order rate constants ($\log k_2$) have been combined with the nucleophilicity parameters of the aryl-stabilized sulfur ylides and of the stabilized carbanions (N , s) to calculate the electrophilicity parameters E of the investigated aldehydes, aldimines, and α,β -unsaturated ketones according to the linear free-energy relationship of eq 1. The data reported in this work provide the first quantitative comparison of the electrophilic reactivities of aldehydes, imines, and enones with carbocations and Michael acceptors within our comprehensive electrophilicity scale (Figure 8).

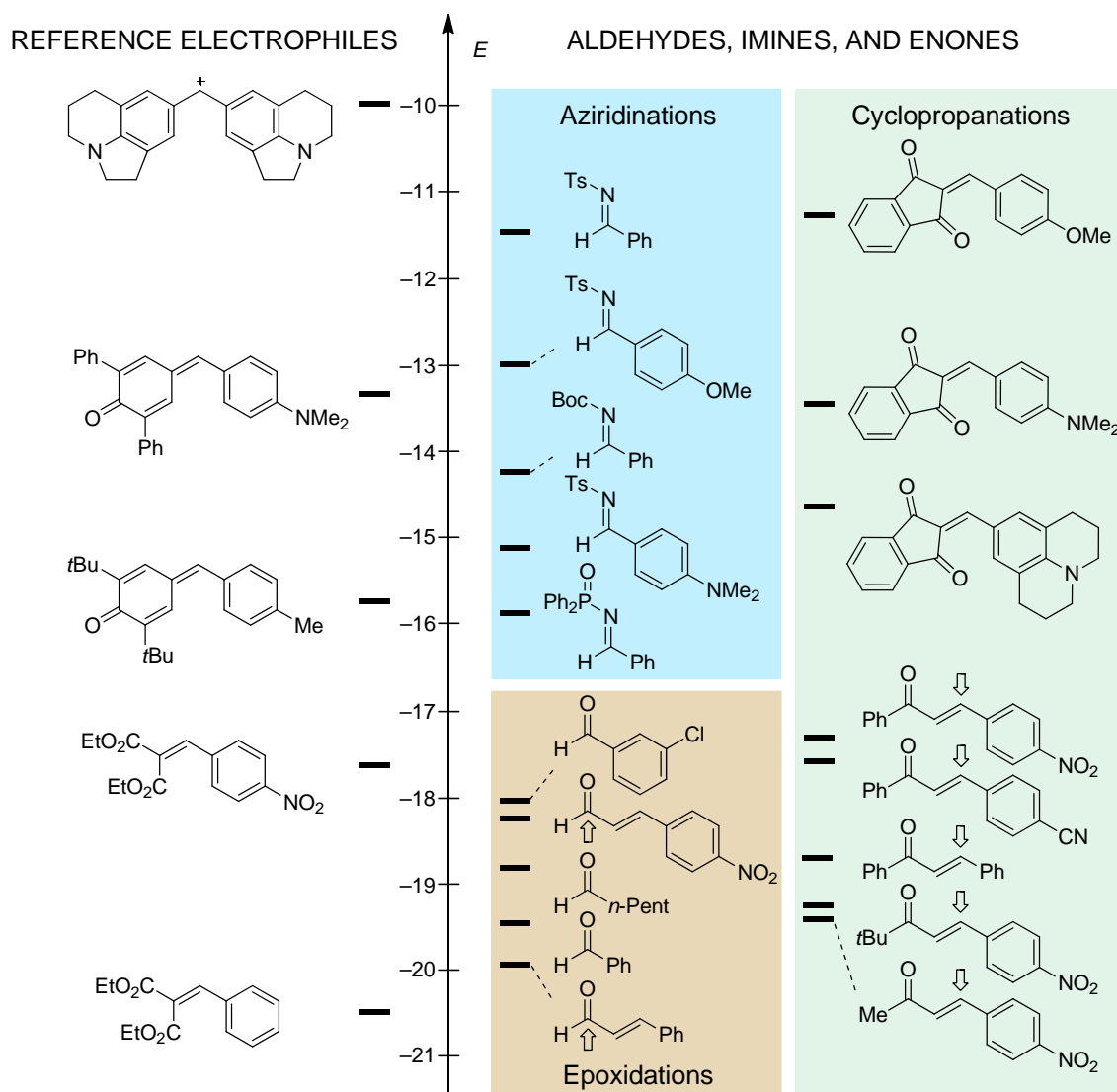


Figure 8. Comparison of the electrophilicity parameters E of aldehydes, imines, and enones with different Michael acceptors in DMSO.

Figure 8 shows that in DMSO, *N*-tosyl-, *N*-*tert*-butoxycarbonyl-, and *N*-phosphinoyl-substituted benzaldimines are significantly more electrophilic than the corresponding benzaldehydes. The α,β -unsaturated ketones depicted in Figure 8 show reactivities comparable to those of diethyl benzylidenemalonates indicating that a single benzoyl group has a similar activating effect on the electrophilicity of a CC double bond as two ethoxycarbonyl groups.

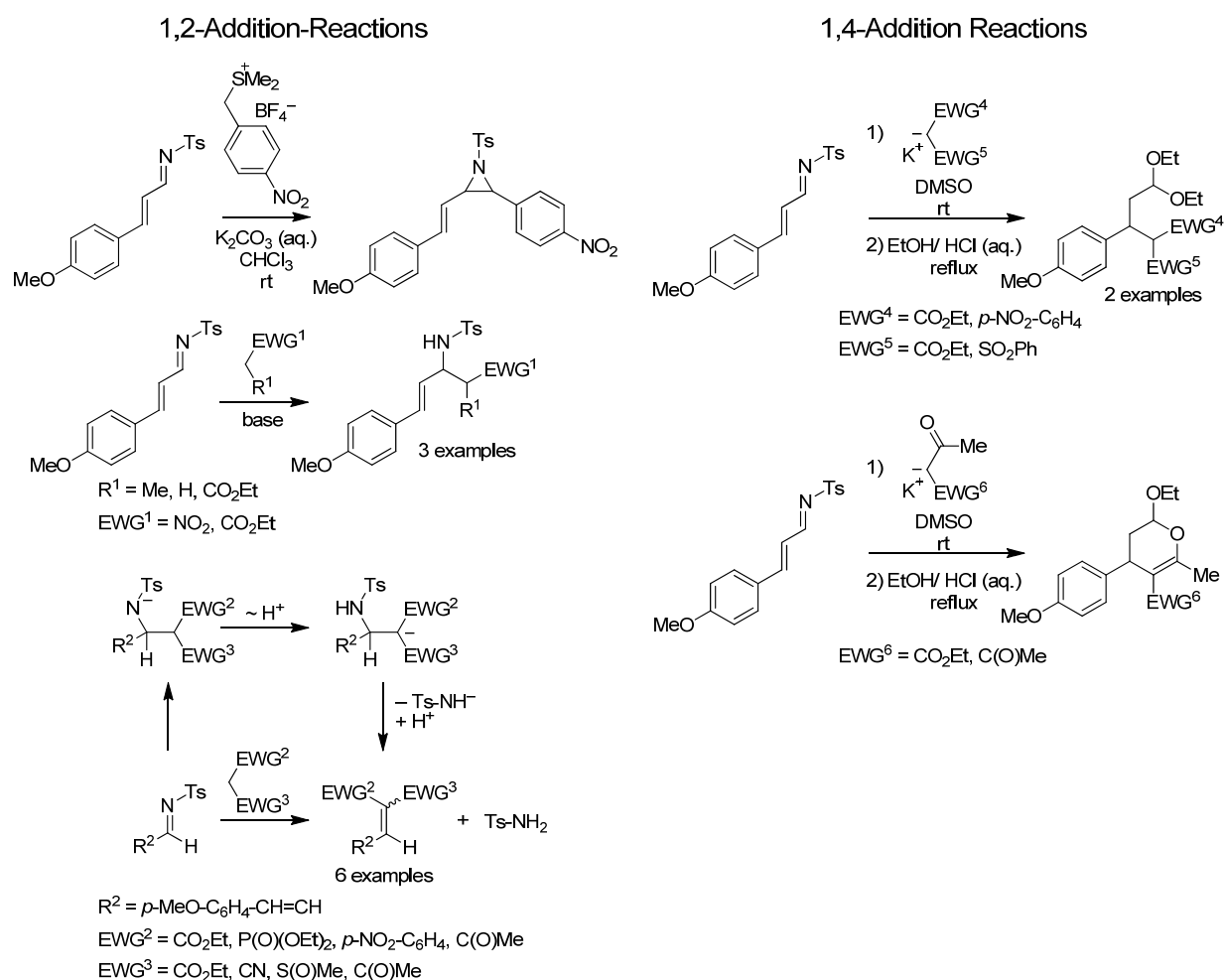
Surprisingly, the rate constants for previously investigated Wittig and Horner-Wadsworth-Emmons reactions could properly be derived from the determined electrophilicity parameters of aldehydes and the N and s parameters of phosphorus-stabilized nucleophiles, which have been derived from their one-bond-forming reactions with benzhydrylium ions and quinone methides. From the agreement between calculated and experimental rate constants of the

investigated olefination reactions, one can conclude that the transition states of the oxaphosphetane formations can only be weakly stabilized by the concerted formation of two new bonds. However, as shown in Figure 3, also cases can be found, where significant differences between the relative reactivities of phosphorus-substituted nucleophiles towards Michael acceptors and benzaldehydes indicate a higher degree of concertedness in Wittig and related olefination reactions. It is presently not clear, in which cases the stabilization of the transition state by concertedness becomes so strong that the approximation by eq 1 is not any longer valid.

7 Ambident Electrophilicity of a Cinnamaldehyde-Derived Imine

Rates and products of the reactions of an α,β -unsaturated imine with a series of carbanions and a sulfur ylide have been studied in order to elucidate the factors which control 1,2- vs. 1,4-additions of α,β -unsaturated carbonyl and related compounds (Scheme 6).

Scheme 6: 1,2- and 1,4-Additions of Several Nucleophiles to an α,β -Unsaturated Imine.



From the kinetic studies, a set of rate constants for both the 1,2-additions as well as for the 1,4-additions could be obtained. Correlation analysis of these rate constants with the corresponding nucleophilicity parameters (N and s) yielded the electrophilicity parameters for both reaction centers of an α,β -unsaturated imine (Figure 9).

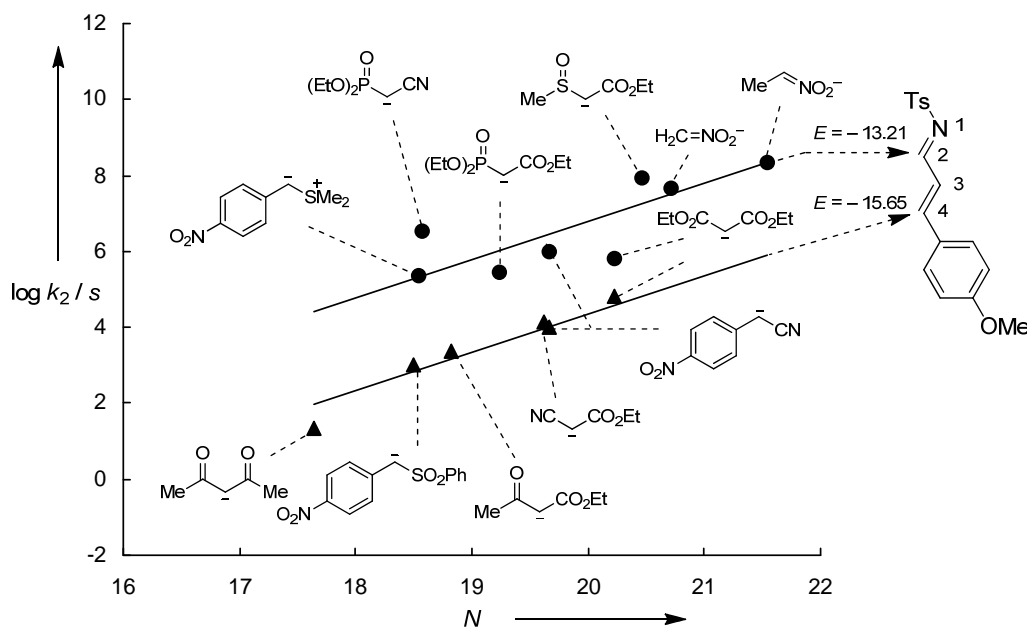
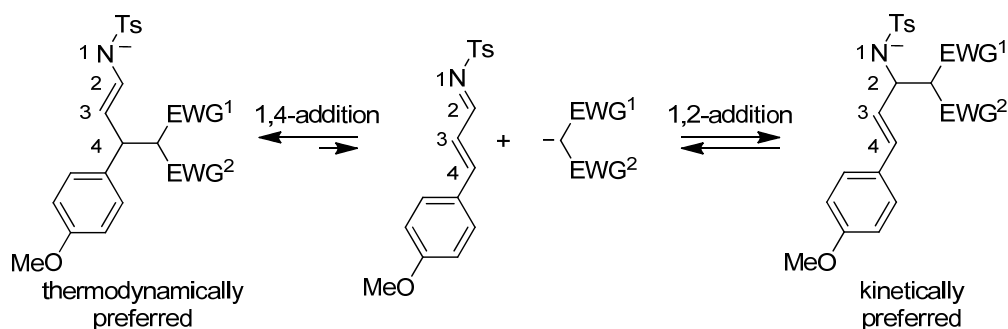


Figure 9: Correlation of $\log k_2 / s$ for the 1,2- and 1,4-additions of several nucleophiles to an α,β -unsaturated imine versus the nucleophilicity parameters N of these nucleophiles in DMSO at 20°C. (The slopes are fixed to one as required by eq 1).

The kinetic and synthetic analyses reveal that 1,2-additions to the investigated α,β -unsaturated imine occur faster than the 1,4-additions, while the 1,4-addition products are thermodynamically preferred (Scheme 7).

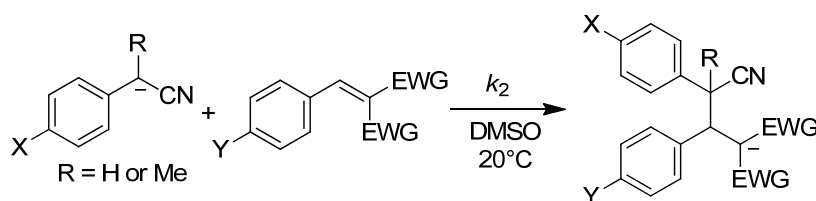
Scheme 7: Rationalization of the Ambident Electrophilic Reactivity of an α,β -Unsaturated Imine by Kinetic and Thermodynamic Control.



8 Nucleophilicities of the Anions of Arylacetonitriles and Arylpropionitriles in Dimethyl Sulfoxide

The rates of the reactions of colored *p*-substituted phenylacetonitrile anions and phenylpropionitrile anions with Michael acceptors were determined by UV-Vis spectroscopy in DMSO at 20°C (Scheme 8).

Scheme 8: Reactions of Phenylacetonitrile and Phenylpropionitrile Anions with Michael Acceptors.



The reactions follow second-order kinetics, and the corresponding rate constants k_2 obey the linear free-energy relationship of eq 1, from which the nucleophile-specific parameters N and s of the investigated carbanions and have been derived. With nucleophilicity parameters from $19 < N < 29$, they are among the most reactive nucleophiles, which have so far been parameterized. Moreover, it has been shown that α -cyano-substituted benzyl anions are several orders of magnitude more nucleophilic than α - SO_2CF_3 - and α - NO_2 -substituted benzyl anions. As colored species of high nucleophilicities, these carbanions complement our series of reference nucleophiles, which can be employed for the photometric determination of electrophilic reactivities (Figure 10).

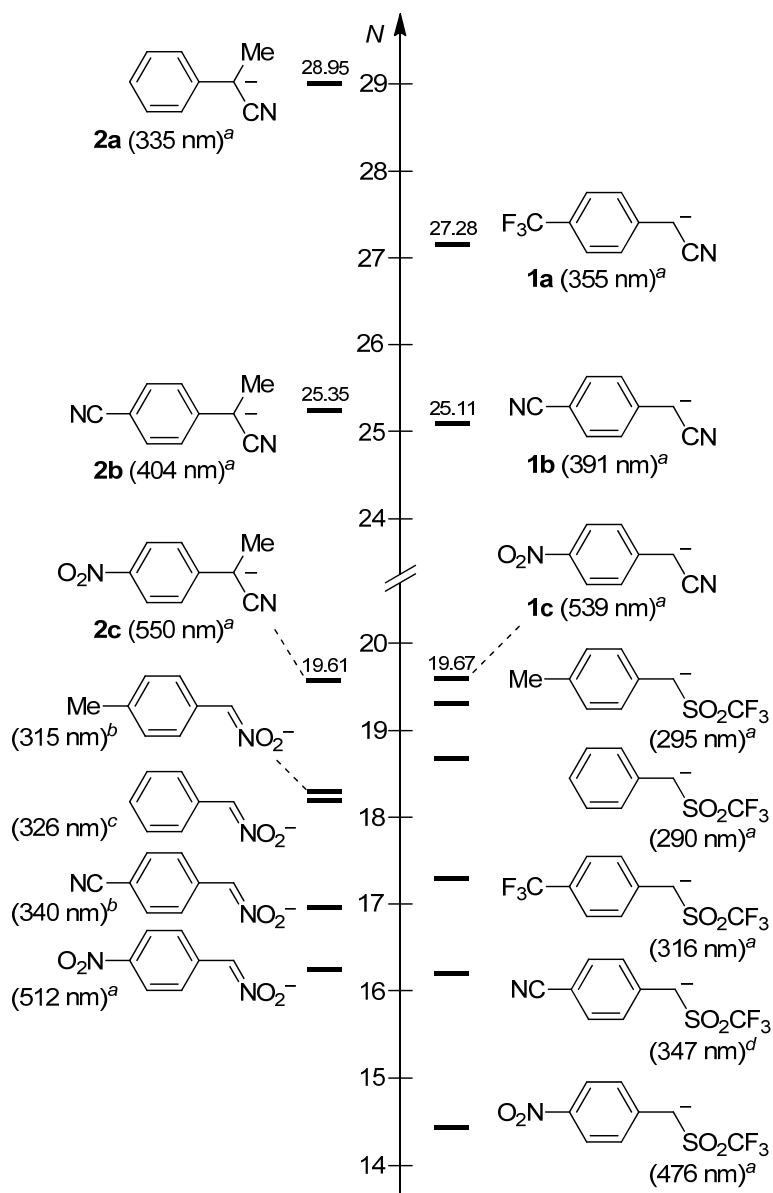
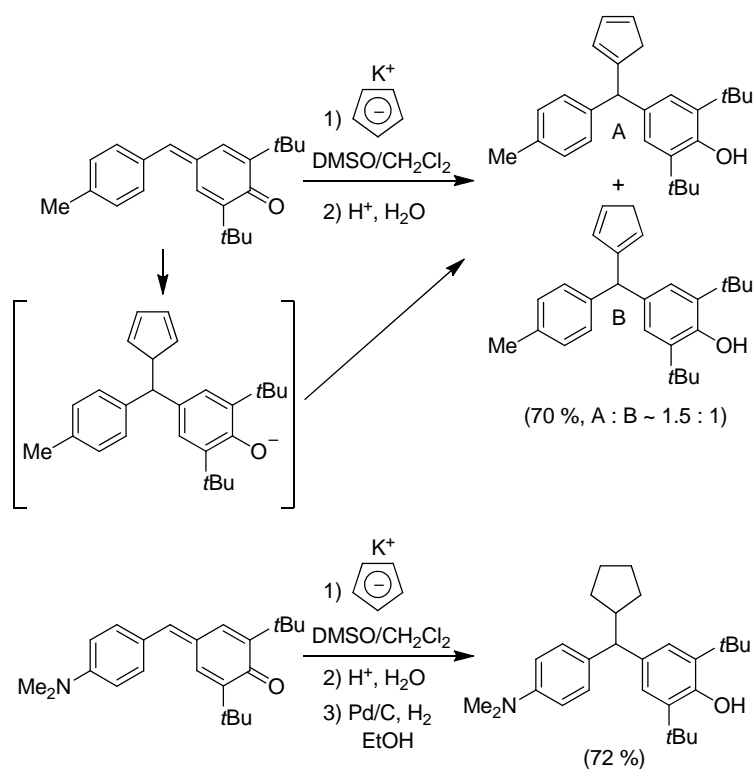


Figure 10: Comparison of the nucleophilicity parameters N of phenylacetone anions and phenylpropionitrile anions with those for α -nitro- and α -trifluoromethylsulfonyl-stabilized carbanions in DMSO. ^a λ_{\max} in DMSO. ^b λ_{\max} in MeOH. ^c λ_{\max} in DMSO/H₂O 10:90 (v/v). ^d λ_{\max} in DMSO/H₂O 30:70 (v/v).

9 Nucleophilic Reactivities of Alkali Cyclopentadienides (CpK, CpNa, CpLi)

The rates of the reactions of potassium-, sodium-, and lithium cyclopentadienides with several Michael acceptors have been determined photometrically. Product studies of potassium cyclopentadienide with quinone methides reveal the formation of two regioisomeric products, which can be hydrogenated to obtain a single product (Scheme 9).

Scheme 9: Reactions of Potassium Cyclopentadienide with Quinone Methides.

By plotting the rate constants of the reactions of the alkali cyclopentadienides against the electrophilicity parameters of the employed electrophiles, their nucleophilicity parameters N and s could be obtained, as exemplarily shown for potassium cyclopentadienide in Figure 11.

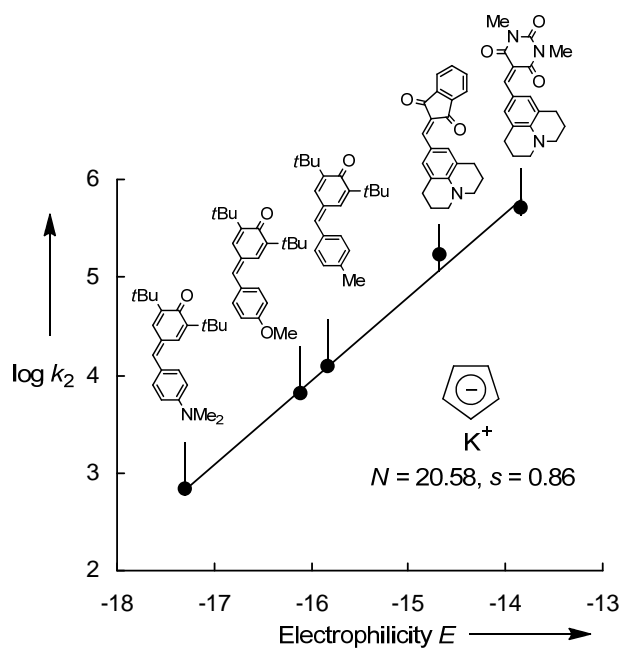


Figure 11: Plot of $\log k_2$ for the reactions of potassium cyclopentadienide with different Michael acceptors at 20°C in DMSO versus their electrophilicity parameters E .

The obtained second-order rate constants for the reactions of the investigated K^+ , Na^+ , and Li^+ cyclopentadienides with Michael acceptors and the resulting nucleophilicity parameters N and s do not differ significantly, when the alkali counterions are changed. As a consequence, we can conclude that all the obtained rate constants reflect the reactivity of the free anion.

Chapter 2: Introduction

1 General

The steady progress in the field of synthetic organic chemistry has led to the discovery of innumerable types of reactions. Considering the large diversity of organic transformations, it is a most challenging task to derive a general concept for the description and prediction of organic reactivity. However, on closer examination it becomes obvious that many organic reactions are combinations of electron-rich reagents with compounds having a lack of electrons. In the 1930s, Ingold introduced the term “nucleophiles” for compounds with a surplus of electrons and the term “electrophiles” for electron-deficient compounds^[1] in order to classify the reactants of these polar organic transformations.

The first systematic approach for quantifying the kinetic terms of nucleophilicity and electrophilicity was reported by Swain and Scott.^[2] By studying the rates of S_N2 reactions, a linear free-energy relationship (eq 1) was found, where nucleophiles are characterized by one parameter (*n*) and electrophiles by two parameters (*s* and log *k*₀). While *n* represents the nucleophilicity of a certain reagent, *s* characterizes the sensitivity of an electrophile towards the variation of nucleophiles and log *k*₀ the rate constant of the electrophile with water. The *s* parameter of methyl bromide was defined as 1.00 and the *n* parameter for water as 0.00.

$$\log (k/k_0) = s n \quad (1)$$

A further important contribution to the quantitative description of polar organic reactivity was reported by Ritchie in 1972.^[3] It was shown that the rates of the reactions of various nucleophiles with carbocations and diazonium ions can be correlated according to eq 2. A given nucleophile in a certain solvent was described by the electrophile-independent nucleophilicity parameter *N*₊, while the electrophilicities of the cations were expressed by their rate constants with water (*k*₀). However, it was shown that eq 2 has a rather limited applicability and better correlations are obtained, when different “families” of electrophiles are treated separately.^[4]

$$\log (k/k_0) = N_+ \quad (2)$$

Based on the rates of the reactions of carbocations, cationic metal- π -complexes, and diazonium ions with n -, π -, and σ -nucleophiles, Mayr and Patz reported a linear free-energy relationship (eq 3), where $k_{20^\circ\text{C}}$ is the second-order rate constant in $\text{M}^{-1} \text{s}^{-1}$, s is a nucleophile-specific sensitivity parameter, N is a nucleophilicity parameter, and E is an electrophilicity parameter.^[5]

$$\log k_{20^\circ\text{C}} = s(N + E) \quad (3)$$

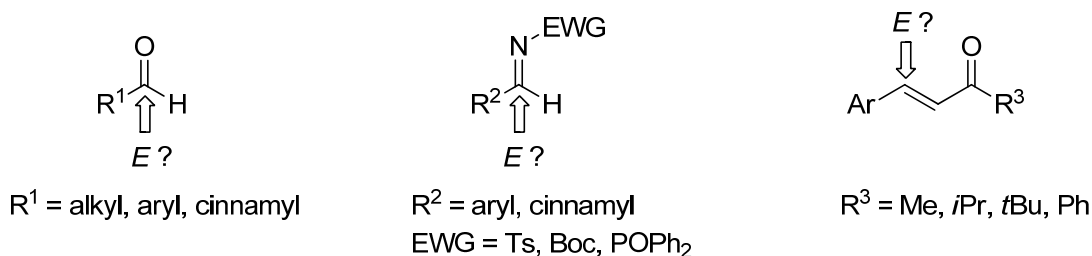
By defining a series of structurally related benzhydrylium ions and Michael acceptors as reference electrophiles having widely variable reactivities, eq 3 was used for the construction of the most comprehensive nucleophilicity and electrophilicity scale presently available.^[6]

The extensive efforts on the determination of reactivity parameters for nucleophiles (N and s) and electrophiles (E) have established a rough ordering principle of polar organic reactivity. With the rule of thumb that nucleophile-electrophile combinations only occur at room temperature when $E + N > -5$ and, diffusion-controlled reactions take place when $E + N > 9$ to 12, a rational planning of organic syntheses with a better understanding of reactivity and selectivity issues has become possible.^[6b,7] Furthermore, a systematic reconsideration of the reactivities of ambident nucleophiles based on eq 3 revealed thermodynamic and kinetic product control as an explanation for the observed regioselectivities, instead of the formerly erroneously employed HSAB treatment of ambident reactivity.^[8] Another important application for organic reactivity parameters was shown in the field of modern organocatalysis. The characterization of the reactivities of key intermediates in these reaction cycles has given useful insights in the complex reaction mechanisms.^[9]

2 Problem Statement

While reactivity parameters (N and s) for many different classes of nucleophiles have already been derived, a considerably smaller amount of electrophiles, mainly carbocations, cationic metal π -complexes, and electron-deficient Michael acceptors, have been characterized according to eq 3.^[6] So far, aldehydes, imines, and enones (Scheme 1), three of the most important classes of electrophiles in organic chemistry, could not be integrated into the electrophilicity scale based on eq 3.

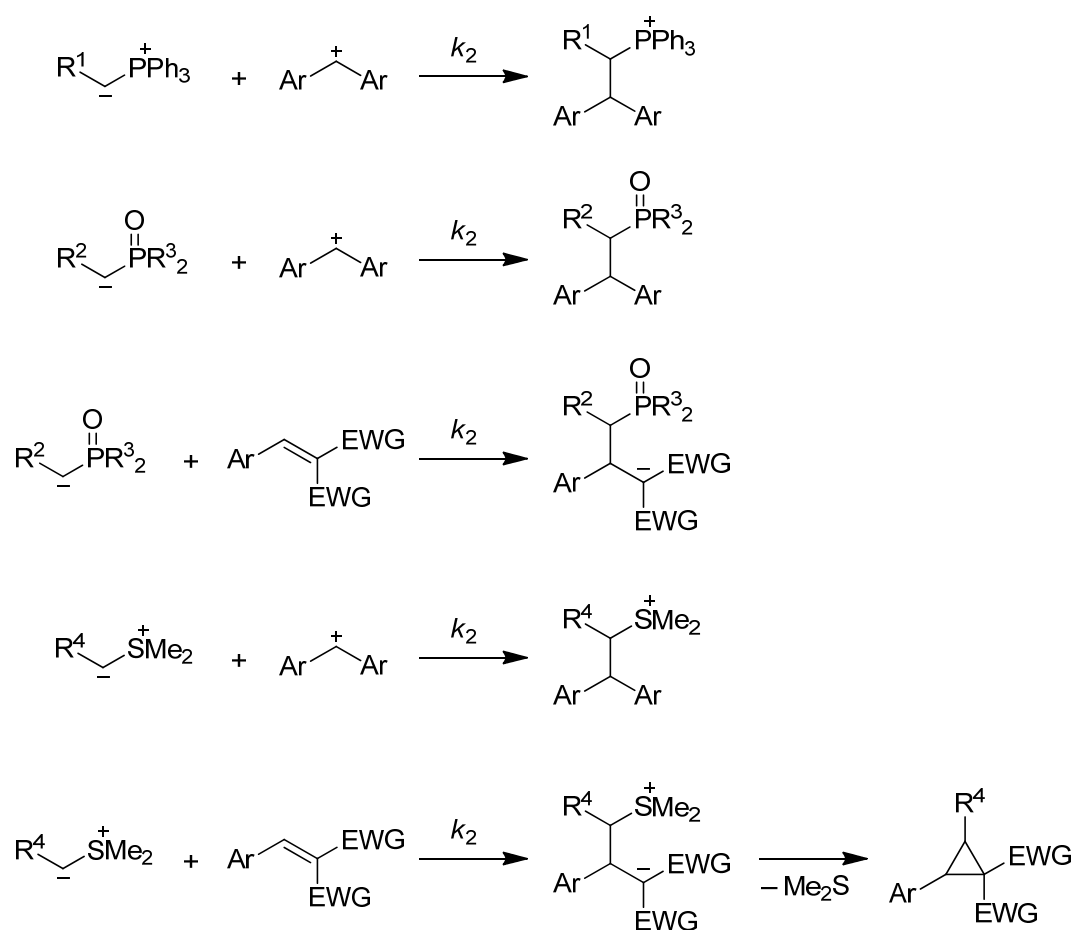
Scheme 1: Aldehydes, Imines, and Enones Investigated in this Work (Ts = *p*-Methylbenzenesulfonyl, Boc = *t*-Butoxycarbonyl).



The electrophilicity parameters E of carbocations and Michael acceptors have previously been derived from the rates of their reactions with carbon-centered nucleophiles (with known N and s parameters), where the CC bond forming step was rate-determining.^[6] As most stabilized carbanions do not react with ordinary aldehydes in DMSO in the absence of a proton source or a strongly coordinating metal ion, an alternative way to achieve irreversible additions of carbon nucleophiles to carbonyl groups had to be found. Therefore, it was necessary to investigate nucleophiles which can trap the intermediate alkoxide anion by an internal electrophile, as it is the case with phosphorus ylides, phosphoryl-stabilized carbanions, and sulfur ylides in Wittig, Horner-Wadsworth-Emmons,^[10] and Corey-Chaykovsky reactions,^[11] respectively.

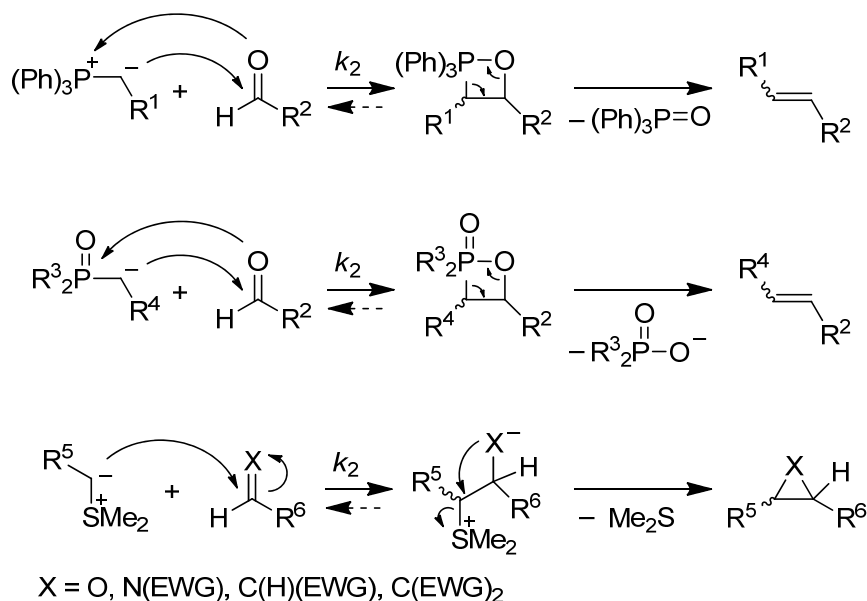
This thesis was set out to integrate phosphorus ylides, sulfur ylides, and related carbanions into the reactivity scale based on eq 3. For this purpose, the rates of their reactions with reference electrophiles (i.e., benzhydrylium ions and Michael acceptors, see Scheme 2) should be determined. The resulting reactivity parameters N and s should allow a direct comparison of the reactivities of these synthetically important nucleophiles.

Scheme 2: Reactions of Phosphorus Ylides, Phosphoryl-Stabilized Carbanions, and Sulfur Ylides with Benzhydrylium Ions and Michael Acceptors.



By combining the nucleophilicity parameters N and s of phosphorus ylides, sulfur ylides, and related carbanions with the rate constants of Wittig, Horner-Wadsworth-Emmons, and sulfur ylide-mediated epoxidation-, aziridination-, and cyclopropanation reactions (Scheme 3), the electrophilic reactivities of aldehydes, imines, and simple Michael acceptors should be quantified systematically. In this context, an investigation of the reactivities of α,β -unsaturated carbonyl compounds and imines should reveal an explanation for the factors controlling the regioselectivities for reactions of these ambident electrophiles (1,2- versus 1,4-addition).

Scheme 3: Wittig Reactions of Phosphorus Ylides, Horner-Wadsworth-Emmons Reactions of Phosphoryl-Stabilized Carbanions, and Sulfur Ylide-Mediated Cyclization Reactions.



In further experiments, the nucleophilic reactivities of different stabilized carbanions (e.g., *p*-substituted phenylacetonitrile anions or the cyclopentadienyl anion) should be determined by studying the rates of their reactions with benzhydrylium ions and Michael acceptors. The change from potassium counterions of stabilized carbanions to stronger coordinating sodium and lithium ions, should provide an insight into the effect of alkali ions on the reactivities of free carbanions. These studies are supposed to pioneer future projects, in which the successive variation of counterions to less electropositive metal cations (Figure 1) should give information about the influence of metal cations on the nucleophilicity of organometallic species.

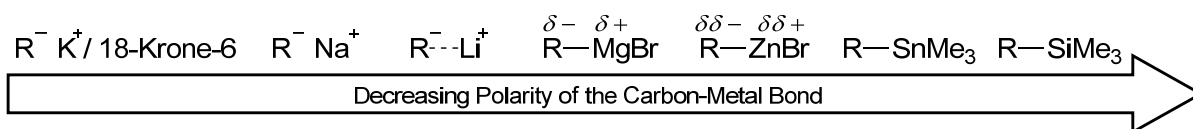


Figure 1: Varying the polarity of carbon-metal bonds by a successive change of the counterion.

As most parts of this thesis have already been published or submitted for publication, individual introductions will be given at the beginning of each chapter. In order to identify my contribution to multiauthor publications, only the kinetic and synthetic experiments, which were performed by me, are described within the corresponding Experimental Sections.

3 References

- [1] (a) Ingold, C. K. *J. Chem. Soc.* **1933**, 1120-1127. (b) Ingold, C. K. *Chem. Rev.* **1934**, *15*, 225-274.
- [2] Swain, C. G.; Scott, C. B. *J. Am. Chem. Soc.* **1953**, *75*, 141-147.
- [3] Ritchie, C. D. *Acc. Chem. Res.* **1972**, *5*, 348-354.
- [4] Ritchie, C. D. *Can. J. Chem.* **1986**, *64*, 2239-2250.
- [5] Mayr, H.; Patz, M. *Angew. Chem.* **1994**, *106*, 990-1010; *Angew. Chem. Int. Ed. Engl.* **1994**, *33*, 938-957.
- [6] (a) Mayr, H.; Bug, T.; Gotta, M. F.; Hering, N.; Irrgang, B.; Janker, B.; Kempf, B.; Loos, R.; Ofial, A. R.; Remennikov, G.; Schimmel, H. *J. Am. Chem. Soc.* **2001**, *123*, 9500-9512. (b) Lucius, R.; Loos, R.; Mayr, H. *Angew. Chem.* **2002**, *114*, 97-102; *Angew. Chem. Int. Ed.* **2002**, *41*, 91-95. (c) Mayr, H.; Kempf, B.; Ofial, A. R. *Acc. Chem. Res.* **2003**, *36*, 66-77. (d) Mayr, H.; Ofial, A. R. *Pure Appl. Chem.* **2005**, *77*, 1807-1821. (e) Mayr, H.; Ofial, A. R. *J. Phys. Org. Chem.* **2008**, *21*, 584-595. (f) For a comprehensive database of nucleophilicity parameters N and electrophilicity parameters E , see <http://www.cup.lmu.de/oc/mayr/>.
- [7] Mayr, H.; Ofial, A. R. *Angew. Chem.* **2006**, *118*, 1876-1886; *Angew. Chem. Int. Ed.* **2006**, *45*, 1844-1854.
- [8] (a) Loos, R.; Kobayashi, S.; Mayr, H. *J. Am. Chem. Soc.* **2003**, *125*, 14126-14132. (b) Bug, T.; Lemek, T.; Mayr, H. *J. Org. Chem.* **2004**, *69*, 7565-7576. (c) Tishkov, A. A.; Mayr, H. *Angew. Chem.* **2005**, *117*, 145-148; *Angew. Chem. Int. Ed.* **2005**, *44*, 142-145. (d) Tishkov, A. A.; Schmidhammer, U.; Roth, S.; Riedle, E.; Mayr, H. *Angew. Chem.* **2005**, *117*, 4699-4703; *Angew. Chem. Int. Ed.* **2005**, *44*, 4623-4626. (e) Schaller, H. F.; Schmidhammer, U.; Riedle, E.; Mayr, H. *Chem. Eur. J.* **2008**, *14*, 3866-3868. (f) Baidya, M.; Kobayashi, S.; Mayr, H. *J. Am. Chem. Soc.* **2010**, *132*, 4796-4805. (g) Breugst, M.; Mayr, H. *J. Am. Chem. Soc.* **2010**, *132*, 15380-15389.
- [9] (a) Lakhdar, S.; Tokuyasu, T.; Mayr, H. *Angew. Chem.* **2008**, *120*, 8851-8854; *Angew. Chem. Int. Ed.* **2008**, *47*, 8723-8726. (b) Baidya, M.; Remennikov, G. Y.; Mayer, P.; Mayr, H. *Chem. Eur. J.* **2010**, *16*, 1365-1371. (c) Lakhdar, S.; Ofial, A. R.; Mayr, H. *J. Phys. Org. Chem.* **2010**, *23*, 886-892. (d) Kanzian, T.; Lakhdar, S.; Mayr, H. *Angew. Chem.* **2010**, *122*, 9717-9720; *Angew. Chem. Int. Ed.* **2010**, *49*, 9526-9529.
- [10] (a) Staudinger, H.; Meyer, J. *Helv. Chim. Acta* **1919**, *2*, 635-646. (b) Wittig, G.; Geissler, G. *Liebigs Ann. Chem.* **1953**, *580*, 44-57. (c) Wittig, G.; Schöllkopf, U. *Chem. Ber.* **1954**, *87*, 1318-1330. (d) Horner, L.; Hoffmann, H.; Wippel, H. G. *Chem. Ber.*

- 1958**, 91, 61-63. (e) Horner, L.; Hoffmann, H.; Wippel, H. G.; Klahre, G. *Chem. Ber.* **1959**, 92, 2499-2505. (f) Wadsworth, W. S.; Emmons, W. D. *J. Am. Chem. Soc.* **1961**, 83, 1733-1738. For a selected review, see: (g) Maryanoff, B. E.; Reitz, A. B. *Chem. Rev.* **1989**, 89, 863-927.
- [11] (a) Johnson, A. W.; LaCount, R. B. *Chem. Ind. (London)* **1958**, 1440-1441. (b) Johnson, A. W.; LaCount, R. B. *J. Am. Chem. Soc.* **1961**, 83, 417-423. (c) Corey, E. J.; Chaykovsky, M. *J. Am. Chem. Soc.* **1962**, 84, 867-868. (d) Corey, E. J.; Chaykovsky, M. *J. Am. Chem. Soc.* **1962**, 84, 3782-3783. For selected reviews, see: (e) Trost, B. M.; Melvin, L. S. *Sulfur Ylides. Emerging Synthetic Intermediates*; Academic Press: New York, 1975. (f) McGarrigle, E. M.; Myers, E. L.; Illa, O.; Shaw, M. A.; Riches, S. L.; Aggarwal, V. K. *Chem. Rev.* **2007**, 107, 5841-5883.

Chapter 3: Nucleophilicity Parameters for Phosphoryl-Stabilized Carbanions and Phosphorus Ylides: Implications for Wittig and Related Olefination Reactions

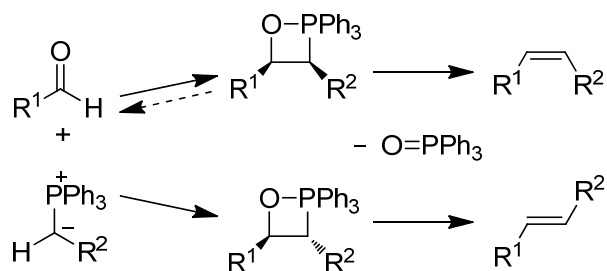
Roland Appel, Robert Loos, and Herbert Mayr

J. Am. Chem. Soc. **2009**, *131*, 704-714.

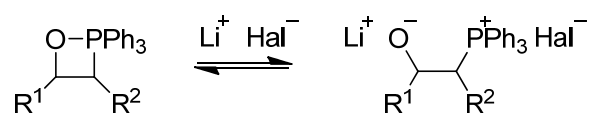
1 Introduction

The Wittig reaction^[1] as well as the related Wittig-Horner^[2] and Horner-Wadsworth-Emmons^[3] reactions are among the most important methods for synthesizing CC double bonds. These olefinations provide access to a wide structural variety and can be carried out with high stereoselectivity.^[4] Detailed mechanistic investigations by Vedejs,^[4e,5] Maryanoff and Reitz,^[6] as well as quantum-chemical approaches by Yamataka,^[7a,b] Aggarwal and Harvey,^[7c,d] and other authors^[8] led to the generally accepted model of salt-free Wittig reactions (Scheme 1). In the first step, an oxaphosphetane is formed via a concerted asynchronous [2+2] cycloaddition with a transition state in which the CC bond formation is more advanced than the PO bond formation. The resulting oxaphosphetane decomposes into the olefin and phosphine oxide. NMR studies showed that the initial oxaphosphetane formation is in general a nonreversible step,^[4a,e,5g,6a,9] although some exceptions have also been reported.^[4a,e,5d,g,10]

Scheme 1: Mechanism of the Salt-Free Wittig Reaction.



In the presence of lithium halides, the oxaphosphetane intermediates can be transferred into betaine intermediates^[5b,11] (Scheme 2), which may be isomerized by additional base before they cyclize, forming the thermodynamically more stable *trans*-oxaphosphetanes, which finally yield the *trans*-olefins selectively.^[4b,e,5g,12] Recently, alternative ionic intermediates have been suggested to account for the stereochemical drift.^[13]

Scheme 2: Betaine Intermediates in the Presence of Lithium Halides.

The mechanistic course of the Horner-Wadsworth-Emmons reactions is closely related to that of the Wittig reaction,^[4b,i,k,l] although it is still controversial, whether the initial attack of the carbanion at the carbonyl group and the oxaphosphetane ring closure proceed in a concerted or stepwise manner and which step is rate-determining in the latter case.^[14] Systematic kinetic investigations for this reaction in ethanol solution by Larsen and Aksnes^[15] led to the conclusion that the oxaphosphetane intermediate is formed in a concerted manner in the rate-determining step.

It is well-known that phosphoryl-substituted carbanions are generally more reactive than phosphorus ylides. A quantitative comparison of these two classes of compounds has, to our knowledge, not been performed to date.

In recent years, we have developed the most comprehensive nucleophilicity scale presently available.^[16] By defining a series of structurally related benzhydrylium ions and quinone methides (some of them are depicted in Table 1) having widely variable reactivities, we have been able to directly compare nucleophiles that differ largely in reactivity.^[16b-f] In this way, we have circumvented the problem that a single reference electrophile does not allow one to compare a large variety of nucleophiles because (1) second-order rate constants $k_2 < 10^{-6} \text{ M}^{-1}\text{s}^{-1}$ cannot easily be determined and (2) the upper limit for the rates of bimolecular reactions is given by diffusion control ($k_2 = 10^9\text{-}10^{10} \text{ M}^{-1}\text{s}^{-1}$ in typical solvents). It has been demonstrated that the nucleophile-specific parameters N and s (defined by eq 1), which are derived from the second-order rate constants (k_2) of a particular nucleophile with a series of benzhydrylium ions and/or quinone methides, correctly predict the reactivity of this nucleophile towards other types of carbocations and Michael acceptors of known electrophilicity E .^[16b-f,17]

$$\log k_{20^\circ\text{C}} = s(N + E) \quad (1)$$

In this work, we have employed this method for characterizing the nucleophilicities of four phosphorus ylides and four phosphoryl-stabilized carbanions (Scheme 3), and we will discuss the impact of these results on carbonyl olefinations. In order to achieve conveniently measurable reactions, the carbanions **1a-d** were predominantly characterized by their

reactions with quinone methides **2i–m** and the least electrophilic benzhydrylium ion **2h**, while the much less nucleophilic phosphorus ylides **1e–h** were almost exclusively characterized through their reactivities towards benzhydrylium ions **2a–h**.

Scheme 3: Phosphoryl-Stabilized Carbanions **1a–d** and Phosphorus Ylides **1e–h** Investigated in this Work.

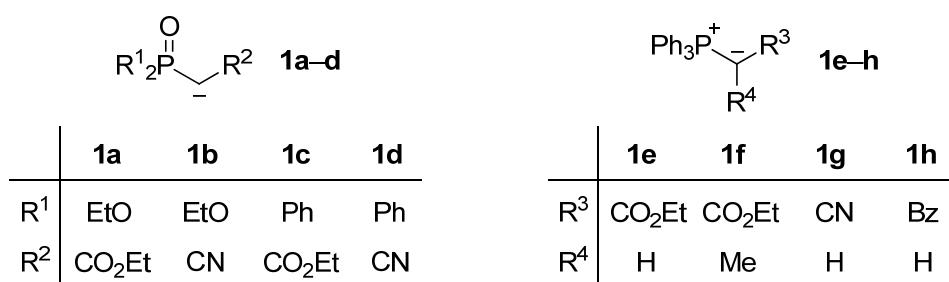
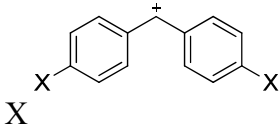
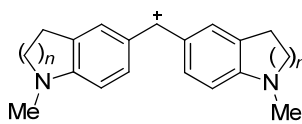
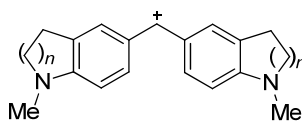
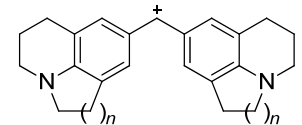
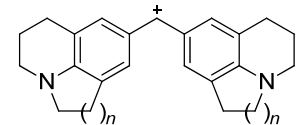
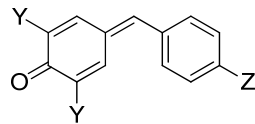
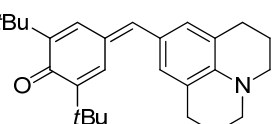


Table 1: Benzhydrylium Ions **2a–h** and Quinone Methides **2i–m** Employed in this Work.

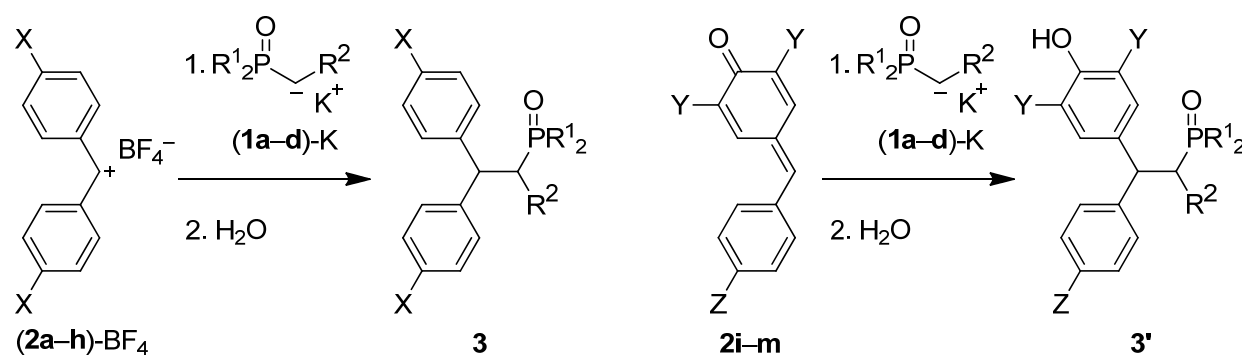
		E^a
2a	NPh ₂	-4.72
2b	N(Ph)(Me)	-5.89
2c	NMe ₂	-7.02
2d	N(CH ₂) ₄	-7.69
2e ($n = 2$)		-8.22
2f ($n = 1$)		-8.76
2g ($n = 2$)		-9.45
2h ($n = 1$)		-10.04
		E^a
2i	Ph OMe	-12.18
2j	<i>t</i> Bu Me	-15.83
2k	<i>t</i> Bu OMe	-16.11
2l	<i>t</i> Bu NMe ₂	-17.29
2m		-17.90

^a E values for **2a–h** were taken from ref 16b and those for **2i–m** from ref 16c.

2 Results

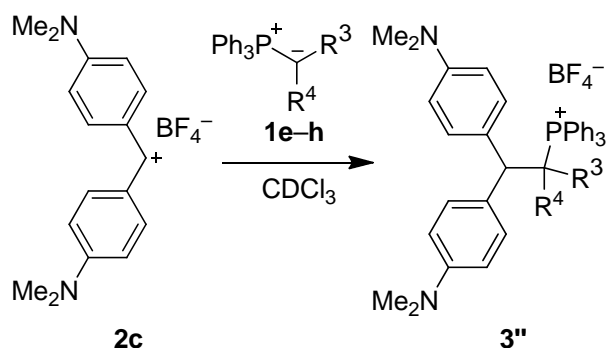
Product Studies. As shown in Scheme 4, the phosphoryl-stabilized carbanions **1a–d** react with the reference electrophiles **2** to give the addition products **3** or **3'**. Solutions of the carbanions **1a–d** were generated either by deprotonating the corresponding CH acids in DMSO with KO t Bu or by isolating the potassium salts (**1a–d**)-K and dissolving them in DMSO or CH₃CN. The particular electrophile, in DMSO or CH₂Cl₂ solution or in a mixture of the two solvents, was then added.

Scheme 4: Reactions of the Phosphoryl-Stabilized Carbanions **1a–d** with the Reference Electrophiles **2**.



The bis(*p*-dimethylamino)benzhydrylium ion **2c** was the only electrophile used for product studies with the phosphorus ylides **1e–h** (Scheme 5). One can assume that variation of the remote aryl substituent of the electrophile does not affect the types of products. The formation of **3''** from **1e–h** and **2c** was studied in CDCl₃ solution by NMR.

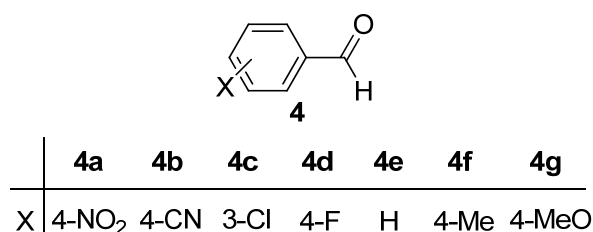
Scheme 5: Reactions of the Phosphorus Ylides **1e–h** with the Reference Electrophile **2c**.



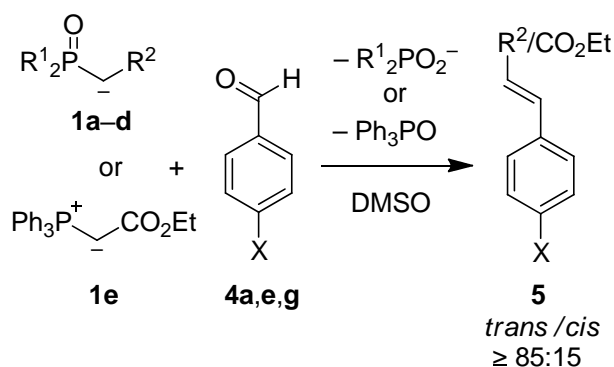
The olefination reactions with the nucleophiles **1a–e** were studied with a series of substituted benzaldehydes **4** (Scheme 6). Representative combinations of the nucleophiles **1a–e** with the benzaldehydes **4a**, **4e**, and **4g** in DMSO showed the expected *trans* selectivity (Scheme 7).

The *cis/trans* ratio of the olefins **5** was determined by GC/MS. In order to exclude that the observed *cis/trans* ratio was changed during workup or purification, samples were taken from the reaction mixtures after different reaction times and analyzed after dilution with acetone. Details are given in the Experimental Section.

Scheme 6: Substituted Benzaldehydes **4** Employed in this Work.



Scheme 7: Reactions of the Phosphoryl-Stabilized Carbanions **1a–d** and the Phosphorus Ylide **1e** with the Benzaldehydes **4a**, **4e** and **4g**.



Kinetic Investigations. For the kinetic measurements, solutions of the carbanions **1a–d** were generated either by deprotonation of the corresponding CH acids with 1.00-1.05 equiv of KO^tBu in DMSO solution or by isolating the potassium salts (**1a–d**)-K and then dissolving them in DMSO. The reactions of the nucleophiles **1a–h** with the reference electrophiles **2a–m** in DMSO or CH₂Cl₂ at 20°C were monitored by UV-Vis spectroscopy at or close to the absorption maxima of the electrophiles. In all of the cases examined, complete consumption of the electrophiles **2** was observed when their solutions were combined with an excess of the carbanions **1a–d**, as shown in Figure 1.

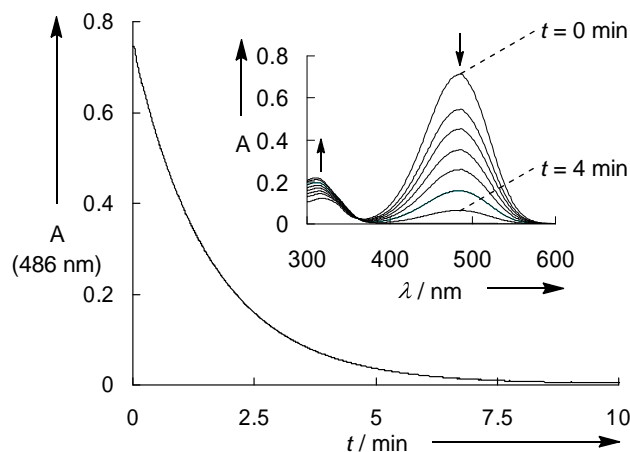


Figure 1: UV-Vis spectroscopic monitoring of the reaction of the phosphoryl-stabilized carbanion **1a** ($7.57 \times 10^{-4} \text{ mol L}^{-1}$) with the quinone methide **2l** ($3.52 \times 10^{-5} \text{ mol L}^{-1}$) at 486 nm in DMSO at 20°C.

Because the nucleophiles **1a–h** were employed in large excess over the electrophiles **2a–m**, their concentration can be considered almost constant throughout the reactions, resulting in first-order kinetics with an exponential decay of the concentrations of the electrophiles **2** (eq 2):

$$-d[\mathbf{2}]/dt = k_{\text{obs}} [\mathbf{2}] \quad (2)$$

The first-order rate constants k_{obs} were obtained by least-squares fitting of the single-exponential $A_t = A_0 \exp(-k_{\text{obs}}t) + C$ to the time-dependent absorbances A of the electrophiles. Second-order rate constants were then obtained as the slopes of plots of k_{obs} versus the concentration of the nucleophile (Figure 2).

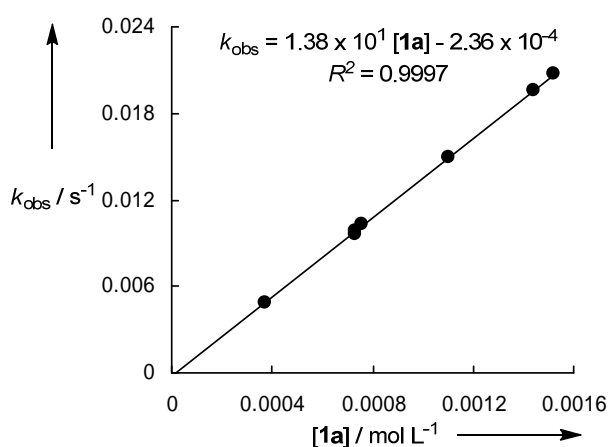
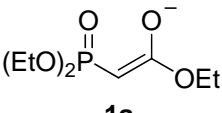
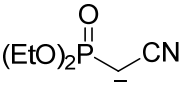
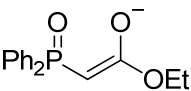
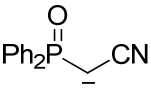


Figure 2: Determination of the second-order rate constant $k_2 = 1.38 \times 10^1 \text{ L mol}^{-1} \text{ s}^{-1}$ for the reaction of the phosphoryl-stabilized carbanion **1a** with the quinone methide **2l** in DMSO at 20°C.

The rate constants listed in Table 2 refer to the reactivities of the free carbanions **1a–d**. Though most of the reactions of (**1a–d**)-K were performed in the presence of 18-crown-6, this additive was not really necessary. In a control experiment, it was found that the rate of the reaction of **1b**-K with **2k** remained constant in the absence of crown ether even when large amounts of KBF₄ (up to 1.6×10^{-2} mol L⁻¹) were added (see Table 52 in the Experimental Section). However, as discussed below, counterion effects were observed when sodium or lithium salts were employed.

Table 2: Second-Order Rate Constants for the Reactions of the Phosphoryl-Stabilized Carbanions **1a–d** and 0-1.3 equiv of 18-Crown-6 with the Reference Electrophiles **2h–m** in DMSO at 20°C.

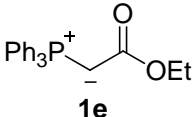
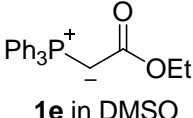
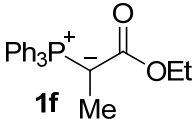
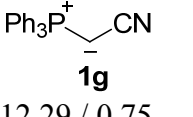
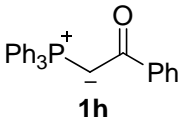
Nucleophile <i>N</i> / <i>s</i> ^a	Counterion	Electrophile	<i>k</i> ₂ / L mol ⁻¹ s ⁻¹
 1a 19.23 / 0.65	K ⁺ /18-crown-6	2h	5.82×10^5
	K ⁺ /18-crown-6	2i	6.06×10^4
	K ⁺	2j	1.99×10^2
	K ⁺ /18-crown-6	2k	1.28×10^2
	K ⁺ /18-crown-6	2l	1.38×10^1
	K ⁺ /18-crown-6	2m	6.02
 1b 18.57 / 0.66	K ⁺ /18-crown-6	2h	3.66×10^5 ^b
	K ⁺ /18-crown-6	2i	2.23×10^4 ^b
	K ⁺ /18-crown-6	2j	6.71×10^1
	K ⁺ /18-crown-6	2k	4.38×10^1 ^b
	K ⁺ /18-crown-6	2l	6.47 ^b
	K ⁺	2m	2.80 ^b
 1c 19.20 / 0.69	K ⁺ /18-crown-6	2h	1.85×10^6 ^b
	K ⁺ /18-crown-6	2i	8.99×10^4 ^b
	K ⁺ /18-crown-6	2j	2.32×10^2 ^b
	K ⁺ /18-crown-6	2k	1.28×10^2 ^b
	K ⁺ /18-crown-6	2l	1.41×10^1 ^b
	K ⁺ /18-crown-6	2m	1.05×10^1
 1d 18.69 / 0.72	K ⁺ /18-crown-6	2h	1.98×10^6 ^b
	K ⁺ /18-crown-6	2i	4.12×10^4 ^b
	K ⁺ /18-crown-6	2j	1.21×10^2 ^b
	K ⁺ /18-crown-6	2k	6.75×10^1 ^b
	K ⁺ /18-crown-6	2l	1.10×10^1 ^b

^a Values of the nucleophilicity parameters *N* and *s* were derived using eq 1, as described in the Discussion.

^b Reaction occurred in the presence of the corresponding conjugate CH acid (**1b–d**)-H.

Analogously, the reactions of the phosphorus ylides **1e–h** with the electrophiles **2** generally proceeded with full conversion of the electrophile. In only a few cases, which are marked in Table 3, was the consumption of the electrophiles **2** not complete, indicating equilibrium situations.

Table 3: Second-Order Rate Constants for the Reactions of the Phosphorus Ylides **1e–h** with the Reference Electrophiles **2a–i** in CH₂Cl₂ at 20°C.

Nucleophile <i>N</i> / <i>s</i> ^a	Electrophile	<i>k</i> ₂ / L mol ⁻¹ s ⁻¹
 1e 12.79 / 0.77	2c	2.65 × 10 ⁴
	2e	3.69 × 10 ³
	2f	1.26 × 10 ³
	2h	1.28 × 10 ²
 1e in DMSO 12.21 / 0.62	2c	1.86 × 10 ³
	2d	6.80 × 10 ²
	2f	1.05 × 10 ²
	2h	2.51 × 10 ¹
	2i	1.06
 1f 13.09 / 0.73	2b	2.03 × 10 ⁵
	2c	2.34 × 10 ⁴
	2e	3.90 × 10 ³
	2g	4.64 × 10 ² ^b
 1g 12.29 / 0.75	2a	4.35 × 10 ⁵
	2c	1.21 × 10 ⁴
	2e	1.21 × 10 ³
	2h	4.33 × 10 ¹ ^b
 1h 9.54 / 0.97	2b	3.37 × 10 ³
	2c	2.73 × 10 ² ^b

^a Values of the nucleophilicity parameters *N* and *s* were derived using eq 1, as described in the Discussion.

^b Incomplete consumption of the electrophile was observed, indicating an equilibrium situation.

The kinetics of the reactions of the nucleophiles **1a–e** with the substituted benzaldehydes **4a–g** were investigated in DMSO at 20°C using large excesses of the nucleophiles. The first-order rate constants *k*_{obs} were usually derived from the single-exponential increase of the

absorbances of the resulting styrenes **5**. As shown in Figure 3 for the reaction of *p*-methoxybenzaldehyde **4g** with the phosphoryl-stabilized carbanion **1b**, the rate of consumption of *p*-methoxybenzaldehyde (monitored at 270 nm) was equal to the rate of formation of *p*-methoxycinnamionitrile (monitored at 310 nm), excluding the formation of a long-lived intermediate during the reaction.

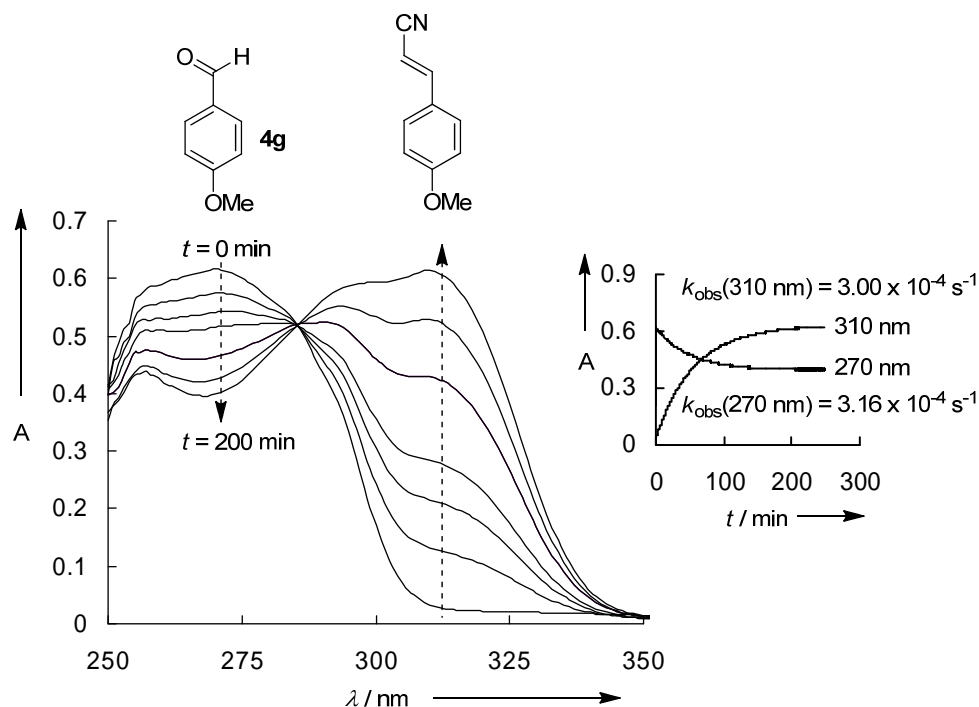


Figure 3: Reaction of *p*-methoxybenzaldehyde **4g** ($5.58 \times 10^{-5} \text{ mol L}^{-1}$) with the phosphoryl-stabilized carbanion **1b** ($7.99 \times 10^{-4} \text{ mol L}^{-1}$) in DMSO at 20°C (the UV absorption of **1b** at $\lambda_{\text{max}} = 257 \text{ nm}$ is partially superimposed by the aldehyde). The inset shows the time traces along with the corresponding k_{obs} values for the single-exponential increase of the reaction product *p*-methoxycinnamionitrile and the single-exponential decrease of the aldehyde **4g**.

Second-order rate constants (Table 4) were again obtained as the slopes of plots of k_{obs} versus the concentration of the nucleophile (Figure 4).

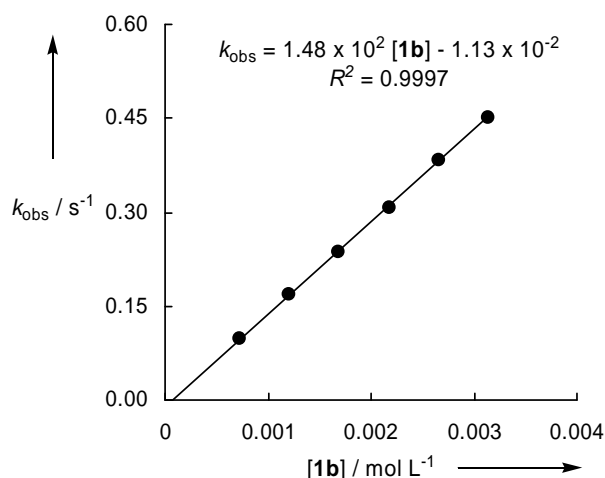
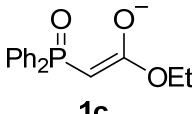
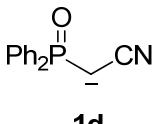
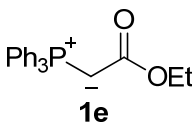


Figure 4: Determination of the second-order rate constant $k_2 = 1.48 \times 10^2 \text{ L mol}^{-1} \text{ s}^{-1}$ for the reaction of the phosphoryl-stabilized carbanion **1b** with *m*-chlorobenzaldehyde **4c** in DMSO at 20°C.

Table 4: Second-Order Rate Constants for the Reactions of the Phosphoryl-Stabilized Carbanions **1a–d** (with K^+ /18-Crown-6 as Counterion) and the Phosphorus Ylide **1e** with the Aldehydes **4a–g** in DMSO at 20°C.

Nucleophile	Electrophile	$k_2 / \text{L mol}^{-1} \text{ s}^{-1}$
 1a	4a	1.20×10^3
	4b	4.78×10^2
	4c	5.73×10^1
	4d	4.05
	4e	2.02
	4f	4.64×10^{-1}
	4g	9.31×10^{-2}
 1b	4a	2.45×10^3
	4b	1.05×10^3
	4c	1.48×10^2
	4d	1.17×10^1
	4e	7.16
	4f	1.73
	4g	3.64×10^{-1}

Table 4: (Continued).

Nucleophile	Electrophile	$k_2 / \text{L mol}^{-1} \text{s}^{-1}$
 1c	4a	2.51×10^1
	4b	1.11×10^1
	4c	1.58
 1d	4a	9.32×10^1
	4b	4.46×10^1
	4c	6.67
	4d	7.08×10^{-1}
	4e	5.52×10^{-1}
 1e	4a	3.07×10^{-1}
	4e	$1.44 \times 10^{-3}{}^a$

^a From ref 23d.

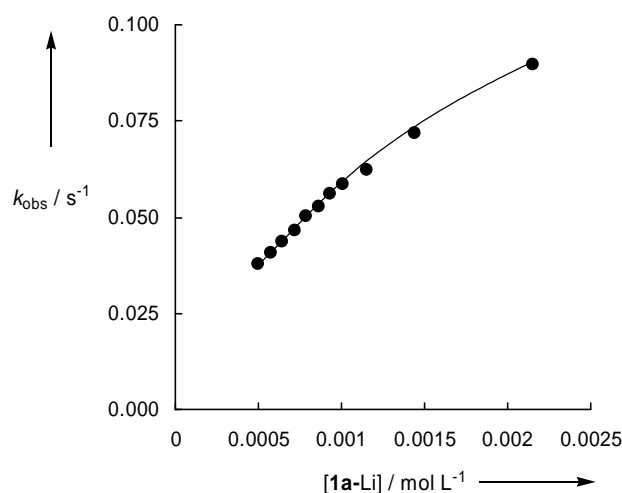
Counterion Effects. In order to gain more insight into the role of the counterions in the reactions of the carbanions **1** with the reference electrophiles **2** as well as with the aldehydes **4**, additional studies in the presence of different alkali cations were performed. For this purpose, the CH acids **1a-H** and **1b-H** were deprotonated with 1.00-1.05 equiv of NaOtBu or LiOtBu in DMSO solution to generate the corresponding sodium or lithium salts **1a-Na** and **1b-Na** or **1a-Li** and **1b-Li**, respectively. Their reactions with the reference electrophiles **2j-m** and the aldehydes **4a**, **4e**, and **4g** were then investigated kinetically using the same method as described above.

All of the reactions, which are listed in Table 5, followed first-order kinetics regardless of the counterion (K^+ , Na^+ , or Li^+) when the carbanions **1a** and **1b** were used in large excess over the electrophiles **2** or **4**. Except for the reactions of **1a-Li**, second-order rate laws were followed, as derived from the linear increase of k_{obs} with the concentrations of **1a** and **1b** (Figures 2 and 4; for details see Tables 34-40, 53-61, and 63-67 in the Experimental Section). In contrast, the plots of k_{obs} versus $[\mathbf{1a-Li}]$ were curved (Figure 5 and Tables 41, 42, and 49 of the Experimental Section), and it was not possible to determine second-order rate constants for the reactions of **1a-Li** with electrophiles.

Table 5: Second-Order Rate Constants k_2 ($\text{L mol}^{-1} \text{s}^{-1}$) for the Reactions of the Phosphoryl-Stabilized Carbanions **1a** and **1b** with the Reference Electrophiles **2h–m** and the Aldehydes **4a**, **4e**, and **4g** in the Presence of Different Counterions in DMSO at 20°C.

Nucleophile	Entry	Electrophile	$k_2 / \text{L mol}^{-1} \text{s}^{-1}$		
			$\text{K}^+ / 18\text{-crown-6}^a$	Na^+	Li^+
 1a	1	2h	5.82×10^5	-	$(1.85 \times 10^5)^b$
	2				$(1.44 \times 10^4)^c$
	3	2j	1.99×10^2	1.47×10^2	$(5.79 \times 10^1)^b$
	4	2k	1.28×10^2	9.56×10^1	$(3.57 \times 10^1)^b$
	5				$(2.49)^c$
	6	2l	1.38×10^1	1.02×10^1	-
	7	2m	6.02	4.43	-
	8	4a	1.20×10^3	1.11×10^3	$(3.25 \times 10^2)^b$
	9	4a			$(4.70 \times 10^1)^c$
	10	4e	2.02	2.53	-
	11	4g	9.31×10^{-2}	1.59×10^{-1}	-
 1b	12	2j	6.71×10^1	6.81×10^1	6.92×10^1
	13	2k	4.38×10^1	4.35×10^1	4.48×10^1
	14	2l	6.47	6.78	6.84
	15	2m	2.80	2.78	2.81
	16	4a	2.45×10^3	2.72×10^3	2.70×10^3
	17	4e	7.16	8.30	8.35
	18	4g	3.64×10^{-1}	4.88×10^{-1}	4.44×10^{-1}

^a Reactions used 0-1.3 equiv of 18-crown-6; data from Tables 2 and 4. ^b No second-order kinetics; $k = k_{\text{obs}} / [\mathbf{1a}]$ at $[\mathbf{1a}] = [\text{Li}^+] = 1 \times 10^{-3} \text{ mol L}^{-1}$. ^c No second-order kinetics; $k = k_{\text{obs}} / [\mathbf{1a}]$ at $[\mathbf{1a}] = 1 \times 10^{-3} \text{ mol L}^{-1}$ and $[\text{Li}^+] = 9 \times 10^{-3} \text{ mol L}^{-1}$.

**Figure 5:** Nonlinear dependence of k_{obs} on the concentration of the nucleophile for the reaction of **1a** with the reference electrophile **2j** in the presence of Li^+ in DMSO at 20°C.

In order to obtain more information about the effect of Li^+ on the reactivity of **1a**, further kinetic studies of the reactions of **1a** with different electrophiles have been performed at variable concentrations of Li^+ . For that purpose, the carbanion concentration [**1a**] (obtained by deprotonation of the corresponding CH acid **1a-H** with 1.00-1.05 equiv of LiOtBu) was kept constant while the Li^+ concentration was modulated by adding various amounts of LiBF_4 . As depicted in Figure 6, the first-order rate constants k_{obs} (s^{-1}) for the reactions of the quinone methide **2k** with **1a** decreased dramatically as the Li^+ concentration was increased.

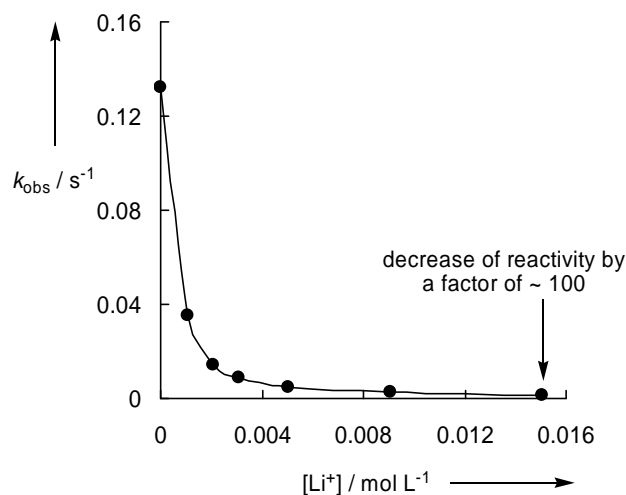


Figure 6: Dependence of k_{obs} on the absolute concentration of Li^+ for the reaction of **1a** ($1 \times 10^{-3} \text{ mol L}^{-1}$) with the quinone methide **2k** ($3 \times 10^{-5} \text{ mol L}^{-1}$) in DMSO at 20°C . (The second-order rate constant $k_2 = 128 \text{ L mol}^{-1} \text{ s}^{-1}$ for the reaction of **1a-K/18-crown-6** with **2k** in DMSO at 20°C (see Table 2) was used to calculate the k_{obs} value for $[\text{Li}^+] = 0 \text{ mol L}^{-1}$).

Li^+ effects on k_{obs} , as depicted in Figure 6, were also observed for the reactions of **1a** with the benzhydrylium ion **2h** (see Tables 47 and 48 in the Experimental Section) and the aldehyde **4a** (see Tables 50 and 51 in the Experimental Section). In contrast, the addition of LiBF_4 had only small effects on the rates of the reactions of the carbanion **1b** with electrophiles. Thus, the reaction of **1b** with the quinone methide **2k** was only 2.3 times slower than the corresponding reaction of the free carbanion **1b** at a high concentration of Li^+ ($[\text{Li}^+] = 1.19 \times 10^{-2} \text{ mol L}^{-1}$ and $[\text{1b}] = 8.02 \times 10^{-4} \text{ mol L}^{-1}$; see Table 62 in the Experimental Section). The rates of the reactions of the phosphorus ylide **1e** with the benzhydrylium ion **2h** as well as with the aldehyde **4a** were not at all affected by the addition of variable amounts of LiBF_4 (see Tables 68-70 in the Experimental Section).

3 Discussion

Counterion Studies. Variation of the counterion of the cyano-stabilized phosphonate **1b** from K^+ via Na^+ to Li^+ revealed (within the error limits of our experiments) no change in the reactivity towards the quinone methides **2j–m** (Table 5, entries 12-15). Consequently, the nucleophilic reactivity of this carbanion, in which the negative charge is mainly localized on the nucleophilic carbon center,^[18] is not affected by the positively charged alkali ions. Even when a 15-fold excess of Li^+ ($[Li^+] = 1.19 \times 10^{-2} \text{ mol L}^{-1}$) over the carbanion **1b** was employed, the reactivity of **1b** towards **2k** decreased only by a factor of 2.3 (see Table 62 in the Experimental Section). The reactions of **1b** with the aldehydes **4a**, **4e**, and **4g** were even 9-34 % faster in the presence of Na^+ and Li^+ counterions (Table 5, entries 16-18) than in the presence of K^+ /18-crown-6. A slight stabilizing coordination of Na^+ and Li^+ with the partial negative charge of the carbonyl oxygen of the aldehyde in the transition state of the olefination reaction may account for this observation.

The situation is different for the ethoxycarbonyl-stabilized carbanion **1a**. In this case, even the Na^+ counterion has a slight decelerating effect (by a factor of 1.35) on the reactions of **1a** with the quinone methides **2j–m** (Table 5, entries 3, 4, 6, and 7). In the olefination reactions, the slight reduction of the nucleophilicity of **1a** by Na^+ is overcompensated by the activation of the aldehydes by Na^+ , and **1a**- Na reacts 1.3 and 1.7 times faster with the aldehydes **4e** and **4g** than the free carbanion (Table 5, entries 10 and 11). As shown in the Experimental Section (e.g., Table 15), K^+ also has a slight activating effect (by a factor of 1.1-1.3) on the olefination reactions of aldehydes when high concentrations of the potassium salts ($[(\mathbf{1a-d})\text{-}K] > 1.30 \times 10^{-3} \text{ mol L}^{-1}$) were employed without crown ether. Below this concentration, the addition of 18-crown-6 did not affect reactivity.

With Li^+ as the counterion, the reactions of **1a** become considerably slower and do not follow simple second-order kinetics (Table 5, entries 1-5, 8, and 9). These findings can be explained by the high charge delocalization in this carbanion, with most of the negative charge residing on the oxygen atom of the carbonyl group (enolate structure). The higher affinity of the (charged) oxygen for the lithium counterion results in the formation of less reactive contact ion pairs even in DMSO (dielectric constant $\epsilon_r = 46.45$). Because the degree of ion-pairing increases with increasing concentration, the nonlinear correlation in Figure 5 can be rationalized. The strong decrease of k_{obs} at constant $[\mathbf{1a}]$ with increasing $[Li^+]$ (Figure 6) can also be explained by the increasing degree of ion-pairing.

According to Table 5, at $[Li^+] = 1 \times 10^{-3} \text{ mol L}^{-1}$, **1a**- Li reacts 3.1-3.7 times more slowly than the free carbanion **1a** with **2h–k** and **4a** (Table 5, entries 1, 3, 4, and 8). At a higher

concentration of Li^+ ($[\text{Li}^+] = 9 \times 10^{-3} \text{ mol L}^{-1}$), **1a**-Li reacts 25-51 times more slowly than the free carbanion with the benzhydrylium ion **2h**, the quinone methide **2k**, and the aldehyde **4a** (Table 5, entries 2, 5, and 9). Because the magnitude of the Li^+ effect depends only slightly on the nature of the electrophile, we have to conclude that under these conditions, the activation of the electrophiles by Li^+ is much less important than the deactivation of the carbanion **1a** by Li^+ coordination.

The reactivity of phosphorus ylide **1e** is not affected by Li^+ ions at all in either the reaction with benzhydrylium ion **2h** or the olefination reaction with *p*-nitrobenzaldehyde (**4a**) (see Tables 68-70 in the Experimental Section).

Nucleophilicity Parameters. As previously shown for many nucleophile-electrophile combinations,^[16,17,19] the second-order rate constants given in Tables 2 and 3 correlate well with the electrophilicity parameters E of the benzhydrylium ions **2a–h** and quinone methides **2i–m**. In Figure 7 these correlations are shown exemplarily for the nucleophiles **1a**, **b**, and **1e–g**. The correlations for the other nucleophiles used in this work (**1c**, **1d**, and **1h**) are of similar quality and allow the calculation of the nucleophile-specific parameters N and s , which are listed in Tables 2 and 3.

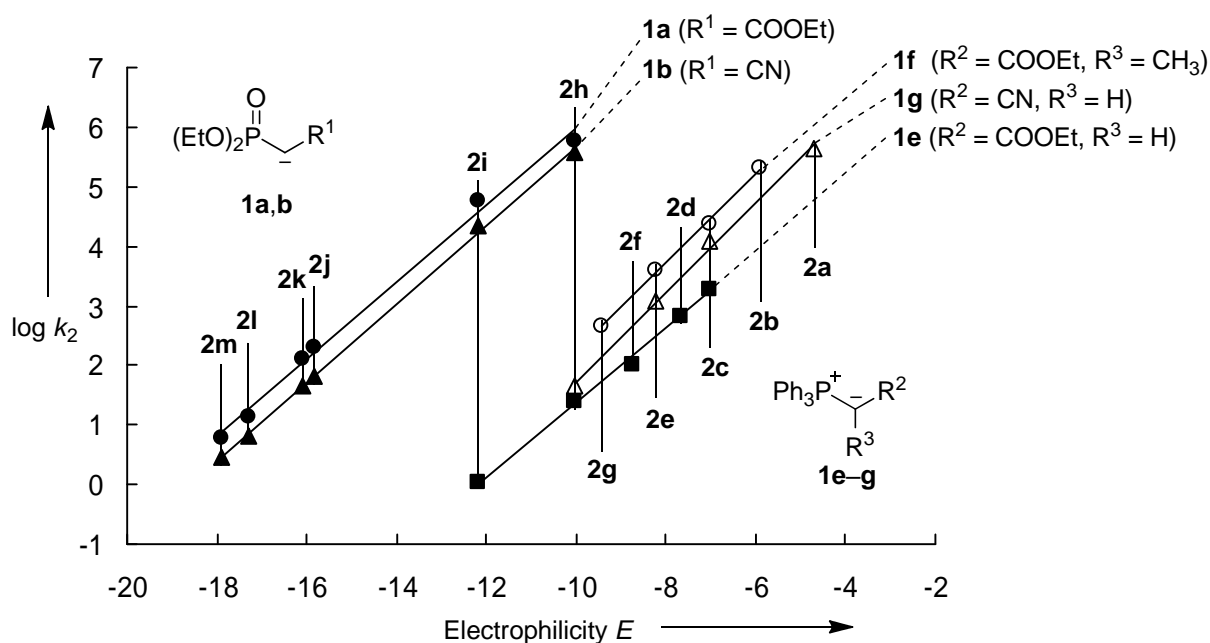


Figure 7: Plots of $\log k_2$ for the reactions of the phosphoryl-stabilized carbanions **1a** and **1b** and the phosphorus ylides **1e–g** with the reference electrophiles **2a–m** at 20°C (filled symbols denote reactions in DMSO, open symbols reactions in CH_2Cl_2) versus the electrophilicity parameters E of **2a–m**.

The similarities of the slopes for the correlations of the nucleophiles **1a–e** in DMSO and for the nucleophiles **1e–g** in CH₂Cl₂ (Figure 7), which are numerically expressed by the *s* parameters in Tables 2 and 3, imply that the relative nucleophilicities of **1a–e** in DMSO and **1e–g** in CH₂Cl₂ depend only slightly on the electrophilicity of the reaction partner. Consequently, the *N* parameters can be used to compare the relative reactivities of these compounds (Figure 8).

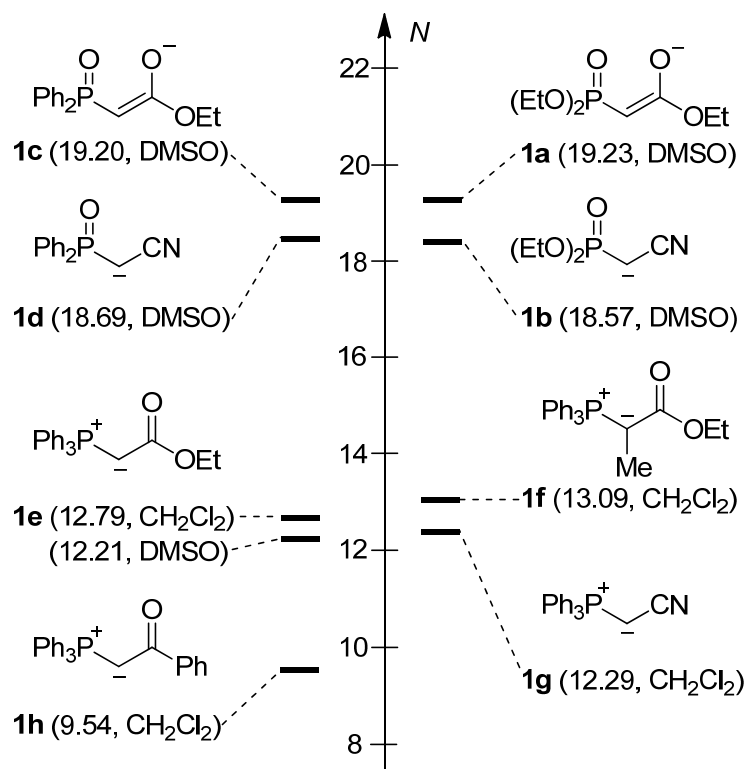


Figure 8: Comparison of the nucleophilicity parameters *N* (in DMSO or CH₂Cl₂) of the phosphorus ylides **1e–h**, the phosphonate-stabilized carbanions **1a** and **1b**, and the phosphine oxide-stabilized carbanions **1c** and **1d**.

Figure 8 shows that phosphonate-stabilized (**1a** and **1b**) and phosphine oxide-stabilized carbanions (**1c** and **1d**) do not differ much in reactivity. This indicates that ethoxy substituents on the phosphorus center have a similar effect on the nucleophilicity of the carbanionic center as phenyl substituents. In analogy to the behavior of other carbanions bearing CN and CO₂R groups,^[16c] the ethoxycarbonyl-substituted carbanions **1a** and **1c** show a slightly higher reactivity than the cyano-stabilized carbanions **1b** and **1d**.

A comparison of the substituent effects on the reactivity (given by the *N* parameters for their reactivities in CH₂Cl₂) of the phosphorus ylides **1e–h** also shows that the ethoxycarbonyl-stabilized ylide **1e** is slightly more reactive than the cyano-stabilized ylide **1g**. Substitution of an α -H-atom of **1e** by a methyl group has almost no effect on the nucleophilic reactivity (cf.

1f vs **1e**). The benzoyl-substituted ylide **1h** is $\sim 10^2$ times less reactive than the structurally analogous phosphorus ylides **1e** and **1f**. Because **1h** could only be investigated with two different reference electrophiles, the atypically high s value of 0.96 is not reliable and shall not be discussed in detail.

It has long been known that the phosphoryl-stabilized carbanions react faster with carbonyl compounds than the Wittig ylides.^[3,20] The N (and s) values for the phosphoryl-stabilized carbanions **1a–d** and the ylides **1e–h** in Figure 8 now provide a quantitative comparison of the reactivities of phosphoryl-stabilized carbanions and phosphorus ylides. A problem in this comparison is the different solvents used for the two classes of compounds. While the carbanions **1a–d** were investigated in DMSO solution, the kinetic investigations of the phosphorus ylides **1e–h** were performed in CH_2Cl_2 . However, the ylide **1e** was investigated in both solvents, showing that the reactivity is less than one order of magnitude higher in CH_2Cl_2 than in DMSO. Comparison of the nucleophilicities of the Wittig ylide **1e** and of the two structurally analogous phosphoryl-stabilized carbanions **1a** and **1c** reveals a difference of nucleophilic reactivity of $\Delta N \approx 7$ (N in DMSO). For an averaged s value of 0.65, this difference implies that the ylide **1e** is 10^4 – 10^5 times less reactive than the carbanions **1a** and **1c**. A similar reactivity ratio can be derived for the comparison of the cyano-substituted carbanions **1b** and **1d** with the cyano-substituted phosphorus ylide **1g**, if one assumes that the change from CH_2Cl_2 to DMSO solution has an effect on the reactivity of **1g** similar to that on **1e**.

Figure 9 shows a rather poor relationship between the rates of the reactions of the benzhydrylium ion **2h** with carbanions^[16c,17a,19a,c] and their $\text{p}K_{\text{aH}}$ values in DMSO.^[21] One can see that the phosphoryl-stabilized carbanions **1a**, **1b**, and **1d** are located in the lower part of this “correlation corridor”. The phosphonate-substituted carbanions **1a** and **1b** are even less reactive than several of the phenyl-substituted nitronates **7-(X)** and the malononitrile anion $(\text{NC})_2\text{CH}^-$, even though the basicities of **1a** and **1b** are 4–8 units higher. It is probably the stabilization of the phosphoryl-stabilized carbanions **1** through dipole-dipole interactions in DMSO that is responsible for the unusually high intrinsic barriers^[22] of their reactions with electrophiles. Because of the low quality of this correlation, we refrain from interpreting the slope.

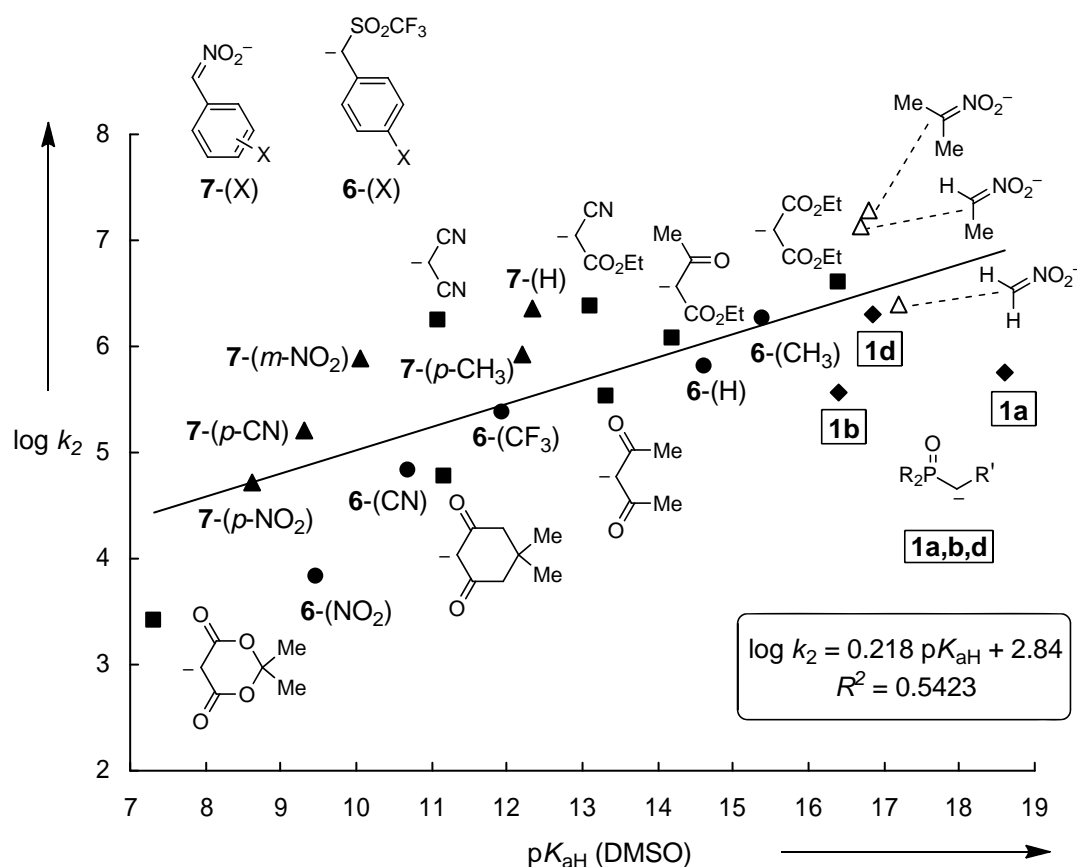


Figure 9: Plot of $\log k_2$ for the reactions of the phosphoryl-stabilized carbanions **1a**, **1b** and **1d** and other classes of carbanions with the benzhydrylium ion **2h** (DMSO, 20°C) versus the corresponding pK_{aH} value of the carbanions (DMSO, 25°C). The second-order rate constants k_2 (filled symbols) were taken from refs 16c, 17a, 19a, and 19c. Second-order rate constants k_2 for the alkyl nitronates (open symbols) were calculated using eq 1. The pK_{aH} -values were taken from ref 21.

Olefination reactions. The kinetic studies on the reactions of the nucleophiles **1a–e** with the benzaldehydes **4** in DMSO (Table 4) showed that in all cases, electron-withdrawing groups at the 3- or 4-positions of the benzaldehydes **4** increase the reaction rates whereas electron-donating substituents decelerate the reaction (Figure 10).

Plots of $\log k_2$ versus the Hammett substituent constants σ are linear (Figure 10) and yield $\rho = 3.4$ – 3.6 for the olefination reactions of the phosphonate-stabilized carbanions **1a** and **1b**, $\rho = 2.7$ – 2.8 for the reactions of the phosphine-oxide stabilized carbanions **1c** and **1d**, and $\rho = 2.9$ for the reactions of the ylide **1e**. Because the correlations with **1c** and **1e** are only based on 3 and 2 data points, respectively, the resulting ρ values for these compounds should be treated with caution. Similar reaction constants ρ have been reported for the Wittig reactions of ester-stabilized triphenylphosphonium ylides with substituted benzaldehydes in benzene at 25°C

($\rho = 2.7$)^[23c] and in acetonitrile at 20°C ($\rho = 2.9$)^[23d] as well as for the Wittig reaction of benzylidene triphenylphosphorane with substituted benzaldehydes in THF at 0°C ($\rho = 2.77$)^[23g]. The substituent effects are in line with a concerted [2+2] cycloaddition in which the formation of the CC bond is more advanced in the transition state than the formation of the PO bond.^[23] In the calculations by Aggarwal and Harvey,^[7c,d] the bond lengths in the transition state for the reaction of benzaldehyde with $\text{Ph}_3\text{PCHCO}_2\text{Me}$ are reported to be 1.86 Å for the CC bond and 2.76 Å for the PO bond.

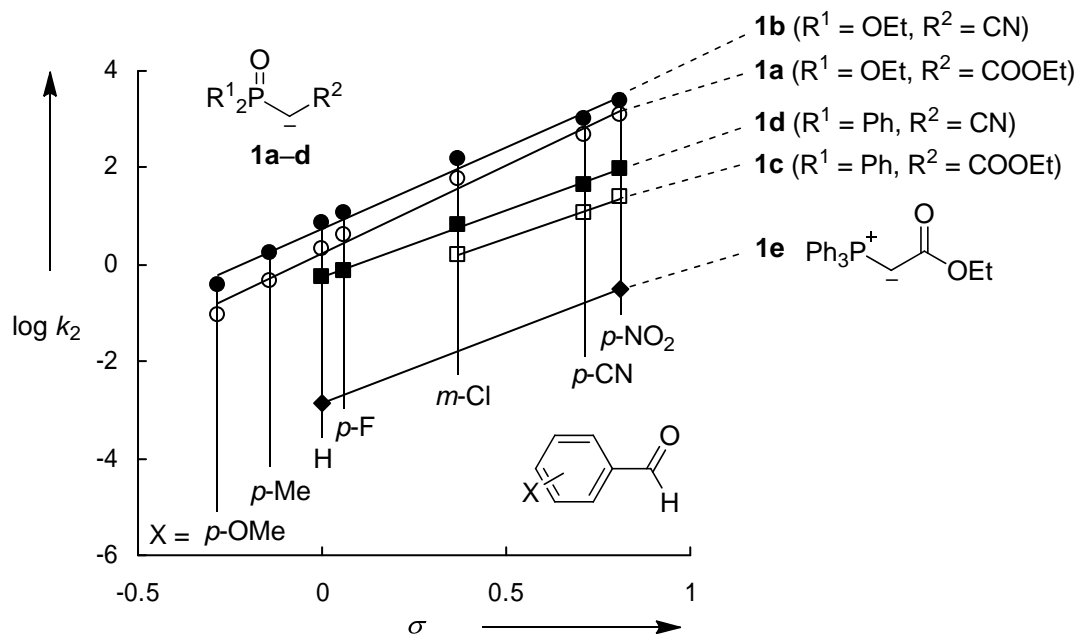


Figure 10: Correlation of the second-order rate constants k_2 for the reactions of the phosphoryl-stabilized carbanions **1a–d** and the phosphorus ylide **1e** with the benzaldehydes **4** in DMSO at 20°C versus Hammett's $\sigma_{\text{p-}}$ or $\sigma_{\text{m-}}$ -values for the substituents of the benzaldehydes: (●) $\log k_2 = 3.38 \sigma + 0.734$, $R^2 = 0.9887$, $n = 7$; (○) $\log k_2 = 3.64 \sigma + 0.214$, $R^2 = 0.9894$, $n = 7$; (■) $\log k_2 = 2.76 \sigma - 0.268$, $R^2 = 0.9978$, $n = 5$; (□) $\log k_2 = 2.67 \sigma - 0.800$, $R^2 = 0.9953$, $n = 3$; (◆) $\log k_2 = 2.87 \sigma - 2.84$, $R^2 = 1$, $n = 2$). The data point for the reaction of **1e** with benzaldehyde (**4e**) was taken from ref 23d.

Whereas the change from ethoxy to phenyl substituents on the phosphorus center of phosphoryl-stabilized carbanions revealed no significant change in reactivity towards the reference electrophiles **2** (Table 2 and Figure 8), the phosphine oxide-stabilized carbanions **1c** and **1d** react considerably more slowly with aldehydes than the corresponding phosphonates **1a** and **1b** (Table 4 and Figure 10).

Figure 11 illustrates significant differences in the relative reactivities towards the Michael acceptor **2i** and the benzaldehyde **4a**. Whereas the phosphine oxide-substituted carbanions **1c**

and **1d** react with **2i** slightly faster (by factors of 1.5 and 1.8, respectively) than the analogous phosphonate-substituted carbanions **1a** and **1b**, **1a** and **1b** are more reactive towards **4a** (by factors of 47 and 26, respectively) than the corresponding phosphine oxide-substituted carbanions **1c** and **1d**. Steric effects may account for this inversion of reactivity. Because in the Horner-Wadsworth-Emmons (HWE) reaction, CC bond formation is accompanied by the formation of the PO bond to yield the oxaphosphetane, the more bulky phenyl groups of the phosphine oxides **1c** and **1d** in comparison with the smaller ethoxy groups of the phosphonates **1a** and **1b** may explain the lower reactivities of **1c** and **1d** in the [2+2] cycloaddition with **4a**. Analogously, the smaller size of CN compared with CO₂Et may account for the finding that the cyano-stabilized carbanions **1b** and **1d** are more reactive in the HWE reaction than the corresponding ethoxycarbonyl-substituted systems **1a** and **1c**, even though their relative reactivities towards the Michael acceptor **2i** are the other way around.

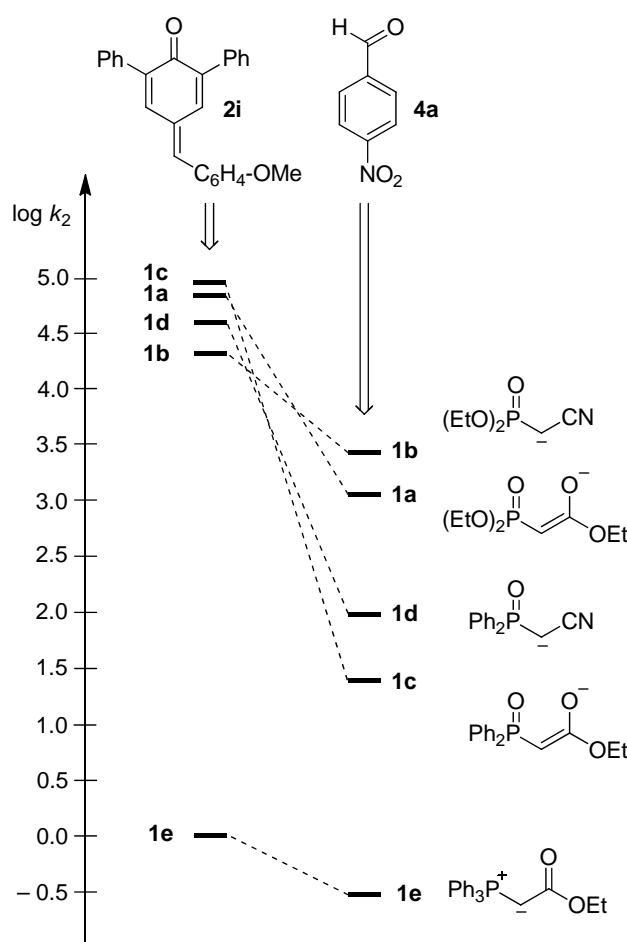
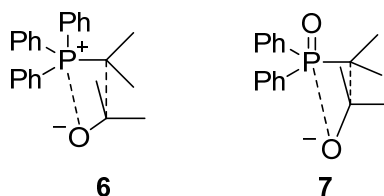


Figure 11: Comparison of the second-order rate constants k_2 for the reactions of the nucleophiles **1a–e** with the quinone methide **2i** (on the left) and *p*-nitrobenzaldehyde **4a** (on the right) in DMSO at 20°C.

A major difference can be seen in the relative reactivities of the ethoxycarbonyl-substituted carbanions **1a** and **1c** on one side and the ethoxycarbonyl-substituted phosphorus ylide **1e** on the other side. Whereas the carbanions **1a** and **1c** are almost 10^5 times more reactive than **1e** in the Michael additions (Figure 11, left), the reactivity ratio shrinks to factors of 100-4000 in the HWE reaction (Figure 11, right). Obviously, the cycloaddition of the phosphorus ylide **1e** profits more from concertedness than the cycloadditions of the carbanions **1a** and **1c**, because the energy gain by forming the PO bond in the transition state **6** is much higher than in transition state **7** (Scheme 8).

Scheme 8: Schematic Transition States for the Reactions of Phosphorus Ylides and Phosphoryl-Substituted Carbanions with Carbonyl Groups.



4 Conclusion

By using benzhydrylium ions and structurally related quinone methides as reference electrophiles, we have been able to directly compare the nucleophilic reactivities of phosphoryl-stabilized carbanions and of stabilized phosphorus ylides. Because the same reference electrophiles have previously been employed for quantifying the reactivities of a large variety of π -, n -, and σ -nucleophiles,^[16,19] we can now integrate the synthetically important phosphorus-substituted nucleophiles **1a–h** into the comprehensive nucleophilicity scale based on equation 1.

Figure 12 compares the effects of $(\text{EtO})_2\text{PO}$, Ph_2PO , and Ph_3P^+ groups on the nucleophilicities of ethoxycarbonyl-substituted carbanions and illustrates that the effect of the phosphoryl group is comparable to that of an acetyl or a cyano group.^[16c]

Since the $\text{p}K_a$ values of the conjugate acids of **1a–d** are much higher than those of ethyl acetoacetate and ethyl cyanoacetate,^[21] we must conclude that the intrinsic barriers for the reactions of the phosphoryl-substituted carbanions are considerably higher than those for the reactions of carbanions stabilized by ester, cyano, and carbonyl groups.

Significant differences between the relative reactivities of the phosphoryl-substituted nucleophiles towards carbocations and Michael acceptors on one side and benzaldehydes on the other side are in line with concerted asynchronous oxaphosphetane formation in the rate-determining step of the olefination reactions.

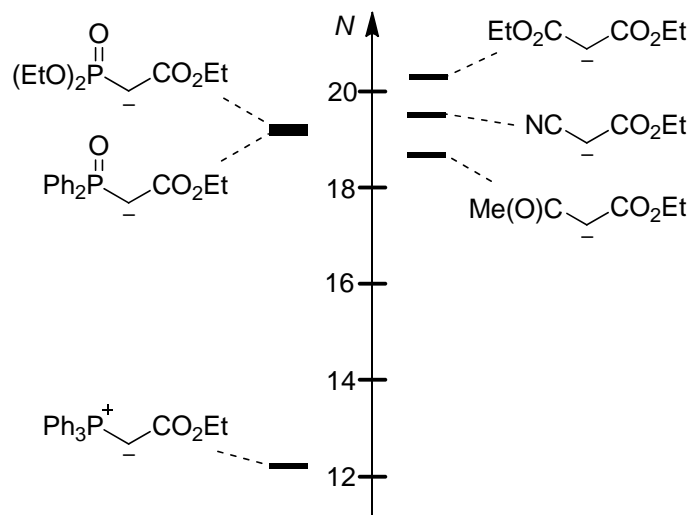


Figure 12: Comparison of the nucleophilicities of different ethoxycarbonyl-stabilized carbanions in DMSO.

5 Experimental Section

In order to identify my contribution to this multiauthor publication, chapter 5.2 and 5.3 of this Experimental Section consist exclusively of the experiments, which were performed by me.

5.1 General

Chemicals. Dimethyl sulfoxide (DMSO) with a H_2O content of < 50 ppm and dry CH_2Cl_2 (freshly distilled over CaH_2) were used for the kinetic experiments. The phosphine oxides **1c-H** and **1d-H** were synthesized according to literature procedure,^[24] as was the phosphorus ylide **1g**.^[25] Benzhydrylium tetrafluoroborates^[16b] (**2a-h**)- BF_4 and quinone methides^[26] **2i-m** were prepared as described previously. All of the other chemicals were purchased from commercial sources and (if necessary) purified by recrystallization or distillation prior to use.

Analyticals. ^1H - and ^{13}C -NMR spectra were recorded on Varian NMR-systems (300, 400, or 600 MHz) in CDCl_3 or $\text{DMSO}-d_6$ and the chemical shifts in ppm refer to TMS (δ_{H} 0.00, δ_{C} 0.00) in CDCl_3 or the solvent residual signal in $\text{DMSO}-d_6$ (δ_{H} 2.50, δ_{C} 39.43) as internal standard. The following abbreviations were used for chemical shift multiplicities: brs = broad singlet, s = singlet, d = doublet, t = triplet, q = quartet, m = multiplet. For reasons of simplicity, the ^1H -NMR signals of AA'BB'-spin systems of *p*-disubstituted aromatic rings were treated as doublets. NMR signal assignments were based on additional 2D-NMR experiments (e.g., COSY-, NOESY-, HSQC-, and HMBC experiments). Diastereomeric ratios (*dr*) were determined by ^1H -NMR. (HR-)MS was performed on a Finnigan MAT 95 (EI) or a

Thermo Finnigan LTQ FT (ESI) mass spectrometer. Melting points were determined on a Büchi B-540 device and are not corrected.

Kinetics. The rates of all of the investigated reactions were determined photometrically. The temperature of the solutions during all kinetic studies was kept constant ($20.0 \pm 0.1^\circ\text{C}$) using a circulating bath thermostat. The reactions with the carbanions in DMSO were carried out either with stock solutions of the potassium salts of the CH acids or by deprotonation of the CH acids with 1.00-1.05 eq of KO t Bu, NaO t Bu, or LiO t Bu in DMSO. The reactions with the ylides in DMSO or CH₂Cl₂ were carried out with solutions of the ylides in the corresponding solvent. The electrophiles were also prepared in stock solutions of the particular solvent and were always employed as the minor component in the reactions with the nucleophiles, resulting in first-order kinetics.

The rates of slow reactions ($\tau_{1/2} > 10$ s) were determined by using a J&M TIDAS diode array spectrophotometer controlled by Labcontrol Spectacle software and connected to Hellma 661.502-QX quartz Suprasil immersion probe (5 mm light path) via fiber-optic cables and standard SMA connectors. For the evaluation of fast kinetics ($\tau_{1/2} < 10$ s) the stopped-flow spectrophotometer systems Hi-Tech SF-61DX2 or Applied Photophysics SX.18MV-R were used.

Rate constants k_{obs} (s^{-1}) were obtained by fitting the single exponential $A_t = A_0 \exp(-k_{\text{obs}}t) + C$ (exponential decrease) or $A_t = A_0 [1 - \exp(-k_{\text{obs}}t)] + C$ (exponential increase) to the observed time-dependent absorbance (averaged from at least four kinetic runs for each nucleophile concentration in the case of applying the stopped-flow method).

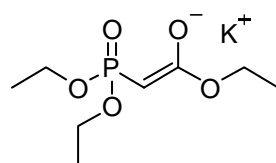
5.2 Syntheses and Product Studies

5.2.1 Synthesis of the Phosphonate-Stabilized Carbanions **1a-K** and **1b-K**

General procedure A. To a stirred solution of KO t Bu in dry ethanol was added the corresponding CH acid (**1a-H** or **1b-H**). After 10 min of stirring, the solvent was evaporated under reduced pressure. The solid residue was washed several times with dry diethyl ether and filtrated under N₂.

Ethyl 2-(diethoxyphosphoryl)acetate potassium salt (1a-K) was obtained from ethyl 2-(diethoxyphosphoryl)acetate **1a-H** (8.29 g, 37.0 mmol) and KO t Bu (4.20 g, 37.4 mmol) in EtOH (15 mL); 7.19 g (27.4 mmol, 74 %); colorless solid.

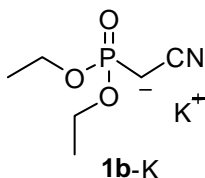
RAS 4

**1a-K**

$^1\text{H-NMR}$ ($\text{d}_6\text{-DMSO}$, 400 MHz): $\delta = 1.03$ (t, $^3J = 7.1$ Hz, 3 H, OCH_2CH_3), 1.12 (t, $^3J = 7.0$ Hz, 6 H, OCH_2CH_3), 1.79 (d, $^2J_{\text{P-H}} = 15.5$ Hz, 0.17 H, CH), 2.19* (d, $^2J_{\text{P-H}} = 15.6$ Hz, 0.80 H, CH), 3.67-3.76 (m, 6 H, OCH_2CH_3). $^{13}\text{C-NMR}$ ($\text{d}_6\text{-DMSO}$, 101 MHz): $\delta = 15.4^*$ (q), 15.5 (q), 16.4* (q, $^3J_{\text{P-C}} = 7.0$ Hz, partially superimposed by the signal of the other isomer), 39.3* (d, d, $^1J_{\text{P-C}} = 220$ Hz), 40.0 (d, d, $^1J_{\text{P-C}} = 213$ Hz), 54.9 (t), 55.2* (t, $^4J_{\text{P-C}} = 3.5$ Hz), 58.4 (t, $^2J_{\text{P-C}} = 4.6$ Hz), 58.5* (t, $^2J_{\text{P-C}} = 4.8$ Hz), 168.9 (s, $^2J_{\text{P-C}} = 12.8$ Hz), 170.1* (s, $^2J_{\text{P-C}} = 22.2$ Hz). $^{31}\text{P-NMR}$ ($\text{d}_6\text{-DMSO}$, 81.0 MHz): $\delta = 37.7, 39.3^*$. HR-MS (ESI $^+$): calc. for $[\text{C}_8\text{H}_{17}\text{KO}_5\text{P}]^+$: 263.0445, found 263.0449. * Major isomer.^[27]

Ethyl cyanomethylphosphonate potassium salt (1b-K) was obtained from ethyl cyanomethylphosphonate **1b-H** (4.57 g, 25.8 mmol) and $\text{KO}t\text{Bu}$ (3.00 g, 26.7 mmol) in EtOH (15 mL); 4.19 g (19.5 mmol, 76 %); pale yellow solid.

RAS 5

**1b-K**

$^1\text{H-NMR}$ ($\text{d}_6\text{-DMSO}$, 400 MHz): $\delta = 0.62$ (d, $^2J_{\text{P-H}} = 5.0$ Hz 1 H, CHCN), 1.13 (t, $^3J = 7.1$ Hz, 6 H, OCH_2CH_3), 3.69-3.79 (m, 4 H, OCH_2CH_3). $^{13}\text{C-NMR}$ ($\text{d}_6\text{-DMSO}$, 101 MHz): $\delta = 3.5$ (d, d, $^1J_{\text{P-C}} = 235$ Hz), 16.4 (q, $^3J_{\text{P-C}} = 7.1$ Hz), 58.7 (t, $^2J_{\text{P-C}} = 4.9$ Hz), 131.1 (s, $^2J_{\text{P-C}} = 11.0$ Hz). $^{31}\text{P-NMR}$ ($\text{d}_6\text{-DMSO}$, 81.0 MHz): $\delta = 43.4$. HR-MS (ESI $^+$): calc. for $[\text{C}_6\text{H}_{12}\text{KNO}_3\text{P}]^+$: 216.0186, found 216.0187.

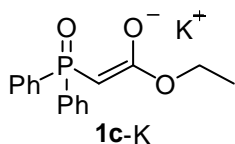
5.2.2 Synthesis of the Phosphine Oxide-Stabilized Carbanions **1c-K** and **1d-K**

General procedure B. To a stirred solution of the corresponding CH acid (**1c-H** or **1d-H**) in CH_2Cl_2 was added finely granulated $\text{KO}t\text{Bu}$. After 30 min of reaction time, the solvent was

evaporated under reduced pressure. The resulting precipitate was washed several times with dry diethyl ether and filtrated under N₂.

Ethyl 2-(diphenylphosphoryl)acetate potassium salt (1c-K) was obtained from ethyl 2-(diphenylphosphoryl)acetate **1c-H** (1.00 g, 3.47 mmol) and KO*t*Bu (430 mg, 3.83 mmol) in CH₂Cl₂ (10 mL); 807 mg (2.47 mmol, 71 %); colorless solid.

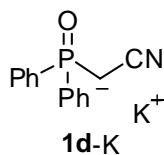
RAS 6



¹H-NMR (d₆-DMSO, 400 MHz): δ = 0.58 (t, ³J = 7.0 Hz, 0.48 H, OCH₂CH₃), 1.08* (t, ³J = 7.1 Hz, 2.52 H, OCH₂CH₃), 2.92* (d, ²J_{P-H} = 22.6 Hz, 0.32 H, CH, Signal for other isomer partially superimposed by DMSO resonance), 3.55 (q, ³J = 7.0 Hz, 0.33 H, OCH₂CH₃), 3.75* (q, ³J = 7.1 Hz, 1.65 H, OCH₂CH₃), 7.26-7.31 (m, 6 H, C-H_{ar}), 7.69-7.74 (m, 4 H, C-H_{ar}). ¹³C-NMR (d₆-DMSO, 101 MHz): δ = 14.8 (q), 15.3* (q), 46.7* (d, d, ¹J_{P-C} = 144 Hz), 49.1 (d, d, ¹J_{P-C} = 138 Hz, very weak signal), 55.0 (t), 55.7* (t, ⁴J_{P-C} = 2.7 Hz), 127.0 (d, ³J_{P-C} = 10.7 Hz), 127.4* (d, ³J_{P-C} = 10.9 Hz), 128.4 (d, ⁴J_{P-C} = 2.3 Hz), 128.8* (d, ⁴J_{P-C} = 2.3 Hz), 130.7* (d, ²J_{P-C} = 8.9 Hz), 131.0 (d, ²J_{P-C} = 8.6 Hz), 140.9* (s, d, ¹J_{P-C} = 103 Hz), 142.0 (s, d, ¹J_{P-C} = 103 Hz), 169.4 (s, ²J_{P-C} = 7.5 Hz), 170.7* (s, ²J_{P-C} = 12.8 Hz). ³¹P-NMR (d₆-DMSO, 81.0 MHz): δ = 23.2, 26.5*. HR-MS (ESI⁺): calc. for [C₁₆H₁₇KO₃P]⁺: 327.0547, found 327.0548. * Major isomer.^[27]

Ethyl 2-(diphenylphosphoryl)acetonitrile potassium salt (1d-K) was obtained from 2-(diphenylphosphoryl)acetonitrile **1d-H** (1.00 g, 4.15 mmol) and KO*t*Bu (550 mg, 4.90 mmol) in CH₂Cl₂ (10 mL); 903 mg (3.22 mmol, 78 %); colorless solid.

RAS 13



¹H-NMR (d₆-DMSO, 400 MHz): δ = 1.24 (d, ²J_{P-H} = 5.7 Hz 1 H, CHCN), 7.29-7.33 (m, 6 H, CH_{ar}), 7.72-7.78 (m, 4 H, CH_{ar}). ¹³C-NMR (d₆-DMSO, 101 MHz): δ = 12.7 (t, ¹J_{P-C} = 145 Hz), 127.3 (d, ³J_{P-C} = 10.9 Hz), 129.0 (d, ⁴J_{P-C} = 2.5 Hz), 131.3 (d, ²J_{P-C} = 8.6 Hz), 131.5 (d,

$^2J_{\text{P-C}} = 6.9$ Hz), 140.7 (s, $^1J_{\text{P-C}} = 105$ Hz). $^{31}\text{P-NMR}$ (d_6 -DMSO, 81.0 MHz): $\delta = 29.3$. HR-MS (ESI⁺): calc. for $[\text{C}_{14}\text{H}_{12}\text{KNOP}]^+$: 280.0288, found 280.0287.

5.2.3 Products for the Reactions of the Nucleophiles **1a–e** with the Aldehydes **4**

General procedure C. Product studies for the reactions of the nucleophiles **1a–d** (0.8–1.0 mmol) with the electrophiles **4** were carried out by mixing the corresponding CH acid (**1a–d**)-H with a slight excess of KO^tBu (1.0–1.3 mmol) in dry DMSO (5 mL). After some minutes, one equiv of the electrophile was added. In case of the triphenylphosphonium ylide **1e** (1.4 mmol) no base for deprotonation was needed. Therefore, nucleophile **1e** was dissolved in dry DMSO and directly mixed with one equiv of the electrophile **4a**. The corresponding reaction mixtures were stirred at room temperature (approximately 20°C) for a certain time and subsequently quenched with aqueous acetic acid solution (2%). Products that precipitated, were filtrated and washed with water. In all other cases, the reaction mixtures were extracted with CH₂Cl₂ or EtOAc. The combined organic layers were washed with water and brine, dried over Na₂SO₄ and evaporated under reduced pressure. The crude products were purified by column chromatography on silica gel (*n*-pentane/EtOAc) and subsequently characterized by ¹H-NMR spectroscopy and GC/MS. Analysis of the products **5** showed that they were formed as a mixture of *cis/trans*-isomers with high selectivity for the *trans* isomer. The *cis/trans* ratio was determined by GC/MS analysis. In order to exclude that the observed *cis/trans* ratio was changed during workup or purification, samples were directly taken from the reaction mixtures (approximately 0.1 mL per sample, diluted with 1 mL of acetone) and analyzed after different reaction times. As no significant change of the *cis/trans* ratios for different reaction times could be observed, only the *cis/trans* ratios after 15 min of reaction times are shown. The yields of the reactions were not optimized, because these studies do not focus on the product formation.

Table 6: Isolated products **5** for the reactions of the nucleophiles **1a–e** with the aldehydes **4** in DMSO at 20°C.

Nucleophile	Electrophile	Product 5	<i>trans/cis</i> ^a	Isolated yield (%)	Reaction time (min)
1a	4a	<i>p</i> -NO ₂ -C ₆ H ₄ CH=CHCO ₂ Et ^b	> 99/1	80	15
1a	4b	<i>p</i> -CN-C ₆ H ₄ CH=CHCO ₂ Et ^c	-	82	15
1a	4c	<i>m</i> -Cl-C ₆ H ₄ CH=CHCO ₂ Et ^d	-	85	15
1a	4d	<i>p</i> -F-C ₆ H ₄ CH=CHCO ₂ Et ^d	-	79	60
1a	4e	C ₆ H ₄ CH=CHCO ₂ Et ^d	> 99/1	80	60
1a	4f	<i>p</i> -Me-C ₆ H ₄ CH=CHCO ₂ Et ^d	-	74	90
1a	4g	<i>p</i> -MeO-C ₆ H ₄ CH=CHCO ₂ Et ^d	> 99/1	78	90
1b	4a	<i>p</i> -NO ₂ -C ₆ H ₄ CH=CHCN ^e	90/10	73	15
1b	4e	C ₆ H ₄ CH=CHCN ^f	92/8	64	60
1b	4g	<i>p</i> -MeO-C ₆ H ₄ CH=CHCN ^g	90/10	76	90
1c	4a	<i>p</i> -NO ₂ -C ₆ H ₄ CH=CHCO ₂ Et ^b	> 99/1	81	30
1d	4a	<i>p</i> -NO ₂ -C ₆ H ₄ CH=CHCN ^e	85/15	71	15
1d	4e	C ₆ H ₄ CH=CHCN ^f	90/10	71	60
1e	4a	<i>p</i> -NO ₂ -C ₆ H ₄ CH=CHCO ₂ Et ^b	95/5	88	150

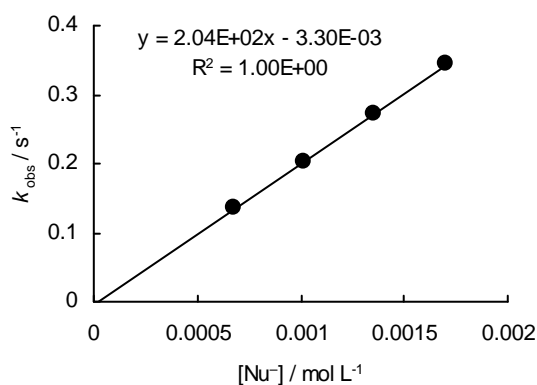
^a Determination see text. ^b ¹H-NMR data are in consistence with those reported in http://riodb01.ibase.aist.go.jp/sdbs/cgi-bin/direct_frame_top.cgi, SDBS-No.: 19530. ^c ¹H-NMR (d₆-DMSO, 400 MHz): δ = 1.26 (t, ³J = 7.1 Hz, 3 H, CH₃), 4.21 (q, ³J = 7.1 Hz, 2 H, CH₂), 6.81 (d, ³J = 16.1 Hz, 1 H, =CH), 7.70 (d, ³J = 16.1 Hz, 1 H, =CH), 7.86-7.88 (m, 2 H, CH_{ar}), 7.91-7.94 (d, 2 H, CH_{ar}). ^d ¹H-NMR-data are in consistence with those reported in Cao, P.; Li, C.; Kang, Y.; Xie, Z.; Sun, X.; Tang, Y. *J. Org. Chem.* **2007**, *72*, 6628-6630. ^e ¹H-NMR (d₆-DMSO, 200 MHz): δ = 6.73 (d, ³J = 16.7 Hz, 1 H, =CH), 7.82 (d, ³J = 16.7 Hz, 1 H, =CH), 7.89-7.95 (m, 2 H, CH_{ar}), 8.25-8.32 (d, 2 H, CH_{ar}). ^f ¹H-NMR-data are in consistence with those reported in Li, H. J.; Wang, L. *Eur. J. Org. Chem.* **2006**, 5099-5102. ^g ¹H-NMR-data are in consistence with those reported in Durantini, E. N. *Synth. Comm.* **1999**, 4201-4222.

5.3 Kinetics

5.3.1 Kinetic Investigations of the Reactions of the Stabilized Carbanions (1a-d)-K with the reference electrophile 2j

Table 7: Kinetics of the reaction of **1a-K** with **2j** in DMSO at 20°C (addition of 0-1.0 equiv 18-crown-6, stopped-flow UV-Vis spectrometer, $\lambda = 371$ nm).

No.	$[E]_0 / \text{mol L}^{-1}$	$[\text{Nu}^-]_0 / \text{mol L}^{-1}$	$[\text{18-crown-6}] / \text{mol L}^{-1}$	$k_{\text{obs}} / \text{s}^{-1}$
RALO 1.1-1	5.60×10^{-5}	6.78×10^{-4}	-	1.36×10^{-1}
RALO 1.1-2	5.60×10^{-5}	1.02×10^{-3}	-	2.04×10^{-1}
RALO 1.1-3	5.60×10^{-5}	1.36×10^{-3}	-	2.73×10^{-1}
RALO 1.1-4	5.60×10^{-5}	1.70×10^{-3}	1.72×10^{-1}	3.44×10^{-1}
$k_2 = 2.04 \times 10^2 \text{ L mol}^{-1} \text{ s}^{-1}$				



The reaction has been performed in order to check the consistency of the data obtained from different experimenters (control experiment). The obtained second-order rate constant is not mentioned in Table 2 and was not used for the calculation of N and s parameters.

Table 8: Kinetics of the reaction of **1b-K** with **2j** in DMSO at 20°C (addition of 0-1.1 equiv 18-crown-6, stopped flow UV-Vis spectrometer, $\lambda = 371$ nm).

No.	$[E]_0 / \text{mol L}^{-1}$	$[\text{Nu}^-]_0 / \text{mol L}^{-1}$	$[\text{18-crown-6}] / \text{mol L}^{-1}$	$k_{\text{obs}} / \text{s}^{-1}$
RALO 2.1-1	5.60×10^{-5}	7.88×10^{-4}	-	5.01×10^{-2}
RALO 2.1-2	5.60×10^{-5}	1.57×10^{-3}	1.72×10^{-3}	1.04×10^{-1}
RALO 2.1-3	5.60×10^{-5}	2.36×10^{-3}	-	1.56×10^{-1}
RALO 2.1-4	5.60×10^{-5}	3.15×10^{-3}	3.45×10^{-3}	2.10×10^{-1}
$k_2 = 6.71 \times 10^1 \text{ L mol}^{-1} \text{ s}^{-1}$				

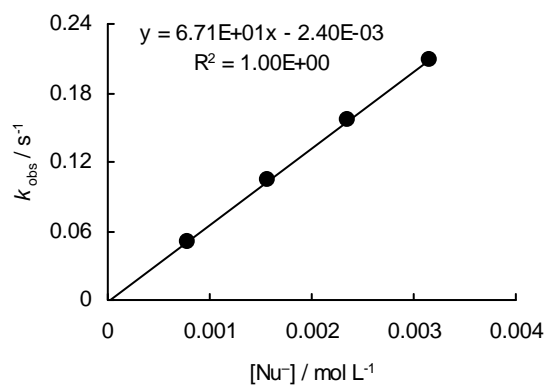
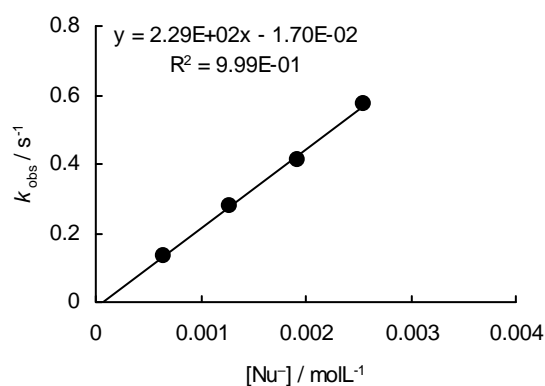


Table 9: Kinetics of the reaction of **1c-K** with **2j** in DMSO at 20°C (addition of 0-1.2 equiv 18-crown-6, stopped-flow UV-Vis spectrometer, $\lambda = 371$ nm).

No.	$[E]_0 / \text{mol L}^{-1}$	$[\text{Nu}^-]_0 / \text{mol L}^{-1}$	$[18\text{-crown-6}] / \text{mol L}^{-1}$	$k_{\text{obs}} / \text{s}^{-1}$
RALO 3.1-1	5.71×10^{-5}	6.40×10^{-4}	-	1.31×10^{-1}
RALO 3.1-2	5.71×10^{-5}	1.28×10^{-3}	1.59×10^{-3}	2.78×10^{-1}
RALO 3.1-3	5.71×10^{-5}	1.92×10^{-3}	-	4.13×10^{-1}
RALO 3.1-4	5.71×10^{-5}	2.56×10^{-3}	2.66×10^{-3}	5.74×10^{-1}

$k_2 = 2.29 \times 10^2 \text{ L mol}^{-1} \text{ s}^{-1}$

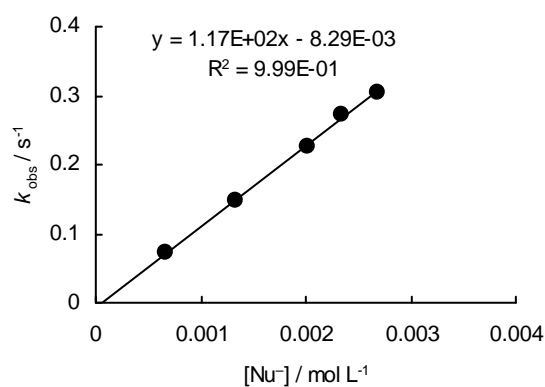


The reaction has been performed in order to check the consistency of the data obtained from different experimenters (control experiment). The obtained second-order rate constant is not mentioned in Table 2 and was not used for the calculation of N and s parameters.

Table 10: Kinetics of the reaction of **1d-K** with **2j** in DMSO at 20°C (addition of 0-1.6 equiv 18-crown-6, stopped-flow UV-Vis spectrometer, $\lambda = 371$ nm).

No.	$[E]_0 / \text{mol L}^{-1}$	$[\text{Nu}^-]_0 / \text{mol L}^{-1}$	$[18\text{-crown-6}] / \text{mol L}^{-1}$	$k_{\text{obs}} / \text{s}^{-1}$
RALO 4.1-1	5.79×10^{-5}	6.71×10^{-4}	-	7.11×10^{-2}
RALO 4.1-2	5.79×10^{-5}	1.34×10^{-3}	2.08×10^{-3}	1.47×10^{-1}
RALO 4.1-3	5.79×10^{-5}	2.01×10^{-3}	-	2.27×10^{-1}
RALO 4.1-4	5.79×10^{-5}	2.35×10^{-3}	2.78×10^{-3}	2.73×10^{-1}
RALO 4.1-5	5.79×10^{-5}	2.69×10^{-3}	-	3.04×10^{-1}

$k_2 = 1.17 \times 10^2 \text{ L mol}^{-1} \text{ s}^{-1}$



The reaction has been performed in order to check the consistency of the data obtained from different experimenters (control experiment). The obtained second-order rate constant is not mentioned in Table 2 and was not used for the calculation of N and s parameters.

5.3.2 Kinetic Investigations of the Reactions of the Stabilized Carbanions (1a–d)-K and the Triphenylphosphonium Ylide 1e with the Aldehydes 4a–g

Kinetic investigations of the reactions of the phosphonate-stabilized carbanion 1a-K with the aldehydes 4a–g in DMSO

Table 11: Kinetics of the reaction of **1a-K** with **4a** in DMSO at 20°C (addition of 0-1.3 equiv 18-crown-6, stopped-flow UV-Vis spectrometer, $\lambda = 310$ nm, data points where counterion effects occurred, i.e., activation effect by K^+ in the absence of 18-crown-6, are not embedded into the correlation and are shown in brackets and open symbols).

No.	$[E]_0 / \text{mol L}^{-1}$	$[\text{Nu}^-]_0 / \text{mol L}^{-1}$	$[18\text{-crown-6}] / \text{mol L}^{-1}$	$k_{\text{obs}} / \text{s}^{-1}$
RAK 7.14-1	5.33×10^{-5}	7.61×10^{-4}	8.55×10^{-4}	8.15×10^{-1}
RAK 7.14-2	5.33×10^{-5}	1.27×10^{-3}	-	1.45
RAK 7.14-3	5.33×10^{-5}	1.77×10^{-3}	2.14×10^{-3}	2.05
RAK 7.14-4	5.33×10^{-5}	2.28×10^{-3}	-	2.70
RAK 7.14-5	5.33×10^{-5}	3.04×10^{-3}	3.21×10^{-3}	3.60
RAK 7.14-6	5.33×10^{-5}	3.55×10^{-3}	-	(4.39)
RAK 7.14-7	5.33×10^{-5}	4.06×10^{-3}	5.34×10^{-3}	4.76
RAK 7.14-8	8.88×10^{-5}	4.56×10^{-3}	-	(5.60)

$k_2 = 1.20 \times 10^3 \text{ L mol}^{-1} \text{ s}^{-1}$

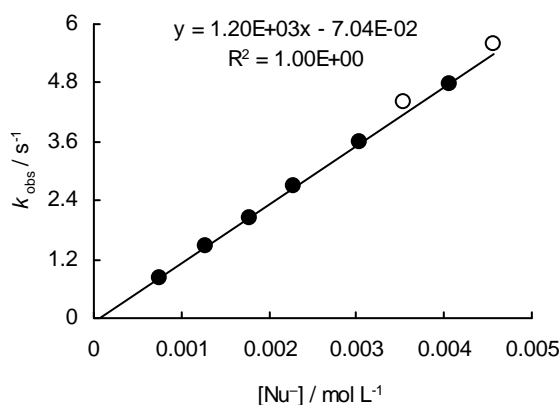


Table 12: Kinetics of the reaction of **1a-K** with **4b** in DMSO at 20°C (addition of 0-1.5 equiv 18-crown-6, stopped-flow UV-Vis spectrometer, $\lambda = 287$ nm, data points where counterion effects occurred, i.e., activation effect by K^+ in the absence of 18-crown-6, are not embedded into the correlation and are shown in brackets and open symbols).

No.	$[E]_0 / \text{mol L}^{-1}$	$[\text{Nu}^-]_0 / \text{mol L}^{-1}$	$[18\text{-crown-6}] / \text{mol L}^{-1}$	$k_{\text{obs}} / \text{s}^{-1}$
RAK 7.15-1	6.14×10^{-5}	7.15×10^{-4}	-	3.20×10^{-1}
RAK 7.15-2	6.14×10^{-5}	1.19×10^{-3}	-	5.56×10^{-1}
RAK 7.15-3	6.14×10^{-5}	1.67×10^{-3}	-	8.06×10^{-1}
RAK 7.15-4	6.14×10^{-5}	2.14×10^{-3}	2.23×10^{-3}	1.01
RAK 7.15-5	6.14×10^{-5}	2.62×10^{-3}	-	(1.30)
RAK 7.15-6	6.14×10^{-5}	3.10×10^{-3}	3.71×10^{-3}	1.47
RAK 7.15-7	6.14×10^{-5}	3.57×10^{-3}	-	(1.82)
RAK 7.15-8	6.14×10^{-5}	4.05×10^{-3}	5.94×10^{-3}	1.92

$k_2 = 4.78 \times 10^2 \text{ L mol}^{-1} \text{ s}^{-1}$

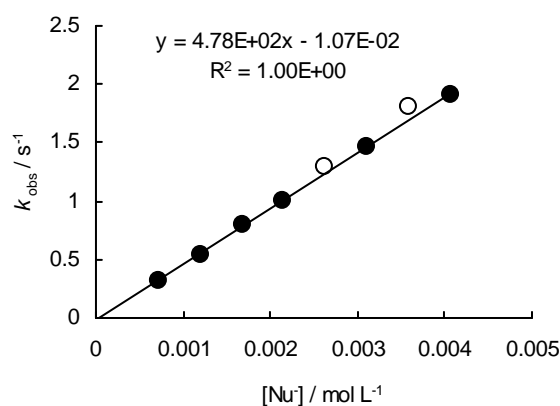


Table 13: Kinetics of the reaction of **1a-K** with **4c** in DMSO at 20°C (addition of 0-1.6 equiv 18-crown-6, stopped-flow UV-Vis spectrometer, $\lambda = 280$ nm, data points where counterion effects occurred, i.e., activation effect by K^+ in the absence of 18-crown-6, are not embedded into the correlation and are shown in brackets and open symbols).

No.	$[E]_0 / \text{mol L}^{-1}$	$[\text{Nu}^-]_0 / \text{mol L}^{-1}$	$[18\text{-crown-6}] / \text{mol L}^{-1}$	$k_{\text{obs}} / \text{s}^{-1}$
RAK 7.19-1	6.02×10^{-5}	1.01×10^{-3}	-	5.56×10^{-2}
RAK 7.19-2	6.02×10^{-5}	1.51×10^{-3}	2.44×10^{-3}	8.40×10^{-2}
RAK 7.19-3	6.02×10^{-5}	2.01×10^{-3}	-	(1.20×10^{-1})
RAK 7.19-4	6.02×10^{-5}	2.52×10^{-3}	3.05×10^{-3}	1.40×10^{-1}
RAK 7.19-5	6.02×10^{-5}	3.02×10^{-3}	-	(1.87×10^{-1})
RAK 7.19-6	6.02×10^{-5}	3.52×10^{-3}	4.57×10^{-3}	2.00×10^{-1}

$k_2 = 5.73 \times 10^1 \text{ L mol}^{-1} \text{ s}^{-1}$

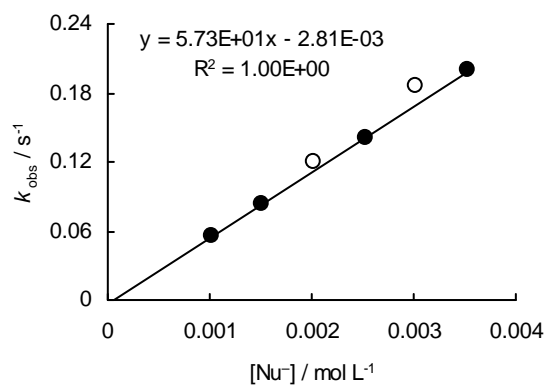


Table 14: Kinetics of the reaction of **1a-K** with **4d** in DMSO at 20°C (addition of 0-1.2 equiv 18-crown-6, diode array UV-Vis spectrometer, $\lambda = 280$ nm, data points where counterion effects occurred, i.e., activation effect by K^+ in the absence of 18-crown-6, are not embedded into the correlation and are shown in brackets and open symbols).

No.	$[E]_0 / \text{mol L}^{-1}$	$[\text{Nu}^-]_0 / \text{mol L}^{-1}$	$[18\text{-crown-6}] / \text{mol L}^{-1}$	$k_{\text{obs}} / \text{s}^{-1}$
RAK 7.13-1	5.40×10^{-5}	8.65×10^{-4}	1.08×10^{-3}	3.18×10^{-3}
RAK 7.13-2	5.42×10^{-5}	1.52×10^{-3}	-	6.21×10^{-3}
RAK 7.13-3	5.09×10^{-5}	2.04×10^{-3}	2.45×10^{-3}	7.89×10^{-3}
RAK 7.13-4	5.29×10^{-5}	2.75×10^{-3}	-	(1.23×10^{-2})
RAK 7.13-5	4.92×10^{-5}	3.15×10^{-3}	3.55×10^{-3}	1.22×10^{-2}
RAK 7.13-7	5.42×10^{-5}	3.60×10^{-3}	3.80×10^{-3}	1.46×10^{-2}
RAK 7.13-6	5.17×10^{-5}	3.93×10^{-3}	-	(1.80×10^{-2})

$k_2 = 4.05 \text{ L mol}^{-1} \text{ s}^{-1}$

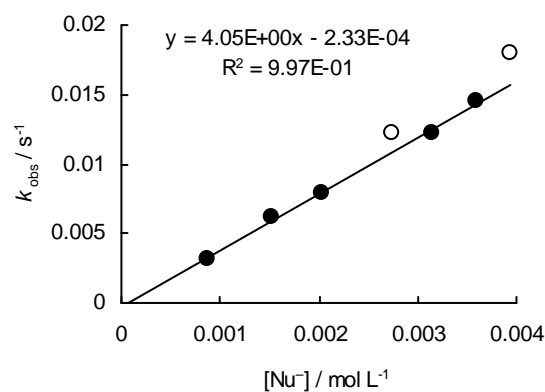


Table 15: Kinetics of the reaction of **1a-K** with **4e** in DMSO at 20°C (addition of 0-1.2 equiv 18-crown-6, diode array UV-Vis spectrometer, $\lambda = 280$ nm data points where counterion effects occurred, i.e., activation effect by K^+ in the absence of 18-crown-6, are not embedded into the correlation and are shown in brackets and open symbols).

No.	$[E]_0 / \text{mol L}^{-1}$	$[\text{Nu}^-]_0 / \text{mol L}^{-1}$	$[\text{18-crown-6}] / \text{mol L}^{-1}$	$k_{\text{obs}} / \text{s}^{-1}$
RAK 7.16-1	5.63×10^{-5}	8.86×10^{-4}	-	1.77×10^{-3}
RAK 7.16-2	5.42×10^{-5}	1.49×10^{-3}	-	(3.40×10^{-3})
RAK 7.16-8	5.55×10^{-5}	1.53×10^{-3}	1.16×10^{-3}	3.07×10^{-3}
RAK 7.16-3	5.73×10^{-5}	2.01×10^{-3}	2.13×10^{-3}	4.01×10^{-3}
RAK 7.16-4	5.41×10^{-5}	2.55×10^{-3}	-	(6.23×10^{-3})
RAK 7.16-5	5.45×10^{-5}	3.05×10^{-3}	3.26×10^{-3}	6.14×10^{-3}
RAK 7.13-6	5.27×10^{-5}	3.52×10^{-3}	-	(9.13×10^{-3})
$k_2 = 2.02 \text{ L mol}^{-1} \text{ s}^{-1}$				

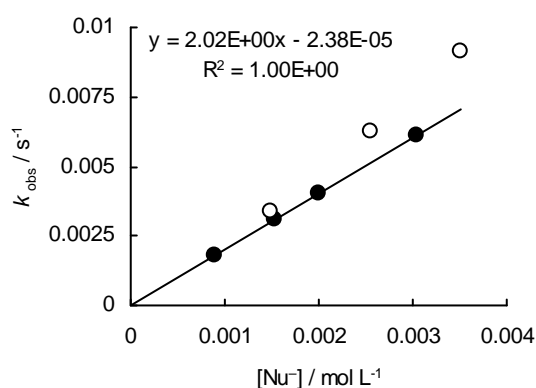


Table 16: Kinetics of the reaction of **1a-K** with **4f** in DMSO at 20°C (addition of 0-1.3 equiv 18-crown-6, diode array UV-Vis spectrometer, $\lambda = 290$ nm, data points where counterion effects occurred, i.e., activation effect by K^+ in the absence of 18-crown-6, are not embedded into the correlation and are shown in brackets and open symbols).

No.	$[E]_0 / \text{mol L}^{-1}$	$[\text{Nu}^-]_0 / \text{mol L}^{-1}$	$[\text{18-crown-6}] / \text{mol L}^{-1}$	$k_{\text{obs}} / \text{s}^{-1}$
RAK 7.17-1	5.96×10^{-5}	8.75×10^{-4}	-	4.29×10^{-4}
RAK 7.17-2	5.56×10^{-5}	1.36×10^{-3}	1.86×10^{-3}	6.24×10^{-4}
RAK 7.17-3	5.43×10^{-5}	1.86×10^{-3}	2.27×10^{-3}	8.64×10^{-4}
RAK 7.17-4	5.47×10^{-5}	2.41×10^{-3}	2.75×10^{-3}	1.12×10^{-3}
RAK 7.17-5	5.73×10^{-5}	2.85×10^{-3}	3.32×10^{-3}	1.35×10^{-3}
RAK 7.17-6	5.58×10^{-5}	3.28×10^{-3}	-	(2.03×10^{-3})
RAK 7.17-7	5.73×10^{-5}	3.85×10^{-3}	5.14×10^{-3}	1.79×10^{-3}
$k_2 = 4.64 \times 10^{-1} \text{ L mol}^{-1} \text{ s}^{-1}$				

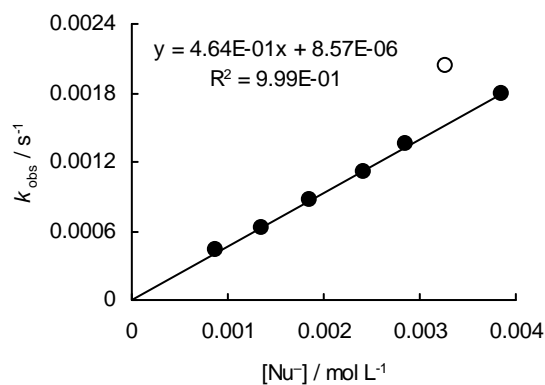
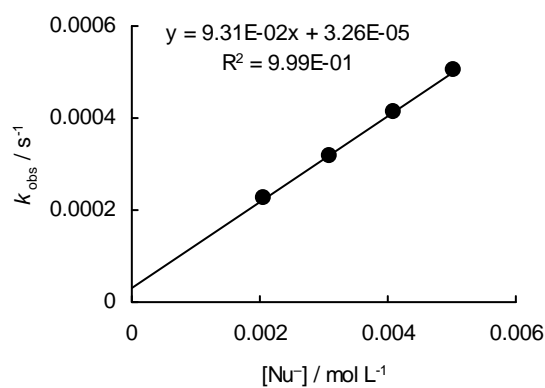


Table 17: Kinetics of the reaction of **1a-K** with **4g** in DMSO at 20°C (addition of 1.1-1.2 equiv 18-crown-6, diode array UV-Vis spectrometer, $\lambda = 315$ nm).

No.	$[E]_0 / \text{mol L}^{-1}$	$[\text{Nu}^-]_0 / \text{mol L}^{-1}$	$[\text{18-crown-6}] / \text{mol L}^{-1}$	$k_{\text{obs}} / \text{s}^{-1}$
RAK 7.18-1	5.30×10^{-5}	2.06×10^{-3}	2.24×10^{-3}	2.27×10^{-4}
RAK 7.18-2	5.33×10^{-5}	3.08×10^{-3}	3.55×10^{-3}	3.16×10^{-4}
RAK 7.18-3	5.88×10^{-5}	4.09×10^{-3}	4.64×10^{-3}	4.12×10^{-4}
RAK 7.18-4	5.83×10^{-5}	5.03×10^{-3}	5.65×10^{-3}	5.02×10^{-4}

$k_2 = 9.31 \times 10^{-2} \text{ L mol}^{-1} \text{ s}^{-1}$



Kinetic investigations of the reactions of the phosphonate-stabilized carbanion **1b-K** with the aldehydes **4a–g** in DMSO

Table 18: Kinetics of the reaction of **1b-K** with **4a** in DMSO at 20°C (addition of 0-1.3 equiv 18-crown-6, stopped-flow UV-Vis spectrometer, $\lambda = 310$ nm).

No.	$[E]_0 / \text{mol L}^{-1}$	$[\text{Nu}^-]_0 / \text{mol L}^{-1}$	$[18\text{-crown-6}] / \text{mol L}^{-1}$	$k_{\text{obs}} / \text{s}^{-1}$
RAK 8.1-1	5.45×10^{-5}	7.88×10^{-4}	-	1.77
RAK 8.1-2	5.45×10^{-5}	1.31×10^{-3}	1.32×10^{-3}	3.04
RAK 8.1-3	5.45×10^{-5}	1.84×10^{-3}	-	4.33
RAK 8.1-4	5.45×10^{-5}	2.36×10^{-3}	-	5.57
RAK 8.1-5	5.45×10^{-5}	2.89×10^{-3}	3.16×10^{-3}	6.85
RAK 8.1-6	5.45×10^{-5}	3.41×10^{-3}	-	8.25
RAK 8.1-7	5.45×10^{-5}	3.94×10^{-3}	5.26×10^{-3}	9.45

$k_2 = 2.45 \times 10^3 \text{ L mol}^{-1} \text{ s}^{-1}$

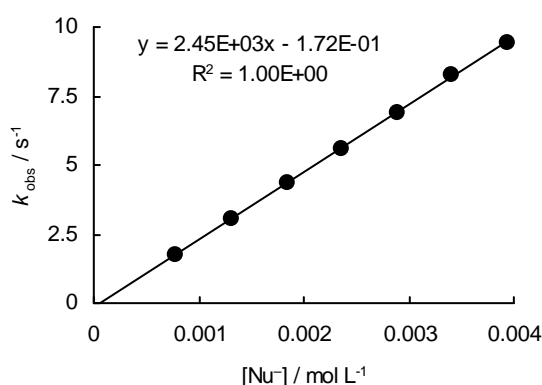


Table 19: Kinetics of the reaction of **1b-K** with **4b** in DMSO at 20°C (addition of 0-1.2 equiv 18-crown-6, stopped-flow UV-Vis spectrometer, $\lambda = 285$ nm, data points where counterion effects occurred, i.e., activation effect by K^+ in the absence of 18-crown-6, are not embedded into the correlation and are shown in brackets and open symbols).

No.	$[E]_0 / \text{mol L}^{-1}$	$[\text{Nu}^-]_0 / \text{mol L}^{-1}$	$[18\text{-crown-6}] / \text{mol L}^{-1}$	$k_{\text{obs}} / \text{s}^{-1}$
RAK 8.6a-1	6.23×10^{-5}	7.25×10^{-4}	-	7.21×10^{-1}
RAK 8.6a-2	6.23×10^{-5}	1.21×10^{-3}	-	1.22
RAK 8.6a-3	6.23×10^{-5}	1.69×10^{-3}	1.79×10^{-3}	1.78
RAK 8.6a-4	6.23×10^{-5}	2.17×10^{-3}	2.23×10^{-3}	2.23
RAK 8.6a-5	6.23×10^{-5}	2.66×10^{-3}	-	(2.93)
RAK 8.6a-6	6.23×10^{-5}	3.14×10^{-3}	3.72×10^{-3}	3.25

$k_2 = 1.05 \times 10^3 \text{ L mol}^{-1} \text{ s}^{-1}$

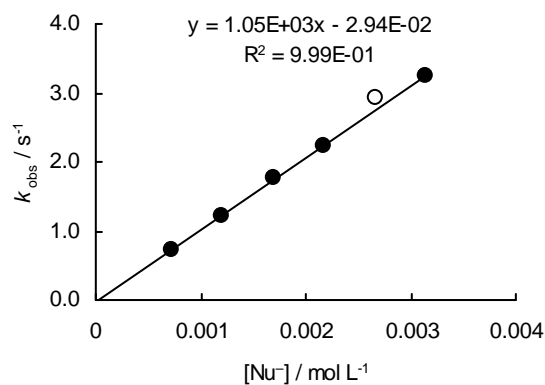


Table 20: Kinetics of the reaction of **1b-K** with **4c** in DMSO at 20°C (addition of 0-1.2 equiv 18-crown-6, stopped-flow UV-Vis spectrometer, $\lambda = 285$ nm).

No.	$[E]_0 / \text{mol L}^{-1}$	$[\text{Nu}^-]_0 / \text{mol L}^{-1}$	$[\text{18-crown-6}] / \text{mol L}^{-1}$	$k_{\text{obs}} / \text{s}^{-1}$
RAK 8.6b-1	6.25×10^{-5}	7.25×10^{-4}	-	9.69×10^{-2}
RAK 8.6b-2	6.25×10^{-5}	1.21×10^{-3}	-	1.68×10^{-1}
RAK 8.6b-3	6.25×10^{-5}	1.69×10^{-3}	1.79×10^{-3}	2.35×10^{-1}
RAK 8.6b-4	6.25×10^{-5}	2.17×10^{-3}	2.23×10^{-3}	3.08×10^{-1}
RAK 8.6b-5	6.25×10^{-5}	2.66×10^{-3}	-	3.84×10^{-1}
RAK 8.6b-6	6.25×10^{-5}	3.14×10^{-3}	3.72×10^{-3}	4.52×10^{-1}

$k_2 = 1.48 \times 10^2 \text{ L mol}^{-1} \text{ s}^{-1}$

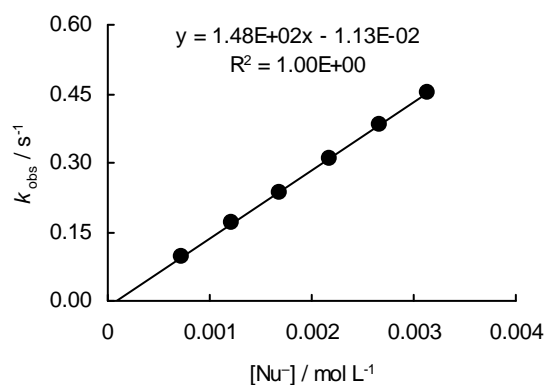
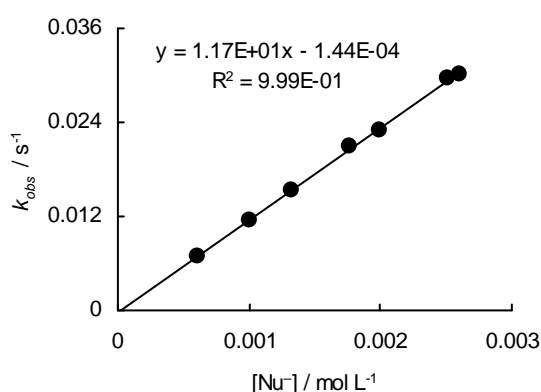


Table 21: Kinetics of the reaction of **1b-K** with **4d** in DMSO at 20°C (addition of 0-1.1 equiv 18-crown-6, diode array UV-Vis spectrometer, $\lambda = 280$ nm).

No.	$[E]_0 / \text{mol L}^{-1}$	$[\text{Nu}^-]_0 / \text{mol L}^{-1}$	$[18\text{-crown-6}] / \text{mol L}^{-1}$	$k_{\text{obs}} / \text{s}^{-1}$
RAK 8.7-1	5.45×10^{-5}	6.07×10^{-4}	-	6.84×10^{-3}
RAK 8.7-2	5.64×10^{-5}	1.00×10^{-3}	-	1.16×10^{-2}
RAK 8.7-3	5.56×10^{-5}	1.33×10^{-3}	1.51×10^{-3}	1.54×10^{-2}
RAK 8.7-4	5.77×10^{-5}	1.77×10^{-3}	-	2.10×10^{-2}
RAK 8.7-5	5.57×10^{-5}	2.00×10^{-3}	2.17×10^{-3}	2.31×10^{-2}
RAK 8.7-6	5.69×10^{-5}	2.52×10^{-3}	-	2.95×10^{-2}
RAK 8.7-7	5.52×10^{-5}	2.61×10^{-3}	2.76×10^{-3}	3.02×10^{-2}

$k_2 = 1.17 \times 10^4 \text{ L mol}^{-1} \text{ s}^{-1}$

**Table 22:** Kinetics of the reaction of **1b-K** with **4e** in DMSO at 20°C (addition of 0-1.2 equiv 18-crown-6, diode array UV-Vis spectrometer, $\lambda = 280$ nm, data points where counterion effects occurred, i.e., activation effect by K^+ in the absence of 18-crown-6, are not embedded into the correlation and are shown in brackets and open symbols).

No.	$[E]_0 / \text{mol L}^{-1}$	$[\text{Nu}^-]_0 / \text{mol L}^{-1}$	$[18\text{-crown-6}] / \text{mol L}^{-1}$	$k_{\text{obs}} / \text{s}^{-1}$
RAK 8.4-1	5.27×10^{-5}	6.17×10^{-4}	-	4.13×10^{-3}
RAK 8.4-2	5.84×10^{-5}	9.88×10^{-4}	1.16×10^{-3}	6.63×10^{-3}
RAK 8.4-3	5.53×10^{-5}	1.40×10^{-3}	-	9.90×10^{-3}
RAK 8.4-7	5.58×10^{-5}	1.42×10^{-3}	1.66×10^{-3}	9.49×10^{-3}
RAK 8.4-4	5.58×10^{-5}	1.70×10^{-3}	1.84×10^{-3}	1.16×10^{-2}
RAK 8.4-5	5.34×10^{-5}	2.13×10^{-3}	-	(1.52×10^{-2})
RAK 8.4-6	5.57×10^{-5}	2.30×10^{-3}	2.59×10^{-3}	1.62×10^{-2}
RAK 8.4-8	5.68×10^{-5}	3.07×10^{-3}	-	(2.22×10^{-2})

$k_2 = 7.16 \text{ L mol}^{-1} \text{ s}^{-1}$

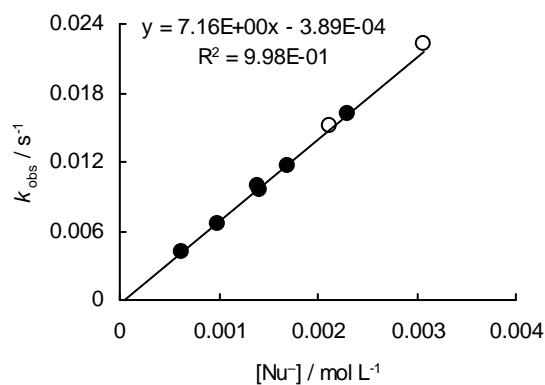


Table 23: Kinetics of the reaction of **1b-K** with **4f** in DMSO at 20°C (addition of 0-1.2 equiv 18-crown-6, diode array UV-Vis spectrometer, $\lambda = 290$ nm, data points where counterion effects occurred, i.e., activation effect by K^+ in the absence of 18-crown-6, are not embedded into the correlation and are shown in brackets and open symbols).

No.	$[E]_0 / \text{mol L}^{-1}$	$[\text{Nu}^-]_0 / \text{mol L}^{-1}$	[18-crown-6] / mol L ⁻¹	$k_{\text{obs}} / \text{s}^{-1}$
RAK 8.2-1	5.56×10^{-5}	8.29×10^{-4}	-	1.38×10^{-3}
RAK 8.2-2	5.58×10^{-5}	1.35×10^{-3}	1.46×10^{-3}	2.31×10^{-3}
RAK 8.2-3	5.70×10^{-5}	1.97×10^{-3}	-	(3.64×10^{-3})
RAK 8.2-4	5.69×10^{-5}	2.39×10^{-3}	2.60×10^{-3}	4.24×10^{-3}
RAK 8.2-5	5.49×10^{-5}	2.84×10^{-3}	3.01×10^{-3}	5.03×10^{-3}
RAK 8.2-6	5.94×10^{-5}	3.45×10^{-3}	-	(6.59×10^{-3})
RAK 8.2-7	5.79×10^{-5}	3.80×10^{-3}	4.67×10^{-3}	6.47×10^{-3}

$k_2 = 1.73 \text{ L mol}^{-1} \text{ s}^{-1}$

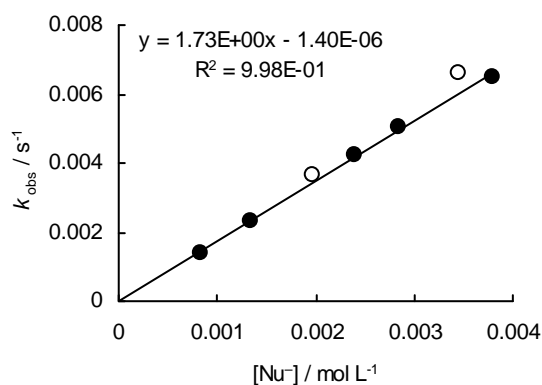
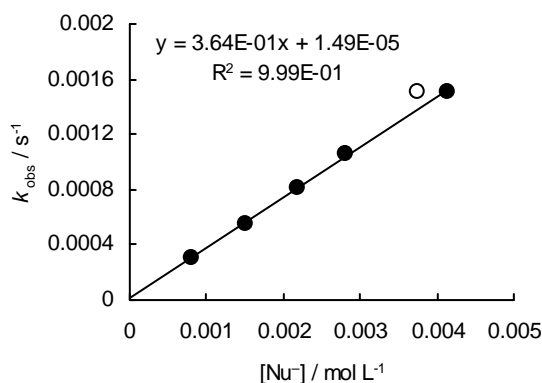


Table 24: Kinetics of the reaction of **1b-K** with **4g** in DMSO at 20°C (addition of 0-1.3 equiv 18-crown-6, diode array UV-Vis spectrometer, $\lambda = 310$ nm, data points where counterion effects occurred, i.e., activation effect by K^+ in the absence of 18-crown-6, are not embedded into the correlation and are shown in brackets and open symbols).

No.	$[E]_0 / \text{mol L}^{-1}$	$[\text{Nu}^-]_0 / \text{mol L}^{-1}$	$[18\text{-crown-6}] / \text{mol L}^{-1}$	$k_{\text{obs}} / \text{s}^{-1}$
RAK 8.3-1	5.58×10^{-5}	7.99×10^{-4}	-	3.00×10^{-4}
RAK 8.3-2	5.70×10^{-5}	1.50×10^{-3}	1.89×10^{-3}	5.56×10^{-4}
RAK 8.3-3	5.92×10^{-5}	2.18×10^{-3}	2.43×10^{-3}	8.12×10^{-4}
RAK 8.3-4	5.74×10^{-5}	2.82×10^{-3}	3.14×10^{-3}	1.06×10^{-3}
RAK 8.3-5	5.68×10^{-5}	3.75×10^{-3}	-	(1.51×10^{-3})
RAK 8.3-6	5.71×10^{-5}	4.14×10^{-3}	4.55×10^{-3}	1.51×10^{-3}

$k_2 = 3.64 \times 10^1 \text{ L mol}^{-1} \text{ s}^{-1}$



Kinetic investigations of the reactions of the phosphine oxide-stabilized carbanion **1c-K** with the aldehydes **4a-c** in DMSO

Table 25: Kinetics of the reaction of **1c-K** with **4a** in DMSO at 20°C (addition of 0-1.1 equiv 18-crown-6, diode array UV-Vis spectrometer, $\lambda = 320$ nm).

No.	$[E]_0 / \text{mol L}^{-1}$	$[\text{Nu}^-]_0 / \text{mol L}^{-1}$	$[18\text{-crown-6}] / \text{mol L}^{-1}$	$k_{\text{obs}} / \text{s}^{-1}$
RAK 9.1-1	4.69×10^{-5}	5.35×10^{-4}	-	1.35×10^{-2}
RAK 9.1-2	4.96×10^{-5}	8.39×10^{-4}	8.95×10^{-4}	2.13×10^{-2}
RAK 9.1-5	5.15×10^{-5}	1.05×10^{-3}	-	2.67×10^{-2}
RAK 9.1-3	5.36×10^{-5}	1.20×10^{-3}	-	3.05×10^{-2}
RAK 9.1-4	5.11×10^{-5}	1.47×10^{-3}	1.57×10^{-3}	3.69×10^{-2}

$k_2 = 2.51 \times 10^1 \text{ L mol}^{-1} \text{ s}^{-1}$

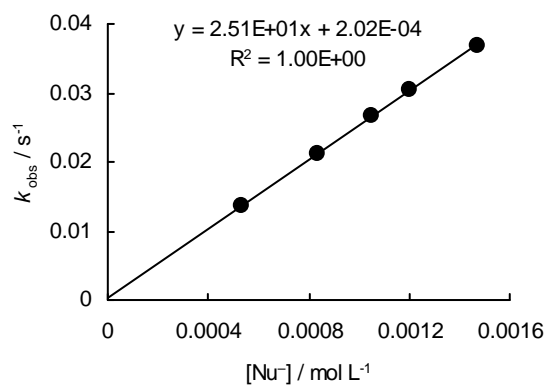


Table 26: Kinetics of the reaction of **1c-K** with **4b** in DMSO at 20°C (addition of 0-1.3 equiv 18-crown-6, diode array UV-Vis spectrometer, $\lambda = 290$ nm, data points where counterion effects occurred, i.e., activation effect by K^+ in the absence of 18-crown-6, are not embedded into the correlation and are shown in brackets and open symbols).

No.	$[E]_0 / \text{mol L}^{-1}$	$[\text{Nu}^-]_0 / \text{mol L}^{-1}$	[18-crown-6] / mol L ⁻¹	$k_{\text{obs}} / \text{s}^{-1}$
RAK 9.2-1	4.96×10^{-5}	5.40×10^{-4}	-	6.16×10^{-3}
RAK 9.2-4	5.26×10^{-5}	6.82×10^{-4}	9.08×10^{-4}	7.78×10^{-3}
RAK 9.2-5	5.11×10^{-5}	8.74×10^{-4}	-	1.04×10^{-2}
RAK 9.2-2	5.14×10^{-5}	1.00×10^{-3}	1.07×10^{-3}	1.14×10^{-2}
RAK 9.2-6	5.16×10^{-5}	1.17×10^{-3}	1.25×10^{-3}	1.34×10^{-2}
RAK 9.2-8	5.08×10^{-5}	1.32×10^{-3}	1.75×10^{-3}	1.48×10^{-2}
RAK 9.2-7	5.07×10^{-5}	1.39×10^{-3}	-	(1.66×10^{-2})
RAK 9.2-3	5.29×10^{-5}	1.54×10^{-3}	-	(1.93×10^{-2})

$k_2 = 1.11 \times 10^4 \text{ L mol}^{-1} \text{ s}^{-1}$

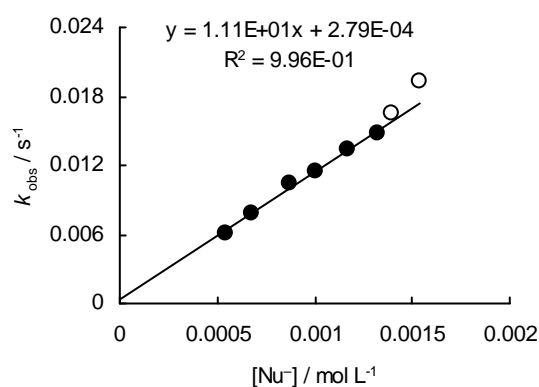
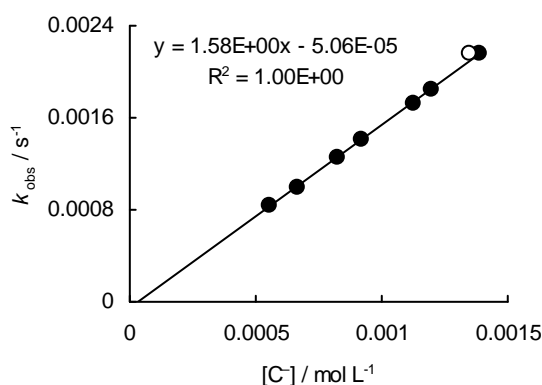


Table 27: Kinetics of the reaction of **1c-K** with **4c** in DMSO at 20°C (addition of 0-1.2 equiv 18-crown-6, diode array UV-Vis spectrometer, $\lambda = 280$ nm, data points where counterion effects occurred, i.e., activation effect by K^+ in the absence of 18-crown-6, are not embedded into the correlation and are shown in brackets and open symbols).

No.	$[E]_0 / \text{mol L}^{-1}$	$[\text{Nu}^-]_0 / \text{mol L}^{-1}$	$[18\text{-crown-6}] / \text{mol L}^{-1}$	$k_{\text{obs}} / \text{s}^{-1}$
RAK 9.4-1	4.88×10^{-5}	5.57×10^{-4}	-	8.40×10^{-4}
RAK 9.4-2	5.15×10^{-5}	6.68×10^{-4}	8.07×10^{-4}	9.98×10^{-4}
RAK 9.4-3	5.30×10^{-5}	8.25×10^{-4}	-	1.26×10^{-3}
RAK 9.4-4	5.53×10^{-5}	9.22×10^{-4}	1.06×10^{-3}	1.41×10^{-3}
RAK 9.4-5	5.42×10^{-5}	1.13×10^{-3}	-	1.72×10^{-3}
RAK 9.4-6	5.59×10^{-5}	1.20×10^{-3}	1.34×10^{-3}	1.85×10^{-3}
RAK 9.4-7	5.21×10^{-5}	1.35×10^{-3}	-	(2.16×10^{-3})
RAK 9.4-8	5.31×10^{-5}	1.39×10^{-3}	1.53×10^{-3}	2.16×10^{-3}

$k_2 = 1.58 \text{ L mol}^{-1} \text{ s}^{-1}$



Kinetic investigations of the reactions of the phosphine oxide-stabilized carbanion **1d-K** with the aldehydes **4a–e** in DMSO

Table 28: Kinetics of the reaction of **1d-K** with **4a** in DMSO at 20°C (addition of 0-1.7 equiv 18-crown-6, stopped-flow UV-Vis spectrometer, $\lambda = 310$ nm, data points where counterion effects occurred i.e., activation effect by K^+ in the absence of 18-crown-6, are not embedded into the correlation and are shown in brackets and open symbols).

No.	$[E]_0 / \text{mol L}^{-1}$	$[\text{Nu}^-]_0 / \text{mol L}^{-1}$	$[18\text{-crown-6}] / \text{mol L}^{-1}$	$k_{\text{obs}} / \text{s}^{-1}$
RAK 10.6-1	6.30×10^{-5}	6.79×10^{-4}	-	5.85×10^{-2}
RAK 10.6-2	6.30×10^{-5}	8.25×10^{-4}	1.15×10^{-3}	7.20×10^{-2}
RAK 10.6-3	6.30×10^{-5}	9.70×10^{-4}	-	8.67×10^{-2}
RAK 10.6-4	6.30×10^{-5}	1.12×10^{-3}	1.85×10^{-3}	9.85×10^{-2}
RAK 10.6-5	6.30×10^{-5}	1.26×10^{-3}	-	(1.21×10^{-1})
RAK 10.6-6	6.30×10^{-5}	1.41×10^{-3}	2.31×10^{-3}	1.27×10^{-1}

$k_2 = 9.32 \times 10^1 \text{ L mol}^{-1} \text{ s}^{-1}$

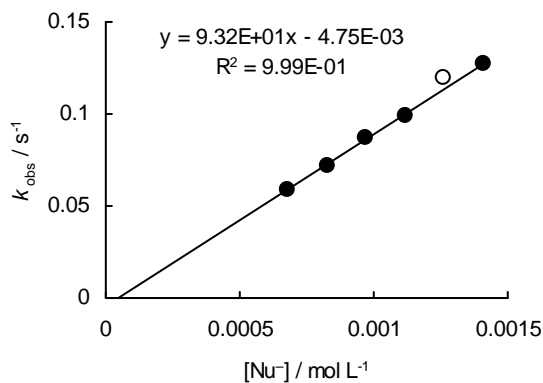


Table 29: Kinetics of the reaction of **1d-K** with **4b** in DMSO at 20°C (addition of 0-1.4 equiv 18-crown-6, diode array UV-Vis spectrometer, $\lambda = 290$ nm, data points where counterion effects occurred, i.e., activation effect by K^+ in the absence of 18-crown-6, are not embedded into the correlation and are shown in brackets and open symbols).

No.	$[E]_0 / \text{mol L}^{-1}$	$[\text{Nu}^-]_0 / \text{mol L}^{-1}$	[18-crown-6] / mol L^{-1}	$k_{\text{obs}} / \text{s}^{-1}$
RAK 10.4-1	4.84×10^{-5}	5.14×10^{-4}	-	2.13×10^{-2}
RAK 10.4-2	4.85×10^{-5}	5.80×10^{-4}	8.19×10^{-4}	2.39×10^{-2}
RAK 10.4-3	5.17×10^{-5}	7.21×10^{-4}	-	3.01×10^{-2}
RAK 10.4-4	4.94×10^{-5}	8.86×10^{-4}	1.26×10^{-3}	3.71×10^{-2}
RAK 10.4-5	5.22×10^{-5}	1.04×10^{-3}	-	4.33×10^{-2}
RAK 10.4-6	5.17×10^{-5}	1.16×10^{-3}	1.39×10^{-3}	4.94×10^{-2}
RAK 10.4-9	5.05×10^{-5}	1.23×10^{-3}	1.60×10^{-3}	5.26×10^{-2}
RAK 10.4-7	5.27×10^{-5}	1.38×10^{-3}	-	(6.40×10^{-2})
RAK 10.4-8	4.89×10^{-5}	1.47×10^{-3}	1.61×10^{-3}	6.43×10^{-2}

$k_2 = 4.46 \times 10^1 \text{ L mol}^{-1} \text{ s}^{-1}$

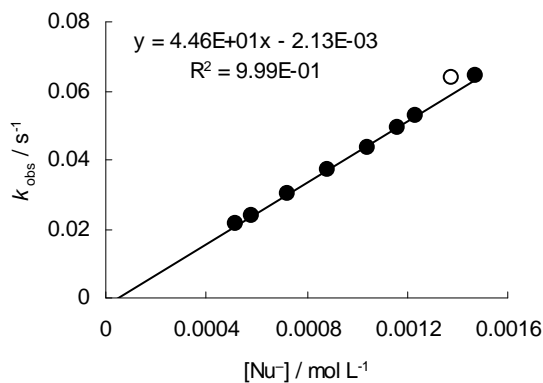
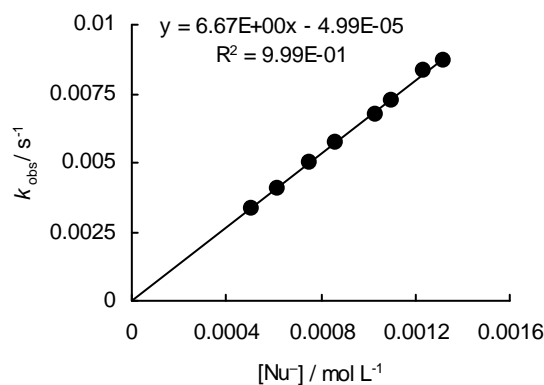


Table 30: Kinetics of the reaction of **1d-K** with **4c** in DMSO at 20°C (addition of 0-1.4 equiv 18-crown-6, diode array UV-Vis spectrometer, $\lambda = 280$ nm).

No.	$[E]_0 / \text{mol L}^{-1}$	$[\text{Nu}^-]_0 / \text{mol L}^{-1}$	$[18\text{-crown-6}] / \text{mol L}^{-1}$	$k_{\text{obs}} / \text{s}^{-1}$
RAK 10.1-1	4.92×10^{-5}	5.10×10^{-4}	-	3.34×10^{-3}
RAK 10.1-2	5.14×10^{-5}	6.18×10^{-4}	1.15×10^{-3}	4.05×10^{-3}
RAK 10.1-3	5.01×10^{-5}	7.50×10^{-4}	-	5.01×10^{-3}
RAK 10.1-4	5.11×10^{-5}	8.61×10^{-4}	1.14×10^{-3}	5.69×10^{-3}
RAK 10.1-5	5.18×10^{-5}	1.03×10^{-3}	-	6.76×10^{-3}
RAK 10.1-6	5.07×10^{-5}	1.10×10^{-3}	1.32×10^{-3}	7.26×10^{-3}
RAK 10.1-7	5.14×10^{-5}	1.24×10^{-3}	-	8.31×10^{-3}
RAK 10.1-8	5.15×10^{-5}	1.32×10^{-3}	1.48×10^{-3}	8.70×10^{-3}
$k_2 = 6.67 \text{ L mol}^{-1} \text{ s}^{-1}$				

**Table 31:** Kinetics of the reaction of **1d-K** with **4d** in DMSO at 20°C (addition of 0-1.4 equiv 18-crown-6, diode array UV-Vis spectrometer, $\lambda = 285$ nm).

No.	$[E]_0 / \text{mol L}^{-1}$	$[\text{Nu}^-]_0 / \text{mol L}^{-1}$	$[18\text{-crown-6}] / \text{mol L}^{-1}$	$k_{\text{obs}} / \text{s}^{-1}$
RAK 10.2-1	5.33×10^{-5}	6.54×10^{-4}	-	4.57×10^{-4}
RAK 10.2-2	5.15×10^{-5}	8.85×10^{-4}	1.23×10^{-3}	6.01×10^{-4}
RAK 10.2-3	5.19×10^{-5}	1.15×10^{-3}	-	7.88×10^{-4}
RAK 10.2-5	5.26×10^{-5}	1.29×10^{-3}	-	8.94×10^{-4}
RAK 10.2-4	5.28×10^{-5}	1.35×10^{-3}	1.59×10^{-3}	9.54×10^{-4}
$k_2 = 7.08 \times 10^{-1} \text{ L mol}^{-1} \text{ s}^{-1}$				

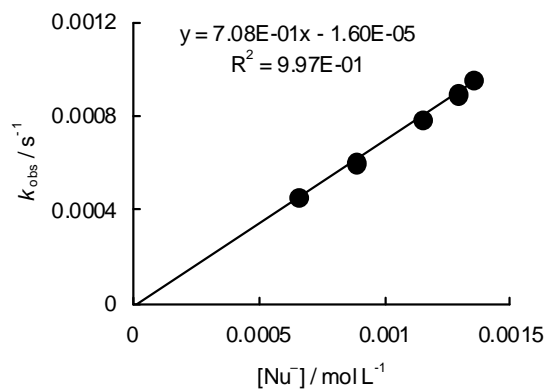
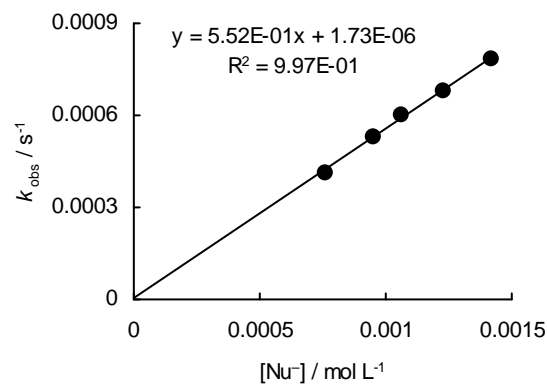


Table 32: Kinetics of the reaction of **1d-K** with **4e** in DMSO at 20°C (addition of 0-1.4 equiv 18-crown-6, diode array UV-Vis spectrometer, $\lambda = 290$ nm).

No.	$[\text{E}]_0 / \text{mol L}^{-1}$	$[\text{Nu}^-]_0 / \text{mol L}^{-1}$	$[\text{18-crown-6}] / \text{mol L}^{-1}$	$k_{\text{obs}} / \text{s}^{-1}$
RAK 10.5-1	5.01×10^{-5}	7.58×10^{-4}	-	4.13×10^{-4}
RAK 10.5-2	5.30×10^{-5}	9.52×10^{-4}	1.03×10^{-3}	5.31×10^{-4}
RAK 10.5-3	5.33×10^{-5}	1.06×10^{-3}	-	5.98×10^{-4}
RAK 10.5-4	5.15×10^{-5}	1.23×10^{-3}	1.76×10^{-3}	6.79×10^{-4}
RAK 10.5-5	5.07×10^{-5}	1.42×10^{-3}	1.98×10^{-3}	7.82×10^{-4}

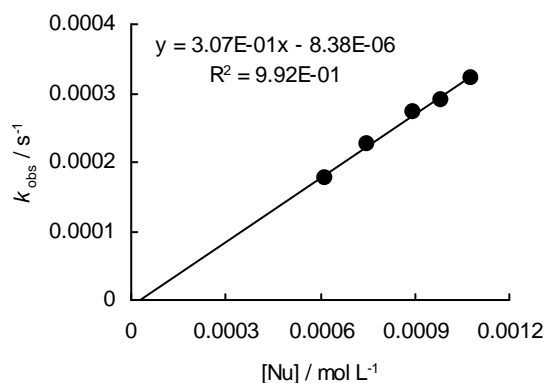
$k_2 = 5.52 \times 10^{-1} \text{ L mol}^{-1} \text{ s}^{-1}$



Kinetic investigation of the reaction of the triphenylphosphonium ylide **1e** with the aldehyde **4a** in DMSO

Table 33: Kinetics of the reaction of **1e** with **4a** in DMSO at 20°C (diode array UV-Vis spectrometer, $\lambda = 330$ nm).

No.	$[E]_0 / \text{mol L}^{-1}$	$[\text{Nu}]_0 / \text{mol L}^{-1}$	$k_{\text{obs}} / \text{s}^{-1}$
RAK 11.1-5	5.04×10^{-5}	6.17×10^{-4}	1.76×10^{-4}
RAK 11.1-4	5.47×10^{-5}	7.50×10^{-4}	2.27×10^{-4}
RAK 11.1-3	5.99×10^{-5}	8.98×10^{-4}	2.73×10^{-4}
RAK 11.1-2	5.60×10^{-5}	9.82×10^{-4}	2.90×10^{-4}
RAK 11.1-1	5.54×10^{-5}	1.08×10^{-3}	3.21×10^{-4}
$k_2 = 3.07 \times 10^{-1} \text{ L mol}^{-1} \text{ s}^{-1}$			



5.3.3 Kinetic investigations of the counterion effects for the phosphonate-stabilized carbanions **1a** and **1b** and the triphenylphosphonium ylide **1e**

Kinetic investigations on the counterion effects for the phosphonate-stabilized carbanion **1a** in DMSO

Counterion effects of Na^+

Table 34: Kinetics of the reaction of **1a-Na** with **2j** in DMSO at 20°C (deprotonation of **1a-H** with 1.00-1.05 equiv of NaOtBu , stopped-flow UV-Vis spectrometer, $\lambda = 371$ nm).

No.	$[E]_0 / \text{mol L}^{-1}$	$[\text{Nu}^-]_0 / \text{mol L}^{-1}$	$k_{\text{obs}} / \text{s}^{-1}$
RALO 1.6.1-1	5.69×10^{-5}	6.36×10^{-4}	9.93×10^{-2}
RALO 1.6.2-1	5.69×10^{-5}	7.69×10^{-4}	1.22×10^{-1}
RALO 1.6.2-2	5.69×10^{-5}	1.03×10^{-3}	1.61×10^{-1}
RALO 1.6.1-2	5.69×10^{-5}	1.06×10^{-3}	1.62×10^{-1}
RALO 1.6.2-3	5.69×10^{-5}	1.28×10^{-3}	1.97×10^{-1}
RALO 1.6.1-3	5.69×10^{-5}	1.48×10^{-3}	2.27×10^{-1}
RALO 1.6.2-2	5.69×10^{-5}	1.54×10^{-3}	2.32×10^{-1}
$k_2 = 1.47 \times 10^2 \text{ L mol}^{-1} \text{ s}^{-1}$			

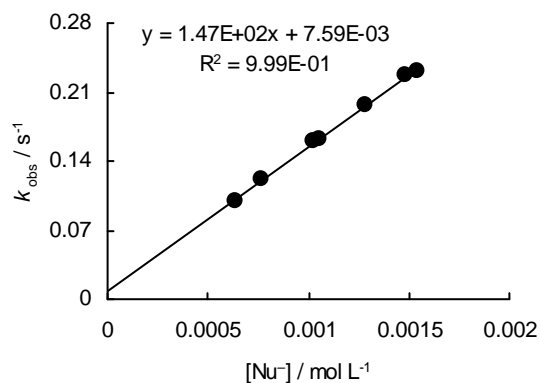
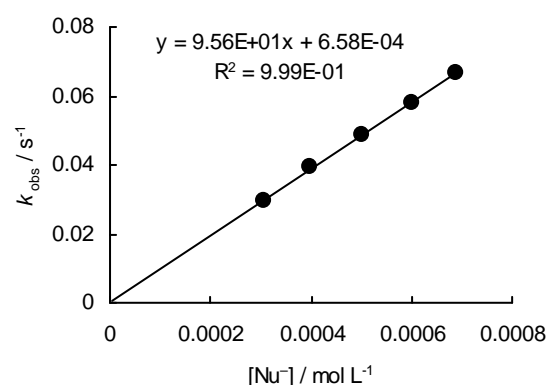
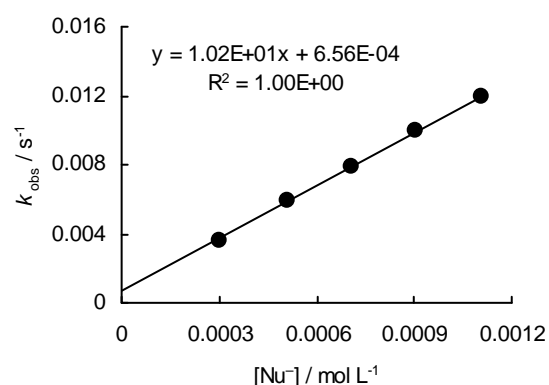


Table 35: Kinetics of the reaction of **1a**-Na with **2k** in DMSO at 20°C (deprotonation of **1a**-H with 1.00-1.05 equiv of NaOtBu, diode array UV-Vis spectrometer, $\lambda = 393$ nm).

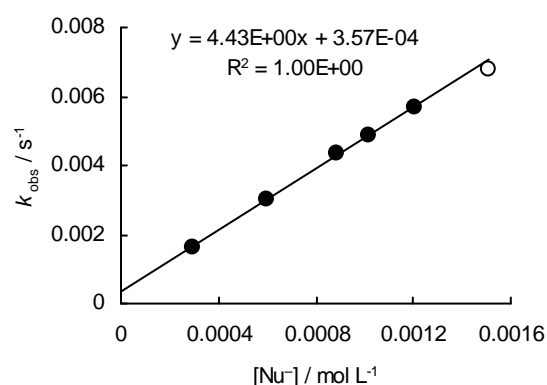
No.	$[E]_0 / \text{mol L}^{-1}$	$[\text{Nu}^-]_0 / \text{mol L}^{-1}$	$k_{\text{obs}} / \text{s}^{-1}$
RALO 1.10-1	2.68×10^{-5}	3.07×10^{-4}	2.95×10^{-2}
RALO 1.10-2	2.91×10^{-5}	3.99×10^{-4}	3.94×10^{-2}
RALO 1.10-3	3.33×10^{-5}	5.03×10^{-4}	4.89×10^{-2}
RALO 1.10-4	3.27×10^{-5}	6.00×10^{-4}	5.81×10^{-2}
RALO 1.10-5	3.28×10^{-5}	6.90×10^{-4}	6.64×10^{-2}
$k_2 = 9.56 \times 10^1 \text{ L mol}^{-1} \text{ s}^{-1}$			

**Table 36:** Kinetics of the reaction of **1a**-Na with **2l** in DMSO at 20°C (deprotonation of **1a**-H with 1.00-1.05 equiv of NaOtBu, diode array UV-Vis spectrometer, $\lambda = 486$ nm).

No.	$[E]_0 / \text{mol L}^{-1}$	$[\text{Nu}^-]_0 / \text{mol L}^{-1}$	$k_{\text{obs}} / \text{s}^{-1}$
RALO 1.8-1	2.03×10^{-5}	3.01×10^{-4}	3.65×10^{-3}
RALO 1.8-2	2.16×10^{-5}	5.08×10^{-4}	5.88×10^{-3}
RALO 1.8-3	2.35×10^{-5}	7.07×10^{-4}	7.93×10^{-3}
RALO 1.8-4	2.31×10^{-5}	9.04×10^{-4}	9.92×10^{-3}
RALO 1.8-5	2.30×10^{-5}	1.11×10^{-3}	1.19×10^{-2}
$k_2 = 1.02 \times 10^1 \text{ L mol}^{-1} \text{ s}^{-1}$			

**Table 37:** Kinetics of the reaction of **1a**-Na with **2m** in DMSO at 20°C (deprotonation of **1a**-H with 1.00-1.05 equiv of NaOtBu, diode array UV-Vis spectrometer, $\lambda = 521$ nm).

No.	$[E]_0 / \text{mol L}^{-1}$	$[\text{Nu}^-]_0 / \text{mol L}^{-1}$	$k_{\text{obs}} / \text{s}^{-1}$
RALO 1.7-1	2.09×10^{-5}	2.95×10^{-4}	1.64×10^{-3}
RALO 1.7-2	2.05×10^{-5}	5.98×10^{-4}	3.03×10^{-3}
RALO 1.7-3	2.01×10^{-5}	8.89×10^{-4}	4.32×10^{-3}
RALO 1.7-6	2.06×10^{-5}	1.02×10^{-3}	4.89×10^{-3}
RALO 1.7-4	2.00×10^{-5}	1.21×10^{-3}	5.69×10^{-3}
RALO 1.7-5	1.98×10^{-5}	1.51×10^{-3}	$(6.78 \times 10^{-4})^*$
$k_2 = 4.43 \text{ L mol}^{-1} \text{ s}^{-1}$			

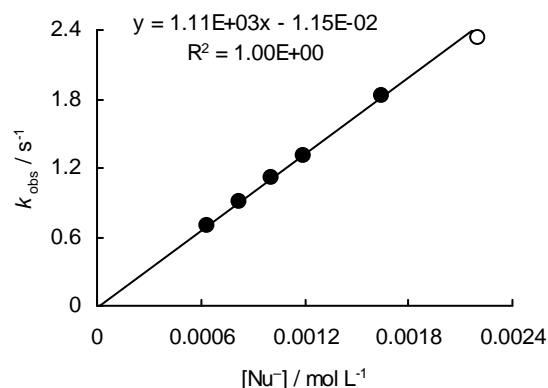


* Data points at high nucleophile concentrations, which deviate from linearity, are not embedded into the correlation.

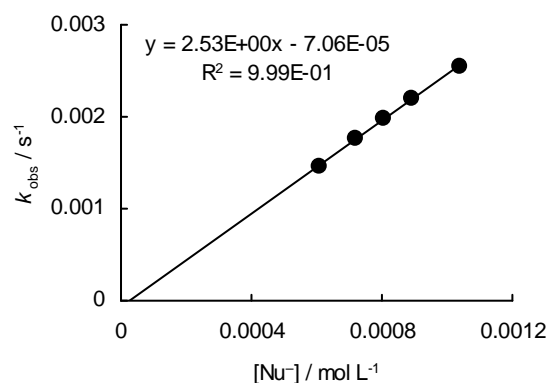
Table 38: Kinetics of the reaction of **1a**-Na with **4a** in DMSO at 20°C (deprotonation of **1a**-H with 1.00-1.05 equiv of NaOtBu, stopped-flow UV-Vis spectrometer, $\lambda = 310$ nm).

No.	$[E]_0 / \text{mol L}^{-1}$	$[\text{Nu}^-]_0 / \text{mol L}^{-1}$	$k_{\text{obs}} / \text{s}^{-1}$
RAK 7.20-1	5.61×10^{-5}	6.42×10^{-4}	7.01×10^{-1}
RAK 7.20-2	5.61×10^{-5}	8.26×10^{-4}	9.02×10^{-1}
RAK 7.20-3	5.61×10^{-5}	1.01×10^{-3}	1.11
RAK 7.20-4	5.61×10^{-5}	1.19×10^{-3}	1.31
RAK 7.20-5	5.61×10^{-5}	1.65×10^{-3}	1.82
RAK 7.20-6	5.61×10^{-5}	2.20×10^{-3}	(2.33) *
$k_2 = 1.11 \times 10^3 \text{ L mol}^{-1} \text{ s}^{-1}$			

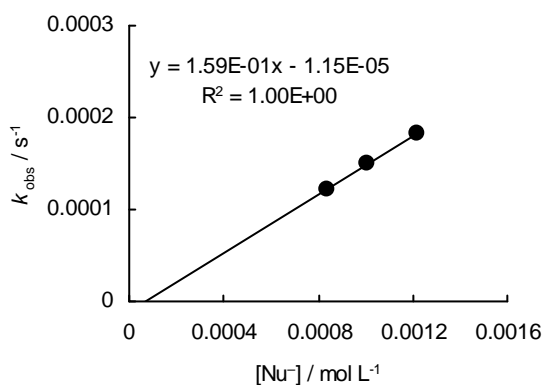
* Data points at high nucleophile concentrations, which deviate from linearity, are not embedded into the correlation.

**Table 39:** Kinetics of the reaction of **1a**-Na with **4e** in DMSO at 20°C (deprotonation of **1a**-H with 1.00-1.05 equiv of NaOtBu, diode array UV-Vis spectrometer, $\lambda = 280$ nm).

No.	$[E]_0 / \text{mol L}^{-1}$	$[\text{Nu}^-]_0 / \text{mol L}^{-1}$	$k_{\text{obs}} / \text{s}^{-1}$
RAK 7.21-1	5.44×10^{-5}	6.11×10^{-4}	1.46×10^{-3}
RAK 7.21-5	5.51×10^{-5}	7.22×10^{-4}	1.77×10^{-3}
RAK 7.21-2	5.40×10^{-5}	8.08×10^{-4}	1.97×10^{-3}
RAK 7.21-4	5.43×10^{-5}	8.94×10^{-4}	2.20×10^{-3}
RAK 7.21-3	5.55×10^{-5}	1.04×10^{-3}	2.55×10^{-3}
$k_2 = 2.53 \text{ L mol}^{-1} \text{ s}^{-1}$			

**Table 40:** Kinetics of the reaction of **1a**-Na with **4g** in DMSO at 20°C (deprotonation of **1a**-H with 1.00-1.05 equiv of NaOtBu, diode array UV-Vis spectrometer, $\lambda = 310$ nm).

No.	$[E]_0 / \text{mol L}^{-1}$	$[\text{Nu}^-]_0 / \text{mol L}^{-1}$	$k_{\text{obs}} / \text{s}^{-1}$
RAK 7.22-3	5.18×10^{-5}	8.42×10^{-4}	1.22×10^{-4}
RAK 7.22-1	5.16×10^{-5}	1.01×10^{-3}	1.49×10^{-4}
RAK 7.22-2	5.34×10^{-5}	1.22×10^{-3}	1.82×10^{-4}
$k_2 = 1.59 \times 10^1 \text{ L mol}^{-1} \text{ s}^{-1}$			

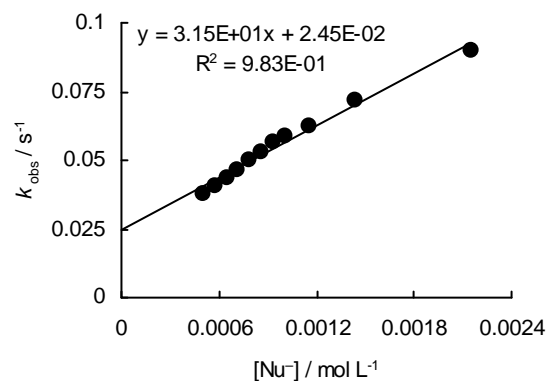


Counterion effects of Li^+ **Table 41:** Kinetics of the reaction of **1a**-Li with **2j** in DMSO at 20°C (deprotonation of **1a**-H with 1.05 equiv of LiOtBu, stopped-flow UV-Vis spectrometer, $\lambda = 371$ nm).

No.	$[\text{E}]_0 / \text{mol L}^{-1}$	$[\text{Nu}^-]_0 / \text{mol L}^{-1}$	$k_{\text{obs}} / \text{s}^{-1}$
RALO 1.12-10	3.70×10^{-5}	5.04×10^{-4}	3.78×10^{-2}
RALO 1.12-11	3.70×10^{-5}	5.75×10^{-4}	4.06×10^{-2}
RALO 1.12-4	4.93×10^{-5}	6.47×10^{-4}	4.37×10^{-2}
RALO 1.12-1	4.93×10^{-5}	7.19×10^{-4}	4.65×10^{-2}
RALO 1.12-5	4.93×10^{-5}	7.91×10^{-4}	5.01×10^{-2}
RALO 1.12-2	4.93×10^{-5}	8.63×10^{-4}	5.29×10^{-2}
RALO 1.12-8	4.93×10^{-5}	9.35×10^{-4}	5.62×10^{-2}
RALO 1.12-3	4.93×10^{-5}	1.01×10^{-3}	5.85×10^{-2}
RALO 1.12-6	4.93×10^{-5}	1.15×10^{-3}	6.22×10^{-2}
RALO 1.12-7	4.93×10^{-5}	1.44×10^{-3}	7.16×10^{-2}
RALO 1.12-9	4.93×10^{-5}	2.16×10^{-3}	8.97×10^{-2}

 $k_2 = -^*$

* No clean second-order kinetics.

**Table 42:** Kinetics of the reaction of **1a**-Li with **2k** in DMSO at 20°C (deprotonation of **1a**-H with 1.05 equiv of LiOtBu, diode array UV-Vis spectrometer, $\lambda = 393$ nm).

No.	$[\text{E}]_0 / \text{mol L}^{-1}$	$[\text{Nu}^-]_0 / \text{mol L}^{-1}$	$k_{\text{obs}} / \text{s}^{-1}$
RALO 1.11-1	2.70×10^{-5}	3.02×10^{-4}	1.70×10^{-2}
RALO 1.11-6	2.84×10^{-5}	4.05×10^{-4}	2.04×10^{-2}
RALO 1.11-2	2.89×10^{-5}	5.04×10^{-4}	2.36×10^{-2}
RALO 1.11-4	3.04×10^{-5}	6.08×10^{-4}	2.65×10^{-2}
RALO 1.11-3	2.96×10^{-5}	6.97×10^{-4}	2.85×10^{-2}
RALO 1.11-8	2.97×10^{-5}	7.86×10^{-4}	3.09×10^{-2}
RALO 1.11-5	3.16×10^{-5}	8.84×10^{-4}	3.40×10^{-2}
RALO 1.11-7	3.13×10^{-5}	9.98×10^{-4}	3.56×10^{-2}

 $k_2 = -^*$

* No clean second-order kinetics.

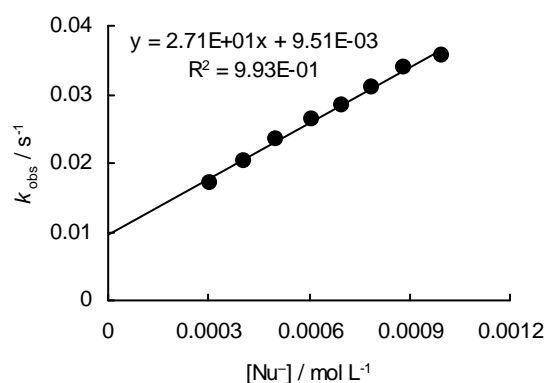
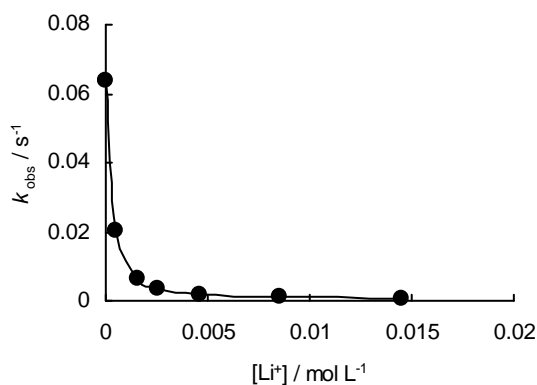


Table 43: Kinetics of the reaction of **1a**-Li with **2k** in DMSO with additional LiBF₄ at 20°C (deprotonation of **1a**-H with 1.05 equiv of LiOtBu, diode array UV-Vis spectrometer, $\lambda = 393$ nm, the data point for [Li⁺] = 0 mol L⁻¹ was calculated from the measurement of **1a**-K with **2k** in DMSO at 20°C).

No.	[E] ₀ / mol L ⁻¹	[Nu ⁻] ₀ / mol L ⁻¹	[LiBF ₄] / mol L ⁻¹	[Li ⁺] / mol L ⁻¹	<i>k</i> _{obs} / s ⁻¹
-	-	-	-	-	6.40 × 10 ⁻² *
RALO 1.14-3-1	3.12 × 10 ⁻⁵	5.00 × 10 ⁻⁴	-	5.25 × 10 ⁻⁴	2.05 × 10 ⁻²
RALO 1.14-3-2	3.54 × 10 ⁻⁵	5.00 × 10 ⁻⁴	1.00 × 10 ⁻³	1.53 × 10 ⁻³	6.42 × 10 ⁻³
RALO 1.14-3-3	3.45 × 10 ⁻⁵	5.00 × 10 ⁻⁴	1.99 × 10 ⁻³	2.52 × 10 ⁻³	3.57 × 10 ⁻³
RALO 1.14-3-4	3.39 × 10 ⁻⁵	5.00 × 10 ⁻⁴	4.06 × 10 ⁻³	4.59 × 10 ⁻³	1.83 × 10 ⁻³
RALO 1.14-3-5	3.25 × 10 ⁻⁵	5.00 × 10 ⁻⁴	7.97 × 10 ⁻³	8.50 × 10 ⁻³	9.02 × 10 ⁻⁴
RALO 1.14-3-6	3.04 × 10 ⁻⁵	5.00 × 10 ⁻⁴	1.40 × 10 ⁻²	1.45 × 10 ⁻²	4.78 × 10 ⁻⁴

* Calculated from the measurement of **1a**-K with **2k** in DMSO at 20°C.**Table 44:** Kinetics of the reaction of **1a**-Li with **2k** in DMSO with additional LiBF₄ at 20°C (deprotonation of **1a**-H with 1.05 equiv of LiOtBu, diode array UV-Vis spectrometer, $\lambda = 393$ nm, the data point for [Li⁺] = 0 mol L⁻¹ was calculated from the measurement of **1a**-K with **2k** in DMSO at 20°C).

No.	[E] ₀ / mol L ⁻¹	[Nu ⁻] ₀ / mol L ⁻¹	[LiBF ₄] / mol L ⁻¹	[Li ⁺] / mol L ⁻¹	<i>k</i> _{obs} / s ⁻¹
-	-	-	-	-	1.32 × 10 ⁻¹ *
RALO 1.14-1-1	3.05 × 10 ⁻⁵	1.03 × 10 ⁻³	-	1.08 × 10 ⁻³	3.52 × 10 ⁻²
RALO 1.14-1-2	3.04 × 10 ⁻⁵	1.03 × 10 ⁻³	1.03 × 10 ⁻³	2.11 × 10 ⁻³	1.41 × 10 ⁻²
RALO 1.14-1-3	3.09 × 10 ⁻⁵	1.03 × 10 ⁻³	2.01 × 10 ⁻³	3.09 × 10 ⁻³	8.56 × 10 ⁻³
RALO 1.14-1-4	3.06 × 10 ⁻⁵	1.03 × 10 ⁻³	3.99 × 10 ⁻³	5.07 × 10 ⁻³	4.73 × 10 ⁻³
RALO 1.14-1-5	2.99 × 10 ⁻⁵	1.03 × 10 ⁻³	8.01 × 10 ⁻³	9.09 × 10 ⁻³	2.49 × 10 ⁻³
RALO 1.14-1-6	2.78 × 10 ⁻⁵	1.03 × 10 ⁻³	1.40 × 10 ⁻²	1.51 × 10 ⁻²	1.40 × 10 ⁻³

* Calculated from the measurement of **1a**-K with **2k** in DMSO at 20°C.

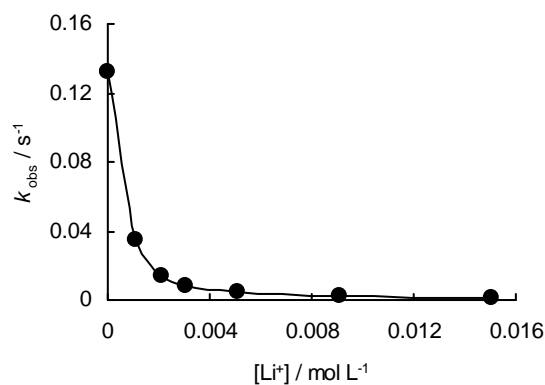


Table 45: Kinetics of the reaction of **1a-Li** with **2k** in DMSO with additional LiBF₄ at 20°C (deprotonation of **1a-H** with 1.05 equiv of LiOtBu, diode array UV-Vis spectrometer, $\lambda = 393$ nm, the data point for [Li⁺] = 0 mol L⁻¹ was calculated from the measurement of **1a-K** with **2k** in DMSO at 20°C).

No.	[E] ₀ / mol L ⁻¹	[Nu ⁻] ₀ / mol L ⁻¹	[LiBF ₄] / mol L ⁻¹	[Li ⁺] / mol L ⁻¹	k _{obs} / s ⁻¹
-	-	-	-	-	1.92 × 10 ⁻¹ *
RALO 1.14-4-1	3.08 × 10 ⁻⁵	1.50 × 10 ⁻³	-	1.58 × 10 ⁻³	4.03 × 10 ⁻²
RALO 1.14-4-2	3.06 × 10 ⁻⁵	1.50 × 10 ⁻³	1.00 × 10 ⁻³	2.58 × 10 ⁻³	1.78 × 10 ⁻²
RALO 1.14-4-3	3.06 × 10 ⁻⁵	1.50 × 10 ⁻³	1.99 × 10 ⁻³	3.57 × 10 ⁻³	1.03 × 10 ⁻²
RALO 1.14-4-4	2.94 × 10 ⁻⁵	1.50 × 10 ⁻³	3.98 × 10 ⁻³	5.56 × 10 ⁻³	6.29 × 10 ⁻³
RALO 1.14-4-5	2.95 × 10 ⁻⁵	1.50 × 10 ⁻³	8.00 × 10 ⁻³	9.58 × 10 ⁻³	3.51 × 10 ⁻³
RALO 1.14-4-6	2.96 × 10 ⁻⁵	1.50 × 10 ⁻³	1.40 × 10 ⁻²	1.56 × 10 ⁻²	2.12 × 10 ⁻³

* Calculated from the measurement of **1a-K** with **2k** in DMSO at 20°C.

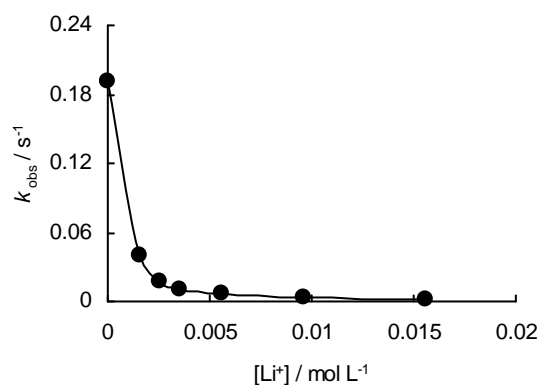
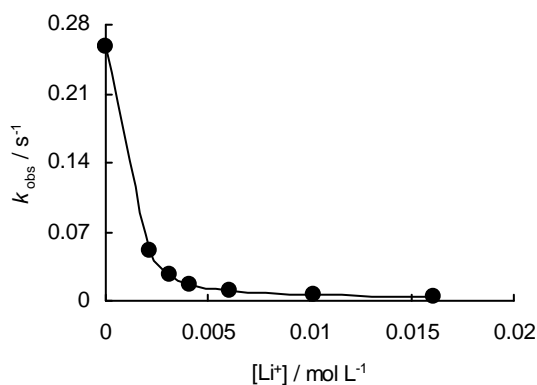


Table 46: Kinetics of the reaction of **1a**-Li with **2k** in DMSO with additional LiBF₄ at 20°C (deprotonation of **1a**-H with 1.05 equiv of LiOtBu, diode array UV-Vis spectrometer, $\lambda = 393$ nm, the data point for [Li⁺] = 0 mol L⁻¹ was calculated from the measurement of **1a**-K with **2k** in DMSO at 20°C).

No.	[E] ₀ / mol L ⁻¹	[Nu ⁻] ₀ / mol L ⁻¹	[LiBF ₄] / mol L ⁻¹	[Li ⁺] / mol L ⁻¹	<i>k</i> _{obs} / s ⁻¹
-	-	-	-	-	2.57 × 10 ⁻¹ *
RALO 1.14-2-1	3.10 × 10 ⁻⁵	2.01 × 10 ⁻³	-	2.11 × 10 ⁻³	5.07 × 10 ⁻²
RALO 1.14-2-2	3.10 × 10 ⁻⁵	2.01 × 10 ⁻³	1.01 × 10 ⁻³	3.12 × 10 ⁻³	2.58 × 10 ⁻²
RALO 1.14-2-3	3.16 × 10 ⁻⁵	2.01 × 10 ⁻³	2.00 × 10 ⁻³	4.11 × 10 ⁻³	1.67 × 10 ⁻²
RALO 1.14-2-4	3.17 × 10 ⁻⁵	2.01 × 10 ⁻³	4.00 × 10 ⁻³	6.11 × 10 ⁻³	9.82 × 10 ⁻³
RALO 1.14-2-5	3.05 × 10 ⁻⁵	2.01 × 10 ⁻³	8.07 × 10 ⁻³	1.02 × 10 ⁻²	5.31 × 10 ⁻³
RALO 1.14-2-6	3.04 × 10 ⁻⁵	2.01 × 10 ⁻³	1.40 × 10 ⁻²	1.61 × 10 ⁻²	3.34 × 10 ⁻³

* Calculated from the measurement of **1a**-K with **2k** in DMSO at 20°C.**Table 47:** Kinetics of the reaction of **1a**-Li with **2h** in DMSO with additional LiBF₄ at 20°C (deprotonation of **1a**-H with 1.05 equiv of LiOtBu, stopped-flow UV-Vis spectrometer, $\lambda = 630$ nm, the data point for [Li⁺] = 0 mol L⁻¹ was calculated from the measurement of **1a**-K with **2h** in DMSO at 20°C).

No.	[E] ₀ / mol L ⁻¹	[Nu ⁻] ₀ / mol L ⁻¹	[LiBF ₄] / mol L ⁻¹	[Li ⁺] / mol L ⁻¹	<i>k</i> _{obs} / s ⁻¹
-	-	-	-	-	3.01 × 10 ² *
RALO 1.15-1-7	2.12 × 10 ⁻⁵	5.18 × 10 ⁻⁴	-	5.44 × 10 ⁻⁴	1.17 × 10 ²
RALO 1.15-1-8	2.12 × 10 ⁻⁵	5.18 × 10 ⁻⁴	1.01 × 10 ⁻³	1.55 × 10 ⁻³	3.16 × 10 ¹
RALO 1.15-1-9	2.12 × 10 ⁻⁵	5.18 × 10 ⁻⁴	2.01 × 10 ⁻³	2.55 × 10 ⁻³	1.64 × 10 ¹
RALO 1.15-1-10	2.12 × 10 ⁻⁵	5.18 × 10 ⁻⁴	4.00 × 10 ⁻³	5.54 × 10 ⁻³	7.41
RALO 1.15-1-11	2.12 × 10 ⁻⁵	5.18 × 10 ⁻⁴	8.00 × 10 ⁻³	8.54 × 10 ⁻³	2.87

* Calculated from the measurement of **1a**-K with **2h** in DMSO at 20°C.

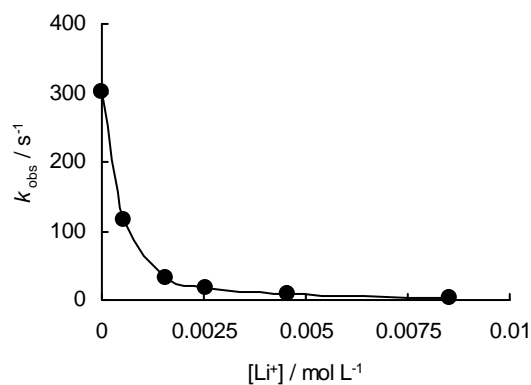


Table 48: Kinetics of the reaction of **1a-Li** with **2h** in DMSO with additional LiBF₄ at 20°C (deprotonation of **1a-H** with 1.05 equiv of LiOtBu, stopped-flow UV-Vis spectrometer, $\lambda = 630$ nm, the data point for [Li⁺] = 0 mol L⁻¹ was calculated from the measurement of **1a-K** with **2h** in DMSO at 20°C).

No.	[E] ₀ / mol L ⁻¹	[Nu ⁻] ₀ / mol L ⁻¹	[LiBF ₄] / mol L ⁻¹	[Li ⁺] / mol L ⁻¹	k _{obs} / s ⁻¹
-	-	-	-	-	5.88 × 10 ² *
RALO 1.15-1-1	2.12 × 10 ⁻⁵	1.01 × 10 ⁻³	-	1.06 × 10 ⁻³	1.85 × 10 ²
RALO 1.15-1-2	2.12 × 10 ⁻⁵	1.01 × 10 ⁻³	1.01 × 10 ⁻³	2.07 × 10 ⁻³	6.34 × 10 ¹
RALO 1.15-1-3	2.12 × 10 ⁻⁵	1.01 × 10 ⁻³	2.01 × 10 ⁻³	3.07 × 10 ⁻³	3.70 × 10 ¹
RALO 1.15-1-4	2.12 × 10 ⁻⁵	1.01 × 10 ⁻³	4.00 × 10 ⁻³	5.06 × 10 ⁻³	2.14 × 10 ¹
RALO 1.15-1-5	2.12 × 10 ⁻⁵	1.01 × 10 ⁻³	8.00 × 10 ⁻³	9.06 × 10 ⁻³	1.44 × 10 ¹
RALO 1.15-1-6	2.12 × 10 ⁻⁵	1.01 × 10 ⁻³	1.40 × 10 ⁻²	1.51 × 10 ⁻²	1.17 × 10 ¹

* Calculated from the measurement of **1a-K** with **2h** in DMSO at 20°C.

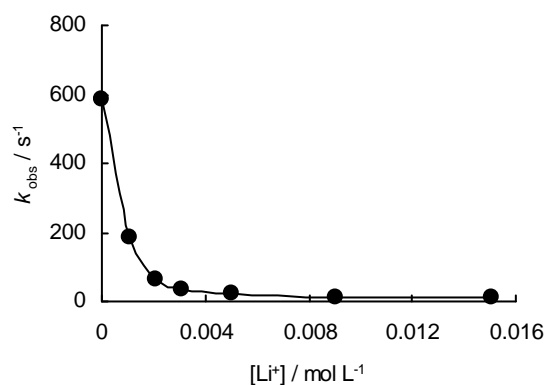
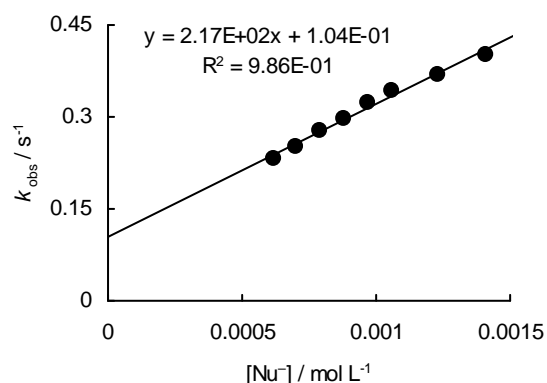


Table 49: Kinetics of the reaction of **1a**-Li with **4a** in DMSO at 20°C (deprotonation of **1a**-H with 1.00-1.05 equiv of LiOtBu, stopped-flow UV-Vis spectrometer, $\lambda = 310$ nm).

No.	$[E]_0 / \text{mol L}^{-1}$	$[\text{Nu}^-]_0 / \text{mol L}^{-1}$	$k_{\text{obs}} / \text{s}^{-1}$
RAK 7.23-8	5.16×10^{-5}	6.17×10^{-4}	2.31×10^{-1}
RAK 7.23-1	5.16×10^{-5}	7.05×10^{-4}	2.52×10^{-1}
RAK 7.23-2	5.16×10^{-5}	7.93×10^{-4}	2.76×10^{-1}
RAK 7.23-3	5.16×10^{-5}	8.81×10^{-4}	2.97×10^{-1}
RAK 7.23-4	5.16×10^{-5}	9.69×10^{-4}	3.23×10^{-1}
RAK 7.23-7	5.16×10^{-5}	1.06×10^{-3}	3.44×10^{-1}
RAK 7.23-6	5.16×10^{-5}	1.23×10^{-3}	3.70×10^{-1}
RAK 7.23-5	5.16×10^{-5}	1.41×10^{-3}	4.01×10^{-1}

$k_2 = -^*$



* No clean second-order kinetics.

Table 50: Kinetics of the reaction of **1a**-Li with **4a** in DMSO with additional LiBF₄ at 20°C (deprotonation of **1a**-H with 1.05 equiv of LiOtBu, stopped-flow UV-Vis spectrometer, $\lambda = 310$ nm, the data point for $[\text{Li}^+] = 0$ mol L⁻¹ was calculated from the measurement of **1a**-K with **4a** in DMSO at 20°C).

No.	$[E]_0 / \text{mol L}^{-1}$	$[\text{Nu}^-]_0 / \text{mol L}^{-1}$	$[\text{LiBF}_4] / \text{mol L}^{-1}$	$[\text{Li}^+] / \text{mol L}^{-1}$	$k_{\text{obs}} / \text{s}^{-1}$
-	-	-	-	-	1.21 *
RAK 7.24-1	5.71×10^{-5}	1.01×10^{-3}	-	1.06×10^{-3}	3.32×10^{-1}
RAK 7.24-2	5.71×10^{-5}	1.01×10^{-3}	1.00×10^{-3}	2.06×10^{-3}	1.56×10^{-1}
RAK 7.24-3	5.71×10^{-5}	1.01×10^{-3}	2.01×10^{-3}	3.07×10^{-3}	1.06×10^{-1}
RAK 7.24-4	5.71×10^{-5}	1.01×10^{-3}	4.02×10^{-3}	5.08×10^{-3}	7.04×10^{-2}
RAK 7.24-5	5.71×10^{-5}	1.01×10^{-3}	8.01×10^{-3}	9.07×10^{-3}	4.70×10^{-2}

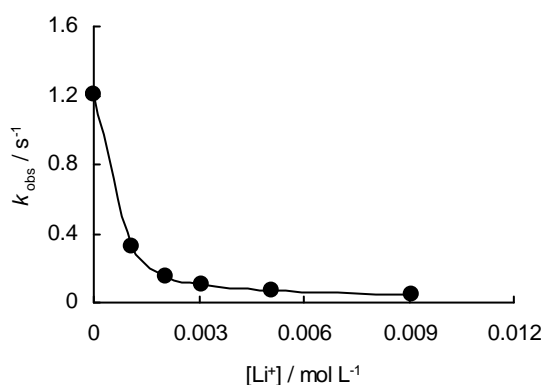
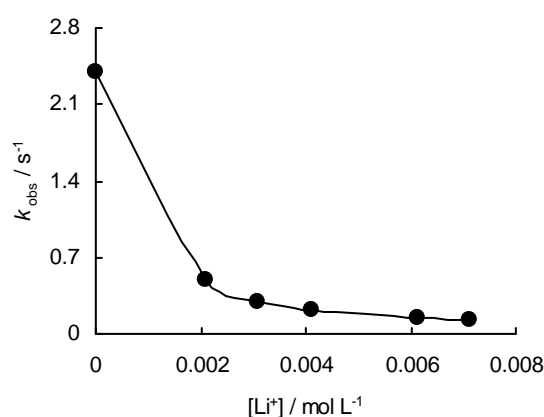
* Calculated from the measurement of **1a**-K with **4a** in DMSO at 20°C.

Table 51: Kinetics of the reaction of **1a**-Li with **4a** in DMSO with additional LiBF₄ at 20°C (deprotonation of **1a**-H with 1.05 equiv of LiOtBu, stopped-flow UV-Vis spectrometer, $\lambda = 310$ nm, the data point for [Li⁺] = 0 mol L⁻¹ was calculated from the measurement of **1a**-K with **4a** in DMSO at 20°C).

No.	[E] ₀ / mol L ⁻¹	[Nu ⁻] ₀ / mol L ⁻¹	[LiBF ₄] / mol L ⁻¹	[Li ⁺] / mol L ⁻¹	<i>k</i> _{obs} / s ⁻¹
-	-	-	-	-	2.40 *
RAK 7.24-6	5.71 × 10 ⁻⁵	2.00 × 10 ⁻³	-	2.10 × 10 ⁻³	4.89 × 10 ⁻¹
RAK 7.24-7	5.71 × 10 ⁻⁵	2.00 × 10 ⁻³	1.00 × 10 ⁻³	3.10 × 10 ⁻³	2.90 × 10 ⁻¹
RAK 7.24-8	5.71 × 10 ⁻⁵	2.00 × 10 ⁻³	2.01 × 10 ⁻³	4.11 × 10 ⁻³	2.13 × 10 ⁻¹
RAK 7.24-9	5.71 × 10 ⁻⁵	2.00 × 10 ⁻³	4.02 × 10 ⁻³	6.12 × 10 ⁻³	1.48 × 10 ⁻¹
RAK 7.24-10	5.71 × 10 ⁻⁵	2.00 × 10 ⁻³	5.02 × 10 ⁻³	7.12 × 10 ⁻³	1.31 × 10 ⁻¹

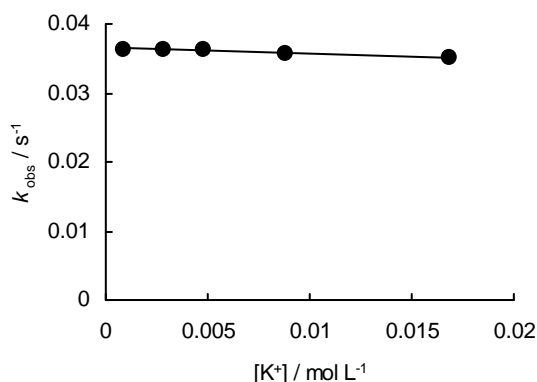
* Calculated from the measurement of **1a**-K with **4a** in DMSO at 20°C.

Kinetic investigations of the counterion effects for the phosphonate-stabilized carbanion **1b**

Counterion effects of K⁺

Table 52: Kinetics of the reaction of **1b**-K with **2k** in DMSO with additional KBF₄ at 20°C (deprotonation of **1b**-H with 1.05 equiv of KOtBu, diode array UV-Vis spectrometer, $\lambda = 393$ nm).

No.	[E] ₀ / mol L ⁻¹	[Nu ⁻] ₀ / mol L ⁻¹	[KBF ₄] / mol L ⁻¹	[K ⁺] / mol L ⁻¹	<i>k</i> _{obs} / s ⁻¹
RALO 2.12-1	3.40 × 10 ⁻⁵	8.02 × 10 ⁻⁴	-	8.42 × 10 ⁻⁴	3.63 × 10 ⁻²
RALO 2.12-2	3.58 × 10 ⁻⁵	8.02 × 10 ⁻⁴	2.02 × 10 ⁻³	2.86 × 10 ⁻³	3.63 × 10 ⁻²
RALO 2.12-3	3.64 × 10 ⁻⁵	8.02 × 10 ⁻⁴	3.99 × 10 ⁻³	4.83 × 10 ⁻³	3.63 × 10 ⁻²
RALO 2.12-4	3.70 × 10 ⁻⁵	8.02 × 10 ⁻⁴	8.00 × 10 ⁻³	8.84 × 10 ⁻³	3.57 × 10 ⁻²
RALO 2.12-5	3.56 × 10 ⁻⁵	8.02 × 10 ⁻⁴	1.60 × 10 ⁻²	1.68 × 10 ⁻²	3.51 × 10 ⁻²



Counterion effects of Na⁺

Table 53: Kinetics of the reaction of **1b**-Na with **2j** in DMSO at 20°C (deprotonation of **1b**-H with 1.00-1.05 equiv of NaOtBu, stopped-flow UV-Vis spectrometer, $\lambda = 371$ nm).

No.	[E] ₀ / mol L ⁻¹	[Nu ⁻] ₀ / mol L ⁻¹	k _{obs} / s ⁻¹
RALO 2.2-1	5.64×10^{-5}	6.33×10^{-4}	4.27×10^{-2}
RALO 2.2-2	5.64×10^{-5}	9.21×10^{-4}	6.17×10^{-2}
RALO 2.2-3	5.64×10^{-5}	1.21×10^{-3}	8.21×10^{-2}
RALO 2.2-4	5.64×10^{-5}	1.50×10^{-3}	1.01×10^{-1}
RALO 2.2-5	5.64×10^{-5}	1.79×10^{-3}	1.22×10^{-1}
RALO 2.2-6	5.64×10^{-5}	2.07×10^{-3}	1.40×10^{-1}
$k_2 = 6.81 \times 10^1 \text{ L mol}^{-1} \text{ s}^{-1}$			

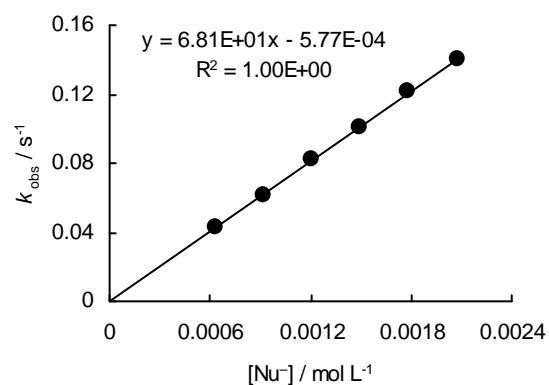


Table 54: Kinetics of the reaction of **1b**-Na with **2k** in DMSO at 20°C (deprotonation of **1b**-H with 1.00-1.05 equiv of NaOtBu, diode array UV-Vis spectrometer, $\lambda = 393$ nm).

No.	[E] ₀ / mol L ⁻¹	[Nu ⁻] ₀ / mol L ⁻¹	k _{obs} / s ⁻¹
RALO 2.6-1	2.34×10^{-5}	4.02×10^{-4}	1.71×10^{-2}
RALO 2.6-2	2.49×10^{-5}	5.10×10^{-4}	2.17×10^{-2}
RALO 2.6-3	2.66×10^{-5}	6.19×10^{-4}	2.68×10^{-2}
RALO 2.6-4	2.64×10^{-5}	7.21×10^{-4}	3.12×10^{-2}
RALO 2.6-5	2.65×10^{-5}	8.04×10^{-4}	3.44×10^{-2}
$k_2 = 4.35 \times 10^1 \text{ L mol}^{-1} \text{ s}^{-1}$			

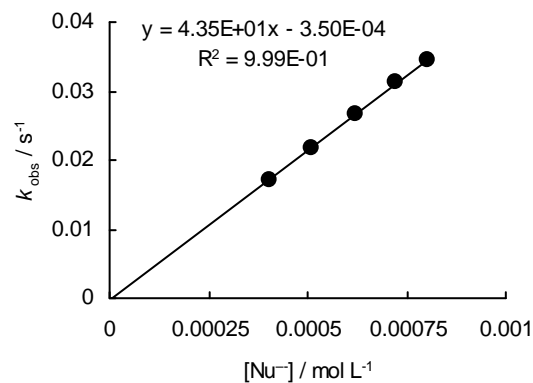
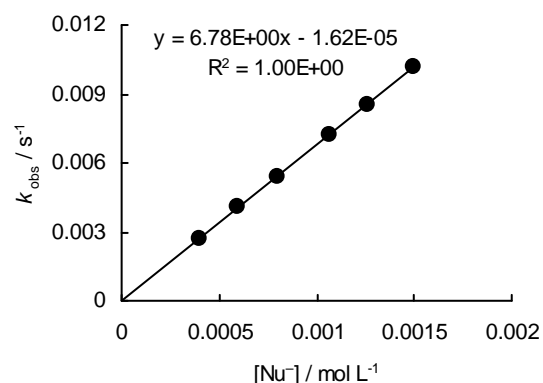
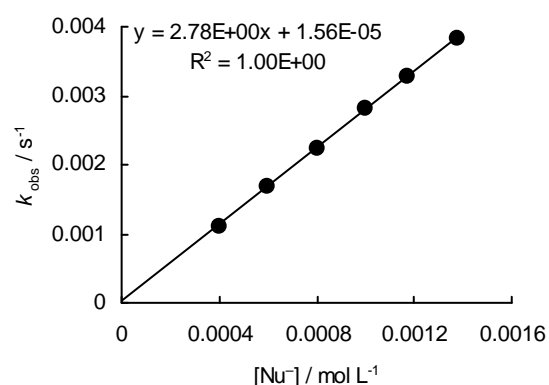


Table 55: Kinetics of the reaction of **1b**-Na with **2l** in DMSO at 20°C (deprotonation of **1b**-H with 1.00-1.05 equiv of NaOtBu, diode array UV-Vis spectrometer, $\lambda = 486$ nm).

No.	$[E]_0 / \text{mol L}^{-1}$	$[\text{Nu}^-]_0 / \text{mol L}^{-1}$	$k_{\text{obs}} / \text{s}^{-1}$
RALO 2.5-1	2.30×10^{-5}	3.95×10^{-4}	2.66×10^{-3}
RALO 2.5-2	2.46×10^{-5}	5.92×10^{-4}	4.06×10^{-3}
RALO 2.5-3	2.42×10^{-5}	8.01×10^{-4}	5.37×10^{-3}
RALO 2.5-4	2.65×10^{-5}	1.07×10^{-3}	7.20×10^{-3}
RALO 2.5-5	2.57×10^{-5}	1.26×10^{-3}	8.51×10^{-3}
RALO 2.5-6	2.56×10^{-5}	1.50×10^{-3}	1.02×10^{-2}
$k_2 = 6.78 \text{ L mol}^{-1} \text{ s}^{-1}$			

**Table 56:** Kinetics of the reaction of **1b**-Na with **2m** in DMSO at 20°C (deprotonation of **1b**-H with 1.00-1.05 equiv of NaOtBu, diode array UV-Vis spectrometer, $\lambda = 521$ nm).

No.	$[E]_0 / \text{mol L}^{-1}$	$[\text{Nu}^-]_0 / \text{mol L}^{-1}$	$k_{\text{obs}} / \text{s}^{-1}$
RALO 2.4-1	4.03×10^{-5}	3.98×10^{-4}	1.11×10^{-3}
RALO 2.4-2	3.89×10^{-5}	5.95×10^{-4}	1.68×10^{-3}
RALO 2.4-3	3.96×10^{-5}	8.02×10^{-4}	2.24×10^{-3}
RALO 2.4-4	3.89×10^{-5}	9.99×10^{-4}	2.80×10^{-3}
RALO 2.4-5	3.84×10^{-5}	1.17×10^{-3}	3.27×10^{-3}
RALO 2.4-6	3.83×10^{-5}	1.38×10^{-3}	3.84×10^{-3}
$k_2 = 2.78 \text{ L mol}^{-1} \text{ s}^{-1}$			

**Table 57:** Kinetics of the reaction of **1b**-Na with **4a** in DMSO at 20°C (deprotonation of **1b**-H with 1.00-1.05 equiv of NaOtBu, stopped-flow UV-Vis spectrometer, $\lambda = 310$ nm).

No.	$[E]_0 / \text{mol L}^{-1}$	$[\text{Nu}^-]_0 / \text{mol L}^{-1}$	$k_{\text{obs}} / \text{s}^{-1}$
RAK 8.8-1	5.61×10^{-5}	6.31×10^{-4}	1.60
RAK 8.8-2	5.61×10^{-5}	8.41×10^{-4}	2.16
RAK 8.8-3	5.61×10^{-5}	1.05×10^{-3}	2.74
RAK 8.8-4	5.61×10^{-5}	1.26×10^{-3}	3.29
RAK 8.8-5	5.61×10^{-5}	1.68×10^{-3}	4.41
RAK 8.8-6	5.61×10^{-5}	2.52×10^{-3}	6.76
$k_2 = 2.72 \times 10^3 \text{ L mol}^{-1} \text{ s}^{-1}$			

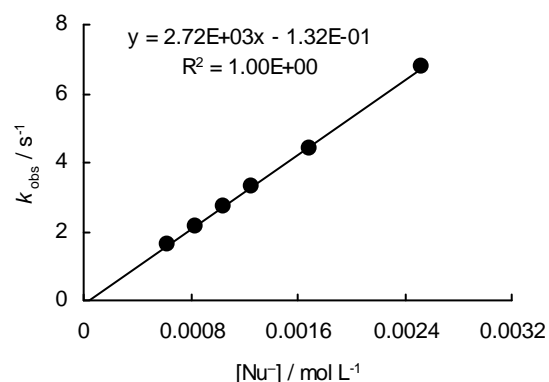
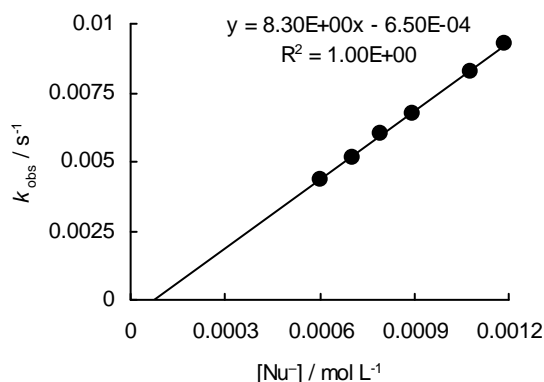
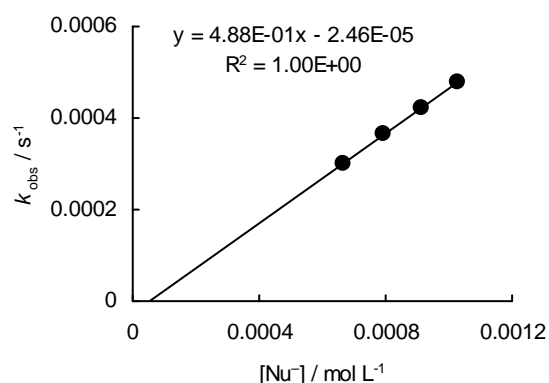


Table 58: Kinetics of the reaction of **1b**-Na with **4e** in DMSO at 20°C (deprotonation of **1b**-H with 1.00-1.05 equiv of NaOtBu, diode array UV-Vis spectrometer, $\lambda = 280$ nm).

No.	$[E]_0 / \text{mol L}^{-1}$	$[\text{Nu}^-]_0 / \text{mol L}^{-1}$	$k_{\text{obs}} / \text{s}^{-1}$
RAK 8.9-1	4.96×10^{-5}	6.01×10^{-4}	4.34×10^{-3}
RAK 8.9-2	4.92×10^{-5}	7.04×10^{-4}	5.17×10^{-3}
RAK 8.9-3	4.96×10^{-5}	7.95×10^{-4}	6.00×10^{-3}
RAK 8.9-4	5.41×10^{-5}	8.94×10^{-4}	6.73×10^{-3}
RAK 8.9-5	5.46×10^{-5}	1.08×10^{-3}	8.28×10^{-3}
RAK 8.9-6	5.47×10^{-5}	1.19×10^{-3}	9.25×10^{-3}
$k_2 = 8.30 \text{ L mol}^{-1} \text{ s}^{-1}$			

**Table 59:** Kinetics of the reaction of **1b**-Na with **4g** in DMSO at 20°C (deprotonation of **1b**-H with 1.00-1.05 eq. of NaOtBu, diode array UV-Vis spectrometer, $\lambda = 310$ nm).

No.	$[E]_0 / \text{mol L}^{-1}$	$[\text{Nu}^-]_0 / \text{mol L}^{-1}$	$k_{\text{obs}} / \text{s}^{-1}$
RAK 8.11-4	4.56×10^{-5}	6.68×10^{-4}	3.01×10^{-4}
RAK 8.11-1	4.61×10^{-5}	7.96×10^{-4}	3.64×10^{-4}
RAK 8.11-2	4.60×10^{-5}	9.12×10^{-4}	4.23×10^{-4}
RAK 8.11-3	4.57×10^{-5}	1.03×10^{-3}	4.77×10^{-4}
$k_2 = 4.88 \times 10^{-1} \text{ L mol}^{-1} \text{ s}^{-1}$			



Counterion effects of Li^+

Table 60: Kinetics of the reaction of **1b**-Li with **2j** in DMSO at 20°C (deprotonation of **1b**-H with 1.05 equiv of LiOtBu, stopped-flow UV-Vis spectrometer, $\lambda = 371$ nm).

No.	$[E]_0 / \text{mol L}^{-1}$	$[\text{Nu}^-]_0 / \text{mol L}^{-1}$	$k_{\text{obs}} / \text{s}^{-1}$
RALO 2.7-1	5.17×10^{-5}	5.41×10^{-4}	3.52×10^{-2}
RALO 2.7-2	5.17×10^{-5}	6.76×10^{-4}	4.51×10^{-2}
RALO 2.7-3	5.17×10^{-5}	8.11×10^{-4}	5.54×10^{-2}
RALO 2.7-4	5.17×10^{-5}	9.46×10^{-4}	6.42×10^{-2}
RALO 2.7-5	5.17×10^{-5}	1.08×10^{-3}	7.40×10^{-2}
RALO 2.7-6	5.17×10^{-5}	1.35×10^{-3}	9.26×10^{-2}
RALO 2.7-7	5.17×10^{-5}	1.62×10^{-3}	1.11×10^{-1}
RALO 2.7-8	5.17×10^{-5}	1.89×10^{-3}	1.29×10^{-1}
$k_2 = 6.92 \times 10^1 \text{ L mol}^{-1} \text{ s}^{-1}$			

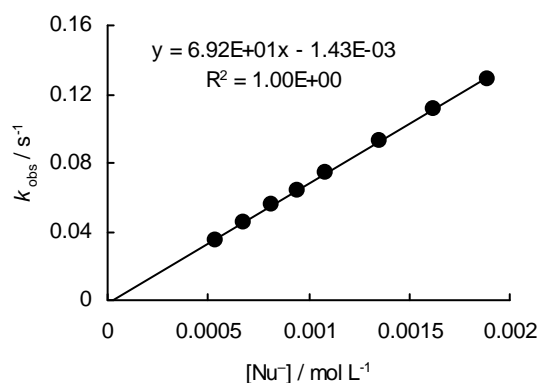
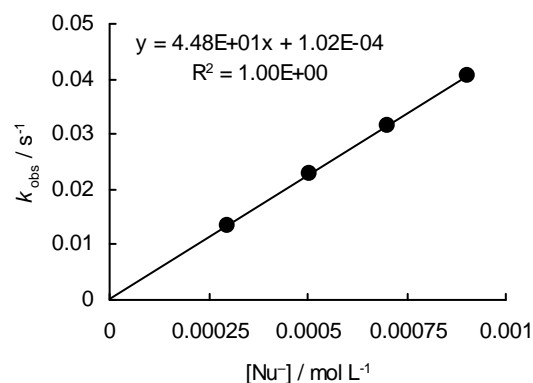


Table 61: Kinetics of the reaction of **1b**-Li with **2k** in DMSO at 20°C (deprotonation of **1b**-H with 1.05 equiv of LiOtBu, diode array UV-Vis spectrometer, $\lambda = 393$ nm).

No.	$[E]_0 / \text{mol L}^{-1}$	$[\text{Nu}^-]_0 / \text{mol L}^{-1}$	$k_{\text{obs}} / \text{s}^{-1}$
RALO 2.9-1	2.64×10^{-5}	2.98×10^{-4}	1.33×10^{-2}
RALO 2.9-2	2.59×10^{-5}	5.03×10^{-4}	2.29×10^{-2}
RALO 2.9-3	2.80×10^{-5}	7.00×10^{-4}	3.14×10^{-2}
RALO 2.9-4	2.78×10^{-5}	9.05×10^{-4}	4.06×10^{-2}
$k_2 = 4.48 \times 10^1 \text{ L mol}^{-1} \text{ s}^{-1}$			

**Table 62:** Kinetics of the reaction of **1b**-Li with **2k** in DMSO with additional LiBF₄ at 20°C (deprotonation of **1b**-H with 1.04 equiv of LiOtBu, diode array UV-Vis spectrometer, $\lambda = 393$ nm, the data point for $[\text{Li}^+] = 0 \text{ mol L}^{-1}$ was calculated from the measurement of **1b**-K with **2k** in DMSO at 20°C).

No.	$[E]_0 / \text{mol L}^{-1}$	$[\text{Nu}^-]_0 / \text{mol L}^{-1}$	$[\text{LiBF}_4] / \text{mol L}^{-1}$	$[\text{Li}^+] / \text{mol L}^{-1}$	$k_{\text{obs}} / \text{s}^{-1}$
-	-	-	-	-	$3.51 \times 10^{-2}^*$
RALO 2.11-1	3.02×10^{-5}	8.02×10^{-4}	-	8.34×10^{-4}	3.40×10^{-2}
RALO 2.11-2	2.86×10^{-5}	8.02×10^{-4}	2.03×10^{-3}	2.86×10^{-3}	3.06×10^{-2}
RALO 2.11-3	2.97×10^{-5}	8.02×10^{-4}	3.98×10^{-3}	4.81×10^{-3}	2.69×10^{-2}
RALO 2.11-4	2.92×10^{-5}	8.02×10^{-4}	8.04×10^{-3}	8.87×10^{-3}	2.02×10^{-2}
RALO 2.11-5	2.80×10^{-5}	8.02×10^{-4}	1.11×10^{-2}	1.19×10^{-2}	1.56×10^{-2}

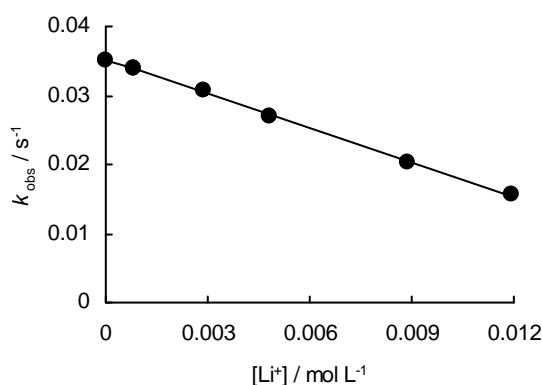
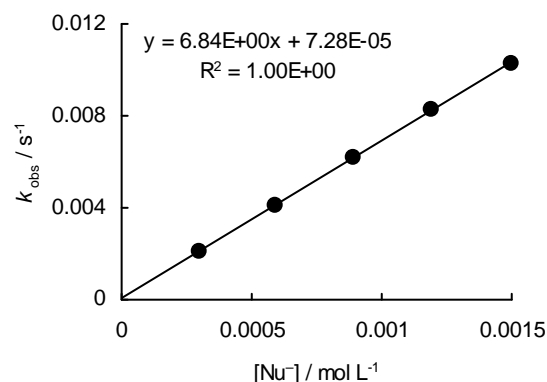
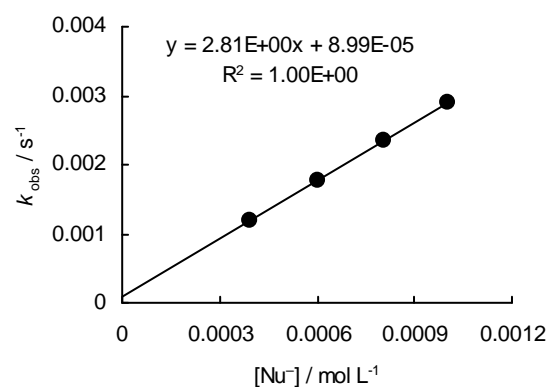
* Calculated from the measurement of **1b**-K with **2k** in DMSO at 20°C.

Table 63: Kinetics of the reaction of **1b**-Li with **2l** in DMSO at 20°C (deprotonation of **1b**-H with 1.05 equiv of LiOtBu, diode array UV-Vis spectrometer, $\lambda = 486$ nm).

No.	$[E]_0 / \text{mol L}^{-1}$	$[\text{Nu}^-]_0 / \text{mol L}^{-1}$	$k_{\text{obs}} / \text{s}^{-1}$
RALO 2.8-1	2.67×10^{-5}	2.99×10^{-4}	2.12×10^{-3}
RALO 2.8-2	2.64×10^{-5}	5.92×10^{-4}	4.11×10^{-3}
RALO 2.8-3	2.60×10^{-5}	8.96×10^{-4}	6.18×10^{-3}
RALO 2.8-4	2.61×10^{-5}	1.19×10^{-3}	8.26×10^{-3}
RALO 2.8-5	2.59×10^{-5}	1.50×10^{-3}	1.03×10^{-2}
$k_2 = 6.84 \text{ L mol}^{-1} \text{ s}^{-1}$			

**Table 64:** Kinetics of the reaction of **1b**-Li with **2m** in DMSO at 20°C (deprotonation of **1b**-H with 1.05 equiv of LiOtBu, diode array UV-Vis spectrometer, $\lambda = 521$ nm).

No.	$[E]_0 / \text{mol L}^{-1}$	$[\text{Nu}^-]_0 / \text{mol L}^{-1}$	$k_{\text{obs}} / \text{s}^{-1}$
RALO 2.10-1	3.16×10^{-5}	3.95×10^{-4}	1.20×10^{-3}
RALO 2.10-2	3.16×10^{-5}	6.01×10^{-4}	1.78×10^{-3}
RALO 2.10-3	3.14×10^{-5}	8.05×10^{-4}	2.36×10^{-3}
RALO 2.10-4	3.11×10^{-5}	1.00×10^{-3}	2.90×10^{-3}
$k_2 = 2.81 \text{ L mol}^{-1} \text{ s}^{-1}$			

**Table 65:** Kinetics of the reaction of **1b**-Li with **4a** in DMSO at 20°C (deprotonation of **1b**-H with 1.05 equiv of LiOtBu, stopped-flow UV-Vis spectrometer, $\lambda = 310$ nm).

No.	$[E]_0 / \text{mol L}^{-1}$	$[\text{Nu}^-]_0 / \text{mol L}^{-1}$	$k_{\text{obs}} / \text{s}^{-1}$
RAK 8.12-1	5.38×10^{-5}	6.15×10^{-4}	1.55
RAK 8.12-2	5.38×10^{-5}	7.38×10^{-4}	1.88
RAK 8.12-3	5.38×10^{-5}	8.61×10^{-4}	2.17
RAK 8.12-4	5.38×10^{-5}	9.83×10^{-4}	2.51
RAK 8.12-5	5.38×10^{-5}	1.11×10^{-3}	2.89
RAK 8.12-9	5.38×10^{-5}	1.23×10^{-3}	3.20
RAK 8.12-6	5.38×10^{-5}	1.72×10^{-3}	4.60
RAK 8.12-7	5.38×10^{-5}	2.21×10^{-3}	5.63
RAK 8.12-8	5.38×10^{-5}	2.95×10^{-3}	7.95
$k_2 = 2.70 \times 10^3 \text{ L mol}^{-1} \text{ s}^{-1}$			

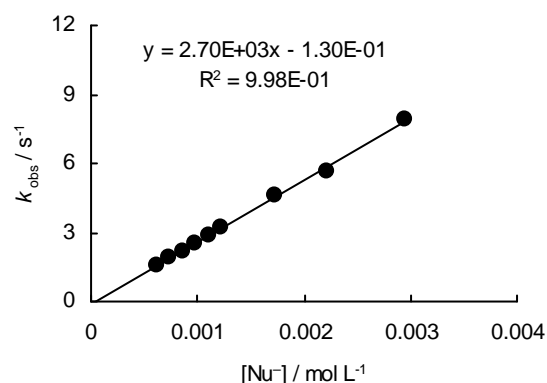
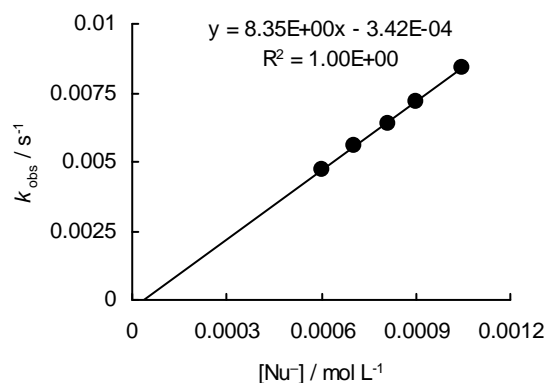
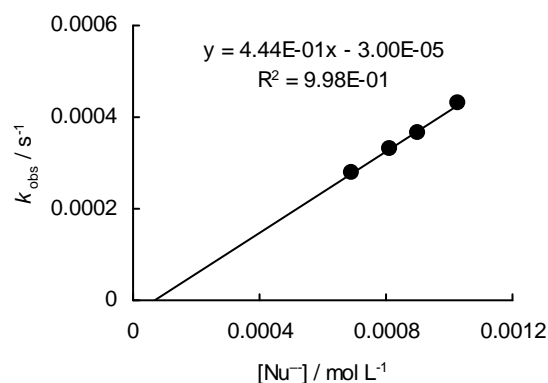


Table 66: Kinetics of the reaction of **1b**-Li with **4e** in DMSO at 20°C (deprotonation of **1b**-H with 1.05 equiv of LiOtBu, diode array UV-Vis spectrometer, $\lambda = 280$ nm).

No.	$[E]_0 / \text{mol L}^{-1}$	$[\text{Nu}^-]_0 / \text{mol L}^{-1}$	$k_{\text{obs}} / \text{s}^{-1}$
RAK 8.13-1	4.98×10^{-5}	6.05×10^{-4}	4.73×10^{-3}
RAK 8.13-2	4.94×10^{-5}	7.07×10^{-4}	5.55×10^{-3}
RAK 8.13-3	4.93×10^{-5}	8.13×10^{-4}	6.41×10^{-3}
RAK 8.13-4	4.95×10^{-5}	9.02×10^{-4}	7.21×10^{-3}
RAK 8.13-5	5.15×10^{-5}	1.05×10^{-3}	8.43×10^{-3}
$k_2 = 8.35 \text{ L mol}^{-1} \text{ s}^{-1}$			

**Table 67:** Kinetics of the reaction of **1b**-Li with **4g** in DMSO at 20°C (deprotonation of **1b**-H with 1.05 equiv of LiOtBu, diode array UV-Vis spectrometer, $\lambda = 310$ nm).

No.	$[E]_0 / \text{mol L}^{-1}$	$[\text{Nu}^-]_0 / \text{mol L}^{-1}$	$k_{\text{obs}} / \text{s}^{-1}$
RAK 8.14-1	5.22×10^{-5}	6.93×10^{-4}	2.78×10^{-4}
RAK 8.14-2	5.25×10^{-5}	8.10×10^{-4}	3.31×10^{-4}
RAK 8.14-3	5.13×10^{-5}	9.00×10^{-4}	3.65×10^{-4}
RAK 8.14-4	5.12×10^{-5}	1.03×10^{-3}	4.29×10^{-4}
$k_2 = 4.44 \times 10^{-1} \text{ L mol}^{-1} \text{ s}^{-1}$			



Kinetic investigation of the counterion effects for the triphenylphosphonium ylide **1e**

Counterion effects of Li^+

Table 68: Kinetics of the reaction of **1e** with **2h** in DMSO with additional LiBF_4 at 20°C (diode array UV-Vis spectrometer, $\lambda = 630$ nm).

No.	$[E]_0 / \text{mol L}^{-1}$	$[\text{Nu}^-]_0 / \text{mol L}^{-1}$	$[\text{LiBF}_4] / \text{mol L}^{-1}$	$k_{\text{obs}} / \text{s}^{-1}$
RALO 5.2-1-1	1.97×10^{-5}	1.02×10^{-3}	-	2.43×10^{-2}
RALO 5.2-1-2	1.96×10^{-5}	1.02×10^{-3}	1.02×10^{-3}	2.51×10^{-2}
RALO 5.2-1-3	2.02×10^{-5}	1.02×10^{-3}	2.03×10^{-3}	2.58×10^{-2}
RALO 5.2-1-4	2.03×10^{-5}	1.02×10^{-3}	4.01×10^{-3}	2.61×10^{-2}
RALO 5.2-1-5	2.00×10^{-5}	1.02×10^{-3}	7.99×10^{-3}	2.68×10^{-2}

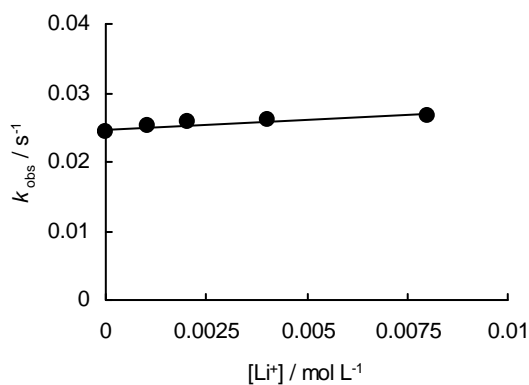


Table 69: Kinetics of the reaction of **1e** with **2h** in DMSO with additional LiBF₄ at 20°C (diode array UV-Vis spectrometer, $\lambda = 630$ nm).

No.	[E] ₀ / mol L ⁻¹	[Nu ⁻] ₀ / mol L ⁻¹	[LiBF ₄] / mol L ⁻¹	k _{obs} / s ⁻¹
RALO 5.2-1-6	1.94×10^{-5}	5.04×10^{-4}	-	1.18×10^{-2}
RALO 5.2-1-7	1.94×10^{-5}	5.04×10^{-4}	1.02×10^{-3}	1.21×10^{-2}
RALO 5.2-1-8	2.00×10^{-5}	5.04×10^{-4}	2.01×10^{-3}	1.22×10^{-2}
RALO 5.2-1-9	1.97×10^{-5}	5.04×10^{-4}	8.07×10^{-3}	1.33×10^{-2}

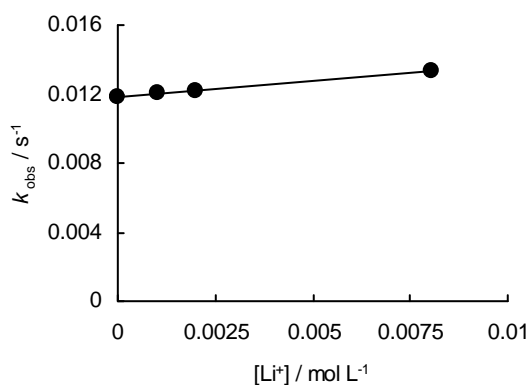
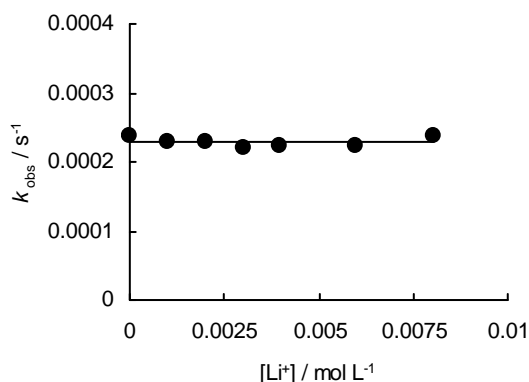


Table 70: Kinetics of the reaction of **1e** with **4a** in DMSO with additional LiBF₄ at 20°C (diode array UV-Vis spectrometer, $\lambda = 330$ nm).

No.	[E] ₀ / mol L ⁻¹	[Nu ⁻] ₀ / mol L ⁻¹	[LiBF ₄] / mol L ⁻¹	k _{obs} / s ⁻¹
RAK 11.2-2-3	5.64×10^{-5}	8.03×10^{-4}	-	2.39×10^{-4}
RAK 11.2-1	5.69×10^{-5}	8.03×10^{-4}	1.02×10^{-3}	2.30×10^{-4}
RAK 11.2-2-1	5.64×10^{-5}	8.03×10^{-4}	2.02×10^{-3}	2.29×10^{-4}
RAK 11.2-3-2	5.77×10^{-5}	8.03×10^{-4}	3.00×10^{-3}	2.20×10^{-4}
RAK 11.2-3-1	5.64×10^{-5}	8.03×10^{-4}	3.98×10^{-3}	2.22×10^{-4}
RAK 11.2-2-2	5.64×10^{-5}	8.03×10^{-4}	6.00×10^{-3}	2.24×10^{-4}
RAK 11.2-3	5.72×10^{-5}	8.03×10^{-4}	8.05×10^{-3}	2.39×10^{-4}



6 References

- [1] (a) Staudinger, H.; Meyer, J. *Helv. Chim. Acta* **1919**, *2*, 635-646. (b) Wittig, G.; Geissler, G. *Liebigs Ann. Chem.* **1953**, *580*, 44-57. (c) Wittig, G.; Schöllkopf, U. *Chem. Ber.* **1954**, *87*, 1318-1330.
- [2] (a) Horner, L.; Hoffmann, H.; Wippel, H. G. *Chem. Ber.* **1958**, *91*, 61-63. (b) Horner, L.; Hoffmann, H.; Wippel, H. G.; Klahre, G. *Chem. Ber.* **1959**, *92*, 2499-2505.
- [3] Wadsworth, W. S.; Emmons, W. D. *J. Am. Chem. Soc.* **1961**, *83*, 1733-1738.
- [4] (a) Maryanoff, B. E.; Reitz, A. B. *Phosphorus, Sulfur Silicon Relat. Elem.* **1986**, *27*, 167-189. (b) Maryanoff, B. E.; Reitz, A. B. *Chem. Rev.* **1989**, *89*, 863-927. (c) Clayden, J.; Warren, S. *Angew. Chem.* **1996**, *108*, 261-291; *Angew. Chem., Int. Ed. Engl.* **1996**, *35*, 241-270. (d) Bojin, M. L.; Barkallah, S.; Evans, S. A. *J. Am. Chem. Soc.* **1996**, *118*, 1549-1550. (e) Vedejs, E.; Peterson, M. J. In *Advances in Carbanion Chemistry*; Snieckus, V., Ed.; JAI Press: London, 1996; Vol. 2, pp 1-85. (f) Nicolaou, K. C.; Härter, M. W.; Gunzner, J. L.; Nadin, A. *Liebigs Ann./Recueil* **1997**, 1283-1301. (g) Kokin, K.; Iitake, K.-I.; Takaguchi, Y.; Aoyama, H.; Hayashi, S.; Motoyoshiya, J. *Phosphorus, Sulfur Silicon Relat. Elem.* **1998**, *133*, 21-40. (h) Kolodiazhnyi, O. I., *Phosphorus Ylides*; Wiley-VCH: Weinheim, 1999; pp 258-358. (i) Clayden, J.; Greeves, N.; Warren, S.; Wothers, P. *Organic Chemistry*; Oxford University Press: New York, 2001; pp 814-818. (j) López-Ortiz, F.; López, J. G.; Manzaneda, R. A.; Álvarez, I. J. P. *Mini-Rev. Org. Chem.* **2004**, *1*, 65-76. (k) Brückner, R. *Reaktionsmechanismen*; 3rd ed.; Elsevier - Spektrum Akademischer Verlag: Heidelberg (Germany), 2004; pp 455-483. (l) Smith, M. B.; March, J. *March's Advanced Organic Chemistry: Reactions, Mechanism, and Structure*; 6th ed.; Wiley: Hoboken (N.J.), 2007; pp 1369-1380.
- [5] (a) Vedejs, E.; Snoble, K. A. *J. Am. Chem. Soc.* **1973**, *95*, 5778-5780. (b) Vedejs, E.; Meier, G. P.; Snoble, K. A. *J. Am. Chem. Soc.* **1981**, *103*, 2823-2831. (c) Vedejs, E.;

- Marth, C. F.; Ruggeri, R. *J. Am. Chem. Soc.* **1988**, *110*, 3940-3948. (d) Vedejs, E.; Marth, C. F. *J. Am. Chem. Soc.* **1988**, *110*, 3948-3958. (e) Vedejs, E.; Fleck, T. J. *J. Am. Chem. Soc.* **1989**, *111*, 5861-5871. (f) Vedejs, E.; Marth, C. F. *J. Am. Chem. Soc.* **1990**, *112*, 3905-3909. (g) Vedejs, E.; Peterson, M. J. *Top. Stereochem.* **1994**, *21*, 1-157.
- [6] (a) Reitz, A. B.; Mutter, M. S.; Maryanoff, B. E. *J. Am. Chem. Soc.* **1984**, *106*, 1873-1875. (b) Maryanoff, B. E.; Reitz, A. B.; Mutter, M. S.; Inners, R. R.; Almond, H. R.; Whittle, R. R.; Olofson, R. A. *J. Am. Chem. Soc.* **1986**, *108*, 7664-7678. (c) Maryanoff, B. E.; Reitz, A. B.; Graden, D. W.; Almond, H. R. *Tetrahedron Lett.* **1989**, *30*, 1361-1364.
- [7] (a) Naito, T.; Nagase, S.; Yamataka, H. *J. Am. Chem. Soc.* **1994**, *116*, 10080-10088. (b) Yamataka, H.; Nagase, S. *J. Am. Chem. Soc.* **1998**, *120*, 7530-7536. (c) Robiette, R.; Richardson, J.; Aggarwal, V. K.; Harvey, J. N. *J. Am. Chem. Soc.* **2005**, *127*, 13468-13469. (d) Robiette, R.; Richardson, J.; Aggarwal, V. K.; Harvey, J. N. *J. Am. Chem. Soc.* **2006**, *128*, 2394-2409.
- [8] For further references on theoretical studies of the Wittig reaction, see: (a) Trindle, C.; Hwang, J.-T.; Carey, F. A. *J. Org. Chem.* **1973**, *38*, 2664-2669. (b) Hoeller, R.; Lischka, H. *J. Am. Chem. Soc.* **1980**, *102*, 4632-4635. (c) Volatron, F.; Eisenstein, O. *J. Am. Chem. Soc.* **1984**, *106*, 6117-6119. (d) Volatron, F.; Eisenstein, O. *J. Am. Chem. Soc.* **1987**, *109*, 1-14. (e) Rzepa, H. S. *J. Chem. Soc., Perkin Trans. 2* **1989**, 2115-2119. (f) Mari, F.; Lahti, P. M.; McEwen, W. E. *Heteroat. Chem.* **1990**, *1*, 255-259. (g) Mari, F.; Lahti, P. M.; McEwen, W. E. *Heteroat. Chem.* **1991**, *2*, 265-276. (h) Mari, F.; Lahti, P. M.; McEwen, W. E. *J. Am. Chem. Soc.* **1992**, *114*, 813-821. (i) Restrepo-Cossio, A. A.; Gonzalez, C. A.; Mari, F. *J. Phys. Chem. A* **1998**, *102*, 6993-7000. (j) Lu, W. C.; Wong, N. B.; Zhang, R. Q. *Theor. Chem. Acc.* **2002**, *107*, 206-210. (k) Seth, M.; Senn, H. M.; Ziegler, T. *J. Phys. Chem. A* **2005**, *109*, 5136-5143.
- [9] Ward, W. J.; McEwen, W. E. *J. Org. Chem.* **1990**, *55*, 493-500.
- [10] Schlosser, M.; Christmann, K. F. *Angew. Chem.* **1965**, *77*, 682-683; *Angew. Chem., Int. Ed. Engl.* **1965**, *4*, 689-690.
- [11] (a) Schlosser, M.; Christmann, K. F. *Synthesis* **1969**, 38-39. (b) Schlosser, M.; Tuong, H. B.; Tarchini, C. *Chimia* **1977**, *31*, 219-220. (c) Schlosser, M.; Tuong, H. B. *Angew. Chem.* **1979**, *91*, 675; *Angew. Chem., Int. Ed. Engl.* **1979**, *18*, 633-634. (d) Neumann, R. A.; Berger, S. *Eur. J. Org. Chem.* **1998**, 1085-1087. (e) Pascariu, A.; Mracec, M.; Berger, S. *Int. J. Quantum Chem.* **2008**, *108*, 1052-1058.

- [12] (a) Schlosser, M.; Christmann, K. F. *Liebigs Ann. Chem.* **1967**, *708*, 1-35. (b) Schlosser, M. *Top. Stereochem.* **1970**, *5*, 1-30. (c) Schlosser, M.; Oi, R.; Schaub, B. *Phosphorus, Sulfur Silicon Relat. Elem.* **1983**, *18*, 171-174.
- [13] Mracec, M.; Pascariu, A.; Berger, S.; Mracec, M. *Int. J. Quantum Chem.* **2007**, *107*, 1782-1793.
- [14] (a) Brandt, P.; Norrby, P. O.; Martin, I.; Rein, T. *J. Org. Chem.* **1998**, *63*, 1280-1289. (b) Ando, K. *J. Org. Chem.* **1999**, *64*, 6815-6821. (c) Norrby, P. O.; Brandt, P.; Rein, T. *J. Org. Chem.* **1999**, *64*, 5845-5852. (d) Motoyoshiya, J.; Kusaura, T.; Kokin, K.; Yokoya, S.-i.; Takaguchi, Y.; Narita, S.; Aoyama, H. *Tetrahedron* **2001**, *57*, 1715-1721.
- [15] (a) Larsen, R. O.; Aksnes, G. *Phosphorus, Sulfur Silicon Relat. Elem.* **1983**, *15*, 219-228. (b) Larsen, R. O.; Aksnes, G. *Phosphorus, Sulfur Silicon Relat. Elem.* **1983**, *15*, 229-237.
- [16] (a) Mayr, H.; Patz, M. *Angew. Chem.* **1994**, *106*, 990-1010; *Angew. Chem., Int. Ed. Engl.*, **1994**, *33*, 938-957. (b) Mayr, H.; Bug, T.; Gotta, M. F.; Hering, N.; Irrgang, B.; Janker, B.; Kempf, B.; Loos, R.; Ofial, A. R.; Remennikov, G.; Schimmel, H. *J. Am. Chem. Soc.* **2001**, *123*, 9500-9512. (c) Lucius, R.; Loos, R.; Mayr, H. *Angew. Chem.* **2002**, *114*, 97-102; *Angew. Chem. Int. Ed.* **2002**, *41*, 91-95. (d) Mayr, H.; Kempf, B.; Ofial, A. R. *Acc. Chem. Res.* **2003**, *36*, 66-77. (e) Mayr, H.; Ofial, A. R. *Pure Appl. Chem.* **2005**, *77*, 1807-1821. (f) Mayr, H.; Ofial, A. R. *J. Phys. Org. Chem.* **2008**, *21*, 584-595.
- [17] (a) Lemek, T.; Mayr, H. *J. Org. Chem.* **2003**, *68*, 6880-6886. (b) Berger, S. T. A.; Seeliger, F. H.; Hofbauer, F.; Mayr, H. *Org. Biomol. Chem.* **2007**, *5*, 3020-3026. (c) Seeliger, F.; Berger, S. T. A.; Remennikov, G. Y.; Polborn, K.; Mayr, H. *J. Org. Chem.* **2007**, *72*, 9170-9180. (d) Kaumanns, O.; Mayr, H. *J. Org. Chem.* **2008**, *73*, 2738-2745.
- [18] (a) Fleming, F. F.; Shook, B. C. *Tetrahedron* **2002**, *58*, 1-23. (b) Fleming, F. F.; Zhang, Z.; Wei, G.; Steward, O. W. *J. Org. Chem.* **2006**, *71*, 1430-1435.
- [19] (a) Bug, T.; Lemek, T.; Mayr, H. *J. Org. Chem.* **2004**, *69*, 7565-7576. (b) Mayr, H.; Ofial, A. R. In *Carbocation Chemistry*; Olah, G. A., Prakash, G. K. S., Eds.; Wiley: Hoboken, NJ, 2004; pp 331-358. (c) Berger, S. T. A.; Ofial, A. R.; Mayr, H. *J. Am. Chem. Soc.* **2007**, *129*, 9753-9761. (d) Brotzel, F.; Chu, Y. C.; Mayr, H. *J. Org. Chem.* **2007**, *72*, 3679-3688. (e) Nigst, T. A.; Westermaier, M.; Ofial, A. R.; Mayr, H. *Eur. J. Org. Chem.* **2008**, 2369-2374.

- [20] (a) Horner, L.; Hoffmann, H.; Klink, W.; Ertel, H.; Toscano, V. G. *Chem. Ber.* **1962**, *95*, 581-601. (b) Boutagy, J.; Thomas, R. *Chem. Rev.* **1974**, *74*, 87-99. (c) Schlosser, M.; Tuong, H. B. *Chimia* **1976**, *30*, 197-199.
- [21] (a) Data taken from <http://www.chem.wisc.edu/areas/reich/pkatable/>. (b) Matthews, W. S.; Bares, J. E.; Bartmess, J. E.; Bordwell, F. G.; Cornforth, F. J.; Drucker, G. E.; Margolin, Z.; McCallum, R. J.; McCollum, G. J.; Vanier, N. R. *J. Am. Chem. Soc.* **1975**, *97*, 7006-7014. (c) Keeffe, J. R.; Morey, J.; Palmer, C. A.; Lee, J. C. *J. Am. Chem. Soc.* **1979**, *101*, 1295-1297. (d) Olmstead, W. N.; Bordwell, F. G. *J. Org. Chem.* **1980**, *45*, 3299-3305. (e) Arnett, E. M.; Harrelson, J. A. *J. Am. Chem. Soc.* **1987**, *109*, 809-812. (f) Bordwell, F. G. *Acc. Chem. Res.* **1988**, *21*, 456-463. (g) Bordwell, F. G.; Bausch, M. J.; Branca, J. C.; Harrelson, J. A. *J. Phys. Org. Chem.* **1988**, *1*, 225-239. (h) Bordwell, F. G.; Branca, J. C.; Bares, J. E.; Filler, R. *J. Org. Chem.* **1988**, *53*, 780-782. (i) Bordwell, F. G.; Harrelson, J. A.; Satish, A. V. *J. Org. Chem.* **1989**, *54*, 3101-3105. (j) Bordwell, F. G.; Satish, A. V. *J. Am. Chem. Soc.* **1994**, *116*, 8885-8889. (k) Goumont, R.; Kizilian, E.; Buncel, E.; Terrier, F. *Org. Biomol. Chem.* **2003**, *1*, 1741-1748.
- [22] (a) Bernasconi, C. F. *Acc. Chem. Res.* **1987**, *20*, 301-308. (b) Bernasconi, C. F. *Acc. Chem. Res.* **1992**, *25*, 9-16.
- [23] (a) Goetz, H.; Nerdel, F.; Michaelis, H. *Naturwissenschaften* **1963**, *50*, 496-497. (b) Speziale, A. J.; Bissing, D. E. *J. Am. Chem. Soc.* **1963**, *85*, 1888-1889. (c) Speziale, A. J.; Bissing, D. E. *J. Am. Chem. Soc.* **1963**, *85*, 3878-3884. (d) Röchardt, C.; Panse, P.; Eichler, S. *Chem. Ber.* **1967**, *100*, 1144-1164. (e) Aksnes, G.; Khalil, F. Y. *Phosphorus* **1972**, *2*, 105-109. (f) Giese, B.; Schoch, J.; Röchardt, C. *Chem. Ber.* **1978**, *111*, 1395-1403. (g) Yamataka, H.; Nagareda, K.; Ando, K.; Hanafusa, T. *J. Org. Chem.* **1992**, *57*, 2865-2869. (h) Li, Z.; He, C.; Yang, M.; Xia, C.; Yu, X. *ARKIVOC* **2005** (i), 98-104.
- [24] (a) Quin, L. D.; Anderson, H. G. *J. Org. Chem.* **1964**, *29*, 1859-1861. (b) Regitz, M.; Anschutz, W. *Chem. Ber.* **1969**, *102*, 2216-2229.
- [25] Mauduit, M.; Kouklovsky, C.; Langlois, Y. *Tetrahedron Lett.* **1998**, *39*, 6857-6860.
- [26] (a) Lucius, R.; Mayr, H. *Angew. Chem.* **2000**, *112*, 2086-2089; *Angew. Chem., Int. Ed.* **2000**, *39*, 1995-1997. (b) Evans, S.; Nesvadba P.; Allenbach S. (Ciba-Geigy AG), EP-B 744392, **1996** [*Chem. Abstr.* **1997**, *126*, 46968v].
- [27] For detailed NMR investigations on the structures of the anion of diethyl [(carbomethoxy)methyl]phosphonate in various solvents, see: Bottin-Strzalko, T.; Corset, J.; Froment, F.; Pouet, M.-J.; Seyden-Penne, J.; Simonnin, M.-P. *J. Org. Chem.* **1980**, *45*, 1270-1276.

Chapter 4: Nucleophilic Reactivities of Sulfur Ylides and Related Carbanions: Comparison with Structurally Related Organophosphorus Compounds

Roland Appel and Herbert Mayr

Chem. Eur. J. **2010**, *16*, 8610-8614.

1 Introduction

Phosphorus and sulfur ylides are two important classes of reagents in organic chemistry. While phosphorus ylides and related phosphoryl-stabilized carbanions are used in the most common olefination reactions, that is, Wittig, Wittig-Horner, and Horner-Wadsworth-Emmons reactions,^[1] sulfur ylides have been introduced as versatile reagents for the syntheses of three-membered carbo- and heterocyclic rings (Corey-Chaykovsky reaction).^[2]

In contrast to their phosphorus-stabilized analogs, sulfinyl- and sulfonyl-stabilized carbanions react with aldehydes to form β -hydroxysulfines and -sulfones,^[3] respectively, or undergo Knoevenagel condensation reactions.^[4] Acylation and subsequent reductive elimination transfers β -hydroxy-sulfones into olefins (Julia and related olefinations).^[5]

Previous investigations on structure-reactivity relationships of sulfur and phosphorus ylides were focused on their basicities^[6] and the different leaving group abilities of R_2S and R_3P .^[7] Owing to the poor correlation between basicities and reactivities of carbon-centered nucleophiles,^[8] a quantitative comparison of the reactivities of sulfur and phosphorus ylides as well as their related carbanions has so far not been possible.

In recent years, we have shown that the rates of the reactions of carbocations and Michael acceptors with n -, π -, and σ -nucleophiles can be described by eq 1, where $k_{20^\circ\text{C}}$ is the second-order rate constant in $\text{M}^{-1} \text{s}^{-1}$, s is a nucleophile-specific slope parameter, N is a nucleophilicity parameter, and E is an electrophilicity parameter.

$$\log k_{20^\circ\text{C}} = s(N + E) \quad (1)$$

By using this methodology, we have developed the most comprehensive nucleophilicity scale presently available and, therefore, were able to directly compare many different classes of nucleophiles.^[8,9] With the rule of thumb that electrophile-nucleophile combinations at room temperature only take place when $(E + N > -5)$, we have been able to establish a rough ordering principle of polar organic reactivity.^[9c]

After determining the nucleophilicities of phosphorus ylides and phosphoryl-stabilized carbanions,^[8c] we have now studied the kinetics of the reactions of the sulfur ylides **1a** and **1b**, the sulfonyl stabilized carbanion **1c**, and the sulfinyl stabilized carbanion **1d** with the benzhydrylium ions **2a–e** and the structurally related quinone methides **2f–k** (Table 1) in DMSO, to derive the nucleophilicity parameters *N* and *s* for the nucleophiles **1** and to compare them with those of analogous phosphorus compounds.

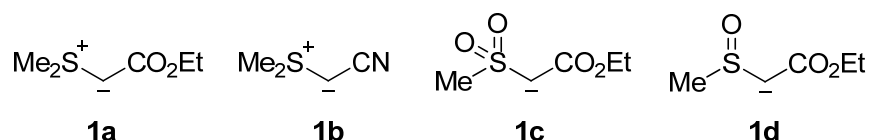


Table 1: Benzhydrylium Ions **2a–e** and Quinone Methides **2f–k** Employed as Reference Electrophiles in this Work.

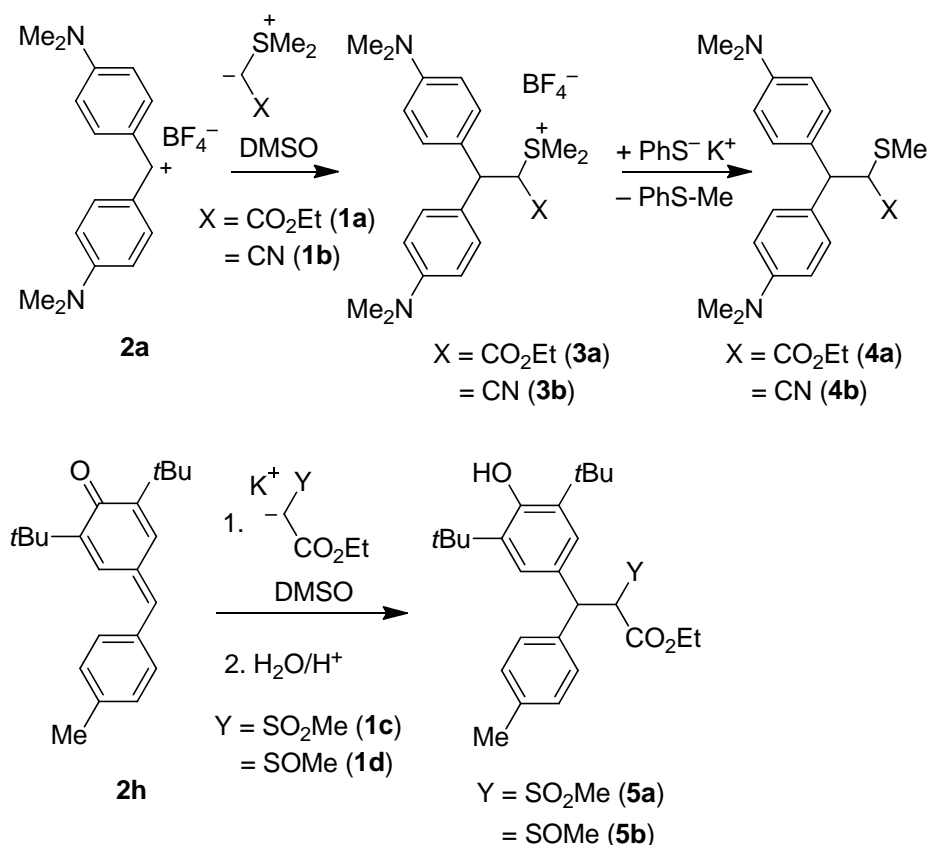
Electrophile		E^a
2a	X = NMe ₂	-7.02
2b	X = N(CH ₂) ₄	-7.69
2c		-8.76
2d (<i>n</i> = 2)		-9.45
2e (<i>n</i> = 1)		-10.04
Electrophile		E^a
2f	Y = Ph Z = OMe	-12.18
2g	Y = Ph Z = NMe ₂	-13.39
2h	Y = <i>t</i> Bu Z = Me	-15.83
2i	Y = <i>t</i> Bu Z = OMe	-16.11
2j	Y = <i>t</i> Bu Z = NMe ₂	-17.29
2k		-17.90

^a *E* for **2a–e** from ref 9b, for **2f–k** from ref 9c.

2 Results

As shown in Scheme 1, the reference electrophiles **2a** and **2h** were employed to elucidate the course of these reactions. Because of the low stability of the addition products **3a,b** obtained from **2a** and the sulfur ylides **1a,b**, the adducts **3a,b** were not isolated but immediately treated with thiophenolate to afford the non-charged products **4a,b**, which were fully characterized. For identifying the products formed from the nucleophiles **1c,d** and the quinone methide **2h**, solutions of the carbanions **1c,d** were generated by deprotonation of the corresponding CH acids (**1c,d**)-H with KO*t*Bu in DMSO, subsequent addition of **2h**, and aqueous acidic workup. The addition products **5a** and **5b** were obtained as mixtures of two and four diastereomers, respectively (^1H - and ^{13}C -NMR spectroscopy).

Scheme 1: Characterization of the Reaction Products.



All kinetic investigations were monitored photometrically by following the disappearance of the colored electrophiles **2** in the presence of more than 10 equiv of the nucleophiles **1** (first-order conditions). Solutions of the ylides **1a,b** in DMSO were freshly prepared before the kinetic experiments; the carbanions **1c,d** were generated by deprotonation of the corresponding CH acids (**1c,d**)-H with 1.00-1.05 equiv of KO*t*Bu in DMSO solution. To

prove that (**1c,d**)-H were quantitatively deprotonated under these conditions, several kinetic experiments have been repeated by using only 0.5-0.6 equiv of KO t Bu for the deprotonation of (**1c,d**)-H. In these experiments, where the concentrations of the carbanions **1c,d** correspond to the amount of KO t Bu used, second-order rate constants were obtained, which agreed within 1-2 % with those obtained with a slight excess of KO t Bu (see Table 2). As the presence of 18-crown-6 did not affect the reactivities of (**1c,d**)-K, one can conclude that the reactivities of the free carbanions **1c,d** were observed.

From the exponential decays of the UV-Vis absorbances of the electrophiles, the first-order rate constants k_{obs} were obtained. Plots of k_{obs} (s^{-1}) against the concentrations of the nucleophiles **1** were linear with negligible intercepts as required by eq 2 (Figure 1).

$$-d[\mathbf{2}]/dt = k_2 [\mathbf{1}] [\mathbf{2}] \text{ for } [\mathbf{1}] \gg [\mathbf{2}] \Rightarrow k_{\text{obs}} = k_2 [\mathbf{1}] \quad (2)$$

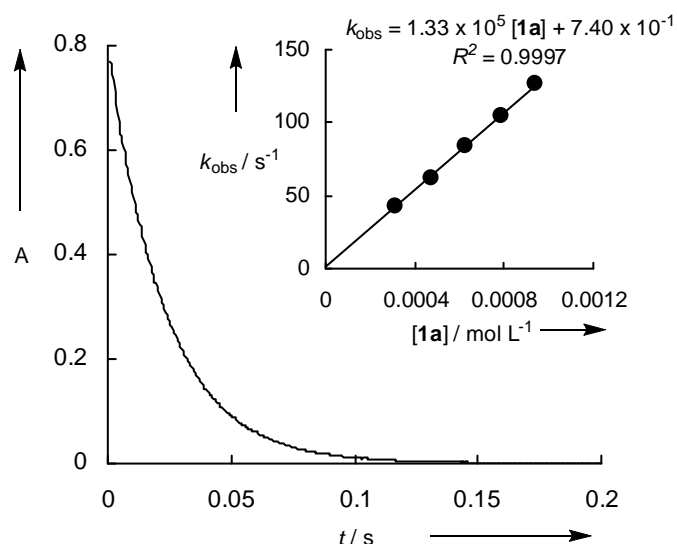
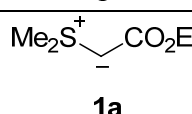
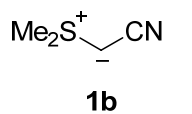
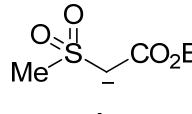
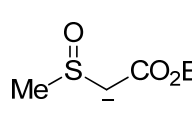


Figure 1: Exponential decay of the absorbance at 624 nm during the reaction of **1a** (3.14×10^{-4} M) with **2b** (2.23×10^{-5} M) at 20°C in DMSO. Insert: Determination of the second-order rate constant $k_2 = 1.33 \times 10^5 \text{ M}^{-1} \text{ s}^{-1}$ from the dependence of the first-order rate constant k_{obs} on the concentration of **1a**.

Table 2: Second-Order Rate Constants for the Reactions of the Sulfur-Stabilized Nucleophiles **1** with the Reference Electrophiles **2** in DMSO at 20°C.

Nucleophile	N / s^a	Electrophile	$k_2 / \text{M}^{-1} \text{s}^{-1}$
 1a	15.85 / 0.61	2a	2.70×10^5
		2b	1.33×10^5
		2c	1.34×10^4
		2d	7.30×10^3
		2e	2.56×10^3
		2f	2.32×10^2
 1b	16.23 / 0.60	2a	3.47×10^5
		2b	2.08×10^5
		2c	1.95×10^4
		2d	9.06×10^3
		2e	3.07×10^3
		2f	4.00×10^2
 1c	18.00 / 0.66	2d	3.38×10^5
		2e	1.61×10^5
		2f	1.04×10^4
		2f	1.02×10^4 ^b
		2g	1.17×10^3
		2h	2.72×10^1
		2i	1.65×10^1
		2j	2.54
 1d	20.61 / 0.64	2f	2.29×10^5
		2g	3.42×10^4
		2g	3.44×10^4 ^b
		2h	1.34×10^3
		2i	8.12×10^2
		2j	1.30×10^2 ^b
	2k	4.43×10^1	

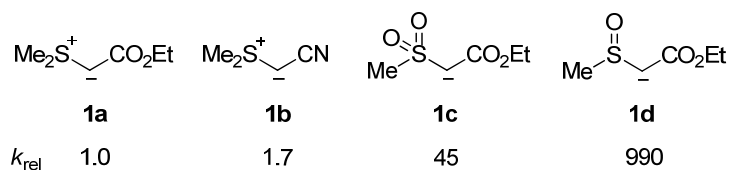
^a Nucleophilicity parameters N and s derived by using eq 1; determination see below. ^b Deprotonation of the conjugate CH acids (**1c,d**)-H with 0.5-0.6 equiv of KO^tBu.

3 Discussion

According to Table 2, the quinone methide **2f** is the only electrophile for which rate constants with all four nucleophiles **1a–d** have been determined. The corresponding rate constants can, therefore, be employed for a direct structure-reactivity analysis. As shown in Scheme 2, the

cyano-substituted sulfur ylide **1b** is marginally more reactive than the ethoxycarbonyl-substituted analog **1a**. However, the methylsulfonyl-stabilized carbanion **1c** is 45 times and the methylsulfinyl-stabilized carbanion **1d** 990 times more reactive than the ylide **1a**. Comparison of the two carbanions **1c,d** moreover shows that the methylsulfinyl-stabilized species **1d** is 22 times more reactive than the analogously substituted methylsulfonyl compound **1c**.

Scheme 2: Relative Reactivities of the Nucleophiles **1a–d** towards the Quinone Methide **2f** (DMSO, 20°C).



To include compounds **1a–d** in our comprehensive nucleophilicity scale, we determined their nucleophilicity parameters N and s . For that purpose, $\log k_2$ for the reactions of the nucleophiles **1** with the electrophiles **2** (Table 2) were plotted against their electrophilicity parameters E as shown in Figure 2. The linearity of the correlations shows the applicability of eq 1, which allows one to derive the nucleophile-specific parameters N and s for the nucleophiles **1a–d**, which are listed in Table 2 and Figure 3.

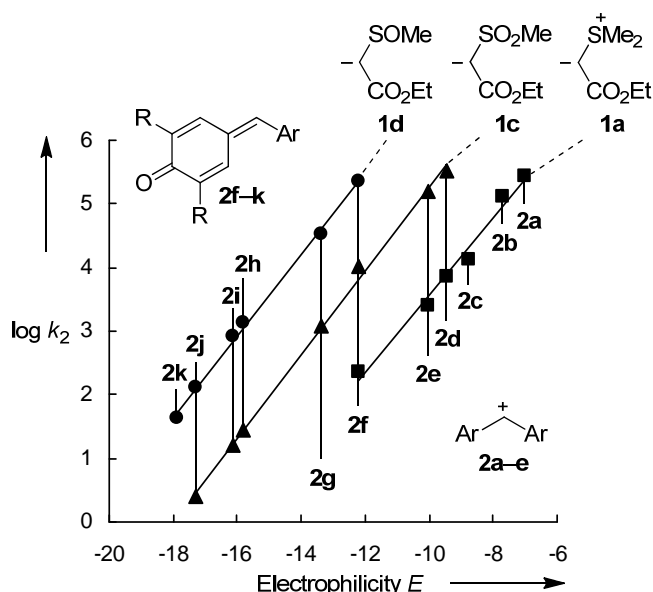


Figure 2: Plots of $\log k_2$ for the reactions of the sulfur ylide **1a** and the sulfur-stabilized carbanions **1c,d** with the reference electrophiles **2a–k** in DMSO at 20°C versus their electrophilicity parameters E . For the sake of clarity, the correlation line for **1b** is not shown (see the Experimental Section).

Among the many comparisons, which are now possible on the basis of N , we will restrict the following discussion on the comparison with the recently investigated phosphoryl-stabilized carbanions and phosphorus ylides (Figure 3).^[8c]

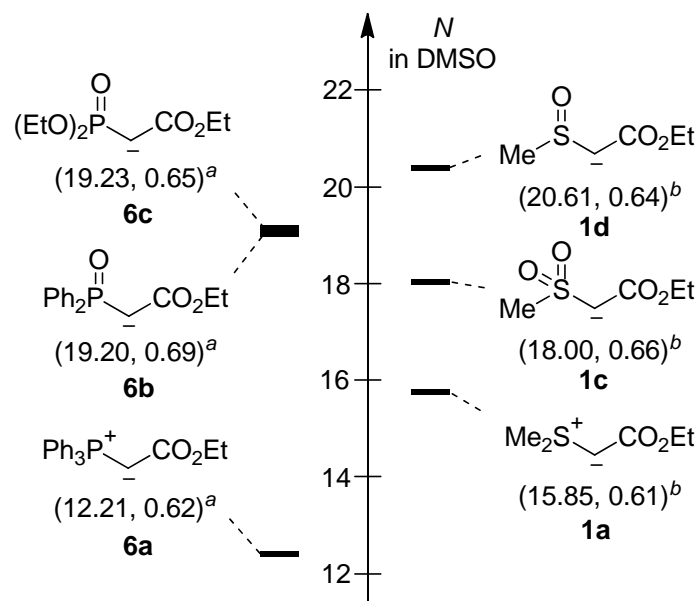


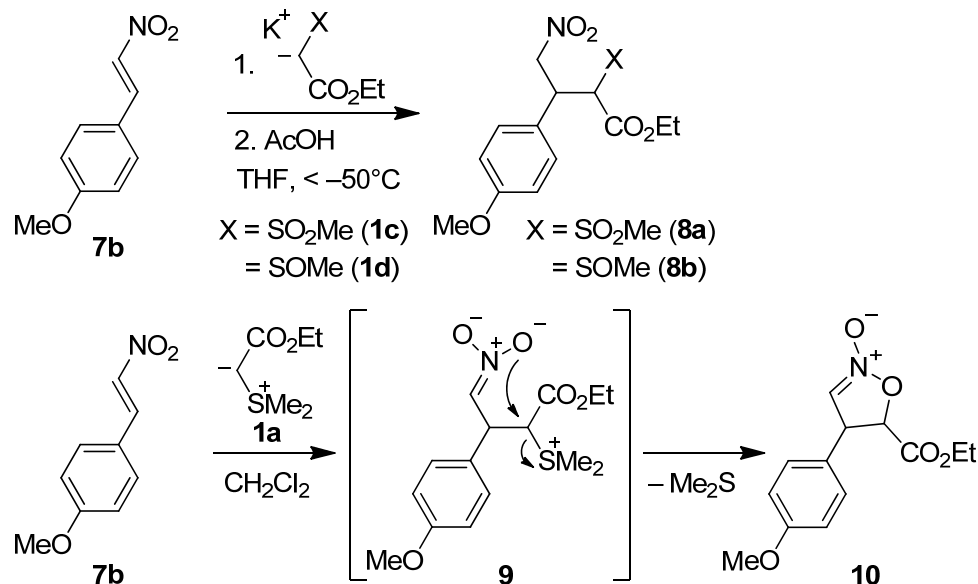
Figure 3: Comparison of the nucleophilicity parameters (N , s) in DMSO of the sulfur-stabilized nucleophiles **1a,c,d** with those of phosphorus ylide **6a** and phosphoryl-stabilized carbanions **6b,c**. ^a Values (N , s) taken from ref 8c. ^b Values (N , s) taken from Table 2.

Figure 3 reveals a difference of nucleophilic reactivity of $\Delta N \approx 3.6$ between the triphenylphosphonium ylide **6a** and the structurally analogous dimethylsulfonium ylide **1a**. For an s value of 0.62, this difference implies that the phosphorus ylide **6a** is 170 times less reactive than the sulfur ylide **1a**. On the other hand, the phosphoryl-stabilized carbanions **6b,c** show nucleophilic reactivities, which lie in between those of the sulfinyl- and sulfonyl-stabilized carbanions **1c,d**. From the nucleophilicities of diethyl malonate anions ($N = 20.22$), ethyl cyanoacetate anions ($N = 19.62$), and ethyl acetoacetate anions ($N = 18.82$),^[9c] one can derive that the ethoxycarbonyl-, cyano-, and acetyl groups have stabilizing abilities, which are also in between those of a methylsulfinyl and a methylsulfonyl group.

To examine the applicability of the N and s parameters of the sulfur-stabilized nucleophiles **1** for reactions with other electrophiles, we have investigated their reactions with *trans*- β -nitrostyrene (**7a**) and *trans*-4-methoxy- β -nitrostyrene (**7b**), whose electrophilicity parameters E have recently been determined.^[10] Whereas the reactions of the carbanions **1c,d** with nitrostyrene **7b** yield the Michael addition products **8a** and **8b**, respectively, the zwitterion **9** initially generated from the sulfur ylide **1a** and **7b**, underwent a subsequent intramolecular nucleophilic displacement of dimethylsulfide to yield the dihydroisoxazole N -oxide **10**

(Scheme 3). The latter compound was not isolated but intercepted by a 1,3-dipolar cycloaddition with dimethyl maleate according to previous reports^[11] and as specified in the Experimental Section.

Scheme 3: Reactions of the Nucleophiles **1a,c,d** with Nitroolefin **7b**.



In line with these mechanisms, the experimental second-order rate constants for the reactions of **1a,c,d** with the nitrostyrenes **7a,b** agree within a factor of 1.1 to 4.3 with those calculated by equation 1 (Table 3). This remarkable agreement demonstrates that rates of the reactions of the nucleophiles **1** with electrophiles of known electrophilicity E can be efficiently predicted by eq 1 using the N/s -parameters reported in Table 2.

Table 3: Experimental and Calculated Second-Order Rate Constants ($M^{-1} s^{-1}$) for the Reactions of the Nucleophiles **1a,c,d** with the Nitrostyrenes **7** in DMSO at 20°C.

Nucleophile	Electrophile	k_2^{exp}	$k_2^{\text{calcd } a}$	$k_2^{\text{exp}} / k_2^{\text{calcd}}$
1a	7b	5.46	5.03	1.1
1c	7a	1.25×10^2	5.48×10^2	0.23
	7b	3.98×10^1	1.51×10^2	0.26
1d	7a	1.21×10^4	2.12×10^4	0.57
	7b	3.48×10^3	6.06×10^3	0.57

^a Calculated by eq 1 using the electrophilicity parameters $E(\mathbf{7a}) = -13.85$ and $E(\mathbf{7b}) = -14.70$ (from ref 10) as well as the N and s values for **1a,c,d** (from Table 2).

As the formation of oxaphosphetanes from phosphorus ylides and carbonyl compounds generally proceeds via concerted [2+2] cycloaddition reactions,^[1a-d,12] the N and s parameters

of phosphorus ylides cannot be employed to determine the *E* parameters of aldehydes.^[8c] On the other hand, sulfur ylides have been demonstrated to react with aldehydes by a stepwise mechanism.^[13] It should, therefore, be possible to use the kinetics of the formation of epoxides via the Corey-Chaykovsky reaction to derive electrophilicity parameters of carbonyl compounds.

4 Experimental Section

4.1 General

Chemicals. The sulfur ylides **1a,b** were synthesized according to literature procedures^[14] as well as ethyl 2-(methylsulfinyl)acetate (**1d**)-H,^[15] and the nitrostyrenes **7a,b**.^[16] Benzhydrylium tetrafluoroborates^[9b] (**2a–e**)-BF₄ and quinone methides^[8a,17] **2f–k** were prepared as described before. All other chemicals were purchased from commercial sources and (if necessary) purified by recrystallization or distillation prior to use.

Analytcs. ¹H- and ¹³C-NMR spectra were recorded on *Varian* NMR-systems (300, 400, or 600 MHz) in CDCl₃ or DMSO-*d*₆ and the chemical shifts in ppm refer to TMS (δ_{H} 0.00, δ_{C} 0.00) in CDCl₃ or the solvent residual signal in DMSO-*d*₆ (δ_{H} 2.50, δ_{C} 39.43) as internal standard. The following abbreviations were used for chemical shift multiplicities: brs = broad singlet, s = singlet, d = doublet, t = triplet, q = quartet, m = multiplet. For reasons of simplicity, the ¹H-NMR signals of AA'BB'-spin systems of *p*-disubstituted aromatic rings were treated as doublets. NMR signal assignments are based on additional 2D-NMR experiments (COSY, NOESY, HSQC, and HMBC). Diastereomeric ratios (*dr*) were determined by ¹H-NMR. (HR-)MS has been performed on a *Finnigan MAT 95* (EI) or a *Thermo Finnigan LTQ FT* (ESI) mass spectrometer. An *Elementar Vario Micro Cube* device was used for elemental analysis. Melting points were determined on a *Büchi B-540* device and are not corrected.

Kinetics. The rates of all investigated reactions were determined photometrically. The temperature of the solutions was kept constant (20.0 ± 0.1°C) during all kinetic studies by using a circulating bath thermostat. The kinetic experiments with ylides **1a,b** were carried out with freshly prepared stock solutions of the ylides in DMSO. If not mentioned otherwise, stock solutions of the carbanions **1c,d** were prepared by deprotonation of the CH acids (**1c,d**)-H with 1.00-1.05 eq of KO^tBu in DMSO. The electrophiles **2** and **7** (also prepared as stock

solutions in DMSO) were always employed as minor component in the reactions with the nucleophiles resulting in first-order kinetics.

The rates of slow reactions ($\tau_{1/2} > 15\text{-}20$ s) were determined by using a J&M TIDAS diode array spectrophotometer controlled by Labcontrol Spectacle software and connected to a Hellma 661.502-QX quartz Suprasil immersion probe (5 mm light path) via fiber optic cables and standard SMA connectors.

For the evaluation of fast kinetics ($\tau_{1/2} < 15\text{-}20$ s) the stopped-flow spectrophotometer systems Hi-Tech SF-61DX2 or Applied Photophysics SX.18MV-R were used.

Rate constants k_{obs} (s^{-1}) were obtained by fitting the single exponential $A_t = A_0 \exp(-k_{\text{obs}}t) + C$ (exponential decrease) to the observed time-dependent absorbance (averaged from at least 3 kinetic runs for each nucleophile concentration in case of stopped-flow method). Second-order rate constants k_2 ($\text{L mol}^{-1} \text{s}^{-1}$) were derived from the slopes of the linear correlations of k_{obs} (s^{-1}) with the concentration of the nucleophiles used in excess ($[\text{Nu}]_0$).

4.2 Product Studies

4.2.1 Reactions of the Ylides **1a,b** and the Carbanions **1c,d** with the Reference Electrophiles **2a,h**

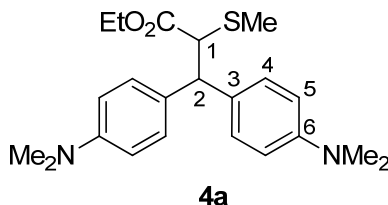
Reactions of the sulfur ylides **1a,b** with the reference electrophile **2a**

General procedure A. Reactions of the ylides **1a,b** with electrophile the **2a** were carried out by dissolving the ylides **1a** or **1b** and the electrophile **2a**-BF₄ in dry DMSO (2-3 mL) at room temperature. The resulting mixture was stirred until complete decolorization occurred (< 1 min) and subsequently treated with a mixture of thiophenol (50 μL , 0.49 mmol) and KO^tBu (37.3 mg, 332 μmol) in dry DMSO (2-3 mL). After 10 min of additional stirring, the reaction was quenched by the addition of water and extracted with CH₂Cl₂. The combined organic layers were washed with water and brine, dried over Na₂SO₄ and evaporated under reduced pressure. The crude products were purified by column chromatography on silica gel (*n*-pentane/EtOAc). Small samples of solid products were recrystallized in appropriate solvent mixtures for the determination of melting points.

Ethyl 3,3-Bis(4-(dimethylamino)phenyl)-2-(methylthio)propanoate (4a) was obtained from ethyl (dimethyl- λ^4 -sulfanylidene)acetate (**1a**, 42.0 mg, 283 μmol) and benzhydrylium

tetrafluoroborate **2a**-BF₄ (94.2 mg, 277 μmol) as a pale yellow solid (95 mg, 0.25 mmol, 90 %).

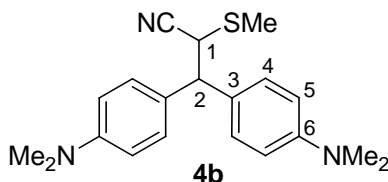
RAP 20.1



R_f (*n*-pentane/EtOAc 4:1, *v/v*): 0.31. Mp. (*n*-pentane/Et₂O): 122-123°C. ¹H-NMR (CDCl₃, 300 MHz): δ = 1.07 (t, 3 H, *J* = 7.1 Hz, OCH₂CH₃), 2.08 (s, 3 H, SCH₃), 2.85 (s, 6 H, N(CH₃)₂), 2.89 (s, 6 H, N(CH₃)₂), 3.96 (d, 1 H, *J* = 12.2 Hz, 1-H), 3.98-4.06 (m, 2 H, OCH₂CH₃), 4.16 (d, 1 H, *J* = 12.2 Hz, 2-H), 6.61 (d, 2 H, *J* = 8.8 Hz, 5-H), 6.66 (d, 2 H, *J* = 8.8 Hz, 5-H), 7.14-7.19 (m, 4 H, 4-H). ¹³C-NMR (CDCl₃, 75.5 MHz): δ = 14.02 (q, SCH₃), 14.04 (q, OCH₂CH₃), 40.6 (q, N(CH₃)₂), 40.7 (q, N(CH₃)₂), 50.3 (d, C-2), 52.5 (d, C-1), 60.7 (t, OCH₂CH₃), 112.6 (d, C-5), 112.8 (d, C-5), 128.1 (d, C-4), 128.5 (d, C-4), 129.8 (s, C-3), 130.9 (s, C-3), 149.2 (s, C-6), 149.3 (s, C-6), 171.5 (s, CO). MS (EI): *m/e* (%) = 386 (1) [M]⁺, 266 (5), 254 (17), 253 (100), 237 (9). HR-MS (EI) [M]⁺: calcd for [C₂₂H₃₀N₂O₂S]⁺: 386.2022, found 386.2025. Anal calcd for C₂₂H₃₀N₂O₂S (386.55): C 68.36, H 7.82, N 7.25, S 8.30, found C 68.31, H 7.66, N 7.33, S 8.69.

3,3-Bis(4-(dimethylamino)phenyl)-2-(methylthio)propanenitrile (4b) was obtained from (dimethyl-λ⁴-sulfanylidene)-acetonitrile (**1b**, 29.0 mg, 287 μmol) and benzhydrylium tetrafluoroborate **2a**-BF₄ (94.2 mg, 277 μmol) as yellow oil (88 mg, 0.26 mmol, 94 %).

RAP 21.1



R_f (*n*-pentane/EtOAc 4:1, *v/v*): 0.25. ¹H-NMR (CDCl₃, 300 MHz): δ = 2.24 (s, 3 H, SCH₃), 2.90 (s, 12 H, 2 × N(CH₃)₂), 4.10-4.17 (m, 2 H, 1-H, 2-H), 6.65-6.69 (m, 4 H, 5-H), 7.14 (d, 2 H, *J* = 8.8 Hz, 4-H), 7.23 (d, 2 H, *J* = 8.8 Hz, 4-H). ¹³C-NMR (CDCl₃, 75.5 MHz): δ = 15.0 (q, SCH₃), 40.45 (q, N(CH₃)₂), 40.47 (q, N(CH₃)₂), 40.52 (d, C-1), 51.5 (d, C-2), 112.4 (d, C-5), 112.5 (d, C-5), 118.5 (s, CN), 127.8 (s, C-3), 128.1 (s, C-3), 128.4 (d, C-4), 128.7 (d, C-4),

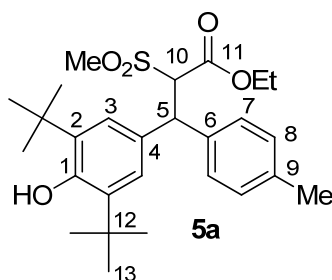
149.6 (s, C-6), 149.7 (s, C-6). MS (EI): m/e (%) = 339 (<1) $[M]^+$, 254 (19), 253 (100), 237 (12), 126 (8). HR-MS (EI) $[M]^+$: calcd for $[C_{20}H_{25}N_3S]^+$: 339.1764, found 339.1765.

Reactions of the carbanions **1c,d** with the reference electrophile **2h**

General procedure B. Reactions of the nucleophiles **1c,d** with the electrophile **2h** were carried out by dissolving the corresponding CH acid (**1c,d**)-H with KO t Bu in dry DMSO (5 mL). After 2 min, a solution of the electrophile **2h** in DMSO (3 mL) was added and the resulting mixture was stirred for additional 5 min. The reaction was quenched by the addition of 1 % aqueous acetic acid solution (30 mL). After extraction with CH₂Cl₂, the combined organic layers were washed with water and brine, dried over Na₂SO₄ and evaporated under reduced pressure. The crude products were purified by column chromatography on silica gel (*n*-pentane/EtOAc).

Ethyl 3-(3,5-di-*tert*-butyl-4-hydroxyphenyl)-2-(methylsulfonyl)-3-*p*-tolylpropanoate (5a) was obtained from ethyl 2-(methylsulfonyl)acetate **1c**-H (90.0 mg, 542 μ mol), KO t Bu (57.0 mg, 508 μ mol), and quinone methide **2h** (150 mg, 486 μ mol) as colorless solid (218 mg, 459 μ mol, 94 %, *dr* ~ 1 : 1.4).

RAP 25.1



¹H-NMR (CDCl₃, 599 MHz): δ = 0.91* (t, 3 H, J = 7.1 Hz, OCH₂CH₃), 1.00[#] (t, 3 H, J = 7.1 Hz, OCH₂CH₃), 1.39, 1.40 (2s, 2 \times 18 H, 2 \times 13-H), 2.22[#] (s, 3 H, SO₂CH₃), 2.28[#] (s, 3 H, Ar-CH₃), 2.30* (s, 3 H, Ar-CH₃), 2.45* (s, 3 H, SO₂CH₃), 3.95-4.08 (m, 2 \times 2 H, 2 \times OCH₂CH₃), 4.64* (d, 1 H, J = 11.9 Hz, 5-H), 4.68-4.72[#] (m, 2 H, 5-H, 10-H), 4.75* (d, 1 H, J = 11.9 Hz, 10-H), 5.09* (s, 1 H, OH), 5.18[#] (s, 1 H, OH), 7.09[#] (d, 2 H, J = 7.9 Hz, 8-H), 7.11* (s, 2 H, 3-H), 7.15* (d, 2 H, J = 7.9 Hz, 8-H), 7.25-7.26[#] (m, 4 H, 3-H, 7-H, superimposed by CDCl₃ residual signal), 7.35* (d, 2 H, J = 8.1 Hz, 7-H). ¹³C-NMR (CDCl₃, 151 MHz): δ = 13.5* (q, OCH₂CH₃), 13.6[#] (q, OCH₂CH₃), 21.0[#] (q, Ar-CH₃), 21.1[#] (q, Ar-

CH₃), 30.2* (q, C-13), 30.3[#] (q, C-13), 34.3* (s, C-12), 34.4[#] (s, C-12), 41.8* (q, SO₂CH₃), 42.2[#] (q, SO₂CH₃), 50.9[#] (d, C-5), 51.0* (d, C-5), 62.1* (t, OCH₂CH₃), 62.3[#] (t, OCH₂CH₃), 75.1* (d, C-10), 75.4[#] (d, C-10), 124.3* (d, C-3), 125.1[#] (d, C-3), 127.6[#] (d, C-7), 128.1* (d, C-7), 129.5[#] (d, C-8), 129.81* (d, C-8), 129.83[#] (s, C-4), 130.8* (s, C-4), 136.0* (s, C-2), 136.7[#] (s, C-2), 136.9[#] (s, C-9), 137.1* (s, C-6), 137.4* (s, C-9), 137.5[#] (s, C-6), 152.9* (s, C-1), 153.3[#] (s, C-1), 164.5[#] (s, C-11), 164.8* (s, C-11). HR-MS (ESI⁻) [M-H]⁻: calc. for [C₂₇H₃₈O₅S]⁻: 473.2367; found 473.2396.

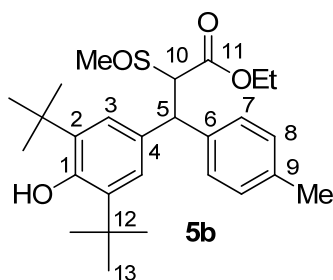
* signal can be assigned to major isomer

[#] signal can be assigned to minor isomer

Ethyl 3-(3,5-di-*tert*-butyl-4-hydroxyphenyl)-2-(methylsulfinyl)-3-*p*-tolylpropanoate (**5b**)

was obtained from ethyl 2-(methylsulfinyl)acetate **1d**-H (82.0 mg, 546 μmol), KO^tBu (57.0 mg, 508 μmol), and quinone methide **2h** (150 mg, 486 μmol) as colorless solid (214 mg, 467 μmol, 96 %, complex mixture of 4 diastereomers, *dr* ~ 1 : 2.0 : 3.8 : 6.0).

RAP 29.1



¹H-NMR (CDCl₃, 599 MHz): δ = 0.92* (t, 3 H, *J* = 7.1 Hz, OCH₂CH₃), 1.00-1.03 (m, 2 × 3 H, OCH₂CH₃), 1.08 (t, 3 H, *J* = 7.1 Hz, OCH₂CH₃), 1.38, 1.390, 1.394*, 1.40 (4s, 4 × 18 H, 13-H), 2.275, 2.280, 2.30 (3s, 4 × 3 H, Ar-CH₃, signal of one diastereomer superimposed), 2.45, 2.52*, 2.63, 2.64 (4s, 4 × 3 H, SOCH₃), 3.93-4.25 (m, 4 × 2 H, 4 × OCH₂CH₃, 4 × 1 H, 2 × 10-H, 2 × 5-H), 4.66-4.69 (m, 2 × 1 H, 2 × 5-H), 4.77-4.81 (m, 2 × 1 H, 2 × 10-H), 5.07, 5.08, 5.13 (3brs, 4 × 1 H, 4 × OH, signal of one diastereomer superimposed), 7.07-7.14 (m, 8 × 2 H, 4 × 3-H, 4 × 8-H), 7.19 (d, 2 H, *J* = 8.1 Hz, 7-H), 7.23-7.24 (m, 2 × 2 H, 2 × 7-H), 7.28* (d, 2 H, *J* = 8.1 Hz, 7-H). ¹³C-NMR (CDCl₃, 151 MHz): δ = 13.85*, 13.99, 14.02, 14.09 (4q, 4 × OCH₂CH₃), 20.98, 20.99, 21.04, 21.07* (4q, 4 × Ar-CH₃), 30.21, 30.26, 30.27 (3q, 4 × C-13, signal of one diastereomer superimposed), 30.05, 33.11 (2q, 2 × SOCH₃), 34.34, 34.35, 34.37, 34.40 (4s, 4 × C-12), 37.32*, 37.76 (2q, 2 × SOCH₃), 48.49*, 48.69, 49.64, 49.77 (4d, 4 × C-5), 61.36*, 61.53, 61.55, 61.68 (4t, 4 × OCH₂CH₃), 69.25, 69.28, 71.10*, 71.76 (4d,

4 × C-10), 123.99, 124.16*, 124.42, 124.80 (4d, 4 × C-3), 127.34, 127.45, 127.71, 128.12* (4d, 4 × C-7), 129.31, 129.43, 129.65 (3d, 3 × C-8), 129.71 (d and/or s, 1 × C-4 and/or 1 × C-8, assignment not possible, C-4 or C-8 signal of one diastereomer superimposed), 130.31, 131.41, 131.92 (3s, 3 × C-4), 135.90, 135.97, 136.22, 136.33, 136.42, 136.43, 136.72, 137.02, 137.15, 137.52, 138.28, 138.68 (12s, 4 × C-2, 4 × C-6, 4 × C-9), 152.66*, 152.80, 153.03, 153.08 (4s, 4 × C-1), 165.85*, 166.03, 167.13, 167.18 (4s, 4 × C-11). HR-MS (ESI⁺) [M+H]⁺: calcd for [C₂₇H₃₉O₄S]⁺: 459.2563; found 459.2549.

* signal can be assigned to major isomer

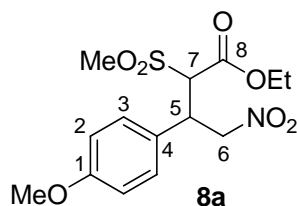
4.2.2 Reactions of the Carbanions **1c,d** and the Ylide **1a** with the Nitrostyrene **7b**

Reactions of the carbanions **1c,d** with nitrostyrene **7b**

General procedure C. Reactions of the nucleophiles **1c,d** with the electrophile **7b** were carried out by dissolving the corresponding CH acid (**1c,d**)-H with KO^tBu in dry THF (4 mL). The resulting mixture was cooled down to -78°C and a solution of electrophile **7b** in dry THF (4-5 mL) was added dropwise. After 3 h of stirring at a temperature below -50°C, the mixture was again cooled down to -78°C and treated with concentrated acetic acid (0.1 mL). The resulting solution was allowed to warm to room temperature. After evaporation of the THF under reduced pressure, the residue was dissolved in CH₂Cl₂ (30-50 mL), washed with water and brine, dried over Na₂SO₄ and again evaporated under reduced pressure. The crude products were purified by column chromatography on silica gel (CH₂Cl₂/EtOAc).

Ethyl 3-(4-methoxyphenyl)-2-(methylsulfonyl)-4-nitrobutanoate (8a) was obtained from ethyl 2-(methylsulfonyl)acetate **1c**-H (130 mg, 782 μmol), KO^tBu (92.0 mg, 820 μmol), and nitrostyrene **7b** (200 mg, 1.12 mmol) as colorless oil after column chromatography (165 mg, 478 μmol, 61 %, *dr* ~ 1 : 1.7). Recrystallization from *n*-pentane/EtOAc yielded a colorless solid still composed of two diastereomers (102 mg, 295 μmol, 38 %, *dr* ~ 1 : 1.9).

RAP 54.7

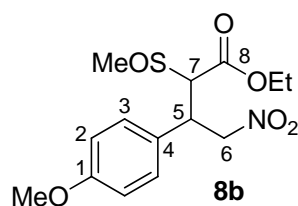


$^1\text{H-NMR}$ (CDCl_3 , 599 MHz): $\delta = 1.00^*$ (t, 3 H, $J = 7.1$ Hz, OCH_2CH_3), $1.33^\#$ (t, 3 H, $J = 7.2$ Hz, OCH_2CH_3), $2.82^\#$ (s, 3 H, SO_2CH_3), 3.11^* (s, 3 H, SO_2CH_3), 3.78^* (s, 3 H, OCH_3), 3.79^* (s, 3 H, OCH_3), $3.96\text{-}4.04^*$ (m, 2 H, OCH_2CH_3), $4.20\text{-}4.27$ (m, 3 H, 5-H * , 7-H * , 7-H $^\#$), $4.29\text{-}4.38^\#$ (m, 2 H, OCH_2CH_3), $4.47^\#$ (ddd, 1 H, $J = 10.3, 6.3, 3.9$ Hz, 5-H), $4.79\text{-}4.83^*$ (m, 1 H, 6-H), $5.01^\#$ (dd, 1 H, $J = 13.7, 3.9$ Hz, 6-H), $5.19^\#$ (dd, 1 H, $J = 13.7, 10.5$ Hz, 6-H'), 5.26^* (dd, 1 H, $J = 13.6, 4.1$ Hz, 6-H'), 6.85^* (d, 2 H, $J = 8.8$ Hz, 2-H), $6.89^\#$ (d, 2 H, $J = 8.8$ Hz, 2-H), 7.15^* (d, 2 H, $J = 8.8$ Hz, 3-H), $7.24^\#$ (d, 2 H, $J = 8.7$ Hz, 3-H). $^{13}\text{C-NMR}$ (CDCl_3 , 151 MHz): $\delta = 13.6^*$ (q, OCH_2CH_3), $14.0^\#$ (q, OCH_2CH_3), 39.4^* (q, SO_2CH_3), $40.5^\#$ (d, C-5), 41.9^* (d, C-5), $42.3^\#$ (q, SO_2CH_3), 55.3 (q, OCH_3 , same chemical shift of signal for both diastereomers), 62.8^* (t, OCH_2CH_3), $63.3^\#$ (t, OCH_2CH_3), 71.5^* (d, C-7), $71.9^\#$ (d, C-7), $76.2^\#$ (t, C-6), 77.6^* (t, C-6), 114.6^* (d, C-2), $114.8^\#$ (d, C-2), 126.1^* (s, C-4), $126.8^\#$ (s, C-4), $129.3^\#$ (d, C-3), 129.5^* (d, C-3), $159.9^\#$ (s, C-1), 160.0^* (s, C-1), $164.3^\#$ (s, C-8), 164.8^* (s, C-8). MS (EI): m/e (%) = 345 (1) $[\text{M}]^+$, 284 (12), 239 (13), 205 (13), 204 (38), 179 (28), 159 (10), 139 (27), 133 (19), 132 (100), 121 (11), 121 (30), 117 (13), 90 (10), 89 (19), 79 (24), 77 (15), 63 (11), 44 (18), 43 (10), 42 (12). HR-MS (EI) $[\text{M}]^+$: calcd for $[\text{C}_{14}\text{H}_{19}\text{NO}_7\text{S}]^+$: 345.0877, found 345.0885. HR-MS (ESI $^-$) $[\text{M-H}]^-$: calcd for $[\text{C}_{14}\text{H}_{18}\text{NO}_7\text{S}]^-$: 344.0810; found 344.0805. Anal calcd for $\text{C}_{14}\text{H}_{19}\text{NO}_7\text{S}$ (345.37): C 48.69, H 5.55, N 4.06, S 9.28, found C 48.57, H 5.52, N 4.03, S 9.49.

* signal can be assigned to major isomer

$^\#$ signal can be assigned to minor isomer

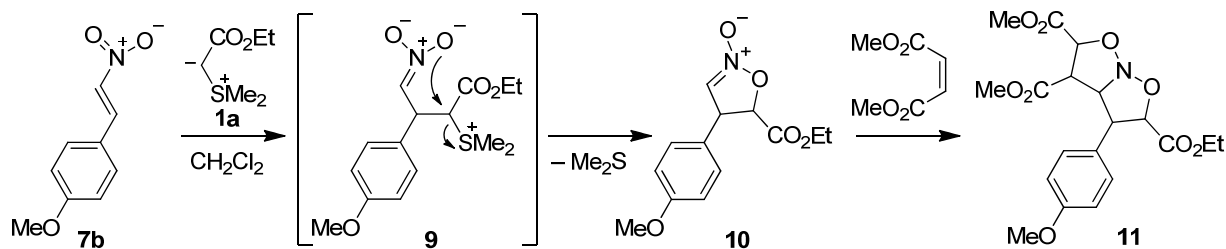
Ethyl 3-(4-methoxyphenyl)-2-(methylsulfinyl)-4-nitrobutanoate (8b) was obtained from ethyl 2-(methylsulfinyl)acetate **1d-H** (120 mg, 799 μmol), $\text{KO}t\text{Bu}$ (94.1 mg, 839 μmol), and nitrostyrene **7b** (200 mg, 1.12 mmol) as colorless oil after column chromatography (161 mg, 489 μmol , 61 %, complex mixture of 4 diastereomers, *d.r.* $\sim 1 : 1.1 : 1.2 : 2.5$). A colorless solid was obtained by recrystallization from *n*-pentane/EtOAc (53 mg, 0.16 mmol, 20 %, only major diastereomer).*



Mp. (*n*-pentane/EtOAc): 136-137°C. ¹H-NMR (CDCl₃, 599 MHz): δ = 1.38 (t, 3 H, *J* = 7.1 Hz, OCH₂CH₃), 2.59 (s, 3 H, SOCH₃), 3.68 (d, 1 H, *J* = 10.9 Hz, 7-H), 3.79 (s, 3 H, OMe), 4.25 (ddd, 1 H, *J* = 11.2, 9.1, 4.1 Hz, 5-H), 4.36-4.42 (m, 2 H, OCH₂CH₃), 4.79 (dd, 1 H, *J* = 12.8, 4.1 Hz, 6-H), 4.88 (dd, 1 H, *J* = 12.8, 8.9 Hz, 6-H), 6.89 (d, 2 H, *J* = 8.6 Hz, 2-H), 7.19 (d, 2 H, *J* = 8.6 Hz, 3-H). ¹³C-NMR (CDCl₃, 151 MHz): δ = 14.4 (q, OCH₂CH₃), 37.9 (q, SOCH₃), 41.8 (d, C-5), 55.3 (q, OMe), 62.5 (t, OCH₂CH₃), 68.2 (d, C-7), 78.2 (t, C-6), 114.8 (d, C-2), 126.8 (s, C-4), 129.3 (d, C-3), 159.9 (s, C-1), 165.1 (s, C-8). MS (EI): *m/e* (%) = 329 (<1) [M]⁺, 220 (17), 219 (18), 205 (47), 191 (18), 179 (60), 177 (16), 147 (22), 134 (18), 133 (25), 132 (100), 121 (21), 118 (18), 117 (17), 105 (27), 90 (15), 89 (24), 88 (51), 77 (26), 64 (20), 63 (32), 59 (19). HR-MS (EI) [M]⁺: calcd for [C₁₄H₁₉NO₆S]⁺: 329.0928, found 329.0942. HR-MS (ESI⁺) [M+H]⁺: calcd for [C₁₄H₂₀NO₆S]⁺: 330.1006, found 330.1005.

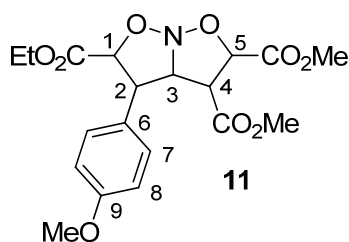
* only NMR signals for major diastereomers given

Reaction of the sulfur ylide 1a with the nitrostyrene 7b



5-Ethyl 2,3-dimethyl 4-(4-methoxyphenyl)tetrahydro-2*H*-isoxazolo[2,3-*b*]isoxazole-2,3,5-tricarboxylate (11). To a stirred solution of ethyl (dimethyl-λ⁴-sulfanylidene)acetate **1a** (65.2 mg, 440 μmol) in CH₂Cl₂ (2 mL) was added dropwise a solution of nitrostyrene **7b** (75.0 mg, 419 μmol) in CH₂Cl₂ (2 mL) and subsequently dimethyl maleate (0.15 mL, 0.90 mmol). After 17 h of stirring at room temperature, the resulting dark red reaction mixture was evaporated under reduced pressure. Purification of the crude product by column chromatography (silica gel, *n*-pentane/EtOAc 3:1 → 2:1) furnished **11** as a colorless oil (21 mg, 51 μmol, 12 %, one diastereomer).

RAP 55.2



R_f (*n*-pentane/EtOAc 2:1, *v/v*): 0.22. ¹H-NMR (DMSO-*d*₆, 400 MHz): δ = 1.17 (t, 3 H, *J* = 7.1 Hz, OCH₂CH₃), 3.57 (s, 3 H, CO₂Me), 3.66 (s, 3 H, CO₂Me), 3.75 (s, 3 H, Ar-OMe), 4.03 (dd, 1 H, *J* = 8.4, 3.4 Hz, 4-H), 4.07-4.16 (m, 3 H, OCH₂CH₃, 2-H), 4.19 (dd, 1 H, *J* = 4.9, 3.5 Hz, 3-H), 4.68 (d, 1 H, *J* = 5.8 Hz, 1-H), 5.29 (d, 1 H, *J* = 8.4 Hz, 5-H), 6.94 (d, 2 H, *J* = 8.8 Hz, 8-H), 7.31 (d, 2 H, *J* = 8.8 Hz, 7-H). ¹³C-NMR (DMSO-*d*₆, 101 MHz): δ = 13.8 (q, OCH₂CH₃), 52.0 (d, C-4), 52.17 (q, CO₂Me), 52.24 (d, C-2), 52.4 (q, CO₂Me), 55.0 (q, Ar-OMe), 61.1 (t, OCH₂CH₃), 77.5 (d, C-5), 79.8 (d, C-3), 83.8 (d, C-1), 114.3 (d, C-8), 128.7 (d, C-7), 131.1 (s, C-6), 158.6 (s, C-9), 168.0 (s, CO from CO₂Me), 169.1 (s, CO from CO₂Et), 169.4 (s, CO from CO₂Me). HR-MS (ESI⁺) [M+H]⁺: calcd for [C₁₉H₂₄NO₉]⁺: 410.1446, found 410.1445.

4.3 Kinetics

4.3.1 Reactions of the Ylides 1a,b and the Carbanions 1c,d with the Reference Electrophiles 2a–k

Table 4: Kinetics of the reaction of **1a** with **2a** in DMSO at 20°C (stopped-flow UV-Vis spectrometer, λ = 613 nm).

No.	[E] ₀ / mol L ⁻¹	[Nu] ₀ / mol L ⁻¹	<i>k</i> _{obs} / s ⁻¹
nfh 36-1	1.26 × 10 ⁻⁵	1.31 × 10 ⁻⁴	4.74 × 10 ¹
nfh 36-2	1.26 × 10 ⁻⁵	1.69 × 10 ⁻⁴	5.68 × 10 ¹
nfh 36-3	1.26 × 10 ⁻⁵	2.06 × 10 ⁻⁴	6.69 × 10 ¹
nfh 36-4	1.26 × 10 ⁻⁵	2.44 × 10 ⁻⁴	7.67 × 10 ¹
nfh 36-5	1.26 × 10 ⁻⁵	2.81 × 10 ⁻⁴	8.80 × 10 ¹

$k_2 = 2.70 \times 10^5 \text{ L mol}^{-1} \text{ s}^{-1}$

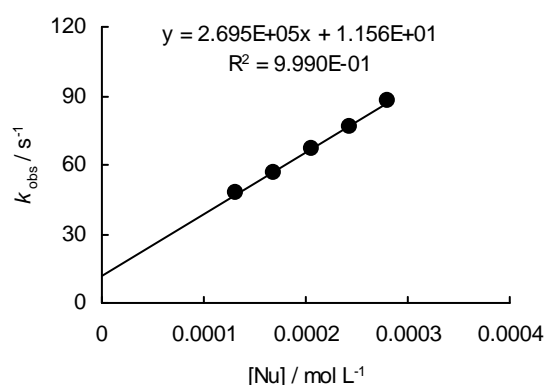
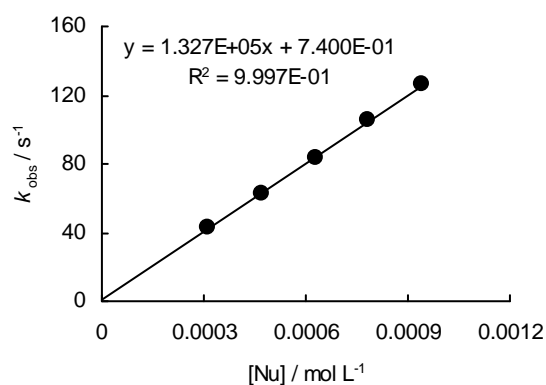


Table 5: Kinetics of the reaction of **1a** with **2b** in DMSO at 20°C (stopped-flow UV-Vis spectrometer, $\lambda = 624$ nm).

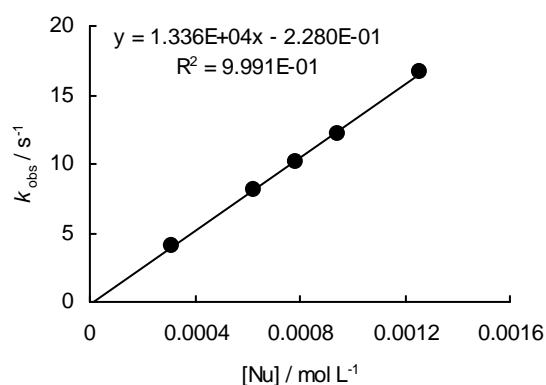
No.	$[E]_0 / \text{mol L}^{-1}$	$[\text{Nu}]_0 / \text{mol L}^{-1}$	$k_{\text{obs}} / \text{s}^{-1}$
nfh 15-1	2.23×10^{-5}	3.14×10^{-4}	4.31×10^1
nfh 15-4	2.23×10^{-5}	4.71×10^{-4}	6.26×10^1
nfh 15-2	2.23×10^{-5}	6.27×10^{-4}	8.34×10^1
nfh 15-5	2.23×10^{-5}	7.84×10^{-4}	1.05×10^2
nfh 15-3	2.23×10^{-5}	9.41×10^{-4}	1.26×10^2

$k_2 = 1.33 \times 10^5 \text{ L mol}^{-1} \text{ s}^{-1}$

**Table 6:** Kinetics of the reaction of **1a** with **2c** in DMSO at 20°C (stopped-flow UV-Vis spectrometer, $\lambda = 624$ nm).

No.	$[E]_0 / \text{mol L}^{-1}$	$[\text{Nu}]_0 / \text{mol L}^{-1}$	$k_{\text{obs}} / \text{s}^{-1}$
nfh 14-1	2.19×10^{-5}	3.14×10^{-4}	4.11
nfh 14-2	2.19×10^{-5}	6.27×10^{-4}	8.05
nfh 14-5	2.19×10^{-5}	7.84×10^{-4}	1.02×10^1
nfh 14-3	2.19×10^{-5}	9.41×10^{-4}	1.22×10^1
nfh 14-4	2.19×10^{-5}	1.26×10^{-3}	1.67×10^1

$k_2 = 1.34 \times 10^4 \text{ L mol}^{-1} \text{ s}^{-1}$

**Table 7:** Kinetics of the reaction of **1a** with **2d** in DMSO at 20°C (stopped-flow UV-Vis spectrometer, $\lambda = 632$ nm).

No.	$[E]_0 / \text{mol L}^{-1}$	$[\text{Nu}]_0 / \text{mol L}^{-1}$	$k_{\text{obs}} / \text{s}^{-1}$
nfh 13-1	1.01×10^{-5}	2.01×10^{-4}	1.21
nfh 13-2	1.01×10^{-5}	6.03×10^{-4}	4.23
nfh 13-3	1.01×10^{-5}	1.01×10^{-3}	7.15
nfh 13-4	1.01×10^{-5}	1.41×10^{-3}	1.00×10^1
nfh 13-5	1.01×10^{-5}	1.81×10^{-3}	1.30×10^1

$k_2 = 7.30 \times 10^3 \text{ L mol}^{-1} \text{ s}^{-1}$

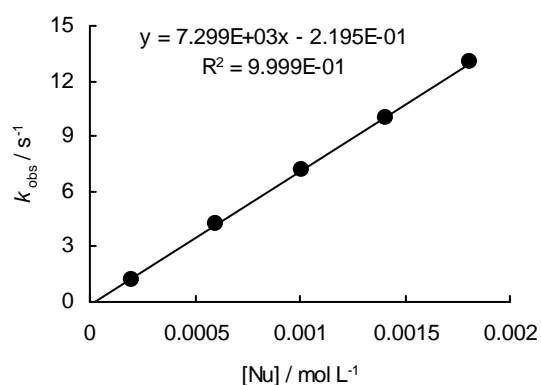
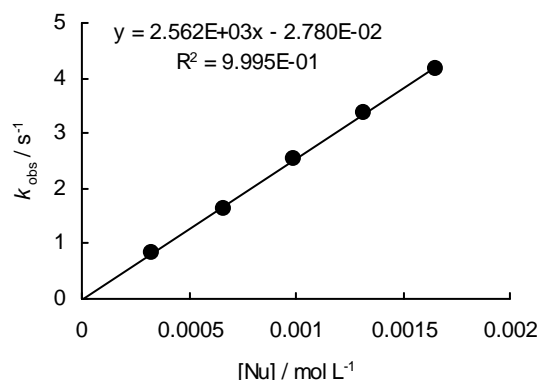


Table 8: Kinetics of the reaction of **1a** with **2e** in DMSO at 20°C (stopped-flow UV-Vis spectrometer, $\lambda = 632$ nm).

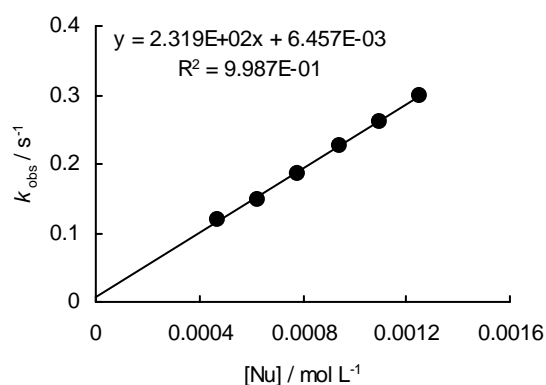
No.	$[E]_0 / \text{mol L}^{-1}$	$[\text{Nu}]_0 / \text{mol L}^{-1}$	$k_{\text{obs}} / \text{s}^{-1}$
nfh 12-1	1.18×10^{-5}	3.30×10^{-4}	8.29×10^{-1}
nfh 12-2	1.18×10^{-5}	6.60×10^{-4}	1.62
nfh 12-3	1.18×10^{-5}	9.90×10^{-4}	2.54
nfh 12-4	1.18×10^{-5}	1.32×10^{-3}	3.37
nfh 12-5	1.18×10^{-5}	1.65×10^{-3}	4.18

$k_2 = 2.56 \times 10^3 \text{ L mol}^{-1} \text{ s}^{-1}$

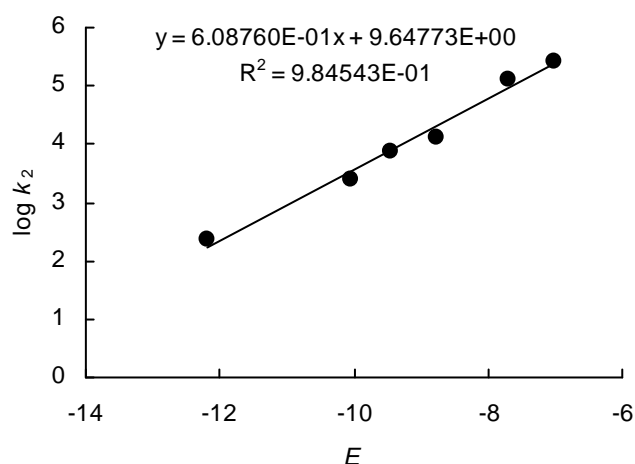
**Table 9:** Kinetics of the reaction of **1a** with **2f** in DMSO at 20°C (stopped-flow UV-Vis spectrometer, $\lambda = 422$ nm).

No.	$[E]_0 / \text{mol L}^{-1}$	$[\text{Nu}]_0 / \text{mol L}^{-1}$	$k_{\text{obs}} / \text{s}^{-1}$
nfh 20-6	3.79×10^{-5}	4.71×10^{-4}	1.19×10^{-1}
nfh 20-1	3.79×10^{-5}	6.27×10^{-4}	1.49×10^{-1}
nfh 20-2	3.79×10^{-5}	7.84×10^{-4}	1.86×10^{-1}
nfh 20-3	3.79×10^{-5}	9.41×10^{-4}	2.26×10^{-1}
nfh 20-4	3.79×10^{-5}	1.10×10^{-3}	2.60×10^{-1}
nfh 20-5	3.79×10^{-5}	1.25×10^{-3}	2.99×10^{-1}

$k_2 = 2.32 \times 10^2 \text{ L mol}^{-1} \text{ s}^{-1}$



Determination of the N -Parameter for **1a**
 (Correlation of $\log k_2$ for the Reactions of **1a** with **2a-f**
 Versus the Electrophilicity Parameters E for **2a-f**)



$$N = 15.85$$

$$s = 0.61$$

Kinetic investigations of the reactions of the ylide **1b** with the reference electrophiles **2a–f** in DMSO

Table 10: Kinetics of the reaction of **1b** with **2a** in DMSO at 20°C (stopped-flow UV-Vis spectrometer, $\lambda = 613$ nm).

No.	$[E]_0 / \text{mol L}^{-1}$	$[\text{Nu}]_0 / \text{mol L}^{-1}$	$k_{\text{obs}} / \text{s}^{-1}$
RAK 15.5-1	1.75×10^{-5}	1.86×10^{-4}	7.68×10^1
RAK 15.5-2	1.75×10^{-5}	2.54×10^{-4}	1.02×10^2
RAK 15.5-3	1.75×10^{-5}	3.22×10^{-4}	1.24×10^2
RAK 15.5-4	1.75×10^{-5}	3.90×10^{-4}	1.47×10^2
RAK 15.5-5	1.75×10^{-5}	4.58×10^{-4}	1.72×10^2
$k_2 = 3.47 \times 10^5 \text{ L mol}^{-1} \text{ s}^{-1}$			

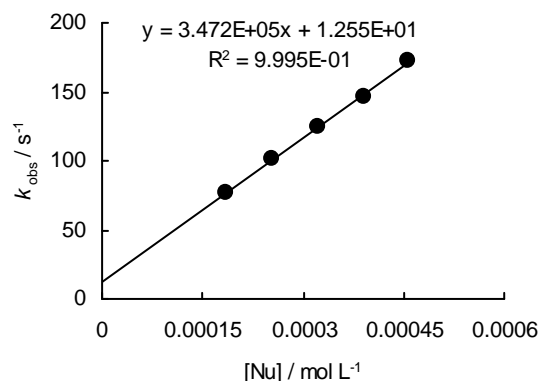


Table 11: Kinetics of the reaction of **1b** with **2b** in DMSO at 20°C (stopped-flow UV-Vis spectrometer, $\lambda = 623$ nm).

No.	$[E]_0 / \text{mol L}^{-1}$	$[\text{Nu}]_0 / \text{mol L}^{-1}$	$k_{\text{obs}} / \text{s}^{-1}$
RAK 15.4-3	2.47×10^{-5}	2.84×10^{-4}	5.97×10^1
RAK 15.4-1	2.47×10^{-5}	3.79×10^{-4}	7.75×10^1
RAK 15.4-4	2.47×10^{-5}	4.73×10^{-4}	9.87×10^1
RAK 15.4-2	2.47×10^{-5}	5.68×10^{-4}	1.18×10^2
RAK 15.4-5	2.47×10^{-5}	6.62×10^{-4}	1.38×10^2
$k_2 = 2.08 \times 10^5 \text{ L mol}^{-1} \text{ s}^{-1}$			

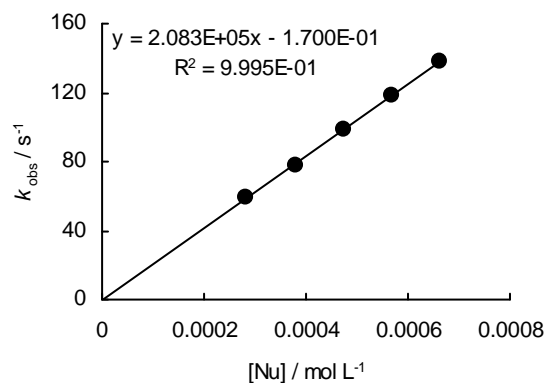


Table 12: Kinetics of the reaction of **1b** with **2c** in DMSO at 20°C (stopped-flow UV-Vis spectrometer, $\lambda = 623$ nm).

No.	$[E]_0 / \text{mol L}^{-1}$	$[\text{Nu}]_0 / \text{mol L}^{-1}$	$k_{\text{obs}} / \text{s}^{-1}$
RAK 15.3-1	2.40×10^{-5}	3.79×10^{-4}	6.94
RAK 15.3-2	2.40×10^{-5}	5.68×10^{-4}	1.07×10^1
RAK 15.3-3	2.40×10^{-5}	7.57×10^{-4}	1.44×10^1
RAK 15.3-4	2.40×10^{-5}	9.46×10^{-4}	1.81×10^1
RAK 15.3-5	2.40×10^{-5}	1.14×10^{-3}	2.17×10^1
$k_2 = 1.95 \times 10^4 \text{ L mol}^{-1} \text{ s}^{-1}$			

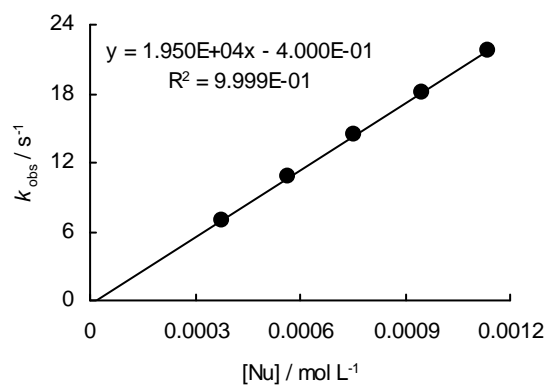
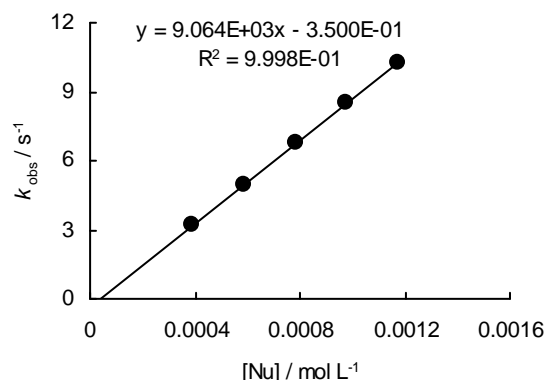
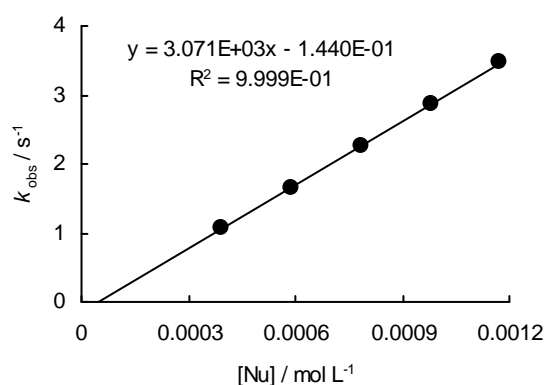


Table 13: Kinetics of the reaction of **1b** with **2d** in DMSO at 20°C (stopped-flow UV-Vis spectrometer, $\lambda = 630$ nm).

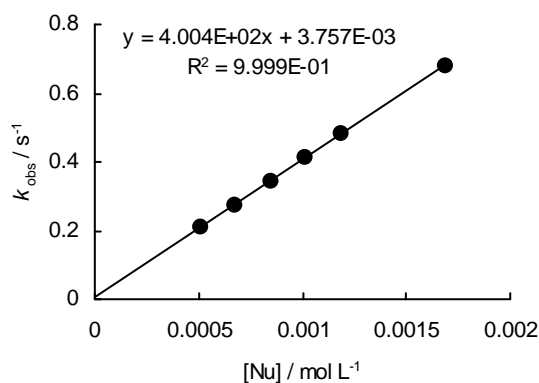
No.	$[E]_0 / \text{mol L}^{-1}$	$[\text{Nu}]_0 / \text{mol L}^{-1}$	$k_{\text{obs}} / \text{s}^{-1}$
RAK 15.2-1	2.35×10^{-5}	3.91×10^{-4}	3.22
RAK 15.2-2	2.35×10^{-5}	5.87×10^{-4}	4.92
RAK 15.2-3	2.35×10^{-5}	7.83×10^{-4}	6.79
RAK 15.2-4	2.35×10^{-5}	9.79×10^{-4}	8.50
RAK 15.2-5	2.35×10^{-5}	1.17×10^{-3}	1.03×10^1
$k_2 = 9.06 \times 10^3 \text{ L mol}^{-1} \text{ s}^{-1}$			

**Table 14:** Kinetics of the reaction of **1b** with **2e** in DMSO at 20°C (stopped-flow UV-Vis spectrometer, $\lambda = 630$ nm).

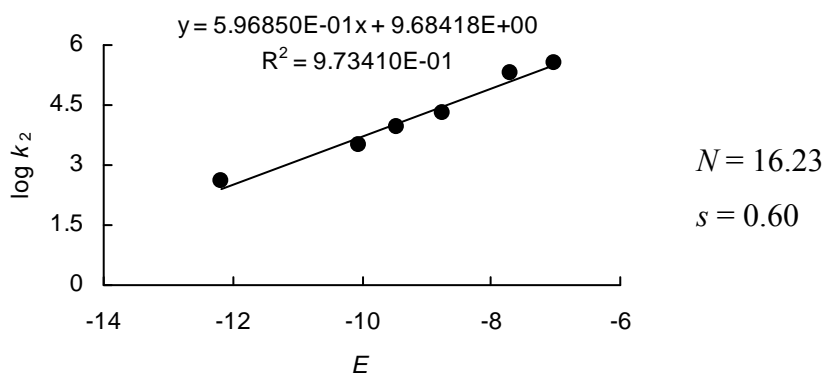
No.	$[E]_0 / \text{mol L}^{-1}$	$[\text{Nu}]_0 / \text{mol L}^{-1}$	$k_{\text{obs}} / \text{s}^{-1}$
RAK 15.1-1	2.30×10^{-5}	3.91×10^{-4}	1.07
RAK 15.1-2	2.30×10^{-5}	5.87×10^{-4}	1.65
RAK 15.1-3	2.30×10^{-5}	7.83×10^{-4}	2.25
RAK 15.1-4	2.30×10^{-5}	9.79×10^{-4}	2.86
RAK 15.1-5	2.30×10^{-5}	1.17×10^{-3}	3.47
$k_2 = 3.07 \times 10^3 \text{ L mol}^{-1} \text{ s}^{-1}$			

**Table 15:** Kinetics of the reaction of **1b** with **2f** in DMSO at 20°C (stopped-flow UV-Vis spectrometer, $\lambda = 422$ nm).

No.	$[E]_0 / \text{mol L}^{-1}$	$[\text{Nu}]_0 / \text{mol L}^{-1}$	$k_{\text{obs}} / \text{s}^{-1}$
RAK 15.6-1	3.98×10^{-5}	5.09×10^{-4}	2.06×10^{-1}
RAK 15.6-2	3.98×10^{-5}	6.78×10^{-4}	2.75×10^{-1}
RAK 15.6-3	3.98×10^{-5}	8.48×10^{-4}	3.43×10^{-1}
RAK 15.6-4	3.98×10^{-5}	1.02×10^{-3}	4.13×10^{-1}
RAK 15.6-5	3.98×10^{-5}	1.19×10^{-3}	4.80×10^{-1}
RAK 15.6-6	3.98×10^{-5}	1.70×10^{-3}	6.81×10^{-1}
$k_2 = 4.00 \times 10^2 \text{ L mol}^{-1} \text{ s}^{-1}$			



Determination of the N -Parameter for **1b**
 (Correlation of $\log k_2$ for the Reactions of **1b** with **2a-f**
 Versus the Electrophilicity Parameters E for **2a-f**)



Kinetic investigations of the reactions of the carbanion **1c** with the reference electrophiles **2d-j** in DMSO

Table 16: Kinetics of the reaction of **1c** with **2d** in DMSO at 20°C (addition of 0-2.0 equiv of 18-crown-6, stopped-flow UV-Vis spectrometer, $\lambda = 633$ nm).

No.	$[E]_0 / \text{mol L}^{-1}$	$[\text{Nu}^-]_0 / \text{mol L}^{-1}$	[18-crown-6] / mol L ⁻¹	$k_{\text{obs}} / \text{s}^{-1}$
RAK 21.4-1	1.08×10^{-5}	1.79×10^{-4}	-	6.14×10^1
RAK 21.4-2	1.08×10^{-5}	2.98×10^{-4}	4.68×10^{-4}	1.04×10^2
RAK 21.4-3	1.08×10^{-5}	4.17×10^{-4}	-	1.45×10^2
RAK 21.4-4	1.08×10^{-5}	5.36×10^{-4}	1.09×10^{-3}	1.83×10^2
RAK 21.4-5	1.08×10^{-5}	6.55×10^{-4}	-	2.23×10^2

$k_2 = 3.38 \times 10^5 \text{ L mol}^{-1} \text{ s}^{-1}$

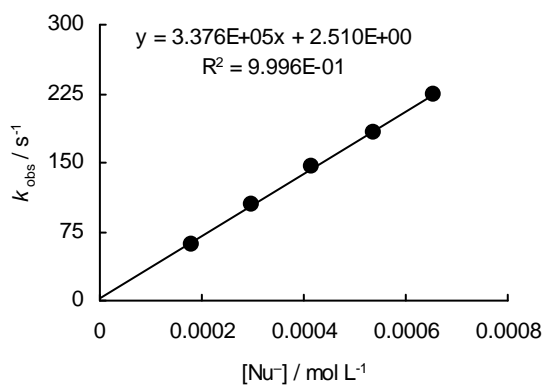
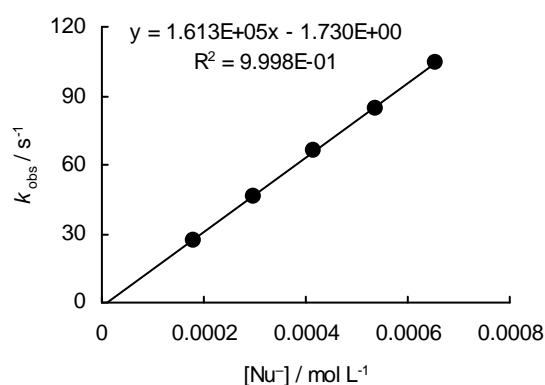


Table 17: Kinetics of the reaction of **1c** with **2e** in DMSO at 20°C (addition of 0-2.0 equiv of 18-crown-6, stopped-flow UV-Vis spectrometer, $\lambda = 633$ nm).

No.	[E] ₀ / mol L ⁻¹	[Nu ⁻] ₀ / mol L ⁻¹	[18-crown-6] / mol L ⁻¹	<i>k</i> _{obs} / s ⁻¹
RAK 21.3-1	1.01×10^{-5}	1.79×10^{-4}	-	2.70×10^1
RAK 21.3-2	1.01×10^{-5}	2.98×10^{-4}	4.68×10^{-4}	4.61×10^1
RAK 21.3-3	1.01×10^{-5}	4.17×10^{-4}	-	6.63×10^1
RAK 21.3-4	1.01×10^{-5}	5.36×10^{-4}	1.09×10^{-3}	8.43×10^1
RAK 21.3-5	1.01×10^{-5}	6.55×10^{-4}	-	1.04×10^2

$k_2 = 1.61 \times 10^5 \text{ L mol}^{-1} \text{ s}^{-1}$

**Table 18:** Kinetics of the reaction of **1c** with **2f** in DMSO at 20°C (addition of 0-1.5 equiv of 18-crown-6, stopped-flow UV-Vis spectrometer, $\lambda = 422$ nm).

No.	[E] ₀ / mol L ⁻¹	[Nu ⁻] ₀ / mol L ⁻¹	[18-crown-6] / mol L ⁻¹	<i>k</i> _{obs} / s ⁻¹
RAK 21.1-1	2.61×10^{-5}	3.57×10^{-4}	-	3.32
RAK 21.1-2	2.61×10^{-5}	5.96×10^{-4}	7.80×10^{-4}	5.73
RAK 21.1-3	2.61×10^{-5}	8.34×10^{-4}	-	8.11
RAK 21.1-4	2.61×10^{-5}	1.07×10^{-3}	1.56×10^{-3}	1.07×10^1
RAK 21.1-5	2.61×10^{-5}	1.31×10^{-3}	-	1.32×10^1

$k_2 = 1.04 \times 10^4 \text{ L mol}^{-1} \text{ s}^{-1}$

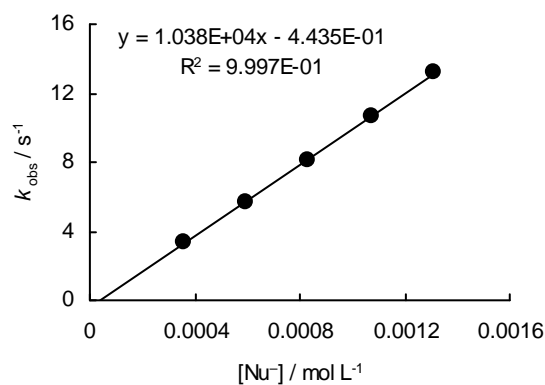
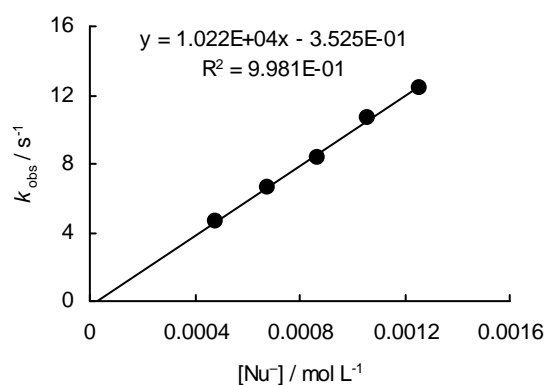


Table 19: Kinetics of the reaction of **1c** with **2f** in DMSO at 20°C (deprotonation of **1c**-H with 0.497 equiv of KO^tBu, addition of 0-1.5 equiv of 18-crown-6, stopped-flow UV-Vis spectrometer, $\lambda = 422$ nm).

No.	[E] ₀ / mol L ⁻¹	[Nu ⁻] ₀ / mol L ⁻¹	[Nu-H] ₀ / mol L ⁻¹	[18-crown-6] / mol L ⁻¹	<i>k</i> _{obs} / s ⁻¹
RAK 21.5-1	2.71×10^{-5}	4.83×10^{-4}	4.88×10^{-4}	-	4.60
RAK 21.5-2	2.71×10^{-5}	6.76×10^{-4}	6.82×10^{-4}	7.80×10^{-4}	6.57
RAK 21.5-3	2.71×10^{-5}	8.69×10^{-4}	8.77×10^{-4}	-	8.36
RAK 21.5-4	2.71×10^{-5}	1.06×10^{-3}	1.07×10^{-3}	1.56×10^{-3}	1.07×10^1
RAK 21.5-5	2.71×10^{-5}	1.25×10^{-3}	1.27×10^{-3}	-	1.24×10^1

$k_2 = 1.02 \times 10^4 \text{ L mol}^{-1} \text{ s}^{-1}$

**Table 20:** Kinetics of the reaction of **1c** with **2g** in DMSO at 20°C (addition of 0-1.6 equiv of 18-crown-6, stopped-flow UV-Vis spectrometer, $\lambda = 533$ nm).

No.	[E] ₀ / mol L ⁻¹	[Nu ⁻] ₀ / mol L ⁻¹	[18-crown-6] / mol L ⁻¹	<i>k</i> _{obs} / s ⁻¹
RAK 21.2-1	2.46×10^{-5}	4.77×10^{-4}	-	5.22×10^{-1}
RAK 21.2-2	2.46×10^{-5}	7.15×10^{-4}	9.36×10^{-4}	7.95×10^{-1}
RAK 21.2-3	2.46×10^{-5}	9.53×10^{-4}	-	1.07
RAK 21.2-4	2.46×10^{-5}	1.19×10^{-3}	1.87×10^{-3}	1.36
RAK 21.2-5	2.46×10^{-5}	1.43×10^{-3}	-	1.63

$k_2 = 1.17 \times 10^3 \text{ L mol}^{-1} \text{ s}^{-1}$

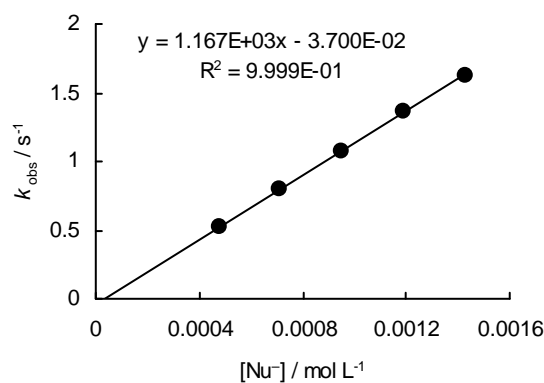
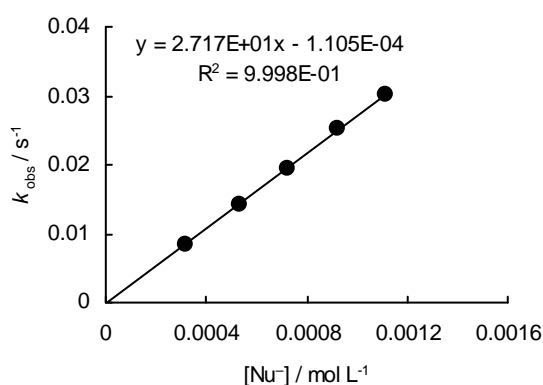


Table 21: Kinetics of the reaction of **1c** with **2h** in DMSO at 20°C (addition of 0-1.7 equiv of 18-crown-6, diode array UV-Vis spectrometer, $\lambda = 371$ nm).

No.	$[E]_0 / \text{mol L}^{-1}$	$[\text{Nu}^-]_0 / \text{mol L}^{-1}$	$[\text{18-crown-6}] / \text{mol L}^{-1}$	$k_{\text{obs}} / \text{s}^{-1}$
RAK 21.6-1	3.07×10^{-5}	3.15×10^{-4}	-	8.50×10^{-3}
RAK 21.6-2	3.28×10^{-5}	5.30×10^{-4}	7.97×10^{-4}	1.43×10^{-2}
RAK 21.6-3	3.63×10^{-5}	7.24×10^{-4}	-	1.94×10^{-2}
RAK 21.6-4	3.75×10^{-5}	9.26×10^{-4}	1.54×10^{-3}	2.52×10^{-2}
RAK 21.6-5	4.16×10^{-5}	1.12×10^{-3}	-	3.02×10^{-2}

$k_2 = 2.72 \times 10^1 \text{ L mol}^{-1} \text{ s}^{-1}$

**Table 22:** Kinetics of the reaction of **1c** with **2i** in DMSO at 20°C (addition of 0-1.5 equiv of 18-crown-6, diode array UV-Vis spectrometer, $\lambda = 393$ nm).

No.	$[E]_0 / \text{mol L}^{-1}$	$[\text{Nu}^-]_0 / \text{mol L}^{-1}$	$[\text{18-crown-6}] / \text{mol L}^{-1}$	$k_{\text{obs}} / \text{s}^{-1}$
RAK 21.7-1	4.11×10^{-5}	4.23×10^{-4}	-	6.87×10^{-3}
RAK 21.7-2	3.97×10^{-5}	6.34×10^{-4}	7.99×10^{-4}	1.04×10^{-2}
RAK 21.7-3	4.07×10^{-5}	8.38×10^{-4}	-	1.37×10^{-2}
RAK 21.7-4	3.85×10^{-5}	1.03×10^{-3}	1.55×10^{-3}	1.70×10^{-2}
RAK 21.7-5	3.99×10^{-5}	1.23×10^{-3}	-	2.02×10^{-2}

$k_2 = 1.65 \times 10^1 \text{ L mol}^{-1} \text{ s}^{-1}$

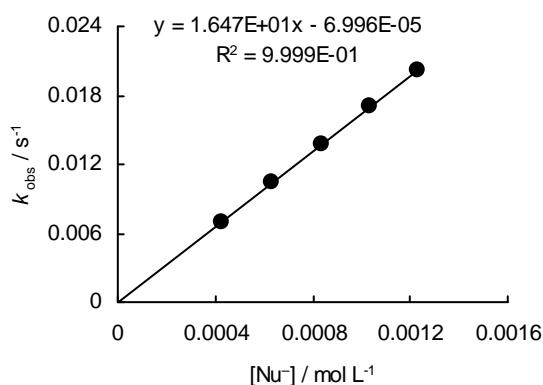
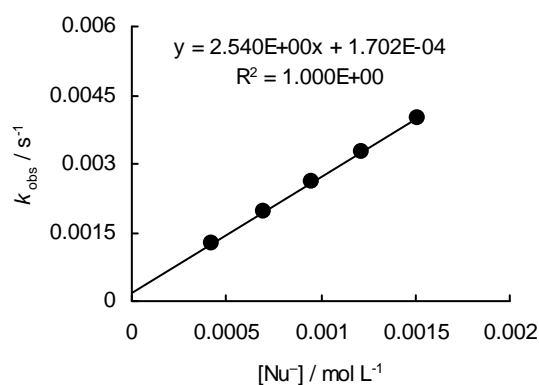


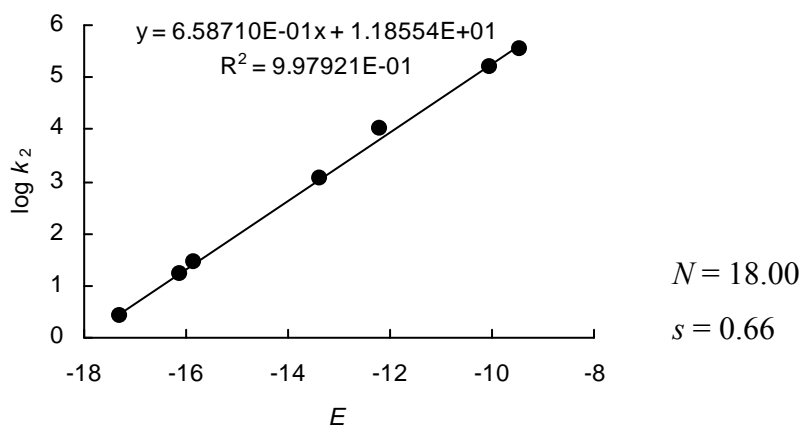
Table 23: Kinetics of the reaction of **1c** with **2j** in DMSO at 20°C (addition of 0-1.5 equiv of 18-crown-6, diode array UV-Vis spectrometer, $\lambda = 486$ nm).

No.	$[E]_0 / \text{mol L}^{-1}$	$[\text{Nu}^-]_0 / \text{mol L}^{-1}$	$[\text{18-crown-6}] / \text{mol L}^{-1}$	$k_{\text{obs}} / \text{s}^{-1}$
RAK 21.8-1	3.62×10^{-5}	4.21×10^{-4}	-	1.24×10^{-3}
RAK 21.8-2	4.18×10^{-5}	7.00×10^{-4}	9.31×10^{-4}	1.95×10^{-3}
RAK 21.8-3	4.24×10^{-5}	9.57×10^{-4}	-	2.60×10^{-3}
RAK 21.8-4	4.11×10^{-5}	1.22×10^{-3}	1.83×10^{-3}	3.26×10^{-3}
RAK 21.8-5	4.26×10^{-5}	1.51×10^{-3}	-	4.01×10^{-3}

$k_2 = 2.54 \text{ L mol}^{-1} \text{ s}^{-1}$



Determination of the N -Parameter for **1c**
 (Correlation of $\log k_2$ for the Reactions of **1c** with **2d-j**
 Versus the Electrophilicity Parameters E for **2d-j**)



Kinetic investigations of the reactions of the carbanion **1d** with the reference electrophiles **2f–k** in DMSO

Table 24: Kinetics of the reaction of **1d** with **2f** in DMSO at 20°C (addition of 0-3.4 equiv of 18-crown-6, stopped-flow UV-Vis spectrometer, $\lambda = 422$ nm).

No.	[E] ₀ / mol L ⁻¹	[Nu ⁻] ₀ / mol L ⁻¹	[18-crown-6] / mol L ⁻¹	<i>k</i> _{obs} / s ⁻¹
RAK 22.1-1	2.72×10^{-5}	2.84×10^{-4}	-	6.43×10^1
RAK 22.1-2	2.72×10^{-5}	4.26×10^{-4}	1.20×10^{-3}	9.63×10^1
RAK 22.1-3	2.72×10^{-5}	5.69×10^{-4}	-	1.29×10^2
RAK 22.1-4	2.72×10^{-5}	7.11×10^{-4}	2.40×10^{-3}	1.62×10^2
RAK 22.1-5	2.72×10^{-5}	8.53×10^{-4}	-	1.94×10^2
$k_2 = 2.29 \times 10^5 \text{ L mol}^{-1} \text{ s}^{-1}$				

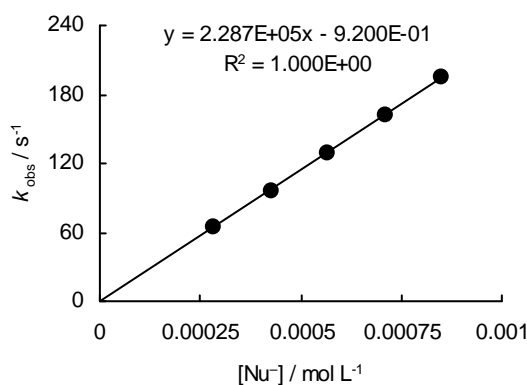


Table 25: Kinetics of the reaction of **1d** with **2g** in DMSO at 20°C (addition of 0-2.1 equiv of 18-crown-6, stopped-flow UV-Vis spectrometer, $\lambda = 533$ nm).

No.	[E] ₀ / mol L ⁻¹	[Nu ⁻] ₀ / mol L ⁻¹	[18-crown-6] / mol L ⁻¹	<i>k</i> _{obs} / s ⁻¹
RAK 22.2-1	2.16×10^{-5}	2.84×10^{-4}	-	9.19
RAK 22.2-2	2.16×10^{-5}	5.69×10^{-4}	1.20×10^{-3}	1.94×10^1
RAK 22.2-3	2.16×10^{-5}	8.53×10^{-4}	-	2.83×10^1
RAK 22.2-4	2.16×10^{-5}	1.14×10^{-3}	2.40×10^{-3}	3.91×10^1
RAK 22.2-5	2.16×10^{-5}	1.42×10^{-3}	-	4.80×10^1
$k_2 = 3.42 \times 10^4 \text{ L mol}^{-1} \text{ s}^{-1}$				

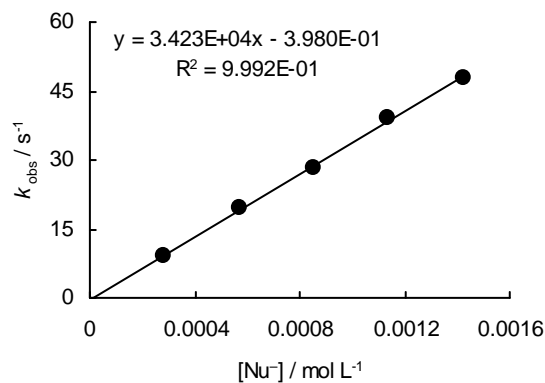


Table 26: Kinetics of the reaction of **1d** with **2g** in DMSO at 20°C (deprotonation of **1d**-H with 0.593 equiv of KO t Bu, addition of 0-2.2 equiv of 18-crown-6, stopped-flow UV-Vis spectrometer, $\lambda = 533$ nm).

No.	$[\text{E}]_0 / \text{mol L}^{-1}$	$[\text{Nu}^-]_0 / \text{mol L}^{-1}$	$[\text{Nu-H}]_0 / \text{mol L}^{-1}$	$[\text{18-crown-6}] / \text{mol L}^{-1}$	$k_{\text{obs}} / \text{s}^{-1}$
RAK 22.5-1	2.16×10^{-5}	2.74×10^{-4}	1.88×10^{-4}	-	9.00
RAK 22.5-2	2.16×10^{-5}	5.49×10^{-4}	3.77×10^{-4}	1.20×10^{-3}	1.92×10^1
RAK 22.5-3	2.16×10^{-5}	8.23×10^{-4}	5.65×10^{-4}	-	2.89×10^1
RAK 22.5-4	2.16×10^{-5}	1.10×10^{-3}	7.54×10^{-4}	2.40×10^{-3}	3.76×10^1
RAK 22.5-5	2.16×10^{-5}	1.37×10^{-3}	9.42×10^{-4}	-	4.70×10^1

$k_2 = 3.44 \times 10^4 \text{ L mol}^{-1} \text{ s}^{-1}$

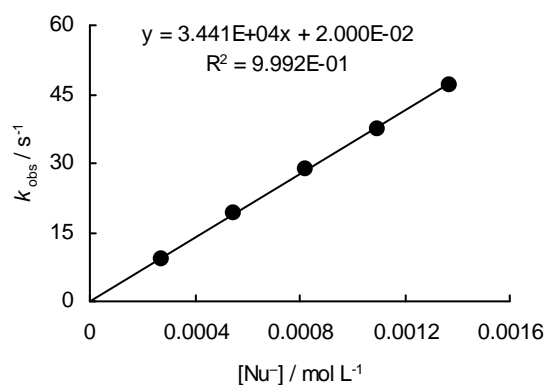
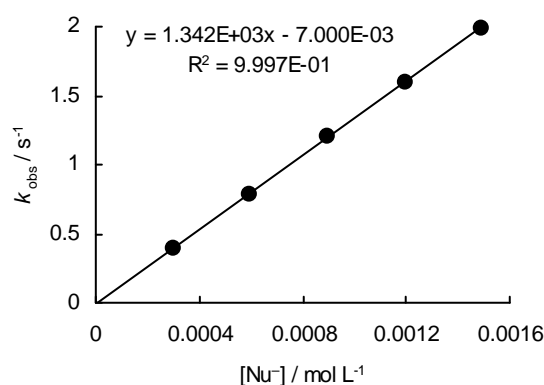


Table 27: Kinetics of the reaction of **1d** with **2h** in DMSO at 20°C (addition of 0-2.0 equiv of 18-crown-6, stopped-flow UV-Vis spectrometer, $\lambda = 380$ nm).

No.	$[E]_0 / \text{mol L}^{-1}$	$[\text{Nu}^-]_0 / \text{mol L}^{-1}$	$[18\text{-crown-6}] / \text{mol L}^{-1}$	$k_{\text{obs}} / \text{s}^{-1}$
RAK 22.3-1	2.76×10^{-5}	2.99×10^{-4}	-	3.95×10^{-1}
RAK 22.3-2	2.76×10^{-5}	5.97×10^{-4}	1.20×10^{-3}	7.82×10^{-1}
RAK 22.3-3	2.76×10^{-5}	8.96×10^{-4}	-	1.21
RAK 22.3-4	2.76×10^{-5}	1.19×10^{-3}	2.40×10^{-3}	1.60
RAK 22.3-5	2.76×10^{-5}	1.49×10^{-3}	-	1.99

$k_2 = 1.34 \times 10^3 \text{ L mol}^{-1} \text{ s}^{-1}$

**Table 28:** Kinetics of the reaction of **1d** with **2i** in DMSO at 20°C (addition of 0-2.0 equiv of 18-crown-6, stopped-flow UV-Vis spectrometer, $\lambda = 380$ nm).

No.	$[E]_0 / \text{mol L}^{-1}$	$[\text{Nu}^-]_0 / \text{mol L}^{-1}$	$[18\text{-crown-6}] / \text{mol L}^{-1}$	$k_{\text{obs}} / \text{s}^{-1}$
RAK 22.4-1	2.75×10^{-5}	2.99×10^{-4}	-	2.38×10^{-1}
RAK 22.4-2	2.75×10^{-5}	5.97×10^{-4}	1.20×10^{-3}	4.81×10^{-1}
RAK 22.4-3	2.75×10^{-5}	8.96×10^{-4}	-	7.38×10^{-1}
RAK 22.4-4	2.75×10^{-5}	1.19×10^{-3}	2.40×10^{-3}	9.82×10^{-1}
RAK 22.4-5	2.75×10^{-5}	1.49×10^{-3}	-	1.20

$k_2 = 8.12 \times 10^2 \text{ L mol}^{-1} \text{ s}^{-1}$

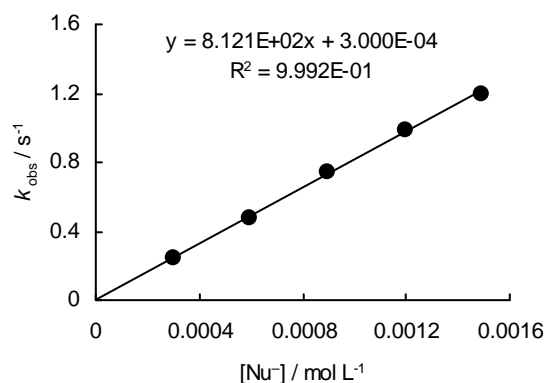
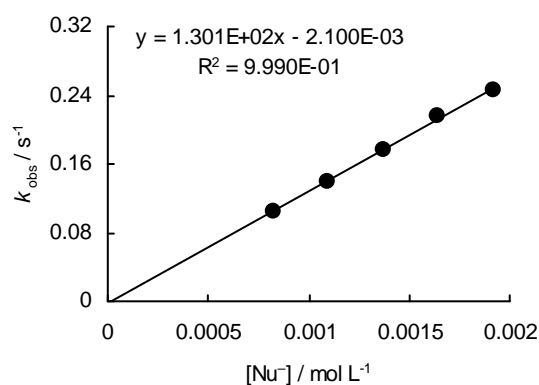


Table 29: Kinetics of the reaction of **1d** with **2j** in DMSO at 20°C (deprotonation of **1d**-H with 0.593 equiv of KOtBu, addition of 0-2.2 equiv of 18-crown-6, stopped-flow UV-Vis spectrometer, $\lambda = 533$ nm).

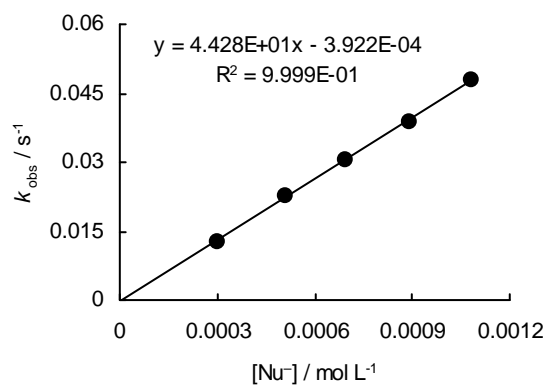
No.	$[E]_0 / \text{mol L}^{-1}$	$[\text{Nu}^-]_0 / \text{mol L}^{-1}$	$[\text{Nu-H}]_0 / \text{mol L}^{-1}$	$[\text{18-crown-6}] / \text{mol L}^{-1}$	$k_{\text{obs}} / \text{s}^{-1}$
RAK 22.6-1	2.64×10^{-5}	8.23×10^{-4}	5.65×10^{-4}	-	1.05×10^{-1}
RAK 22.6-2	2.64×10^{-5}	1.10×10^{-3}	7.54×10^{-4}	2.40×10^{-3}	1.40×10^{-1}
RAK 22.6-3	2.64×10^{-5}	1.37×10^{-3}	9.42×10^{-4}	-	1.76×10^{-1}
RAK 22.6-4	2.64×10^{-5}	1.65×10^{-3}	1.13×10^{-3}	2.40×10^{-3}	2.15×10^{-1}
RAK 22.6-5	2.64×10^{-5}	1.92×10^{-3}	1.32×10^{-3}	-	2.46×10^{-1}

$k_2 = 1.30 \times 10^2 \text{ L mol}^{-1} \text{ s}^{-1}$

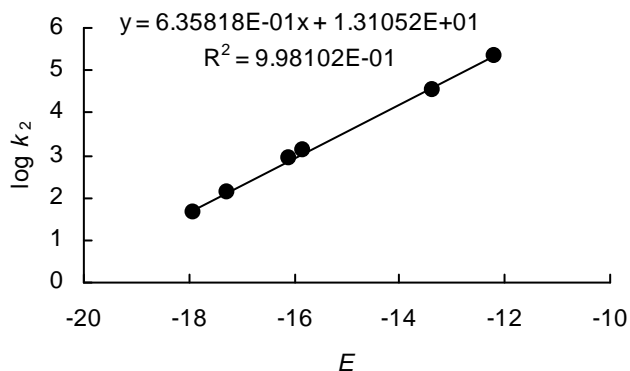
**Table 30:** Kinetics of the reaction of **1d** with **2k** in DMSO at 20°C (addition of 0-2.0 equiv of 18-crown-6, diode array UV-Vis spectrometer, $\lambda = 521$ nm).

No.	$[E]_0 / \text{mol L}^{-1}$	$[\text{Nu}^-]_0 / \text{mol L}^{-1}$	$[\text{18-crown-6}] / \text{mol L}^{-1}$	$k_{\text{obs}} / \text{s}^{-1}$
RAK 22.7-1	2.26×10^{-5}	3.00×10^{-4}	-	1.28×10^{-2}
RAK 22.7-2	2.95×10^{-5}	5.11×10^{-4}	9.34×10^{-4}	2.24×10^{-2}
RAK 22.7-3	2.99×10^{-5}	6.96×10^{-4}	-	3.05×10^{-2}
RAK 22.7-4	3.56×10^{-5}	8.92×10^{-4}	1.80×10^{-3}	3.89×10^{-2}
RAK 22.7-5	3.70×10^{-5}	1.08×10^{-3}	-	4.77×10^{-2}

$k_2 = 4.43 \times 10^1 \text{ L mol}^{-1} \text{ s}^{-1}$



Determination of the N -Parameter for **1d**
 (Correlation of $\log k_2$ for the Reactions of **1d** with **2f-k**
 Versus the Electrophilicity Parameters E for **2f-k**)



$$N = 20.61$$

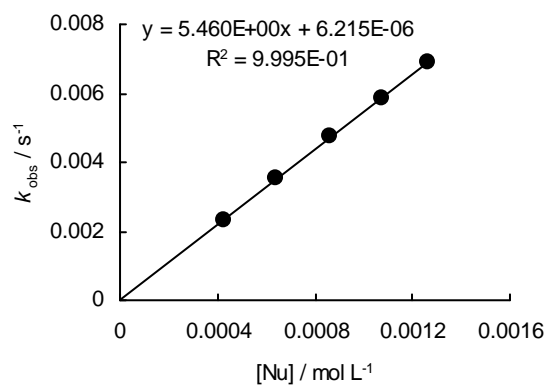
$$s = 0.64$$

4.3.2 Reactions of the Ylide **1a** and the Carbanions **1c,d** with the Nitrostyrenes **7a,b**

Kinetic investigation of the reaction of the ylide **1a** with nitrostyrene **7b** in DMSO

Table 31: Kinetics of the reaction of **1a** with nitrostyrene **7b** in DMSO at 20°C (diode array UV-Vis spectrometer, $\lambda = 363$ nm).

No.	$[E]_0 / \text{mol L}^{-1}$	$[\text{Nu}]_0 / \text{mol L}^{-1}$	$k_{\text{obs}} / \text{s}^{-1}$
RAK 23.3-2-1	4.16×10^{-5}	4.29×10^{-4}	2.30×10^{-3}
RAK 23.3-2-2	4.86×10^{-5}	6.41×10^{-4}	3.55×10^{-3}
RAK 23.3-2-3	4.90×10^{-5}	8.61×10^{-4}	4.75×10^{-3}
RAK 23.3-2-4	4.88×10^{-5}	1.07×10^{-3}	5.84×10^{-3}
RAK 23.3-2-5	4.79×10^{-5}	1.26×10^{-3}	6.88×10^{-3}
$k_2 = 5.46 \text{ L mol}^{-1} \text{ s}^{-1}$			



Kinetic investigations of the reactions of the carbanion **1c** with the nitrostyrenes **7** in DMSO

Table 32: Kinetics of the reaction of **1c** with nitrostyrene **7a** in DMSO at 20°C (stopped-flow UV-Vis spectrometer, $\lambda = 330$ nm).

No.	$[E]_0 / \text{mol L}^{-1}$	$[\text{Nu}^-]_0 / \text{mol L}^{-1}$	$k_{\text{obs}} / \text{s}^{-1}$
RAK 21.9-1	3.76×10^{-5}	5.08×10^{-4}	5.88×10^{-2}
RAK 21.9-2	3.76×10^{-5}	7.62×10^{-4}	8.90×10^{-2}
RAK 21.9-3	3.76×10^{-5}	1.02×10^{-3}	1.21×10^{-1}
RAK 21.9-4	3.76×10^{-5}	1.27×10^{-3}	1.57×10^{-1}
RAK 21.9-5	3.76×10^{-5}	1.52×10^{-3}	1.83×10^{-1}
$k_2 = 1.25 \times 10^2 \text{ L mol}^{-1} \text{ s}^{-1}$			

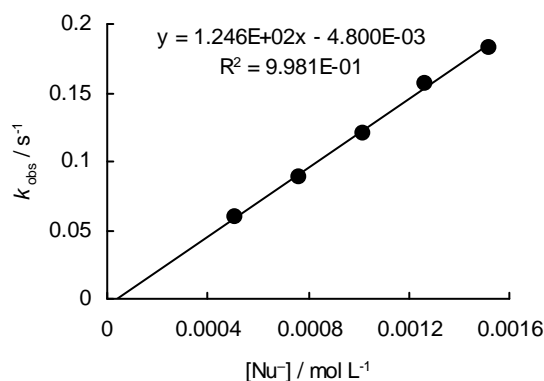
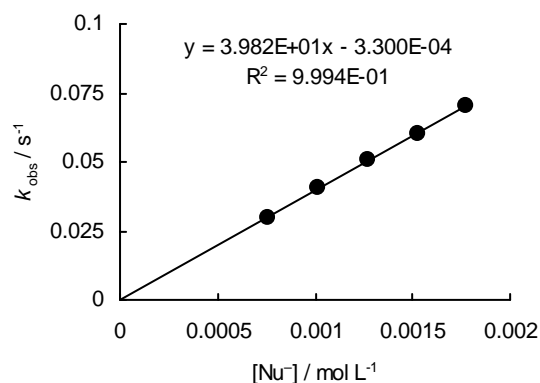


Table 33: Kinetics of the reaction of **1c** with nitrostyrene **7b** in DMSO at 20°C (stopped-flow UV-Vis spectrometer, $\lambda = 360$ nm).

No.	$[E]_0 / \text{mol L}^{-1}$	$[\text{Nu}^-]_0 / \text{mol L}^{-1}$	$k_{\text{obs}} / \text{s}^{-1}$
RAK 21.10-1	3.74×10^{-5}	7.62×10^{-4}	2.96×10^{-2}
RAK 21.10-2	3.74×10^{-5}	1.02×10^{-3}	4.03×10^{-2}
RAK 21.10-3	3.74×10^{-5}	1.27×10^{-3}	5.08×10^{-2}
RAK 21.10-4	3.74×10^{-5}	1.52×10^{-3}	6.02×10^{-2}
RAK 21.10-5	3.74×10^{-5}	1.78×10^{-3}	7.02×10^{-2}
$k_2 = 3.98 \times 10^1 \text{ L mol}^{-1} \text{ s}^{-1}$			



Kinetic investigations of the reactions of the carbanion **1d** with the nitrostyrenes **7** in DMSO

Table 34: Kinetics of the reaction of **1d** with nitrostyrene **7a** in DMSO at 20°C (stopped-flow UV-Vis spectrometer, $\lambda = 330$ nm).

No.	$[E]_0 / \text{mol L}^{-1}$	$[\text{Nu}^-]_0 / \text{mol L}^{-1}$	$k_{\text{obs}} / \text{s}^{-1}$
RAK 22.8-1	3.96×10^{-5}	4.53×10^{-4}	4.85
RAK 22.8-2	3.96×10^{-5}	6.80×10^{-4}	7.77
RAK 22.8-3	3.96×10^{-5}	9.07×10^{-4}	1.04×10^1
RAK 22.8-4	3.96×10^{-5}	1.13×10^{-3}	1.32×10^1
RAK 22.8-5	3.96×10^{-5}	1.36×10^{-3}	1.59×10^1
$k_2 = 1.21 \times 10^4 \text{ L mol}^{-1} \text{ s}^{-1}$			

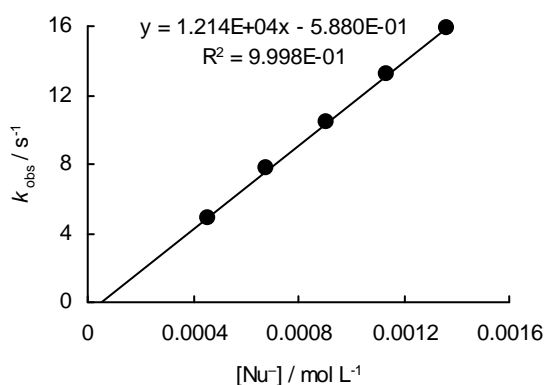
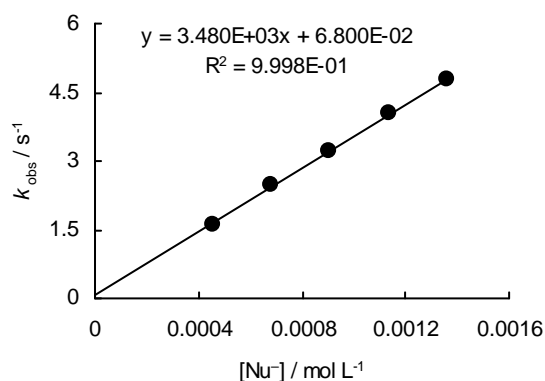


Table 35: Kinetics of the reaction of **1d** with nitrostyrene **7b** in DMSO at 20°C (stopped-flow UV-Vis spectrometer, $\lambda = 360$ nm).

No.	$[E]_0 / \text{mol L}^{-1}$	$[\text{Nu}^-]_0 / \text{mol L}^{-1}$	$k_{\text{obs}} / \text{s}^{-1}$
RAK 22.9-1	3.82×10^{-5}	4.53×10^{-4}	1.63
RAK 22.9-2	3.82×10^{-5}	6.80×10^{-4}	2.46
RAK 22.9-3	3.82×10^{-5}	9.07×10^{-4}	3.21
RAK 22.9-4	3.82×10^{-5}	1.13×10^{-3}	4.03
RAK 22.9-5	3.82×10^{-5}	1.36×10^{-3}	4.79
$k_2 = 3.48 \times 10^3 \text{ L mol}^{-1} \text{ s}^{-1}$			



5 References

- [1] For selected reviews, see: (a) Maryanoff, B. E.; Reitz, A. B. *Phosphorus, Sulfur Silicon Relat. Elem.* **1986**, *27*, 167-189. (b) Maryanoff, B. E.; Reitz, A. B. *Chem. Rev.* **1989**, *89*, 863-927. (c) Vedejs, E.; Peterson, M. J. *Top. Stereochem.* **1994**, *21*, 1-157. (d) Vedejs, E.; Peterson, M. J. In *Advances in Carbanion Chemistry*; Snieckus, V., Ed.; JAI Press: London, 1996; Vol. 2, pp 1-85. (e) Nicolaou, K. C.; Härter, M. W.; Gunzner, J. L.; Nadin, A. *Liebigs Ann./Recueil* **1997**, 1283-1301. (f) Kolodiazhnyi, O. I., *Phosphorus Ylides*; Wiley-VCH: Weinheim, 1999; pp 258-358.
- [2] (a) Johnson, A. W.; LaCount, R. B. *Chem. Ind. (London)* **1958**, 1440-1441. (b) Johnson, A. W.; LaCount, R. B. *J. Am. Chem. Soc.* **1961**, *83*, 417-423. (c) Corey, E. J.; Chaykovsky, M. *J. Am. Chem. Soc.* **1962**, *84*, 867-868. (d) Corey, E. J.; Chaykovsky, M. *J. Am. Chem. Soc.* **1962**, *84*, 3782-3783. (e) Franzen, V.; Driessen, H.-E. *Tetrahedron Lett.* **1962**, *3*, 661-662. For selected reviews, see: (f) Trost, B. M.; Melvin, L. S. *Sulfur Ylides. Emerging Synthetic Intermediates*; Academic Press: New York, 1975. (g) Li, A.-H.; Dai, L.-X.; Aggarwal, V. K. *Chem. Rev.* **1997**, *97*, 2341-2372. (h) Clark, J. S. In *Nitrogen, Oxygen and Sulfur Ylide Chemistry*; Clark, J. S., Ed.; Oxford University Press: New York, 2002; pp 1-114. (i) Aggarwal, V. K.; Richardson, J. In *Science of Synthesis*; Georg Thieme Verlag: Stuttgart, 2004; Vol. 27, pp 21-104. (j) Aggarwal, V. K.; Winn, C. L. *Acc. Chem. Res.* **2004**, *37*, 611-620. (k) Aggarwal, V. K.; Richardson, J.; Winn, C. L. In *Science of Synthesis*, Georg Thieme Verlag: Stuttgart, 2005; Vol. 22, pp 11-73. (l) McGarrigle, E. M.; Aggarwal, V. K. In *Enantioselective Organocatalysis*; Dalko, P. I., Ed.; Wiley-VCH: Weinheim, 2007; pp 357-390. (m) McGarrigle, E. M.; Myers, E. L.; Illa, O.; Shaw, M. A.; Riches, S. L.; Aggarwal, V. K. *Chem. Rev.* **2007**, *107*, 5841-5883. (n) Aggarwal, V. K.; Crimmin, M.; Riches, S. In

- Science of Synthesis*; Georg Thieme Verlag: Stuttgart, 2008; Vol. 37, pp 321-406. (o) Brière, J.-F.; Metzner, P. In *Organosulfur Chemistry in Asymmetric Synthesis*; Toru, T., Bolm, C., Eds.; Wiley-VCH: Weinheim, 2008; pp 179-208.
- [3] (a) Stowell, J. C. *Carbanions in Organic Synthesis*, John Wiley & Sons: New York, 1979. (b) Gais, H. J.; Hellmann, G. *J. Am. Chem. Soc.* **1992**, *114*, 4439-4440. (c) Solladié-Cavallo, A.; Roche, D.; Fischer, J.; De Cian, A. *J. Org. Chem.* **1996**, *61*, 2690-2694. (d) Gais, H.-J.; v. Gumpel, M.; Raabe, G.; Müller, J.; Braun, S.; Lindner, H. J.; Rohs, S.; Runsink, J. *Eur. J. Org. Chem.* **1999**, 1627-1651. (e) Volonterio, A.; Zanda, M.; In *Organosulfur Chemistry in Asymmetric Synthesis*; Toru, T., Bolm, C., Eds.; Wiley-VCH: Weinheim, 2008; pp. 351-374. (f) Gais, H.-J. In *Organosulfur Chemistry in Asymmetric Synthesis*; Toru, T., Bolm, C., Eds.; Wiley-VCH: Weinheim, 2008; pp. 375-398.
- [4] (a) Happer, D. A. R.; Steenson, B. E. *Synthesis* **1980**, 806-807. (b) Tanikaga, R.; Tamura, T.; Nozaki, Y.; Kaji, A. *J. Chem. Soc., Chem. Commun.* **1984**, 87-88. (c) Tanikaga, R.; Konya, N.; Tamura, T.; Kaji, A. *J. Chem. Soc., Perkin Trans. I* **1987**, 825-830.
- [5] (a) Julia, M.; Paris, J.-M. *Tetrahedron Lett.* **1973**, *14*, 4833-4836. (b) Kocienski, P. J.; Lythgoe, B.; Ruston, S. *J. Chem. Soc., Perkin Trans. I* **1978**, 829-834. (c) Julia, M. *Pure Appl. Chem.* **1985**, *57*, 763-768. (d) Blakemore, P. R. *J. Chem. Soc., Perkin Trans. I* **2002**, 2563-2585.
- [6] (a) Ratts, K. W. *J. Org. Chem.* **1972**, *37*, 848-851. (b) Zhang, X.-M.; Bordwell, F. G. *J. Am. Chem. Soc.* **1994**, *116*, 968-972. (c) Cheng, J.-P.; Liu, B.; Zhang, X.-M. *J. Org. Chem.* **1998**, *63*, 7574-7575. (d) Cheng, J.-P.; Liu, B.; Zhao, Y.; Sun, Y.; Zhang, X.-M.; Lu, Y. *J. Org. Chem.* **1999**, *64*, 604-610. (e) Fu, Y.; Wang, H.-J.; Chong, S.-S.; Guo, Q.-X.; Liu, L. *J. Org. Chem.* **2009**, *74*, 810-819.
- [7] (a) Volatron, F.; Eisenstein, O. *J. Am. Chem. Soc.* **1987**, *109*, 1-14. (b) Aggarwal, V. K.; Harvey, J. N.; Robiette, R. *Angew. Chem.* **2005**, *117*, 5604-5607; *Angew. Chem. Int. Ed.* **2005**, *44*, 5468-5471.
- [8] (a) Lucius, R.; Mayr, H. *Angew. Chem.* **2000**, *112*, 2086-2089; *Angew. Chem. Int. Ed.* **2000**, *39*, 1995-1997. (b) Berger, S. T. A.; Ofial, A. R.; Mayr, H. *J. Am. Chem. Soc.* **2007**, *129*, 9753-9761. (c) Appel, R.; Loos, R.; Mayr, H. *J. Am. Chem. Soc.* **2009**, *131*, 704-714.
- [9] (a) Mayr, H.; Patz, M. *Angew. Chem.* **1994**, *106*, 990-1010; *Angew. Chem. Int. Ed. Engl.* **1994**, *33*, 938-957. (b) Mayr, H.; Bug, T.; Gotta, M. F.; Hering, N.; Irrgang, B.; Janker,

- B.; Kempf, B.; Loos, R.; Ofial, A. R.; Remennikov, G.; Schimmel, H. *J. Am. Chem. Soc.* **2001**, *123*, 9500-9512. (c) Lucius, R.; Loos, R.; Mayr, H. *Angew. Chem.* **2002**, *114*, 97-102; *Angew. Chem. Int. Ed.* **2002**, *41*, 91-95. (d) Mayr, H.; Kempf, B.; Ofial, A. R. *Acc. Chem. Res.* **2003**, *36*, 66-77. (e) Mayr, H.; Ofial, A. R. *Pure Appl. Chem.* **2005**, *77*, 1807-1821. (f) Mayr, H.; Ofial, A. R. *J. Phys. Org. Chem.* **2008**, *21*, 584-595.
- [10] Zenz, I.; Mayr, H. unpublished results.
- [11] (a) Lu, L.-Q.; Cao, Y.-J.; Liu, X.-P.; An, J.; Yao, C.-J.; Ming, Z.-H.; Xiao, W.-J. *J. Am. Chem. Soc.* **2008**, *130*, 6946-6948. (b) Lu, L.-Q.; Li, F.; An, J.; Zhang, J.-J.; An, X.-L.; Hua, Q.-L.; Xiao, W.-J. *Angew. Chem.* **2009**, *121*, 9706-9709; *Angew. Chem. Int. Ed.* **2009**, *48*, 9542-9545.
- [12] Robiette, R.; Richardson, J.; Aggarwal, V. K.; Harvey, J. N. *J. Am. Chem. Soc.* **2006**, *128*, 2394-2409.
- [13] (a) Aggarwal, V. K.; Calamai, S.; Ford, J. G. *J. Chem. Soc., Perkin Trans. 1* **1997**, 593-599. (b) Aggarwal, V. K.; Harvey, J. N.; Richardson, J. *J. Am. Chem. Soc.* **2002**, *124*, 5747-5756. (c) Edwards, D. R.; Montoya-Peleaz, P.; Crudden, C. M. *Org. Lett.* **2007**, *9*, 5481-5484.
- [14] (a) Payne, G. B. *J. Org. Chem.* **1967**, *32*, 3351-3355. (b) Jeckel, D.; Gosselck, J. *Tetrahedron Lett.* **1972**, *13*, 2101-2104.
- [15] (a) Labuschagne, A. J. H.; Malherbe, J. S.; Meyer, C. J.; Schneider, D. F. *J. Chem. Soc., Perkin Trans. 1* **1978**, 955-961. (b) Coppola, G. M.; Hardtmann, G. E. *J. Heterocycl. Chem.* **1979**, *16*, 1605-1610.
- [16] Gairaud, C. B.; Lappin, G. R. *J. Org. Chem.* **1953**, *18*, 1-3.
- [17] (a) Evans, S.; Nesvadba, P.; Allenbach S. (Ciba-Geigy AG), EP-B 744392, **1996** [*Chem. Abstr.* **1997**, *126*, 46968v]. (b) Richter, D.; Hampel, N.; Singer, T.; Ofial, A. R.; Mayr, H. *Eur. J. Org. Chem.* **2009**, 3203-3211.
- [18] Based on a comparable procedure; see: Seebach, D.; Leitz, H.F. *Angew. Chem.* **1971**, *83*, 542-544; *Angew. Chem. Int. Ed. Engl.* **1971**, *10*, 501-503.

Chapter 5: Scope and Limitations of Cyclopropanations with Sulfur Ylides

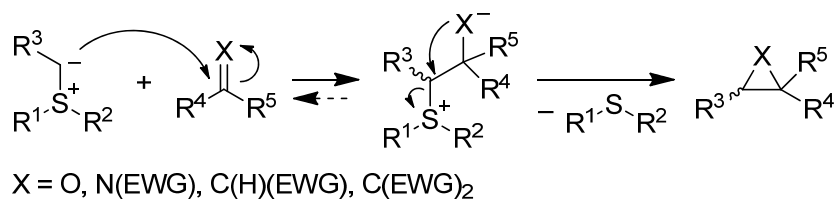
Roland Appel, Nicolai Hartmann, and Herbert Mayr

J. Am. Chem. Soc. **2010**, *132*, 17894-17900.

1 Introduction

Sulfur ylides have emerged to an important class of reagents in organic synthesis. Though the first report on the isolation of a sulfur ylide by Ingold and Jessop was already published in 1930,^[1] a systematic investigation of sulfur ylides started only in the 1960s when these compounds were recognized as versatile reagents for the preparation of three-membered carbo- and heterocycles.^[2] Eventually, the use of chiral sulfur ylides or chiral electrophilic substrates gave rise to a variety of stereoselective sulfur ylide-mediated cyclization reactions.^[3] Detailed investigations of epoxidation,^[4] cyclopropanation,^[4b,5] and aziridination reactions^[6] revealed a common mechanistic course. In all cases, the sulfur ylide initially attacks at an electrophilic carbon center (i.e., aldehyde, imine, or Michael acceptor) to form a betaine intermediate, which undergoes an intramolecular nucleophilic displacement to yield an epoxide, an aziridine, or a cyclopropane, respectively (Scheme 1).

Scheme 1: Mechanism of the Sulfur Ylide-Mediated Epoxidation-, Aziridination-, and Cyclopropanation Reaction (Corey-Chaykovsky Reaction).^[4,5,6]



Depending on the reactivities of the sulfur ylides, the initial addition step of the sulfur ylide to an aldehyde or an imine has been shown to be reversible or irreversible.^[2k,4b,k-n,6a,c,d] Stabilized sulfur ylides, i.e., acetyl-, benzoyl-, and ester-substituted sulfur ylides, are considerably less reactive than the so-called semistabilized sulfur ylides, i.e., aryl-substituted sulfur ylides, and do not undergo epoxidation reactions with aldehydes or react only under harsh conditions.^[2k,p,4k] Obviously, the nucleophilicities of the ylides play an important role for their synthetic applicability. Previous rationalizations of structure-reactivity relationships of sulfur ylides focused on their basicities.^[5d,7] However, due to the small amount of available

pK_{aH} values of sulfur ylides and the poor correlation between basicity and nucleophilicity of carbon-centered nucleophiles,^[8] a quantitative comparison of the nucleophilicities of variably substituted sulfur ylides as well as a comparison with other classes of nucleophiles has so far not been possible.

In recent years, we have shown that the rates of the reactions of carbocations and Michael acceptors (some of them are depicted in Table 1) with n -, π -, and σ -nucleophiles can be described by eq 1, where $k_{20^\circ\text{C}}$ is the second-order rate constant in $\text{M}^{-1} \text{s}^{-1}$, s is a nucleophile-specific sensitivity parameter, N is a nucleophilicity parameter, and E is an electrophilicity parameter.

$$\log k_{20^\circ\text{C}} = s(N + E) \quad (1)$$

On the basis of this linear free-energy relationship, we have developed the most comprehensive nucleophilicity and electrophilicity scale presently available.^[8,9] We have now employed this method for characterizing the nucleophilicities of stabilized and semistabilized sulfur ylides **1a–g** (Scheme 2), and we will discuss the impact of these results for predicting scope and limitations of cyclopropanation reactions of Michael acceptors with sulfur ylides.

Scheme 2: Benzoyl-Stabilized Sulfur Ylides **1a–d**, Semistabilized Sulfur Ylides **1e–g**, and Ester-Stabilized Sulfur Ylide **1h**.

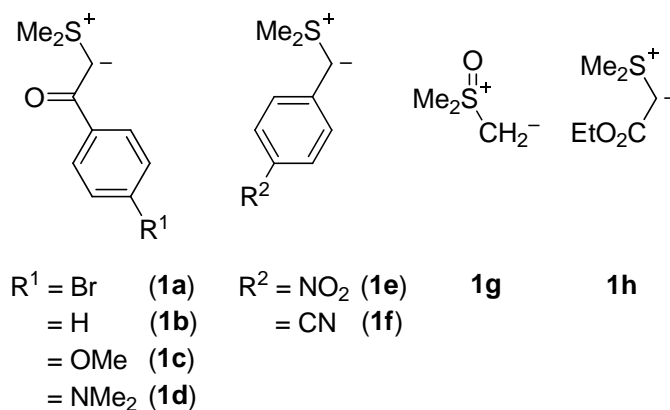
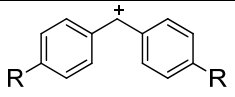
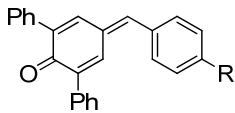
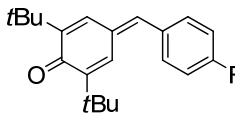
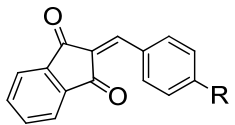
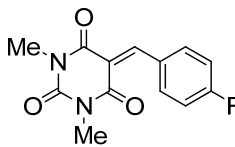
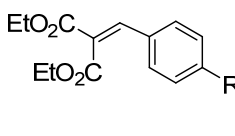
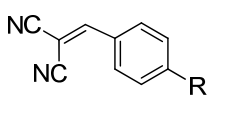
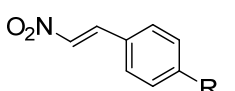
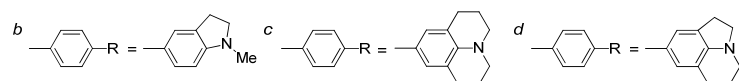


Table 1: Benzhydrylium Ions **2a–e**, Michael Acceptors **2f–v**, and their Electrophilicity Parameters E .

Electrophile	R	E^a
	2a	NMe ₂ -7.02
	2b	N(CH ₂) ₄ -7.69
	2c	ind ^b -8.76
	2d	jul ^c -9.45
	2e	lil ^d -10.04
	2f	OMe -12.18
	2g	NMe ₂ -13.39
	2h	Me -15.83
	2i	OMe -16.11
	2j	NMe ₂ -17.29
	2k	jul ^c -17.90
	2l	OMe -11.32
	2m	NMe ₂ -13.56
	2n	jul ^c -14.68
	2o	OMe -10.37
	2p	NMe ₂ -12.76
	2q	jul ^c -13.84
	2r	NO ₂ -17.67
	2s	CN -18.06
	2t	<i>m</i> Cl -18.98
	2u	NMe ₂ -13.30
	2v	OMe -14.70

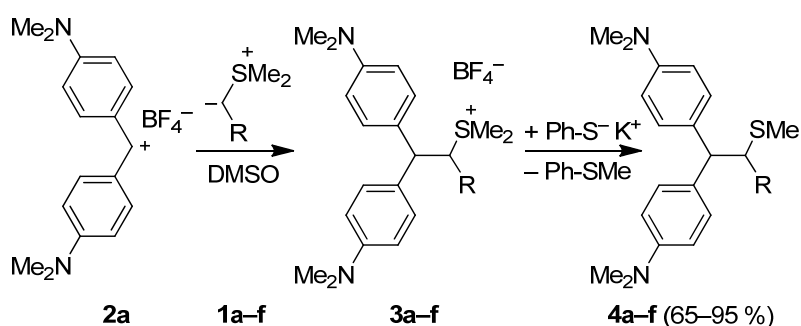
^a Electrophilicity parameters E of **2a–e** were taken from ref 9b, of **2f–k** from ref 9c, of **2l–n** from ref 9g, **2o–q** from ref 9h, of **2r–t** from ref 9i, of **2u** from 9d, and of **2v** from ref 9k.



2 Results

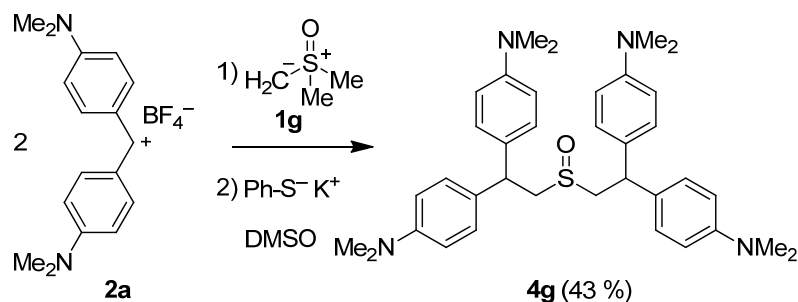
Reactions with Benzhydrylium Ions. In order to establish the course of the reactions, which were studied kinetically, we have characterized products of the reactions of the sulfur ylides **1a–g** with the benzhydrylium ion **2a**. Owing to their low stability, the initially formed addition products **3a–f** were not isolated but immediately treated with thiophenolate to afford the neutral addition products **4a–f**, which are fully characterized in the Experimental Section (Scheme 3).

Scheme 3: Reactions of the Sulfur Ylides **1a–f** with Benzhydrylium Tetrafluoroborate **2a**-BF₄.



Treatment of **2a** with the dimethylsulfoxonium ylide **1g** and subsequent addition of thiophenolate yielded the 2:1-product **4g** (Scheme 4). Obviously, the initially generated 1:1-addition product from **2a** and **1g** is rapidly deprotonated to give another sulfur ylide which reacts with a second molecule of the electrophile **2a**. Eventually, demethylation by thiophenolate (according to Scheme 3) yields **4g**.

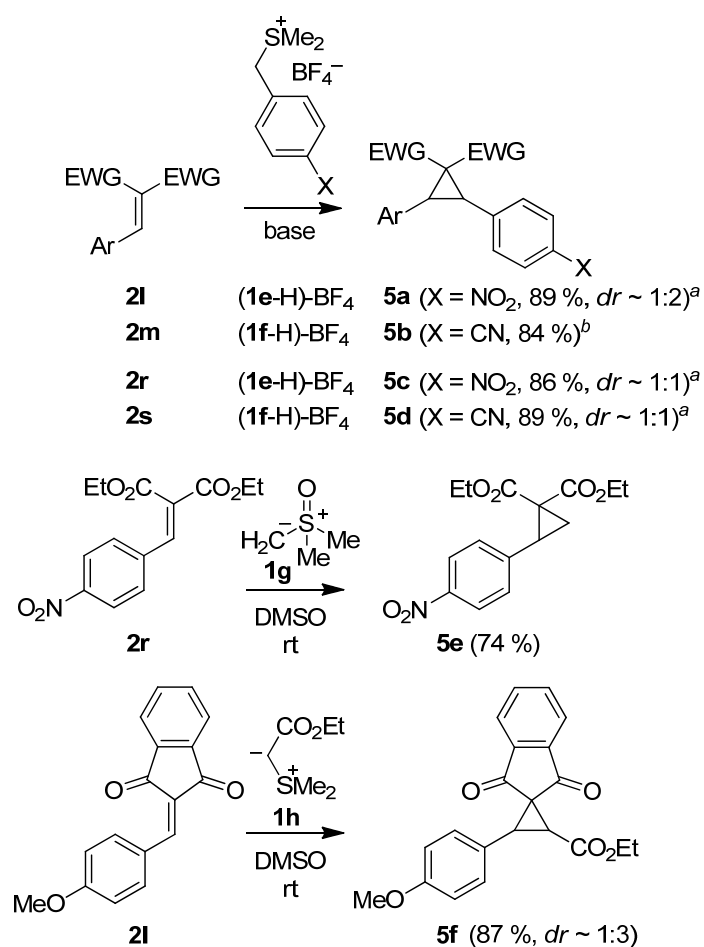
Scheme 4: Reaction of the Sulfur Ylide **1g** with Benzhydrylium Tetrafluoroborate **2a**-BF₄.



Reactions with Michael Acceptors. As the reactions of sulfur ylides with Michael acceptors had already been known to yield cyclopropane derivatives (Scheme 1), product analyses have only been performed for representative combinations of the sulfur ylides **1** with Michael acceptors. The reactions of the semistabilized sulfur ylides **1e–g** with the

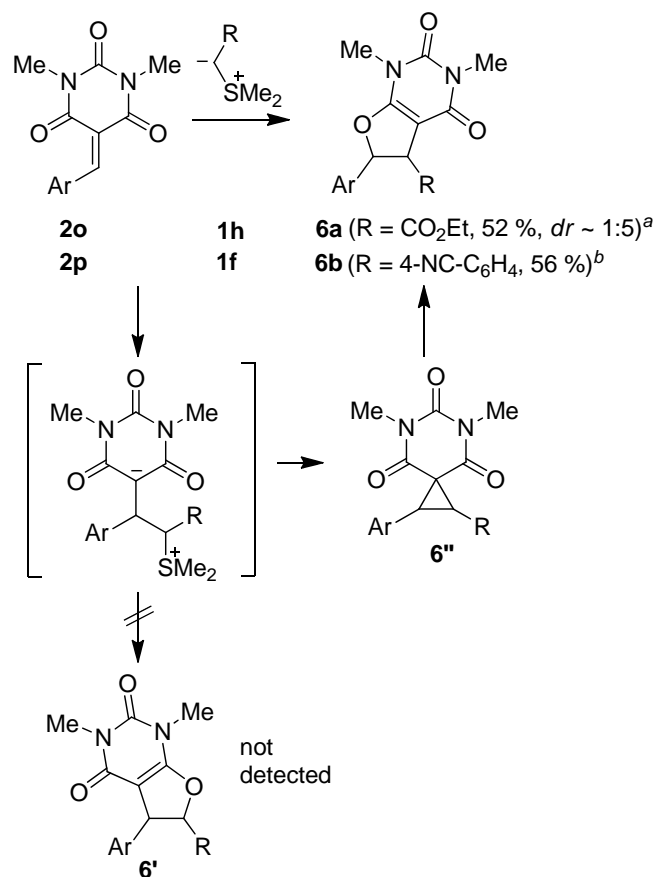
benzylideneindandiones **2l,m** and the diethyl benzylidenemalonates **2r,s** as well as the reaction of the stabilized sulfur ylide **1h** with benzylideneindandione **2l** yielded the expected cyclopropane derivatives **5** (Scheme 5). Due to the high tendency of dimethylsulfoxonium ylide **1g** for multiple addition (see Scheme 4), complex mixtures of products were formed in the reactions of **1g** with the other types of Michael acceptors. The treatment of the benzylidenebarbituric acids **2o,p** with the sulfur ylides **1f** and **1h** did not yield cyclopropanes, but the dihydrofuran derivatives **6a,b**. As indicated in Scheme 6, the direct nucleophilic displacement of dimethylsulfide by a carbonyl oxygen of the initially formed zwitterion would lead to dihydrofurans **6'**, which have a different substitution pattern than was actually found for the compounds **6a,b** (derived by 2D-NMR experiments). These findings suggest that the dihydrofurans **6a,b** are formed via a rearrangement of an intermediate cyclopropane species **6''**.

Scheme 5: Reactions of the Semistabilized Sulfur Ylides **1e–g** and the Stabilized Sulfur Ylide **1h** with Different Michael Acceptors.



^a Reaction conditions: KO^tBu, DMSO, rt. ^b Reaction conditions: K₂CO₃ (aq.)/CHCl₃, rt; only one diastereomer isolated.

Scheme 6: Reactions of the Sulfur Ylides **1f** and **1h** with the Benzylidenebarbituric Acids **2o** and **2p**.



^a Reaction conditions: **1h**, DMSO, rt. ^b Reaction conditions: (**1f-H**)-BF₄, K₂CO₃ (aq.)/CHCl₃, rt; only one diastereomer isolated.

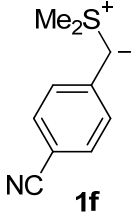
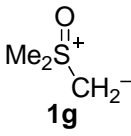
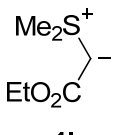
In analogy to previous reports,^[10,11] the reaction of the benzoyl-stabilized sulfur ylide **1c** with *trans*-4-methoxy- β -nitrostyrene (**2v**) does not give a cyclopropane but a dihydroisoxazole *N*-oxide, which has been identified as described in the Experimental Section.

Kinetic Investigations have been performed in analogy to earlier studies.^[10] However, because of the low stability of the semistabilized ylides **1e,f**, several modifications were needed as described in detail in the Experimental Section. Table 2 shows a summary of the second-order rate constants, which have been determined for the reactions of the sulfur ylides **1a–h** with the benzhydrylium ions **2a–e** and the Michael acceptors **2f–v**.

Table 2: Experimental and Calculated Second-Order Rate Constants ($M^{-1}s^{-1}$) for the Reactions of the Sulfur Ylides **1** with the Electrophiles **2** in DMSO at 20°C.

Nucleophile N/s^a	Electrophile	k_2^{exp}	$k_2^{calcd}^b$
 1a 13.78 / 0.72	2a	5.71×10^4	7.37×10^4
	2b	3.34×10^4	2.43×10^4
	2c	3.03×10^3	4.12×10^3
	2d	1.73×10^3	1.31×10^3
	2e	5.72×10^2	4.93×10^2
	2f	1.23×10^1	1.42×10^1
 1b 13.95 / 0.69	2a	5.15×10^4	6.05×10^4
	2b	3.06×10^4	2.09×10^4
	2c	2.98×10^3	3.81×10^3
	2d	1.53×10^3	1.27×10^3
	2e	5.18×10^2	4.99×10^2
	2f	1.62×10^1	1.66×10^1
 1c 14.48 / 0.71	2a	1.46×10^5	1.98×10^5
	2b	7.54×10^4	6.62×10^4
	2c	8.06×10^3	1.15×10^4
	2d	4.61×10^3	3.73×10^3
	2e	1.50×10^3	1.42×10^3
	2f	5.01×10^1	4.30×10^1
 1d 15.68 / 0.65	2a	3.83×10^5	4.26×10^5
	2b	2.02×10^5	1.56×10^5
	2c	2.29×10^4	3.15×10^4
	2d	1.31×10^4	1.12×10^4
	2e	5.05×10^3	4.63×10^3
	2f	1.82×10^2	1.88×10^2
 1e 18.42 / 0.65	2e	2.28×10^5	2.80×10^5
	2h	5.16×10^1	4.83×10^1
	2i	3.27×10^1	3.17×10^1
	2l	5.96×10^4	4.12×10^4
	2r	2.81	3.07

Table 2: (Continued).

Nucleophile N/s^a	Electrophile	k_2^{exp}	$k_2^{\text{calcd } b}$
 1f 21.07 / 0.68	2j	3.97×10^2	3.72×10^2
	2m	1.77×10^5	1.28×10^5
	2p	3.70×10^5	4.48×10^5
	2r	1.51×10^2	2.05×10^2
	2s	9.69×10^1	1.11×10^2
	2t	3.48×10^1	2.64×10^1
 1g 21.29 / 0.47	2d	1.63×10^5	3.67×10^5
	2e	6.38×10^4	1.94×10^5
	2e	$6.36 \times 10^4^c$	1.94×10^5
	2f	1.65×10^4	1.91×10^4
	2g	3.53×10^3	5.16×10^3
	2h	2.19×10^2	3.68×10^2
	2i	1.36×10^2	2.72×10^2
	2j	3.51×10^1	7.59×10^1
	2k	1.82×10^1	3.92×10^1
	2m	8.27×10^3	4.30×10^3
	2n	2.47×10^3	1.28×10^3
	2p	3.27×10^4	1.02×10^4
	2q	9.55×10^3	3.17×10^3
	2r	7.84×10^1	5.03×10^1
2u	6.69×10^3	5.69×10^3	
 1h (15.85 / 0.61) ^d	2l	2.41×10^3	5.80×10^2
	2m	1.14×10^2	2.49×10^1
	2o	1.06×10^4	2.20×10^3

^a Nucleophilicity parameters N and s derived by using eq 1, determination see below. ^b Calculated by using eq 1 and the N and s parameters for the ylides **1** (column 1 of this Table) as well as the electrophilicity parameters E for the benzhydrylium ions **2a–e** and the Michael acceptors **2f–v** (see Table 1). ^c Deprotonation of the conjugate CH acid $\text{Me}_3\text{SO}^+ \Gamma$ with 0.482 equiv of $\text{KO}t\text{Bu}$ (for details see Experimental Section). ^d Taken from ref 10.

3 Discussion

Correlation Analysis. In order to determine the nucleophile-specific parameters N and s of the sulfur ylides **1a–g**, the second-order rate constants ($\log k_2$) of their reactions with the electrophiles **2** (see Table 2) were plotted against the electrophilicity parameters E of **2a–v**, which have previously been derived from the rates of the reactions of **2a–v** with electron-rich ethylenes and carbanions.^[9b–d,g–i,k] In Figure 1 these correlations are shown exemplarily for the stabilized sulfur ylides **1b,d** and the semistabilized sulfur ylides **1e,f**. The correlations for the other nucleophiles investigated in this work (**1a,c,g**) are of similar quality (see Table 2 and Experimental Section) and allow the calculation of the nucleophile-specific parameters N and s , which are listed in Table 2. The small deviations between the calculated and experimental rate constants in Table 2 (72 % less than a factor of 1.5, 87 % less than a factor of 3.0, and 100 % less than a factor of 5) confirms that the rate-determining step of these reactions is analogous to that from which the electrophilicity parameters E of **2a–v** have been derived. The same electrophilicity parameters E of carbocations and Michael acceptors, which have previously been demonstrated to be suitable for predicting the rates of their reactions with aliphatic and aromatic π -systems, carbanions, hydride donors, phosphines, and amines^[8,9] have thus been found to be also suitable for predicting the rates of their reactions with stabilized and semistabilized sulfur ylides.

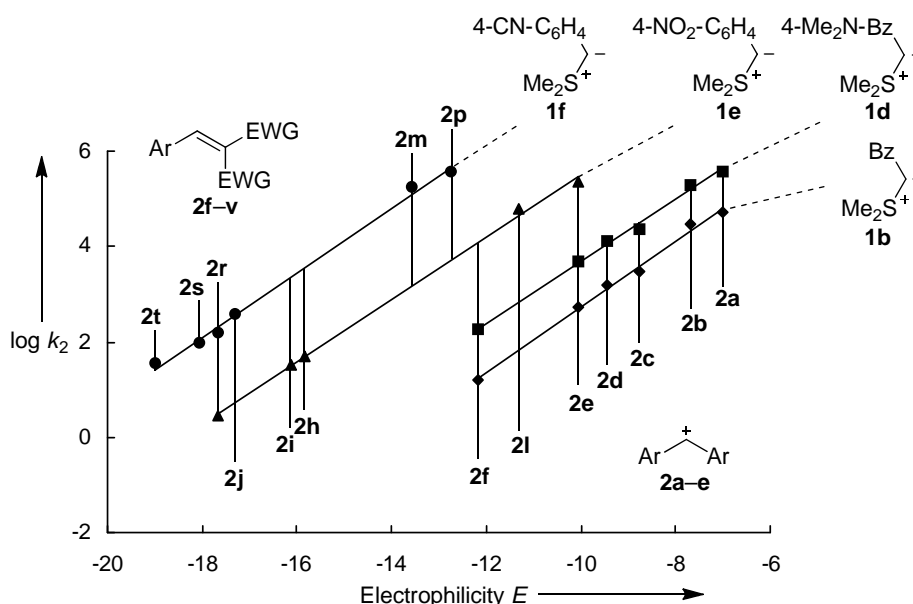


Figure 1: Plots of $\log k_2$ for the reactions of the stabilized sulfur ylides **1b,d** and the semistabilized sulfur ylides **1e,f** with the electrophiles **2** (in DMSO at 20°C) versus the electrophilicity parameters E of **2**. For the sake of clarity, the correlation lines for the ylides **1a,c,g** are only shown in the Experimental Section.

The similarities of the slopes of the correlations for the dimethylsulfonium ylides **1a–f** (Figure 1 and Experimental Section), which are numerically expressed by the *s* parameters in Table 2, imply that the relative nucleophilicities of the dimethylsulfonium ylides **1a–f** depend only slightly on the electrophilicity of the reaction partners. Consequently, the *N* parameters can be used to compare the relative reactivities of these compounds (Figure 2). The considerably lower *s* parameter for the dimethylsulfoxonium ylide **1g** indicates that the rates of its reactions are less influenced by a change of the electrophilicity of the reaction partners than the corresponding reactions of the dimethylsulfonium ylides **1a–f**. As a consequence, the relative reactivities of dimethylsulfonium ylides **1a–f** in comparison to dimethylsulfoxonium ylide **1g** depend on the electrophilicity of the reaction partner.

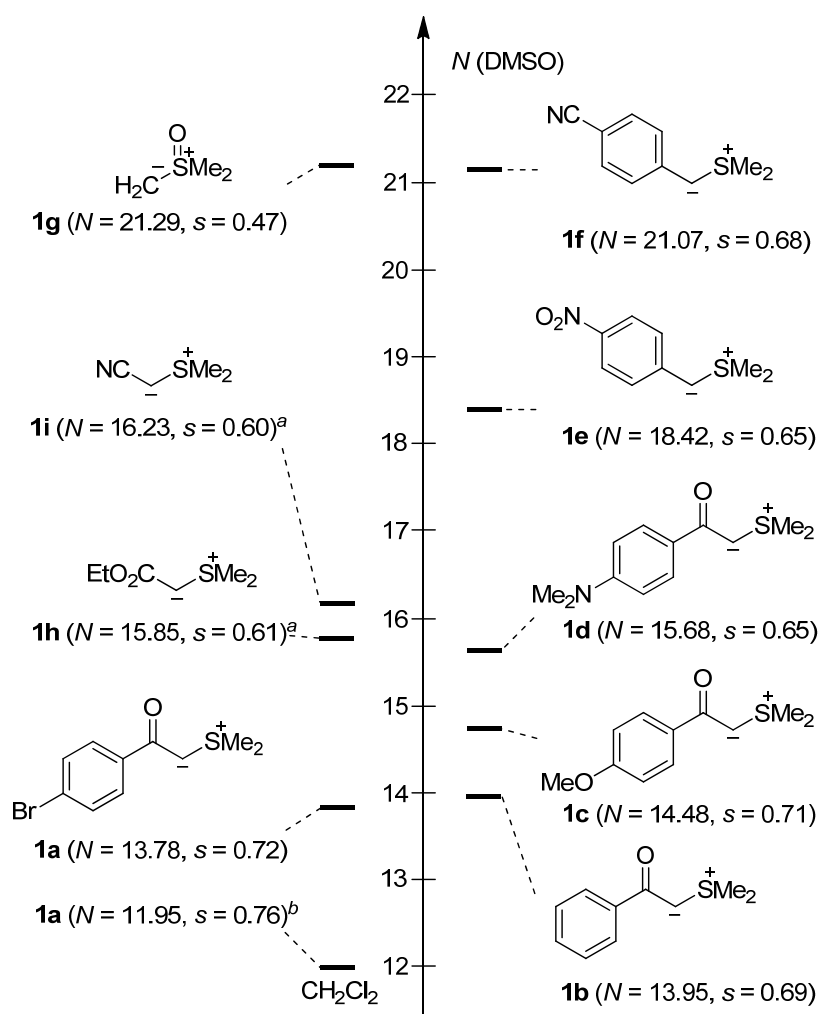


Figure 2: Comparison of the nucleophilicity parameters *N* (in DMSO at 20°C) of stabilized sulfur ylides (**1a–d,h,i**) and semistabilized sulfur ylides (**1e–g**). ^a Taken from ref 10. ^b Taken from ref 12.

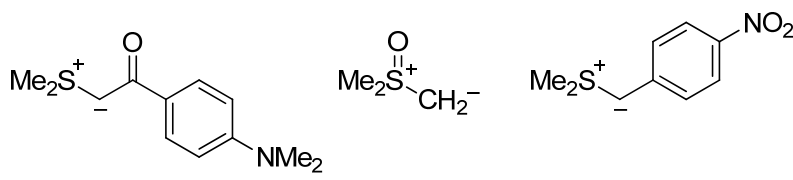
Structure-Reactivity Relationships. As shown in Figure 2, the nucleophilic reactivities of the sulfur ylides **1a–i** in DMSO cover a range of seven orders of magnitude.

The reactivities of the benzoyl-stabilized ylides **1a–d**, which are the least reactive species in this series, correlate moderately with Hammett's σ_p as shown on p. 171 in the Experimental Section. For $s = 0.7$, one derives a Hammett reaction constant of $\rho = -1.3$ which indicates a moderate increase of reactivity by electron-donating substituents.

The ethoxycarbonyl- and cyano-substituted ylides **1h** and **1i** show nucleophilic reactivities, which lie in between those of benzoyl- and aryl-substituted ylides. The semistabilized ylides **1e,f** are the strongest nucleophiles in this series despite the presence of strongly electron-withdrawing groups at the *p*-position of the phenyl ring.

As the nucleophile-specific slope parameter s of the dimethylsulfoxonium ylide **1g** differs significantly from those of the dimethylsulfonium ylides **1a–f,h,i**, the relative nucleophilic reactivities of these different types of sulfur ylides have to be compared with respect to a certain reaction partner. Scheme 7 thus shows that **1g** reacts 13 times faster with the benzhydrylium ion **2e** than the most reactive benzoyl-stabilized ylide **1d**, but 3 times more slowly than the benzylic ylide **1e**. In reactions with the weaker electrophile **2h**, **1g** exceeds the reactivity of the benzoyl-substituted sulfur ylide **1d** by more than 10^2 and is even more reactive than the aryl-stabilized sulfur ylide **1e** (Scheme 7).

Scheme 7. Relative Reactivities of the Nucleophiles **1d,e,g** towards the Benzhydrylium Ion **2e** and the Quinone Methide **2h** (DMSO, 20°C).



	1d	1g	1e
k_{rel} (toward 2e)	1.0	13	45
k_{rel} (toward 2h)	1.0 ^a	274	65

^a Absolute rate constant ($k_2 = 0.799 \text{ M}^{-1} \text{ s}^{-1}$) calculated by eq 1 using $N = 15.68$ and $s = 0.65$ for ylide **1d** as well as the electrophilicity parameters $E = -15.83$ for the electrophile **2h**.

As indicated in Figure 2, the sulfur ylide **1a** is significantly more nucleophilic in DMSO ($\epsilon = 46.45$)¹³ than in CH_2Cl_2 ($\epsilon = 8.93$)¹³ solution.¹² Obviously, the formation of a sulfonium ion from a delocalized benzhydrylium ion and a sulfur ylide is accompanied by a significant

localization of charge; as a result the rates of the reactions of **1a** with benzhydrylium ions increase with increasing solvent polarity.

Figure 3 compares the nucleophilic reactivities of ethoxycarbonyl- and *p*-nitro-phenyl-stabilized sulfur ylides with those of analogously substituted carbanions. Both columns show that Me_2S^+ substitution reduces the nucleophilicity of a carbanionic center more than a cyano group. The right column indicates that a nitro group reduces the reactivity even more than a dimethylsulfonium group. It should be noted, however, that relative stabilizing effects of different groups thus derived, cannot be generalized, because geminal substituent effects are not strictly additive.

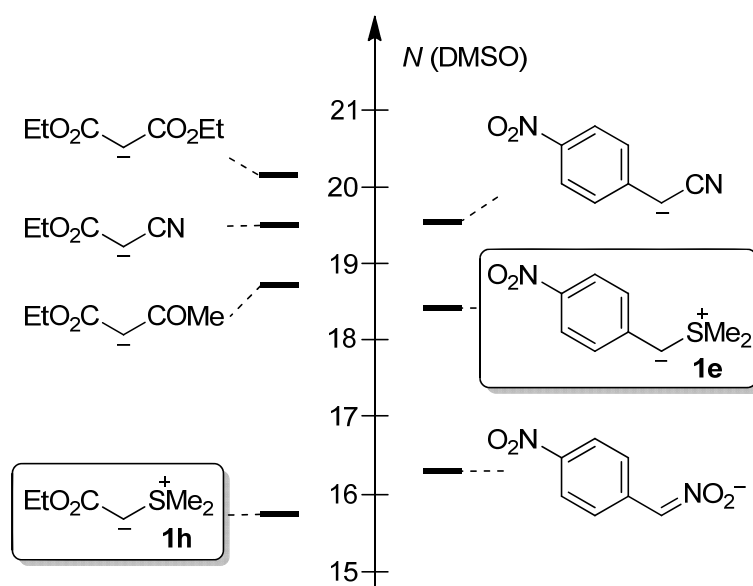


Figure 3. Comparison of the nucleophilic reactivities of different ethoxycarbonyl- and *p*-nitro-phenyl-stabilized carbanions and sulfur ylides in DMSO at 20°C.

A rather poor correlation is found between the nucleophilic reactivities of different classes of carbanions and ylides^[8,9c,14] and their $\text{p}K_{\text{aH}}$ values^[7c,15] (Figure 6 in the Experimental Section). Thus Brønsted basicities are also a poor guide for the prediction of nucleophilicities for ylides, as previously shown for acceptor-stabilized carbanions^[8] as well as for amide and imide anions.^[16]

4 Conclusion

Though the reactions of sulfur ylides with carbocations (see Schemes 3 and 4) yield products which differ from those obtained with Michael acceptors (see Schemes 5 and 6), the rate constants for both types of reactions lie on the same correlation lines (Table 2 and Figure 1),

which allow us to include sulfur ylides into the nucleophilicity scale on the basis of eq 1 (Figure 4).

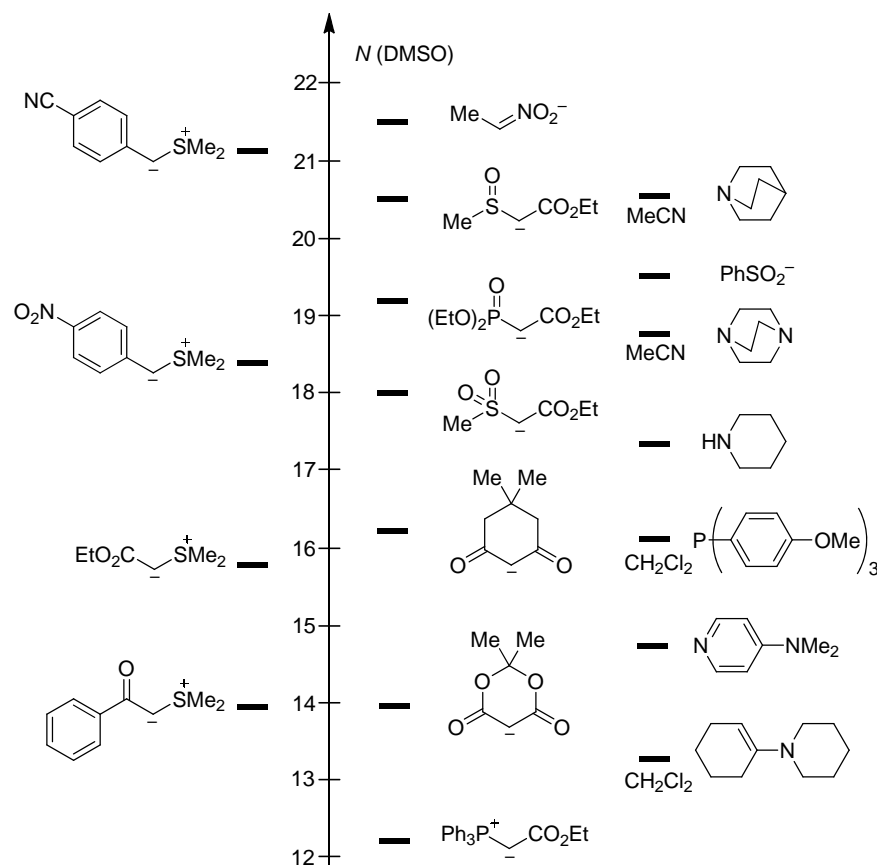


Figure 4: Comparison of the nucleophilicity parameters N (in DMSO at 20°C) of different sulfur ylides with other classes of nucleophiles (data referring to other solvents are marked).

The common correlation lines for carbocations and Michael acceptors furthermore imply that the rate-determining step of the investigated sulfur ylide-mediated cyclopropanations is the same as that for additions of sulfur ylides to carbocations. These findings are in line with a stepwise or highly asynchronous mechanism for the cyclopropanation of Michael acceptors with sulfur ylides, in which the formation of the first CC bond is rate-determining.^[5b,e] As a consequence, eq 1 and the derived nucleophilicity parameters N (and s) of sulfur ylides **1** can efficiently predict the rates of their reactions with Michael acceptors of known electrophilicity E . As previous mechanistic investigations have shown that cyclopropanation reactions with sulfur ylides usually proceed with rate-determining addition steps, followed by fast cyclizations (sometimes accompanied by preceding fast proton-transfer reactions),^[5b,e] the rule of thumb that nucleophile-electrophile combinations at room temperature only occur when $E + N > -5$ can be employed^[9c] to predict whether a certain cyclopropanation reaction is likely to take place.

5 Experimental Section

5.1 General

Chemicals. Sulfur ylides **1a–d,h** were obtained from the corresponding 2-bromoacetophenones or ethyl bromoacetate and dimethylsulfide according to literature procedures.^[2j,n,17]

Analytical data for **1d**: Mp. (*n*-pentane/CH₂Cl₂): >107°C (decomp.). ¹H-NMR (CDCl₃, 300 MHz): δ = 2.96 (s, 12 H, NMe₂, S⁺Me₂), 4.21 (brs, 1 H, S⁺CH⁻), 6.64 (d, 2 H, *J* = 8.9 Hz, CH_{aryl}), 7.71 (d, 2 H, *J* = 8.6 Hz, CH_{aryl}). ¹³C-NMR (CDCl₃, 75.5 MHz): δ = 28.9 (q, S⁺Me₂), 40.3 (q, NMe₂), 47.9 (d, S⁺CH⁻), 111.1 (d, C_{aryl}), 127.6 (d, C_{aryl}), 128.9 (s, C_{aryl}), 151.5 (s, C_{aryl}), 183.4 (s, CO). HR-MS (ESI⁺) [M+H]⁺: calcd for [C₁₂H₁₈NOS]⁺: 224.1103, found 224.1102.

The sulfonium tetrafluoroborates (**1e,f-H**)-BF₄ were prepared according to a procedure for benzyldimethylsulfonium tetrafluoroborate.^[18]

Analytical data for (**1e-H**)-BF₄: Mp. (Et₂O/acetone): 137-139°C. ¹H-NMR (DMSO-*d*₆, 400 MHz): δ = 2.84 (s, 6 H, S⁺Me₂), 4.77 (s, 2 H, CH₂), 7.74 (d, 2 H, *J* = 8.8 Hz, CH_{aryl}), 8.34 (d, 2 H, *J* = 8.8 Hz, CH_{aryl}). ¹³C-NMR (DMSO-*d*₆, 101 MHz): δ = 24.0 (q, S⁺Me₂), 44.7 (t, CH₂), 124.2 (d, C_{aryl}), 132.0 (d, C_{aryl}), 135.8 (s, C_{aryl}), 148.0 (s, C_{aryl}). HR-MS (ESI⁻) [M+BF₄]⁻: calcd for [C₉H₁₂B₂F₈NO₂S]⁻: 372.0653, found 372.0650.

Analytical data for (**1f-H**)-BF₄: Mp. (Et₂O/acetone): 124-126°C. ¹H-NMR (DMSO-*d*₆, 400 MHz): δ = 2.82 (s, 6 H, S⁺Me₂), 4.71 (s, 2 H, CH₂), 7.66 (d, 2 H, *J* = 8.4 Hz, CH_{aryl}), 7.96 (d, 2 H, *J* = 8.3 Hz, CH_{aryl}). ¹³C-NMR (DMSO-*d*₆, 101 MHz): δ = 23.9 (q, S⁺Me₂), 45.0 (t, CH₂), 112.2 (s, C_{aryl}), 118.2 (s, CN), 131.5 (d, C_{aryl}), 133.0 (d, C_{aryl}), 133.8 (s, C_{aryl}). MS (EI): *m/e* (%) = 265 (<1) [M]⁺, 230 (10), 229 (7), 163 (33), 162 (35), 146 (5), 135 (12), 134 (19), 117 (13), 116 (100), 89 (13), 62 (13), 61 (9), 49 (11), 47 (10), 44 (6). HR-MS (EI) [M]⁺: calcd for [C₁₀H₁₂BF₄NS]⁺: 265.0714, found 265.0719. HR-MS (ESI⁻) [M+BF₄]⁻: calcd for [C₁₀H₁₂B₂F₈NS]⁻: 352.0754, found 352.0761.

The Michael acceptors **2l–v** have also been prepared by known procedures.^[19] Benzydrylium tetrafluoroborates^[9b] (**2a–e**)-BF₄ and quinone methides^[8a,20] **2f–k** were prepared as described

before. All other chemicals were purchased from commercial sources and (if necessary) purified by recrystallization or distillation prior to use.

Analyticals. ^1H - and ^{13}C -NMR spectra were recorded on Varian NMR-systems (300, 400, or 600 MHz) in CDCl_3 or $\text{DMSO-}d_6$ and the chemical shifts in ppm refer to TMS (δ_{H} 0.00, δ_{C} 0.00), CDCl_3 (δ_{H} 7.26, δ_{C} 77.0), or $\text{DMSO-}d_6$ (δ_{H} 2.50, δ_{C} 39.43) as internal standard. The following abbreviations were used for chemical shift multiplicities: brs = broad singlet, s = singlet, d = doublet, t = triplet, q = quartet, m = multiplet. For reasons of simplicity, the ^1H -NMR signals of AA'BB'-spin systems of *p*-disubstituted aromatic rings were treated as doublets. NMR signal assignments were based on additional 2D-NMR experiments (e.g., COSY-, NOESY-, HSQC-, and HMBC experiments). Diastereomeric ratios (*dr*) were determined by ^1H -NMR. (HR-)MS were performed on a Finnigan MAT 95 (EI) or a Thermo Finnigan LTQ FT (ESI) mass spectrometer. Melting points were determined on a Büchi B-540 device and are not corrected.

Kinetics. All kinetic investigations were performed in DMSO solution (H_2O content < 50 ppm) at 20°C. Kinetic experiments with the stabilized ylides **1a–d,h** were carried out with freshly prepared solutions of the ylides in DMSO. As the aryl-stabilized sulfur ylides **1e,f** are only persistent for a short time at room temperature, they were prepared by deprotonation of the corresponding CH acids (**1e,f-H**)- BF_4 in dry THF at $\leq -50^\circ\text{C}$ with 1.00-1.05 equiv of $\text{KO}t\text{Bu}$. Small amounts of these solutions were dissolved in DMSO at room temperature directly before each kinetic experiment. Stable stock solutions of dimethylsulfoxonium methylide (**1g**) were prepared by deprotonation of trimethylsulfoxonium iodide ($\text{Me}_3\text{SO}^+ \Gamma$) with 1.00-1.05 equiv of $\text{KO}t\text{Bu}$ in DMSO at room temperature. In order to confirm that $\text{Me}_3\text{SO}^+ \Gamma$ was quantitatively deprotonated under these conditions, the kinetic study of the reaction of **1g** with **2e** was repeated by using only 0.482 equiv of $\text{KO}t\text{Bu}$ for the deprotonation of $\text{Me}_3\text{SO}^+ \Gamma$. In these experiments, in which the concentration of the ylide **1g** corresponds to the amount of $\text{KO}t\text{Bu}$ used, a second-order rate constant was obtained, which agreed within <1 % with that obtained with a slight excess of $\text{KO}t\text{Bu}$ (see Table 2).

All kinetic investigations were monitored photometrically, either by following the disappearance of the colored electrophiles **2** or of the colored aryl-stabilized sulfur ylides **1e,f** at or close to their absorption maxima. All reactions of the sulfur ylides **1a–d,g,h** with **2** were performed under first-order conditions using at least 10 equiv of **1a–d,g,h**. Vice versa, the first-order kinetics for the reactions of the aryl-stabilized ylides **1e,f** with **2** were realized by

using at least 10 equiv of the electrophiles **2**. As the absolute concentration of the minor component is not crucial for the determination of the pseudo-first-order rate constants k_{obs} (eqs 2 and 3), we have thus circumvented the problem that the absolute concentrations of the semistabilized ylides **1e,f** cannot precisely be determined due to their low stability.

From the exponential decays of the UV-Vis absorbances of the electrophiles **2** (Figure 5) or of the sulfur ylides **1e,f**, the first-order rate constants k_{obs} were obtained. Plots of k_{obs} (s^{-1}) against the concentrations of the reaction partners used in excess were linear with negligible intercepts as required by the relation $k_{\text{obs}} = k_2[\text{Nu}]_0$ (eq 2, Figure 5) or $k_{\text{obs}} = k_2[\text{E}]_0$ (eq 3), respectively. Therefore, the slopes of these linear correlations yielded the second-order rate constants of the corresponding reactions.

$$-d[\text{E}]/dt = k_2 [\text{Nu}] [\text{E}] \quad \text{for } [\text{Nu}]_0 \gg [\text{E}]_0 \Rightarrow k_{\text{obs}} = k_2 [\text{Nu}]_0 \quad (2)$$

$$-d[\text{Nu}]/dt = k_2 [\text{Nu}] [\text{E}] \quad \text{for } [\text{E}]_0 \gg [\text{Nu}]_0 \Rightarrow k_{\text{obs}} = k_2 [\text{E}]_0 \quad (3)$$

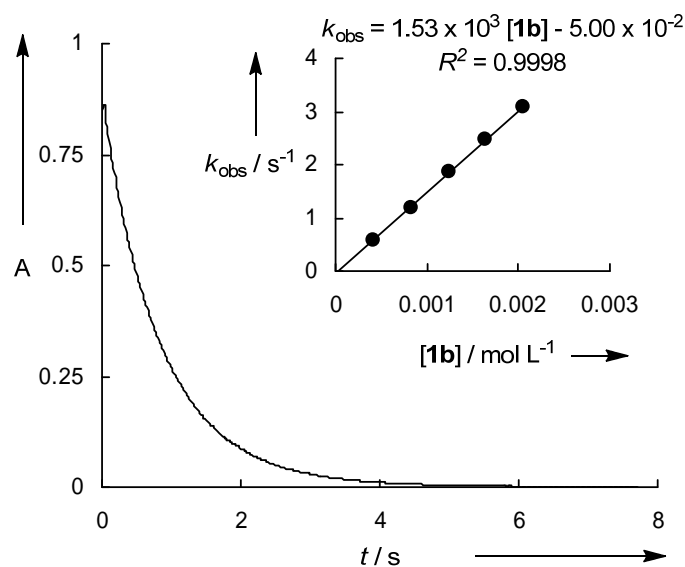


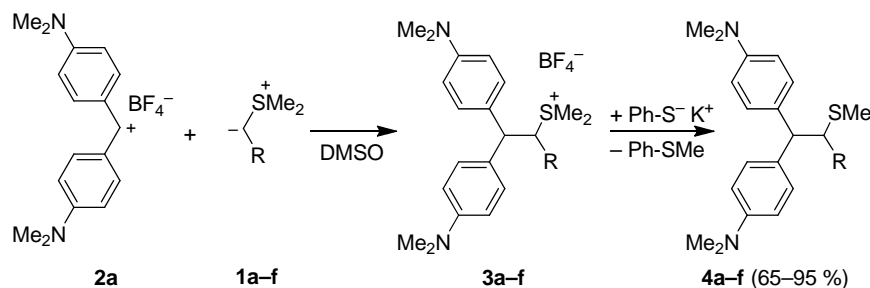
Figure 5: UV-Vis spectroscopic monitoring of the reaction of the benzoyl-stabilized sulfur ylide **1b** ($8.24 \times 10^{-4} \text{ mol L}^{-1}$) with the benzhydrylium ion **2d** ($1.05 \times 10^{-5} \text{ mol L}^{-1}$) at 632 nm in DMSO at 20°C. Insert: Determination of the second-order rate constant $k_2 = 1.53 \times 10^3 \text{ L mol}^{-1} \text{ s}^{-1}$ from the dependence of the first-order rate constant k_{obs} on the concentration of **1b**.

The rates of slow reactions ($\tau_{1/2} > 15\text{-}20 \text{ s}$) were determined by using a J&M TIDAS diode array spectrophotometer controlled by Labcontrol Spectacle software and connected to a Hellma 661.502-QX quartz Suprasil immersion probe (5 mm light path) via fiber optic cables and standard SMA connectors. For the evaluation of fast kinetics ($\tau_{1/2} < 15\text{-}20 \text{ s}$) the stopped-flow spectrophotometer systems Hi-Tech SF-61DX2 or Applied Photophysics SX.18MV-R

were used. First-order rate constants k_{obs} (s^{-1}) were obtained by fitting the single exponential $A_t = A_0 \exp(-k_{\text{obs}}t) + C$ (exponential decrease) to the observed time-dependent absorbance (averaged from at least 3 kinetic runs for each nucleophile concentration in case of the stopped-flow method).

5.2 Product Analysis

5.2.1 Reactions of the Ylides **1** with the Benzhydrylium Ion **2a**

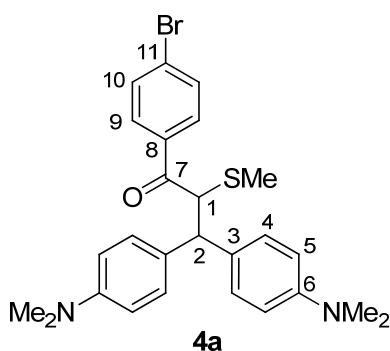


Product studies for the reactions of the stabilized sulfur ylides **1a–d** with the reference electrophile **2a** in DMSO

General Procedure A. Reactions of the nucleophiles **1a–d** with the electrophile **2a** were carried out by dissolving the ylides **1a–d** and the benzhydrylium tetrafluoroborate (**2a**)-BF₄ in dry DMSO (2–3 mL) at room temperature. The resulting mixture was stirred until complete decolorization occurred (usually < 1 min) and subsequently treated with a mixture of thiophenol (50 μL , 0.49 mmol) and KO^tBu (37 mg, 0.33 mmol) in dry DMSO (2–3 mL). After 10 min of stirring, the reaction was quenched by the addition of water and extracted with CH₂Cl₂. The combined organic layers were washed with water and brine, dried over Na₂SO₄ and evaporated under reduced pressure. The crude products were purified by column chromatography on silica gel (*n*-pentane/EtOAc) and subsequently characterized by ¹H- and ¹³C-NMR spectroscopy and MS. Signal assignments were based on additional COSY, HSQC and HMBC experiments. Small samples of solid products were recrystallized in appropriate solvent mixtures for the determination of melting points.

1-(4-Bromophenyl)-3,3-bis(4-(dimethylamino)phenyl)-2-(methylthio)propan-1-one (4a) was obtained from 1-(4-bromophenyl)-2-(dimethyl- λ^4 -sulfanylidene)-ethanone **1a** (73.0 mg, 282 μmol) and (**2a**)-BF₄ (94.2 mg, 277 μmol) as yellow solid (131 mg, 263 μmol , 95 %).

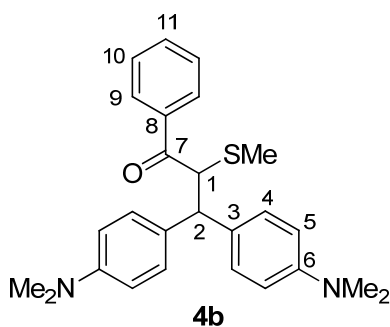
RAP 18.1



R_f (*n*-pentane/EtOAc 4:1, *v/v*): 0.30. Mp. (Et₂O/CH₂Cl₂): 190-192°C. ¹H-NMR (CDCl₃, 599 MHz): δ = 1.91 (s, 3 H, SCH₃), 2.80 (s, 6 H, N(CH₃)₂), 2.91 (s, 6 H, N(CH₃)₂), 4.47 (d, 1 H, *J* = 11.8 Hz, 2-H), 4.82 (d, 1 H, *J* = 11.8 Hz, 1-H), 6.55 (d, 2 H, *J* = 6.8 Hz, 5-H), 6.73 (d, 2 H, *J* = 6.6 Hz, 5-H), 7.09 (d, 2 H, *J* = 8.8 Hz, 4-H), 7.25 (d, 2 H, *J* = 8.5 Hz, 4-H, superimposed by CDCl₃ residual signal), 7.55 (d, 2 H, *J* = 8.7 Hz, 10-H), 7.79 (d, 2 H, *J* = 8.7 Hz, 9-H). ¹³C-NMR (CDCl₃, 151 MHz): δ = 11.5 (q, SCH₃), 40.7 (q, 2 × N(CH₃)₂), 47.5 (d, C-2), 50.5 (d, C-1), 112.8 (d, C-5), 113.0 (d, C-5), 127.7 (s, C-11), 128.1 (d, C-4), 128.8 (d, C-4), 129.8 (d, C-9), 130.3 (s, C-3, broadened signal), 131.5 (s, C-3, broadened signal), 131.8 (d, C-10), 135.4 (s, C-8), 148.8 (s, C-6, broadened signal), 149.0 (s, C-6, broadened signal), 191.8 (s, C-7). MS (EI): *m/e* (%) = 496 (<1) [M]⁺, 266 (4), 254 (17), 253 (100), 237 (8). HR-MS (EI) [M]⁺: calcd for [C₂₆H₂₉BrN₂OS]⁺: 496.1179, found 496.1182.

3,3-Bis(4-(dimethylamino)phenyl)-2-(methylthio)-1-phenylpropan-1-one (4b) was obtained from 2-(dimethyl-λ⁴-sulfanylidene)-1-phenyl-ethanone **1b** (50.0 mg, 277 μmol) and (2a)-BF₄ (94.2 mg, 277 μmol) as pale yellow solid (99 mg, 0.24 mmol, 87 %).

RAP 16.1

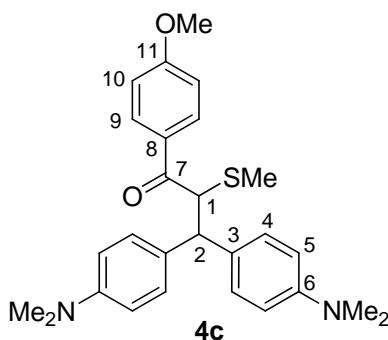


R_f (*n*-pentane/EtOAc 4:1, *v/v*): 0.19. Mp. (*n*-pentane/CH₂Cl₂): 164-165°C. ¹H-NMR (CDCl₃, 300 MHz): δ = 1.93 (s, 3 H, SCH₃), 2.79 (s, 6 H, N(CH₃)₂), 2.91 (s, 6 H, N(CH₃)₂), 4.49 (d, 1 H, *J* = 11.8 Hz, 2-H), 4.91 (d, 1 H, *J* = 11.8 Hz, 1-H), 6.53 (d, 2 H, *J* = 8.7 Hz, 5-H), 6.71

(d, 2 H, $J = 8.7$ Hz, 5-H), 7.12 (d, 2 H, $J = 8.8$ Hz, 4-H), 7.27 (d, 2 H, $J = 9.1$ Hz, 4-H, superimposed by CDCl_3 residual signal), 7.39-7.44 (m, 2 H, 10-H), 7.48-7.53 (m, 1 H, 11-H), 7.92-7.95 (m, 2 H, 9-H). ^{13}C -NMR (CDCl_3 , 75.5 MHz): $\delta = 11.4$ (q, SCH_3), 40.6 (q, $2 \times \text{N}(\text{CH}_3)_2$), 47.5 (d, C-2), 50.4 (d, C-1), 112.6 (d, C-5), 112.9 (d, C-5), 128.1 (d, C-4), 128.2 (d, C-9), 128.5 (d, C-10), 128.8 (d, C-4), 130.5 (s, C-3), 131.5 (s, C-3), 132.6 (d, C-11), 136.6 (s, C-8), 148.9 (s, C-6), 149.1 (s, C-6), 192.8 (s, C-7). MS (EI): m/e (%) = 418 (<1) $[\text{M}]^+$, 266 (4), 254 (17), 253 (100), 237 (9), 127 (4), 126 (5). HR-MS (EI) $[\text{M}]^+$: calcd for $[\text{C}_{26}\text{H}_{30}\text{N}_2\text{OS}]^+$: 418.2073, found 418.2079. HR-MS (ESI $^+$): calc. for $[\text{C}_{26}\text{H}_{31}\text{N}_2\text{OS}]^+$: 419.2151, found 419.2139.

3,3-Bis(4-(dimethylamino)phenyl)-1-(4-methoxyphenyl)-2-(methylthio)propan-1-one (4c) was obtained from 2-(dimethyl- λ^4 -sulfanylidene)-1-(4-(methoxy)phenyl)-ethanone **1c** (60.0 mg, 285 μmol) and (**2a**)- BF_4 (94.2 mg, 277 μmol) as yellow solid (111 mg, 247 μmol , 89 %).

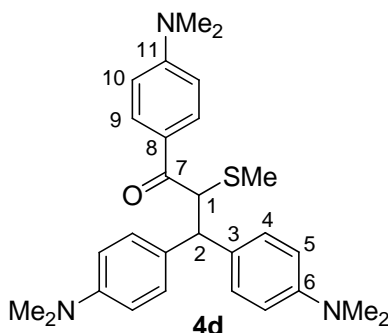
RAP 19.1



R_f (*n*-pentane/EtOAc 3:1, v/v): 0.18. Mp. (*n*-pentane/Et $_2$ O): $> 130^\circ\text{C}$ (decomp.). ^1H -NMR (CDCl_3 , 599 MHz): $\delta = 1.92$ (s, 3 H, SCH_3), 2.78 (s, 6 H, $\text{N}(\text{CH}_3)_2$), 2.90 (s, 6 H, $\text{N}(\text{CH}_3)_2$), 3.83 (s, 3 H, OCH_3), 4.50 (d, 1 H, $J = 11.7$ Hz, 2-H), 4.88 (d, 1 H, $J = 11.7$ Hz, 1-H), 6.51 (d, 2 H, $J = 8.7$ Hz, 5-H), 6.70 (d, 2 H, $J = 8.7$ Hz, 5-H), 6.89 (d, 2 H, $J = 8.9$ Hz, 10-H), 7.11 (d, 2 H, $J = 8.8$ Hz, 4-H), 7.26 (d, 2 H, $J = 8.7$ Hz, 4-H), 7.94 (d, 2 H, $J = 8.9$ Hz, 9-H). ^{13}C -NMR (CDCl_3 , 151 MHz): $\delta = 11.6$ (q, SCH_3), 40.58 (q, $\text{N}(\text{CH}_3)_2$), 40.61 (q, $\text{N}(\text{CH}_3)_2$), 47.7 (d, C-2), 50.0 (d, C-1), 55.4 (q, OCH_3), 112.6 (d, C-5), 112.9 (d, C-5), 113.7 (d, C-10), 128.1 (d, C-4), 128.8 (d, C-4), 129.4 (s, C-8), 130.5 (d, C-9), 130.7 (s, C-3), 131.6 (s, C-3), 148.9 (s, C-6), 149.2 (s, C-6), 163.2 (s, C-11), 191.8 (s, C-7). MS (EI): m/e (%) = 448 (<1) $[\text{M}]^+$, 254 (18), 253 (100), 237 (8), 135 (4). HR-MS (EI) $[\text{M}]^+$: calcd for $[\text{C}_{27}\text{H}_{32}\text{N}_2\text{O}_2\text{S}]^+$: 448.2180, found 448.2186.

1,3,3-Tris(4-(dimethylamino)phenyl)-2-(methylthio)propan-1-one (4d) was obtained from 1-(4-dimethylamino-phenyl)-2-(dimethyl- λ^4 -sulfanylidene)-ethanone **1d** (63.0 mg, 282 μ mol) and (**2a**)-BF₄ (94.2 mg, 277 μ mol) as yellow solid (106 mg, 230 μ mol, 83 %).

RAP 17.1



R_f (*n*-pentane/EtOAc 3:1, *v/v*): 0.11. Mp. (*n*-pentane/EtOAc): >200°C (decomp.). ¹H-NMR (CDCl₃, 300 MHz): δ = 1.93 (s, 3 H, SCH₃), 2.78 (s, 6 H, N(CH₃)₂), 2.90 (s, 6 H, N(CH₃)₂), 3.03 (s, 6 H, N(CH₃)₂), 4.52 (d, 1 H, *J* = 11.7 Hz, 2-H), 4.89 (d, 1 H, *J* = 11.7 Hz, 1-H), 6.52 (d, 2 H, *J* = 8.8 Hz, 5-H), 6.63 (d, 2 H, *J* = 9.1 Hz, 10-H), 6.70 (d, 2 H, *J* = 8.8 Hz, 5-H), 7.12 (d, 2 H, *J* = 8.7 Hz, 4-H), 7.26 (d, 2 H, *J* = 8.1 Hz, 4-H, superimposed by CDCl₃ residual signal), 7.90 (d, 2 H, *J* = 9.2 Hz, 9-H). ¹³C-NMR (CDCl₃, 75.5 MHz): δ = 11.8 (q, SCH₃), 40.0 (q, N(CH₃)₂), 40.7 (q, 2 \times N(CH₃)₂), 47.8 (d, C-2), 49.5 (d, C-1), 110.7 (d, C-10), 112.6 (d, C-5), 113.0 (d, C-5), 124.1 (s, C-8), 128.1 (d, C-4), 128.8 (d, C-4), 130.4 (d, C-9), 131.3 (s, C-3), 132.0 (s, C-3), 148.8 (s, C-6), 149.1 (s, C-6), 153.2 (s, C-11), 191.7 (s, C-7). MS (EI): *m/e* (%) = 461 (<1) [M]⁺, 254 (20), 253 (100), 239 (4), 237 (10), 148 (11). HR-MS (EI) [M]⁺: calcd for [C₂₈H₃₅N₃OS]⁺: 461.2496, found 461.2489.

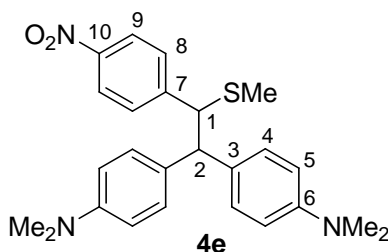
Product studies for the reactions of the semistabilized sulfur ylides **1e,f** with the reference electrophile **2a** in DMSO

General procedure B. The ylides **1e,f** were generated by the addition of KO^{*t*}Bu (dissolved in 2-3 mL DMSO) to a vigorously stirred solution of the sulfonium tetrafluoroborates (**1e,f**)-BF₄ in dry DMSO (2-3 mL) at room temperature. The benzhydrylium tetrafluoroborate (**2a**)-BF₄ (dissolved in 2-3 mL DMSO) was then added in one portion. The resulting mixture was stirred for 1 min and subsequently treated with a mixture of thiophenol (50 μ L, 0.49 mmol) and KO^{*t*}Bu (37 mg, 0.33 mmol) in dry DMSO (2-3 mL). After 10 min of stirring, the reaction was quenched by the addition of water and extracted with CH₂Cl₂. The combined organic layers were washed with water and brine, dried over Na₂SO₄ and evaporated under reduced

pressure. The crude products were purified by column chromatography on silica gel (*n*-pentane/EtOAc) and subsequently characterized by ^1H - and ^{13}C -NMR spectroscopy and MS. Signal assignments were based on additional COSY, HSQC and HMBC experiments. Small samples of the solid products were recrystallized in appropriate solvent mixtures for the determination of melting points.

4,4'-(2-(Methylthio)-2-(4-nitrophenyl)ethane-1,1-diyl)bis(*N,N*-dimethylaniline) (4e) was obtained from dimethyl(4-nitrobenzyl)sulfonium tetrafluoroborate (**1e-H**)-BF₄ (197 mg, 691 μmol), KO t Bu (77.5 mg, 691 μmol) and (**2a**)-BF₄ (94.2 mg, 277 μmol) as a red solid (91 mg, 0.21 mmol, 76 %).

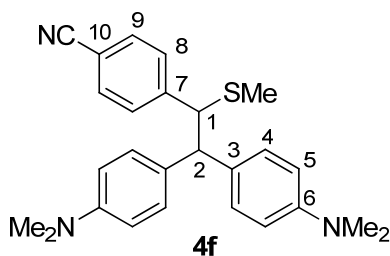
RAP 23.3



R_f (*n*-pentane/EtOAc 4:1, *v/v*): 0.24. Mp. (*n*-pentane/EtOAc): 191-192°C. ^1H -NMR (CDCl₃, 599 MHz): δ = 1.72 (s, 3 H, SCH₃), 2.79 (s, 6 H, N(CH₃)₂), 2.91 (s, 6 H, N(CH₃)₂), 4.14 (d, 1 H, *J* = 11.4 Hz, 2-H), 4.53 (d, 1 H, *J* = 11.4 Hz, 1-H), 6.46 (d, 2 H, *J* = 7.1 Hz, 5-H), 6.72 (d, 2 H, *J* = 6.3 Hz, 5-H), 6.93 (d, 2 H, *J* = 8.7 Hz, 4-H), 7.28 (d, 2 H, *J* = 8.7 Hz, 4-H), 7.42 (d, 2 H, *J* = 8.8 Hz, 8-H), 8.04 (d, 2 H, *J* = 8.8 Hz, 9-H). ^{13}C -NMR (CDCl₃, 151 MHz): δ = 15.0 (q, SCH₃), 40.5 (q, N(CH₃)₂), 40.7 (q, N(CH₃)₂), 56.0 (d, C-2), 56.1 (d, C-1), 112.6 (d, 2 \times C-5), 123.4 (d, C-9), 128.4 (d, C-4), 128.7 (d, C-4), 129.4 (d, C-8), 130.5 (s, 2 \times C-3, broadened signal), 146.4 (s, C-10), 148.7 (s, C-6, broadened signal), 149.2 (s, C-6, broadened signal), 149.9 (s, C-7). HR-MS (ESI⁺) [M+H]⁺: calcd for [C₂₅H₃₀N₃O₂S]⁺: 436.2053, found 436.2038.

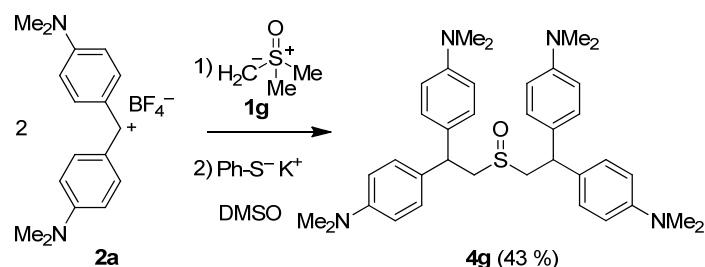
4,4'-(2-(Methylthio)-2-(4-cyanophenyl)ethane-1,1-diyl)bis(*N,N*-dimethylaniline) (4f) was obtained from dimethyl(4-cyanobenzyl)sulfonium tetrafluoroborate (**1f-H**)-BF₄ (265 mg, 1.00 mmol), KO t Bu (113 mg, 1.01 mmol), and (**2a**)-BF₄ (94.2 mg, 277 μmol) as a pale yellow solid (75 mg, 0.18 mmol, 65 %).

RAP 28.1



R_f (*n*-pentane/EtOAc 4:1, *v/v*): 0.19. Mp. (*n*-pentane/EtOAc): 197-198°C. $^1\text{H-NMR}$ (CDCl_3 , 599 MHz): δ = 1.71 (s, 3 H, SCH₃), 2.80 (s, 6 H, N(CH₃)₂), 2.91 (s, 6 H, N(CH₃)₂), 4.10 (d, 1 H, J = 11.4 Hz, 2-H), 4.46 (d, 1 H, J = 11.4 Hz, 1-H), 6.46 (d, 2 H, J = 8.4 Hz, 5-H), 6.71 (d, 2 H, J = 8.4 Hz, 5-H), 6.90 (d, 2 H, J = 8.8 Hz, 4-H), 7.26 (d, 2 H, J = 8.7 Hz, 4-H), 7.36 (d, 2 H, J = 8.4 Hz, 8-H), 7.46 (d, 2 H, J = 8.4 Hz, 9-H). $^{13}\text{C-NMR}$ (CDCl_3 , 151 MHz): δ = 15.0 (q, SCH₃), 40.6 (q, N(CH₃)₂), 40.7 (q, N(CH₃)₂), 55.9 (d, C-2), 56.4 (d, C-1), 110.2 (s, C-10), 112.6 (d, 2 × C-5), 118.9 (s, CN), 128.4 (d, C-4), 128.7 (d, C-4), 129.4 (d, C-8), 130.5 (s, C-3, broadened signal), 130.7 (s, C-3, broadened signal), 131.9 (d, C-9), 147.7 (s, C-7), 148.7 (s, C-6, broadened signal), 149.2 (s, C-6, broadened signal). HR-MS (ESI⁺) [$\text{M}+\text{H}$]⁺: calcd for [C₂₆H₃₀N₃S]⁺: 416.2155, found 416.2141.

Product study for the reaction of dimethylsulfoxonium methylide (**1g**) with the reference electrophile **2a** in DMSO

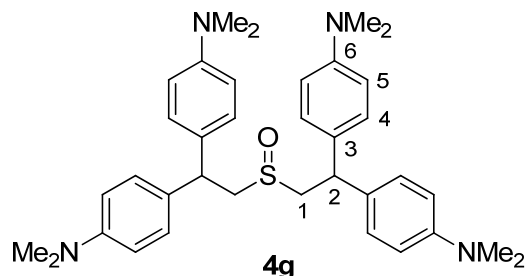


4,4',4'',4'''-(Sulfinylbis(ethane-2,1,1-triyl))tetrakis(*N,N*-dimethylaniline) (**4g**).

Trimethylsulfoxonium iodide ($\text{Me}_3\text{SO}^+\text{I}^-$, 150 mg, 682 μmol) and KO t Bu (76.5 mg, 682 μmol) were dissolved in dry DMSO (5 mL). After the addition of the benzhydrylium tetrafluoroborate (**2a**)-BF₄ (102 mg, 300 μmol , dissolved in 3 mL of DMSO), the reaction mixture was immediately treated with a mixture of thiophenol (50 μL , 0.49 mmol) and KO t Bu (37 mg, 0.33 mmol) in dry DMSO (2-3 mL). After 10 min of stirring, the reaction was quenched by the addition of water and extracted with CH₂Cl₂. The combined organic layers were washed with water and brine, dried over Na₂SO₄ and evaporated under reduced pressure. Purification of the crude product by column chromatography on silica gel (*n*-pentane/EtOAc) furnished **4g** as colorless solid (38 mg, 65 μmol , 43%), which was subsequently

characterized by ^1H - and ^{13}C -NMR spectroscopy and MS. Signal assignments were based on additional COSY, HSQC and HMBC experiments. A small sample of the solid product was recrystallized from *n*-pentane/acetone for the determination of the melting point.

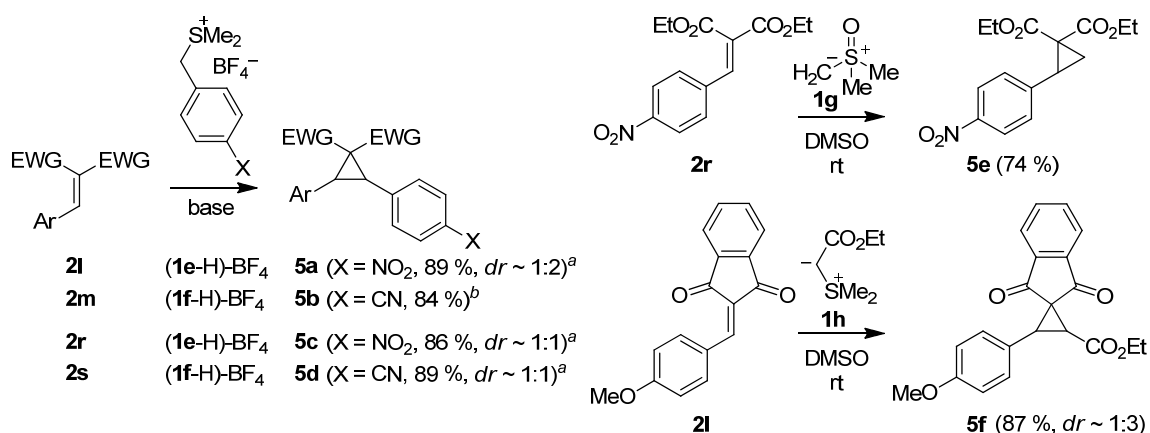
RAP 24.3



R_f (*n*-pentane/EtOAc 1:10, *v/v*): 0.30. Mp. (*n*-pentane/acetone): $>194^\circ\text{C}$ (decomp.). ^1H -NMR (CDCl_3 , 599 MHz): $\delta = 2.90$ (s, 12 H, NMe_2), 2.91 (s, 12 H, NMe_2), 3.26 (d, 4 H, $J = 8.0$ Hz, 1-H), 4.37 (t, 2 H, $J = 8.0$ Hz, 2-H), 6.67 (d, 8 H, $J = 5.7$ Hz, 5-H), 7.01-7.05 (m, 8 H, 4-H). ^{13}C -NMR (CDCl_3 , 151 MHz): $\delta = 40.8$ (q, NMe_2), 43.2 (d, C-2), 60.1 (t, C-1), 113.0 (d, C-5), 128.2 (d, C-4), 128.7 (d, C-4), 130.5 (s, C-3, broadened signal), 131.9 (s, C-3, broadened signal), 149.1 (s, C-6). HR-MS (ESI $^+$) $[\text{M}+\text{Na}]^+$: calcd for $[\text{C}_{36}\text{H}_{46}\text{N}_4\text{NaOS}]^+$: 605.3285; found 605.3291.

5.2.2 Reactions of the Ylides 1 with Different Michael Acceptors

Product studies for the reactions of the semistabilized sulfur ylides **1e–g** and the stabilized sulfur ylide **1h** with the benzylidenemalonates **2r,s** and the benzylideneindandiones **2l,m**

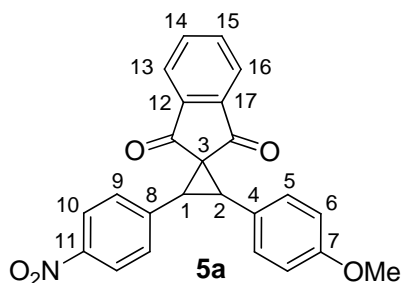


^a Reaction conditions: $\text{KO}t\text{Bu}$, DMSO, rt. ^b Reaction conditions: K_2CO_3 (aq.)/ CHCl_3 , rt; only one diastereomer isolated.

General procedure C. The ylides **1e,f** were generated by the addition of KO t Bu (dissolved in 2-3 mL DMSO) to a vigorously stirred solution of the sulfonium tetrafluoroborates (**1e,f-H**)-BF $_4$ in dry DMSO (2-3 mL) at room temperature. The Michael acceptors **2l,r,s** (dissolved in 2-3 mL of DMSO) were then added in one portion. The resulting mixtures were stirred for 5-10 min at room temperature and subsequently quenched by the addition of water followed by the extraction with CH $_2$ Cl $_2$. The combined organic layers were washed with water and brine, dried over Na $_2$ SO $_4$ and evaporated under reduced pressure. The crude products were purified by column chromatography on silica gel (*n*-pentane/EtOAc) and subsequently characterized by 1 H- and 13 C-NMR spectroscopy and MS. Signal assignments were based on additional COSY, HSQC and HMBC experiments.

2-(4-Methoxyphenyl)-3-(4-nitrophenyl)spiro[cyclopropane-1,2'-indene]-1',3'-dione (5a) was obtained from dimethyl(4-nitrobenzyl)sulfonium tetrafluoroborate (**1e-H**)-BF $_4$ (200 mg, 702 μ mol), KO t Bu (78.8 mg, 702 μ mol), and benzylideneindandione **2l** (92.5 mg, 350 μ mol) as a yellow solid (124 mg, 310 μ mol, 89 %, *dr* ~ 1 : 1.7).

RAP 47.2



1 H-NMR (CDCl $_3$, 599 MHz): δ = 3.78 $^{\#}$ (s, 3 H, OMe), 3.79-3.81 (m, 4 H, OMe * , 1-H $^{\#}$), 3.85 $^{\#}$ (d, 1 H, J = 10.0 Hz, 2-H), 4.12 * (d, 1 H, J = 9.2 Hz, 2-H), 4.17 * (d, 1 H, J = 9.2 Hz, 1-H), 6.79 $^{\#}$ (d, 2 H, J = 8.8 Hz, 6-H), 6.88 * (d, 2 H, J = 8.7 Hz, 6-H), 7.01 $^{\#}$ (d, 2 H, J = 8.7 Hz, 5-H), 7.31 * (d, 2 H, J = 8.6 Hz, 5-H), 7.35 $^{\#}$ (d, 2 H, J = 8.7 Hz, 9-H), 7.56 * (d, 2 H, J = 8.6 Hz, 9-H), 7.77-7.78 * (m, 2 H, 14-H, 15-H), 7.81-7.89 (m, 5 H, 13-H * , 13-H $^{\#}$ or 16-H $^{\#}$, 14-H $^{\#}$, 15-H $^{\#}$, 16-H *), 8.00-8.02 $^{\#}$ (m, 1 H, 13-H or 16-H), 8.08 $^{\#}$ (d, 2 H, J = 8.8 Hz, 10-H), 8.19 * (d, 2 H, J = 8.7 Hz, 10-H). 13 C-NMR (CDCl $_3$, 151 MHz): δ = 41.5 * (d, C-1), 41.8 $^{\#}$ (d, C-1), 42.8 $^{\#}$ (d, C-2), 43.6 * (d, C-2), 45.5 $^{\#}$ (s, C-3), 48.5 * (s, C-3), 55.20 $^{\#}$ (q, OMe), 55.25 * (q, OMe), 113.5 $^{\#}$ (d, C-6), 113.9 * (d, C-6), 122.6, 122.66, 122.70, 122.75, 122.77, 122.78 (s, C-4 $^{\#}$, d, C-10 $^{\#}$, d, C-13 * , d, C-13 $^{\#}$, d, C-16 * , d, C-16 $^{\#}$), 123.5 * (d, C-10), 124.7 * (s, C-4), 130.20 * , 130.24 * (2d, C-5, C-9), 131.9 $^{\#}$, 132.0 $^{\#}$ (2d, C-5, C-9), 135.0 * (d, C-14 or C-15), 135.07 $^{\#}$ (d, C-14 or C-15), 135.10 * (d, C-14 or C-15), 135.3 $^{\#}$ (d, C-14 or C-15), 140.0 $^{\#}$ (s, C-8), 140.4 $^{\#}$ (s, C-12 or C-17),

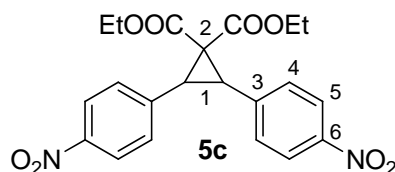
141.6* (s, C-8), 141.9* (s, C-12 or C-17), 142.0* (s, C-12 or C-17), 143.3# (s, C-12 or C-17), 147.0# (s, C-11), 147.3* (s, C-11), 159.1# (s, C-7), 159.4* (s, C-7), 194.4# (s, CO), 194.7* (s, CO), 195.2* (s, CO), 197.4# (s, CO). MS (EI): m/e (%) = 400 (29), 399 (100) $[M]^+$, 382 (26), 369 (17), 368 (26), 352 (28), 266 (21), 263 (16), 252 (15), 133 (19), 57 (18). HR-MS (EI) $[M]^+$: calcd for $[C_{24}H_{17}NO_5]^+$: 399.1102, found 399.1106.

* signal can be assigned to major diastereomer

signal can be assigned to minor diastereomer

Diethyl 2,3-bis(4-nitrophenyl)cyclopropane-1,1-dicarboxylate (5c) was obtained from dimethyl(4-nitrobenzyl)sulfonium tetrafluoroborate (**1e-H**)- BF_4 (200 mg, 702 μ mol), $KOtBu$ (78.8 mg, 702 μ mol), and diethyl benzylidenemalonate **2r** (100 mg, 341 μ mol) as a pale yellow oil (125 mg, 292 μ mol, 86 %, $dr \sim 1 : 1.2$).

RAP 15.2



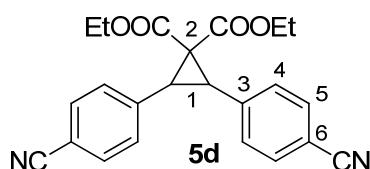
1H -NMR ($CDCl_3$, 599 MHz): δ = 1.00-1.05 (m, 9 H, $2 \times OCH_2CH_3^*$, $OCH_2CH_3^\#$), 1.37# (t, 3 H, $J = 7.2$ Hz, OCH_2CH_3), 3.45# (s, 2 H, 1-H), 3.92* (s, 2 H, 1-H), 3.95-4.08 (m, 6 H, $2 \times OCH_2CH_3^*$, $OCH_2CH_3^\#$), 4.35# (q, 2 H, $J = 7.2$ Hz, OCH_2CH_3), 7.22# (d, 4 H, $J = 8.9$ Hz, 4-H), 7.52* (d, 4 H, $J = 8.8$ Hz, 4-H), 8.07# (d, 4 H, $J = 9.0$ Hz, 5-H), 8.20* (d, 4 H, $J = 8.8$ Hz, 5-H). ^{13}C -NMR ($CDCl_3$, 151 MHz): δ = 13.7# (q, OCH_2CH_3), 13.9* (q, OCH_2CH_3), 14.1# (q, OCH_2CH_3), 34.1* (d, C-1), 34.8# (d, C-1), 41.8# (s, C-2), 46.2* (s, C-2), 61.8# (t, OCH_2CH_3), 62.2* (t, OCH_2CH_3), 63.0# (t, OCH_2CH_3), 122.9# (d, C-5), 123.6* (d, C-5), 129.7* (d, C-4), 131.4# (d, C-4), 139.8# (s, C-3), 141.4* (s, C-3), 147.0# (s, C-6), 147.5* (s, C-6), 165.0# (s, CO), 165.5* (s, CO), 169.3# (s, CO). MS (EI): m/e (%) = 428 (12) $[M]^+$, 383 (30), 382 (100), 336 (26), 326 (36), 236 (32), 189 (38), 180 (22), 152 (28). HR-MS (EI) $[M]^+$: calcd for $[C_{21}H_{20}N_2O_8]^+$: 428.1214, found 428.1219.

* signal can be assigned to *trans*-diastereomer

signal can be assigned to *cis*-diastereomer

Diethyl 2,3-bis(4-cyanophenyl)cyclopropane-1,1-dicarboxylate (5d) was obtained from dimethyl(4-cyanobenzyl)sulfonium tetrafluoroborate (**1f-H**)-BF₄ (300 mg, 1.13 mmol), KO^tBu (127 mg, 1.13 mmol), and diethyl benzylidenemalonate **2s** (124 mg, 454 μmol) as a pale yellow oil (157 mg, 404 μmol, 89 %, *dr* ~ 1 : 1.0).

RAP 14.3



¹H-NMR (CDCl₃, 599 MHz): δ = 0.97-1.02 (m, 9 H, 2 × OCH₂CH₃^{*}, OCH₂CH₃[#]), 1.35[#] (t, 3 H, *J* = 7.2 Hz, OCH₂CH₃), 3.38[#] (s, 2 H, 1-H), 3.85^{*} (s, 2 H, 1-H), 3.94-4.05 (m, 6 H, 2 × OCH₂CH₃^{*}, OCH₂CH₃[#]), 4.33[#] (q, 2 H, *J* = 7.2 Hz, OCH₂CH₃), 7.15[#] (d, 4 H, *J* = 8.5 Hz, 4-H), 7.45^{*} (d, 4 H, *J* = 8.5 Hz, 4-H), 7.50[#] (d, 4 H, *J* = 8.6 Hz, 5-H), 7.63^{*} (d, 4 H, *J* = 8.5 Hz, 5-H). ¹³C-NMR (CDCl₃, 151 MHz): δ = 13.6[#] (q, OCH₂CH₃), 13.9^{*} (q, OCH₂CH₃), 14.0[#] (q, OCH₂CH₃), 34.1^{*} (d, C-1), 34.9[#] (d, C-1), 41.6[#] (s, C-2), 46.0^{*} (s, C-2), 61.6[#] (t, OCH₂CH₃), 62.1^{*} (t, OCH₂CH₃), 62.8[#] (t, OCH₂CH₃), 111.2[#] (s, C-6), 111.7^{*} (s, C-6), 118.4^{*} (s, CN), 118.5[#] (s, CN), 129.6^{*} (d, C-4), 131.3[#] (d, C-4), 131.4[#] (d, C-5), 132.2^{*} (d, C-5), 137.8[#] (s, C-3), 139.4^{*} (s, C-3), 165.0[#] (s, CO), 165.5^{*} (s, CO), 169.4[#] (s, CO). MS (EI): *m/e* (%) = 388 (13) [M]⁺, 343 (29), 342 (100), 315 (15), 314 (17), 297 (35), 296 (44), 286 (25), 271 (15), 269 (20), 268 (18), 243 (25), 242 (68), 241 (49), 228 (16), 160 (36), 132 (23). HR-MS (EI) [M]⁺: calcd for [C₂₃H₂₀N₂O₄]⁺: 388.1417, found 388.1416.

* signal can be assigned to *trans*-diastereomer

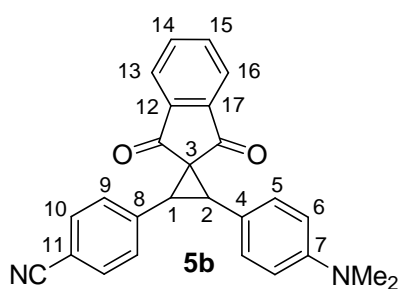
signal can be assigned to *cis*-diastereomer

Product study for the reaction of the semistabilized sulfur ylide **1f** with the Michael acceptor **2m**

4-(2-(4-(Dimethylamino)phenyl)-1',3'-dioxo-1',3'-dihydrospiro[cyclopropane-1,2'-inden]-3-yl)benzotrile (5b). A vigorously stirred solution of sulfonium tetrafluoroborate (**1f-H**)-BF₄ (159 mg, 600 μmol) and benzylideneindandione **2m** (111 mg, 400 μmol) in CHCl₃ (15 mL) was treated with saturated aqueous K₂CO₃-solution (5 mL). This biphasic mixture was vigorously stirred for 3 h. During this reaction further portions of (**1f-H**)-BF₄

(53 mg, 200 μmol) were added after 1 h and 2.5 h. The reaction was subsequently treated with water (50 mL), the organic layer was separated and the aqueous phase additionally extracted by CHCl_3 . The combined organic layers were washed with water and brine, dried over Na_2SO_4 and evaporated under reduced pressure. Purification of the crude product by column chromatography on silica gel (*n*-pentane/EtOAc) furnished **5b** as yellow solid (131 mg, 334 μmol , 84 %, one diastereomer), which was subsequently characterized by $^1\text{H}/^{13}\text{C}$ -NMR spectroscopy, and MS. Signal assignments were based on additional COSY, HSQC and HMBC experiments.

RAP 48.3



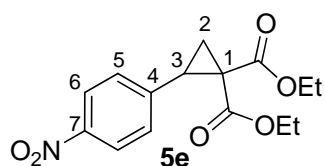
R_f (*n*-pentane/EtOAc 2:1, *v/v*): 0.44. Mp.: $>104^\circ\text{C}$ (decomp.). ^1H -NMR (CDCl_3 , 599 MHz): δ = 2.95 (s, 6 H, NMe_2), 4.08 (d, 1 H, $J = 9.4$ Hz, 2-H), 4.17 (d, 1 H, $J = 9.4$ Hz, 1-H), 6.68 (d, 2 H, $J = 8.7$ Hz, 6-H), 7.24 (d, 2 H, $J = 8.7$ Hz, 5-H), 7.50 (d, 2 H, $J = 8.1$ Hz, 9-H), 7.62 (d, 2 H, $J = 8.4$ Hz, 10-H), 7.74-7.75 (m, 2 H, 14-H, 15-H), 7.82-7.84 (m, 2 H, 13-H, 16-H). ^{13}C -NMR (CDCl_3 , 151 MHz): δ = 40.4 (q, NMe_2), 41.8 (d, C-1), 44.8 (d, C-2), 49.1 (s, C-3), 111.4 (s, C-11), 111.9 (d, C-6), 118.7 (s, CN), 119.8 (s, C-4), 122.5 (d, C-13 or C-16), 122.6 (d, C-13 or C-16), 129.9 (d, C-5), 130.1 (d, C-9), 132.0 (d, C-10), 134.8 (d, C-14 or C-15), 134.9 (d, C-14 or C-15), 139.9 (s, C-8), 141.98 (s, C-12 or C-17), 142.04 (s, C-12 or C-17), 150.2 (s, C-7), 194.8 (s, CO), 195.5 (s, CO). HR-MS (ESI^+) $[\text{M}+\text{H}]^+$: calcd for $[\text{C}_{26}\text{H}_{21}\text{N}_2\text{O}_2]^+$: 393.1598, found 393.1598.

Product study for the reaction of dimethylsulfoxonium methylide (1g) with the Michael acceptor 2r in DMSO

Diethyl 2-(4-nitrophenyl)cyclopropane-1,1-dicarboxylate (5e). Trimethylsulfoxonium iodide ($\text{Me}_3\text{SO}^+ \text{I}^-$, 135 mg, 613 μmol) and $\text{KO}t\text{Bu}$ (68.8 mg, 613 μmol) were dissolved in dry DMSO (3 mL). After the addition of electrophile **2r** (150 mg, 511 μmol , dissolved in 3 mL DMSO) at room temperature, the reaction mixture was stirred for additional 10 min,

subsequently quenched by the addition of water and then extracted with CH_2Cl_2 . The combined organic layers were washed with water and brine, dried over Na_2SO_4 and evaporated under reduced pressure. Purification of the crude product by column chromatography on silica gel (*n*-pentane/EtOAc) furnished **5e** as colorless solid (116 mg, 377 μmol , 74 %), which was subsequently characterized by ^1H - and ^{13}C -NMR spectroscopy and MS. Signal assignments were based on additional COSY, HSQC and HMBC experiments. A small sample of the solid product was recrystallized from *n*-pentane/ Et_2O for the determination of the melting point.

RAP 45.1



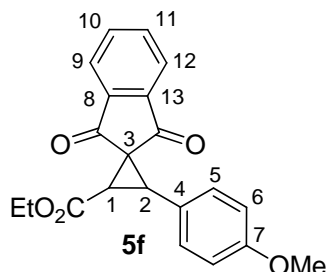
R_f (*n*-pentane/EtOAc 5:1, *v/v*): 0.43. Mp. (*n*-pentane/ Et_2O): 72–73°C. ^1H -NMR (CDCl_3 , 599 MHz): δ = 0.93 (t, 3 H, J = 7.1 Hz, OCH_2CH_3), 1.31 (t, 3 H, J = 7.2 Hz, OCH_2CH_3), 1.80 (dd, 1 H, J = 9.1 Hz, J = 5.4 Hz, 2-H), 2.20 (dd, 1 H, J = 8.0 Hz, J = 5.4 Hz, 2-H), 3.27 (dd, 1 H, J = 8.5 Hz, J = 8.5 Hz, 3-H), 3.83–3.95 (m, 2 H, OCH_2CH_3), 4.21–4.32 (m, 2 H, OCH_2CH_3), 7.38 (d, 2 H, J = 8.5 Hz, 5-H), 8.14 (d, 2 H, J = 8.8 Hz, 6-H). ^{13}C -NMR (CDCl_3 , 151 MHz): δ = 13.8 (q, OCH_2CH_3), 14.1 (q, OCH_2CH_3), 19.0 (t, C-2) 31.2 (d, C-3), 38.0 (s, C-1), 61.5 (t, OCH_2CH_3), 62.1 (t, OCH_2CH_3), 123.3 (d, C-6), 129.4 (d, C-5), 142.6 (s, C-4), 147.2 (s, C-7), 166.1 (s, CO), 169.1 (s, CO). HR-MS (ESI $^-$) [$\text{M}-\text{H}$] $^-$: calcd for [$\text{C}_{15}\text{H}_{16}\text{NO}_6$] $^-$: 306.0983, found 306.0995.

Product study for the reaction of the stabilized sulfur ylide **1h** with the Michael acceptor **2l**

Ethyl 3-(4-methoxyphenyl)-1',3'-dioxo-1',3'-dihydrospiro[cyclopropane-1,2'-indene]-2-carboxylate (5f). The benzylideneindandione **2l** (267 mg, 1.01 mmol, dissolved in 7 mL of dry DMSO) was added to a solution of ethyl (dimethyl- λ^4 -sulfanylidene)acetate (**1h**, 150 mg, 1.01 mmol) in dry DMSO (2–3 mL) at room temperature. The resulting mixture was stirred for 5 min and subsequently quenched by the addition of water followed by the extraction with CH_2Cl_2 . The combined organic layers were washed with water and brine, dried over Na_2SO_4 and evaporated under reduced pressure. Purification by column chromatography on silica gel (*n*-pentane/EtOAc) yielded **5f** as a yellow oil (308 mg, 879 μmol , 87 %, *dr* ~ 1 : 2.6), which

was subsequently characterized by ^1H - and ^{13}C -NMR spectroscopy and MS. Signal assignments were based on additional COSY, HSQC and HMBC experiments.

RAP 82.1

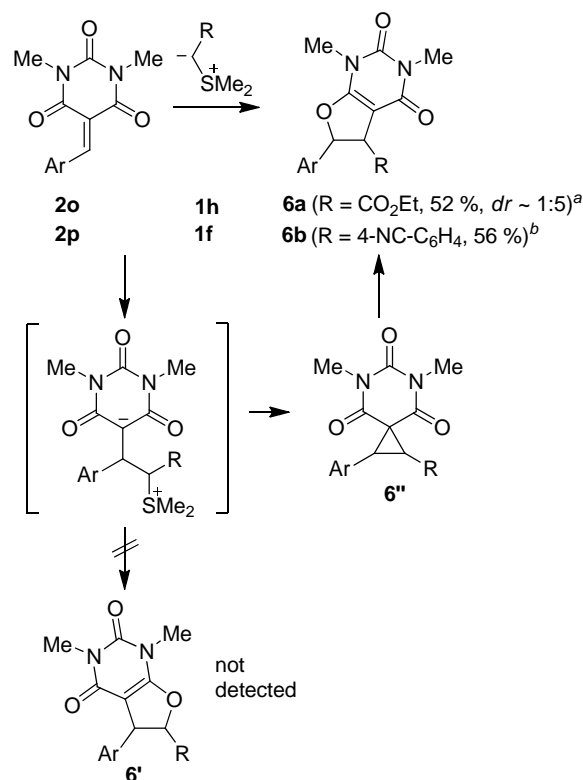


^1H -NMR (CDCl_3 , 599 MHz): δ = 1.20[#] (t, 3 H, J = 7.1 Hz, OCH_2CH_3), 1.30^{*} (t, 3 H, J = 7.1 Hz, OCH_2CH_3), 3.28[#] (d, 1 H, J = 10.1 Hz, 1-H), 3.52[#] (d, 1 H, J = 10.1 Hz, 2-H), 3.59^{*} (d, 1 H, J = 8.8 Hz, 1-H), 3.76 (s, 6 H, OMe^* , $\text{OMe}^\#$), 3.97^{*} (d, 1 H, J = 8.8 Hz, 2-H), 4.18[#] (q, 2 H, J = 7.1 Hz, OCH_2CH_3), 4.21-4.30^{*} (m, 2 H, OCH_2CH_3), 6.80-6.83 (m, 4 H, 6-H^{*}, 6-H[#]), 7.21^{*} (d, 2 H, J = 8.8 Hz, 5-H), 7.27[#] (d, 2 H, J = 8.8 Hz, 5-H), 7.73-7.81 (m, 5 H, 9-H^{*} or 12-H^{*}, 10-H^{*}, 10-H[#], 11-H^{*}, 11-H[#]), 7.91-7.93[#] (m, 1 H, 9-H[#] or 12-H[#]), 7.95-7.99 (m, 2 H, 9-H^{*} or 12-H^{*}, 9-H[#] or 12-H[#]). ^{13}C -NMR (CDCl_3 , 151 MHz): δ = 14.0[#] (q, OCH_2CH_3), 14.1^{*} (q, OCH_2CH_3), 36.8^{*} (d, C-1), 37.0[#] (d, C-1), 40.6[#] (d, C-2), 42.2^{*} (d, C-2), 42.8[#] (s, C-3), 46.1^{*} (s, C-3), 55.09[#] (q, OMe), 55.14^{*} (q, OMe), 61.3[#] (t, OCH_2CH_3), 61.7^{*} (t, OCH_2CH_3), 113.2[#] (d, C-6), 113.6^{*} (d, C-6), 122.70, 122.73, 122.74, 122.8, 122.9 (s, C-4[#], d, C-9^{*}, d, C-9[#], d, C-12^{*}, d, C-12[#]), 123.8^{*} (s, C-4), 130.2^{*} (d, C-5), 131.6[#] (d, C-5), 134.9[#] (d, C-10 or C-11), 135.0^{*} (d, C-10 or C-11), 135.1^{*} (d, C-10 or C-11), 135.3[#] (d, C-10 or C-11), 140.8[#] (s, C-8 or C-13), 141.9^{*} (s, C-8 or C-13), 142.0^{*} (s, C-8 or C-13), 143.3[#] (s, C-8 or C-13), 159.0[#] (s, C-7), 159.3^{*} (s, C-7), 165.4[#] (s, CO_2), 166.5^{*} (s, CO_2), 192.9[#] (s, CO), 193.6^{*} (s, CO), 194.7^{*} (s, CO), 196.9[#] (s, CO). MS (EI): m/e (%) = 350 (36) $[\text{M}]^+$, 305 (21), 304 (35), 278 (26), 277 (100), 276 (69), 262 (12), 261 (12), 234 (11). HR-MS (EI) $[\text{M}]^+$: calcd for $[\text{C}_{21}\text{H}_{18}\text{O}_5]^+$: 350.1149, found 350.1148.

* signal can be assigned to major diastereomer

signal can be assigned to minor diastereomer

Product study for the reaction of the stabilized sulfur ylide **1h and the semistabilized sulfur ylide **1f** with the benzylidenebarbituric acids **2o** and **2p****



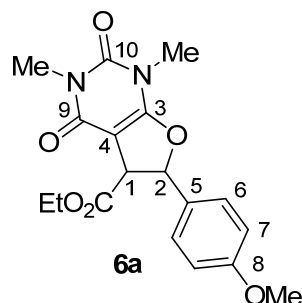
^a Reaction conditions: **1h**, DMSO, rt. ^b Reaction conditions: (**1f**-H)-BF₄, K₂CO₃ (aq.)/CHCl₃, rt; only one diastereomer isolated.

Product study for the reaction of the stabilized sulfur ylide **1h with the Michael acceptor **2o****

Ethyl 6-(4-methoxyphenyl)-1,3-dimethyl-2,4-dioxo-1,2,3,4,5,6-hexahydrofuro[2,3-d]pyrimidine-5-carboxylate (6a**).** The benzylidenebarbituric acid **2o** (275 mg, 1.00 mmol, dissolved in 7 mL of dry DMSO) was added to a solution of ethyl (dimethyl- λ^4 -sulfanylidene)acetate (**1h**, 160 mg, 1.08 mmol) in dry DMSO (2-3 mL) at room temperature. The resulting mixture was stirred for 5 min and subsequently quenched by the addition of water followed by the extraction with CH₂Cl₂. The combined organic layers were washed with water and brine, dried over Na₂SO₄ and evaporated under reduced pressure. The dihydrofuran **6a** was obtained as a mixture of diastereomers (*dr* ~ 1:5), which were separated by column chromatography on silica gel (*n*-pentane/EtOAc). After recrystallisation from Et₂O/EtOAc, diastereomer 1 was obtained as colorless solid (120 mg, 333 μ mol, 33 %). Recrystallisation from *n*-pentane/EtOAc yielded diastereomer 2 also as colorless solid (67 mg, 0.19 mmol, 19 %). The two diastereomers were subsequently characterized by ¹H-

and ^{13}C -NMR spectroscopy and MS. Signal assignments were based on additional COSY, HSQC and HMBC experiments.

RAP 83.2



Diastereomer 1:

R_f (*n*-pentane/EtOAc 2:3, v/v): 0.34. Mp.: 170-171°C (Et₂O/EtOAc). ^1H -NMR (CDCl₃, 300 MHz): δ = 1.31 (t, 3 H, J = 7.1 Hz, OCH₂CH₃), 3.33 (s, 3 H, NMe), 3.36 (s, 3 H, NMe), 3.83 (s, 3 H, OMe), 4.22-4.32 (m, 3 H, 1-H, OCH₂CH₃), 5.99 (d, 1 H, J = 6.2 Hz, 2-H), 6.94 (d, 2 H, J = 8.8 Hz, 7-H), 7.29 (d, 2 H, J = 8.6 Hz, 6-H). ^{13}C -NMR (CDCl₃, 75.5 MHz): δ = 14.2 (q, OCH₂CH₃), 28.1 (q, NMe), 29.7 (q, NMe), 52.4 (d, C-1), 55.4 (q, OMe), 62.0 (t, OCH₂CH₃), 86.2 (s, C-4), 90.5 (d, C-2), 114.5 (d, C-7), 127.7 (d, C-6), 129.5 (s, C-5), 151.6 (s, C-10), 159.3 (s, C-3 or C-9), 160.7 (s, C-8), 162.0 (s, C-3 or C-9), 171.6 (s, CO₂). MS (EI): m/e (%) = 360 (22) [M]⁺, 315 (21), 314 (100), 288 (11), 287 (46), 286 (19), 229 (24). HR-MS (EI): calc. for [C₁₈H₂₀N₂O₆]⁺: 360.1316, found 360.1317.

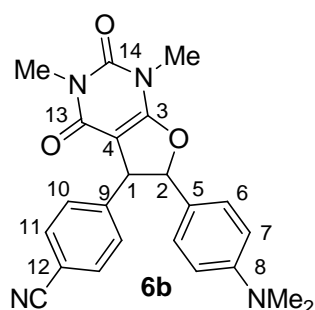
Diastereomer 2:

R_f (*n*-pentane/EtOAc 2:3, v/v): 0.22. Mp.: 151-153°C (*n*-pentane/EtOAc). ^1H -NMR (CDCl₃, 300 MHz): δ = 0.83 (t, 3 H, J = 7.2 Hz, OCH₂CH₃), 3.34 (s, 3 H, NMe), 3.42 (s, 3 H, NMe), 3.60-3.79 (m, 2 H, OCH₂CH₃), 3.81 (s, 3 H, OMe), 4.39 (d, 1 H, J = 10.1 Hz, 1-H), 6.09 (d, 1 H, J = 10.0 Hz, 2-H), 6.90 (d, 2 H, J = 8.8 Hz, 7-H), 7.26 (d, 2 H, J = 8.4 Hz, 6-H). ^{13}C -NMR (CDCl₃, 75.5 MHz): δ = 13.7 (q, OCH₂CH₃), 28.1 (q, NMe), 29.7 (q, NMe), 50.8 (d, C-1), 55.4 (q, OMe), 61.2 (t, OCH₂CH₃), 86.8 (s, C-4), 88.9 (d, C-2), 113.8 (d, C-7), 126.0 (s, C-5), 128.0 (d, C-6), 151.6 (s, C-10), 159.7 (s, C-3 or C-9), 160.3 (s, C-8), 162.8 (s, C-3 or C-9), 169.1 (s, CO₂). MS (EI): m/e (%) = 360 (21) [M]⁺, 315 (20), 314 (100), 287 (33), 286 (20), 229 (25), 132 (10). HR-MS (EI): calc. for [C₁₈H₂₀N₂O₆]⁺: 360.1316, found 360.1317.

Product study for the reaction of the semistabilized sulfur ylide **1f** with the Michael acceptor **2p**

4-(6-(4-(Dimethylamino)phenyl)-1,3-dimethyl-2,4-dioxo-1,2,3,4,5,6-hexahydrofuro[2,3-*d*]pyrimidin-5-yl)benzonitrile (6b). A vigorously stirred solution of sulfonium tetrafluoroborate (**1f-H**)-BF₄ (530 mg, 2.00 mmol) and benzylidenebarbituric acid **2p** (288 mg, 1.00 mmol) in CHCl₃ (25 mL) was treated with saturated aqueous K₂CO₃-solution (10 mL). This biphasic mixture was vigorously stirred for 2 h. During this reaction further portions of (**1f-H**)-BF₄ (265 mg, 1.00 mmol) were added after 1 h and 1.5 h. The reaction was subsequently treated with water (50 mL), the organic layer was separated and the aqueous phase additionally extracted by CHCl₃. The combined organic layers were washed with water and brine, dried over Na₂SO₄ and evaporated under reduced pressure. Purification of the crude product by column chromatography on silica gel (*n*-pentane/EtOAc) furnished **6b** as yellow solid (225 mg, 559 μmol, 56 %, one diastereomer), which was subsequently characterized by ¹H- and ¹³C-NMR spectroscopy and MS. Signal assignments were based on additional COSY, HSQC and HMBC experiments.

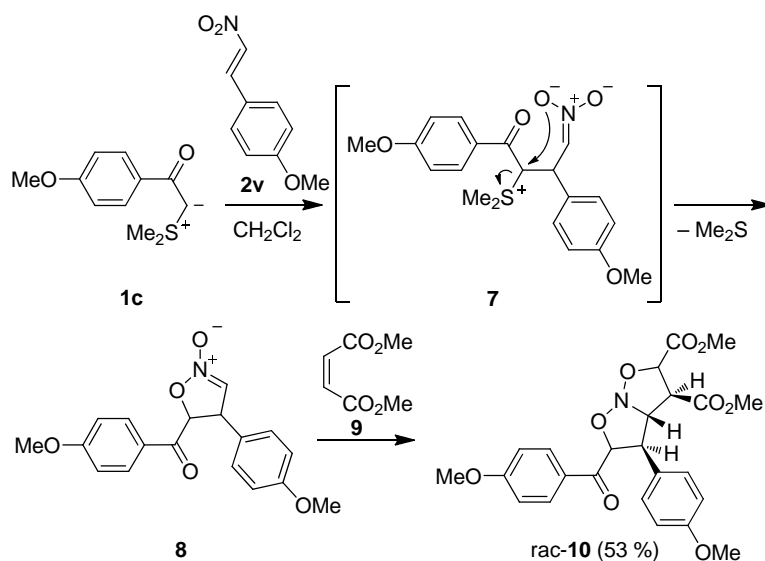
RAP 49.4



R_f (*n*-pentane/EtOAc 1:1, *v/v*): 0.43. Mp.: >97°C (decomp.). ¹H-NMR (CDCl₃, 599 MHz): δ = 3.01 (s, 6 H, NMe₂), 3.32 (s, 3 H, NMe), 3.39 (s, 3 H, NMe), 4.74 (d, 1 H, *J* = 6.9 Hz, 1-H), 5.47 (d, 1 H, *J* = 7.2 Hz, 2-H), 6.75 (d, 2 H, *J* = 6.6 Hz, 7-H), 7.22 (d, 2 H, *J* = 8.7 Hz, 6-H), 7.32 (d, 2 H, *J* = 7.9 Hz, 10-H), 7.62 (d, 2 H, *J* = 8.3 Hz, 11-H). ¹³C-NMR (CDCl₃, 151 MHz): δ = 28.0 (q, NMe), 29.6 (q, NMe), 40.4 (q, NMe₂), 53.2 (d, C-1), 88.3 (s, C-4), 96.4 (d, C-2), 111.4 (s, C-12), 112.4 (d, C-7, broadened signal), 118.7 (s, CN), 123.8 (s, C-5, broadened signal), 128.2 (2 × d, C-6, C-10), 132.7 (d, C-11), 145.9 (s, C-9), 151.3 (s, C-8, broadened signal), 151.7 (s, C-14), 159.7, 162.0 (2s, C-3, C-13). MS (EI): *m/e* (%) = 403 (23), 402 (100) [M]⁺, 286 (11), 246 (14), 134 (35). HR-MS (EI): calc. for [C₂₃H₂₂N₄O₃]⁺: 402.1687, found 402.1685.

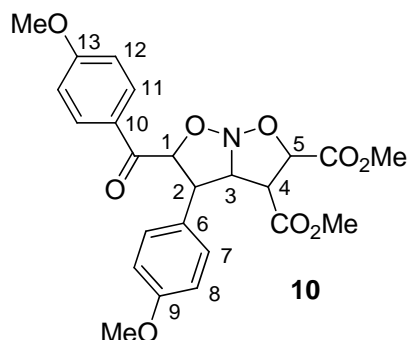
Product study for the reaction of the stabilized sulfur ylide **1c with nitrostyrene **2v****

The reaction of the benzoyl-stabilized sulfur ylide **1c** with *trans*-4-methoxy- β -nitrostyrene (**2v**) initially generates the zwitterion **7**, which undergoes a subsequent intramolecular nucleophilic displacement of dimethylsulfide to yield the dihydroisoxazole *N*-oxide **8**. The latter compound was not isolated but intercepted by a 1,3-dipolar cycloaddition with dimethyl maleate (**9**) according to previous reports (see references 10 and 11 of original manuscript), which yields compound **10** as a single diastereomer. A tentative assignment of the relative stereochemistry of *rac*-**10** is based on NOE experiments (see below).



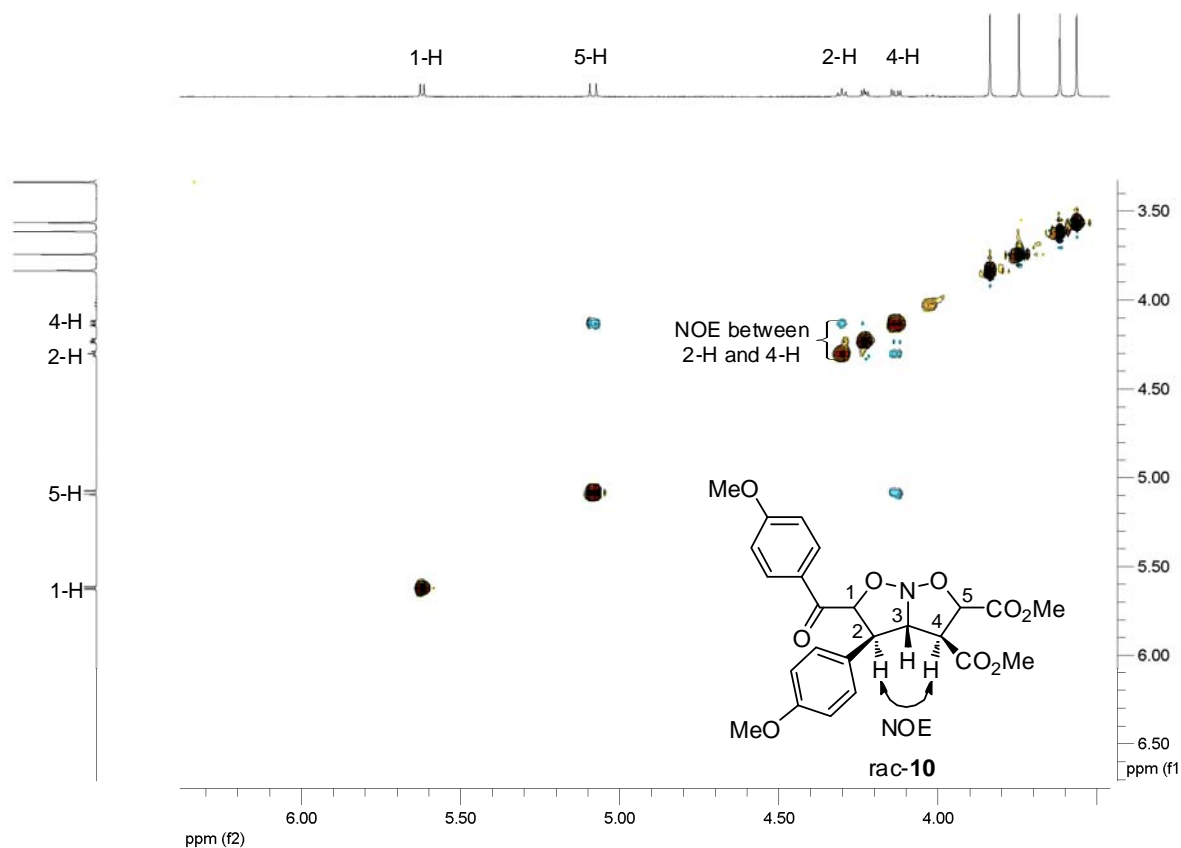
Dimethyl 5-(4-methoxybenzoyl)-4-(4-methoxyphenyl)tetrahydro-2*H*-isoxazolo[2,3-*b*]isoxazole-2,3-dicarboxylate (10**).** The nitrostyrene **2v** (53.8 mg, 300 μmol , dissolved in 2 mL of CH_2Cl_2) was added dropwise to a stirred solution of 2-(dimethyl- λ^4 -sulfanylidene)-1-(4-(methoxy)phenyl)-ethanone (**1c**, 69.0 mg, 328 μmol) in CH_2Cl_2 (2 mL) followed by the addition of dimethyl maleate (0.15 mL, 0.90 mmol). After 2 d of stirring at room temperature, the volatile components of the reaction mixture were evaporated under reduced pressure. Purification of the crude product by column chromatography on silica gel (*n*-pentane/EtOAc) furnished **10** as a colorless oil (74 mg, 0.16 mmol, 53 %, one diastereomer), which was characterized by ^1H - and ^{13}C -NMR spectroscopy and MS. Signal assignments were based on additional COSY, NOESY, HSQC and HMBC experiments.

RAP 53.4



R_f (*n*-pentane/EtOAc 2:1, *v/v*): 0.34. $^1\text{H-NMR}$ (DMSO- d_6 , 400 MHz): δ = 3.56 (s, 3 H, CO₂Me), 3.62 (s, 3 H, CO₂Me), 3.75 (s, 3 H, Ar-OMe), 3.84 (s, 3 H, Ar-OMe), 4.13 (dd, 1 H, J = 8.1, 3.0 Hz, 4-H), 4.23 (dd, 1 H, J = 5.0, 3.1 Hz, 3-H), 4.30 (dd, 1 H, J = 5.0, 5.0 Hz, 2-H), 5.08 (d, 1 H, J = 8.1 Hz, 5-H), 5.62 (d, 1 H, J = 4.9 Hz, 1-H), 6.95 (d, 2 H, J = 8.8 Hz, 8-H), 7.03 (d, 2 H, J = 9.0 Hz, 12-H), 7.36 (d, 2 H, J = 8.8 Hz, 7-H), 7.89 (d, 2 H, J = 9.0 Hz, 11-H). $^{13}\text{C-NMR}$ (DMSO- d_6 , 101 MHz): δ = 49.7 (d, C-2), 52.1 (q, CO₂Me), 52.2 (d, C-4), 52.4 (q, CO₂Me), 55.0 (q, Ar-OMe), 55.5 (q, Ar-OMe), 76.8 (d, C-5), 80.7 (d, C-3), 87.9 (d, C-1), 113.8 (d, C-12), 114.3 (d, C-8), 127.5 (s, C-10), 128.9 (d, C-7), 131.59, 131.60 (d, C-11, s, C-6), 158.5 (s, C-9), 163.4 (s, C-13), 168.2 (s, CO₂), 169.4 (s, CO₂), 192.8 (s, CO). HR-MS (ESI⁺) [M+H]⁺: calcd for [C₂₄H₂₆NO₉]⁺: 472.1602, found 472.1600.

NOESY of compound **10** (DMSO- d_6 , 400 MHz):



5.3 Kinetics

Kinetic investigation of the reactions of the sulfur ylide **1a** with the electrophiles **2a-f** in DMSO

Table 3: Kinetics of the reaction of **1a** with **2a** in DMSO at 20°C (stopped-flow UV-Vis spectrometer, $\lambda = 613$ nm).

No.	$[E]_0 / \text{mol L}^{-1}$	$[\text{Nu}]_0 / \text{mol L}^{-1}$	$k_{\text{obs}} / \text{s}^{-1}$
RAK 12.7-1	1.42×10^{-5}	4.74×10^{-4}	3.49×10^1
RAK 12.7-2	1.42×10^{-5}	9.48×10^{-4}	6.13×10^1
RAK 12.7-3	1.42×10^{-5}	1.42×10^{-3}	8.87×10^1
RAK 12.7-4	1.42×10^{-5}	1.90×10^{-3}	1.16×10^2
$k_2 = 5.71 \times 10^4 \text{ L mol}^{-1} \text{ s}^{-1}$			

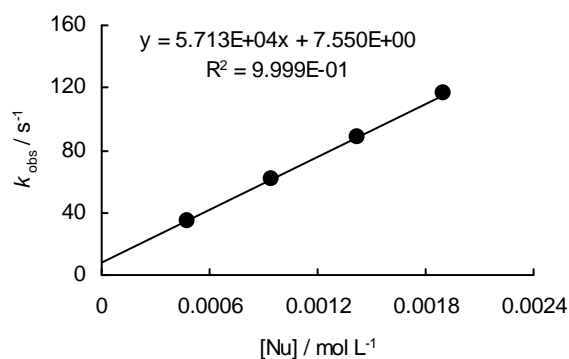


Table 4: Kinetics of the reaction of **1a** with **2b** in DMSO at 20°C (stopped-flow UV-Vis spectrometer, $\lambda = 623$ nm).

No.	$[E]_0 / \text{mol L}^{-1}$	$[\text{Nu}]_0 / \text{mol L}^{-1}$	$k_{\text{obs}} / \text{s}^{-1}$
RAK 12.6-1	2.57×10^{-5}	4.79×10^{-4}	1.84×10^1
RAK 12.6-2	2.57×10^{-5}	9.59×10^{-4}	3.50×10^1
RAK 12.6-3	2.57×10^{-5}	1.44×10^{-3}	5.08×10^1
RAK 12.6-4	2.57×10^{-5}	1.92×10^{-3}	6.64×10^1
RAK 12.6-5	2.57×10^{-5}	2.40×10^{-3}	8.27×10^1
$k_2 = 3.34 \times 10^4 \text{ L mol}^{-1} \text{ s}^{-1}$			

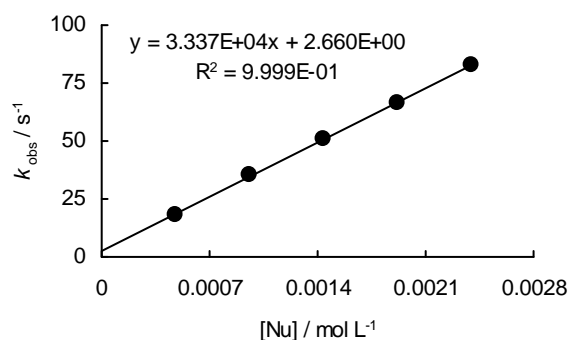


Table 5: Kinetics of the reaction of **1a** with **2c** in DMSO at 20°C (stopped-flow UV-Vis spectrometer, $\lambda = 623$ nm).

No.	$[E]_0 / \text{mol L}^{-1}$	$[\text{Nu}]_0 / \text{mol L}^{-1}$	$k_{\text{obs}} / \text{s}^{-1}$
RAK 12.5-1	1.94×10^{-5}	7.27×10^{-4}	2.19
RAK 12.5-2	1.94×10^{-5}	1.46×10^{-3}	4.37
RAK 12.5-3	1.94×10^{-5}	2.18×10^{-3}	6.60
RAK 12.5-4	1.94×10^{-5}	2.91×10^{-3}	8.80
RAK 12.5-5	1.94×10^{-5}	3.64×10^{-3}	1.10×10^1
$k_2 = 3.03 \times 10^3 \text{ L mol}^{-1} \text{ s}^{-1}$			

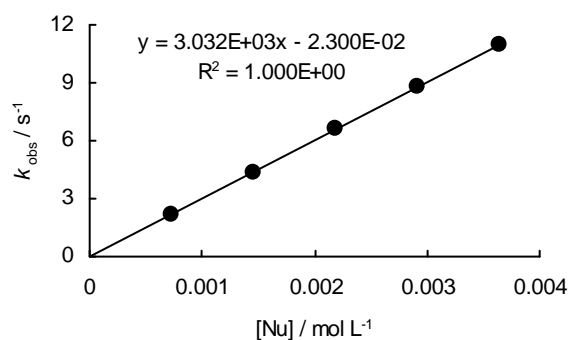
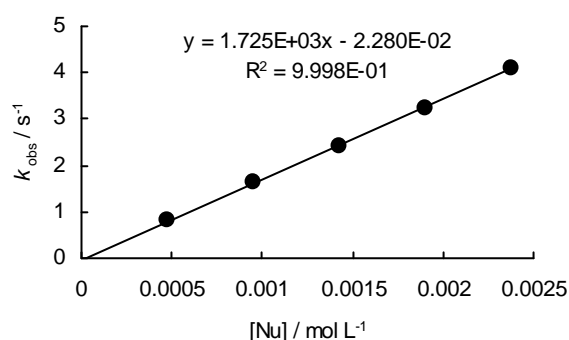
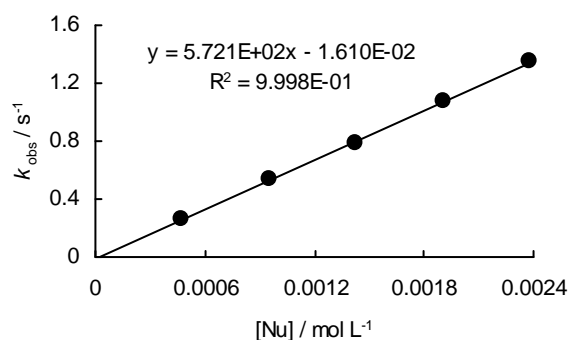


Table 6: Kinetics of the reaction of **1a** with **2d** in DMSO at 20°C (stopped-flow UV-Vis spectrometer, $\lambda = 630$ nm).

No.	$[E]_0 / \text{mol L}^{-1}$	$[\text{Nu}]_0 / \text{mol L}^{-1}$	$k_{\text{obs}} / \text{s}^{-1}$
RAK 12.3-1	2.57×10^{-5}	4.76×10^{-4}	8.09×10^{-1}
RAK 12.3-2	2.57×10^{-5}	9.51×10^{-4}	1.62
RAK 12.3-3	2.57×10^{-5}	1.43×10^{-3}	2.42
RAK 12.3-4	2.57×10^{-5}	1.90×10^{-3}	3.24
RAK 12.3-5	2.57×10^{-5}	2.38×10^{-3}	4.10
$k_2 = 1.73 \times 10^3 \text{ L mol}^{-1} \text{ s}^{-1}$			

**Table 7:** Kinetics of the reaction of **1a** with **2e** in DMSO at 20°C (stopped-flow UV-Vis spectrometer, $\lambda = 630$ nm).

No.	$[E]_0 / \text{mol L}^{-1}$	$[\text{Nu}]_0 / \text{mol L}^{-1}$	$k_{\text{obs}} / \text{s}^{-1}$
RAK 12.2-1	2.59×10^{-5}	4.76×10^{-4}	2.58×10^{-1}
RAK 12.2-2	2.59×10^{-5}	9.51×10^{-4}	5.33×10^{-1}
RAK 12.2-3	2.59×10^{-5}	1.43×10^{-3}	7.90×10^{-1}
RAK 12.2-4	2.59×10^{-5}	1.90×10^{-3}	1.07
RAK 12.2-5	2.59×10^{-5}	2.38×10^{-3}	1.35
$k_2 = 5.72 \times 10^2 \text{ L mol}^{-1} \text{ s}^{-1}$			

**Table 8:** Kinetics of the reaction of **1a** with **2f** in DMSO at 20°C (diode array UV-Vis spectrometer, $\lambda = 422$ nm).

No.	$[E]_0 / \text{mol L}^{-1}$	$[\text{Nu}]_0 / \text{mol L}^{-1}$	$k_{\text{obs}} / \text{s}^{-1}$
RAK 12.4-1	3.60×10^{-5}	5.06×10^{-4}	6.14×10^{-3}
RAK 12.4-2	3.79×10^{-5}	1.00×10^{-3}	1.23×10^{-2}
RAK 12.4-3	3.78×10^{-5}	1.49×10^{-3}	1.84×10^{-2}
RAK 12.4-4	3.83×10^{-5}	1.96×10^{-3}	2.41×10^{-2}
RAK 12.4-5	3.93×10^{-5}	2.50×10^{-3}	3.07×10^{-2}
$k_2 = 1.23 \times 10^1 \text{ L mol}^{-1} \text{ s}^{-1}$			

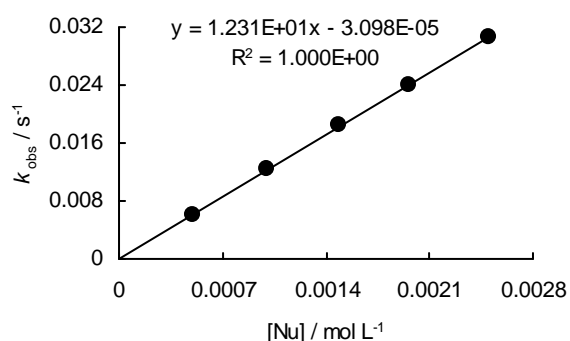
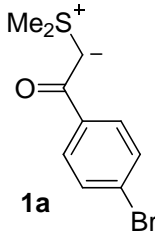
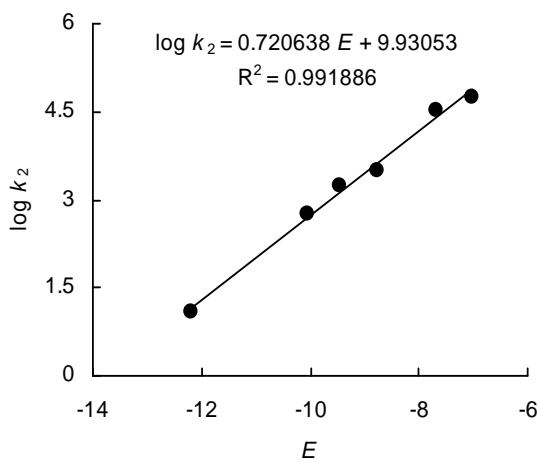


Table 9: Determination of the nucleophilicity parameters N , s for **1a** (correlation of $\log k_2$ for the reactions of **1a** with **2a–f** versus the electrophilicity parameters E for **2a–f**).

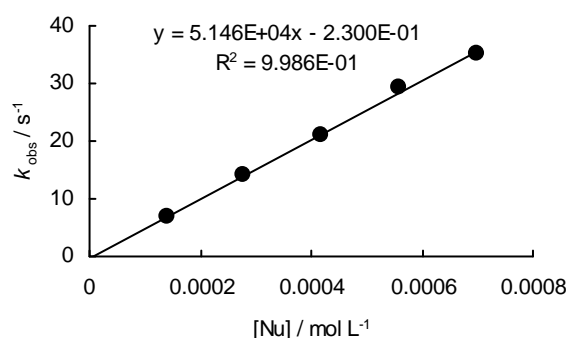
Nucleophile	Electrophile (E)	$k_2 / \text{L mol}^{-1} \text{s}^{-1}$
 1a	2a (-7.02)	5.71×10^4
	2b (-7.69)	3.34×10^4
	2c (-8.76)	3.03×10^3
	2d (-9.45)	1.73×10^3
	2e (-10.04)	5.72×10^2
	2f (-12.18)	1.23×10^1
$N = 13.78, s = 0.72$		



Kinetic investigation of the reactions of the sulfur ylide **1b** with the electrophiles **2a–f** in DMSO

Table 10: Kinetics of the reaction of **1b** with **2a** in DMSO at 20°C (stopped-flow UV-Vis spectrometer, $\lambda = 613 \text{ nm}$).

No.	$[E]_0 / \text{mol L}^{-1}$	$[\text{Nu}]_0 / \text{mol L}^{-1}$	$k_{\text{obs}} / \text{s}^{-1}$
NFH 10-1	1.09×10^{-5}	1.40×10^{-4}	6.85
NFH 10-2	1.09×10^{-5}	2.79×10^{-4}	1.41×10^1
NFH 10-3	1.09×10^{-5}	4.19×10^{-4}	2.12×10^1
NFH 10-4	1.09×10^{-5}	5.58×10^{-4}	2.92×10^1
NFH 10-5	1.09×10^{-5}	6.98×10^{-4}	3.52×10^1
$k_2 = 5.15 \times 10^4 \text{ L mol}^{-1} \text{s}^{-1}$			

**Table 11:** Kinetics of the reaction of **1b** with **2b** in DMSO at 20°C (stopped-flow UV-Vis spectrometer, $\lambda = 624 \text{ nm}$).

No.	$[E]_0 / \text{mol L}^{-1}$	$[\text{Nu}]_0 / \text{mol L}^{-1}$	$k_{\text{obs}} / \text{s}^{-1}$
NFH 9-1	1.08×10^{-5}	2.82×10^{-4}	7.72
NFH 9-2	1.08×10^{-5}	5.65×10^{-4}	1.66×10^1
NFH 9-3	1.08×10^{-5}	8.47×10^{-3}	2.53×10^1
NFH 9-4	1.08×10^{-5}	1.13×10^{-3}	3.35×10^1
NFH 9-5	1.08×10^{-5}	1.41×10^{-3}	4.24×10^1
$k_2 = 3.06 \times 10^4 \text{ L mol}^{-1} \text{s}^{-1}$			

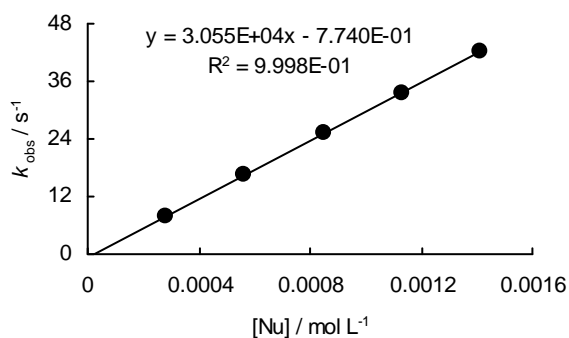
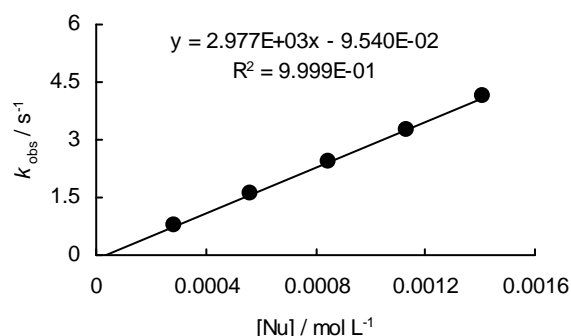
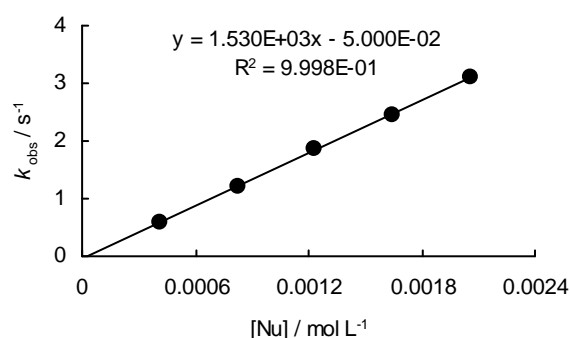


Table 12: Kinetics of the reaction of **1b** with **2c** in DMSO at 20°C (stopped-flow UV-Vis spectrometer, $\lambda = 624$ nm).

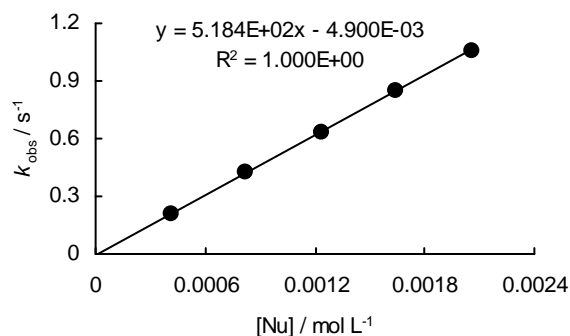
No.	$[E]_0 / \text{mol L}^{-1}$	$[\text{Nu}]_0 / \text{mol L}^{-1}$	$k_{\text{obs}} / \text{s}^{-1}$
NFH 8-1	1.11×10^{-5}	2.82×10^{-4}	7.52×10^{-1}
NFH 8-2	1.11×10^{-5}	5.65×10^{-4}	1.59
NFH 8-3	1.11×10^{-5}	8.47×10^{-4}	2.41
NFH 8-4	1.11×10^{-5}	1.13×10^{-3}	3.26
NFH 8-5	1.11×10^{-5}	1.41×10^{-3}	4.12
$k_2 = 2.98 \times 10^3 \text{ L mol}^{-1} \text{ s}^{-1}$			

**Table 13:** Kinetics of the reaction of **1b** with **2d** in DMSO at 20°C (stopped-flow UV-Vis spectrometer, $\lambda = 632$ nm).

No.	$[E]_0 / \text{mol L}^{-1}$	$[\text{Nu}]_0 / \text{mol L}^{-1}$	$k_{\text{obs}} / \text{s}^{-1}$
NFH 7-1	1.05×10^{-5}	4.12×10^{-4}	5.80×10^{-1}
NFH 7-2	1.05×10^{-5}	8.24×10^{-4}	1.20
NFH 7-3	1.05×10^{-5}	1.24×10^{-3}	1.86
NFH 7-4	1.05×10^{-5}	1.65×10^{-3}	2.46
NFH 7-5	1.05×10^{-5}	2.06×10^{-3}	3.10
$k_2 = 1.53 \times 10^3 \text{ L mol}^{-1} \text{ s}^{-1}$			

**Table 14:** Kinetics of the reaction of **1b** with **2e** in DMSO at 20°C (stopped-flow UV-Vis spectrometer, $\lambda = 632$ nm).

No.	$[E]_0 / \text{mol L}^{-1}$	$[\text{Nu}]_0 / \text{mol L}^{-1}$	$k_{\text{obs}} / \text{s}^{-1}$
NFH 6-1	1.08×10^{-5}	4.12×10^{-4}	2.07×10^{-1}
NFH 6-2	1.08×10^{-5}	8.24×10^{-4}	4.23×10^{-1}
NFH 6-3	1.08×10^{-5}	1.24×10^{-3}	6.36×10^{-1}
NFH 6-4	1.08×10^{-5}	1.65×10^{-3}	8.52×10^{-1}
NFH 6-5	1.08×10^{-5}	2.06×10^{-3}	1.06
$k_2 = 5.18 \times 10^2 \text{ L mol}^{-1} \text{ s}^{-1}$			

**Table 15:** Kinetics of the reaction of **1b** with **2f** in DMSO at 20°C (diode array UV-Vis spectrometer, $\lambda = 422$ nm).

No.	$[E]_0 / \text{mol L}^{-1}$	$[\text{Nu}]_0 / \text{mol L}^{-1}$	$k_{\text{obs}} / \text{s}^{-1}$
NFH 19-1	3.36×10^{-5}	4.57×10^{-4}	7.38×10^{-3}
NFH 19-2	3.31×10^{-5}	6.55×10^{-4}	1.08×10^{-2}
NFH 19-3	3.55×10^{-5}	8.87×10^{-4}	1.45×10^{-2}
NFH 19-4	3.67×10^{-5}	1.12×10^{-3}	1.82×10^{-2}
NFH 19-5	3.60×10^{-5}	1.28×10^{-3}	2.08×10^{-2}
$k_2 = 1.62 \times 10^1 \text{ L mol}^{-1} \text{ s}^{-1}$			

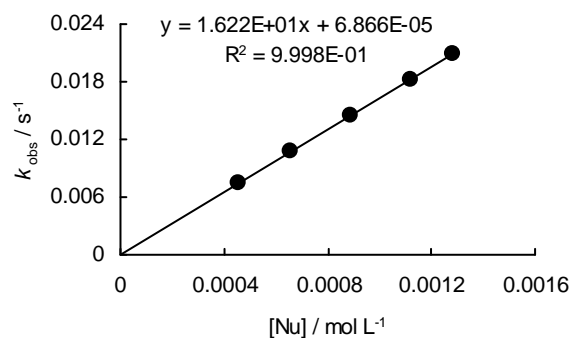
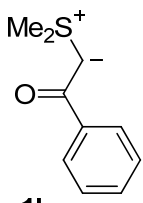
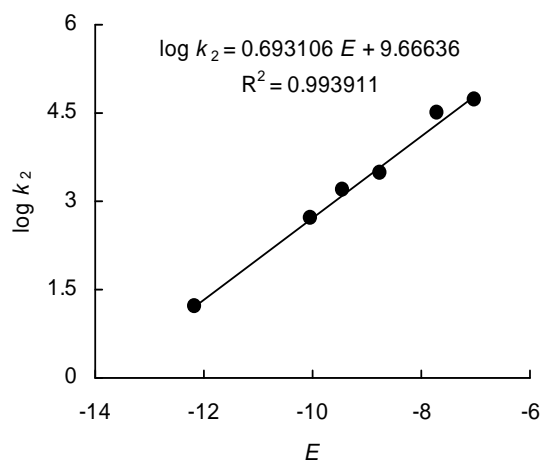


Table 16: Determination of the nucleophilicity parameters N , s for **1b** (correlation of $\log k_2$ for the reactions of **1b** with **2a–f** versus the electrophilicity parameters E for **2a–f**).

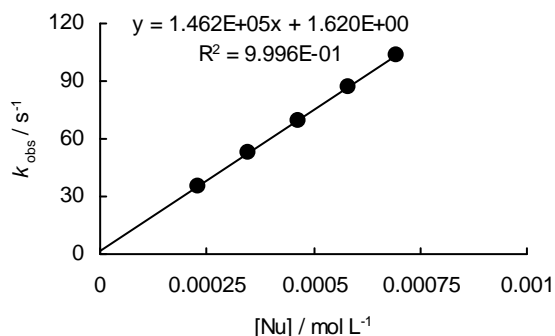
Nucleophile	Electrophile (E)	$k_2 / \text{L mol}^{-1} \text{s}^{-1}$
 1b	2a (-7.02)	5.15×10^4
	2b (-7.69)	3.06×10^4
	2c (-8.76)	2.98×10^3
	2d (-9.45)	1.53×10^3
	2e (-10.04)	5.18×10^2
	2f (-12.18)	1.62×10^1
$N = 13.95, s = 0.69$		



Kinetic investigation of the reactions of the sulfur ylide **1c** with the electrophiles **2a–f,v** in DMSO

Table 17: Kinetics of the reaction of **1c** with **2a** in DMSO at 20°C (stopped-flow UV-Vis spectrometer, $\lambda = 613 \text{ nm}$).

No.	$[E]_0 / \text{mol L}^{-1}$	$[\text{Nu}]_0 / \text{mol L}^{-1}$	$k_{\text{obs}} / \text{s}^{-1}$
NFH 32-1	2.06×10^{-5}	2.32×10^{-4}	3.50×10^1
NFH 32-2	2.06×10^{-5}	3.48×10^{-4}	5.32×10^1
NFH 32-3	2.06×10^{-5}	4.64×10^{-4}	6.93×10^1
NFH 32-4	2.06×10^{-5}	5.80×10^{-4}	8.68×10^1
NFH 32-5	2.06×10^{-5}	6.96×10^{-4}	1.03×10^2
$k_2 = 1.46 \times 10^5 \text{ L mol}^{-1} \text{s}^{-1}$			

**Table 18:** Kinetics of the reaction of **1c** with **2b** in DMSO at 20°C (stopped-flow UV-Vis spectrometer, $\lambda = 624 \text{ nm}$).

No.	$[E]_0 / \text{mol L}^{-1}$	$[\text{Nu}]_0 / \text{mol L}^{-1}$	$k_{\text{obs}} / \text{s}^{-1}$
NFH 30-1	2.09×10^{-5}	2.39×10^{-4}	1.93×10^1
NFH 30-2	2.09×10^{-5}	4.77×10^{-4}	3.69×10^1
NFH 30-3	2.09×10^{-5}	7.16×10^{-4}	5.41×10^1
NFH 30-4	2.09×10^{-5}	9.55×10^{-4}	7.19×10^1
NFH 30-5	2.09×10^{-5}	1.19×10^{-3}	9.18×10^1
$k_2 = 7.54 \times 10^4 \text{ L mol}^{-1} \text{s}^{-1}$			

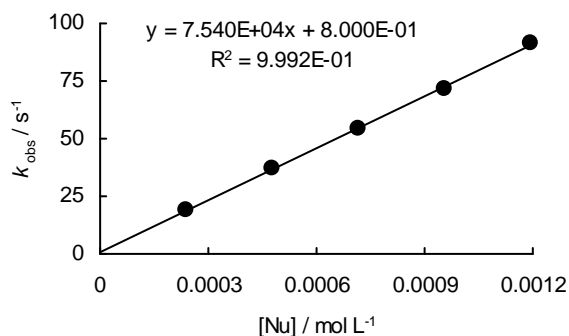
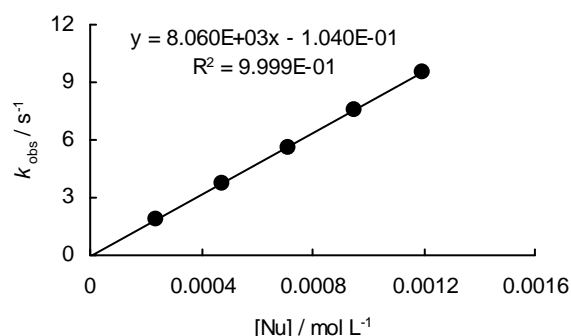
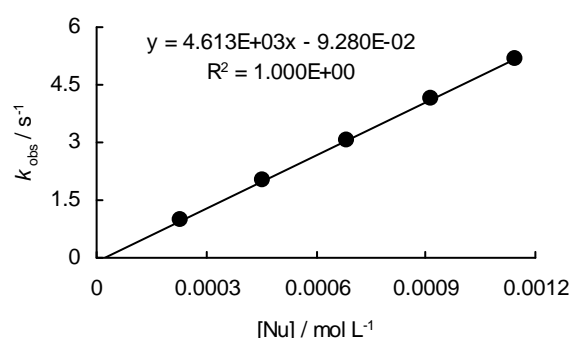


Table 19: Kinetics of the reaction of **1c** with **2c** in DMSO at 20°C (stopped-flow UV-Vis spectrometer, $\lambda = 624$ nm).

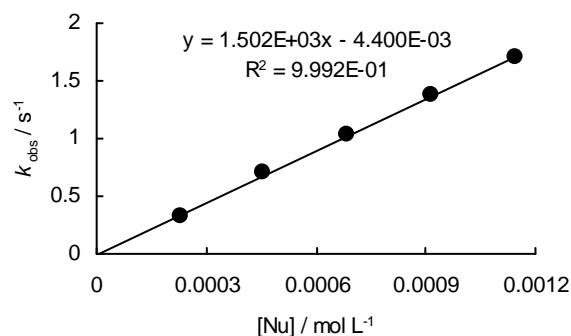
No.	[E] ₀ / mol L ⁻¹	[Nu] ₀ / mol L ⁻¹	<i>k</i> _{obs} / s ⁻¹
NFH 29-1	2.10 × 10 ⁻⁵	2.39 × 10 ⁻⁴	1.83
NFH 29-2	2.10 × 10 ⁻⁵	4.77 × 10 ⁻⁴	3.77
NFH 29-3	2.10 × 10 ⁻⁵	7.16 × 10 ⁻⁴	5.62
NFH 29-4	2.10 × 10 ⁻⁵	9.55 × 10 ⁻⁴	7.57
NFH 29-5	2.10 × 10 ⁻⁵	1.19 × 10 ⁻³	9.55
<i>k</i>₂ = 8.06 × 10³ L mol⁻¹ s⁻¹			

**Table 20:** Kinetics of the reaction of **1c** with **2d** in DMSO at 20°C (stopped-flow UV-Vis spectrometer, $\lambda = 633$ nm).

No.	[E] ₀ / mol L ⁻¹	[Nu] ₀ / mol L ⁻¹	<i>k</i> _{obs} / s ⁻¹
NFH 28-1	2.08 × 10 ⁻⁵	2.29 × 10 ⁻⁴	9.64 × 10 ⁻¹
NFH 28-2	2.08 × 10 ⁻⁵	4.57 × 10 ⁻⁴	2.02
NFH 28-3	2.08 × 10 ⁻⁵	6.86 × 10 ⁻⁴	3.06
NFH 28-4	2.08 × 10 ⁻⁵	9.15 × 10 ⁻⁴	4.14
NFH 28-5	2.08 × 10 ⁻⁵	1.14 × 10 ⁻³	5.18
<i>k</i>₂ = 4.61 × 10³ L mol⁻¹ s⁻¹			

**Table 21:** Kinetics of the reaction of **1c** with **2e** in DMSO at 20°C (stopped-flow UV-Vis spectrometer, $\lambda = 633$ nm).

No.	[E] ₀ / mol L ⁻¹	[Nu] ₀ / mol L ⁻¹	<i>k</i> _{obs} / s ⁻¹
NFH 27-1	2.12 × 10 ⁻⁵	2.29 × 10 ⁻⁴	3.22 × 10 ⁻¹
NFH 27-2	2.12 × 10 ⁻⁵	4.57 × 10 ⁻⁴	7.00 × 10 ⁻¹
NFH 27-3	2.12 × 10 ⁻⁵	6.86 × 10 ⁻⁴	1.03
NFH 27-4	2.12 × 10 ⁻⁵	9.15 × 10 ⁻⁴	1.38
NFH 27-5	2.12 × 10 ⁻⁵	1.14 × 10 ⁻³	1.70
<i>k</i>₂ = 1.50 × 10³ L mol⁻¹ s⁻¹			

**Table 22:** Kinetics of the reaction of **1c** with **2f** in DMSO at 20°C (stopped-flow UV-Vis spectrometer, $\lambda = 422$ nm).

No.	[E] ₀ / mol L ⁻¹	[Nu] ₀ / mol L ⁻¹	<i>k</i> _{obs} / s ⁻¹
NFH 33-1	3.75 × 10 ⁻⁵	4.64 × 10 ⁻⁴	2.32 × 10 ⁻²
NFH 33-2	3.75 × 10 ⁻⁵	9.28 × 10 ⁻⁴	4.57 × 10 ⁻²
NFH 33-3	3.75 × 10 ⁻⁵	1.39 × 10 ⁻³	6.86 × 10 ⁻²
NFH 33-6	3.75 × 10 ⁻⁵	1.51 × 10 ⁻³	7.49 × 10 ⁻²
NFH 33-4	3.75 × 10 ⁻⁵	1.86 × 10 ⁻³	9.27 × 10 ⁻²
NFH 33-5	3.75 × 10 ⁻⁵	2.32 × 10 ⁻³	1.16 × 10 ⁻¹
<i>k</i>₂ = 5.01 × 10¹ L mol⁻¹ s⁻¹			

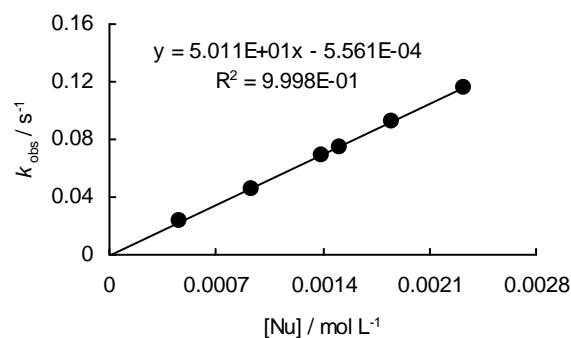
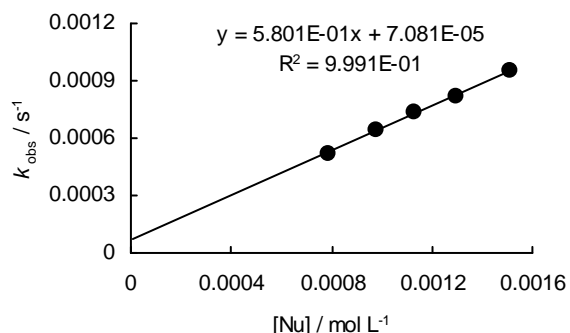
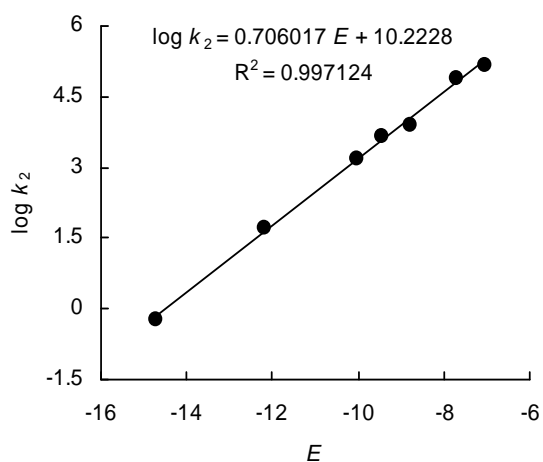


Table 23: Kinetics of the reaction of **1c** with **2v** in DMSO at 20°C (diode array UV-Vis spectrometer, $\lambda = 375$ nm).

No.	$[E]_0 / \text{mol L}^{-1}$	$[\text{Nu}]_0 / \text{mol L}^{-1}$	$k_{\text{obs}} / \text{s}^{-1}$
RAK 23.2-1	4.20×10^{-5}	7.87×10^{-4}	5.22×10^{-4}
RAK 23.2-2	4.52×10^{-5}	9.78×10^{-4}	6.42×10^{-4}
RAK 23.2-3	4.68×10^{-5}	1.13×10^{-3}	7.32×10^{-4}
RAK 23.2-4	4.62×10^{-5}	1.30×10^{-3}	8.22×10^{-4}
RAK 23.2-5	4.71×10^{-5}	1.51×10^{-3}	9.47×10^{-4}
$k_2 = 5.80 \times 10^{-1} \text{ L mol}^{-1} \text{ s}^{-1}$			

**Table 24:** Determination of the nucleophilicity parameters N , s for **1c** (correlation of $\log k_2$ for the reactions of **1c** with **2a–f,v** versus the electrophilicity parameters E for **2a–f,v**).

Nucleophile	Electrophile (E)	$k_2 / \text{L mol}^{-1} \text{ s}^{-1}$
 1c	2a (-7.02)	1.46×10^5
	2b (-7.69)	7.54×10^4
	2c (-8.76)	8.06×10^3
	2d (-9.45)	4.61×10^3
	2e (-10.04)	1.50×10^3
	2f (-12.18)	5.01×10^1
	2v (-14.70)	5.80×10^{-1}
$N = 14.48, s = 0.71$		



Kinetic investigation of the reactions of the sulfur ylide **1d** with the electrophiles **2a–f** in DMSO

Table 25: Kinetics of the reaction of **1d** with **2a** in DMSO at 20°C (stopped-flow UV-Vis spectrometer, $\lambda = 617$ nm).

No.	$[E]_0 / \text{mol L}^{-1}$	$[\text{Nu}]_0 / \text{mol L}^{-1}$	$k_{\text{obs}} / \text{s}^{-1}$
NFH 4-2	9.88×10^{-6}	1.16×10^{-4}	4.98×10^1
NFH 4-4	9.88×10^{-6}	1.74×10^{-4}	7.41×10^1
NFH 4-1	9.88×10^{-6}	2.32×10^{-4}	9.42×10^1
NFH 4-5	9.88×10^{-6}	2.90×10^{-4}	1.18×10^2
NFH 4-3	9.88×10^{-6}	3.49×10^{-4}	1.39×10^2
$k_2 = 3.83 \times 10^5 \text{ L mol}^{-1} \text{ s}^{-1}$			

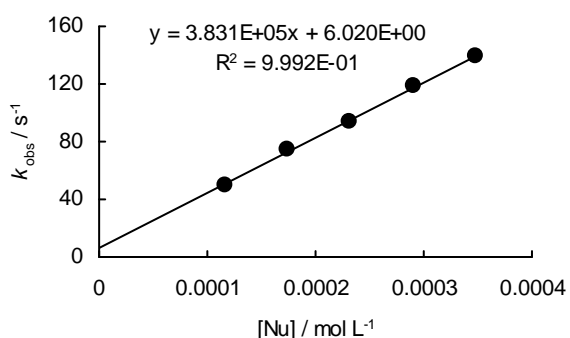
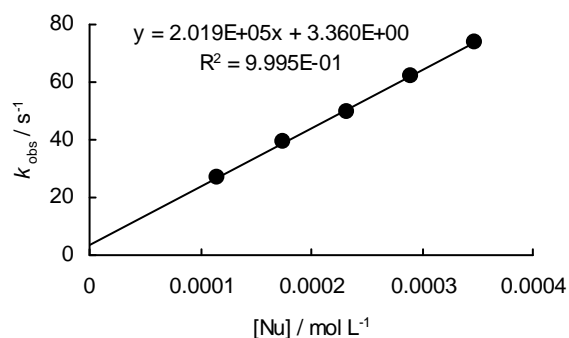
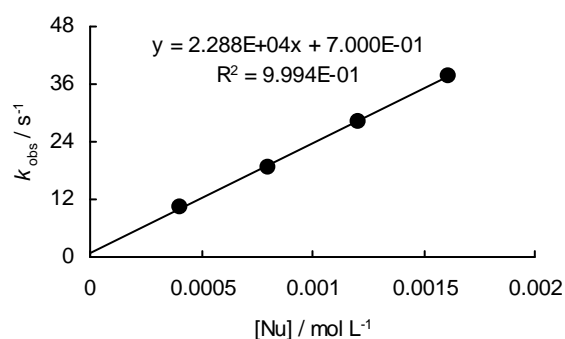


Table 26: Kinetics of the reaction of **1d** with **2b** in DMSO at 20°C (stopped-flow UV-Vis spectrometer, $\lambda = 617$ nm).

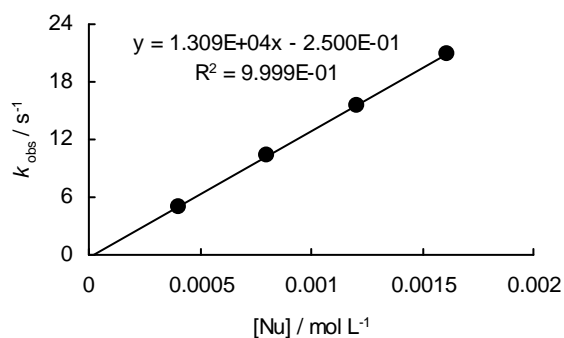
No.	$[E]_0 / \text{mol L}^{-1}$	$[\text{Nu}]_0 / \text{mol L}^{-1}$	$k_{\text{obs}} / \text{s}^{-1}$
NFH 3-2	9.99×10^{-6}	1.16×10^{-4}	2.68×10^1
NFH 3-4	9.99×10^{-6}	1.74×10^{-4}	3.90×10^1
NFH 3-1	9.99×10^{-6}	2.32×10^{-4}	4.96×10^1
NFH 3-5	9.99×10^{-6}	2.90×10^{-4}	6.21×10^1
NFH 3-3	9.99×10^{-6}	3.49×10^{-4}	7.39×10^1
$k_2 = 2.02 \times 10^5 \text{ L mol}^{-1} \text{ s}^{-1}$			

**Table 27:** Kinetics of the reaction of **1d** with **2c** in DMSO at 20°C (stopped-flow UV-Vis spectrometer, $\lambda = 630$ nm).

No.	$[E]_0 / \text{mol L}^{-1}$	$[\text{Nu}]_0 / \text{mol L}^{-1}$	$k_{\text{obs}} / \text{s}^{-1}$
NFH 2-1	2.02×10^{-5}	4.03×10^{-4}	1.02×10^1
NFH 2-2	2.02×10^{-5}	8.06×10^{-4}	1.88×10^1
NFH 2-3	2.02×10^{-5}	1.21×10^{-3}	2.82×10^1
NFH 2-4	2.02×10^{-5}	1.61×10^{-3}	3.78×10^1
$k_2 = 2.29 \times 10^4 \text{ L mol}^{-1} \text{ s}^{-1}$			

**Table 28:** Kinetics of the reaction of **1d** with **2d** in DMSO at 20°C (stopped-flow UV-Vis spectrometer, $\lambda = 630$ nm).

No.	$[E]_0 / \text{mol L}^{-1}$	$[\text{Nu}]_0 / \text{mol L}^{-1}$	$k_{\text{obs}} / \text{s}^{-1}$
NFH 1-1	2.22×10^{-5}	4.03×10^{-4}	5.05
NFH 1-2	2.22×10^{-5}	8.06×10^{-4}	1.03×10^1
NFH 1-3	2.22×10^{-5}	1.21×10^{-3}	1.55×10^1
NFH 1-4	2.22×10^{-5}	1.61×10^{-3}	2.09×10^1
$k_2 = 1.31 \times 10^4 \text{ L mol}^{-1} \text{ s}^{-1}$			

**Table 29:** Kinetics of the reaction of **1d** with **2e** in DMSO at 20°C (stopped-flow UV-Vis spectrometer, $\lambda = 630$ nm).

No.	$[E]_0 / \text{mol L}^{-1}$	$[\text{Nu}]_0 / \text{mol L}^{-1}$	$k_{\text{obs}} / \text{s}^{-1}$
RAK 13.1-1	1.38×10^{-5}	2.91×10^{-4}	1.37
RAK 13.1-2	1.38×10^{-5}	5.82×10^{-4}	2.80
RAK 13.1-3	1.38×10^{-5}	8.73×10^{-4}	4.29
RAK 13.1-4	1.38×10^{-5}	1.16×10^{-3}	5.81
RAK 13.1-5	1.38×10^{-5}	1.46×10^{-3}	7.19
RAK 13.1-6	1.38×10^{-5}	2.91×10^{-3}	1.46×10^1
$k_2 = 5.05 \times 10^3 \text{ L mol}^{-1} \text{ s}^{-1}$			

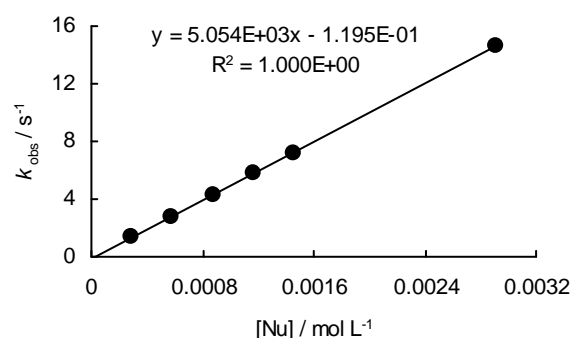
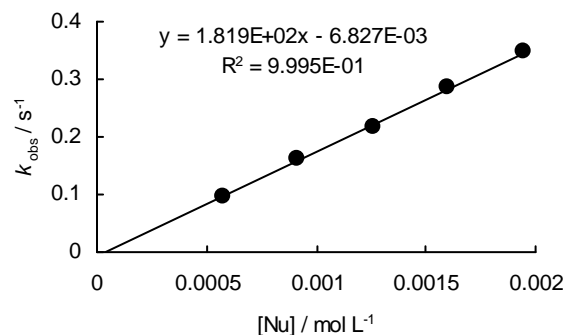


Table 30: Kinetics of the reaction of **1d** with **2f** in DMSO at 20°C (stopped-flow UV-Vis spectrometer, $\lambda = 422$ nm).

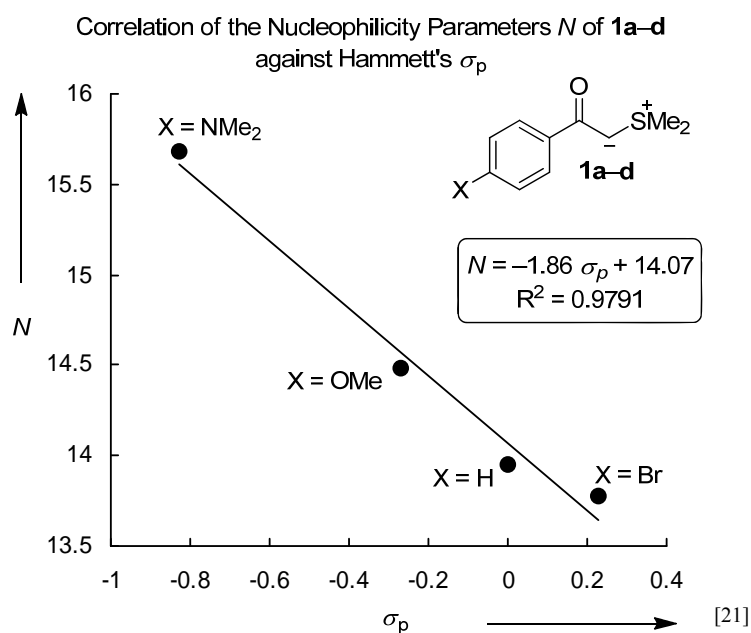
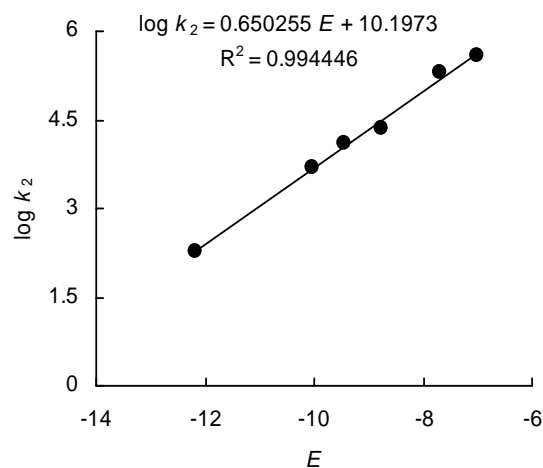
No.	$[E]_0 / \text{mol L}^{-1}$	$[\text{Nu}]_0 / \text{mol L}^{-1}$	$k_{\text{obs}} / \text{s}^{-1}$
NFH 5-1	1.96×10^{-5}	5.71×10^{-4}	9.74×10^{-2}
NFH 5-2	1.96×10^{-5}	9.13×10^{-4}	1.61×10^{-1}
NFH 5-3	1.96×10^{-5}	1.26×10^{-3}	2.18×10^{-1}
NFH 5-4	1.96×10^{-5}	1.60×10^{-3}	2.85×10^{-1}
NFH 5-5	1.96×10^{-5}	1.94×10^{-3}	3.47×10^{-1}

$k_2 = 1.82 \times 10^2 \text{ L mol}^{-1} \text{ s}^{-1}$

**Table 31:** Determination of the nucleophilicity parameters N , s for **1d** (correlation of $\log k_2$ for the reactions of **1d** with **2a–f** versus the electrophilicity parameters E for **2a–f**).

Nucleophile	Electrophile (E)	$k_2 / \text{L mol}^{-1} \text{ s}^{-1}$
 1d	2a (-7.02)	3.83×10^5
	2b (-7.69)	2.02×10^5
	2c (-8.76)	2.29×10^4
	2d (-9.45)	1.31×10^4
	2e (-10.04)	5.05×10^3
	2f (-12.18)	1.82×10^2

$N = 15.68, s = 0.65$



Kinetic investigation of the reactions of the sulfur ylide **1e** with the electrophiles **2e,h,i,l,r** in DMSO

Table 32: Kinetics of the reaction of **1e** with **2e** in DMSO at 20°C (stopped-flow UV-Vis spectrometer, $\lambda = 470$ nm).

No.	[Nu] ₀ / mol L ⁻¹ *	[E] ₀ / mol L ⁻¹	<i>k</i> _{obs} / s ⁻¹
RAK 16.4-3	$< 5 \times 10^{-5}$	5.56×10^{-4}	1.20×10^2
RAK 16.4-1	$< 5 \times 10^{-5}$	6.17×10^{-4}	1.31×10^2
RAK 16.4-4	$< 5 \times 10^{-5}$	6.79×10^{-4}	1.48×10^2
RAK 16.4-2	$< 5 \times 10^{-5}$	7.41×10^{-4}	1.62×10^2
RAK 16.4-5	$< 5 \times 10^{-5}$	8.03×10^{-4}	1.75×10^2

$$k_2 = 2.28 \times 10^5 \text{ L mol}^{-1} \text{ s}^{-1}$$

* Only approximate values are given for the initial concentration of the nucleophile (see general comments).

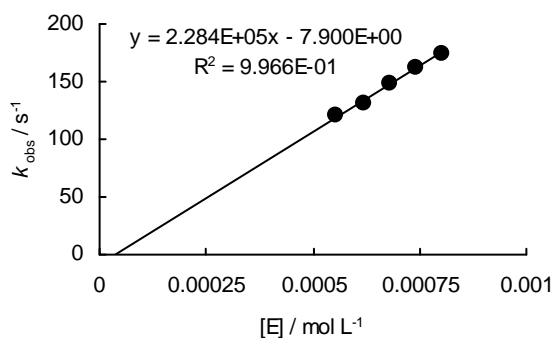


Table 33: Kinetics of the reaction of **1e** with **2h** in DMSO at 20°C (diode array UV-Vis spectrometer, $\lambda = 520$ nm).

No.	[Nu] ₀ / mol L ⁻¹ *	[E] ₀ / mol L ⁻¹	<i>k</i> _{obs} / s ⁻¹
RAK 16.6-1	$< 3 \times 10^{-5}$	3.83×10^{-4}	1.85×10^{-2}
RAK 16.6-2	$< 4 \times 10^{-5}$	4.53×10^{-4}	2.24×10^{-2}
RAK 16.6-3	$< 4 \times 10^{-5}$	5.17×10^{-4}	2.55×10^{-2}
RAK 16.6-4	$< 4 \times 10^{-5}$	5.75×10^{-4}	2.85×10^{-2}
RAK 16.6-5	$< 4 \times 10^{-5}$	6.37×10^{-4}	3.17×10^{-2}

$$k_2 = 5.16 \times 10^1 \text{ L mol}^{-1} \text{ s}^{-1}$$

* Only approximate values are given for the initial concentration of the nucleophile (see general comments).

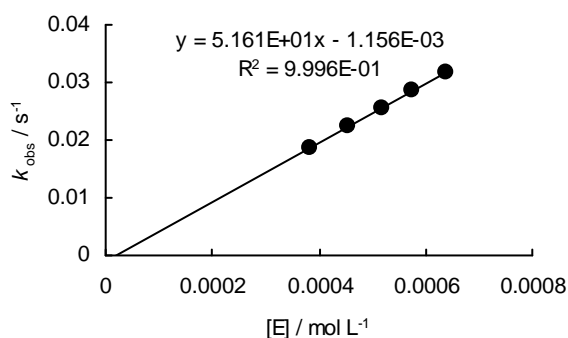


Table 34: Kinetics of the reaction of **1e** with **2i** in DMSO at 20°C (diode array UV-Vis spectrometer, $\lambda = 520$ nm).

No.	[Nu] ₀ / mol L ⁻¹ *	[E] ₀ / mol L ⁻¹	<i>k</i> _{obs} / s ⁻¹
RAK 16.8-1	$< 4 \times 10^{-5}$	4.27×10^{-4}	1.35×10^{-2}
RAK 16.8-2	$< 4 \times 10^{-5}$	5.77×10^{-4}	1.85×10^{-2}
RAK 16.8-3	$< 4 \times 10^{-5}$	7.11×10^{-4}	2.30×10^{-2}
RAK 16.8-4	$< 4 \times 10^{-5}$	8.53×10^{-4}	2.74×10^{-2}

$$k_2 = 3.27 \times 10^1 \text{ L mol}^{-1} \text{ s}^{-1}$$

* Only approximate values are given for the initial concentration of the nucleophile (see general comments).

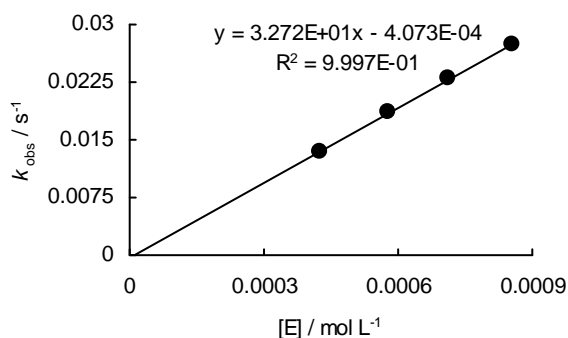
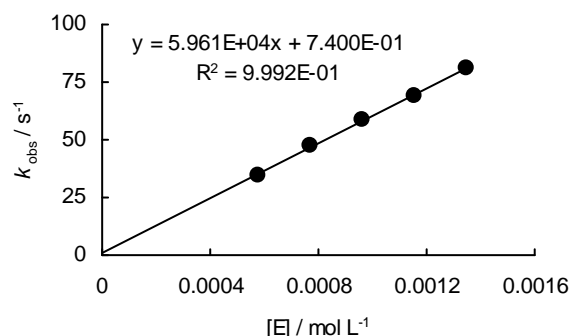


Table 35: Kinetics of the reaction of **1e** with **2l** in DMSO at 20°C (stopped-flow UV-Vis spectrometer, $\lambda = 530$ nm).

No.	[Nu] ₀ / mol L ⁻¹ *	[E] ₀ / mol L ⁻¹	<i>k</i> _{obs} / s ⁻¹
RAK 16.12-1	< 4 × 10 ⁻⁵	5.78 × 10 ⁻⁴	3.48 × 10 ¹
RAK 16.12-2	< 4 × 10 ⁻⁵	7.70 × 10 ⁻⁴	4.71 × 10 ¹
RAK 16.12-3	< 4 × 10 ⁻⁵	9.63 × 10 ⁻⁴	5.86 × 10 ¹
RAK 16.12-4	< 4 × 10 ⁻⁵	1.16 × 10 ⁻³	6.89 × 10 ¹
RAK 16.12-5	< 4 × 10 ⁻⁵	1.35 × 10 ⁻³	8.13 × 10 ¹

$k_2 = 5.96 \times 10^4 \text{ L mol}^{-1} \text{ s}^{-1}$

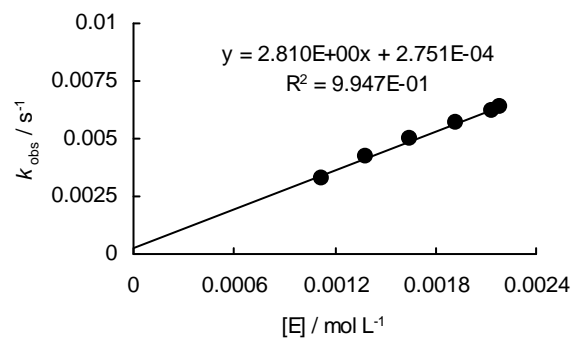
* Only approximate values are given for the initial concentration of the nucleophile (see general comments).

**Table 36:** Kinetics of the reaction of **1e** with **2r** in DMSO at 20°C (diode array UV-Vis spectrometer, $\lambda = 520$ nm).

No.	[Nu] ₀ / mol L ⁻¹ *	[E] ₀ / mol L ⁻¹	<i>k</i> _{obs} / s ⁻¹
RAK 16.10-1	< 4 × 10 ⁻⁵	1.12 × 10 ⁻³	3.31 × 10 ⁻³
RAK 16.10-2	< 4 × 10 ⁻⁵	1.38 × 10 ⁻³	4.25 × 10 ⁻³
RAK 16.10-3	< 4 × 10 ⁻⁵	1.65 × 10 ⁻³	4.98 × 10 ⁻³
RAK 16.10-4	< 4 × 10 ⁻⁵	1.92 × 10 ⁻³	5.71 × 10 ⁻³
RAK 16.10-6	< 5 × 10 ⁻⁵	2.14 × 10 ⁻³	6.19 × 10 ⁻³
RAK 16.10-6	< 5 × 10 ⁻⁵	2.18 × 10 ⁻³	6.41 × 10 ⁻³

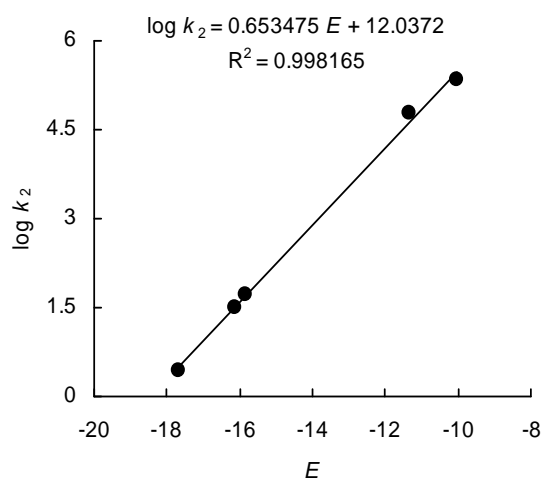
$k_2 = 2.81 \text{ L mol}^{-1} \text{ s}^{-1}$

* Only approximate values are given for the initial concentration of the nucleophile (see general comments).

**Table 37:** Determination of the nucleophilicity parameters *N*, *s* for **1e** (correlation of log *k*₂ for the reactions of **1e** with **2e,h,i,l,r** versus the electrophilicity parameters *E* for **2e,h,i,l,r**)

Nucleophile	Electrophile (<i>E</i>)	<i>k</i> ₂ / L mol ⁻¹ s ⁻¹
 1e	2e (-10.04)	2.28 × 10 ⁵
	2h (-15.83)	5.16 × 10 ¹
	2i (-16.11)	3.27 × 10 ¹
	2l (-11.32)	5.96 × 10 ⁴
	2r (-17.67)	2.81

$N = 18.42, s = 0.65$



Kinetic investigation of the reactions of the sulfur ylide **1f** with the electrophiles **2j,m,p,r-t** in DMSO

Table 38: Kinetics of the reaction of **1f** with **2j** in DMSO at 20°C (stopped-flow UV-Vis spectrometer, $\lambda = 380$ nm).

No.	[Nu] ₀ / mol L ⁻¹ *	[E] ₀ / mol L ⁻¹	<i>k</i> _{obs} / s ⁻¹
RAK 17.7-1	$< 6 \times 10^{-5}$	5.91×10^{-4}	2.27×10^{-1}
RAK 17.7-2	$< 6 \times 10^{-5}$	7.88×10^{-4}	3.06×10^{-1}
RAK 17.7-3	$< 6 \times 10^{-5}$	9.85×10^{-4}	3.84×10^{-1}
RAK 17.7-4	$< 6 \times 10^{-5}$	1.18×10^{-3}	4.62×10^{-1}
$k_2 = 3.97 \times 10^2$ L mol⁻¹ s⁻¹			

* Only approximate values are given for the initial concentration of the nucleophile (see general comments).

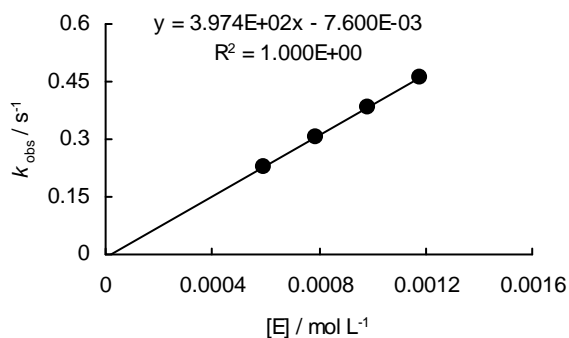


Table 39: Kinetics of the reaction of **1f** with **2m** in DMSO at 20°C (stopped-flow UV-Vis spectrometer, $\lambda = 380$ nm).

No.	[Nu] ₀ / mol L ⁻¹ *	[E] ₀ / mol L ⁻¹	<i>k</i> _{obs} / s ⁻¹
RAK 17.11-1	$< 6 \times 10^{-5}$	6.56×10^{-4}	1.00×10^2
RAK 17.11-4	$< 6 \times 10^{-5}$	7.09×10^{-4}	1.13×10^2
RAK 17.11-2	$< 6 \times 10^{-5}$	7.88×10^{-4}	1.23×10^2
RAK 17.11-5	$< 6 \times 10^{-5}$	8.40×10^{-4}	1.36×10^2
RAK 17.11-3	$< 6 \times 10^{-5}$	9.19×10^{-4}	1.47×10^2
$k_2 = 1.77 \times 10^5$ L mol⁻¹ s⁻¹			

* Only approximate values are given for the initial concentration of the nucleophile (see general comments).

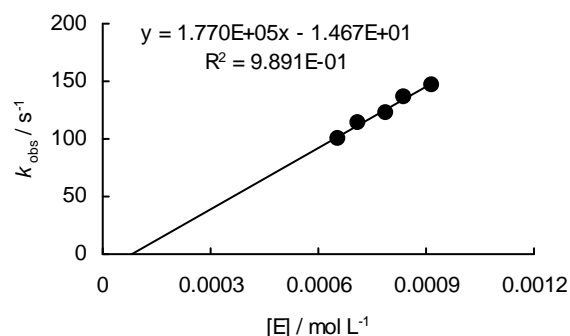


Table 40: Kinetics of the reaction of **1f** with **2p** in DMSO at 20°C (stopped-flow UV-Vis spectrometer, $\lambda = 360$ nm).

No.	[Nu] ₀ / mol L ⁻¹ *	[E] ₀ / mol L ⁻¹	<i>k</i> _{obs} / s ⁻¹
RAK 17.3-2	$< 5 \times 10^{-5}$	4.46×10^{-4}	1.53×10^2
RAK 17.3-4	$< 5 \times 10^{-5}$	5.01×10^{-4}	1.79×10^2
RAK 17.3-1	$< 5 \times 10^{-5}$	5.57×10^{-4}	1.98×10^2
RAK 17.3-5	$< 5 \times 10^{-5}$	6.13×10^{-4}	2.15×10^2
RAK 17.3-3	$< 5 \times 10^{-5}$	6.68×10^{-4}	2.38×10^2
$k_2 = 3.70 \times 10^5$ L mol⁻¹ s⁻¹			

* Only approximate values are given for the initial concentration of the nucleophile (see general comments).

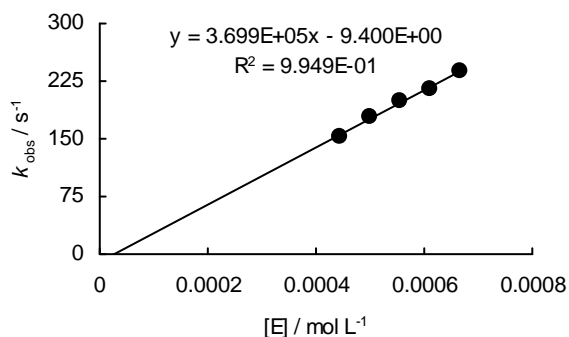
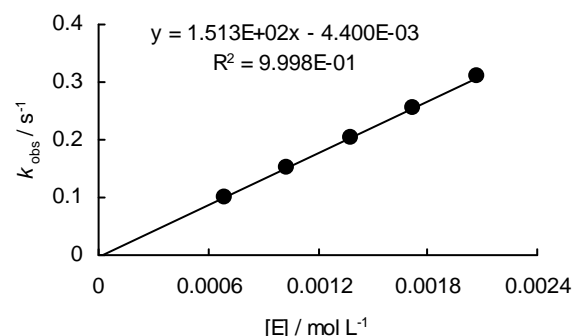


Table 41: Kinetics of the reaction of **1f** with **2r** in DMSO at 20°C (stopped-flow UV-Vis spectrometer, $\lambda = 390$ nm).

No.	[Nu] ₀ / mol L ⁻¹ *	[E] ₀ / mol L ⁻¹	k _{obs} / s ⁻¹
RAK 17.6-1	< 7 × 10 ⁻⁵	6.89 × 10 ⁻⁴	1.00 × 10 ⁻¹
RAK 17.6-2	< 7 × 10 ⁻⁵	1.03 × 10 ⁻³	1.53 × 10 ⁻¹
RAK 17.6-3	< 7 × 10 ⁻⁵	1.38 × 10 ⁻³	2.02 × 10 ⁻¹
RAK 17.6-4	< 7 × 10 ⁻⁵	1.72 × 10 ⁻³	2.56 × 10 ⁻¹
RAK 17.6-5	< 7 × 10 ⁻⁵	2.07 × 10 ⁻³	3.09 × 10 ⁻¹

$k_2 = 1.51 \times 10^2 \text{ L mol}^{-1} \text{ s}^{-1}$

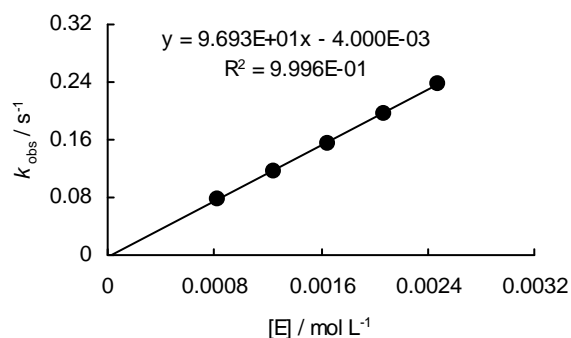
* Only approximate values are given for the initial concentration of the nucleophile (see general comments).

**Table 42:** Kinetics of the reaction of **1f** with **2s** in DMSO at 20°C (stopped-flow UV-Vis spectrometer, $\lambda = 390$ nm).

No.	[Nu] ₀ / mol L ⁻¹ *	[E] ₀ / mol L ⁻¹	k _{obs} / s ⁻¹
RAK 17.8-1	< 8 × 10 ⁻⁵	8.27 × 10 ⁻⁴	7.76 × 10 ⁻²
RAK 17.8-2	< 8 × 10 ⁻⁵	1.24 × 10 ⁻³	1.15 × 10 ⁻¹
RAK 17.8-3	< 8 × 10 ⁻⁵	1.65 × 10 ⁻³	1.55 × 10 ⁻¹
RAK 17.8-4	< 8 × 10 ⁻⁵	2.07 × 10 ⁻³	1.97 × 10 ⁻¹
RAK 17.8-5	< 8 × 10 ⁻⁵	2.48 × 10 ⁻³	2.37 × 10 ⁻¹

$k_2 = 9.69 \times 10^1 \text{ L mol}^{-1} \text{ s}^{-1}$

* Only approximate values are given for the initial concentration of the nucleophile (see general comments).

**Table 43:** Kinetics of the reaction of **1f** with **2t** in DMSO at 20°C (diode array UV-Vis spectrometer, $\lambda = 380$ nm).

No.	[Nu] ₀ / mol L ⁻¹ *	[E] ₀ / mol L ⁻¹	k _{obs} / s ⁻¹
RAK 17.1-5	< 5 × 10 ⁻⁵	4.61 × 10 ⁻⁴	1.86 × 10 ⁻²
RAK 17.1-1	< 5 × 10 ⁻⁵	6.16 × 10 ⁻⁴	2.50 × 10 ⁻²
RAK 17.1-2	< 6 × 10 ⁻⁵	7.68 × 10 ⁻⁴	2.99 × 10 ⁻²
RAK 17.1-3	< 7 × 10 ⁻⁵	9.02 × 10 ⁻⁴	3.42 × 10 ⁻²
RAK 17.1-4	< 7 × 10 ⁻⁵	1.04 × 10 ⁻³	3.91 × 10 ⁻²

$k_2 = 3.48 \times 10^1 \text{ L mol}^{-1} \text{ s}^{-1}$

* Only approximate values are given for the initial concentration of the nucleophile (see general comments).

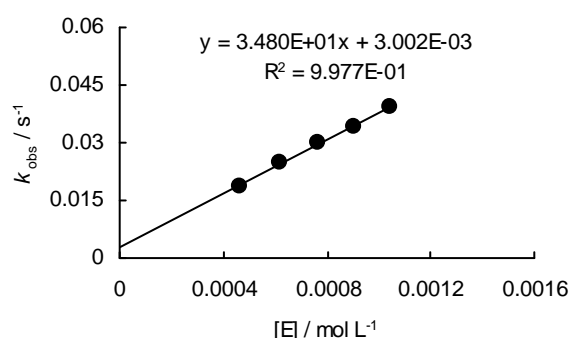
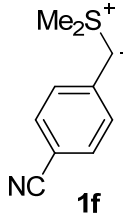
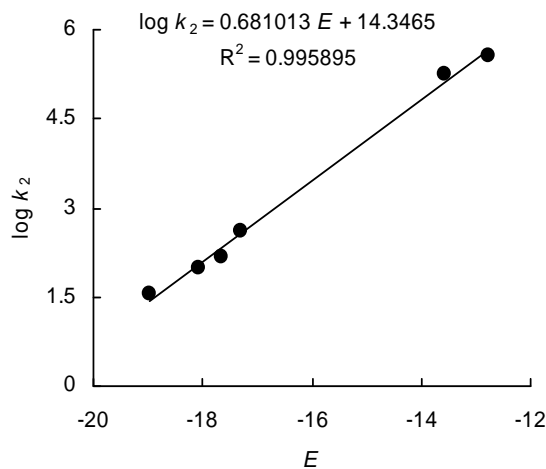


Table 44: Determination of the nucleophilicity parameters N , s for **1f** (correlation of $\log k_2$ for the reactions of **1f** with **2j,m,p,r-t** versus the electrophilicity parameters E for **2j,m,p,r-t**)

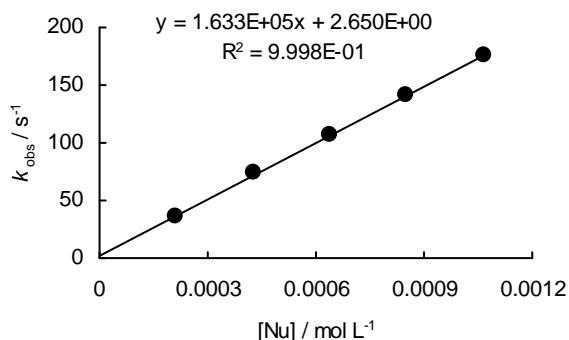
Nucleophile	Electrophile (E)	$k_2 / \text{L mol}^{-1} \text{s}^{-1}$
 1f	2j (-17.29)	3.97×10^2
	2m (-13.56)	1.77×10^5
	2p (-12.76)	3.70×10^5
	2r (-17.67)	1.51×10^2
	2s (-18.06)	9.69×10^1
	2t (-18.98)	3.48×10^1
$N = 21.07, s = 0.68$		



Kinetic investigation of the reactions of the sulfur ylide **1g** with the electrophiles **2d–k,m,n,p,q,r,u** in DMSO

Table 45: Kinetics of the reaction of **1g** with **2d** in DMSO at 20°C (stopped-flow UV-Vis spectrometer, $\lambda = 633 \text{ nm}$).

No.	$[E]_0 / \text{mol L}^{-1}$	$[\text{Nu}]_0 / \text{mol L}^{-1}$	$k_{\text{obs}} / \text{s}^{-1}$
RAK 20.13-1	1.92×10^{-5}	2.13×10^{-4}	3.65×10^1
RAK 20.13-2	1.92×10^{-5}	4.26×10^{-4}	7.33×10^1
RAK 20.13-3	1.92×10^{-5}	6.39×10^{-4}	1.07×10^2
RAK 20.13-4	1.92×10^{-5}	8.52×10^{-4}	1.42×10^2
RAK 20.13-5	1.92×10^{-5}	1.06×10^{-3}	1.76×10^2
$k_2 = 1.63 \times 10^5 \text{ L mol}^{-1} \text{s}^{-1}$			

**Table 46:** Kinetics of the reaction of **1g** with **2e** in DMSO at 20°C (stopped-flow UV-Vis spectrometer, $\lambda = 633 \text{ nm}$).

No.	$[E]_0 / \text{mol L}^{-1}$	$[\text{Nu}]_0 / \text{mol L}^{-1}$	$k_{\text{obs}} / \text{s}^{-1}$
RAK 20.12-1	1.82×10^{-5}	2.13×10^{-4}	1.39×10^1
RAK 20.12-2	1.82×10^{-5}	4.26×10^{-4}	2.81×10^1
RAK 20.12-3	1.82×10^{-5}	6.39×10^{-4}	4.16×10^1
RAK 20.12-4	1.82×10^{-5}	8.52×10^{-4}	5.51×10^1
RAK 20.12-5	1.82×10^{-5}	1.06×10^{-3}	6.83×10^1
$k_2 = 6.38 \times 10^4 \text{ L mol}^{-1} \text{s}^{-1}$			

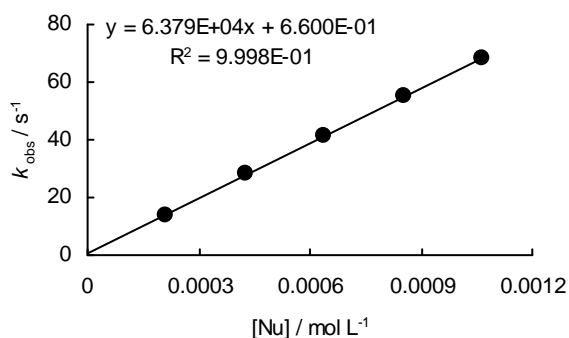
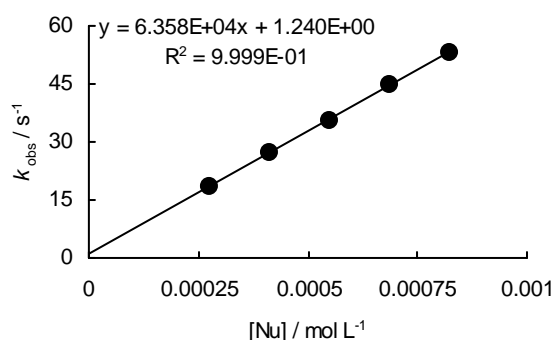


Table 47: Kinetics of the reaction of **1g** with **2e** in DMSO at 20°C (deprotonation of the CH acid $\text{Me}_3\text{SO}^+ \Gamma$ with 0.482 equiv of KOtBu, stopped-flow UV-Vis spectrometer, $\lambda = 633 \text{ nm}$).

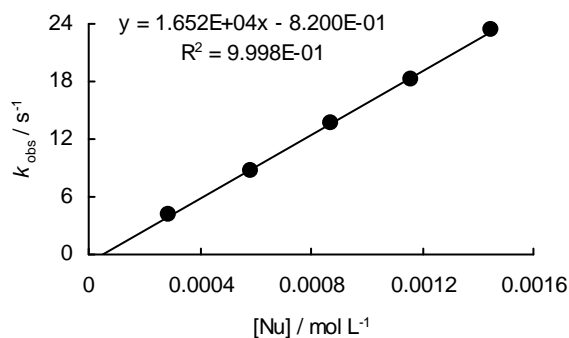
No.	$[\text{E}]_0 / \text{mol L}^{-1}$	$[\text{Nu}]_0 / \text{mol L}^{-1}$	$[(\text{Nu-H})-\text{I}] / \text{mol L}^{-1}$	$k_{\text{obs}} / \text{s}^{-1}$
RAK 20.15-1	1.48×10^{-5}	2.74×10^{-4}	2.94×10^{-4}	1.87×10^1
RAK 20.15-2	1.48×10^{-5}	4.11×10^{-4}	4.41×10^{-4}	2.74×10^1
RAK 20.15-3	1.48×10^{-5}	5.48×10^{-4}	5.88×10^{-4}	3.59×10^1
RAK 20.15-4	1.48×10^{-5}	6.85×10^{-4}	7.35×10^{-4}	4.49×10^1
RAK 20.15-5	1.48×10^{-5}	8.22×10^{-4}	8.82×10^{-4}	5.35×10^1

$k_2 = 6.36 \times 10^4 \text{ L mol}^{-1} \text{ s}^{-1}$

**Table 48:** Kinetics of the reaction of **1g** with **2f** in DMSO at 20°C (stopped-flow UV-Vis spectrometer, $\lambda = 422 \text{ nm}$).

No.	$[\text{E}]_0 / \text{mol L}^{-1}$	$[\text{Nu}]_0 / \text{mol L}^{-1}$	$k_{\text{obs}} / \text{s}^{-1}$
RAK 20.1-1	2.68×10^{-5}	2.90×10^{-4}	4.05
RAK 20.1-2	2.68×10^{-5}	5.81×10^{-4}	8.72
RAK 20.1-3	2.68×10^{-5}	8.71×10^{-4}	1.36×10^1
RAK 20.1-4	2.68×10^{-5}	1.16×10^{-3}	1.82×10^1
RAK 20.1-5	2.68×10^{-5}	1.45×10^{-3}	2.33×10^1

$k_2 = 1.65 \times 10^4 \text{ L mol}^{-1} \text{ s}^{-1}$

**Table 49:** Kinetics of the reaction of **1g** with **2g** in DMSO at 20°C (stopped-flow UV-Vis spectrometer, $\lambda = 533 \text{ nm}$).

No.	$[\text{E}]_0 / \text{mol L}^{-1}$	$[\text{Nu}]_0 / \text{mol L}^{-1}$	$k_{\text{obs}} / \text{s}^{-1}$
RAK 20.2-1	2.55×10^{-5}	3.87×10^{-4}	1.15
RAK 20.2-2	2.55×10^{-5}	7.74×10^{-4}	2.48
RAK 20.2-3	2.55×10^{-5}	1.16×10^{-3}	3.83
RAK 20.2-4	2.55×10^{-5}	1.55×10^{-3}	5.24
RAK 20.2-5	2.55×10^{-5}	1.94×10^{-3}	6.60

$k_2 = 3.53 \times 10^3 \text{ L mol}^{-1} \text{ s}^{-1}$

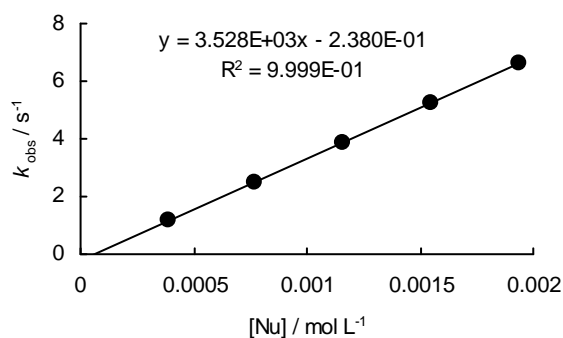
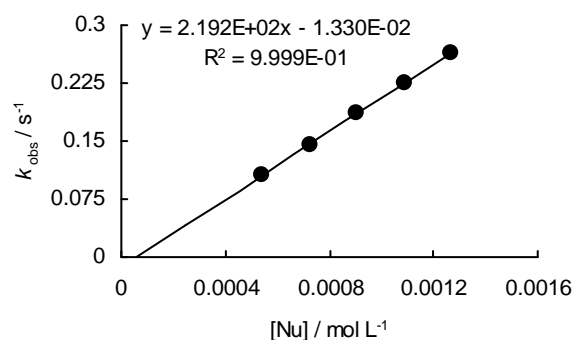
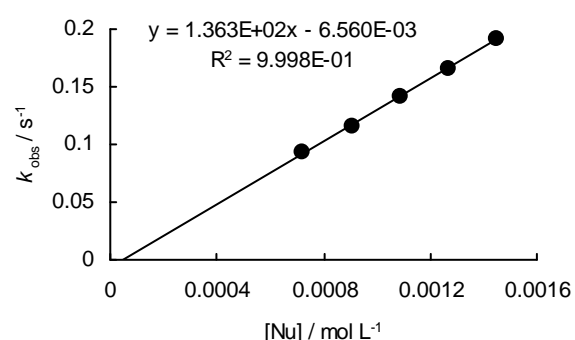


Table 50: Kinetics of the reaction of **1g** with **2h** in DMSO at 20°C (stopped-flow UV-Vis spectrometer, $\lambda = 371$ nm).

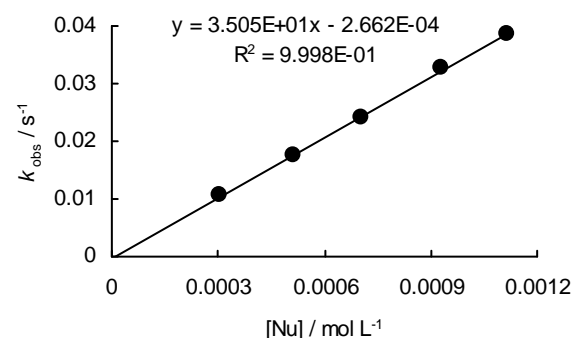
No.	$[E]_0 / \text{mol L}^{-1}$	$[\text{Nu}]_0 / \text{mol L}^{-1}$	$k_{\text{obs}} / \text{s}^{-1}$
RAK 20.7-1	2.37×10^{-5}	5.43×10^{-4}	1.06×10^{-1}
RAK 20.7-2	2.37×10^{-5}	7.24×10^{-4}	1.45×10^{-1}
RAK 20.7-3	2.37×10^{-5}	9.05×10^{-4}	1.85×10^{-1}
RAK 20.7-4	2.37×10^{-5}	1.09×10^{-3}	2.26×10^{-1}
RAK 20.7-5	2.37×10^{-5}	1.27×10^{-3}	2.64×10^{-1}
$k_2 = 2.19 \times 10^2 \text{ L mol}^{-1} \text{ s}^{-1}$			

**Table 51:** Kinetics of the reaction of **1g** with **2i** in DMSO at 20°C (stopped-flow UV-Vis spectrometer, $\lambda = 393$ nm).

No.	$[E]_0 / \text{mol L}^{-1}$	$[\text{Nu}]_0 / \text{mol L}^{-1}$	$k_{\text{obs}} / \text{s}^{-1}$
RAK 20.8-1	2.33×10^{-5}	7.24×10^{-4}	9.26×10^{-2}
RAK 20.8-2	2.33×10^{-5}	9.05×10^{-4}	1.16×10^{-1}
RAK 20.8-3	2.33×10^{-5}	1.09×10^{-3}	1.42×10^{-1}
RAK 20.8-4	2.33×10^{-5}	1.27×10^{-3}	1.66×10^{-1}
RAK 20.8-5	2.33×10^{-5}	1.45×10^{-3}	1.91×10^{-1}
$k_2 = 1.36 \times 10^2 \text{ L mol}^{-1} \text{ s}^{-1}$			

**Table 52:** Kinetics of the reaction of **1g** with **2j** in DMSO at 20°C (diode array UV-Vis spectrometer, $\lambda = 486$ nm).

No.	$[E]_0 / \text{mol L}^{-1}$	$[\text{Nu}]_0 / \text{mol L}^{-1}$	$k_{\text{obs}} / \text{s}^{-1}$
RAK 20.9-1	2.82×10^{-5}	3.06×10^{-4}	1.06×10^{-2}
RAK 20.9-2	3.54×10^{-5}	5.13×10^{-4}	1.76×10^{-2}
RAK 20.9-3	3.48×10^{-5}	7.06×10^{-4}	2.43×10^{-2}
RAK 20.9-4	3.57×10^{-5}	9.31×10^{-4}	3.26×10^{-2}
RAK 20.9-5	3.49×10^{-5}	1.11×10^{-3}	3.87×10^{-2}
$k_2 = 3.51 \times 10^1 \text{ L mol}^{-1} \text{ s}^{-1}$			

**Table 53:** Kinetics of the reaction of **1g** with **2k** in DMSO at 20°C (diode array UV-Vis spectrometer, $\lambda = 521$ nm).

No.	$[E]_0 / \text{mol L}^{-1}$	$[\text{Nu}]_0 / \text{mol L}^{-1}$	$k_{\text{obs}} / \text{s}^{-1}$
RAK 20.10-1	3.53×10^{-5}	6.08×10^{-4}	1.04×10^{-2}
RAK 20.10-2	4.12×10^{-5}	8.02×10^{-4}	1.37×10^{-2}
RAK 20.10-3	4.14×10^{-5}	1.01×10^{-3}	1.75×10^{-2}
RAK 20.10-4	4.10×10^{-5}	1.20×10^{-3}	2.11×10^{-2}
RAK 20.10-5	4.10×10^{-5}	1.40×10^{-3}	2.46×10^{-2}
$k_2 = 1.82 \times 10^1 \text{ L mol}^{-1} \text{ s}^{-1}$			

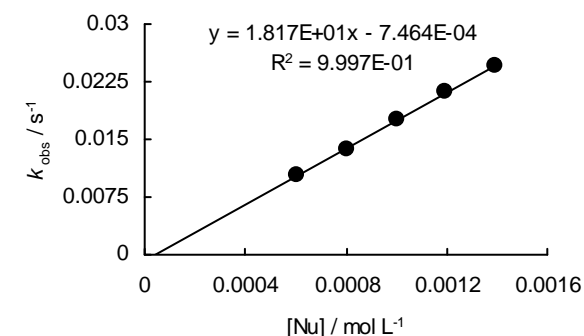
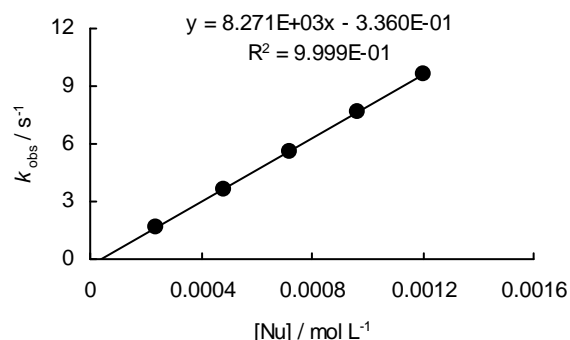
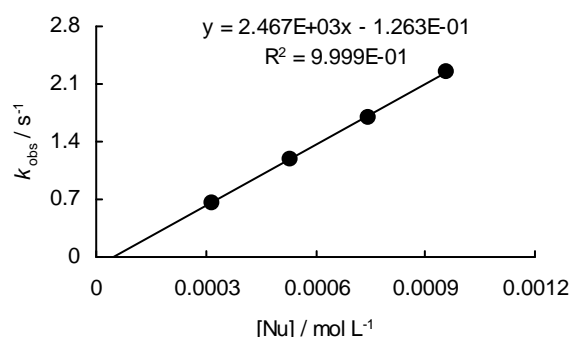


Table 54: Kinetics of the reaction of **1g** with **2m** in DMSO at 20°C (stopped-flow UV-Vis spectrometer, $\lambda = 470$ nm).

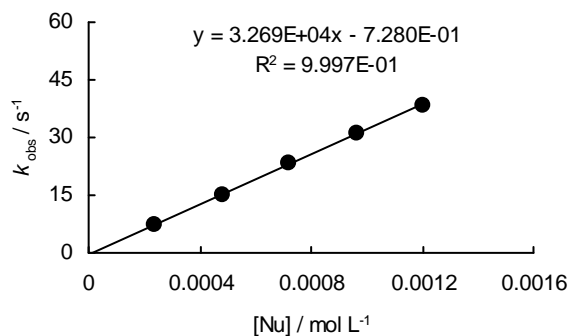
No.	$[E]_0 / \text{mol L}^{-1}$	$[\text{Nu}]_0 / \text{mol L}^{-1}$	$k_{\text{obs}} / \text{s}^{-1}$
RAK 20.4-1	2.34×10^{-5}	2.41×10^{-4}	1.67
RAK 20.4-2	2.34×10^{-5}	4.82×10^{-4}	3.63
RAK 20.4-3	2.34×10^{-5}	7.22×10^{-4}	5.62
RAK 20.4-4	2.34×10^{-5}	9.63×10^{-4}	7.67
RAK 20.4-5	2.34×10^{-5}	1.20×10^{-3}	9.61
$k_2 = 8.27 \times 10^3 \text{ L mol}^{-1} \text{ s}^{-1}$			

**Table 55:** Kinetics of the reaction of **1g** with **2n** in DMSO at 20°C (stopped-flow UV-Vis spectrometer, $\lambda = 520$ nm).

No.	$[E]_0 / \text{mol L}^{-1}$	$[\text{Nu}]_0 / \text{mol L}^{-1}$	$k_{\text{obs}} / \text{s}^{-1}$
RAK 20.6-1	2.58×10^{-5}	3.19×10^{-4}	6.61×10^{-1}
RAK 20.6-2	2.58×10^{-5}	5.32×10^{-4}	1.19
RAK 20.6-3	2.58×10^{-5}	7.44×10^{-4}	1.70
RAK 20.6-4	2.58×10^{-5}	9.57×10^{-4}	2.24
$k_2 = 2.47 \times 10^3 \text{ L mol}^{-1} \text{ s}^{-1}$			

**Table 56:** Kinetics of the reaction of **1g** with **2p** in DMSO at 20°C (stopped-flow UV-Vis spectrometer, $\lambda = 470$ nm).

No.	$[E]_0 / \text{mol L}^{-1}$	$[\text{Nu}]_0 / \text{mol L}^{-1}$	$k_{\text{obs}} / \text{s}^{-1}$
RAK 20.3-1	2.40×10^{-5}	2.41×10^{-4}	7.14
RAK 20.3-2	2.40×10^{-5}	4.82×10^{-4}	1.48×10^1
RAK 20.3-3	2.40×10^{-5}	7.22×10^{-4}	2.32×10^1
RAK 20.3-4	2.40×10^{-5}	9.63×10^{-4}	3.08×10^1
RAK 20.3-5	2.40×10^{-5}	1.20×10^{-3}	3.85×10^1
$k_2 = 3.27 \times 10^4 \text{ L mol}^{-1} \text{ s}^{-1}$			

**Table 57:** Kinetics of the reaction of **1g** with **2q** in DMSO at 20°C (stopped-flow UV-Vis spectrometer, $\lambda = 520$ nm).

No.	$[E]_0 / \text{mol L}^{-1}$	$[\text{Nu}]_0 / \text{mol L}^{-1}$	$k_{\text{obs}} / \text{s}^{-1}$
RAK 20.5-1	2.48×10^{-5}	3.19×10^{-4}	2.65
RAK 20.5-2	2.48×10^{-5}	5.32×10^{-4}	4.68
RAK 20.5-3	2.48×10^{-5}	7.44×10^{-4}	6.68
RAK 20.5-4	2.48×10^{-5}	9.57×10^{-4}	8.75
$k_2 = 9.55 \times 10^3 \text{ L mol}^{-1} \text{ s}^{-1}$			

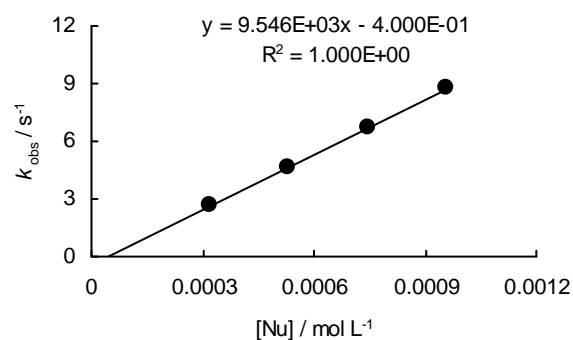
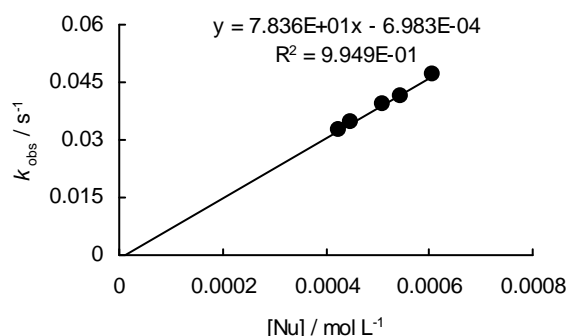
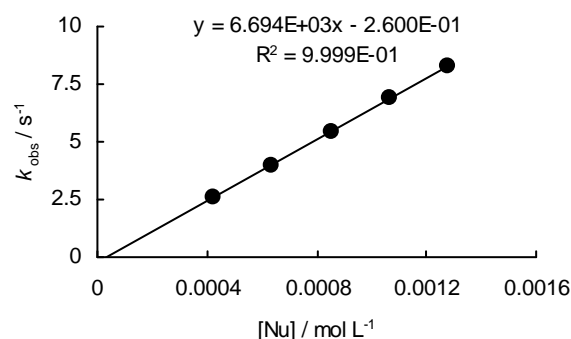


Table 58: Kinetics of the reaction of **1g** with **2r** in DMSO at 20°C (diode array UV-Vis spectrometer, $\lambda = 310$ nm).

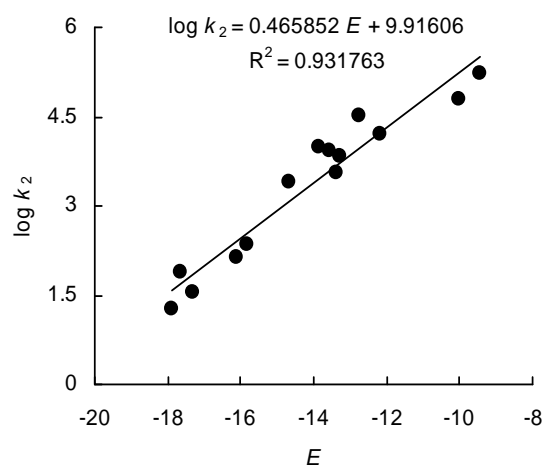
No.	$[E]_0 / \text{mol L}^{-1}$	$[\text{Nu}]_0 / \text{mol L}^{-1}$	$k_{\text{obs}} / \text{s}^{-1}$
RAK 20.11-1	3.98×10^{-5}	4.25×10^{-4}	3.27×10^{-2}
RAK 20.11-4	4.07×10^{-5}	4.48×10^{-4}	3.44×10^{-2}
RAK 20.11-2	4.06×10^{-5}	5.08×10^{-4}	3.94×10^{-2}
RAK 20.11-5	4.04×10^{-5}	5.46×10^{-4}	4.14×10^{-2}
RAK 20.11-3	4.29×10^{-5}	6.06×10^{-4}	4.71×10^{-2}
$k_2 = 7.84 \times 10^1 \text{ L mol}^{-1} \text{ s}^{-1}$			

**Table 59:** Kinetics of the reaction of **1g** with **2u** in DMSO at 20°C (stopped-flow UV-Vis spectrometer, $\lambda = 441$ nm).

No.	$[E]_0 / \text{mol L}^{-1}$	$[\text{Nu}]_0 / \text{mol L}^{-1}$	$k_{\text{obs}} / \text{s}^{-1}$
RAK 20.14-1	2.12×10^{-5}	4.26×10^{-4}	2.61
RAK 20.14-2	2.12×10^{-5}	6.39×10^{-4}	4.00
RAK 20.14-3	2.12×10^{-5}	8.52×10^{-4}	5.41
RAK 20.14-4	2.12×10^{-5}	1.06×10^{-3}	6.89
RAK 20.14-5	2.12×10^{-5}	1.28×10^{-3}	8.29
$k_2 = 6.69 \times 10^3 \text{ L mol}^{-1} \text{ s}^{-1}$			

**Table 60:** Determination of the nucleophilicity parameters N , s for **1g** (correlation of $\log k_2$ for the reactions of **1g** with **2d–k,m,n,p,q,r,u** versus the electrophilicity parameters E for **2d–k,m,n,p,q,r,u**).

Nucleophile	Electrophile (E)	$k_2 / \text{L mol}^{-1} \text{ s}^{-1}$
 1g	2d (-9.45)	1.63×10^5
	2e (-10.04)	6.38×10^4
	2f (-12.18)	1.65×10^4
	2g (-13.39)	3.53×10^3
	2h (-15.83)	2.19×10^2
	2i (-16.11)	1.36×10^2
	2j (-17.29)	3.51×10^1
	2k (-17.90)	1.82×10^1
	2m (-13.56)	8.27×10^3
	2n (-14.68)	2.47×10^3
	2p (-12.76)	3.27×10^4
	2q (-13.84)	9.55×10^3
	2r (-17.67)	7.84×10^1
	2u (-13.30)	6.69×10^3
	$N = 21.29, s = 0.47$	



Kinetic investigation of the reactions of the sulfur ylide **1h** with the Michael acceptors **2l,m,o** in DMSO

Table 61: Kinetics of the reaction of **1h** with **2l** in DMSO at 20°C (stopped-flow UV-Vis spectrometer, $\lambda = 375$ nm).

No.	$[E]_0 / \text{mol L}^{-1}$	$[\text{Nu}]_0 / \text{mol L}^{-1}$	$k_{\text{obs}} / \text{s}^{-1}$
RAK 23.50-1	4.56×10^{-5}	4.91×10^{-4}	1.08
RAK 23.50-2	4.56×10^{-5}	6.54×10^{-4}	1.50
RAK 23.50-3	4.56×10^{-5}	8.18×10^{-4}	1.89
RAK 23.50-4	4.56×10^{-5}	9.82×10^{-4}	2.27
RAK 23.50-5	4.56×10^{-5}	1.15×10^{-3}	2.67
$k_2 = 2.41 \times 10^3 \text{ L mol}^{-1} \text{ s}^{-1}$			

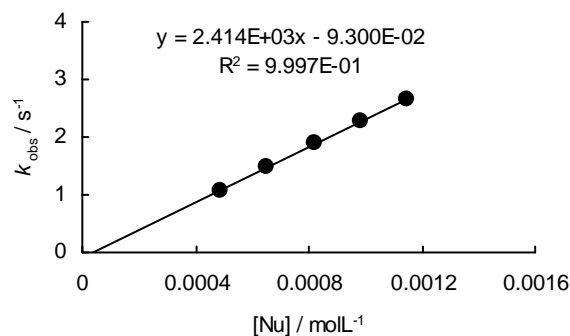


Table 62: Kinetics of the reaction of **1h** with **2m** in DMSO at 20°C (diode array UV-Vis spectrometer, $\lambda = 493$ nm).

No.	$[E]_0 / \text{mol L}^{-1}$	$[\text{Nu}]_0 / \text{mol L}^{-1}$	$k_{\text{obs}} / \text{s}^{-1}$
RAK 23.52-1	2.15×10^{-5}	2.18×10^{-4}	2.39×10^{-2}
RAK 23.52-2	2.30×10^{-5}	3.28×10^{-4}	3.59×10^{-2}
RAK 23.52-3	2.29×10^{-5}	4.34×10^{-4}	4.89×10^{-2}
RAK 23.52-4	2.27×10^{-5}	5.39×10^{-4}	6.11×10^{-2}
RAK 23.52-5	2.27×10^{-5}	6.45×10^{-4}	7.21×10^{-2}
$k_2 = 1.14 \times 10^2 \text{ L mol}^{-1} \text{ s}^{-1}$			

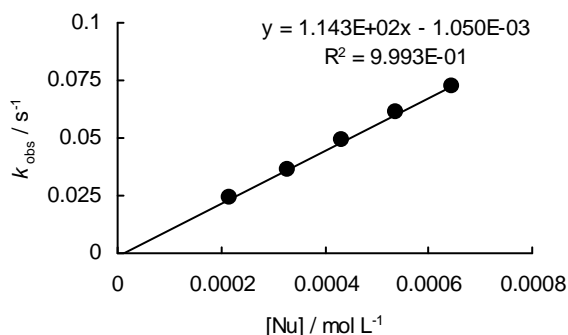
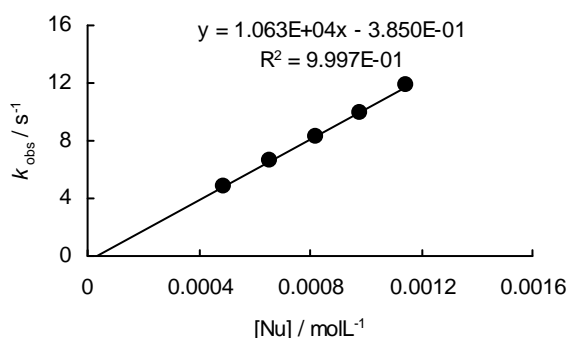


Table 63: Kinetics of the reaction of **1h** with **2o** in DMSO at 20°C (stopped-flow UV-Vis spectrometer, $\lambda = 375$ nm).

No.	$[E]_0 / \text{mol L}^{-1}$	$[\text{Nu}]_0 / \text{mol L}^{-1}$	$k_{\text{obs}} / \text{s}^{-1}$
RAK 23.51-1	4.38×10^{-5}	4.91×10^{-4}	4.79
RAK 23.51-2	4.38×10^{-5}	6.54×10^{-4}	6.63
RAK 23.51-3	4.38×10^{-5}	8.18×10^{-4}	8.33
RAK 23.51-4	4.38×10^{-5}	9.82×10^{-4}	1.00×10^1
RAK 23.51-5	4.38×10^{-5}	1.15×10^{-3}	1.18×10^1
$k_2 = 1.06 \times 10^4 \text{ L mol}^{-1} \text{ s}^{-1}$			



5.4 Comparison of Basicity and Nucleophilicity

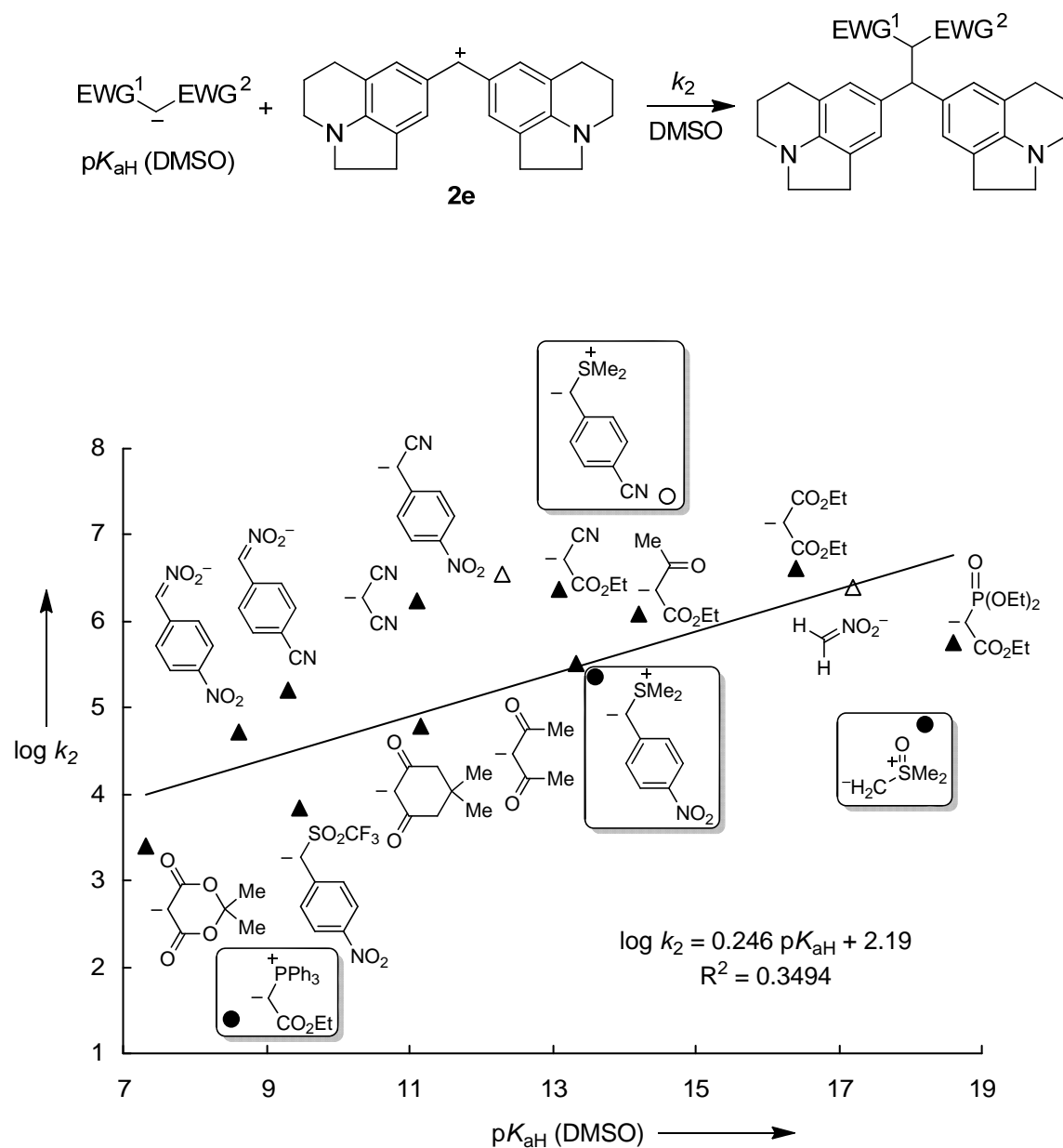


Figure 6: Plot of $\log k_2$ for the reactions of different classes of ylides and carbanions with the benzhydrylium ion **2e** (DMSO, 20°C) versus the $\text{p}K_{\text{aH}}$ values of the corresponding CH acids (DMSO, 25°C). The second-order rate constants k_2 (filled symbols) are taken from refs 8, 9c, and 14 of the original manuscript. Second-order rate constants k_2 for data points with open symbols are calculated by using equation 1. The $\text{p}K_{\text{aH}}$ values are taken from refs 7c and 15 of the original manuscript.

6 References

- [1] Ingold, C. K.; Jessop, J. A. *J. Chem. Soc.* **1930**, 713-718.
- [2] (a) Johnson, A. W.; LaCount, R. B. *Chem. Ind. (London)* **1958**, 1440-1441. (b) Johnson, A. W.; LaCount, R. B. *J. Am. Chem. Soc.* **1961**, *83*, 417-423. (c) Corey, E. J.; Chaykovsky, M. *J. Am. Chem. Soc.* **1962**, *84*, 867-868. (d) Corey, E. J.; Chaykovsky, M. *J. Am. Chem. Soc.* **1962**, *84*, 3782-3783. (e) Franzen, V.; Driessen, H.-E. *Tetrahedron Lett.* **1962**, *3*, 661-662. (f) Franzen, V.; Driessen, H.-E. *Chem. Ber.* **1963**, *96*, 1881-1890. (g) Johnson, A. W.; Hruby, V. J.; Williams, J. L. *J. Am. Chem. Soc.* **1964**, *86*, 918-922. (h) Corey, E. J.; Chaykovsky, M. *J. Am. Chem. Soc.* **1965**, *87*, 1353-1364. (i) Johnson, A. W.; Amel, R. T. *Tetrahedron Lett.* **1966**, *7*, 819-823. (j) Ratts, K. W.; Yao, A. N. *J. Org. Chem.* **1966**, *31*, 1185-1188. (k) Ratts, K. W.; Yao, A. N. *J. Org. Chem.* **1966**, *31*, 1689-1693. (l) Casanova, J.; Rutolo, D. A. *Chem. Commun. (London)* **1967**, 1224-1225. (m) Nozaki, H.; Tunemoto, D.; Matubara, S.; Kondô, K. *Tetrahedron* **1967**, *23*, 545-551. (n) Payne, G. B. *J. Org. Chem.* **1967**, *32*, 3351-3355. (o) Trost, B. M. *J. Am. Chem. Soc.* **1967**, *89*, 138-142. (p) Johnson, A. W.; Amel, R. T. *J. Org. Chem.* **1969**, *34*, 1240-1247. (q) Adams, J.; Hoffman, L.; Trost, B. M. *J. Org. Chem.* **1970**, *35*, 1600-1604. (r) Jeckel, D.; Gosselck, J. *Tetrahedron Lett.* **1972**, *13*, 2101-2104. (s) Trost, B. M.; Melvin, L. S. *Sulfur Ylides. Emerging Synthetic Intermediates*; Academic Press: New York, 1975.
- [3] For selected reviews, see: (a) Li, A.-H.; Dai, L.-X.; Aggarwal, V. K. *Chem. Rev.* **1997**, *97*, 2341-2372. (b) Dai, L.-X.; Hou, X.-L.; Zhou, Y.-G. *Pure Appl. Chem.* **1999**, *71*, 369-376. (c) Clark, J. S. In *Nitrogen, Oxygen and Sulfur Ylide Chemistry*; Clark, J. S., Ed.; Oxford University Press: New York, 2002; pp 1-114. (d) Aggarwal, V. K.; Richardson, J. In *Science of Synthesis*; Georg Thieme Verlag: Stuttgart, 2004; Vol. 27, pp 21-104. (e) Aggarwal, V. K.; Winn, C. L. *Acc. Chem. Res.* **2004**, *37*, 611-620. (f) Aggarwal, V. K.; Badine, D. M.; Moorthie, V. A. In *Aziridines and Epoxides in Organic Synthesis*; Yudin, A. K., Ed.; Wiley-VCH: Weinheim, 2006; pp 1-35. (g) McGarrigle, E. M.; Aggarwal, V. K. In *Enantioselective Organocatalysis*; Dalko, P. I., Ed.; Wiley-VCH: Weinheim, 2007; pp 357-390. (h) McGarrigle, E. M.; Myers, E. L.; Illa, O.; Shaw, M. A.; Riches, S. L.; Aggarwal, V. K. *Chem. Rev.* **2007**, *107*, 5841-5883. (i) Aggarwal, V. K.; Crimmin, M.; Riches, S. In *Science of Synthesis*; Georg Thieme Verlag: Stuttgart, 2008; Vol. 37, pp 321-406. (j) Brière, J.-F.; Metzner, P. In *Organosulfur Chemistry in Asymmetric Synthesis*; Toru, T., Bolm, C., Eds.; Wiley-

- VCH: Weinheim, 2008; pp 179-208. (k) Sun, X.-L.; Tang, Y. *Acc. Chem. Res.* **2008**, *41*, 937-948.
- [4] (a) Yoshimine, M.; Hatch, M. J. *J. Am. Chem. Soc.* **1967**, *89*, 5831-5838. (b) Johnson, C. R.; Schroeck, C. W. *J. Am. Chem. Soc.* **1971**, *93*, 5303-5305. (c) Volatron, F.; Eisenstein, O. *J. Am. Chem. Soc.* **1987**, *109*, 1-14. (d) For the special case of a Corey-Chaykovsky reaction with oxathietane formation, see: Kawashima, T.; Ohno, F.; Okazaki, R.; Ikeda, H.; Inagaki, S. *J. Am. Chem. Soc.* **1996**, *118*, 12455-12456. (e) Aggarwal, V. K.; Calamai, S.; Ford, J. G. *J. Chem. Soc., Perkin Trans. 1* **1997**, 593-599. (f) Lindvall, M. K.; Koskinen, A. M. P. *J. Org. Chem.* **1999**, *64*, 4596-4606. (g) Myllymäki, V. T.; Lindvall, M. K.; Koskinen, A. M. P. *Tetrahedron* **2001**, *57*, 4629-4635. (h) Aggarwal, V. K.; Harvey, J. N.; Richardson, J. *J. Am. Chem. Soc.* **2002**, *124*, 5747-5756. (i) Silva, M. A.; Bellenie, B. R.; Goodman, J. M. *Org. Lett.* **2004**, *6*, 2559-2562. (j) Aggarwal, V. K.; Bi, J. *Beilstein J. Org. Chem.* **2005**, *1*, doi: 10.1186/1860-5397-1-4. (k) Aggarwal, V. K.; Hebach, C. *Org. Biomol. Chem.* **2005**, *3*, 1419-1427. (l) Aggarwal, V. K.; Charmant, J. P. H.; Fuentes, D.; Harvey, J. N.; Hynd, G.; Ohara, D.; Picoul, W.; Robiette, R.; Smith, C.; Vasse, J.-L.; Winn, C. L. *J. Am. Chem. Soc.* **2006**, *128*, 2105-2114. (m) Edwards, D. R.; Du, J.; Crudden, C. M. *Org. Lett.* **2007**, *9*, 2397-2400. (n) Edwards, D. R.; Montoya-Peleaz, P.; Crudden, C. M. *Org. Lett.* **2007**, *9*, 5481-5484.
- [5] (a) Midura, W. H.; Krysiak, J. A.; Cypryk, M.; Mikołajczyk, M.; Wieczorek, M. W.; Filipczak, A. D. *Eur. J. Org. Chem.* **2005**, 653-662. (b) Aggarwal, V. K.; Grange, E. *Chem. Eur. J.* **2006**, *12*, 568-575. (c) Deng, X.-M.; Cai, P.; Ye, S.; Sun, X.-L.; Liao, W.-W.; Li, K.; Tang, Y.; Wu, Y.-D.; Dai, L.-X. *J. Am. Chem. Soc.* **2006**, *128*, 9730-9740. (d) Janardanan, D.; Sunoj, R. B. *J. Org. Chem.* **2007**, *72*, 331-341. (e) Riches, S. L.; Saha, C.; Filgueira, N. F.; Grange, E.; McGarrigle, E. M.; Aggarwal, V. K. *J. Am. Chem. Soc.* **2010**, *132*, 7626-7630.
- [6] (a) Aggarwal, V. K.; Charmant, J. P. H.; Ciampi, C.; Hornby, J. M.; O'Brien, C. J.; Hynd, G.; Parsons, R. *J. Chem. Soc., Perkin Trans. 1* **2001**, 3159-3166. (b) Yang, X.-F.; Zhang, M.-J.; Hou, X.-L.; Dai, L.-X. *J. Org. Chem.* **2002**, *67*, 8097-8103. (c) Robiette, R. *J. Org. Chem.* **2006**, *71*, 2726-2734. (d) Janardanan, D.; Sunoj, R. B. *Chem. Eur. J.* **2007**, *13*, 4805-4815. (e) Janardanan, D.; Sunoj, R. B. *J. Org. Chem.* **2008**, *73*, 8163-8174.
- [7] (a) Ratts, K. W. *J. Org. Chem.* **1972**, *37*, 848-851. (b) Cheng, J.-P.; Liu, B.; Zhang, X.-M. *J. Org. Chem.* **1998**, *63*, 7574-7575. (c) Cheng, J.-P.; Liu, B.; Zhao, Y.; Sun, Y.;

- Zhang, X.-M.; Lu, Y. *J. Org. Chem.* **1999**, *64*, 604-610. (d) Fu, Y.; Wang, H.-J.; Chong, S.-S.; Guo, Q.-X.; Liu, L. *J. Org. Chem.* **2009**, *74*, 810-819.
- [8] (a) Lucius, R.; Mayr, H. *Angew. Chem.* **2000**, *112*, 2086-2089; *Angew. Chem. Int. Ed.* **2000**, *39*, 1995-1997. (b) Berger, S. T. A.; Ofial, A. R.; Mayr, H. *J. Am. Chem. Soc.* **2007**, *129*, 9753-9761. (c) Appel, R.; Loos, R.; Mayr, H. *J. Am. Chem. Soc.* **2009**, *131*, 704-714. (d) Kaumanns, O.; Appel, R.; Lemek, T.; Seeliger, F.; Mayr, H. *J. Org. Chem.* **2009**, *74*, 75-81.
- [9] (a) Mayr, H.; Patz, M. *Angew. Chem.* **1994**, *106*, 990-1010; *Angew. Chem. Int. Ed. Engl.* **1994**, *33*, 938-957. (b) Mayr, H.; Bug, T.; Gotta, M. F.; Hering, N.; Irrgang, B.; Janker, B.; Kempf, B.; Loos, R.; Ofial, A. R.; Remennikov, G.; Schimmel, H. *J. Am. Chem. Soc.* **2001**, *123*, 9500-9512. (c) Lucius, R.; Loos, R.; Mayr, H. *Angew. Chem.* **2002**, *114*, 97-102; *Angew. Chem. Int. Ed.* **2002**, *41*, 91-95. (d) Lemek, T.; Mayr, H. *J. Org. Chem.* **2003**, *68*, 6880-6886. (e) Mayr, H.; Kempf, B.; Ofial, A. R. *Acc. Chem. Res.* **2003**, *36*, 66-77. (f) Mayr, H.; Ofial, A. R. *Pure Appl. Chem.* **2005**, *77*, 1807-1821. (g) Berger, S. T. A.; Seeliger, F. H.; Hofbauer, F.; Mayr, H. *Org. Biomol. Chem.* **2007**, *5*, 3020-3026. (h) Seeliger, F.; Berger, S. T. A.; Remennikov, G. Y.; Polborn, K.; Mayr, H. *J. Org. Chem.* **2007**, *72*, 9170-9180. (i) Kaumanns, O.; Lucius, R.; Mayr, H. *Chem. Eur. J.* **2008**, *14*, 9675-9682. (j) Mayr, H.; Ofial, A. R. *J. Phys. Org. Chem.* **2008**, *21*, 584-595. (k) Zenz, I.; Mayr, H. *unpublished results* **2010**. (l) For a comprehensive database of nucleophilicity parameters N and electrophilicity parameters E , see <http://www.cup.lmu.de/oc/mayr/>.
- [10] Appel, R.; Mayr, H. *Chem. Eur. J.* **2010**, *16*, 8610-8614.
- [11] (a) Lu, L.-Q.; Cao, Y.-J.; Liu, X.-P.; An, J.; Yao, C.-J.; Ming, Z.-H.; Xiao, W.-J. *J. Am. Chem. Soc.* **2008**, *130*, 6946-6948. (b) Lu, L.-Q.; Li, F.; An, J.; Zhang, J.-J.; An, X.-L.; Hua, Q.-L.; Xiao, W.-J. *Angew. Chem.* **2009**, *121*, 9706-9709; *Angew. Chem. Int. Ed.* **2009**, *48*, 9542-9545.
- [12] Lakhdar, S.; Appel, R.; Mayr, H. *Angew. Chem.* **2009**, *121*, 5134-5137; *Angew. Chem. Int. Ed.* **2009**, *48*, 5034-5037.
- [13] Reichardt, C. *Solvents and Solvent Effects in Organic Chemistry*; Wiley-VCH: Weinheim, 2003.
- [14] Bug, T.; Lemek, T.; Mayr, H. *J. Org. Chem.* **2004**, *69*, 7565-7576.
- [15] (a) Keeffe, J. R.; Morey, J.; Palmer, C. A.; Lee, J. C. *J. Am. Chem. Soc.* **1979**, *101*, 1295-1297. (b) Olmstead, W. N.; Bordwell, F. G. *J. Org. Chem.* **1980**, *45*, 3299-3305. (c) Arnett, E. M.; Harrelson, J. A. *J. Am. Chem. Soc.* **1987**, *109*, 809-812. (d) Bordwell,

- F. G. *Acc. Chem. Res.* **1988**, *21*, 456-463. (e) Bordwell, F. G.; Branca, J. C.; Bares, J. E.; Filler, R. *J. Org. Chem.* **1988**, *53*, 780-782. (f) Bordwell, F. G.; Cheng, J.-P.; Bausch, M. J.; Bares, J. E. *J. Phys. Org. Chem.* **1988**, *1*, 209-223. (g) Bordwell, F. G.; Harrelson, J. A.; Satish, A. V. *J. Org. Chem.* **1989**, *54*, 3101-3105. (h) Zhang, X.-M.; Bordwell, F. G. *J. Am. Chem. Soc.* **1994**, *116*, 968-972. (i) Bordwell, F. G.; Satish, A. V. *J. Am. Chem. Soc.* **1994**, *116*, 8885-8889. (j) Goumont, R.; Kizilian, E.; Buncel, E.; Terrier, F. *Org. Biomol. Chem.* **2003**, *1*, 1741-1748. (k) For a comprehensive database of pK_a -values in DMSO, see <http://www.chem.wisc.edu/areas/reich/pkatable/>.
- [16] Breugst, M.; Tokuyasu, T.; Mayr, H. *J. Org. Chem.* **2010**, *75*, 5250-5258.
- [17] 2-Bromo-4'-(dimethylamino)acetophenone was synthesized according to Diwu, Z.; Beachdel, C.; Klaubert, D. H. *Tetrahedron Lett.* **1998**, *39*, 4987-4990.
- [18] Forrester, J.; Jones, R. V. H.; Newton, L.; Preston, P. N. *Tetrahedron* **2001**, *57*, 2871-2884.
- [19] (a) Corson, B. B.; Stoughton, R. W. *J. Am. Chem. Soc.* **1928**, *50*, 2825-2837 (benzylidenmalononitrile **2u**). (b) Gairaud, C. B.; Lappin, G. R. *J. Org. Chem.*, **1953**, *18*, 1-3 (nitrostyrene **2v**). (c) Zabicky, J. *J. Chem. Soc.* **1961**, 683-687. (diethyl benzylidenemalonates **2r-t**). (d) Behera, R. K.; Nayak, A. *Indian J. Chem. B* **1976**, *14*, 223-224 (benzylideneindandiones **2l-n**). (e) Xu, Y.; Dolbier, W. R. *Tetrahedron* **1998**, *54*, 6319-6328. (benzylidenebarbituric acids **2o-q**).
- [20] (a) Evans, S.; Nesvadba, P.; Allenbach, S. (Ciba-Geigy AG), EP-B 744392, **1996** [*Chem. Abstr.* **1997**, *126*, 46968v]. (c) Richter, D.; Hampel, N.; Singer, T.; Ofial, A. R.; Mayr, H. *Eur. J. Org. Chem.* **2009**, 3203-3211.
- [21] σ_p -values taken from: Hansch, C.; Leo, A.; Taft, R. W. *Chem. Rev.* **1991**, *91*, 165-195.

Chapter 6: How Does Electrostatic Activation Control Iminium Catalyzed Cyclopropanations?

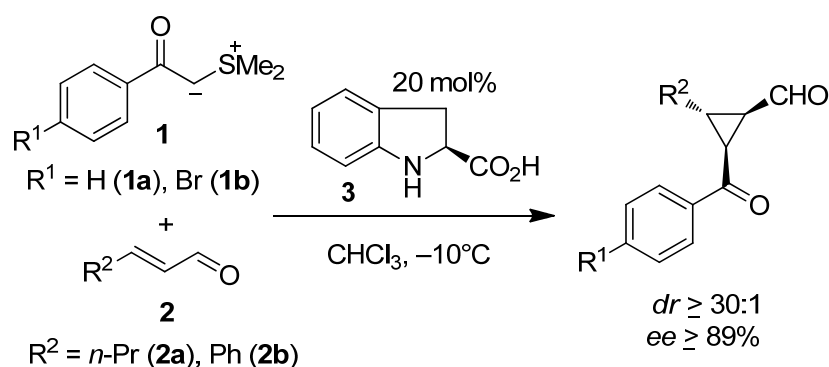
Sami Lakhdar, Roland Appel, and Herbert Mayr

Angew. Chem. **2009**, *121*, 5134-5137; *Angew. Chem. Int. Ed.* **2009**, *48*, 5034-5037.

1 Introduction

Three-membered carbocycles are versatile building blocks in organic chemistry and are found in numerous natural products.^[1] The use of sulfur ylides for their syntheses from α,β -unsaturated carbonyl compounds has been introduced in the 1960s by Corey and Chaykovsky.^[2] Since then, numerous syntheses of cyclopropanes have emerged that often provide excellent levels of both enantio- and diastereocontrol.^[3,4] In 2005 MacMillan and Kunz reported an enantioselective cyclopropanation reaction by using chiral indoline-2-carboxylic acid (**3**) as a catalyst (Scheme 1).^[5]

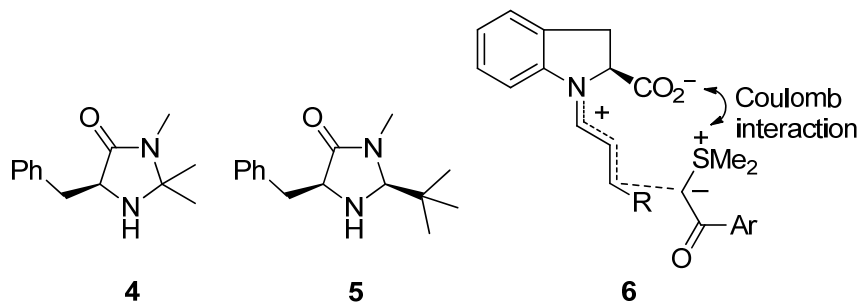
Scheme 1: Diastereo- and Enantioselective Organocatalytic Ylide Cyclopropanation with Indoline-2-Carboxylic Acid (**3**) by MacMillan and Kunz.^[5]



From the observation that the imidazolidinones **4**·TFA and **5**·TFA (Scheme 2, TFA = trifluoroacetic acid) did not catalyze the reaction of (*E*)-hex-2-enal (**2a**) with the sulfur ylide **1a** (0 % conversion), MacMillan and Kunz concluded that the iminium ions derived from **2a** and **4** or **5** are inert to the ylides **1**. Electrostatic stabilization of the transition state **6** (Scheme 2), that is, Coulombic attraction between the negatively charged carboxylate group and the positively charged sulfonium fragment, was suggested to account for the high reactivity and selectivity of the iminium ions derived from **3**.^[5,6] On the other hand, Cao et al. reported the highly diastereoselective and enantioselective cyclopropanation of cinnamaldehyde (**2b**) with

the triphenylarsonium analogue of **1a** when the diphenylprolinol trimethylsilyl ether was used as the catalyst.^[7]

Scheme 2: Imidazolidinones **4** and **5** and Transition State **6** for the Cyclopropanation of Iminium Ions derived from **3** with Sulfur Ylides.

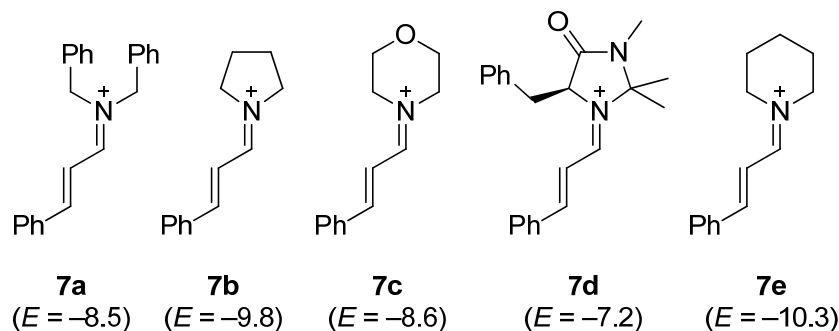


In previous work we have shown that the rates of the reactions of carbocations and Michael acceptors with n -, π -, and σ -nucleophiles can be described by eq 1, where $k_{20^\circ\text{C}}$ is the second-order rate constant in $\text{M}^{-1} \text{s}^{-1}$, s is the nucleophile-specific slope parameter, N is the nucleophilicity parameter, and E is the electrophilicity parameter.^[8]

$$\log k_{20^\circ\text{C}} = s(N + E) \quad (1)$$

Based on reactivity parameters of sulfur ylides and the recently reported electrophilicity parameters of iminium ions (Scheme 3),^[9] we had expected that in contrast to MacMillan's statement,^[5] the reactions of cinnamaldehyde-derived iminium ions **7** with sulfur ylide **1b** should proceed readily, as predicted by eq 1.

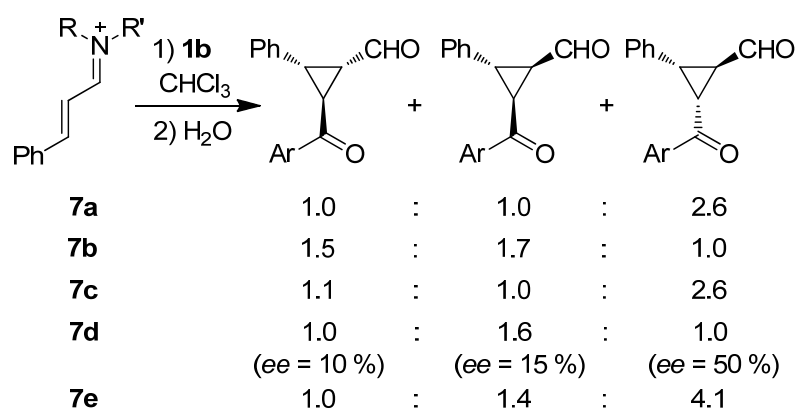
Scheme 3: Iminium Ions **7** Derived from Cinnamaldehyde (**2b**) and their Electrophilicity Parameters E (from ref 9).



2 Results and Discussion

Accordingly, treatment of the iminium triflates (**7a–e**)-OTf with the sulfur ylide **1b** yielded cyclopropane derivatives in 42–77 % yield. However, in contrast to MacMillan's conditions,^[5] which gave only two diastereomers in a ratio of 33:1 and high enantioselectivity, no significant stereoselectivity was observed (Scheme 4). None of the diastereoisomers obtained with **7d** was formed with high enantioselectivity.

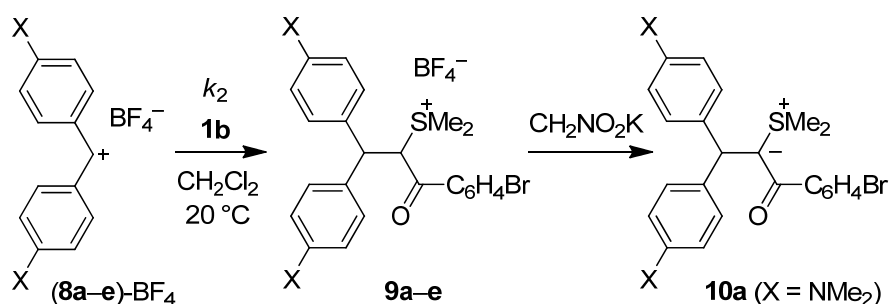
Scheme 4: Reactions of Iminium Triflates **7** with the Sulfur Ylide **1b** (Ar = *p*-Br-C₆H₄-).



To elucidate whether electrostatic activation really accounts for the catalytic activity of **3** in cyclopropanation reactions with sulfur ylides, we determined the nucleophilicity parameter of **1b** as well as the electrophilicity parameter of the zwitterion **7f[±]** derived from chiral indoline-2-carboxylic acid (**3**) and cinnamaldehyde (**2b**).

The nucleophile-specific parameters *N* and *s* of the sulfur ylide **1b** were derived from the second-order rate constants *k*₂ of the reactions of **1b** with the reference electrophiles **8a–e** (see Table 1),^[8b] which gave the addition products **9a–e** as confirmed by the isolation and characterization of the ylide **10a** (Scheme 5, for details see the Experimental Section).

Scheme 5: Reactions of the Sulfur Ylide **1b** with the Reference Electrophiles **8** in CH₂Cl₂ at 20°C.



The kinetics were monitored photometrically by following the disappearance of the colored benzhydrylium ions **8** as described previously^[8,10] and specified in the Experimental Section. As required by eq 1, $\log k_2$ for the reactions of **1b** with **8a–e** correlated linearly with the electrophilicity parameters E of **8a–e** (Table 1) and yielded the nucleophile-specific parameters $N(\mathbf{1b}) = 11.95$ and $s(\mathbf{1b}) = 0.76$ (Figure 1). The nucleophilicity of sulfur ylide **1b** is thus similar to that of an alkoxy-carbonyl- or cyano-stabilized triphenylphosphonium ylide,^[10] and **1b** is more nucleophilic than indoles,^[8e] pyrroles,^[8g] and dihydropyridines,^[8h] which have previously been employed as substrates in iminium-catalyzed reactions.

Table 1: Second-Order Rate Constants for the Reactions of the Benzhydrylium Ions **8a–e** with the Sulfur Ylide **1b** (CH_2Cl_2 , 20°C).

Electrophile	E^a	$k_2 / \text{M}^{-1} \text{s}^{-1}$
8a X = N(Me) ₂	-7.02	5.82×10^3
8b X = N(CH ₂) ₄	-7.69	1.84×10^3
8c	-8.76	2.45×10^2
8d ($n = 2$)	-9.45	8.40×10^1
8e ($n = 1$)	-10.04	2.91×10^1

^a E from ref 8b.

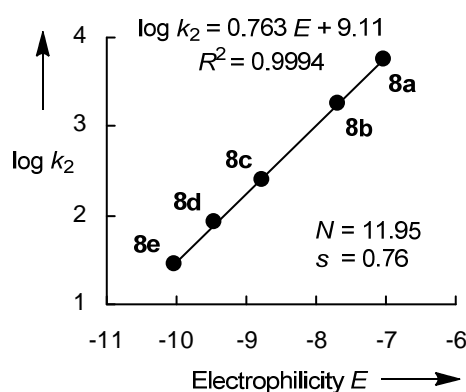


Figure 1: Plot of $\log k_2$ for the reactions of the sulfur ylide **1b** with the benzhydrylium ions **8a–e** in CH_2Cl_2 at 20°C versus the electrophilicity parameters E of **8a–e**.

The observation made by MacMillan and Kunz that 4-H^+ fails to catalyze the reaction of **1** with **2** thus cannot be explained by the low nucleophilicity of sulfur ylides. Instead it can be rationalized by the high basicity of sulfur ylides, which inhibits the formation of iminium

The zwitterion **7f[±]** reacts about 10^2 times more slowly with the ketene acetals **11** and **12** than the iminium ion **7d** derived from MacMillan's catalyst **4**.^[9] Substitution of the *N* and *s* parameters for the reference nucleophiles **11** and **12** and of the second-order rate constants from Scheme 7 into eq 1 gave $E(\mathbf{7f}^{\pm}) = -9.5$ by least-squares minimization. A comparison with the iminium ions **7a–e** (Scheme 3) shows that **7f[±]** is one of the weakest electrophiles derived from cinnamaldehyde. Yet, **3** was reported to be the most effective catalyst for the organocatalytic cyclopropanation reactions of unsaturated aldehydes with sulfur ylides **1**.^[5] In order to rationalize this discrepancy, we have investigated the kinetics of the reactions of the sulfur ylide **1b** with the iminium ions **7a–e** and the zwitterion **7f[±]**.

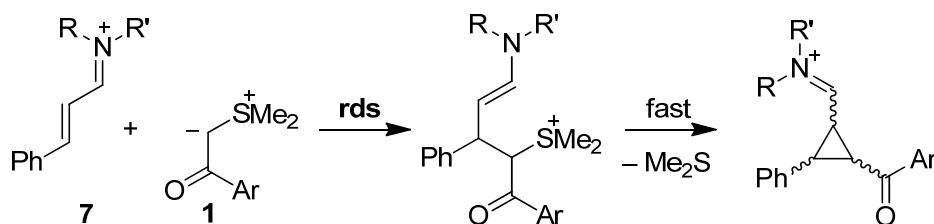
Table 2: Experimental and Calculated Second-Order Rate Constants ($\text{M}^{-1} \text{s}^{-1}$) for the Reactions of the Sulfur Ylide **1b** with the Iminium Ions **7a–e** and with **7f[±]** in CH_2Cl_2 at 20°C .

Iminium Ion	k_2^{exp}	$k_2^{\text{calcd } a}$	$k_2^{\text{exp}}/k_2^{\text{calcd}}$
7a	1.08×10^4	4.19×10^2	26
7b	1.19×10^2	4.31×10^1	2.8
7c	4.01×10^3	3.52×10^2	11
7d	1.31×10^5	4.07×10^3	32
7e	1.22×10^2	1.79×10^1	6.8
7f[±]	$\gg 10^7$ ^b	7.15×10^1	$\gg 10^5$

^a Calculated by eq 1 using the electrophilicity parameters *E* for **7a–e** (from ref 9) and **7f[±]** ($E = -9.5$, see above) as well as the *N* and *s* values for **1b** (from Figure 1). ^b Too fast for our instrumentation.

Table 2 shows that the experimental rate constants for the reactions of iminium ions **7a–e** with the sulfur ylide **1b** agree within a factor of 3 to 32 with those calculated by eq 1 from $E(\mathbf{7a})-E(\mathbf{7e})$ ^[9] and the nucleophile-specific parameters *N* and *s* for **1b** given in Figure 1. This agreement is quite remarkable in view of the simplicity of eq 1 and the reactivity range of 40 orders of magnitude covered by this correlation, and it demonstrates the applicability of our nucleophilicity parameters *N/s* for exploring the scope of iminium catalyzed reactions.^[11] The similarity of calculated and experimental rate constants suggests, moreover, that the cyclopropanation reactions between iminium ions **7a–e** and the sulfur ylide **1b** proceed by a stepwise mechanism, in which the formation of the first CC bond is rate-determining (Scheme 8).

Scheme 8: Stepwise Mechanism for the Cyclopropanation of Iminium Ions **7** with Sulfur Ylides **1** (rds = rate-determining step).



While good agreement between observed and calculated rate constants has also been observed for the reactions of **7d** with pyrroles, indoles and furans,^[12] the situation changes dramatically for the reaction of the ylide **1b** with the zwitterion **7f^z**. Now, the observed rate constant is more than 10^5 times (!) higher than predicted by eq 1 (last entry in Table 2). Obviously, the reaction of **7f^z** with **1b** is accelerated by a special factor which is not taken into account when we parametrized the nucleophilicity of **1b** through its reactions with the reference electrophiles **8a–e** and when parametrizing the electrophilicity of **7f^z** through its reactions with the reference nucleophiles **11** and **12**. Electrostatic interaction between the carboxyl group of **7f^z** and the sulfonium group of **1b**, as depicted in transition state **6** (Scheme 2), may account for this more than 10^5 -fold acceleration. The remarkable magnitude of this electrostatic activation moreover rationalizes the high stereoselectivity of the cyclopropanation reaction depicted in Scheme 1. As described in Scheme 4, only low diastereoselectivity and enantioselectivity were observed in the reaction of **7d** with **1b** where this electrostatic activation is absent.

3 Conclusion

In conclusion, we have shown that electrostatic activation is, indeed, responsible for the more than 10^5 -fold acceleration of the reaction of the zwitterion **7f^z** with the sulfur ylide **1b** and the high stereoselectivity of this reaction. However, in contrast to previous statements,^[5] also iminium ions **7a–e** react readily with the benzoyl-stabilized sulfur ylide **1b**, though with low stereoselectivity. The previously reported failure of **4-H⁺** to catalyze the cyclopropanation of α,β -unsaturated aldehydes with sulfur ylides thus is not a result of the low rate of the reaction **7d** + **1b** but because of the high basicity of sulfur ylides, which inhibits the formation of iminium ions.

4 Experimental Section

In order to identify my contribution to this multiauthor publication, chapter 4.2 and 4.3 of this Experimental Section consist exclusively of the experiments, which were performed by me.

4.1 General

Chemicals. Solvents were dried over the indicated drying agents and freshly distilled prior to use: dichloromethane (CaH₂), diethyl ether (Na/benzophenone). Ketene acetals **11** and **12** were prepared by reported methods.^[13] Cinnamaldehyde (**2b**) was purified by distillation before use and stored under nitrogen. The iminium salts (**7a–e**)-OTf^[9] as well as the benzhydrylium tetrafluoroborates (**8a–e**)-BF₄^[8b] were prepared as described before. The sulfur ylide **1b** was synthesized according to a literature procedure.^[14] All other chemicals were purchased from commercial sources and (if necessary) purified by recrystallization or distillation prior to use.

Analytcs. ¹H- and ¹³C-NMR spectra were recorded in CDCl₃ or CD₃OD on 200, 300, 400 or 600 MHz NMR spectrometers. The following abbreviations were used to designate chemical shift multiplicities: brs = broad singlet, s = singlet, d = doublet, t = triplet, m = multiplet. For reasons of simplicity, the ¹H-NMR signals of AA'BB'-spin systems of *p*-disubstituted aromatic rings were treated as doublets. The assignments of individual NMR signals were based on additional 2D-NMR experiments and stereochemical assignments were made on the basis of NOESY experiments. Diastereomeric ratios (*dr*) were determined by ¹H-NMR. HR-MS were recorded on a Finnigan MAT 95 Q mass spectrometer. An Agilent 1200 system was employed for the HPLC analyses.

Kinetics. The rates of all of the investigated reactions were determined photometrically under first-order conditions (i.e., one reaction partner in high excess). The temperature of the solutions during all kinetic studies was kept constant (20.0 ± 0.1°C) using a circulating bath thermostat. The kinetic runs were initiated by mixing CH₂Cl₂ solutions of the nucleophiles and electrophiles in a 1/1 ratio. As **7f[±]** possesses only a low solubility in CH₂Cl₂, 20 Vol% MeOH were used as a cosolvent for the preparation of solutions of this electrophile in CH₂Cl₂. As a consequence, the reactions of **7f[±]** with nucleophiles were studied in 9/1 CH₂Cl₂/MeOH mixtures, which resulted after the 1/1 mixing of the **7f[±]** solution with the nucleophile solution in pure CH₂Cl₂.

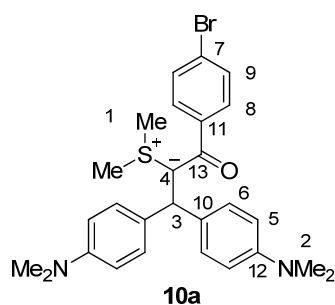
The rates of slow reactions ($\tau_{1/2} > 10$ s) were determined by using a J&M TIDAS diode array spectrophotometer controlled by Labcontrol Spectacle software and connected to Hellma

661.502-QX quartz Suprasil immersion probe (5 mm light path) via fiber-optic cables and standard SMA connectors. For the evaluation of fast kinetics ($\tau_{1/2} < 10$ s) the stopped-flow spectrophotometer systems Hi-Tech SF-61DX2 or Applied Photophysics SX.18MV-R were used. Rate constants k_{obs} (s^{-1}) were obtained by fitting the single exponential $A_t = A_0 \exp(-k_{\text{obs}}t) + C$ (exponential decrease) to the observed time-dependent absorbance (averaged from at least four kinetic runs for each nucleophile concentration in the case of applying the stopped-flow method). Second-order rate constants k_2 ($\text{L mol}^{-1} \text{s}^{-1}$) were derived from the slopes of the linear correlations of k_{obs} (s^{-1}) with the concentration of the reaction partner used in excess.

4.2 Synthesis of Ylide 10a

1-(4-Bromo-phenyl)-3,3-bis(4-(dimethylamino)phenyl)-2-(dimethyl- λ^4 -sulfanylidene)-propan-1-one (10a): The benzhydrylium tetrafluoroborate **8a**-BF₄ (135 mg, 397 μmol , dissolved in 5 mL of dry DMSO) was added in one portion to a stirred solution of 1-(4-bromo-phenyl)-2-(dimethyl- λ^4 -sulfanylidene)-ethanone (**1b**, 103 mg, 397 μmol) in dry DMSO (2 mL). The resulting mixture was immediately quenched with a solution of nitromethane (43.6 mg, 714 μmol) and KO^tBu (66.9 mg, 596 μmol) in dry DMSO (2 mL). After 10 min of stirring, water (40 mL) was added and the resulting suspension was extracted with CH₂Cl₂ (2 \times 50 mL). The combined organic layers were washed with water (2 \times 50 mL) and brine (1 \times 50 mL), dried (Na₂SO₄), and evaporated under reduced pressure. Purification of the crude product by column chromatography (neutral aluminum oxide, EtOAc \rightarrow CHCl₃/MeOH = 15/1) furnished **10a** as a yellow solid (182 mg, 356 μmol , 90 %). NMR signal assignments were based on additional 2D-NMR experiments.

RAP 11.9



R_f (CHCl₃/MeOH = 15:1) = 0.61. Mp: 90-93°C (decomp.). ¹H-NMR (CDCl₃, 600 MHz): δ = 7.39 (d, ³J = 8.3 Hz, 2 H, 9-H), 7.31 (d, ³J = 8.3 Hz, 2 H, 8-H), 6.97 (d, ³J = 8.7 Hz, 4 H, 6-H), 6.66 (d, ³J = 8.7 Hz, 4 H, 5-H), 5.07 (brs, 1 H, 3-H), 2.93 (s, 12 H, 2-H), 2.87 ppm (s, 6 H,

1-H). ^{13}C -NMR (CDCl_3 , 151 MHz): δ = 181.7 (s, C-13), 148.9 (s, C-12), 142.3 (s, C-11), 132.8 (s, C-10), 130.8 (d, C-9), 129.4 (d, C-6), 129.0 (d, C-8), 122.0 (s, C-7), 112.4 (d, C-5), 74.0 (s, C-4), 50.2 (d, C-3), 40.7 (q, C-2), 25.1 ppm (q, C-1). MS (EI): m/z (%) = 510 (1), 450 (91), 448 (85), 265 (100), 253 (46). HRMS (EI): m/z calcd for $[\text{C}_{27}\text{H}_{31}^{79}\text{BrN}_2\text{O}^{32}\text{S}]^+$: 510.1335, found 510.1334. HRMS (ESI+): m/z calcd for $[\text{C}_{27}\text{H}_{32}^{79}\text{BrN}_2\text{O}^{32}\text{S}]^+$: 511.1413, found 511.1428.

4.3 Kinetics of the Reactions of the Sulfur Ylide **1b** with the Benzhydrylium Ions **8**

The kinetics were monitored photometrically by following the disappearance of the colored benzhydrylium ions **8** at or close to their absorption maxima under first-order conditions using at least 12 equiv of **1b** over **8**. From the exponential decays of the UV-Vis absorbances of the electrophiles, the first-order rate constants k_{obs} were obtained. Plots of k_{obs} (s^{-1}) against the concentrations of the nucleophile **1b** were linear with negligible intercepts as required by the relation $k_{\text{obs}} = k_2[\mathbf{1b}]$ (2).

$$-d[\mathbf{8}]/dt = k_2 [\mathbf{8}] [\mathbf{1b}] \quad \text{for } [\mathbf{1b}] \gg [\mathbf{8}] \Rightarrow k_{\text{obs}} = k_2 [\mathbf{1b}] \quad (2)$$

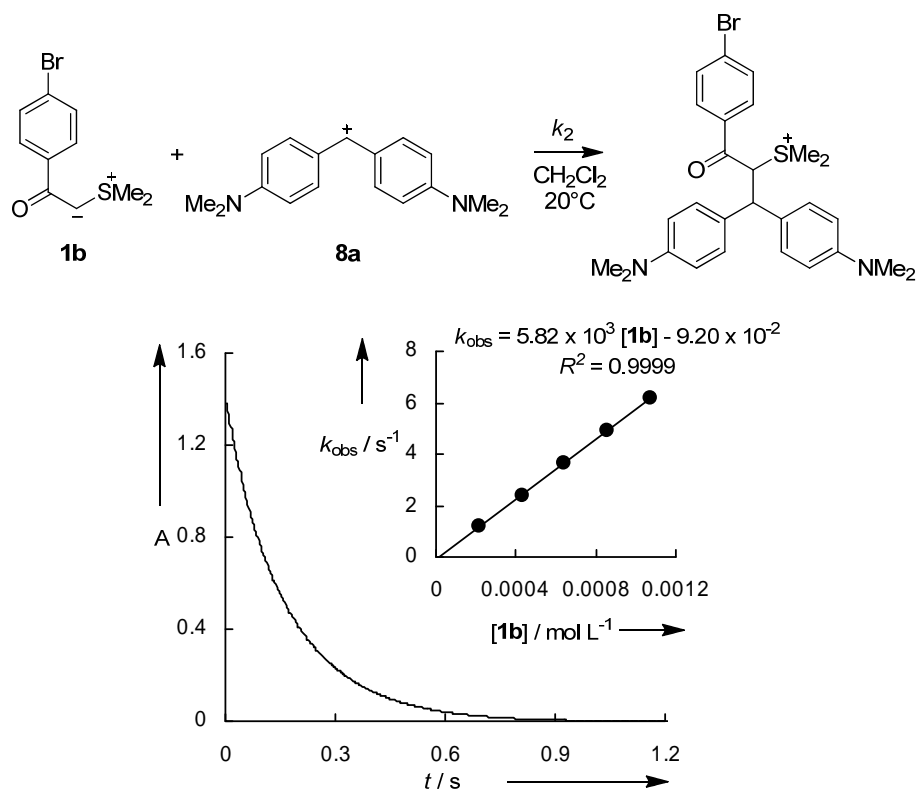
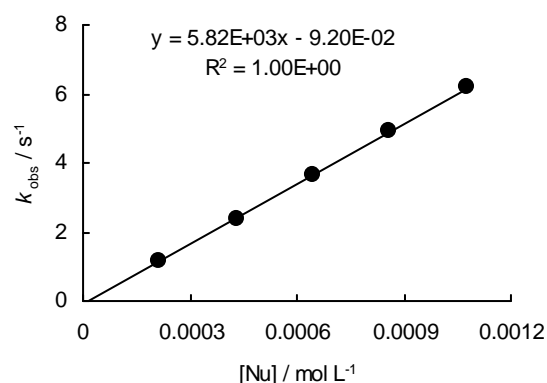


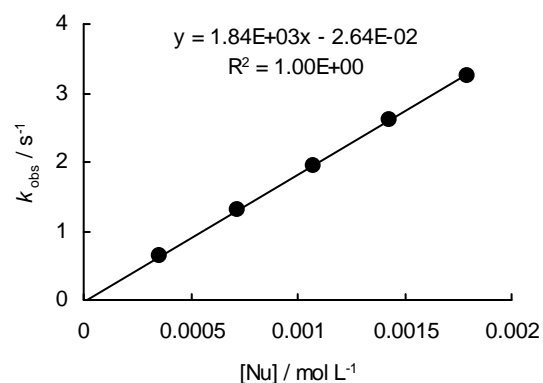
Figure 2: Exponential decay of the absorbance at 613 nm during the reaction of **1b** ($1.08 \times 10^{-3}\text{ M}$) with **8a** ($7.61 \times 10^{-6}\text{ M}$) at 20°C in CH_2Cl_2 . Insert: Determination of the second-order rate constant $k_2 = 5.82 \times 10^3\text{ M}^{-1}\text{s}^{-1}$ from the dependence of the first-order rate constant k_{obs} on the concentration of **1b**.

Table 3: Kinetics of the reaction of **8a**-BF₄ with sulfur ylide **1b** in CH₂Cl₂ at 20°C (stopped-flow UV-Vis spectrometer, λ = 613 nm).

Nr.	[E] ₀ / mol L ⁻¹	[Nu] ₀ / mol L ⁻¹	k _{obs} / s ⁻¹
RAK 12.11-1	7.61 × 10 ⁻⁶	2.15 × 10 ⁻⁴	1.18
RAK 12.11-2	7.61 × 10 ⁻⁶	4.30 × 10 ⁻⁴	2.40
RAK 12.11-3	7.61 × 10 ⁻⁶	6.45 × 10 ⁻⁴	3.63
RAK 12.11-4	7.61 × 10 ⁻⁶	8.60 × 10 ⁻⁴	4.90
RAK 12.11-5	7.61 × 10 ⁻⁶	1.08 × 10 ⁻³	6.18
k₂ = 5.82 × 10³ M⁻¹ s⁻¹			

**Table 4:** Kinetics of the reaction of **8b**-BF₄ with sulfur ylide **1b** in CH₂Cl₂ at 20°C (stopped-flow UV-Vis spectrometer, λ = 623 nm).

Nr.	[E] ₀ / mol L ⁻¹	[Nu] ₀ / mol L ⁻¹	k _{obs} / s ⁻¹
RAK 12.10-1	9.48 × 10 ⁻⁶	3.58 × 10 ⁻⁴	6.30 × 10 ⁻¹
RAK 12.10-2	9.48 × 10 ⁻⁶	7.17 × 10 ⁻⁴	1.29
RAK 12.10-3	9.48 × 10 ⁻⁶	1.08 × 10 ⁻³	1.95
RAK 12.10-4	9.48 × 10 ⁻⁶	1.43 × 10 ⁻³	2.61
RAK 12.10-5	9.48 × 10 ⁻⁶	1.79 × 10 ⁻³	3.26
k₂ = 1.84 × 10³ M⁻¹ s⁻¹			

**Table 5:** Kinetics of the reaction of **8c**-BF₄ with sulfur ylide **1b** in CH₂Cl₂ at 20°C (stopped-flow UV-Vis spectrometer, λ = 623 nm).

Nr.	[E] ₀ / mol L ⁻¹	[Nu] ₀ / mol L ⁻¹	k _{obs} / s ⁻¹
RAK 12.9-1	9.39 × 10 ⁻⁶	3.58 × 10 ⁻⁴	8.69 × 10 ⁻²
RAK 12.9-2	9.39 × 10 ⁻⁶	7.17 × 10 ⁻⁴	1.73 × 10 ⁻¹
RAK 12.9-3	9.39 × 10 ⁻⁶	1.08 × 10 ⁻³	2.60 × 10 ⁻¹
RAK 12.9-4	9.39 × 10 ⁻⁶	1.43 × 10 ⁻³	3.49 × 10 ⁻¹
RAK 12.9-5	9.39 × 10 ⁻⁶	1.79 × 10 ⁻³	4.37 × 10 ⁻¹
k₂ = 2.45 × 10² M⁻¹ s⁻¹			

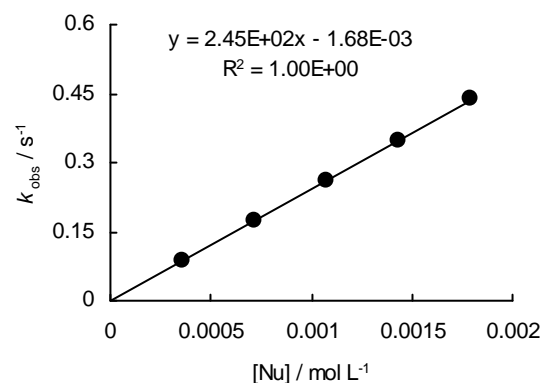
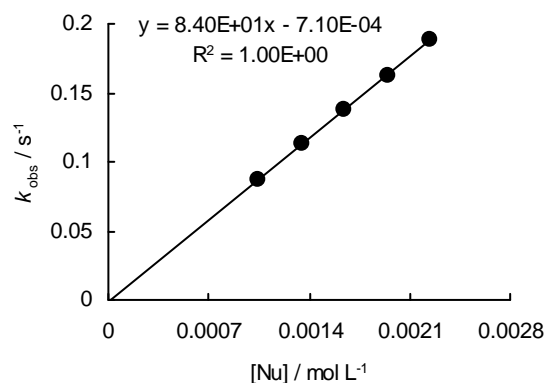
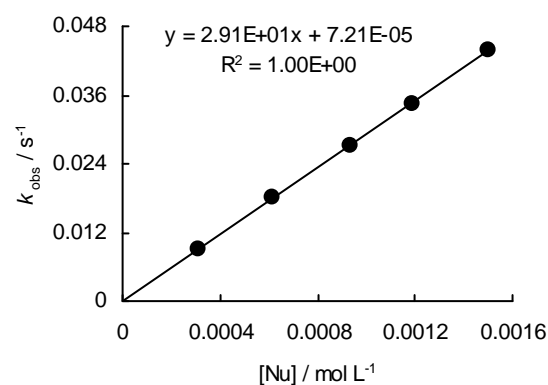


Table 6: Kinetics of the reaction of **8d**-BF₄ with sulfur ylide **1b** in CH₂Cl₂ at 20°C (stopped-flow UV-Vis spectrometer, λ = 640 nm).

Nr.	[E] ₀ / mol L ⁻¹	[Nu] ₀ / mol L ⁻¹	k _{obs} / s ⁻¹
RAK 12.8-1	1.02 × 10 ⁻⁵	1.05 × 10 ⁻³	8.68 × 10 ⁻²
RAK 12.8-2	1.02 × 10 ⁻⁵	1.35 × 10 ⁻³	1.13 × 10 ⁻¹
RAK 12.8-3	1.02 × 10 ⁻⁵	1.65 × 10 ⁻³	1.38 × 10 ⁻¹
RAK 12.8-4	1.02 × 10 ⁻⁵	1.95 × 10 ⁻³	1.62 × 10 ⁻¹
RAK 12.8-5	1.02 × 10 ⁻⁵	2.25 × 10 ⁻³	1.88 × 10 ⁻¹
k₂ = 8.40 × 10¹ M⁻¹ s⁻¹			

**Table 7:** Kinetics of the reaction of **8e**-BF₄ with sulfur ylide **1b** in CH₂Cl₂ at 20°C (diode array UV-Vis spectrometer, λ = 640 nm).

Nr.	[E] ₀ / mol L ⁻¹	[Nu] ₀ / mol L ⁻¹	k _{obs} / s ⁻¹
RAK 12.12-1	1.09 × 10 ⁻⁵	3.11 × 10 ⁻⁴	9.08 × 10 ⁻³
RAK 12.12-2	1.01 × 10 ⁻⁵	6.14 × 10 ⁻⁴	1.81 × 10 ⁻²
RAK 12.12-3	1.03 × 10 ⁻⁵	9.34 × 10 ⁻⁴	2.73 × 10 ⁻²
RAK 12.12-4	1.03 × 10 ⁻⁵	1.19 × 10 ⁻³	3.45 × 10 ⁻²
RAK 12.12-5	1.04 × 10 ⁻⁵	1.50 × 10 ⁻³	4.39 × 10 ⁻²
k₂ = 2.91 × 10¹ M⁻¹ s⁻¹			



5 References

- [1] Reviews: (a) Salaun, J. *Chem. Rev.* **1989**, *89*, 1247-1270. (b) Li, A.-H.; Dai, L.-X.; Aggarwal, V. K. *Chem. Rev.* **1997**, *97*, 2341-2372. (c) Pfaltz, A.; In *Comprehensive Asymmetric Catalysis*; Jacobsen, E. N., Pfaltz, A., Yamamoto Y., Eds.; Springer: Heidelberg, 1999; pp. 513-538. (d) Faust, R. *Angew. Chem.* **2001**, *113*, 2312-2314; *Angew. Chem. Int. Ed.* **2001**, *40*, 2251-2253. (e) Reissig, H.-U.; Zimmer, R. *Chem. Rev.* **2003**, *103*, 1151-1196.
- [2] (a) Corey, E. J.; Chaykovsky, M. *J. Am. Chem. Soc.* **1962**, *84*, 867-868. (b) Corey, E. J.; Chaykovsky, M. *J. Am. Chem. Soc.* **1962**, *84*, 3782-3783. (c) Corey, E. J.; Chaykovsky, M. *J. Am. Chem. Soc.* **1965**, *87*, 1353-1364.
- [3] For selected recent examples on organocatalytic ylide cyclizations, see: (a) Bremeyer, N.; Smith, S. C.; Ley, S. V.; Gaunt, M. J. *Angew. Chem.* **2004**, *116*, 2735-2738; *Angew. Chem. Int. Ed.* **2004**, *43*, 2681-2684. (b) Papageorgiou, C. D.; De Dios, M. A.; Ley, S. V.; Gaunt, M. J. *Angew. Chem.* **2004**, *116*, 4741-4744; *Angew. Chem. Int. Ed.* **2004**, *43*, 4641-4644. (c) Johansson, C. C. C.; Bremeyer, N.; Ley, S. V.; Owen, D. R.; Smith, S.

- C.; Gaunt, M. J. *Angew. Chem.* **2006**, *118*, 6170-6175; *Angew. Chem. Int. Ed.* **2006**, *45*, 6024-6028. (d) Gaunt, M. J.; Johansson, C. C. C.; *Chem. Rev.* **2007**, *107*, 5596-5605. (e) Sun, X. L.; Tang, Y.; *Acc. Chem. Res.* **2008**, *41*, 937-948.
- [4] For stereoselective cyclopropanations, see: (a) Charette, A. B.; Lebel, H. *J. Org. Chem.* **1995**, *60*, 2966-2967. (b) Lebel, H.; Marcoux, J.-F.; Molinaro, C.; Charette, A. B. *Chem. Rev.* **2003**, *103*, 977-1050.
- [5] Kunz, R. K.; MacMillan, D. W. C. *J. Am. Chem. Soc.* **2005**, *127*, 3240-3241.
- [6] For related electrostatic activation, see: Hartikka, A.; Arvidsson, P. I. *J. Org. Chem.* **2007**, *72*, 5874-5877.
- [7] Zhao, Y.-H.; Zhao, G.; Cao, W.-G. *Tetrahedron: Asymmetry* **2007**, *18*, 2462-2467.
- [8] (a) Mayr, H.; Patz, M.; *Angew. Chem.* **1994**, *106*, 990-1010; *Angew. Chem. Int. Ed. Engl.* **1994**, *33*, 938-957. (b) Mayr, H.; Bug, T.; Gotta, M. F.; Hering, N.; Irrgang, B.; Janker, B.; Kempf, B.; Loos, R.; Ofial, A. R.; Remennikov, G.; Schimmel, H. *J. Am. Chem. Soc.* **2001**, *123*, 9500-9512. (c) Mayr, H.; Kempf, B.; Ofial, A. R. *Acc. Chem. Res.* **2003**, *36*, 66-77. (d) Mayr, H.; Ofial, A. R. *Pure Appl. Chem.* **2005**, *77*, 1807-1821. (e) Lakhdar, S.; Westermaier, M.; Terrier, F.; Goumont, R.; Boubaker, T.; Ofial, A. R.; Mayr, H. *J. Org. Chem.* **2006**, *71*, 9088-9095. (f) Mayr, H.; Ofial, A. R. *J. Phys. Org. Chem.* **2008**, *21*, 584-595. (g) Nigst, T. A.; Westermaier, M.; Ofial, A. R.; Mayr, H. *Eur. J. Org. Chem.* **2008**, 2369-2374. (h) Richter, D.; Mayr, H. *Angew. Chem.* **2009**, *121*, 1922-1995; *Angew. Chem. Int. Ed.* **2009**, *48*, 1958-1961.
- [9] Lakhdar, S.; Tokuyasu, T.; Mayr, H. *Angew. Chem.* **2008**, *120*, 8851-8854; *Angew. Chem. Int. Ed.* **2008**, *47*, 8723-8725.
- [10] Appel, R.; Loos, R.; Mayr, H. *J. Am. Chem. Soc.* **2009**, *131*, 704-714.
- [11] Reviews: (a) Berkessel, A.; Gröger, H. *Asymmetric Organocatalysis*, Wiley-VCH: Weinheim, 2004. (b) Seayad, J.; List, B. *Org. Biomol. Chem.* **2005**, *3*, 719-724. (c) Lelais, G.; MacMillan, D. W. C. *Aldrichim. Acta* **2006**, *39*, 79-87. (d) *Enantioselective Organocatalysis*; Dalko, P. I., Ed.; Wiley-VCH: Weinheim, 2007. (e) Erkkilä, A.; Majander, I.; Pihko, P. M. *Chem. Rev.* **2007**, *107*, 5416-5470. (f) Gaunt, M. J.; Johansson, C. C. C.; McNally, A.; Vo, N. C. *Drug Discovery Today* **2007**, *12*, 8-27. (g) Tsogoeva, S. B. *Eur. J. Org. Chem.* **2007**, 1701-1716. (h) MacMillan, D. W. C. *Nature* **2008**, *455*, 304-308. (i) Melchiorre, P.; Marigo, M.; Carlone, A.; Bartoli, G. *Angew. Chem.* **2008**, *120*, 6232-6265; *Angew. Chem. Int. Ed.* **2008**, *47*, 6138-6171. For structural investigations of α,β -unsaturated iminium ions: (j) Seebach, D.; Groselj, U.; Badine, D. M.; Schweizer, W. B.; Beck, A. K. *Helv. Chim. Acta* **2008**, *91*, 1999-2034.

- (k) Groselj, U.; Schweizer, W. B.; Ebert, M.-O.; Seebach, D. *Helv. Chim. Acta* **2009**, *92*, 1-13.
- [12] (a) Lakhdar, S.; Mayr, H. *Chem. Commun.* **2011**, Advance Article (b) Lakhdar, S.; Mayr, H. unpublished results.
- [13] Oisaki, K.; Suto, Y.; Kanai, M.; Shibasaki, M. *J. Am. Chem. Soc.* **2003**, *125*, 5644-5645.
- [14] Ratts, K. W.; Yao, A. N. *J. Org. Chem.* **1966**, *31*, 1185-1188.

Chapter 7: Quantification of the Electrophilic Reactivities of Aldehydes, Imines, and Enones

Roland Appel and Herbert Mayr

J. Am. Chem. Soc., submitted.

1 Introduction

Eq 1, where $k_{20^\circ\text{C}}$ is the second-order rate constant in $\text{L mol}^{-1} \text{s}^{-1}$, s is a nucleophile-specific sensitivity parameter, N is a nucleophilicity parameter, and E is an electrophilicity parameter, has been employed for the construction of the most comprehensive nucleophilicity scale presently available.^[1]

$$\log k_{20^\circ\text{C}} = s(N + E) \quad (1)$$

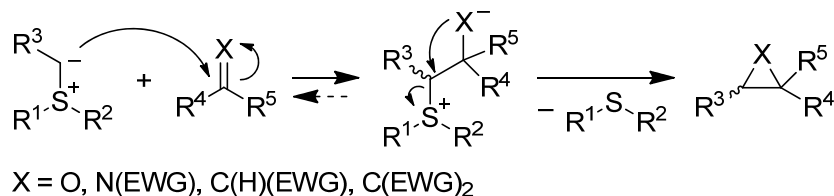
While N and s parameters have been determined for the most important classes of nucleophiles, including aliphatic and aromatic π -systems, hydride donors, and n-nucleophiles such as alkoxides and amines, there is a striking shortage of electrophilicity parameters.^[1g] Carbocations, including benzhydrylium ions,^[1b,d] cationic metal π -complexes,^[1d] and iminium ions^[1d,2f] as well as highly electron-deficient Michael acceptors^[1c,2] have so far been the only compounds for which electrophilicity parameters E have been determined. Most remarkably, E parameters have neither been reported for imines nor for ordinary carbonyl compounds, two of the most important classes of electrophiles.

Electrophilicity parameters of carbocations and Michael acceptors have previously been derived from the rates of their reactions with carbon-centered nucleophiles (with known N and s parameters),^[1,2] where the CC bond forming step is rate-determining. Attempts to determine E parameters of aldehydes analogously failed, because stabilized carbanions (e.g., *p*-substituted phenylacetonitrile anions) do not react with ordinary aldehydes (e.g., PhCHO) in DMSO in the absence of a proton source or a strongly coordinating metal ion. Obviously, stabilization of the developing alkoxide is needed to suppress the fast reverse reaction.

An alternative way to achieve irreversible additions of carbon nucleophiles to carbonyl groups is the rapid trapping of the intermediate alkoxide anion by an internal electrophile, which is encountered in the reactions of sulfur ylides with carbonyl compounds (Scheme 1). Detailed investigations revealed a common mechanistic course of these epoxidation reactions^[3] and the analogous aziridination^[4] and cyclopropanation reactions.^[3b,5] In all cases, the sulfur ylide initially attacks at an electrophilic carbon center to form a betaine intermediate, which then

undergoes an intramolecular nucleophilic displacement to yield an epoxide, an aziridine, or a cyclopropane, respectively (Scheme 1).

Scheme 1: Mechanism of Sulfur Ylide-Mediated Epoxidations, Aziridinations, and Cyclopropanations (Corey-Chaykovsky Reaction).^[3,4,5]



As the formation of the betaine intermediate is often irreversible and rate-determining,^[3e,h,n,4a,c,d,5b,e,6] the kinetics of the reactions of the sulfur ylides **4a,b** (Table 1) with the aldehydes **1a-i**, the *N*-activated imines **2a-e**, and the α,β -unsaturated ketones **3a-f** (Scheme 2) will now be employed to determine the electrophilicity parameters *E* for these synthetically important compounds.

Scheme 2: Aldehydes **1a-i**, Imines **2a-e**, and Enones **3a-f** Investigated in this Work (Ts = *p*-Methylbenzenesulfonyl, Boc = *t*-Butoxycarbonyl).

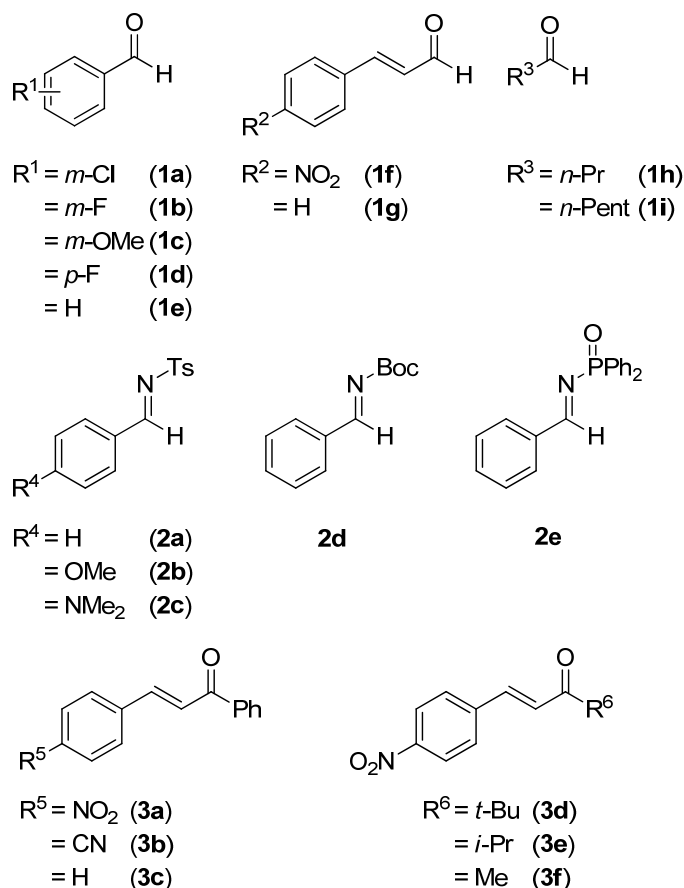
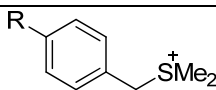
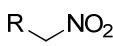
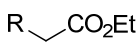
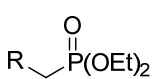


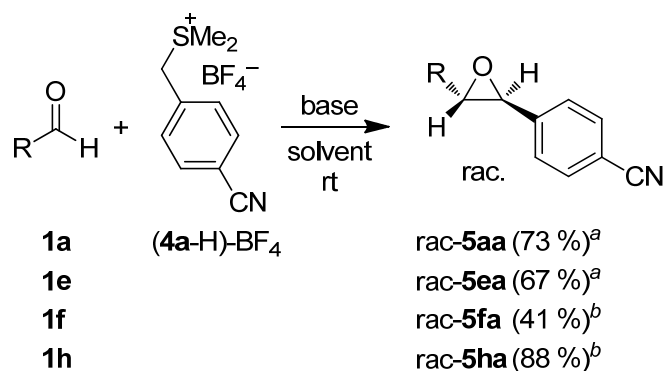
Table 1: Sulfur Ylides **4a,b**, Carbanions **4c–h**, and their Nucleophilicity Parameters N and s in DMSO.

Nucleophile	R	$N (s)^a$
	4a CN	21.07 (0.68)
	4b NO ₂	18.42 (0.65)
	4c Me	21.54 (0.62)
	4d H	20.71 (0.60)
	4e S(O)Me	20.61 (0.64)
	4f CO ₂ Et	20.22 (0.65)
	4g CO ₂ Et	19.23 (0.65)
	4h CN	18.57 (0.66)

^a Nucleophilicity parameters N and s for **4a,b** were taken from ref 6b, for **4c,d** from ref 7, for **4e** from ref 8, for **4f** from ref 1c, and for **4g,h** from ref 9.

2 Results

Product Studies. In line with earlier investigations,^[3e,h,n] the semistabilized sulfur ylide **4a**, which was used for most kinetic investigations, was found to give *trans*-epoxides **5** with the benzaldehydes **1a** and **1e** as well as with the cinnamaldehyde **1f** and butanal (**1h**) (Scheme 3).

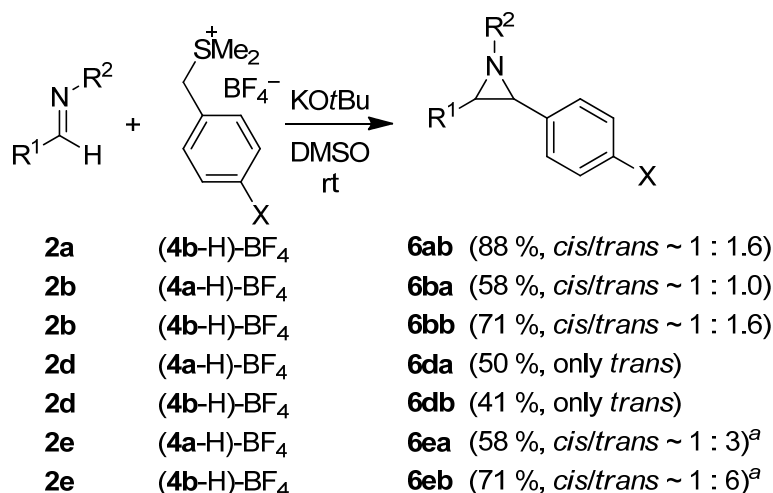
Scheme 3: Reactions of Sulfur Ylide **4a** with the Aldehydes **1a,e,f,h**.

^a KO^tBu, DMSO. ^b K₂CO₃ (aq.), CHCl₃.

The reactions of the sulfur ylides **4a,b** with all imines **2** examined yielded the expected aziridines **6** (Scheme 4). While the *N*-tosyl-substituted aziridines **6ab**, **6ba**, and **6bb** were formed as mixtures of *cis*- and *trans*-isomers, exclusively *trans*-isomers were isolated from the *N*-*tert*-butoxycarbonyl-substituted imine **2d**. NMR studies of the crude products obtained

from the *N*-diphenylphosphinoyl-substituted imine **2e** showed the formation of **6ea** (*cis/trans* 1 : 3) and **6eb** (*cis/trans* 1 : 6) as mixtures of diastereomers, which were separated by column chromatography. The corresponding *trans*-products were isolated and characterized, while the *cis*-products could not be obtained in pure form. Detailed descriptions of the experimental procedures and the characterizations of the isolated compounds are given in the Experimental Section.

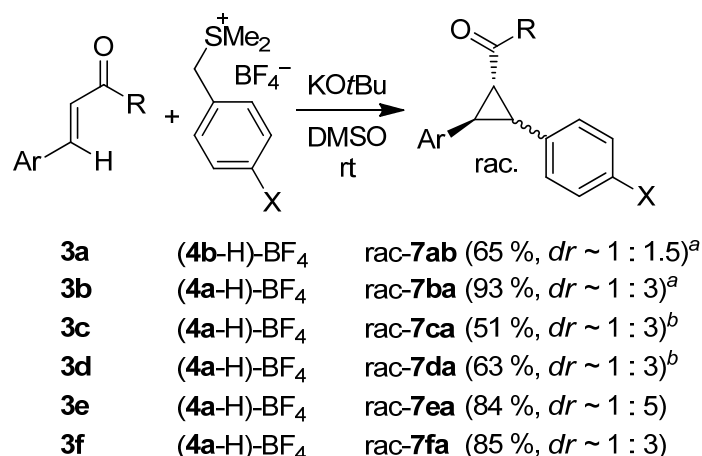
Scheme 4: Reactions of the Sulfur Ylides **4a,b** with the Imines **2a,b,d,e** (*cis/trans*-Ratios Correspond to the Isolated Products).



^a Yield isolated refers to *trans*-isomer; *cis/trans*-ratio corresponds to the crude product.

In line with previous reports on the reactivity of cinnamaldehyde with aryl-stabilized sulfur ylides,^[10] Scheme 3 shows that *p*-nitrocinnamaldehyde (**1f**) reacts exclusively at the carbonyl group with **4a**. In contrast, the α,β -unsaturated ketones **3a–f** reacted selectively at the CC double bond to yield the cyclopropanes **7** as mixtures of diastereomers (Scheme 5). The diastereomers of the cyclopropanes **7ca** and **7da** were separated, and the major isomers were isolated and characterized. The relative configurations of the cyclopropanes **7** have been defined by the characteristic coupling constants of the corresponding cyclopropane protons in the ¹H-NMR spectra. Detailed descriptions of the experimental procedures and the characterizations of the isolated compounds are given in the Experimental Section.

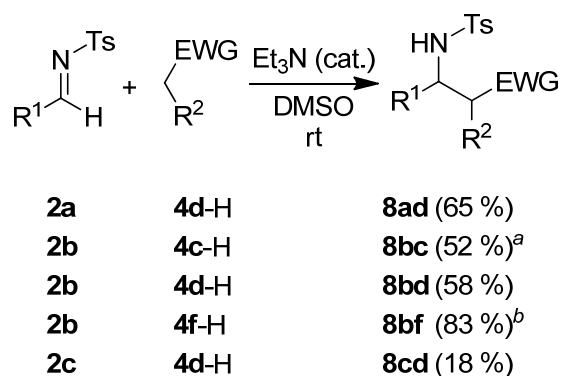
Scheme 5: Reactions of the Sulfur Ylides **4a,b** with the Michael Acceptors **3a–f** (Diastereomeric Ratios *dr* Correspond to the Isolated Products).



^a Minor diastereomer is a meso compound. ^b Yield isolated refers to major diastereomer; *dr* corresponds to the crude product.

In contrast to the *N*-Boc and *N*-diphenylphoshyloxy-substituted imines **2d** and **2e**, which reacted only with the sulfur ylides **4a,b** (see above), the *N*-tosyl-substituted imines **2a–c** also reacted with the carbanions **4c–h** in DMSO. As depicted in Scheme 6, the addition products **8** were obtained from the reactions of the *N*-tosyl-activated imines **2a–c** with the nitronates **4c,d** and the diethyl malonate anion (**4f**).

Scheme 6: Reactions of the Carbanions **4c,d,f** with the Imines **2a–c**.



^a *dr* ~ 1 : 3 for the crude product; only major diastereomer isolated and characterized. ^b Reaction conditions: KOtBu, THF, –80 to –40°C.

The methylsulfinyl-stabilized carbanion **4e** and the phosphonate-stabilized carbanions **4g,h** did not yield simple addition products with the imine **2b**. Instead, Knoevenagel-type condensation reactions took place with the formation of the olefins **9** (Figure 1 and Scheme 7), as previously described for the reactions of **4g** and **4h** with *N*-tosyl-substituted imines.^[11]

UV-Vis spectroscopic monitoring of these reactions showed that the fast additions of the carbanions to the imine **2b** are followed by slow eliminations of the tosylamide group to give the Knoevenagel products **9** (Figure 1 and Tables 21, 24, and 26 of the Experimental Section).

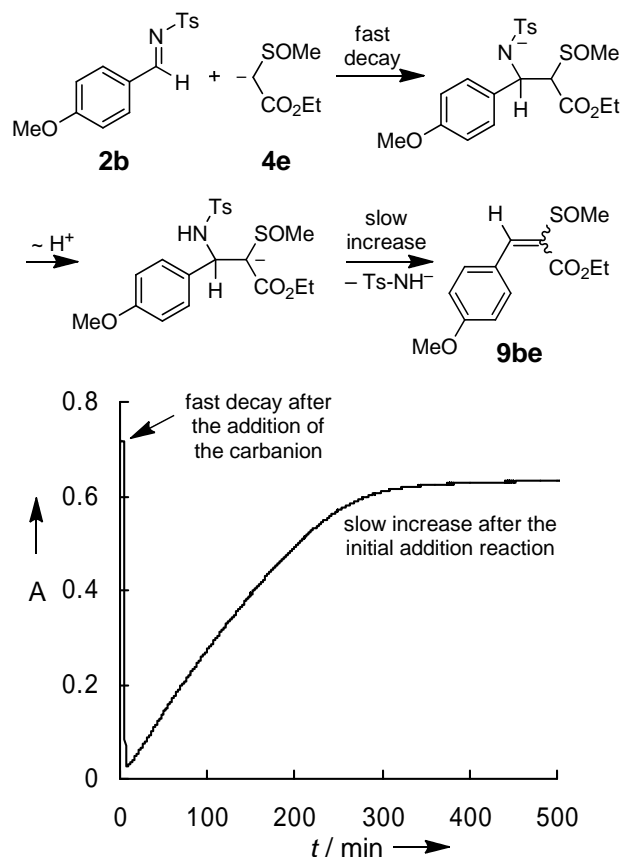
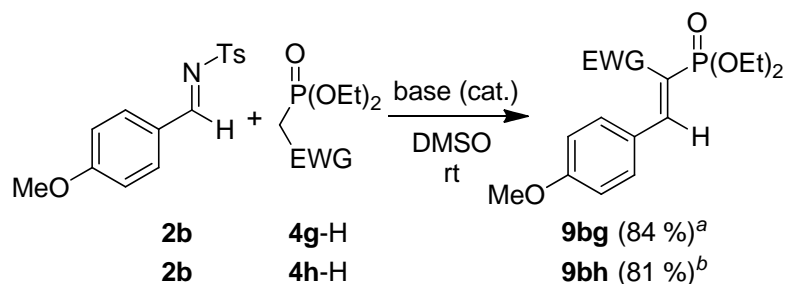


Figure 1: UV-Vis spectroscopic monitoring at 318 nm of the reaction of imine **2b** ($4.73 \times 10^{-5} \text{ mol L}^{-1}$) with the methanesulfonyl-stabilized carbanion **4e** ($8.03 \times 10^{-5} \text{ mol L}^{-1}$) in DMSO at 20°C.

In all investigated Knoevenagel-type condensation reactions, only one stereoisomer was obtained. In the case of compound **9be** (Figure 1) the configuration of the double bond was not determined. However, the *E*-configurations of the olefins **9bg** and **9bh** (Scheme 7) were derived from the characteristic coupling constant of the olefinic proton with the phosphorus nucleus ($J_{\text{HP}} = 24$ and 21 Hz, respectively).^[11,12] Detailed reaction conditions for the preparation of the compounds **9be**, **9bg**, and **9bh** are given in the Experimental Section.

Scheme 7: Condensation Products from the Phosphoryl-Stabilized Carbanions **4g,h** and Imine **2b**.



^a KO^tBu (18 mol-%). ^b Et₃N (18 mol-%).

Kinetic Investigations. All kinetic investigations were performed in DMSO solution at 20°C. As reported earlier,^[6b] the aryl-stabilized sulfur ylides **4a,b** decompose slowly at room temperature and were, therefore, prepared by deprotonation of the corresponding CH acids (**4a,b-H**)-BF₄ with 1.00-1.05 equiv of KO^tBu in dry THF at $\leq -50^\circ\text{C}$. Small amounts of these solutions were dissolved in DMSO at room temperature directly before each kinetic experiment. Stock solutions of the carbanions **4c-h** were prepared by deprotonation of the corresponding CH acids (**4c-h**)-H with 1.00-1.05 equiv of KO^tBu in DMSO. All kinetic investigations were monitored photometrically, either by following the disappearance of the colored imines **2a-c** or of the colored aryl-stabilized sulfur ylides **4a,b** at or close to their absorption maxima. The kinetic investigations of the reactions of the carbanions **4c-h** with the imines **2a-c** (also prepared as stock solutions in DMSO) were performed with a high excess of the carbanions over the imines to achieve first-order kinetics. Vice versa, first-order kinetics for the reactions of the aryl-stabilized ylides **4a,b** with the electrophiles **1-3** were realized by using at least 10 equiv of the electrophiles **1-3**. As the absolute concentration of the minor component is not crucial for the determination of the pseudo-first-order rate constants k_{obs} (eqs 2a and 2b) when the rate of decomposition is much slower than the reaction under consideration, we have thus circumvented the problem that the absolute concentrations of the semistabilized ylides **4a,b** cannot precisely be determined due to their low stability.

From the exponential decays of the UV-Vis absorbances of the imines **2a-c** (Figure 2) or of the sulfur ylides **4a,b**, the first-order rate constants k_{obs} were obtained. Plots of k_{obs} (s⁻¹) against the concentrations of the reaction partners used in excess were linear with negligible intercepts as required by the relation $k_{\text{obs}} = k_2[\text{Nu}]_0$ (eq 2a and Figure 2) or $k_{\text{obs}} = k_2[\text{E}]_0$ (eq 2b), respectively. Only in the reactions of the carbanions **4f-h** with **2b** incomplete consumption of the imine **2b** as well as positive intercepts of plots of k_{obs} vs [**4**] were

observed due to the high reversibility of the additions. However, in all cases the second-order rate constants could be derived from the slopes of the linear correlations of k_{obs} versus $[\text{Nu}]_0$ or $[\text{E}]_0$, respectively (Table 2).

$$-d[\text{E}]/dt = k_2 [\text{Nu}] [\text{E}] \quad (2)$$

$$\text{for } [\text{Nu}]_0 \gg [\text{E}]_0 \Rightarrow k_{\text{obs}} = k_2 [\text{Nu}]_0 \quad (2a)$$

$$\text{for } [\text{E}]_0 \gg [\text{Nu}]_0 \Rightarrow k_{\text{obs}} = k_2 [\text{E}]_0 \quad (2b)$$

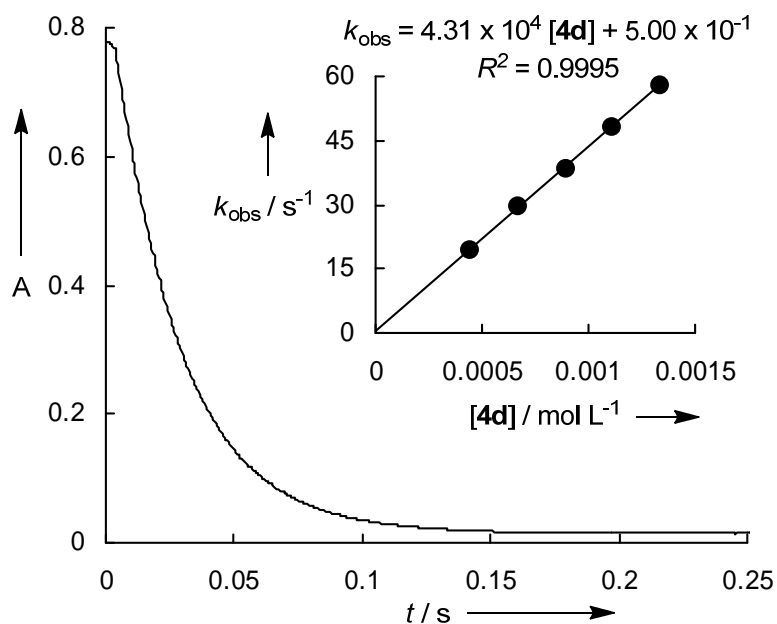


Figure 2: UV-Vis spectroscopic monitoring of the reaction of the nitromethyl anion (**4d**, $4.44 \times 10^{-4} \text{ mol L}^{-1}$) with the imine **2b** ($3.77 \times 10^{-5} \text{ mol L}^{-1}$) at 330 nm in DMSO at 20°C. Insert: Determination of the second-order rate constant $k_2 = 4.31 \times 10^4 \text{ L mol}^{-1} \text{ s}^{-1}$ from the dependence of the first-order rate constant k_{obs} on the concentration of **4d**.

Table 2: Experimental and Calculated Second-Order Rate Constants ($\text{L mol}^{-1}\text{s}^{-1}$) for the Reactions of the Sulfur Ylides **4a,b** and the Carbanions **4c–h** with the Aldehydes **1**, the Imines **2**, and the Michael Acceptors **3** in DMSO at 20°C.

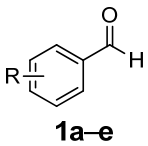
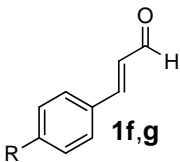
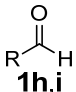
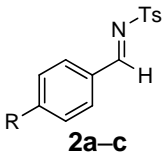
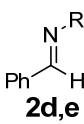
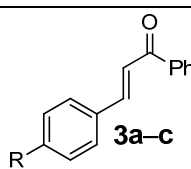
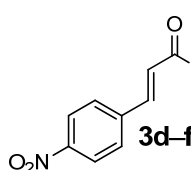
Electrophile	E^a	Nucleophile	Identified Product	k_2^{exp}	$k_2^{\text{calcd } c}$		
 1a–e	1a (R = <i>m</i> -Cl)	-18.03	4a	5aa	1.17×10^2	identical ^d	
	1b (R = <i>m</i> -F)	-18.27	4a		8.06×10^1	identical ^d	
	1c (R = <i>m</i> -OMe)	-19.32	4a		1.54×10^1	identical ^d	
	1d (R = <i>p</i> -F)	-19.42	4a		1.32×10^1	identical ^d	
	1e (R = H)	-19.52	4a	5ea	1.13×10^1	identical ^d	
 1f,g	1f (R = NO ₂)	-18.19	4a	5fa	9.04×10^1	identical ^d	
	1g (R = H)	-19.92	4a		6.03	identical ^d	
 1h,i	1h (R = <i>n</i> -Pr)	-18.72	4a	5ha	3.98×10^1	identical ^d	
	1i (R = <i>n</i> -Pent)	-18.76	4a		3.72×10^1	identical ^d	
 2a–c	2a (R = H)	-11.50	4b	6ab	4.15×10^4	3.15×10^4	
		4d	8ad	2.50×10^5	3.36×10^5		
		2b (R = OMe)	-13.05	4a	6ba	3.21×10^5	2.84×10^5
		4b	6bb	6.19×10^3	3.09×10^3		
		4c	8bc	2.62×10^5	1.84×10^5		
		4d	8bd	4.31×10^4	3.94×10^4		
		4e	9be	1.33×10^5	6.89×10^4		
		4f	8bf	7.65×10^3 ^b	4.58×10^4		
		4g	9bg	2.35×10^3 ^b	1.04×10^4		
		4h	9bh	1.63×10^4 ^b	4.40×10^3		
2c (R = NMe ₂)	-15.09	4c		1.03×10^4	9.98×10^3		
	4d	8cd	1.58×10^3	2.36×10^3			
	4e		4.79×10^3	3.41×10^3			
 2d,e	2d (R = Boc)	-14.22	4a	6da	3.97×10^4	4.55×10^4	
		4b	6db	6.17×10^2	5.37×10^2		
	2e (R = POPh ₂)	-15.89	4a	6ea	4.46×10^3	3.33×10^3	
		4b	6eb	3.21×10^1	4.41×10^1		

Table 2: (Continued).

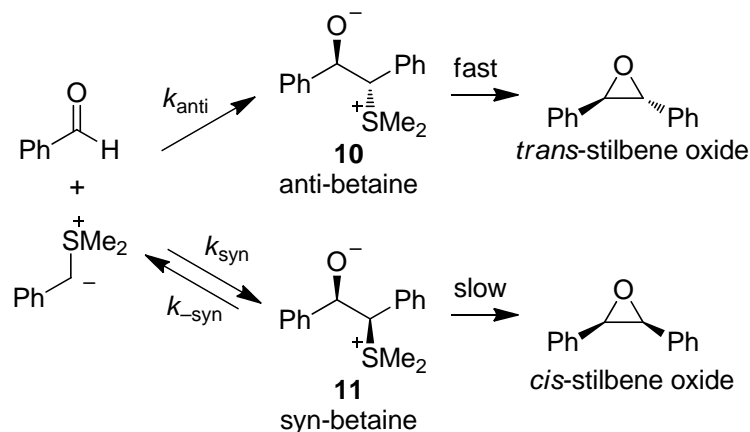
Electrophile	E^a	Nucleophile	Identified Product	k_2^{exp}	$k_2^{\text{calcd } c}$
 3a-c	3a (R = NO ₂)	-17.33	4a	3.46×10^2	3.49×10^2
	3b (R = CN)	-17.64	4a 4b	5.22 2.41 × 10 ²	5.11 2.15 × 10 ²
	3c (R = H)	-18.82	4a	2.89	3.21
 3d-f	3d (R = <i>t</i> -Bu)	-19.15	4a	3.41×10^1	identical ^d
	3e (R = <i>i</i> -Pr)	-19.17	4a	2.02×10^1	identical ^d
	3f (R = Me)	-19.36	4a	1.97×10^1	identical ^d
			4b	1.45×10^1	identical ^d

^a Determination see text, Tables 13, 30, 35, 41, 45, and Figures 9–11 of the Experimental Section. ^b Incomplete consumption of the electrophile was observed indicating an equilibrium situation. ^c Calculated from eq 1 with the N and s parameters for the nucleophiles **4** (Table 1) and the electrophilicity parameters E for the imines **2a–e** and the enones **3a,b** (column 2 of this Table). ^d Only one k_2 value used for the determination of E .

3 Discussion

Epoxidation Reactions. Elegant cross-over experiments by Aggarwal and co-workers^[3e] have shown that the independently generated anti-betaine **10** underwent fast cyclization with exclusive formation of *trans*-stilbene oxide (Scheme 8). The analogous generation of the syn-betaine **11** led to retro-addition, however, and the regenerated sulfur ylide could be trapped by the more electrophilic *p*-nitrobenzaldehyde.

Scheme 8: Mechanism Accounting for the High *trans* Selectivity in the Epoxidation Reaction of Benzaldehyde with Semistabilized Sulfur Ylides.^[3e,h]



Analogous cross-over experiments showed that also in acetonitrile the anti-betaine does not cleave to sulfur ylide and aldehyde but gives the *trans* stilbene oxide selectively.^[3n]

As a consequence, the selective formation of *trans*-epoxide from benzaldehyde and semistabilized sulfur ylides (Scheme 8) must either be due to selective formation of the anti-betaine **10** ($k_{\text{anti}} \gg k_{\text{syn}}$) or to the parallel formation of both betaines ($k_{\text{anti}} \approx k_{\text{syn}}$), followed by cyclization of the anti-betaine **10** and retro-addition of the syn-betaine **11**. The second mechanism is only compatible with the observed second-order kinetics if the retro-addition of the syn-betaine ($k_{\text{-syn}}$) is very fast. If significant equilibrium concentrations of the syn-betaine would build up during the reaction, deviations from the second-order rate law would be expected, as the UV-Vis monitored sulfur ylide **4a** would continuously be regenerated from the reservoir of the syn-betaine. No matter whether the syn-betaine is formed as a short-lived intermediate or not, the rate constants listed in Table 2 reflect the rate-determining formation of the anti-betaine (k_{anti}) as exemplified in Scheme 8.^[13]

As shown in Table 2, the rates of the reactions of the sulfur ylide **4a** with the aldehydes **1a–e** increase with the increasing electron-withdrawing properties of the groups bound to the 3- or 4-positions of the benzaldehydes **1a–e**. From the fair correlation of $\log k_2$ versus Hammett's substituent constants σ shown in Figure 3 one can derive a reaction constant of $\rho = 2.8$ in line with a rate-determining nucleophilic addition of sulfur ylide **4a** to the aldehydes **1a–e**. A similar reaction constant of $\rho = 2.5$ was reported for the epoxidations of various benzaldehydes with dimethylsulfonium benzylide in CD_3CN .^[3n]

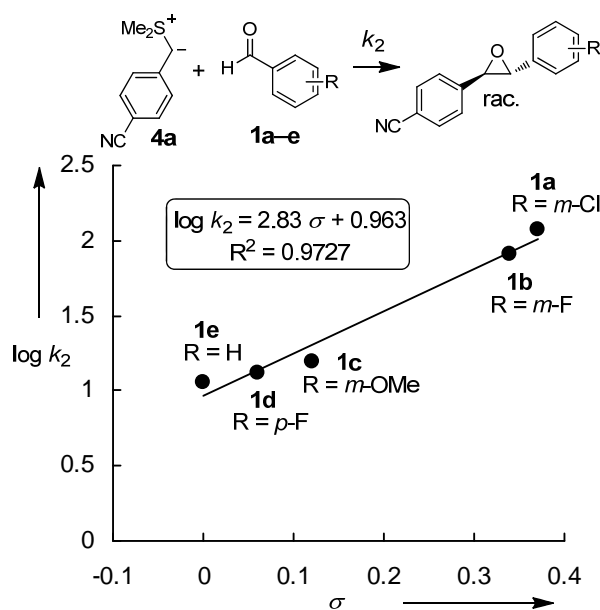


Figure 3: Correlation of the second-order rate constants k_2 for the reactions of the sulfur ylide **4a** with the benzaldehydes **1a–e** in DMSO at 20°C versus Hammett's σ (taken from ref 14).

As the second-order rate constants (Table 2) for the reactions of sulfur ylide **4a** with the aldehydes **1a–i** reflect the rate of attack of a carbon nucleophile at a carbonyl group, they can be used for a quantitative comparison of the electrophilic reactivities of the different aldehydes **1a–i**. Figure 4 shows that the reactivities of the aldehydes **1a–i** cover only 1.5 orders of magnitude. The least reactive compound in this series is the unsubstituted cinnamaldehyde (**1g**), which is approximately half as reactive as benzaldehyde (**1e**). The aliphatic aldehydes **1h** and **1i** are 3 times more electrophilic than benzaldehyde. Substitution of these rate constants and the N and s parameters of sulfur ylide **4a** into eq 1 allows to calculate the electrophilicity parameters E of **1a–i**, which are listed in Table 2.

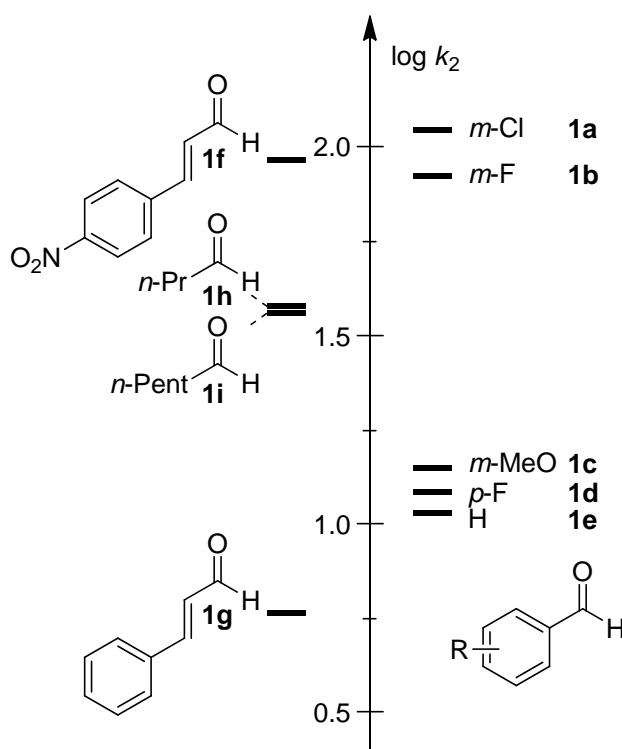
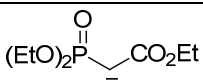
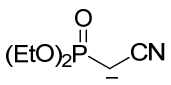
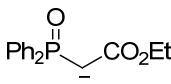
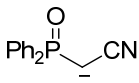
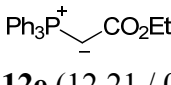


Figure 4: Comparison of the rate constants ($\log k_2$) for the reactions of the aldehydes **1a–i** with sulfur ylide **4a** in DMSO at 20°C.

In previous work we have determined rate constants for the olefination reactions of aromatic aldehydes with phosphoryl-stabilized carbanions and with phosphorus ylides.^[9] Table 3 compares the experimental rate constants with those calculated by eq 1 from the E values of the aldehydes in Table 2 and the previously reported N and s parameters^[9] for phosphorus ylides and phosphoryl-substituted carbanions.

Table 3: Comparison of the Experimental and Calculated Second-Order Rate Constants ($\text{L mol}^{-1}\text{s}^{-1}$) for the Olefination Reactions of the Benzaldehydes **1a,d,e** with Phosphoryl-Stabilized Carbanions **12a–d** and Phosphorus Ylide **12e** in DMSO at 20°C .^{a,b}

Nucleophile (<i>N</i> / <i>s</i>)		1a	1d	1e
 12a (19.23 / 0.65)	k_2^{exp}	5.73×10^1	4.05	2.02
	k_2^{calcd}	6.03	7.52×10^{-1}	6.48×10^{-1}
	$k_2^{\text{exp}}/k_2^{\text{calcd}}$	9.5	5.4	3.1
 12b (18.57 / 0.66)	k_2^{exp}	1.48×10^2	1.17×10^1	7.16
	k_2^{calcd}	2.27	2.75×10^{-1}	2.36×10^{-1}
	$k_2^{\text{exp}}/k_2^{\text{calcd}}$	65	43	30
 12c (19.20 / 0.69)	k_2^{exp}	1.58		
	k_2^{calcd}	6.42		
	$k_2^{\text{exp}}/k_2^{\text{calcd}}$	0.25		
 12d (18.69 / 0.72)	k_2^{exp}	6.67	7.08×10^{-1}	5.52×10^{-1}
	k_2^{calcd}	2.99	2.98×10^{-1}	2.53×10^{-1}
	$k_2^{\text{exp}}/k_2^{\text{calcd}}$	2.2	2.4	2.2
 12e (12.21 / 0.62)	k_2^{exp}			1.44×10^{-3} ^c
	k_2^{calcd}			2.94×10^{-5}
	$k_2^{\text{exp}}/k_2^{\text{calcd}}$			49

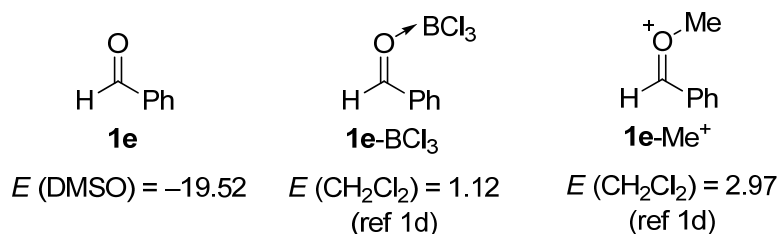
^a *N* and *s* parameters and rate constants k_2^{exp} (DMSO, 20°C) taken from ref 9 if not indicated otherwise. ^b Rate constants k_2^{calcd} were calculated by using eq 1, the *N* and *s* parameters for the nucleophiles (column 1 of this Table), and the electrophilicity parameters *E* for **1a,d,e** (Table 2). ^c Taken from ref 15.

In view of the generally accepted model for salt-free Wittig reactions, which involves concerted oxaphosphetane formation,^[16,17] the coincidence of k_2^{exp} and k_2^{calcd} in Table 3 is unexpected and remarkable: All rate constants calculated by using eq 1 for the reactions of the phosphoryl-stabilized carbanions **12a–d** and the phosphorus ylide **12e** listed in Table 3 with the benzaldehydes **1a,d,e** deviate by less than a factor of 66 from the corresponding experimental values. As the confidence limit of eq 1, which uses only three parameters to predict absolute rate constants in a reactivity range of 40 orders of magnitude, is a factor of 10–100, one cannot unambiguously assign the origin of these deviations. In any case, the small $k_2^{\text{exp}}/k_2^{\text{calcd}}$ ratios in Table 3 prove that the transition states of the oxaphosphetane formations in these reactions can only weakly be stabilized by the concerted formation of the PO bonds. One might conclude, therefore, that the *N* and *s* parameters of phosphoryl-stabilized carbanions and phosphorus ylides can generally be combined with the *E* parameters

of carbonyl compounds to predict scope and limitations of Wittig and Horner-Wadsworth-Emmons reactions. In previous work we have demonstrated, however, that the reactivity ratio of **12c** and **12e** towards quinone methides ($\approx 8.5 \times 10^4$) decreases to 82 in the reaction towards *p*-nitrobenzaldehyde, which was assigned to a higher degree of concertedness in the reaction of the phosphorus ylide.^[9] It is presently not clear, in which cases the stabilization of the transition state by concertedness becomes so strong that the approximation by eq 1 is not any longer valid.

While the electrophilicity parameters for aldehydes (Table 2) reflect the intrinsic reactivities of aldehydes in DMSO, Scheme 9 demonstrates the striking increase of the electrophilic reactivity of benzaldehyde (**1e**), when its carbonyl group is activated by a Lewis acid or by O-methylation. Accordingly, the boron trichloride complex **1e-BCl₃** is more than 20 orders and the carboxonium ion **1e-Me⁺** is more than 22 orders of magnitude more reactive than benzaldehyde (**1e**). The mild conditions for many Knoevenagel^[18] and Henry^[19] reactions indicate, however, that the electrophilicities of aldehydes increase significantly in aqueous or alcoholic solvents.

Scheme 9: Comparison of the Electrophilic Reactivity *E* of Benzaldehyde **1e** in DMSO with those of the Boron Trichloride Complex **1e-BCl₃** and the Carboxonium Ion **1e-Me⁺** in CH₂Cl₂.



Reactions with Imines. Previous mechanistic studies revealed the aziridination reactions of *N*-tosyl-substituted aldimines (e.g., imines **2a–c**) with aryl-stabilized sulfur ylides (e.g., **4a,b**) to proceed stepwise via initial irreversible nucleophilic attack.^[4a,c,d] Thus, a single CC bond is generated in the rate-determining step, with the consequence that eq 1 should be applicable. Therefore, we have calculated the electrophilicity parameters *E* for **2a–c** by least-squares minimization of $\Delta^2 = \sum(\log k_2 - s(N + E))^2$ using the second-order rate constants k_2 given in Table 2 and the *N* and *s* parameters of **4a–h** from Table 1. The comparison between calculated and experimental rate constants in Table 2 shows a remarkable agreement. Though the nucleophile-specific parameters *N* and *s* of the sulfur ylides **4a,b** and of the carbanions **4c–h** have been derived from the rates of their reactions with benzhydrylium ions and

Michael acceptors, they can be combined with the electrophilicity parameters of the *N*-tosyl-substituted benzaldimines **2a–c** to calculate the rate constants for the aziridination reactions as well as for the addition reactions of the carbanions to the CN double bond. In 5 of 8 cases, the agreement between calculated and experimental reactivities of **2b** is better than factor 2.1, and in all other cases better than factor 6. In Figure 5 the consistency of the obtained reactivity parameters is further visualized by the good match of the data points for the reactions of the aryl-stabilized sulfur ylides **4a,b** and the carbanion **4d** with the imines **2a–e** to the correlation lines, which were obtained from the rate constants of the reactions of **4a,b,d** with reference electrophiles (i.e., benzhydrylium ions and Michael acceptors).

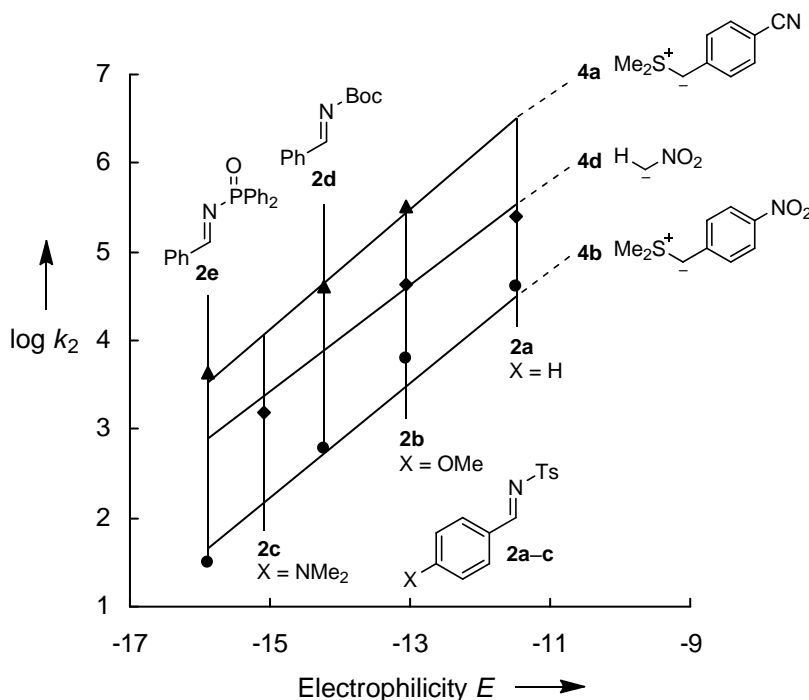


Figure 5: Match of the rate constants for the reactions of the aryl-stabilized sulfur ylides **4a,b** and the carbanion **4d** with the imines **2a–e** ($\log k_2$ versus E (**2a–e**)) to the correlation lines derived from the reactions of **4a,b,d** with benzhydrylium ions and Michael acceptors (DMSO, 20°C).

Figure 5 illustrates that the electrophilic reactivities of the *N*-tosyl-activated imines **2a–c** increase with decreasing electron-donating effects of the *p*-substituents. A correlation of the rate constants for the reactions of **2a–c** with **4d** vs Hammett's σ_p is shown on p. 258 in the Experimental Section. One derives a Hammett reaction constant of $\rho = 2.6$, which is similar to that obtained for the reactions of the benzaldehydes **1a–e** with sulfur ylide **4a** ($\rho = 2.8$, see above). When the tosyl group of the imine **2a** is replaced by less electron-withdrawing substituents, i.e., the *tert*-butoxycarbonyl group in case of **2d** and the diphenylphosphinoyl

group in case of **2e**, the electrophilic reactivity towards **4b** decreases by a factor of 67 and 1290, respectively.

Cyclopropanation Reactions. In previous work, we have observed that the rate constants of the cyclopropanation reactions of Michael acceptors with sulfur ylides fit the same correlations of $\log k_2$ versus electrophilicity E as the corresponding reactions of sulfur ylides with benzhydrylium ions.^[6b] A stepwise formation of the cyclopropanes with rate-determining formation of the intermediate zwitterion was thus indicated. Figure 6 shows that the relative reactivities of the sulfur ylides **4a** and **4b** towards the chalcones **3a** and **3b** are identical to those previously derived from the rates of their reactions with reference electrophiles which again indicates analogous reaction mechanisms. From the corresponding correlations shown in Figure 6 we have derived the E parameters of **3a–f** listed in Table 2.

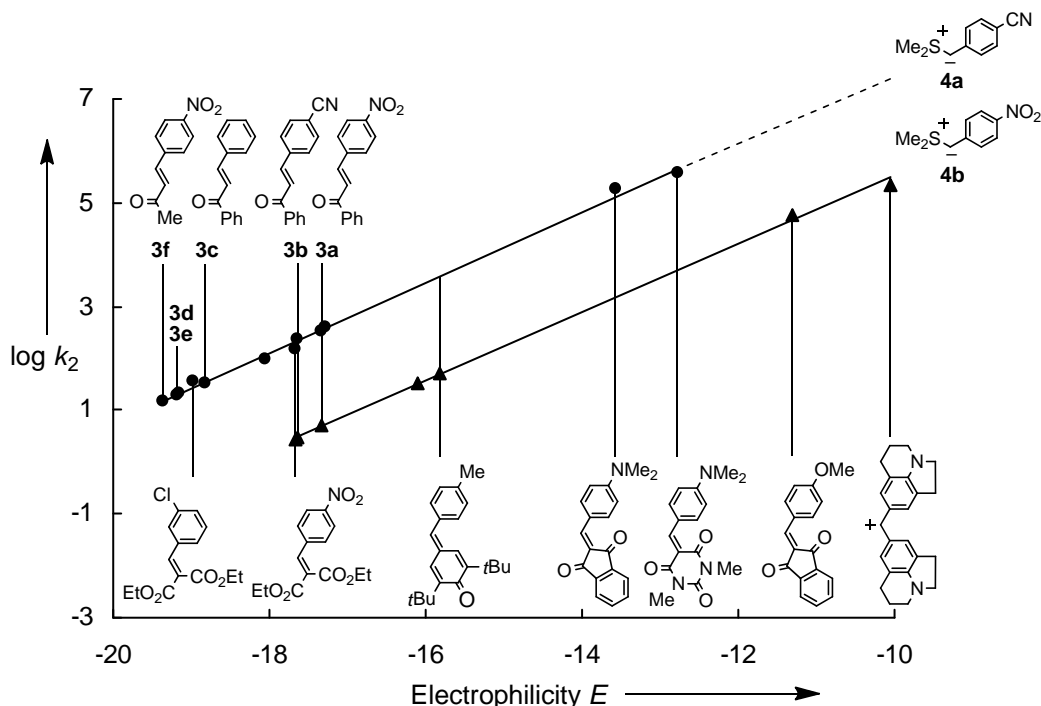


Figure 6: Match of the rate constants for the reactions of the semistabilized sulfur ylides **4a,b** with the enones **3a–f** ($\log k_2$ versus E (**3a–f**)) to the correlation lines of **4a,b** derived from their reactions with a benzhydrylium ion and several types of Michael acceptors (DMSO, 20°C). (Rate constants and E parameters were taken from Table 2 and ref 6b).

From the Hammett correlation one derives a reaction constant of $\rho = 1.3$ for the reactions of the enones **3a–c** with sulfur ylide **4a** indicating a moderate increase of reactivity by electron-withdrawing substituents (see p. 264 in the Experimental Section). As illustrated in Figure 7, the reactivities of the α,β -unsaturated ketones **3a–f** differ by less than a factor of 25. While

variation of the alkyl group in the ketones **3d–f** has almost no effect on the reactivities of the CC double bond, the corresponding phenyl compound **3a** is 24 times more reactive than **3f**, despite the opposite ordering of the Hammett substituent constants (σ_p (COMe) = 0.50 and σ_p (COPh) = 0.43).^[14]

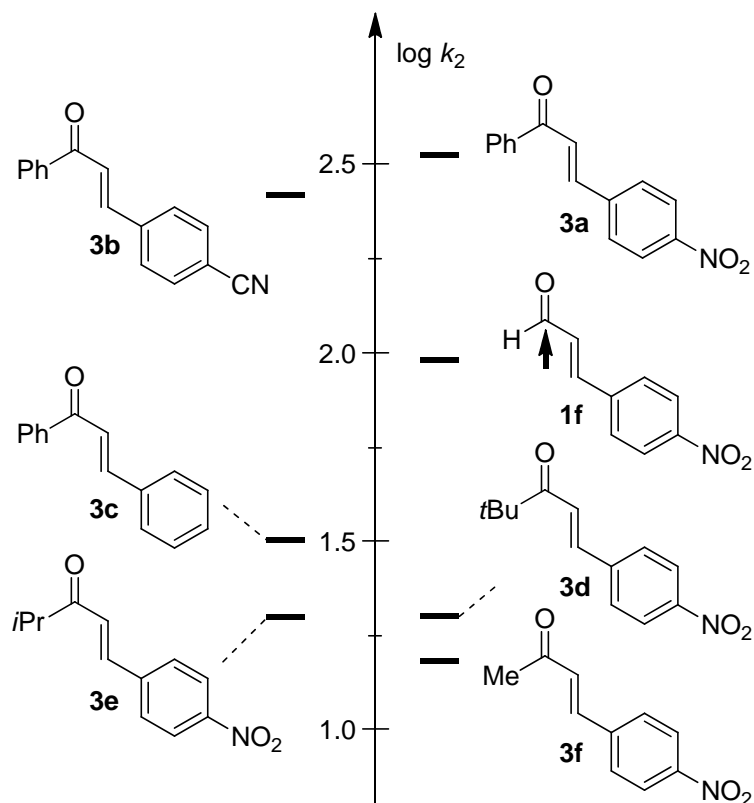


Figure 7: Comparison of the rate constants ($\log k_2$) for the reactions of the enones **3a–f** and *p*-nitrocinnamaldehyde (**1f**) with sulfur ylide **4a** in DMSO at 20°C.

Product analysis of the reaction of *p*-nitrocinnamaldehyde (**1f**) with the sulfur ylide **4a** (Scheme 3) as well as several literature reports on reactions of semistabilized sulfur ylides with α,β -unsaturated aldehydes^[10] show that epoxide formation is generally preferred over the cyclopropane formation when α,β -unsaturated aldehydes are used as reactants. The attack at the carbonyl group of **1f** (i.e., epoxidation) is kinetically preferred over the attack to the conjugate position (i.e., cyclopropanation). This selectivity indicates that the formyl group activates the conjugate addition less than acetyl and benzoyl groups despite the similar magnitudes of Hammett's σ_p values (σ_p (CHO) = 0.42).^[14]

4 Conclusion

Epoxidation, aziridination, and cyclopropanation reactions of aldehydes, imines, and Michael acceptors with sulfur ylides, which proceed stepwise with rate-determining formation of an intermediate zwitterion (Scheme 1) have been investigated kinetically. As the first step of these reactions is mechanistically related to the electrophile-nucleophile combinations, which have been employed to derive eq 1,^[1,2] the resulting second-order rate constants ($\log k_2$) could be combined with the previously published N and s parameters of sulfur ylides^[6b] to calculate the corresponding reactivity parameters E of these electrophiles.

Figure 8 shows that in DMSO, N -tosyl-, N -*tert*-butoxycarbonyl-, and N -phosphinoyl-substituted benzaldimines are significantly more electrophilic than the corresponding benzaldehydes. While the reactions of most aldehydes and imines with stabilized carbanions are highly reversible and cannot be investigated in aprotic solvents, the strong electron-withdrawing effect of the N -tosyl group in the benzaldimines **2a–c** allowed us also to measure the rate constants of their reactions with ordinary carbanions. In line with the stepwise mechanism for the aziridinations, the rates of the reactions of sulfur ylides and carbanions with imines were found on the same correlation lines, which were obtained from the rate constants of the reactions of these nucleophiles with reference electrophiles (i.e., benzhydrylium ions and Michael acceptors) in Figure 5. This finding furthermore justifies the use of sulfur ylides as references for deriving the electrophilicity parameters E for the imines **2**.

Though rate constants for the reactions of phosphorus ylides and phosphoryl-substituted carbanions with aldehydes have already been published previously,^[9] we have been reluctant to use these data for determining electrophilicity parameters of aldehydes, because of the evidence for concerted formation of the oxaphosphetanes.^[9,16,17] We were, therefore, surprised that the rate constants for the Wittig and Horner-Wadsworth-Emmons reactions listed in Table 3 can properly be derived from the electrophilicity parameters of aldehydes in Table 2 and the N and s parameters of the phosphorus-stabilized nucleophiles, which have previously been derived from their one-bond-forming reactions with benzhydrylium ions and quinone methides.^[9] From the agreement between calculated and experimental rate constants of these olefination reactions, we can conclude that the transition states of the oxaphosphetane formations for the combinations described in Table 3 can only be weakly stabilized by the concerted formation of two new bonds. Presently, it is not yet clear, in which cases the transition states for the oxaphosphetane formations are unsymmetrical enough that the corresponding rate constants can be predicted by eq 1.

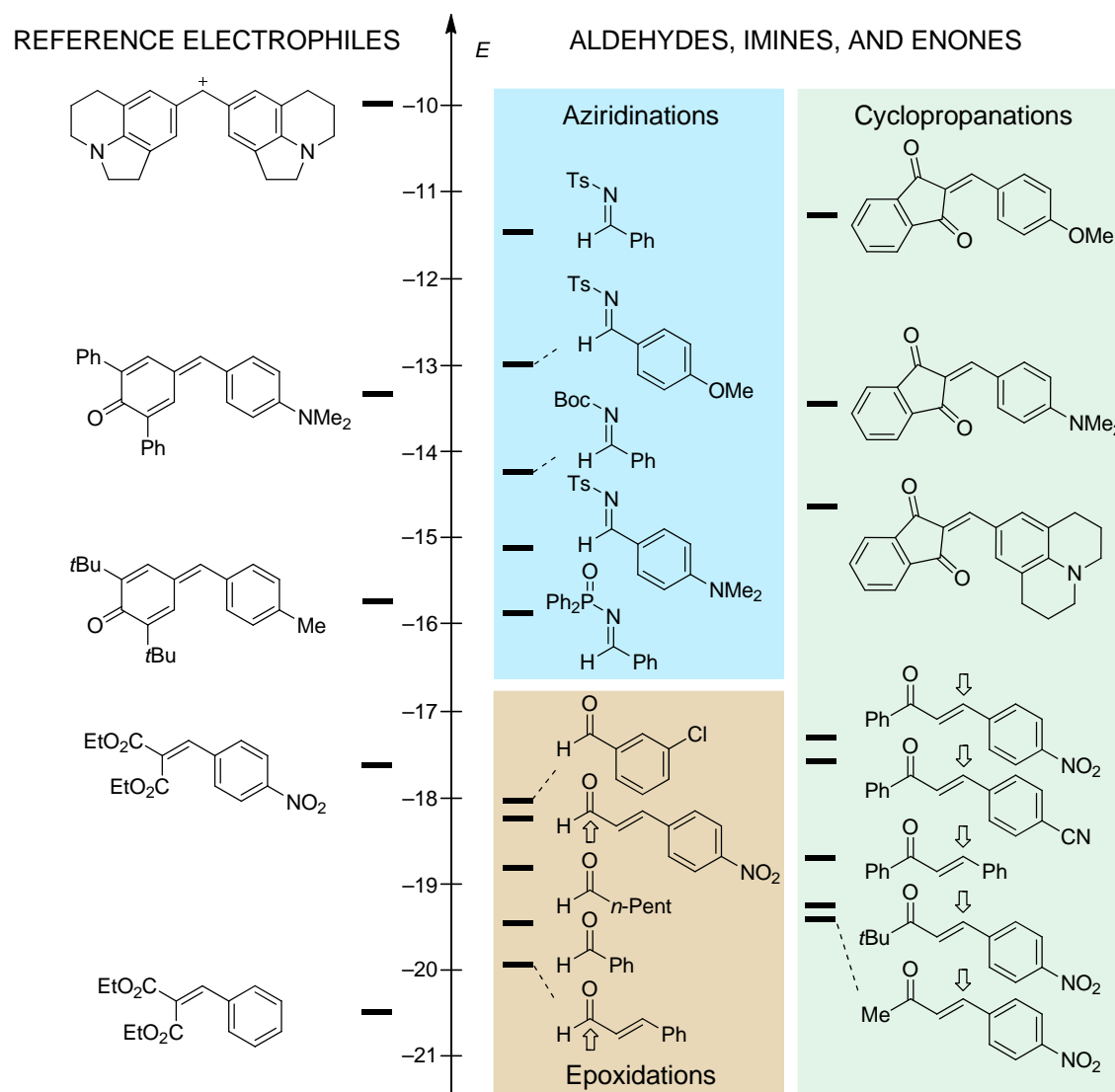


Figure 8: Comparison of the electrophilicity parameters E of aldehydes, imines, and enones with different Michael acceptors in DMSO.

In previous work we have shown that the electrophilicity parameters E of our reference electrophiles (benzhydrylium ions and quinone methides), which were derived from reactions in dichloromethane or DMSO, can also be employed for reactions in other solvents, e. g., acetonitrile, methanol, and water.^[1,2] We, therefore, concluded that these reference electrophiles do not experience differential solvation, implying that the changes of their solvation energies in different solvents are linearly correlated with E . By using solvent-independent electrophilicity parameters E for the reference electrophiles, solvent effects have been shifted into the solvent-dependent nucleophile-specific parameters N and s of eq 1, which allowed us to develop a comprehensive nucleophilicity scale.^[1]

Absence of differential solvation cannot generally be expected for ordinary carbonyl compounds and imines, because strong interactions of the polar CO or CN double bonds with

protic solvents may increase the corresponding electrophilicity parameters E in Figure 8,^[20] which restricts use of the E parameters for these compounds to DMSO solution. Furthermore, the derived reactivity parameters for aldehydes and imines may only hold for their reactions with carbon nucleophiles. In reactions with oxygen- or nitrogen-centered nucleophiles, the well-known anomeric stabilization^[21] of the resulting products may already affect the transition states. As anomeric effects are not included in the reactivity parameters N , s , and E , amines and alkoxides can be expected to react faster with aldehydes and imines than predicted by eq 1.

The α,β -unsaturated ketones depicted in Figure 8 show reactivities comparable to those of diethyl benzylidenemalonates indicating that a single benzoyl group has a similar activating effect on the electrophilicity of a CC double bond as two ethoxycarbonyl groups. Obviously, the electrophilicities of these Michael acceptors are not closely correlated with the pK_{aH} values of the resulting carbanions, demonstrating the need for a systematic investigation of their electrophilicities.^[22]

5 Experimental Section

5.1 General

Chemicals. The sulfonium tetrafluoroborates (**4a,b-H**)-BF₄ were prepared by treatment of the corresponding benzylic alcohols with HBF₄/Et₂O and dimethyl sulfide as reported earlier.^[6b] According to literature reports, 2-(methylsulfinyl)acetate (**4e**)-H was prepared by the oxidation of ethyl 2-(methylthio)acetate with NaIO₄,^[23] *p*-nitrocinnamaldehyde by aldol condensation of *p*-nitrobenzaldehyde with acetaldehyde^[24] (**1f**), the enone **3b** by aldol condensation of *p*-cyanobenzaldehyde with acetophenone,^[25] the imines **2a–c,e** by titanium tetrachloride induced reaction of the corresponding benzaldehydes with *p*-methylbenzenesulfonamide or diphenylphosphinic amide,^[26] imine **2d** by a procedure starting from benzaldehyde, *t*-butyl carbamate, sodium benzene sulfinate, and formic acid.^[27] The enones **3e,f** were prepared according to analogous aldol condensations as for *p*-nitrocinnamaldehyde (**1f**). The syntheses of the enones **3a,d** were achieved according to the same procedure as for compound **3b**. All other chemicals were purchased from commercial sources and (if necessary) purified by recrystallization or distillation prior to use.

Analytics. ¹H- and ¹³C-NMR spectra were recorded on Varian NMR-systems (300, 400, or 600 MHz) in CDCl₃ or CD₃CN and the chemical shifts in ppm refer to TMS (δ_H 0.00, δ_C

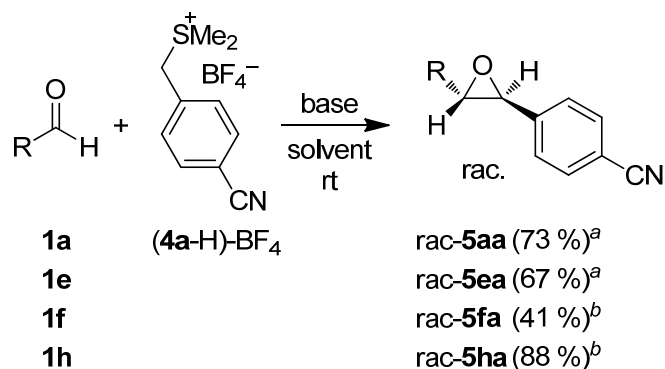
0.00) or CD₃CN (δ_{H} 1.94, δ_{C} 1.24) as internal standard. The following abbreviations were used for chemical shift multiplicities: brs = broad singlet, s = singlet, d = doublet, t = triplet, q = quartet, m = multiplet. For reasons of simplicity, the ¹H-NMR signals of AA'BB'-spin systems of *p*-disubstituted aromatic rings were treated as doublets. NMR signal assignments were based on additional 2D-NMR experiments (e.g., COSY-, NOESY-, HSQC-, and HMBC experiments). Diastereomeric ratios (*dr*) were determined by ¹H-NMR (³¹P-NMR for compounds **6ea** and **6eb**). (HR-)MS was performed on a Finnigan MAT 95 (EI) or a Thermo Finnigan LTQ FT (ESI) mass spectrometer. An Elementar Vario Micro Cube or an Elementar vario EL device was used for elemental analysis. Melting points were determined on a Büchi B-540.

Kinetics. The rates of all reactions were determined photometrically. The temperature was kept constant (20.0 ± 0.1°C) by using a circulating bath thermostat. Stock solutions of the semi-stabilized ylides **4a,b** were prepared by deprotonation of the corresponding CH acids (**4a,b-H**)-BF₄ in dry THF at ≤ -50°C with 1.00-1.05 equiv of KO^{*t*}Bu. Small amounts of these stock solutions were dissolved in DMSO at room temperature directly before each kinetic experiment. The stock solutions of the carbanions **4c-h** were prepared by deprotonation of the corresponding CH acids (**4c-h**)-H with 1.00-1.05 equiv of KO^{*t*}Bu in DMSO. The kinetic investigations of the reactions of the carbanions **4c-h** with the electrophiles **2a-c** (also prepared as stock solutions in DMSO) were performed with a high excess of the nucleophiles over the electrophiles resulting in first-order kinetics. As the absolute concentrations of the semi-stabilized sulfur ylides **4a,b** cannot be determined precisely (low stability, side reactions during the deprotonation of the CH acids), these compounds have been used as minor components in the reactions with the electrophiles **1-3** also resulting in first-order kinetics. The rates of slow reactions ($\tau_{1/2} > 15\text{-}20$ s) were determined by using a J&M TIDAS diode array spectrophotometer controlled by Labcontrol Spectacle software and connected to a Hellma 661.502-QX quartz Suprasil immersion probe (5 mm light path) via fiber optic cables and standard SMA connectors. For the evaluation of fast kinetics ($\tau_{1/2} < 15\text{-}20$ s) the stopped-flow spectrophotometer systems Hi-Tech SF-61DX2 or Applied Photophysics SX.18MV-R were used. First-order rate constants k_{obs} (s⁻¹) were obtained by fitting the single exponential $A_t = A_0 \exp(-k_{\text{obs}}t) + C$ (exponential decrease) to the observed time-dependent absorbance (averaged from at least 3 kinetic runs for each nucleophile concentration in case of stopped-flow method). Second-order rate constants k_2 (L mol⁻¹ s⁻¹) were derived from the slopes of the

linear correlations of k_{obs} with the concentration of the reaction partner used in excess ($[\text{Nu}]_0$ or $[\text{E}]_0$).

5.2 Product Analysis

5.2.1 Reactions of the Sulfur Ylide **4a** with the Aldehydes **1a,e,f,h**

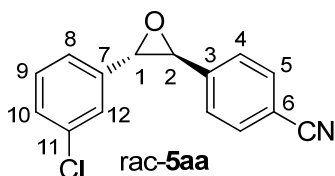


^a KO^tBu, DMSO. ^b K₂CO₃ (aq.), CHCl₃.

Product studies for the reactions of the sulfur ylide **4a** with the aromatic aldehydes **1a,e**

General procedure A. The ylide **4a** was generated by the addition of KO^tBu (dissolved in 2-3 mL DMSO) to a vigorously stirred solution of the sulfonium tetrafluoroborate (**4a-H**)-BF₄ in dry DMSO (2-3 mL) at room temperature. The corresponding aldehyde **1a** or **1e** (dissolved in 2-3 mL DMSO) was then added in one portion. After 10 min of stirring, the reaction was quenched by the addition of water and extracted with CH₂Cl₂. The combined organic layers were washed with water and brine, dried over Na₂SO₄ and evaporated under reduced pressure. The crude products were purified by column chromatography on silica gel (*n*-pentane/EtOAc or *i*-hexane/EtOAc) and subsequently characterized by ¹H- and ¹³C-NMR spectroscopy and MS. Signal assignments were based on additional COSY, HSQC and HMBC experiments. Small samples of solid products were recrystallized in appropriate solvent mixtures for the determination of melting points.

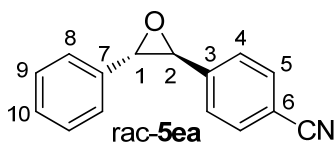
4-(3-(3-Chlorophenyl)oxiran-2-yl)benzotrile (5aa) was obtained from (4-cyanobenzyl)dimethylsulfonium tetrafluoroborate (**4a-H**)-BF₄ (300 mg, 1.13 mmol), KO^tBu (127 mg, 1.13 mmol), and *m*-chlorobenzaldehyde (**1a**, 48.0 mg, 341 μmol) as a colorless solid (65 mg, 0.25 mmol, 73 %, only *trans*-isomer).



R_f (*i*-hexane/EtOAc 12:1, *v/v*): 0.14. Mp. (*n*-pentane/Et₂O): 110-111°C. ¹H-NMR (CDCl₃, 300 MHz): δ = 3.81 (d, 1 H, *J* = 1.8 Hz, 1-H), 3.88 (d, 1 H, *J* = 1.8 Hz, 2-H), 7.21-7.24 (m, 1 H, 12-H), 7.32-7.33 (m, 3 H, 8-H, 9-H, 10-H), 7.44 (d, 2 H, *J* = 8.2 Hz, 4-H), 7.68 (d, 2 H, *J* = 8.4 Hz, 5-H). ¹³C-NMR (CDCl₃, 75.5 MHz): δ = 61.8 (d, C-2), 62.4 (d, C-1), 112.3 (s, C-6), 118.5 (s, CN), 123.8 (d, C-12), 125.5 (d, C-8), 126.2 (d, C-4), 128.9 (d, C-10), 130.0 (d, C-9), 132.5 (d, C-5), 134.9 (s, C-11), 138.3 (s, C-7), 141.9 (s, C-3). MS (EI): *m/e* (%) = 257 (28), 256 (20), 255 (89) [M]⁺, 237 (23), 226 (44), 220 (100), 192 (44), 191 (29), 190 (36), 115 (24), 89 (51). HR-MS (EI): calcd for [C₁₅H₁₀ClNO]⁺: 255.0445, found 255.0447.

4-(3-Phenyloxiran-2-yl)benzonitrile (5ea) was obtained from (4-cyanobenzyl)dimethylsulfonium tetrafluoroborate (**4a-H**)-BF₄ (300 mg, 1.13 mmol), KO^{*t*}Bu (127 mg, 1.13 mmol), and benzaldehyde (**1e**, 31.8 mg, 300 μ mol) as a colorless oil (45 mg, 0.20 mmol, 67 %, only *trans*-isomer).

RAP 35.1



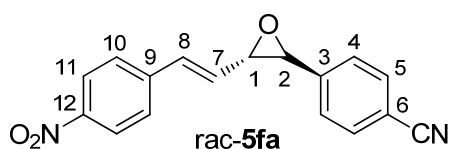
R_f (*n*-pentane/EtOAc 8:1, *v/v*): 0.50. ¹H-NMR (CDCl₃, 300 MHz): δ = 3.83 (d, 1 H, *J* = 1.8 Hz, 1-H), 3.92 (d, 1 H, *J* = 1.8 Hz, 2-H), 7.32-7.42 (m, 5 H, 7-H, 8-H, 9-H, 10-H), 7.45 (d, 2 H, *J* = 8.2 Hz, 4-H), 7.67 (d, 2 H, *J* = 8.4 Hz, 5-H). ¹³C-NMR (CDCl₃, 75.5 MHz): δ = 61.8 (d, C-2), 63.2 (d, C-1), 112.1 (s, C-6), 118.6 (s, CN), 125.5 (d, C-8), 126.1 (d, C-4), 128.7 (d, C-9), 128.8 (d, C-10), 132.4 (d, C-5), 136.2 (s, C-7), 142.5 (s, C-3). MS (EI): *m/e* (%) = 221 [M]⁺ (61), 220 (33), 204 (19), 203 (23), 193 (54), 192 (100), 191 (15), 190 (27), 165 (34), 130 (23), 115 (16), 91 (18), 90 (68), 89 (51), 77 (19), 63 (19). HR-MS (EI): calcd for [C₁₅H₁₁NO]⁺: 221.0835, found 221.0834.

NMR-signals are in agreement with those reported in the literature.^[10c,28]

Product studies for the reactions of the sulfur ylide 4a with the aldehydes 1f,h

(E)-4-(3-(4-Nitrostyryl)oxiran-2-yl)benzonitrile (5fa). Saturated aqueous K_2CO_3 -solution (5 mL) was added to a vigorously stirred solution of sulfonium tetrafluoroborate (**4a-H**)- BF_4 (150 mg, 566 μ mol) and *p*-nitrocinnamaldehyde (**1f**, 100 mg, 564 μ mol) in $CHCl_3$ (15 mL). The resulting biphasic mixture was vigorously stirred for 3 h. During this reaction further portions of (**4a-H**)- BF_4 were added after 1 h (150 mg, 566 μ mol) and 2.5 h (75.0 mg, 283 μ mol). The reaction was subsequently treated with water, the organic layer was separated and the aqueous phase additionally extracted by $CHCl_3$. The combined organic layers were washed with water and brine, dried over Na_2SO_4 , and evaporated under reduced pressure. Purification of the crude product by column chromatography on silica gel (*n*-pentane/EtOAc) furnished **5fa** as a yellow solid (97.0 mg, 0.33 mmol, 59 %, only *trans*-isomer). Recrystallization from *n*-pentane/EtOAc yielded **5fa** as yellow solid (67.0 mg, 0.23 mmol, 41 %, only *trans*-isomer), which was subsequently characterized by 1H - and ^{13}C -NMR spectroscopy, MS, and elemental analysis. Signal assignments were based on additional COSY, HSQC and HMBC experiments.

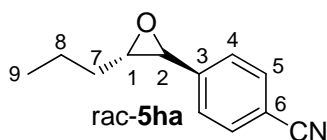
RAP 37.3



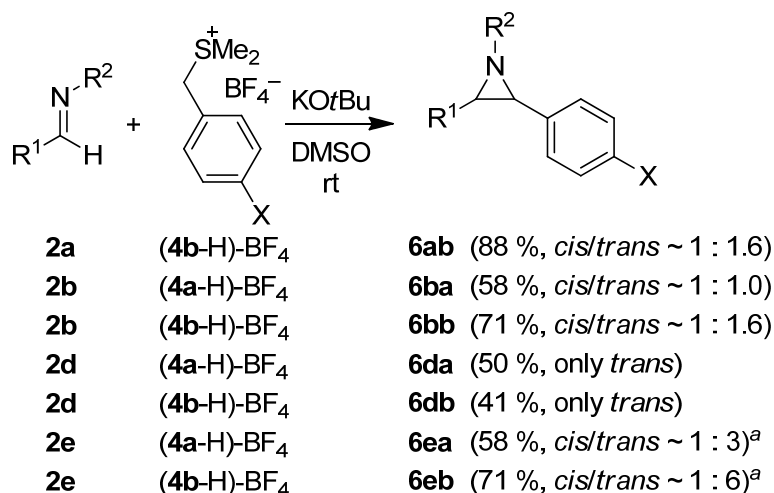
R_f (*n*-pentane/EtOAc 5:1, *v/v*): 0.35. Mp. (*n*-pentane/EtOAc): 175-177°C. 1H -NMR ($CDCl_3$, 400 MHz): δ = 3.51-3.54 (m, 1 H, 1-H), 3.96 (d, 1 H, J = 1.7 Hz, 2-H), 6.26 (dd, 1 H, J = 16.0, 7.3 Hz, 7-H), 6.90 (d, 1 H, J = 16.0 Hz, 8-H), 7.44 (d, 2 H, J = 8.5 Hz, 4-H), 7.54 (d, 2 H, J = 8.9 Hz, 10-H), 7.68 (d, 2 H, J = 8.3 Hz, 5-H), 8.21 (d, 2 H, J = 8.8 Hz, 11-H). ^{13}C -NMR ($CDCl_3$, 101 MHz): δ = 60.0 (d, C-2), 62.7 (d, C-1), 112.3 (s, C-6), 118.5 (s, CN), 124.2 (d, C-11), 126.1 (d, C-4), 127.1 (d, C-10), 130.1 (d, C-7), 132.5 (d, C-5), 132.6 (d, C-8), 141.9, 142.0 (2s, C-3, C-9), 147.4 (s, C-12). MS (EI): m/e (%) = 292 (7) $[M]^+$, 275 (7), 264 (14), 263 (79), 246 (10), 245 (11), 218 (18), 217 (100), 216 (15), 130 (49), 116 (10), 115 (47), 114 (13), 102 (17), 89 (13), 77 (9), 63 (8). HR-MS (EI) $[M]^+$: calcd for $[C_{17}H_{12}N_2O_3]^+$: 292.0843, found 292.0848. Anal. calcd for $C_{17}H_{12}N_2O_3$ (292.29): C 69.86, H 4.14, N 9.58, found C 69.62, H 3.99, N 9.42.

4-(3-Propyloxiran-2-yl)benzonitrile (5ha). Saturated aqueous K_2CO_3 -solution (5 mL) was added to a vigorously stirred solution of the sulfonium tetrafluoroborate (**4a-H**)- BF_4 (300 mg, 1.13 mmol) and butyraldehyde (**1h**, 1.0 mL, 11 mmol) in $CHCl_3$ (5 mL). The resulting biphasic mixture was vigorously stirred for 3 h. The reaction was subsequently treated with water, the organic layer was separated and the aqueous phase additionally extracted by $CHCl_3$. The combined organic layers were washed with water and brine, dried over Na_2SO_4 , and evaporated under reduced pressure. Purification of the crude product by column chromatography on aluminum oxide (*i*-hexane/EtOAc) furnished **5ha** as a colorless oil (187 mg, 999 μ mol, 88 %, only *trans*-isomer), which was subsequently characterized by 1H - and ^{13}C -NMR spectroscopy and MS. Signal assignments were based on additional COSY, HSQC and HMBC experiments.

RAP 46.2



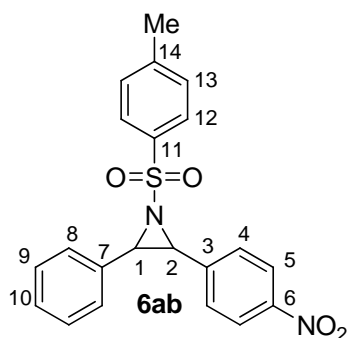
R_f (*i*-hexane/EtOAc 12:1, *v/v*): 0.42. 1H -NMR ($CDCl_3$, 300 MHz): δ = 1.00 (t, 3 H, J = 7.3 Hz, 9-H), 1.52-1.61 (m, 2 H, 8-H), 1.64-1.73 (m, 2 H, 7-H), 2.90 (td, 1 H, J = 5.5, 2.0 Hz, 1-H), 3.65 (d, 1 H, J = 1.9 Hz, 2-H), 7.37 (d, 2 H, J = 8.4 Hz, 4-H), 7.62 (d, 2 H, J = 8.4 Hz, 5-H). ^{13}C -NMR ($CDCl_3$, 75.5 MHz): δ = 13.9 (q, C-9), 19.2 (t, C-8), 34.2 (t, C-7), 57.6 (d, C-2), 63.7 (d, C-1), 111.7 (s, C-6), 118.7 (s, CN), 126.1 (d, C-4), 132.3 (d, C-5), 143.6 (s, C-3). MS (EI): m/e (%) = 187 [M] $^+$ (79), 186 (36), 158 (89), 145 (25), 144 (24), 132 (81), 130 (100), 117 (30), 116 (67), 115 (79), 114 (25), 104 (47), 102 (20), 56 (47), 41 (37). HR-MS (EI) [M] $^+$: calcd for $[C_{12}H_{13}NO]^+$: 187.0992, found 187.0984.

5.2.2 Reactions of the Sulfur Ylides **4a,b** with the Imines **2a,b,d,e**

^a Yield isolated refers to *trans*-isomer; *cis/trans*-ratio corresponds to the crude product.

General procedure B. The ylides **4a,b** were generated by the addition of KOtBu (dissolved in 2-3 mL DMSO) to a vigorously stirred solution of the sulfonium tetrafluoroborates (**4a,b-H**)-BF₄ in dry DMSO (2-3 mL) at room temperature. The electrophiles **2a,b,d,e** (dissolved in 2-3 mL DMSO) were then added in one portion. The resulting mixtures were stirred for 5-15 min at room temperature and subsequently quenched by addition of water followed by extraction with CH₂Cl₂. The combined organic layers were washed with water and brine, dried over Na₂SO₄, and evaporated under reduced pressure. The crude products were purified by column chromatography on silica gel (*n*-pentane/EtOAc or *i*-hexane/EtOAc) and subsequently characterized by ¹H- and ¹³C-NMR spectroscopy and MS. Signal assignments were based on additional COSY, HSQC and HMBC experiments. If not mentioned otherwise, the diastereomeric ratios of the purified products did not differ significantly from those of the crude mixtures before column chromatography. Additional purifications by recrystallization from appropriate solvent mixtures were sometimes performed and are indicated in the corresponding section.

2-(4-Nitrophenyl)-3-phenyl-1-tosylaziridine (6ab) was obtained from dimethyl(4-nitrobenzyl)sulfonium tetrafluoroborate (**4b-H**)-BF₄ (200 mg, 702 μmol), KOtBu (78.8 mg, 702 μmol), and imine **2a** (90.0 mg, 347 μmol) as a pale yellow solid (121 mg, 307 μmol, 88 %, *dr* ~ 1 : 1.6 *cis* / *trans*).



$^1\text{H-NMR}$ (CDCl_3 , 599 MHz): $\delta = 2.40^*$ (s, 3 H, Ar-Me), $2.46^\#$ (s, 3 H, Ar-Me), 4.21^* (d, 1 H, $J = 4.5$ Hz, 1-H), $4.27^\#$ (d, 1 H, $J = 7.3$ Hz, 2-H), $4.30^\#$ (d, 1 H, $J = 7.3$ Hz, 1-H), 4.35^* (d, 1 H, $J = 4.5$ Hz, 2-H), $7.00\text{-}7.02^\#$ (m, 2 H, 8-H), $7.12\text{-}7.13^\#$ (m, 3 H, 9-H, 10-H), $7.23\text{-}7.24$ (m, 4 H, 4-H $^\#$, 13-H *), $7.36\text{-}7.42$ (m, 7 H, 8-H * , 9-H * , 10-H * , 13-H $^\#$), 7.61^* (d, 2 H, $J = 8.8$ Hz, 4-H), 7.65^* (d, 2 H, $J = 8.4$ Hz, 12-H), $7.95\text{-}7.98^\#$ (m, 4 H, 5-H, 12-H), 8.21^* (d, 2 H, $J = 8.8$ Hz, 5-H). $^{13}\text{C-NMR}$ (CDCl_3 , 151 MHz): $\delta = 21.6^*$ (q, Ar-Me), $21.7^\#$ (q, Ar-Me), $46.2^\#$ (d, C-2), $47.9^\#$ (d, C-1), 48.4^* (d, C-2), 51.6^* (d, C-1), $123.2^\#$ (d, C-5), 123.7^* (d, C-5), 127.5 (2d, C-12 * , C-8 $^\#$), $128.1^\#$ (d, C-12), $128.2^\#$ (d, C-10), $128.3^\#$ (d, C-9), 128.4^* , 128.59^* (2d, C-8, C-9), $128.64^\#$ (d, C-4), 129.0^* (d, C-4), 129.1^* (d, C-10), 129.6^* (d, C-13), $130.0^\#$ (d, C-13), $131.1^\#$ (s, C-7), 131.9^* (s, C-7), $134.4^\#$ (s, C-11), 136.6^* (s, C-11), $139.6^\#$ (s, C-3), 140.9^* (s, C-3), 144.5^* (s, C-14), $145.3^\#$ (s, C-14), $147.5^\#$ (s, C-6), 148.0^* (s, C-6). HR-MS (ESI^+) $[\text{M}+\text{H}]^+$: calcd for $[\text{C}_{21}\text{H}_{19}\text{N}_2\text{O}_4\text{S}]^+$: 395.1060; found 395.1060.

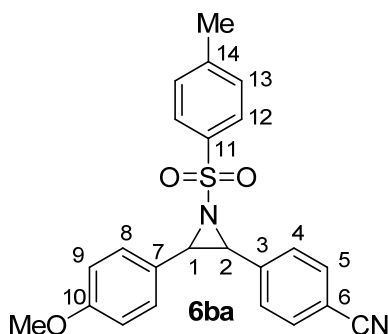
* signal can be assigned to *trans*-diastereomer

$^\#$ signal can be assigned to *cis*-diastereomer

NMR-signals of the *trans*-isomer are in agreement with those reported in the literature.^[29]

4-(3-(4-Methoxyphenyl)-1-tosylaziridin-2-yl)benzotrile (6ba) was obtained from (4-cyanobenzyl)dimethylsulfonium tetrafluoroborate (**4a-H**)- BF_4 (265 mg, 1.00 mmol), $\text{KO}t\text{Bu}$ (113 mg, 1.01 mmol), and imine **2b** (100 mg, 346 μmol) as a colorless solid (82 mg, 0.20 mmol, 58 %, *dr* $\sim 1 : 1.0$ *cis* / *trans*).

RAP 68.2



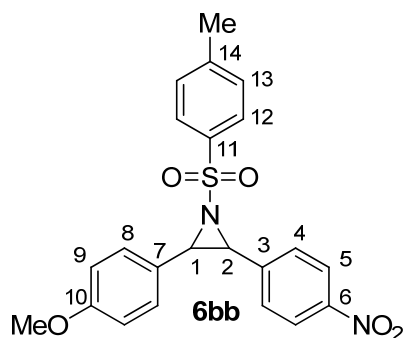
$^1\text{H-NMR}$ (CDCl_3 , 400 MHz): $\delta = 2.39^*$ (s, 3 H, Ar-Me), $2.44^\#$ (s, 3 H, Ar-Me), $3.68^\#$ (s, 3 H, OMe), 3.81^* (s, 3 H, OMe), 4.07^* (d, 1 H, $J = 4.4$ Hz, 1-H), $4.18^\#$ (d, 1 H, $J = 7.2$ Hz, 2-H), $4.21^\#$ (d, 1 H, $J = 7.3$ Hz, 1-H), 4.36^* (d, 1 H, $J = 4.5$ Hz, 2-H), $6.64^\#$ (d, 2 H, $J = 8.3$ Hz, 9-H), $6.86\text{-}6.90$ (m, 4 H, 9-H * , 8-H $^\#$), $7.17^\#$ (d, 2 H, $J = 8.4$ Hz, 4-H), 7.22^* (d, 2 H, $J = 8.2$ Hz, 13-H), $7.32\text{-}7.37$ (m, 4 H, 8-H * , 13-H $^\#$), $7.41^\#$ (d, 2 H, $J = 8.1$ Hz, 5-H), 7.50^* (d, 2 H, $J = 8.3$ Hz, 4-H), $7.61\text{-}7.64$ (m, 4 H, 5-H * , 12-H *), $7.93^\#$ (d, 2 H, $J = 8.2$ Hz, 12-H). $^{13}\text{C-NMR}$ (CDCl_3 , 101 MHz): $\delta = 21.6^*$ (q, Ar-Me), $21.7^\#$ (q, Ar-Me), $46.5^\#$ (d, C-2), $47.6^\#$ (d, C-1), 47.8^* (d, C-2), 52.2^* (d, C-1), $55.1^\#$ (q, OMe), 55.3^* (q, OMe), $111.6^\#$ (s, C-6), 112.3^* (s, C-6), $113.7^\#$ (d, C-9), 113.9^* (d, C-9), 118.4 , 118.5 (2s, CN * , CN $^\#$), $123.1^\#$ (s, C-7), 123.3^* (s, C-7), 127.4^* (d, C-12), $128.0^\#$ (d, C-12), 128.4^* (d, C-4), $128.5^\#$ (d, C-4), $128.7^\#$ (d, C-8), 129.5^* (d, C-13), 130.0 , 130.1 (2d, C-8 * , C-13 $^\#$), $131.8^\#$ (d, C-5), 132.3^* (d, C-5), $134.5^\#$ (s, C-11), 136.8^* (s, C-11), $137.8^\#$ (s, C-3), 139.5^* (s, C-3), 144.3^* (s, C-14), $145.1^\#$ (s, C-14), $159.4^\#$ (s, C-10), 160.2^* (s, C-10). HR-MS (ESI $^+$) $[\text{M}+\text{H}]^+$: calcd for $[\text{C}_{23}\text{H}_{21}\text{N}_2\text{O}_3\text{S}]^+$: 405.1267 ; found 405.1266.

* signal can be assigned to *trans*-diastereomer

$^\#$ signal can be assigned to *cis*-diastereomer

2-(4-Methoxyphenyl)-3-(4-nitrophenyl)-1-tosylaziridine (6bb) was obtained from dimethyl(4-nitrobenzyl)sulfonium tetrafluoroborate (**4b-H**)- BF_4 (200 mg, 702 μmol), $\text{KO}t\text{Bu}$ (78.8 mg, 702 μmol), and imine **2b** (100 mg, 346 μmol) as a yellow solid (105 mg, 247 μmol , 71 %, *dr* $\sim 1 : 1.6$ *cis* / *trans*).

RAP 62.1



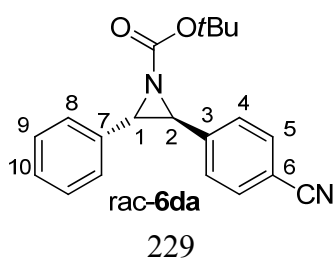
$^1\text{H-NMR}$ (CDCl_3 , 599 MHz): $\delta = 2.39^*$ (s, 3 H, Ar-Me), $2.45^\#$ (s, 3 H, Ar-Me), $3.67^\#$ (s, 3 H, OMe), 3.81^* (s, 3 H, OMe), 4.09^* (d, 1 H, $J = 4.6$ Hz, 1-H), $4.22^\#$ (d, 1 H, $J = 7.3$ Hz, 2-H), $4.24^\#$ (d, 1 H, $J = 7.3$ Hz, 1-H), 4.42^* (d, 1 H, $J = 4.6$ Hz, 2-H), $6.64^\#$ (d, 2 H, $J = 8.7$ Hz, 9-H), 6.88^* (d, 2 H, $J = 8.7$ Hz, 9-H), $6.91^\#$ (d, 2 H, $J = 8.8$ Hz, 8-H), $7.22\text{--}7.24$ (m, 4 H, 4-H $^\#$, 13-H *), $7.35\text{--}7.38$ (m, 4 H, 8-H * , 13-H $^\#$), 7.56^* (d, 2 H, $J = 8.8$ Hz, 4-H), 7.64^* (d, 2 H, $J = 8.3$ Hz, 12-H), $7.95^\#$ (d, 2 H, $J = 8.3$ Hz, 12-H), $7.97^\#$ (d, 2 H, $J = 8.8$ Hz, 5-H), 8.18^* (d, 2 H, $J = 8.8$ Hz, 5-H). $^{13}\text{C-NMR}$ (CDCl_3 , 151 MHz): $\delta = 21.6^*$ (q, Ar-Me), $21.7^\#$ (q, Ar-Me), $46.3^\#$ (d, C-2), 47.5^* (d, C-2), $47.6^\#$ (d, C-1), 52.4^* (d, C-1), $55.1^\#$ (q, OMe), 55.3^* (q, OMe), $113.7^\#$ (d, C-9), 113.9^* (d, C-9), $123.0^\#$ (s, C-7), 123.16^* (s, C-7), $123.23^\#$ (d, C-5), 123.7^* (d, C-5), 127.5^* (d, C-12), $128.0^\#$ (d, C-12), 128.6^* (d, C-4), $128.69^\#$, $128.70^\#$ (2d, C-4, C-8), 129.6^* (d, C-13), $130.0^\#$ (d, C-13), 130.1^* (d, C-8), $134.4^\#$ (s, C-11), 136.7^* (s, C-11), $139.8^\#$ (s, C-3), 141.5^* (s, C-3), 144.4^* (s, C-14), $145.2^\#$ (s, C-14), $147.4^\#$ (s, C-6), 147.9^* (s, C-6), $159.4^\#$ (s, C-10), 160.2^* (s, C-10). HR-MS (ESI $^+$) $[\text{M}+\text{H}]^+$: calcd for $[\text{C}_{22}\text{H}_{21}\text{N}_2\text{O}_5\text{S}]^+$: 425.1166; found 425.1165.

* signal can be assigned to *trans*-diastereomer

$^\#$ signal can be assigned to *cis*-diastereomer

***tert*-Butyl 2-(4-cyanophenyl)-3-phenylaziridine-1-carboxylate (6da)** was obtained from (4-cyanobenzyl)dimethylsulfonium tetrafluoroborate (**4a-H**)- BF_4 (300 mg, 1.13 mmol), KOtBu (127 mg, 1.13 mmol), and imine **2d** (90.0 mg, 438 μmol) as a colorless oil (72 mg, 0.22 mmol, 50 %, only *trans* diastereomer).

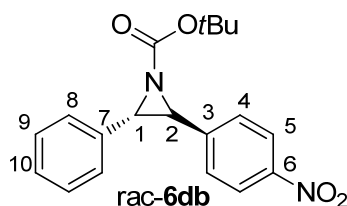
RAP 73.1



R_f (*n*-pentane/EtOAc 9:1, *v/v*): 0.38. $^1\text{H-NMR}$ (CDCl_3 , 599 MHz): δ = 1.20 (s, 9 H, *Ot*Bu), 3.62 (d, 1 H, J = 3.1 Hz, 1-H), 3.92 (d, 1 H, J = 3.1 Hz, 2-H), 7.31-7.33 (m, 2 H, 8-H), 7.34-7.39 (m, 3 H, 9-H, 10-H), 7.48 (d, 2 H, J = 8.4 Hz, 4-H), 7.65 (d, 2 H, J = 8.5 Hz, 5-H). $^{13}\text{C-NMR}$ (CDCl_3 , 151 MHz): δ = 27.6 (q, *Ot*Bu), 45.2 (d, C-2), 49.8 (d, C-1), 82.0 (s, *Ot*Bu), 111.7 (s, C-6), 118.6 (s, CN), 127.3 (d, C-8), 127.4 (d, C-4), 128.61 (d, C-10), 128.62 (d, C-9), 132.3 (s, C-5), 134.0 (s, C-7), 141.8 (s, C-3), 158.8 (s, CO). HR-MS (ESI^+) $[\text{M}+\text{H}]^+$: calcd for $[\text{C}_{20}\text{H}_{21}\text{N}_2\text{O}_2]^+$: 321.1598; found 321.1599.

***tert*-Butyl 2-(4-nitrophenyl)-3-phenylaziridine-1-carboxylate (6db)** was obtained from dimethyl(4-nitrobenzyl)sulfonium tetrafluoroborate (**4b-H**)- BF_4 (200 mg, 702 μmol), KOtBu (78.8 mg, 702 μmol), and imine **2d** (80.0 mg, 390 μmol) as a pale yellow oil (54 mg, 0.16 mmol, 41 %, only *trans* diastereomer).

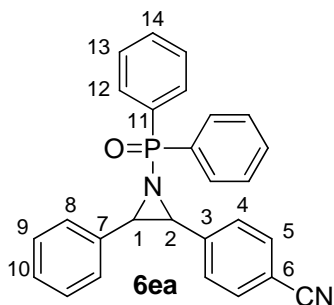
RAP 72.1



R_f (*n*-pentane/EtOAc 9:1, *v/v*): 0.43. $^1\text{H-NMR}$ (CDCl_3 , 599 MHz): δ = 1.21 (s, 9 H, *Ot*Bu), 3.63 (d, 1 H, J = 3.1 Hz, 1-H), 3.99 (d, 1 H, J = 3.1 Hz, 2-H), 7.32-7.33 (m, 2 H, 8-H), 7.35-7.40 (m, 3 H, 9-H, 10-H), 7.54 (d, 2 H, J = 8.9 Hz, 4-H), 8.22 (d, 2 H, J = 8.9 Hz, 5-H). $^{13}\text{C-NMR}$ (CDCl_3 , 151 MHz): δ = 27.6 (q, *Ot*Bu), 44.8 (d, C-2), 50.3 (d, C-1), 82.1 (s, *Ot*Bu), 123.8 (d, C-5), 127.3 (d, C-8), 127.4 (d, C-4), 128.65 (d, C-9), 128.70 (d, C-10), 133.8 (s, C-7), 144.0 (s, C-3), 147.6 (s, C-6), 158.7 (s, CO). HR-MS (ESI^+) $[\text{M}+\text{H}]^+$: calcd for $[\text{C}_{19}\text{H}_{21}\text{N}_2\text{O}_4]^+$: 341.1496; found 341.1495.

4-(1-(Diphenylphosphoryl)-3-phenylaziridin-2-yl)benzotrile (6ea) was obtained from (4-cyanobenzyl)dimethylsulfonium tetrafluoroborate (**4a-H**)- BF_4 (265 mg, 1.00 mmol), KOtBu (113 mg, 1.01 mmol), and imine **2e** (100 mg, 328 μmol). Based on the $^{31}\text{P-NMR}$ signals, the crude product (before column chromatography) shows a *dr* \sim 1 : 3 (*cis* / *trans*). The two diastereomers were separated by column chromatography. After recrystallization from *n*-pentane/EtOAc, the major (*trans*) diastereomer was isolated as a colorless solid (81 mg, 0.19 mmol, 58 %, only *trans* diastereomer). As the minor (*cis*) diastereomer could not be isolated in pure form, only characteristic NMR-signals are given for this compound.

RAP 70.1



Major (*trans*) diastereomer:

R_f (*n*-pentane/EtOAc 2:3, *v/v*): 0.35. Mp. (*n*-pentane/EtOAc): 180-182°C. $^1\text{H-NMR}$ (CDCl_3 , 300 MHz): δ = 4.06-4.14 (m, 2 H, 1-H, 2-H), 7.25-7.44 (m, 11 H, 8-H, 9-H, 10-H, 13-H, 14-H), 7.48 (d, 2 H, J = 8.4 Hz, 4-H), 7.54 (d, 2 H, J = 8.4 Hz, 5-H), 7.60-7.66 (m, 2 H, 12-H), 7.82-7.89 (m, 2 H, 12-H). $^{13}\text{C-NMR}$ (CDCl_3 , 75.5 MHz): δ = 46.5 (d, d, J_{PC} = 6.8 Hz, C-2), 47.5 (d, d, J_{PC} = 6.7 Hz, C-1), 111.7 (s, C-6), 118.6 (s, CN), 127.6 (d, C-8), 128.2 (d, d, J_{PC} = 12.6 Hz, C-13), 128.31 (d, C-10, superimposed by one of the signals of C-13), 128.37 (d, C-9), 128.40 (d, d, J_{PC} = 12.6 Hz, C-13), 128.6 (d, C-4), 131.3 (d, d, J_{PC} = 9.5 Hz, C-12), 131.50 (d, d, J_{PC} = 9.4 Hz, C-12), 131.7 (d, d, J_{PC} = 2.7 Hz, C-14), 131.8 (d, d, J_{PC} = 2.8 Hz, C-14), 132.0 (d, C-5), 132.3 (s, d, J_{PC} = 125 Hz, C-11), 133.8 (s, d, J_{PC} = 134 Hz, C-11), 134.8 (s, d, J_{PC} = 5.1 Hz, C-7, two signals of C-7 and C-11 superimposed), 141.1 (s, d, J_{PC} = 5.4 Hz, C-3). $^{31}\text{P-NMR}$ (CDCl_3 , 81.0 MHz): δ = 28.9. HR-MS (ESI $^+$) $[\text{M}+\text{H}]^+$: calcd for $[\text{C}_{27}\text{H}_{22}\text{N}_2\text{OP}]^+$: 421.1464; found 421.1462.

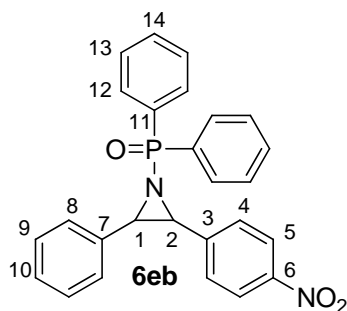
Minor (*cis*) diastereomer (only characteristic signals):

R_f (*n*-pentane/EtOAc 2:3, *v/v*): 0.20. $^1\text{H-NMR}$ (CDCl_3 , 599 MHz): δ = 4.22 (dd, 1 H, J = 16.0, 6.2 Hz), 4.30 (dd, 1 H, J = 16.2, 6.2 Hz). $^{13}\text{C-NMR}$ (CDCl_3 , 151 MHz): δ = 43.0 (d, d, J_{PC} = 5.6 Hz), 44.1 (d, d, J_{PC} = 5.7 Hz). $^{31}\text{P-NMR}$ (CDCl_3 , 81.0 MHz): δ = 34.7.

(2-(4-Nitrophenyl)-3-phenylaziridin-1-yl)diphenylphosphine oxide (6eb) was obtained from dimethyl(4-nitrobenzyl)sulfonium tetrafluoroborate (**4b-H**)- BF_4 (200 mg, 702 μmol), $\text{KO}t\text{Bu}$ (78.8 mg, 702 μmol), and imine **2e** (100 mg, 328 μmol). Based on the $^{31}\text{P-NMR}$ signals, the crude product (before column chromatography) shows a $dr \sim 1 : 6$ (*cis* / *trans*). The two diastereomers were separated by column chromatography. After recrystallization

from *n*-pentane/EtOAc, the major (*trans*) diastereomer was isolated as a pale yellow solid (102 mg, 232 μ mol, 71 %, only *trans* diastereomer). As the minor (*cis*) diastereomer could not be isolated in pure form, only characteristic NMR-signals are given for this compound.

RAP 71.1

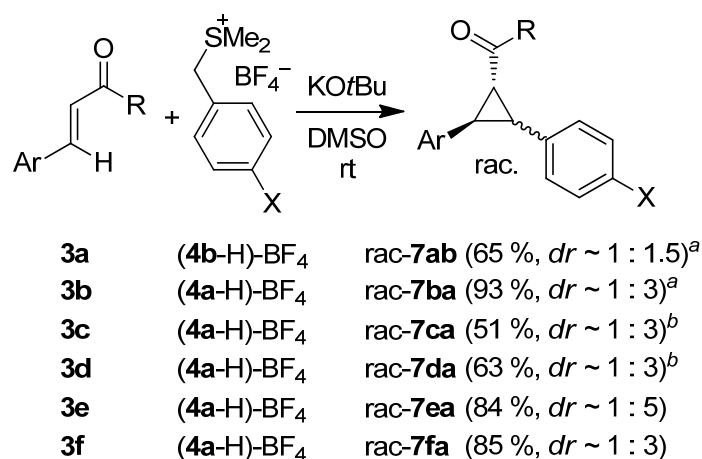


Major (*trans*) diastereomer:

R_f (*n*-pentane/EtOAc 1:1, v/v): 0.38. Mp. (*n*-pentane/EtOAc): 156-157°C. $^1\text{H-NMR}$ (CDCl_3 , 599 MHz): δ = 4.12 (dd, 1 H, J = 14.2, 3.1 Hz, 1-H), 4.17 (dd, 1 H, J = 13.8, 3.1 Hz, 2-H), 7.28-7.32 (m, 5 H, 9-H, 10-H, 13-H), 7.33-7.38 (m, 4 H, 8-H, 13-H), 7.40-7.43 (m, 2 H, 14-H), 7.54 (d, 2 H, J = 8.7 Hz, 4-H), 7.63-7.67 (m, 2 H, 12-H), 7.85-7.89 (m, 2 H, 12-H), 8.11 (d, 2 H, J = 8.8 Hz, 5-H). $^{13}\text{C-NMR}$ (CDCl_3 , 151 MHz): δ = 46.1 (d, d, J_{PC} = 6.7 Hz, C-2), 47.9 (d, d, J_{PC} = 6.7 Hz, C-1), 123.4 (d, C-5), 127.7 (d, C-8), 128.2 (d, d, J_{PC} = 12.6 Hz, C-13), 128.37 (d, C-10, superimposed by one of the signals of C-13), 128.39 (d, C-9), 128.42 (d, d, J_{PC} = 13.0 Hz, C-13), 128.7 (d, C-4), 131.3 (d, d, J_{PC} = 9.5 Hz, C-12), 131.5 (d, d, J_{PC} = 9.4 Hz, C-12), 131.7 (d, d, J_{PC} = 2.8 Hz, C-14), 131.8 (d, d, J_{PC} = 2.8 Hz, C-14), 132.3 (s, d, J_{PC} = 125 Hz, C-11), 133.7 (s, d, J_{PC} = 134 Hz, C-11), 134.6 (s, d, J_{PC} = 5.1 Hz, C-7), 143.2 (s, d, J_{PC} = 5.3 Hz, C-3), 147.5 (s, C-6). $^{31}\text{P-NMR}$ (CDCl_3 , 81.0 MHz): δ = 29.0. HR-MS (ESI $^+$) $[\text{M}+\text{H}]^+$: calcd for $[\text{C}_{26}\text{H}_{22}\text{N}_2\text{O}_3\text{P}]^+$: 441.1362; found 441.1359.

Minor (*cis*) diastereomer (only characteristic signals):

R_f (*n*-pentane/EtOAc 1:1, v/v): 0.22. $^1\text{H-NMR}$ (CDCl_3 , 599 MHz): δ = 4.26 (dd, 1 H, J = 16.0, 6.3 Hz), 4.32 (dd, 1 H, J = 16.2, 6.3 Hz). $^{13}\text{C-NMR}$ (CDCl_3 , 151 MHz): δ = 42.8 (d, d, J_{PC} = 5.7 Hz), 44.2 (d, d, J_{PC} = 5.9 Hz). $^{31}\text{P-NMR}$ (CDCl_3 , 81.0 MHz): δ = 34.7.

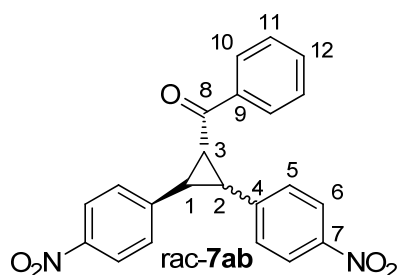
5.2.3 Reactions of the Sulfur Ylides **4a,b** with the Enones **3a–f**

^a Minor diastereomer is a meso compound. ^b Yield isolated refers to major diastereomer; *dr* corresponds to the crude product.

General procedure C. The ylides **4a,b** were generated by the addition of KO*t*Bu (dissolved in 2-3 mL DMSO) to a vigorously stirred solution of the sulfonium tetrafluoroborates (**4a,b-H**)-BF₄ in dry DMSO (2-3 mL) at room temperature. The electrophiles **3a–f** (dissolved in 2-3 mL DMSO) were then added in one portion. The resulting mixtures were stirred for 5-15 min at room temperature and subsequently quenched by the addition of water followed by the extraction with CH₂Cl₂. The combined organic layers were washed with water and brine, dried over Na₂SO₄, and evaporated under reduced pressure. The crude products were purified by column chromatography on silica gel (*n*-pentane/EtOAc or *i*-hexane/EtOAc) and subsequently characterized by ¹H- and ¹³C-NMR spectroscopy and MS. Signal assignments were based on additional COSY, HSQC and HMBC experiments. If not mentioned otherwise, the diastereomeric ratios of the purified products did not differ significantly from those of the crude mixtures before column chromatography. Additional purifications by recrystallization from appropriate solvent mixtures were sometimes performed and are indicated in the corresponding section.

(**2,3-Bis(4-nitrophenyl)cyclopropyl**)(phenyl)methanone (**7ab**) was obtained from dimethyl(4-nitrobenzyl)sulfonium tetrafluoroborate (**4b-H**)-BF₄ (197 mg, 691 μmol), KO*t*Bu (77.5 mg, 691 μmol), and enone **3a** (70.0 mg, 276 μmol) as a yellow solid (70 mg, 0.18 mmol, 65 %, *dr* ~ 1 : 1.5).

RAP 31.1



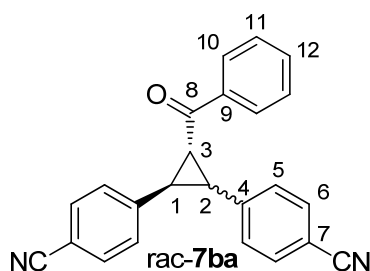
$^1\text{H-NMR}$ (CDCl_3 , 599 MHz): $\delta = 3.36^*$ (dd, 1 H, $J = 9.4$ Hz, $J = 7.2$ Hz, 2-H), $3.45^\#$ (d, 2 H, $J = 5.3$ Hz, 1-H, 2-H), 3.59^* (dd, 1 H, $J = 9.7$ Hz, $J = 5.3$ Hz, 3-H), 3.72 - 3.74 (m, 2 H, 1- H^* , 3- $\text{H}^\#$), $7.19^\#$ (d, 4 H, $J = 8.7$ Hz, 5-H), 7.44 - 7.50^* (m, 6 H, 5-H, 11-H), 7.55 - 7.60 (m, 3 H, 11- $\text{H}^\#$, 12- H^*), 7.66 - $7.68^\#$ (m, 1 H, 12-H), 7.95^* (d, 2 H, $J = 7.3$ Hz, 10-H), $8.05^\#$ (d, 4 H, $J = 8.8$ Hz, 6-H), 8.09 - 8.12 (m, 4 H, 10- $\text{H}^\#$, 6- H^*), 8.23^* (d, 2 H, $J = 8.7$ Hz, 6-H). $^{13}\text{C-NMR}$ (CDCl_3 , 151 MHz): $\delta = 29.9^*$ (d, C-1), $31.7^\#$ (d, C-3), $35.4^\#$ (d, C-1, C-2), 37.0^* (d, C-3), 37.1^* (d, C-2), 123.5^* (d, C-6), $123.6^\#$ (d, C-6), 124.1^* (d, C-6), 127.5^* (d, C-5), 128.1^* (d, C-10), $128.2^\#$ (d, C-10), 128.8^* (d, C-11), $129.0^\#$ (d, C-11), $129.5^\#$ (d, C-5), 129.8^* (d, C-5), 133.6^* (d, C-12), $133.9^\#$ (d, C-12), $136.9^\#$ (s, C-9), 137.4^* (s, C-9), 142.4^* (s, C-4), $142.9^\#$ (s, C-4), 146.7^* (s, C-4), $146.9^\#$ (s, C-7), 146.96^* (s, C-7), 147.01^* (s, C-7), 193.5^* (s, C-8), $196.5^\#$ (s, C-8). MS (EI): m/e (%) = 388 (5) $[\text{M}]^+$, 191 (21), 190 (19), 189 (37), 106 (31), 105 (52), 179 (28), 77 (100). HR-MS (EI) $[\text{M}]^+$: calcd for $[\text{C}_{22}\text{H}_{16}\text{N}_2\text{O}_5]^+$: 388.1054, found 388.1055.

* signal can be assigned to the major diastereomer (1,2-*trans*)

$^\#$ signal can be assigned to the minor diastereomer (1,2-*cis*, meso compound)

4,4'-(3-Benzoylcyclopropane-1,2-diyl)dibenzonitrile (7ba) was obtained from (4-cyanobenzyl)dimethylsulfonium tetrafluoroborate (**4a-H**)- BF_4 (300 mg, 1.13 mmol), $\text{KO}t\text{Bu}$ (127 mg, 1.13 mmol), and enone **3b** (70.0 mg, 300 μmol) as a colorless solid (97 mg, 0.28 mmol, 93 %, *dr* \sim 1 : 3).

RAP 33.2



$^1\text{H-NMR}$ (CDCl_3 , 400 MHz): $\delta = 3.28^*$ (dd, 1 H, $J = 9.5$ Hz, $J = 7.1$ Hz, 2-H), $3.38^\#$ (d, 2 H, $J = 5.3$ Hz, 1-H, 2-H), 3.51^* (dd, 1 H, $J = 9.7$ Hz, $J = 5.4$ Hz, 3-H), 3.62 - 3.65 (m, 2 H, 1- H^* , 3-

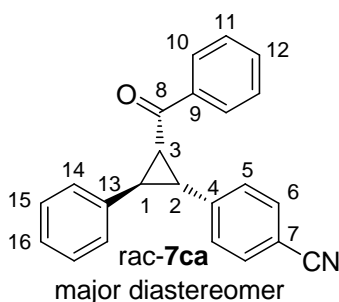
H[#]), 7.11[#] (d, 4 H, $J = 8.1$ Hz, 5-H), 7.37^{*} (d, 2 H, $J = 8.1$ Hz, 5-H), 7.41-7.49 (m, 8 H, 5-H^{*}, 6-H[#], 11-H^{*}), 7.51-7.59 (m, 5 H, 6-H^{*}, 11-H[#], 12-H^{*}), 7.64-7.69 (m, 3 H, 6-H^{*}, 12-H[#]), 7.93^{*} (d, 2 H, $J = 7.5$ Hz, 10-H), 8.09[#] (d, 2 H, $J = 7.4$ Hz, 10-H). ¹³C-NMR (CDCl₃, 101 MHz): $\delta = 29.9^*$ (d, C-1), 31.52[#] (d, C-3), 35.54[#] (d, C-1, C-2) 36.7^{*} (d, C-3), 37.2^{*} (d, C-2), 110.9^{*} (s, C-7), 111.0[#] (s, C-7), 111.1^{*} (s, C-7), 118.4[#] (s, CN), 118.59^{*} (s, CN), 118.62^{*} (s, CN), 127.5^{*} (d, C-5), 128.1^{*} (d, C-10), 128.2[#] (d, C-10), 128.8^{*} (d, C-11), 129.0[#] (d, C-11), 129.5[#] (d, C-5), 129.7^{*} (d, C-5), 132.0^{*} (d, C-6), 132.1[#] (d, C-6), 132.6^{*} (d, C-6), 133.5^{*} (d, C-12), 133.8[#] (d, C-12), 137.0[#] (s, C-9), 137.5^{*} (s, C-9), 140.4^{*} (s, C-4), 140.9[#] (s, C-4), 144.7^{*} (s, C-4), 193.6^{*} (s, C-8), 196.7[#] (s, C-8). MS (EI): m/e (%) = 348 (1) [M]⁺, 217 (5) 106 (6), 105 (100), 77 (18). HR-MS (EI) [M]⁺: calcd for [C₂₄H₁₆N₂O]⁺: 348.1257, found 348.1249.

* signal can be assigned to the major diastereomer (1,2-*trans*)

signal can be assigned to the minor diastereomer (1,2-*cis*, meso compound)

4-(2-Benzoyl-3-phenylcyclopropyl)benzonitrile (7ca) was obtained from (4-cyanobenzyl)dimethylsulfonium tetrafluoroborate (**4a-H**)-BF₄ (300 mg, 1.13 mmol), KO^tBu (127 mg, 1.13 mmol), and enone **3c** (90.0 mg, 432 μ mol) as a colorless oil (*dr* ~ 1 : 3) still containing impurities. After recrystallization from *n*-pentane/EtOAc, **7ca** was obtained as a colorless solid (72 mg, 0.22 mmol, 51 %, only major diastereomer).

RAP 99.1

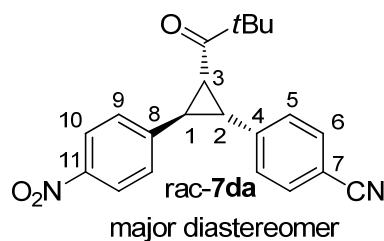


R_f (*i*-hexane/EtOAc 6:1, *v/v*): 0.29. Mp. (*n*-pentane/EtOAc): 134-135°C. ¹H-NMR (CDCl₃, 300 MHz): $\delta = 3.26$ (dd, 1 H, $J = 9.5, 7.1$ Hz, 2-H), 3.46 (dd, 1 H, $J = 9.5, 5.4$ Hz, 3-H), 3.60 (dd, 1 H, $J = 6.8, 5.6$ Hz, 1-H), 7.25-7.58 (m, 12 H, 5-H, 6-H, 11-H, 12-H, 14-H, 15-H, 16-H), 7.91-7.94 (m, 2 H, 10-H). ¹³C-NMR (CDCl₃, 75.5 MHz): $\delta = 30.5$ (d, C-1), 36.4 (d, C-3), 37.1 (d, C-2), 110.7 (s, C-7), 118.8 (s, CN), 126.8 (d, C-14), 127.1 (d, C-16), 128.0 (d, C-10), 128.7, 128.8 (2d, C-11, C-15), 129.9 (d, C-5), 131.9 (d, C-6), 133.2 (d, C-12), 137.9 (s, C-9),

139.0 (s, C-13), 141.1 (s, C-4), 194.5 (s, C-8). MS (EI): m/e (%) = 323 (1) $[M]^+$, 217 (7) 106 (8), 105 (100), 77 (22). HR-MS (EI) $[M]^+$: calcd for $[C_{23}H_{17}NO]^+$: 323.1304, found 323.1305.

4-(2-(4-Nitrophenyl)-3-pivaloylcyclopropyl)benzonitrile (7da) was obtained from (4-cyanobenzyl)dimethylsulfonium tetrafluoroborate (**4a-H**)- BF_4 (300 mg, 1.13 mmol), $KOtBu$ (127 mg, 1.13 mmol), and enone **3d** (100 mg, 429 μ mol) as a yellow solid ($dr \sim 1 : 8$, before column chromatography: 1 : 3), still containing impurities. After recrystallization from *n*-pentane/EtOAc, **7da** was obtained as a pale yellow solid (95 mg, 0.27 mmol, 63 %, only major diastereomer).

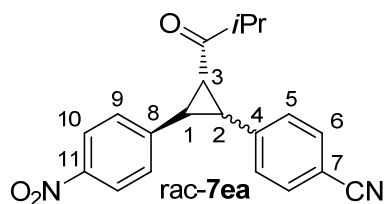
RAP 97.1



R_f (*n*-pentane/EtOAc 5:1, v/v): 0.23. Mp. (*n*-pentane/EtOAc): 209-210°C. 1H -NMR (CD_3CN , 400 MHz): δ = 1.04 (s, 9 H, *t*Bu), 3.23-3.25 (m, 2 H, 2-H, 3-H), 3.42 (dd, 1 H, J = 6.2, 6.2 Hz, 1-H), 7.46 (d, 2 H, J = 8.2 Hz, 5-H), 7.53 (d, 2 H, J = 8.6 Hz, 9-H), 7.64 (d, 2 H, J = 8.6 Hz, 6-H), 8.18 (d, 2 H, J = 8.9 Hz, 10-H). ^{13}C -NMR (CD_3CN , 101 MHz): δ = 25.9 (q, *t*Bu), 30.6 (d, C-1), 36.7 (d, C-3), 38.2 (d, C-2), 44.6 (s, *t*Bu), 111.1 (s, C-7), 119.6 (s, CN), 124.5 (d, C-10), 128.6 (d, C-9), 131.0 (d, C-5), 132.6 (d, C-6), 142.5 (s, C-4), 147.7 (s, C-8), 148.8 (s, C-11), 209.0 (s, CO). MS (EI): m/e (%) = 348 (<1) $[M]^+$, 290 (7), 264 (8), 245 (6), 217 (13), 216 (9), 190 (5), 85 (14), 57 (100). HR-MS (EI) $[M]^+$: calcd for $[C_{21}H_{20}N_2O_3]^+$: 348.1468 found 348.1465.

4-(2-Isobutyryl-3-(4-nitrophenyl)cyclopropyl)benzonitrile (7ea) was obtained from (4-cyanobenzyl)dimethylsulfonium tetrafluoroborate (**4a-H**)- BF_4 (300 mg, 1.13 mmol), $KOtBu$ (127 mg, 1.13 mmol), and enone **3e** (90.0 mg, 411 μ mol) as a colorless solid (115 mg, 344 μ mol, 84 %, $dr \sim 1 : 5$, before column chromatography: 1 : 3).

RAP 96.1



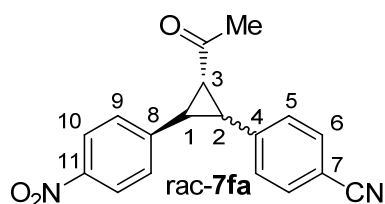
$^1\text{H-NMR}$ (CDCl_3 , 400 MHz): $\delta = 1.01^*$ (d, 3 H, $J = 7.0$ Hz, CH_3 from *iPr*), 1.05^* (d, 3 H, $J = 6.8$ Hz, CH_3 from *iPr*), $1.278^\#$ (d, 3 H, $J = 6.9$ Hz, CH_3 from *iPr*), $1.281^\#$ (d, 3 H, $J = 6.9$ Hz, CH_3 from *iPr*), 2.71^* (sept, 1 H, $J = 6.9$ Hz, CH from *iPr*), $2.93\text{--}3.04$ (m, 3 H, 3-H^* , CH from *iPr* $^\#$, $3\text{-H}^\#$), $3.11\text{--}3.18$ (m, 3 H, 2-H^* , $1\text{-H}^\#$, $2\text{-H}^\#$), 3.44^* (dd, 1 H, $J = 7.0, 5.3$ Hz, 1-H), $7.07^\#$ (d, 2 H, $J = 8.4$ Hz, 5-H), $7.09^\#$ (d, 2 H, $J = 8.8$ Hz, 9-H), 7.40^* (d, 4 H, $J = 8.7$ Hz, 5-H, 9-H, signals identical), $7.46^\#$ (d, 2 H, $J = 8.4$ Hz, 6-H), 7.59^* (d, 2 H, $J = 8.4$ Hz, 6-H), $8.02^\#$ (d, 2 H, $J = 8.8$ Hz, 10-H), 8.19^* (d, 2 H, $J = 8.8$ Hz, 10-H). $^{13}\text{C-NMR}$ (CDCl_3 , 101 MHz): $\delta = 17.4^*$ (q, CH_3 from *iPr*), 17.6^* (q, CH_3 from *iPr*), $17.98^\#$ (q, CH_3 from *iPr*), $18.01^\#$ (q, CH_3 from *iPr*), 29.8^* (d, C-1), $32.9^\#$ (d, C-3), $34.8^\#$, $35.2^\#$ (2d, C-1, C-2), 37.2^* (d, C-2), 38.4^* (d, C-3), 42.1^* (d, CH from *iPr*), $42.2^\#$ (d, CH from *iPr*), $110.9^\#$ (s, C-7), 111.0^* (s, C-7), $118.4^\#$ (s, CN), 118.7^* (s, CN), $123.5^\#$ (d, C-10), 124.0^* (d, C-10), 127.3^* (d, C-9), $129.4^\#$, $129.5^\#$ (2d, C-5, C-9), 129.7^* (d, C-5), 131.9^* (d, C-6), $132.1^\#$ (d, C-6), 140.4^* (s, C-4), $140.7^\#$ (s, C-4), $143.0^\#$ (s, C-8), $146.8^\#$ (s, C-11), 146.86^* , 146.87^* (2s, C-8, C-11), 207.0^* (s, CO), $210.4^\#$ (s, CO). MS (EI): m/e (%) = 334 (1) $[\text{M}]^+$, 217 (34), 216 (25), 214 (10), 190 (15), 71 (100), 43 (72). HR-MS (EI) $[\text{M}]^+$: calcd for $[\text{C}_{20}\text{H}_{18}\text{N}_2\text{O}_3]^+$: 334.1312, found 334.1303. MS HR-MS (ESI) $[\text{M-H}]^-$: calcd for $[\text{C}_{20}\text{H}_{17}\text{N}_2\text{O}_3]^-$: 333.1245, found 333.1240.

* signal can be assigned to major diastereomer (1,2-*trans*)

$^\#$ signal can be assigned to minor diastereomer (1,2-*cis*)

4-(2-Acetyl-3-(4-nitrophenyl)cyclopropyl)benzonitrile (7fa) was obtained from (4-cyanobenzyl)dimethylsulfonium tetrafluoroborate (**4a-H**)- BF_4 (300 mg, 1.13 mmol), $\text{KO}t\text{Bu}$ (127 mg, 1.13 mmol), and enone **3f** (80.0 mg, 418 μmol) as a pale yellow solid (109 mg, 356 μmol , 85 %, *dr* $\sim 1 : 3$).

RAP 42.1



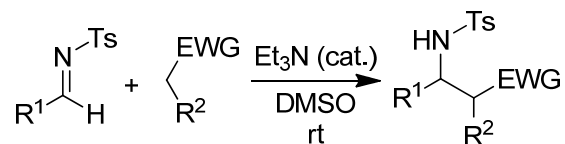
$^1\text{H-NMR}$ (CDCl_3 , 599 MHz): $\delta = 2.22^*$ (s, 3 H, Me), $2.51^\#$ (s, 3 H, Me), 2.92^* (dd, 1 H, $J = 9.7, 5.3$ Hz, 3-H), $2.99^\#$ (dd, 1 H, $J = 5.3, 5.3$ Hz, 3-H), 3.13^* (dd, 1 H, $J = 9.6, 7.1$ Hz, 2-H), $3.19\text{-}3.23^\#$ (m, 2 H, 1-H, 2-H), 3.43^* (dd, 1 H, $J = 6.9, 5.4$ Hz, 1-H), $7.05^\#$ (d, 2 H, $J = 8.3$ Hz, 5-H), $7.08^\#$ (d, 2 H, $J = 8.7$ Hz, 9-H), $7.37\text{-}7.41^*$ (m, 4 H, 5-H, 9-H), $7.46^\#$ (d, 2 H, $J = 8.4$ Hz, 6-H), 7.60^* (d, 2 H, $J = 8.4$ Hz, 6-H), $8.02^\#$ (d, 2 H, $J = 8.8$ Hz, 10-H), 8.20^* (d, 2 H, $J = 8.8$ Hz, 10-H). $^{13}\text{C-NMR}$ (CDCl_3 , 151 MHz): $\delta = 29.8^*$ (d, C-1), $31.3^\#$ (q, Me), 31.9^* (q, Me), $34.9^\#$, $35.0^\#$, $35.4^\#$ (3d, C-1, C-2, C-3), 37.0^* (d, C-2), 40.1^* (d, C-3), $111.0^\#$ (s, C-7), 111.2^* (s, C-7), $118.4^\#$ (s, CN), 118.6^* (s, CN), $123.5^\#$ (d, C-10), 124.0^* (d, C-10), 127.2^* (d, C-9), $129.4^\#$, $129.5^\#$ (2d, C-5, C-9), 129.7^* (d, C-5), 132.0^* (d, C-6), $132.1^\#$ (d, C-6), 140.1^* (s, C-4), $140.4^\#$ (s, C-4), $142.7^\#$ (s, C-8), 146.6^* (s, C-8), $146.8^\#$ (s, C-11), 146.9^* (s, C-11), 201.5^* (s, CO), $204.7^\#$ (s, CO). MS HR-MS (ESI $^-$) $[\text{M-H}]^-$: calcd for $[\text{C}_{18}\text{H}_{13}\text{N}_2\text{O}_3]^-$: 305.0932, found 305.0941.

* signal can be assigned to major diastereomer (1,2-*trans*)

$^\#$ signal can be assigned to minor diastereomer (1,2-*cis*)

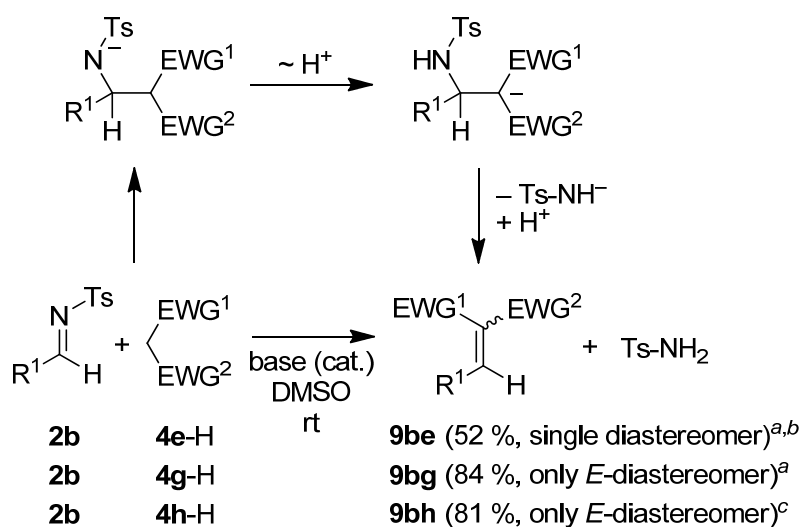
5.2.4 Reactions of the Carbanions 4c–h with the Imines 2a–c

Reactions of the carbanions 4c,d,f with the imines 2a–c



2a	4d-H	8ad (65 %)
2b	4c-H	8bc (52 %) ^a
2b	4d-H	8bd (58 %)
2b	4f-H	8bf (83 %) ^b
2c	4d-H	8cd (18 %)

^a *dr* ~ 1 : 3 for the crude product; only major diastereomer isolated and characterized. ^b Reaction conditions: KO t Bu, THF, -80 to -40°C .

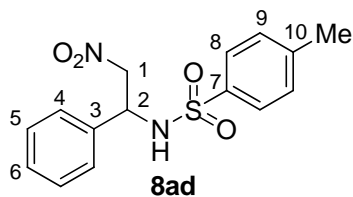
Reactions of the carbanions **4e,g,h** with the imine **2b**

^a KO^tBu (14–18 mol-%), rt. ^b Configuration (*E* or *Z*) was not determined. ^c Et₃N (18 mol-%), rt.

General procedure D. The CH acids (**4c–h**)-H were dissolved with the corresponding imine **2a–c** in dry DMSO (2–3 mL). After the addition of a catalytic amount of base (Et₃N or KO^tBu) the reaction mixtures were stirred for an appropriate time at rt. The reactions were subsequently quenched by addition of water and brine, followed by extraction with CH₂Cl₂. The combined organic layers were washed with water and brine, dried over Na₂SO₄, and evaporated under reduced pressure. The crude products were purified by column chromatography on silica gel (*n*-pentane/EtOAc) and subsequently characterized by ¹H- and ¹³C-NMR (if possible also ³¹P-NMR) spectroscopy and MS. Signal assignments were based on additional COSY, HSQC and HMBC experiments. If not mentioned otherwise, the diastereomeric ratios of the purified products did not differ significantly from those of the crude mixtures before column chromatography. Additional purifications by recrystallization from appropriate solvent mixtures were sometimes performed and are indicated in the corresponding section.

4-Methyl-*N*-(2-nitro-1-phenylethyl)benzenesulfonamide (8ad) was obtained from nitromethane (**4d**-H, 100 mg, 1.64 mmol), the imine **2a** (100 mg, 386 μmol), and Et₃N (7.4 mg, 73 μmol, 19 mol-%) after 1.5 h of reaction time as a colorless solid (91 mg, 0.28 mmol, 73 %). Recrystallization from *n*-pentane/EtOAc yielded **8ad** as colorless needles (79 mg, 0.25 mmol, 65 %).

RAP 63.1

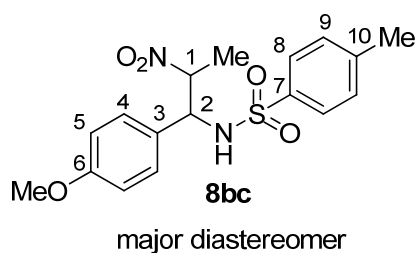


R_f (*n*-pentane/EtOAc 3:1, *v/v*): 0.34. Mp. (*n*-pentane/EtOAc): 154-156°C (Lit.: 155-157°C).^[30] $^1\text{H-NMR}$ (CDCl_3 , 300 MHz): $\delta = 2.39$ (s, 3 H, Ar-Me), 4.65 (dd, 1 H, $J = 13.0$, 6.4 Hz, 1-H), 4.81 (dd, 1 H, $J = 13.1$, 6.8 Hz, 1-H), 4.97-5.04 (m, 1 H, 2-H), 5.60 (d, 1 H, $J = 7.8$ Hz, NH), 7.07-7.10 (m, 2 H, 4-H), 7.20-7.26 (m, 5 H, 5-H, 6-H, 9-H), 7.64 (d, 2 H, $J = 8.4$ Hz, 8-H). $^{13}\text{C-NMR}$ (CDCl_3 , 75.5 MHz): $\delta = 21.5$ (q, Ar-Me), 55.5 (d, C-2), 79.0 (t, C-1), 126.5 (d, C-4), 127.1 (d, C-8), 129.0 (d, C-6), 129.2 (d, C-5), 129.7 (d, C-9), 135.3 (s, C-3), 136.5 (s, C-7), 144.0 (s, C-10).

$^1\text{H-NMR}$ signals are in agreement with those reported in the literature.^[30]

***N*-(1-(4-Methoxyphenyl)-2-nitropropyl)-4-methylbenzenesulfonamide (8bc)** was obtained from nitroethane (**4c-H**, 60.0 mg, 799 μmol), the imine **2b** (100 mg, 346 μmol), and Et_3N (6.0 mg, 59 μmol , 17 mol-%) after 2 h of reaction time as a colorless solid (*dr* ~ 1 : 3.4) still containing impurities. Twice recrystallization from *n*-pentane/EtOAc yielded **8bc** as colorless solid (65 mg, 0.18 mmol, 52 %, only one diastereomer).

RAP 92.2

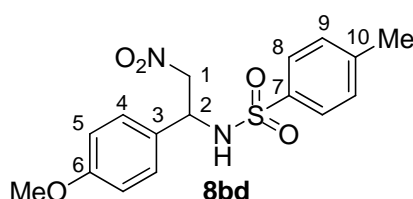


R_f (*n*-pentane/EtOAc 2:1, *v/v*): 0.43. Mp. (*n*-pentane/EtOAc): 188-190°C. $^1\text{H-NMR}$ (CDCl_3 , 300 MHz): $\delta = 1.41$ (d, 3 H, $J = 6.6$ Hz, Me), 2.34 (s, 3 H, Ar-Me), 3.73 (s, 3 H, OMe), 4.69-4.86 (m, 2 H, 1-H, 2-H), 5.95 (d, 1 H, $J = 9.2$ Hz, NH), 6.68 (d, 2 H, $J = 8.7$ Hz, 5-H), 6.92 (d, 2 H, $J = 8.7$ Hz, 4-H), 7.10 (d, 2 H, $J = 8.3$ Hz, 9-H), 7.52 (d, 2 H, $J = 8.3$ Hz, 8-H). $^{13}\text{C-NMR}$ (CDCl_3 , 75.5 MHz): $\delta = 16.8$ (q, Me), 21.4 (q, Ar-Me), 55.3 (q, OMe), 60.1 (d, C-2), 86.9 (d, C-1), 114.3 (d, C-5), 127.1 (d, C-8), 127.3 (s, C-3), 128.0 (d, C-4), 129.4 (d, C-9), 137.0 (s, C-7), 143.4 (s, C-10), 159.7 (s, C-6). MS (EI): m/e (%) = 364 (1) $[\text{M}]^+$, 291 (10), 290 (50), 289

(46), 155 (33), 134 (78), 133 (16), 92 (17), 91 (100), 77 (12), 65 (16). HR-MS (EI) $[M]^+$: calcd for $[C_{17}H_{20}N_2O_5S]^+$: 364.1087, found 364.1087.

N-(1-(4-Methoxyphenyl)-2-nitroethyl)-4-methylbenzenesulfonamide (8bd) was obtained from nitromethane (**4d-H**, 100 mg, 1.64 mmol), the imine **2b** (100 mg, 346 μ mol), and Et_3N (5.3 mg, 52 μ mol, 15 mol-%) after 1.5 h of reaction time as a colorless solid still containing impurities. Recrystallization from *n*-pentane/EtOAc yielded **8bd** as colorless solid (71 mg, 0.20 mmol, 58 %).

RAP 59.1



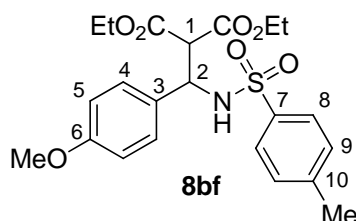
R_f (*n*-pentane/EtOAc 2:1, *v/v*): 0.37. Mp. (*n*-pentane/EtOAc): 174-175°C (Lit.: 142.4°C).^[30b]
 1H -NMR ($CDCl_3$, 599 MHz): δ = 2.41 (s, 3 H, Ar-Me), 3.75 (s, 3 H, OMe), 4.63 (dd, 1 H, J = 13.0, 6.7 Hz, 1-H), 4.82 (dd, 1 H, J = 13.0, 6.7 Hz, 1-H), 4.91-4.94 (m, 1 H, 2-H), 5.43 (d, 1 H, J = 7.2 Hz, NH), 6.75 (d, 2 H, J = 8.7 Hz, 5-H), 6.99 (d, 2 H, J = 8.7 Hz, 4-H), 7.24 (d, 2 H, J = 8.0 Hz, 9-H), 7.64 (d, 2 H, J = 8.3 Hz, 8-H). ^{13}C -NMR ($CDCl_3$, 151 MHz): δ = 21.6 (q, Ar-Me), 55.0 (d, C-2), 55.3 (q, OMe), 79.0 (t, C-1), 114.5 (d, C-5), 127.17 (d, C-8), 127.21 (s, C-3), 127.8 (d, C-4), 129.7 (d, C-9), 136.5 (s, C-7), 144.0 (s, C-10), 160.0 (s, C-6).

1H -NMR signals are in agreement with those reported in the literature.^[30b]

Diethyl 2-((4-methoxyphenyl)(4-methylphenylsulfonamido)methyl)malonate (8bf) could not be obtained by *General Procedure D* because of the high reversibility of the addition of carbanion **4f** to imine **2b**. Instead, the following procedure was used for the synthesis of **8bf**: Diethyl malonate (**4f-H**, 73.0 mg, 456 μ mol) and $KOtBu$ (51.0 mg, 455 μ mol) were dissolved in 5 mL of dry THF at rt. The resulting suspension was cooled down to $-80^\circ C$ and the imine **2b** (120 mg, 415 μ mol, dissolved in 5 mL of dry THF) was added dropwise. After 4 h of stirring at a temperature below $-40^\circ C$, the mixture was again cooled down to $-80^\circ C$ and treated first with concentrated acetic acid (0.1 mL) then with water. The crude mixture was extracted with CH_2Cl_2 and the combined organic layers were washed with water and brine, dried over Na_2SO_4 , and evaporated under reduced pressure. The crude product was purified

by recrystallization from *n*-pentane/Et₂O and yielded **8bf** as a colorless solid (155 mg, 345 μmol, 83 %), which was subsequently characterized by ¹H- and ¹³C-NMR spectroscopy, MS, and elemental analysis. Signal assignments were based on additional COSY, HSQC and HMBC experiments.

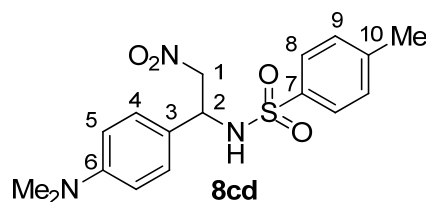
RAP 94.6



Mp. (*n*-pentane/Et₂O): 107.8-108.4°C. ¹H-NMR (CDCl₃, 300 MHz): δ = 1.13-1.20 (m, 6 H, OCH₂CH₃), 2.33 (s, 3 H, Ar-Me), 3.73-3.74 (m, 4 H, 1-H, OMe), 3.96-4.19 (m, 4 H, OCH₂CH₃), 5.09 (dd, 1 H, *J* = 9.2, 5.7 Hz, 2-H), 6.27 (d, 1 H, *J* = 9.3 Hz, NH), 6.65 (d, 2 H, *J* = 8.6 Hz, 5-H), 7.02 (d, 2 H, *J* = 8.7 Hz, 4-H), 7.08 (d, 2 H, *J* = 8.4 Hz, 9-H), 7.50 (d, 2 H, *J* = 8.2 Hz, 8-H). ¹³C-NMR (CDCl₃, 75.5 MHz): δ = 13.86 (q, OCH₂CH₃), 13.90 (q, OCH₂CH₃), 21.4 (q, Ar-Me), 55.2 (q, OMe), 56.6 (d, C-2), 57.9 (d, d, C-1), 61.9 (t, OCH₂CH₃), 62.1 (t, OCH₂CH₃), 113.7 (d, C-5), 127.0 (d, C-8), 128.0 (d, C-4), 129.1 (d, C-9), 129.7 (s, C-3), 138.0 (s, C-7), 142.8 (s, C-10), 159.1 (s, C-6), 166.4 (s, CO), 167.8 (s, CO). MS (EI): *m/e* (%) = 449 (<1) [M]⁺, 302 (11), 301 (55), 155 (28), 134 (77), 133 (18), 92 (16), 91 (100), 77 (10), 65 (13). HR-MS (EI) [M]⁺: calcd for [C₂₂H₂₇NO₇S]⁺: 449.1502, found 449.1514. HR-MS (ESI⁺) [M+Na]⁺: calcd for [C₂₂H₂₇NO₇SNa]⁺: 472.1401, found 472.1400. Anal calcd for C₂₂H₂₇NO₇S (449.52): C 58.78, H 6.05, N 3.12, S 7.31, found C 58.72, H 6.03, N 3.10, S 7.14.

***N*-(1-(4-(Dimethylamino)phenyl)-2-nitroethyl)-4-methylbenzenesulfonamide (8cd)** was obtained from nitromethane (**4d-H**, 100 mg, 1.64 mmol), the imine **2c** (100 mg, 331 μmol), and Et₃N (6.0 mg, 59 μmol, 18 mol-%) after 3.5 h of reaction time as a yellow solid still containing impurities. Recrystallization from *n*-pentane/CH₂Cl₂ yielded **8cd** as yellow solid (22 mg, 61 μmol, 18 %).

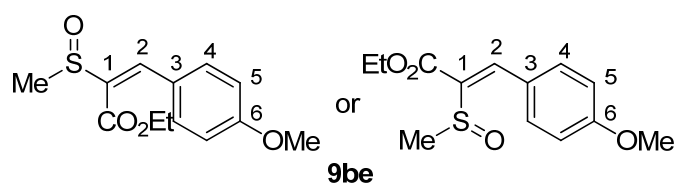
RAP 65.1



R_f (*n*-pentane/EtOAc 2:1, *v/v*): 0.33. Mp. (*n*-pentane/ CH_2Cl_2): 152-153°C. $^1\text{H-NMR}$ (CDCl_3 , 599 MHz): δ = 2.41 (s, 3 H, Ar-Me), 2.90 (s, 6 H, NMe_2), 4.64 (dd, 1 H, J = 15.0, 9.4 Hz, 1-H), 4.83-4.86 (m, 2 H, 1-H, 2-H), 5.29 (d, 1 H, J = 5.6 Hz, NH), 6.54 (d, 2 H, J = 8.3 Hz, 5-H), 6.90 (d, 2 H, J = 8.8 Hz, 4-H), 7.24 (d, 2 H, J = 7.9 Hz, 9-H), 7.66 (d, 2 H, J = 8.3 Hz, 8-H). $^{13}\text{C-NMR}$ (CDCl_3 , 151 MHz): δ = 21.6 (q, Ar-Me), 40.3 (q, NMe_2), 55.2 (d, C-2), 79.0 (t, C-1), 112.5 (d, C-5), 122.3 (s, C-3), 127.2 (d, C-8), 127.4 (d, C-4), 129.7 (d, C-9), 136.5 (s, C-7), 143.8 (s, C-10), 150.7 (s, C-6). HR-MS (ESI^+) $[\text{M}+\text{H}]^+$: calcd for $[\text{C}_{17}\text{H}_{22}\text{N}_3\text{O}_4\text{S}]^+$: 364.1325, found 364.1325.

Ethyl 3-(4-Methoxyphenyl)-2-(methylsulfinyl)acrylate (9be) was obtained from ethyl 2-(methylsulfinyl)acetate (**4e-H**, 75.0 mg, 499 μmol), the imine **2b** (100 mg, 346 μmol), and $\text{KO}t\text{Bu}$ (5.6 mg, 50 μmol , 14 mol-%) after 2.5 h of reaction time as a pale yellow oil (48 mg, 0.18 mmol, 52%). A NOESY experiment did not give conclusive results about the configuration of the olefinic double bond.

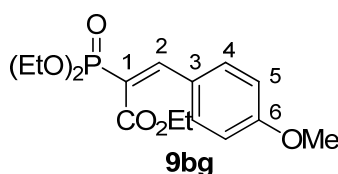
RAP 91.2



R_f (*n*-pentane/EtOAc 2:3, *v/v*): 0.33. $^1\text{H-NMR}$ (CDCl_3 , 300 MHz): δ = 1.32 (t, 3 H, J = 7.1 Hz, OCH_2CH_3), 2.76 (s, 3 H, SOMe), 3.85 (s, 3 H, OMe), 4.32 (q, 2 H, J = 7.1 Hz, OCH_2CH_3), 6.92 (d, 2 H, J = 8.9 Hz, 5-H), 7.52 (s, 1 H, 2-H), 7.73 (d, 2 H, J = 9.0 Hz, 4-H). $^{13}\text{C-NMR}$ (CDCl_3 , 75.5 MHz): δ = 14.0 (q, OCH_2CH_3), 42.0 (q, SOMe), 55.4 (q, OMe), 61.6 (t, OCH_2CH_3), 113.8 (d, C-5), 125.3 (s, C-3), 133.05 (s, C-1), 133.11 (d, C-4), 140.6 (d, C-2), 161.6 (s, C-6), 163.4 (s, CO). MS (EI): m/e (%) = 268 (3) $[\text{M}]^+$, 206 (11), 205 (100), 177 (25), 159 (20), 132 (47), 89 (10). HR-MS (EI) $[\text{M}]^+$: calcd for $[\text{C}_{13}\text{H}_{16}\text{O}_4\text{S}]^+$: 268.0764, found 268.0774.

(E)-Ethyl 2-(diethoxyphosphoryl)-3-(4-methoxyphenyl)acrylate (9bg) was obtained from ethyl 2-(diethoxyphosphoryl)acetate (**4g-H**, 150 mg, 669 μmol), the imine **2b** (100 mg, 346 μmol), and $\text{KO}t\text{Bu}$ (7.2 mg, 64 μmol , 18 mol-%) after 1 h of reaction time as a colorless oil (100 mg, 292 μmol , 84%).

RAP 66.2

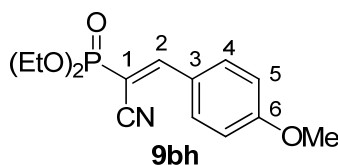


R_f (*n*-pentane/EtOAc 1:2, *v/v*): 0.31. $^1\text{H-NMR}$ (CDCl_3 , 599 MHz): δ = 1.29 (t, 3 H, J = 7.2 Hz, $\text{CO}_2\text{CH}_2\text{CH}_3$), 1.36 (td, 6 H, J = 7.1, 0.6 Hz, $2 \times \text{POCH}_2\text{CH}_3$), 3.83 (s, 3 H, OMe), 4.13-4.22 (m, 4 H, $2 \times \text{POCH}_2\text{CH}_3$), 4.31 (q, 2 H, J = 7.2 Hz, $\text{CO}_2\text{CH}_2\text{CH}_3$), 6.88 (d, 2 H, J = 8.9 Hz, 5-H), 7.42 (d, 2 H, J = 8.9 Hz, 4-H), 7.58 (d, 1 H, J = 24.4 Hz, 2-H). $^{13}\text{C-NMR}$ (CDCl_3 , 151 MHz): δ = 14.0 (q, $\text{CO}_2\text{CH}_2\text{CH}_3$), 16.2 (q, d, J_{PC} = 6.8 Hz, POCH_2CH_3), 55.4 (q, OMe), 61.6 (t, $\text{CO}_2\text{CH}_2\text{CH}_3$), 62.6 (t, d, J_{PC} = 5.1 Hz, POCH_2CH_3), 114.1 (d, C-5), 121.1 (s, d, J_{PC} = 180 Hz, C-1), 126.1 (s, d, J_{PC} = 20.5 Hz, C-3), 131.5 (d, d, J_{PC} = 1.2 Hz, C-4), 148.0 (d, d, J_{PC} = 6.7 Hz, C-2), 161.5 (s, C-6), 166.8 (s, d, J_{PC} = 12.6 Hz, CO). $^{31}\text{P-NMR}$ (CDCl_3 , 81.0 MHz): δ = 16.1.

$^1\text{H-NMR}$ signals are in agreement with those reported in the literature.^[11]

(E)-Diethyl (1-cyano-2-(4-methoxyphenyl)vinyl)phosphonate (9bh) was obtained from diethyl (cyanomethyl)phosphonate (**4h-H**, 120 mg, 677 μmol), the imine **2b** (100 mg, 346 μmol), and Et_3N (6.5 mg, 64 μmol , 18 mol-%) after 3 h of reaction time as a colorless oil (83 mg, 0.28 mmol, 81%).

RAP 64.1



R_f (*n*-pentane/EtOAc 1:2, *v/v*): 0.31. $^1\text{H-NMR}$ (CDCl_3 , 599 MHz): δ = 1.41 (td, 6 H, J = 7.1, 0.6 Hz, $2 \times \text{OCH}_2\text{CH}_3$), 3.89 (s, 3 H, OMe), 4.17-4.27 (m, 4 H, $2 \times \text{OCH}_2\text{CH}_3$), 6.99 (d, 2 H, J = 8.9 Hz, 5-H), 7.93 (d, 1 H, J = 21.3 Hz, 2-H), 7.97 (d, 2 H, J = 8.9 Hz, 4-H). $^{13}\text{C-NMR}$

(CDCl₃, 151 MHz): δ = 16.3 (q, d, J_{PC} = 6.4 Hz, OCH₂CH₃), 55.6 (q, OMe), 63.4 (t, d, J_{PC} = 5.8 Hz, OCH₂CH₃), 95.7 (s, d, J_{PC} = 200 Hz, C-1), 114.7 (d, C-5), 116.1 (s, d, J_{PC} = 10.4 Hz, CN), 125.5 (s, d, J_{PC} = 18.2 Hz, C-3), 133.0 (d, d, J_{PC} = 1.1 Hz, C-4), 158.3 (d, d, J_{PC} = 7.4 Hz, C-2), 163.5 (s, C-6). ³¹P-NMR (CDCl₃, 81.0 MHz): δ = 13.5.

¹H-NMR signals are in agreement with those reported in the literature.^[11]

5.3 Kinetics

5.3.1 Reactions of the Sulfur Ylide 4a with the Aldehydes 1a–i

Reactions of sulfur ylide 4a with the benzaldehydes 1a–e

Table 4: Kinetics of the reaction of **4a** with **1a** in DMSO at 20°C (diode array UV-Vis spectrometer, λ = 380 nm).

No.	[4a] ₀ / mol L ⁻¹ *	[1a] ₀ / mol L ⁻¹	$k_{\text{obs}} / \text{s}^{-1}$
RAK 23.22-1	$\approx 4 \times 10^{-5}$	3.95×10^{-4}	4.54×10^{-2}
RAK 23.22-2	$\approx 4 \times 10^{-5}$	4.28×10^{-4}	4.83×10^{-2}
RAK 23.22-3	$\approx 5 \times 10^{-5}$	4.73×10^{-4}	5.43×10^{-2}
RAK 23.22-4	$\approx 5 \times 10^{-5}$	5.22×10^{-4}	5.98×10^{-2}
RAK 23.22-5	$\approx 6 \times 10^{-5}$	5.68×10^{-4}	6.53×10^{-2}
$k_2 = 1.17 \times 10^2 \text{ L mol}^{-1} \text{ s}^{-1}$			

* Only approximate values are given for the initial concentration of the nucleophile (see general comments).

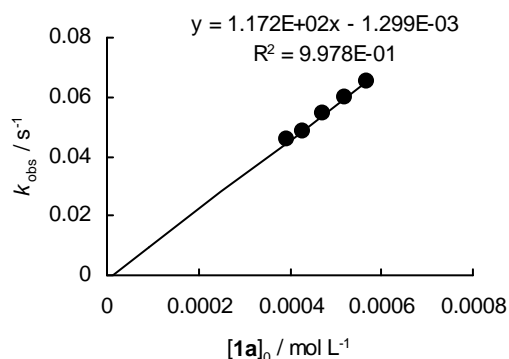


Table 5: Kinetics of the reaction of **4a** with **1b** in DMSO at 20°C (diode array UV-Vis spectrometer, λ = 380 nm).

No.	[4a] ₀ / mol L ⁻¹ *	[1b] ₀ / mol L ⁻¹	$k_{\text{obs}} / \text{s}^{-1}$
RAK 23.27-1	$\approx 4 \times 10^{-5}$	4.12×10^{-4}	3.33×10^{-2}
RAK 23.27-5	$\approx 5 \times 10^{-5}$	4.96×10^{-4}	3.92×10^{-2}
RAK 23.27-2	$\approx 5 \times 10^{-5}$	5.48×10^{-4}	4.25×10^{-2}
RAK 23.27-3	$\approx 5 \times 10^{-5}$	6.81×10^{-4}	5.45×10^{-2}
RAK 23.27-4	$\approx 5 \times 10^{-5}$	8.19×10^{-4}	6.56×10^{-2}
$k_2 = 8.06 \times 10^1 \text{ L mol}^{-1} \text{ s}^{-1}$			

* Only approximate values are given for the initial concentration of the nucleophile (see general comments).

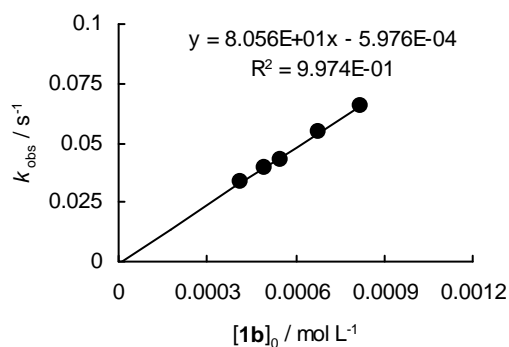
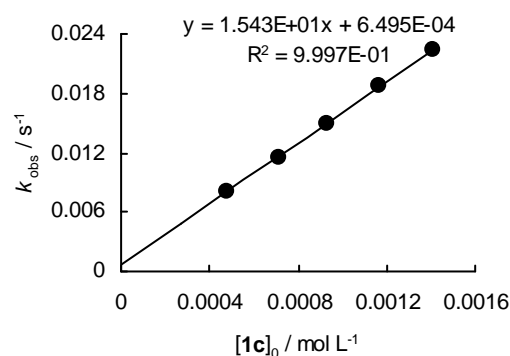


Table 6: Kinetics of the reaction of **4a** with **1c** in DMSO at 20°C (diode array UV-Vis spectrometer, $\lambda = 380$ nm).

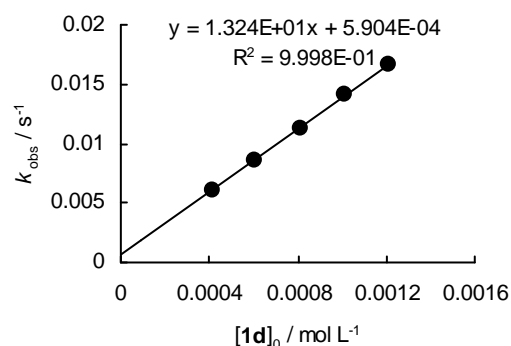
No.	[4a] ₀ / mol L ⁻¹ *	[1c] ₀ / mol L ⁻¹	$k_{\text{obs}} / \text{s}^{-1}$
RAK 23.29-1	$\approx 5 \times 10^{-5}$	4.78×10^{-4}	8.14×10^{-3}
RAK 23.29-2	$\approx 5 \times 10^{-5}$	7.12×10^{-4}	1.15×10^{-2}
RAK 23.29-3	$\approx 5 \times 10^{-5}$	9.34×10^{-4}	1.50×10^{-2}
RAK 23.29-4	$\approx 5 \times 10^{-5}$	1.17×10^{-3}	1.87×10^{-2}
RAK 23.29-5	$\approx 5 \times 10^{-5}$	1.41×10^{-3}	2.24×10^{-2}
$k_2 = 1.54 \times 10^1 \text{ L mol}^{-1} \text{ s}^{-1}$			

* Only approximate values are given for the initial concentration of the nucleophile (see general comments).

**Table 7:** Kinetics of the reaction of **4a** with **1d** in DMSO at 20°C (diode array UV-Vis spectrometer, $\lambda = 380$ nm).

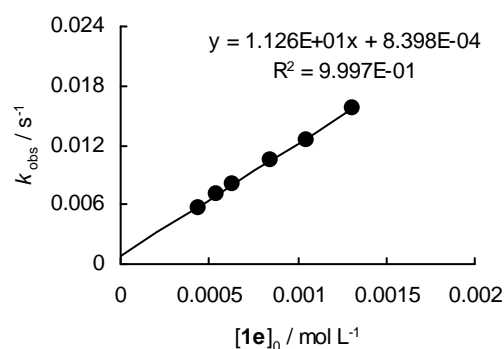
No.	[4a] ₀ / mol L ⁻¹ *	[1d] ₀ / mol L ⁻¹	$k_{\text{obs}} / \text{s}^{-1}$
RAK 23.26-1	$\approx 4 \times 10^{-5}$	4.11×10^{-4}	6.10×10^{-3}
RAK 23.26-2	$\approx 5 \times 10^{-5}$	6.07×10^{-4}	8.54×10^{-3}
RAK 23.26-3	$\approx 5 \times 10^{-5}$	8.11×10^{-4}	1.13×10^{-2}
RAK 23.26-4	$\approx 5 \times 10^{-5}$	1.02×10^{-3}	1.41×10^{-2}
RAK 23.26-5	$\approx 5 \times 10^{-5}$	1.21×10^{-3}	1.66×10^{-2}
$k_2 = 1.32 \times 10^1 \text{ L mol}^{-1} \text{ s}^{-1}$			

* Only approximate values are given for the initial concentration of the nucleophile (see general comments).

**Table 8:** Kinetics of the reaction of **4a** with **1e** in DMSO at 20°C (diode array UV-Vis spectrometer, $\lambda = 380$ nm).

No.	[4a] ₀ / mol L ⁻¹ *	[1e] ₀ / mol L ⁻¹	$k_{\text{obs}} / \text{s}^{-1}$
RAK 23.23-1	$\approx 4 \times 10^{-5}$	4.36×10^{-4}	5.74×10^{-3}
RAK 23.23-6	$\approx 5 \times 10^{-5}$	5.44×10^{-4}	6.97×10^{-3}
RAK 23.23-2	$\approx 5 \times 10^{-5}$	6.35×10^{-4}	8.04×10^{-3}
RAK 23.23-3	$\approx 5 \times 10^{-5}$	8.49×10^{-4}	1.04×10^{-2}
RAK 23.23-4	$\approx 5 \times 10^{-5}$	1.05×10^{-3}	1.26×10^{-2}
RAK 23.26-5	$\approx 5 \times 10^{-5}$	1.31×10^{-3}	1.57×10^{-2}
$k_2 = 1.13 \times 10^1 \text{ L mol}^{-1} \text{ s}^{-1}$			

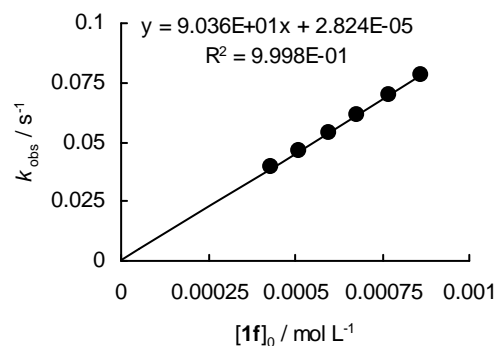
* Only approximate values are given for the initial concentration of the nucleophile (see general comments).



Reactions of sulfur ylide **4a** with the cinnamaldehydes **1f,g****Table 9:** Kinetics of the reaction of **4a** with **1f** in DMSO at 20°C (diode array UV-Vis spectrometer, $\lambda = 380$ nm).

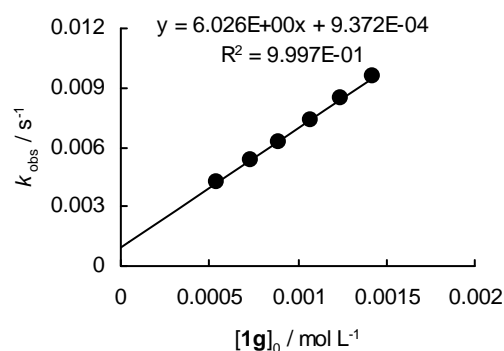
No.	[4a] ₀ / mol L ⁻¹ *	[1f] ₀ / mol L ⁻¹	$k_{\text{obs}} / \text{s}^{-1}$
RAK 23.18-6	$\approx 4 \times 10^{-5}$	4.30×10^{-4}	3.91×10^{-2}
RAK 23.18-1	$\approx 5 \times 10^{-5}$	5.12×10^{-4}	4.59×10^{-2}
RAK 23.18-4	$\approx 5 \times 10^{-5}$	5.95×10^{-4}	5.38×10^{-2}
RAK 23.18-2	$\approx 5 \times 10^{-5}$	6.78×10^{-4}	6.14×10^{-2}
RAK 23.18-5	$\approx 5 \times 10^{-5}$	7.72×10^{-4}	6.99×10^{-2}
RAK 23.18-3	$\approx 6 \times 10^{-5}$	8.63×10^{-4}	7.79×10^{-2}
$k_2 = 9.04 \times 10^1 \text{ L mol}^{-1} \text{ s}^{-1}$			

* Only approximate values are given for the initial concentration of the nucleophile (see general comments).

**Table 10:** Kinetics of the reaction of **4a** with **1g** in DMSO at 20°C (diode array UV-Vis spectrometer, $\lambda = 380$ nm).

No.	[4a] ₀ / mol L ⁻¹ *	[1g] ₀ / mol L ⁻¹	$k_{\text{obs}} / \text{s}^{-1}$
RAK 23.24-1	$\approx 5 \times 10^{-5}$	5.45×10^{-4}	4.24×10^{-3}
RAK 23.24-2	$\approx 6 \times 10^{-5}$	7.32×10^{-4}	5.37×10^{-3}
RAK 23.24-3	$\approx 5 \times 10^{-5}$	8.92×10^{-4}	6.29×10^{-3}
RAK 23.24-4	$\approx 6 \times 10^{-5}$	1.08×10^{-3}	7.37×10^{-3}
RAK 23.24-5	$\approx 5 \times 10^{-5}$	1.25×10^{-3}	8.48×10^{-3}
RAK 23.24-6	$\approx 5 \times 10^{-5}$	1.42×10^{-3}	9.54×10^{-3}
$k_2 = 6.03 \text{ L mol}^{-1} \text{ s}^{-1}$			

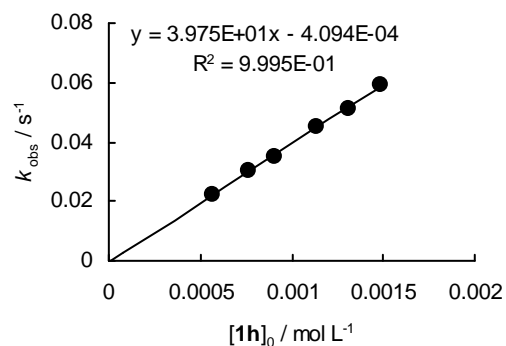
* Only approximate values are given for the initial concentration of the nucleophile (see general comments).



Reactions of sulfur ylide **4a** with the aliphatic aldehydes **1h,i****Table 11:** Kinetics of the reaction of **4a** with **1h** in DMSO at 20°C (diode array UV-Vis spectrometer, $\lambda = 380$ nm).

No.	[4a] ₀ / mol L ⁻¹ *	[1h] ₀ / mol L ⁻¹	k_{obs} / s ⁻¹
RAK 23.20-1	$\approx 6 \times 10^{-5}$	5.69×10^{-4}	2.24×10^{-2}
RAK 23.20-2	$\approx 6 \times 10^{-5}$	7.66×10^{-4}	3.00×10^{-2}
RAK 23.20-3	$\approx 7 \times 10^{-5}$	9.06×10^{-4}	3.52×10^{-2}
RAK 23.20-4	$\approx 7 \times 10^{-5}$	1.14×10^{-3}	4.52×10^{-2}
RAK 23.20-5	$\approx 7 \times 10^{-5}$	1.31×10^{-3}	5.12×10^{-2}
RAK 23.20-6	$\approx 7 \times 10^{-5}$	1.49×10^{-3}	5.90×10^{-2}
$k_2 = 3.98 \times 10^1 \text{ L mol}^{-1} \text{ s}^{-1}$			

* Only approximate values are given for the initial concentration of the nucleophile (see general comments).

**Table 12:** Kinetics of the reaction of **4a** with **1i** in DMSO at 20°C (diode array UV-Vis spectrometer, $\lambda = 380$ nm).

No.	[4a] ₀ / mol L ⁻¹ *	[1i] ₀ / mol L ⁻¹	k_{obs} / s ⁻¹
RAK 23.28-1	$\approx 5 \times 10^{-5}$	6.16×10^{-4}	2.51×10^{-2}
RAK 23.28-2	$\approx 6 \times 10^{-5}$	8.20×10^{-4}	3.28×10^{-2}
RAK 23.28-3	$\approx 6 \times 10^{-5}$	1.01×10^{-3}	3.96×10^{-2}
RAK 23.28-4	$\approx 6 \times 10^{-5}$	1.22×10^{-3}	4.73×10^{-2}
RAK 23.28-5	$\approx 6 \times 10^{-5}$	1.42×10^{-3}	5.54×10^{-2}
$k_2 = 3.72 \times 10^1 \text{ L mol}^{-1} \text{ s}^{-1}$			

* Only approximate values are given for the initial concentration of the nucleophile (see general comments).

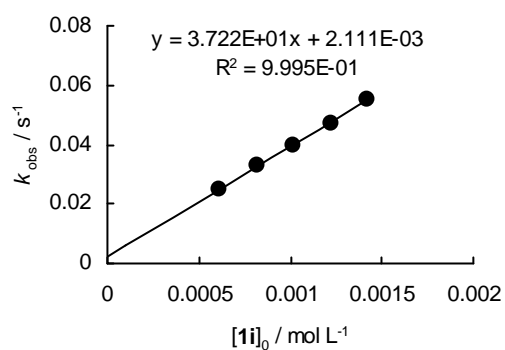
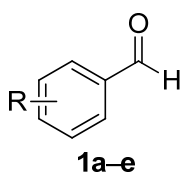
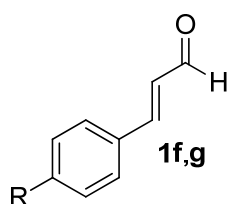
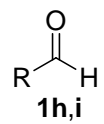


Table 13: Calculation of the electrophilicity parameters E for **1a–i** using the second-order rate constants for their reactions with sulfur ylide **4a** ($N = 21.07$, $s = 0.68$) and correlation equation $\log k_2 = s(N + E)$.

Electrophile	$k_2 / \text{L mol}^{-1} \text{s}^{-1}$	Electrophilicity E
 1a–e	1a (R = m-Cl) 1.17×10^2	E (1a) = -18.03
	1b (R = m-F) 8.06×10^1	E (1b) = -18.27
	1c (R = m-OMe) 1.54×10^1	E (1c) = -19.32
	1d (R = p-F) 1.32×10^1	E (1d) = -19.42
	1e (R = H) 1.13×10^1	E (1e) = -19.52
 1f,g	1f (R = NO ₂) 9.04×10^1	E (1f) = -18.19
	1g (R = H) 6.03	E (1g) = -19.92
 1h,i	1h (R = <i>n</i> -Pr) 3.98×10^1	E (1h) = -18.72
	1i (R = <i>n</i> -Pent) 3.72×10^1	E (1i) = -18.76

5.3.2 Reactions of the Sulfur Ylides **4a,b** and the Carbanions **4c–h** with the Imines **2a–e**

Reactions of sulfur ylide **4b** and the carbanion **4e** with imine **2a**

Table 14: Kinetics of the reaction of **4b** with **2a** in DMSO at 20°C (stopped-flow UV-Vis spectrometer, $\lambda = 530$ nm).

No.	$[\mathbf{4b}]_0 / \text{mol L}^{-1}$ *	$[\mathbf{2a}]_0 / \text{mol L}^{-1}$	$k_{\text{obs}} / \text{s}^{-1}$
RAK 23.33-1	$\approx 4 \times 10^{-5}$	4.55×10^{-4}	1.91×10^1
RAK 23.33-2	$\approx 4 \times 10^{-5}$	6.83×10^{-4}	2.88×10^1
RAK 23.33-3	$\approx 4 \times 10^{-5}$	9.10×10^{-4}	3.79×10^1
RAK 23.33-4	$\approx 4 \times 10^{-5}$	1.14×10^{-3}	4.71×10^1
RAK 23.33-5	$\approx 4 \times 10^{-5}$	1.37×10^{-3}	5.71×10^1

$k_2 = 4.15 \times 10^4 \text{ L mol}^{-1} \text{ s}^{-1}$

* Only approximate values are given for the initial concentration of the nucleophile (see general comments).

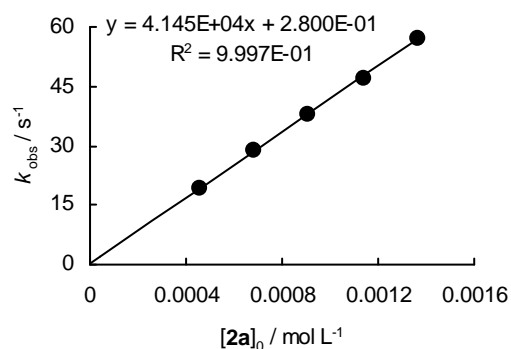
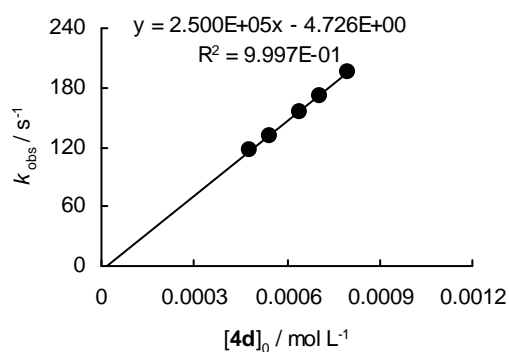


Table 15: Kinetics of the reaction of **4d** with **2a** in DMSO at 20°C (addition of 0-1.8 equiv of 18-crown-6, stopped-flow UV-Vis spectrometer, $\lambda = 300$ nm).

No.	[2a] ₀ / mol L ⁻¹	[4d] ₀ / mol L ⁻¹	[18-crown-6] / mol L ⁻¹	$k_{\text{obs}} / \text{s}^{-1}$
RAK 26.1-1	3.82×10^{-5}	4.80×10^{-4}	-	1.16×10^2
RAK 26.1-4	3.82×10^{-5}	5.44×10^{-4}	-	1.31×10^2
RAK 26.1-2	3.82×10^{-5}	6.41×10^{-4}	-	1.55×10^2
RAK 26.1-5	3.82×10^{-5}	7.05×10^{-4}	-	1.71×10^2
RAK 26.1-3	3.82×10^{-5}	8.01×10^{-4}	1.48×10^{-3}	1.96×10^2

$k_2 = 2.50 \times 10^5 \text{ L mol}^{-1} \text{ s}^{-1}$



Reactions of the sulfur ylides **4a,b** and the carbanions **4c–h** with imine **2b**

Table 16: Kinetics of the reaction of **4a** with **2b** in DMSO at 20°C (stopped-flow UV-Vis spectrometer, $\lambda = 380$ nm).

No.	[4a] ₀ / mol L ⁻¹ *	[2b] ₀ / mol L ⁻¹	$k_{\text{obs}} / \text{s}^{-1}$
RAK 23.36-4	$\approx 4 \times 10^{-5}$	3.32×10^{-4}	1.04×10^2
RAK 23.36-1	$\approx 4 \times 10^{-5}$	4.43×10^{-4}	1.38×10^2
RAK 23.36-2	$\approx 4 \times 10^{-5}$	5.54×10^{-4}	1.75×10^2
RAK 23.36-3	$\approx 4 \times 10^{-5}$	6.65×10^{-4}	2.11×10^2
RAK 23.36-5	$\approx 4 \times 10^{-5}$	7.75×10^{-4}	2.45×10^2

$k_2 = 3.21 \times 10^5 \text{ L mol}^{-1} \text{ s}^{-1}$

* Only approximate values are given for the initial concentration of the nucleophile (see general comments).

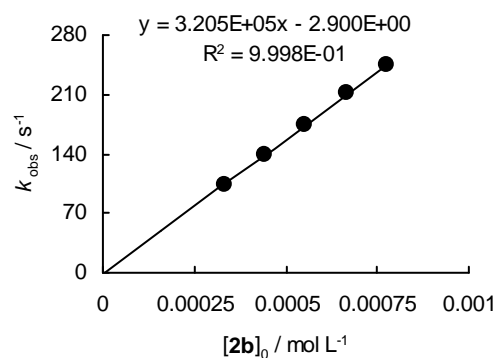
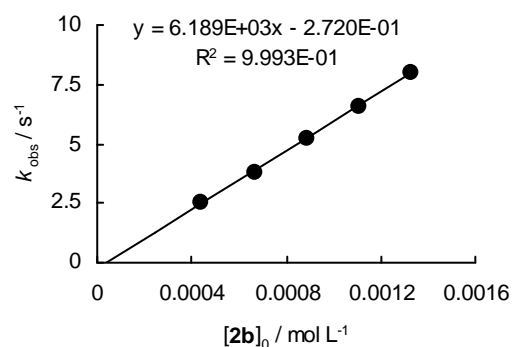


Table 17: Kinetics of the reaction of **4b** with **2b** in DMSO at 20°C (stopped-flow UV-Vis spectrometer, $\lambda = 530$ nm).

No.	[4b] ₀ / mol L ⁻¹ *	[2b] ₀ / mol L ⁻¹	$k_{\text{obs}} / \text{s}^{-1}$
RAK 23.35-2-1	$\approx 4 \times 10^{-5}$	4.43×10^{-4}	2.53
RAK 23.35-2-2	$\approx 4 \times 10^{-5}$	6.65×10^{-4}	3.78
RAK 23.35-2-3	$\approx 4 \times 10^{-5}$	8.86×10^{-4}	5.21
RAK 23.35-2-4	$\approx 4 \times 10^{-5}$	1.11×10^{-3}	6.53
RAK 23.35-2-5	$\approx 4 \times 10^{-5}$	1.33×10^{-3}	8.01

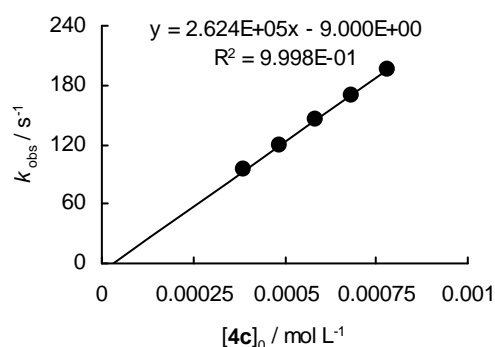
$$k_2 = 6.19 \times 10^3 \text{ L mol}^{-1} \text{ s}^{-1}$$

* Only approximate values are given for the initial concentration of the nucleophile (see general comments).

**Table 18:** Kinetics of the reaction of **4c** with **2b** in DMSO at 20°C (stopped-flow UV-Vis spectrometer, $\lambda = 330$ nm).

No.	[2b] ₀ / mol L ⁻¹	[4c] ₀ / mol L ⁻¹	$k_{\text{obs}} / \text{s}^{-1}$
RAK 25.3-1	3.89×10^{-5}	3.90×10^{-4}	9.40×10^1
RAK 25.3-2	3.89×10^{-5}	4.88×10^{-4}	1.18×10^2
RAK 25.3-3	3.89×10^{-5}	5.85×10^{-4}	1.45×10^2
RAK 25.3-4	3.89×10^{-5}	6.83×10^{-4}	1.70×10^2
RAK 25.3-5	3.89×10^{-5}	7.81×10^{-4}	1.96×10^2

$$k_2 = 2.62 \times 10^5 \text{ L mol}^{-1} \text{ s}^{-1}$$

**Table 19:** Kinetics of the reaction of **4d** with **2b** in DMSO at 20°C (stopped-flow UV-Vis spectrometer, $\lambda = 330$ nm).

No.	[2b] ₀ / mol L ⁻¹	[4d] ₀ / mol L ⁻¹	$k_{\text{obs}} / \text{s}^{-1}$
RAK 25.1-1	3.77×10^{-5}	4.44×10^{-4}	1.95×10^1
RAK 25.1-2	3.77×10^{-5}	6.66×10^{-4}	2.97×10^1
RAK 25.1-3	3.77×10^{-5}	8.88×10^{-4}	3.84×10^1
RAK 25.1-4	3.77×10^{-5}	1.11×10^{-3}	4.82×10^1
RAK 25.1-5	3.77×10^{-5}	1.33×10^{-3}	5.81×10^1

$$k_2 = 4.31 \times 10^4 \text{ L mol}^{-1} \text{ s}^{-1}$$

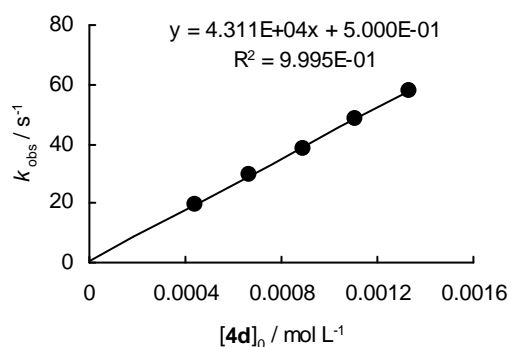
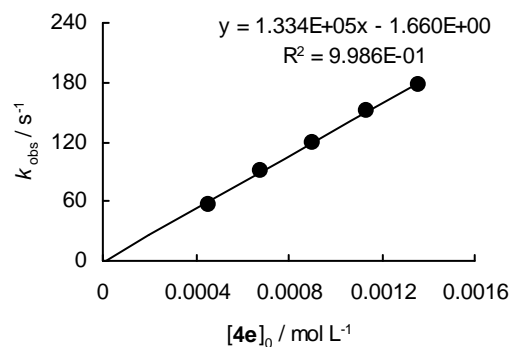
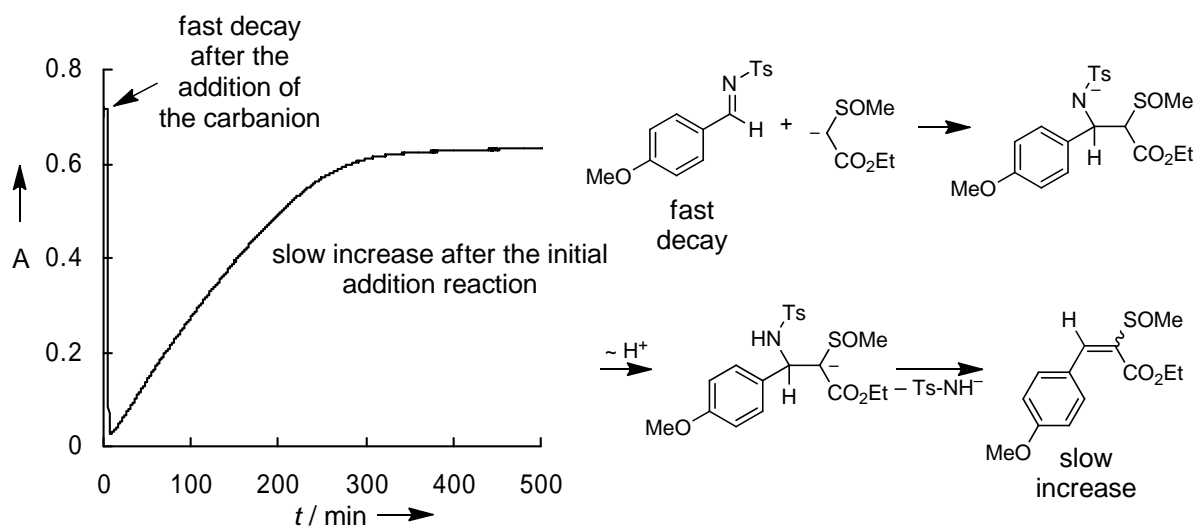


Table 20: Kinetics of the reaction of **4e** with **2b** in DMSO at 20°C (stopped-flow UV-Vis spectrometer, $\lambda = 330$ nm).

No.	$[2b]_0 / \text{mol L}^{-1}$	$[4e]_0 / \text{mol L}^{-1}$	$k_{\text{obs}} / \text{s}^{-1}$
RAK 25.5-1	3.87×10^{-5}	4.53×10^{-4}	5.68×10^1
RAK 25.5-2	3.87×10^{-5}	6.80×10^{-4}	9.09×10^1
RAK 25.5-3	3.87×10^{-5}	9.07×10^{-4}	1.20×10^2
RAK 25.5-4	3.87×10^{-5}	1.13×10^{-3}	1.51×10^2
RAK 25.5-5	3.87×10^{-5}	1.36×10^{-3}	1.78×10^2
$k_2 = 1.33 \times 10^5 \text{ L mol}^{-1} \text{ s}^{-1}$			

**Table 21:** Mechanistic study for the reaction of **4e** with **2b** in DMSO at 20°C (diode array UV-Vis spectrometer, $\lambda = 318$ nm).

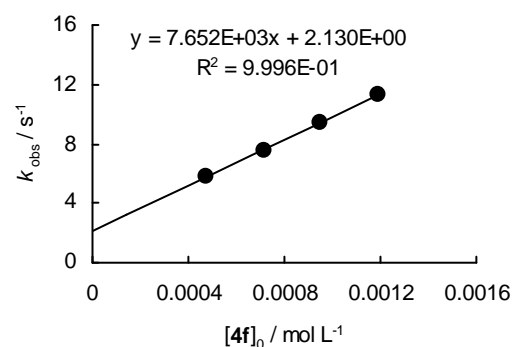
No.	$[2b]_0 / \text{mol L}^{-1}$	$[4e]_0 / \text{mol L}^{-1}$
RAME4	4.73×10^{-5}	8.03×10^{-5}



The imine **2b** reacts with the carbanion **4e** in a fast addition step (fast decay when carbanion is added, for the second-order rate constant see Table 20). The subsequent slow increase of the absorbance indicates a slow formation of the condensation product.

Table 22: Kinetics of the reaction of **4f** with **2b** in DMSO at 20°C (stopped-flow UV-Vis spectrometer, $\lambda = 330$ nm).

No.	[2b] ₀ / mol L ⁻¹	[4f] ₀ / mol L ⁻¹	<i>k</i> _{obs} / s ⁻¹
RAK 25.2-2-1	3.98×10^{-5}	4.77×10^{-4}	5.81
RAK 25.2-2-2	3.98×10^{-5}	7.15×10^{-4}	7.59
RAK 25.2-2-3	3.98×10^{-5}	9.54×10^{-4}	9.37
RAK 25.2-2-4	3.98×10^{-5}	1.19×10^{-3}	1.13×10^1
$k_2 = 7.65 \times 10^3 \text{ L mol}^{-1} \text{ s}^{-1}$			

**Table 23:** Kinetics of the reaction of **4g** with **2b** in DMSO at 20°C (addition of 0-1.6 equiv of 18-crown-6, stopped-flow UV-Vis spectrometer, $\lambda = 330$ nm).

No.	[2b] ₀ / mol L ⁻¹	[4g] ₀ / mol L ⁻¹	[18-crown-6] / mol L ⁻¹	<i>k</i> _{obs} / s ⁻¹
RAK 25.7-1	3.80×10^{-5}	4.59×10^{-4}	-	1.33
RAK 25.7-2	3.80×10^{-5}	6.89×10^{-4}	-	1.84
RAK 25.7-3	3.80×10^{-5}	9.19×10^{-4}	1.48×10^{-3}	2.49
RAK 25.7-4	3.80×10^{-5}	1.15×10^{-3}	-	2.91
RAK 25.7-5	3.80×10^{-5}	1.38×10^{-3}	-	3.49
$k_2 = 2.35 \times 10^3 \text{ L mol}^{-1} \text{ s}^{-1}$				

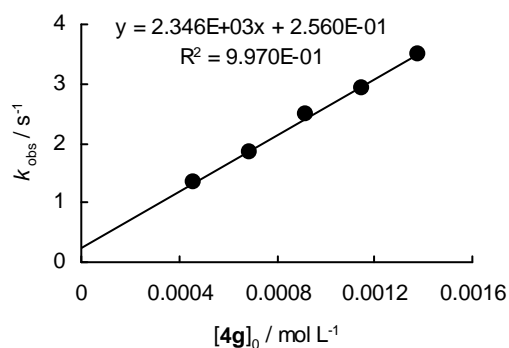
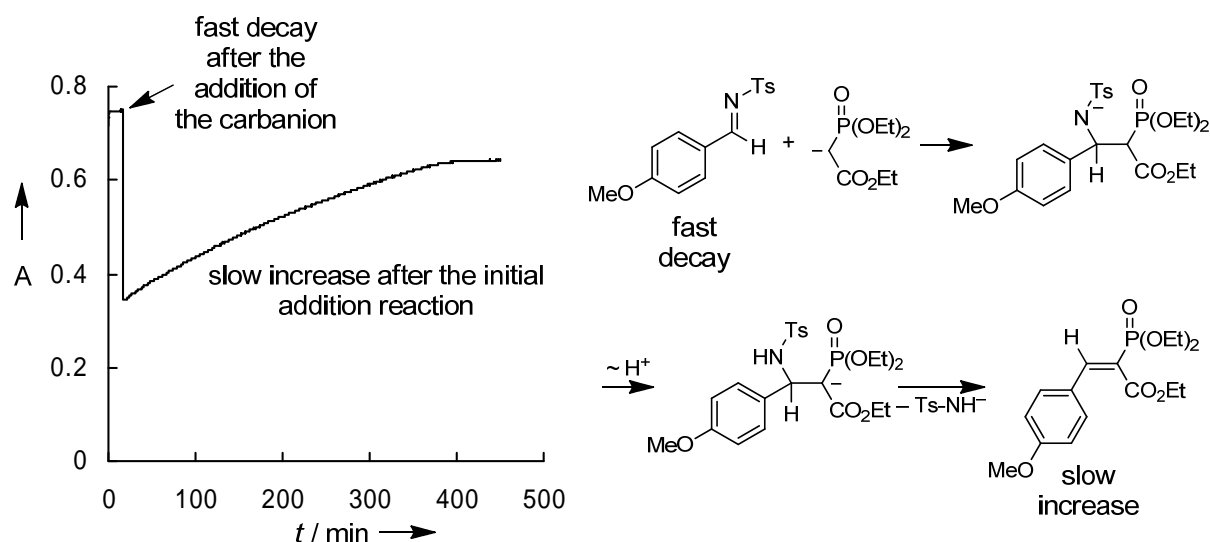


Table 24: Mechanistic study for the reaction of **4g** with **2b** in DMSO at 20°C (diode array UV-Vis spectrometer, $\lambda = 318$ nm).

No.	[2b] ₀ / mol L ⁻¹	[4g] ₀ / mol L ⁻¹
RAME3-2	4.89×10^{-5}	1.11×10^{-4}



The imine **2b** reacts with the carbanion **4g** in a fast addition step (fast decay when carbanion is added, for the second-order rate constant see Table 23). The subsequent slow increase of the absorbance indicates a slow formation of the condensation product.

Table 25: Kinetics of the reaction of **4h** with **2b** in DMSO at 20°C (stopped-flow UV-Vis spectrometer, $\lambda = 330$ nm).

No.	[2h] ₀ / mol L ⁻¹	[4h] ₀ / mol L ⁻¹	$k_{\text{obs}} / \text{s}^{-1}$
RAK 25.6-1	3.87×10^{-5}	4.00×10^{-4}	8.82
RAK 25.6-2	3.87×10^{-5}	6.00×10^{-4}	1.22×10^1
RAK 25.6-3	3.87×10^{-5}	7.99×10^{-4}	1.53×10^1
RAK 25.6-4	3.87×10^{-5}	9.99×10^{-4}	1.85×10^1
RAK 25.6-5	3.87×10^{-5}	1.20×10^{-3}	2.20×10^1
$k_2 = 1.63 \times 10^4 \text{ L mol}^{-1} \text{ s}^{-1}$			

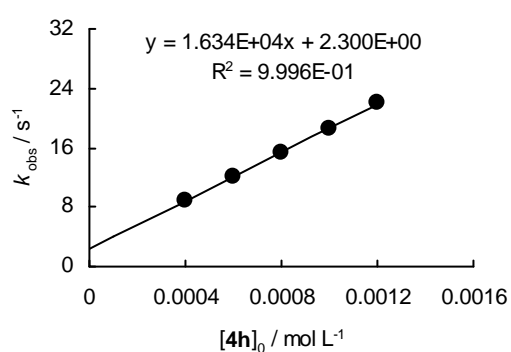
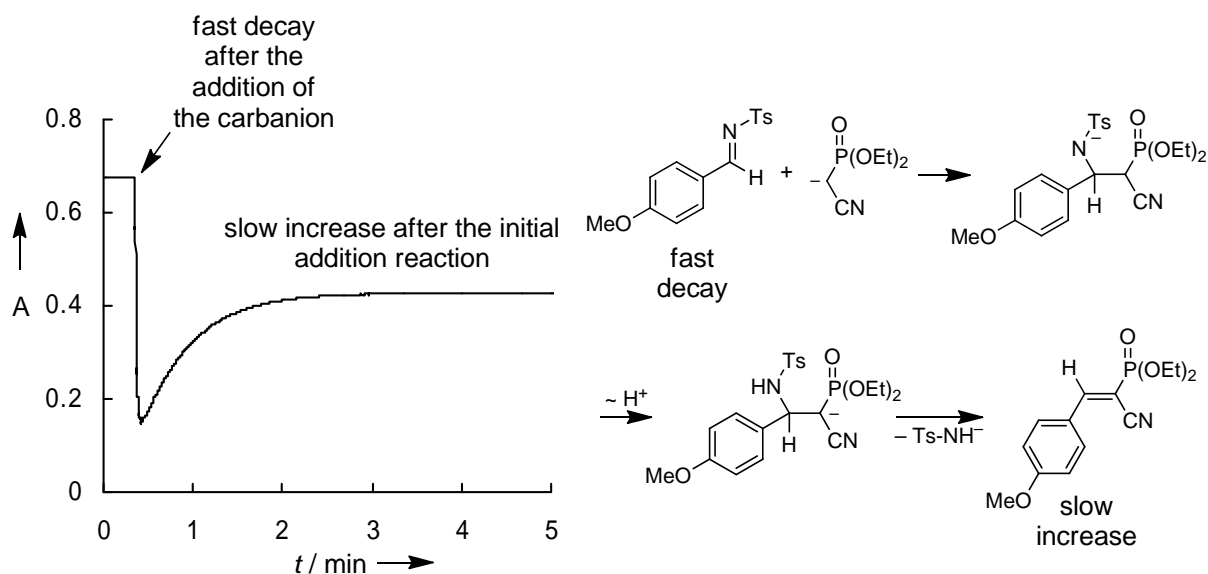


Table 26: Mechanistic study for the reaction of **4h** with **2b** in DMSO at 20°C (diode array UV-Vis spectrometer, $\lambda = 318$ nm).

No.	[2b] ₀ / mol L ⁻¹	[4h] ₀ / mol L ⁻¹
RAME2-1b	4.29×10^{-5}	7.07×10^{-4}



The imine **2b** reacts with the carbanion **4h** in a fast addition step (fast decay when carbanion is added, for the second-order rate constant see Table 25). The subsequent slow increase of the absorbance indicates a slow formation of the condensation product.

Reactions of the carbanions **4c–e** with imine **2c**

Table 27: Kinetics of the reaction of **4c** with **2c** in DMSO at 20°C (addition of 0–1.4 equiv 18-crown-6, stopped-flow UV-Vis spectrometer, $\lambda = 394$ nm).

No.	[2c] ₀ / mol L ⁻¹	[4c] ₀ / mol L ⁻¹	[18-crown-6] / mol L ⁻¹	$k_{\text{obs}} / \text{s}^{-1}$
RAK 27.2-1	3.27×10^{-5}	3.96×10^{-4}	-	4.68
RAK 27.2-2	3.27×10^{-5}	5.93×10^{-4}	-	6.53
RAK 27.2-3	3.27×10^{-5}	7.91×10^{-4}	1.10×10^{-3}	8.76
RAK 27.2-4	3.27×10^{-5}	9.89×10^{-4}	-	1.07×10^1
RAK 27.2-5	3.27×10^{-5}	1.19×10^{-3}	-	1.28×10^1
$k_2 = 1.03 \times 10^4 \text{ L mol}^{-1} \text{ s}^{-1}$				

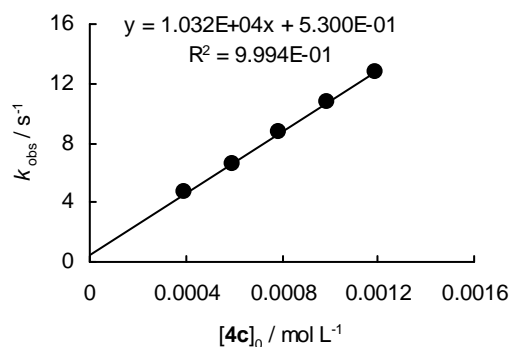


Table 28: Kinetics of the reaction of **4d** with **2c** in DMSO at 20°C (addition of 0-1.3 equiv 18-crown-6, stopped-flow UV-Vis spectrometer, $\lambda = 394$ nm).

No.	$[2c]_0 / \text{mol L}^{-1}$	$[4d]_0 / \text{mol L}^{-1}$	$[18\text{-crown-6}] / \text{mol L}^{-1}$	$k_{\text{obs}} / \text{s}^{-1}$
RAK 27.1-1	3.70×10^{-5}	4.80×10^{-4}	-	7.88×10^{-1}
RAK 27.1-2	3.70×10^{-5}	8.01×10^{-4}	-	1.28
RAK 27.1-3	3.70×10^{-5}	1.12×10^{-3}	1.48×10^{-3}	1.83
RAK 27.1-4	3.70×10^{-5}	1.44×10^{-3}	-	2.29
RAK 27.1-5	3.70×10^{-5}	1.76×10^{-3}	-	2.82
$k_2 = 1.58 \times 10^3 \text{ L mol}^{-1} \text{ s}^{-1}$				

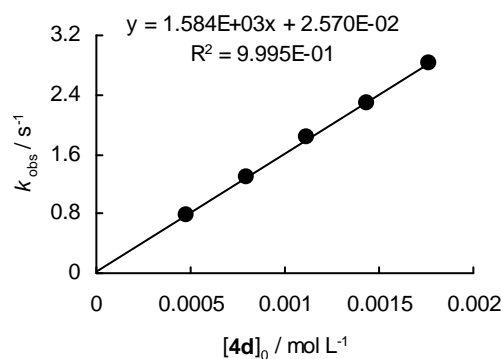


Table 29: Kinetics of the reaction of **4e** with **2c** in DMSO at 20°C (addition of 0-1.5 equiv 18-crown-6, stopped-flow UV-Vis spectrometer, $\lambda = 394$ nm).

No.	$[2c]_0 / \text{mol L}^{-1}$	$[4e]_0 / \text{mol L}^{-1}$	$[18\text{-crown-6}] / \text{mol L}^{-1}$	$k_{\text{obs}} / \text{s}^{-1}$
RAK 27.3-1	3.27×10^{-5}	4.78×10^{-4}	-	2.79
RAK 27.3-2	3.27×10^{-5}	7.17×10^{-4}	-	3.92
RAK 27.3-3	3.27×10^{-5}	9.56×10^{-4}	1.10×10^{-3}	5.14
RAK 27.3-4	3.27×10^{-5}	1.20×10^{-3}	-	6.22
RAK 27.3-5	3.27×10^{-5}	1.43×10^{-3}	-	7.31
RAK 27.3-5M	3.27×10^{-5}	1.43×10^{-3}	2.21×10^{-3}	7.43
$k_2 = 4.79 \times 10^3 \text{ L mol}^{-1} \text{ s}^{-1}$				

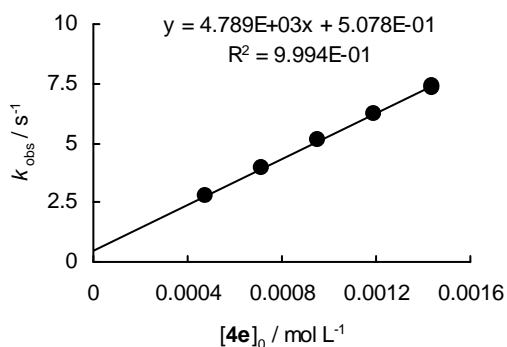
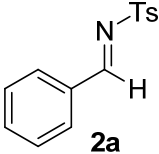
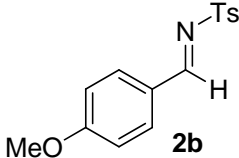
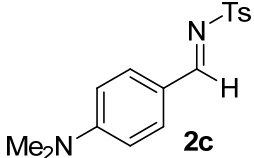


Table 30: Determination of the electrophilicity parameters E for **2a–c** (least-squares minimization of $\Delta^2 = \sum(\log k_2 - s(N + E))^2$ for the correlation of $\log k_2 / s$ of the reactions of **2a–c** with **4a–h** versus the nucleophilicity parameters N for **4a–h**).

Electrophile	Nucleophile (N, s)	$k_2 / \text{L mol}^{-1} \text{s}^{-1}$	Electrophilicity E
 2a	4b (18.42, 0.65)	4.15×10^4	E (2a) = -11.50
	4d (20.71, 0.60)	2.50×10^5	
 2b	4a (21.07, 0.68)	3.21×10^5	E (2b) = -13.05
	4b (18.42, 0.65)	6.19×10^3	
	4c (21.54, 0.62)	2.62×10^5	
	4d (20.71, 0.60)	4.31×10^4	
	4e (20.61, 0.64)	1.33×10^5	
	4f (20.22, 0.65)	7.65×10^3	
	4g (19.23, 0.65)	2.35×10^3	
4h (18.57, 0.65)	1.63×10^4		
 2c	4c (21.54, 0.62)	1.03×10^4	E (2c) = -15.09
	4d (20.71, 0.60)	1.58×10^3	
	4e (20.61, 0.64)	4.79×10^3	

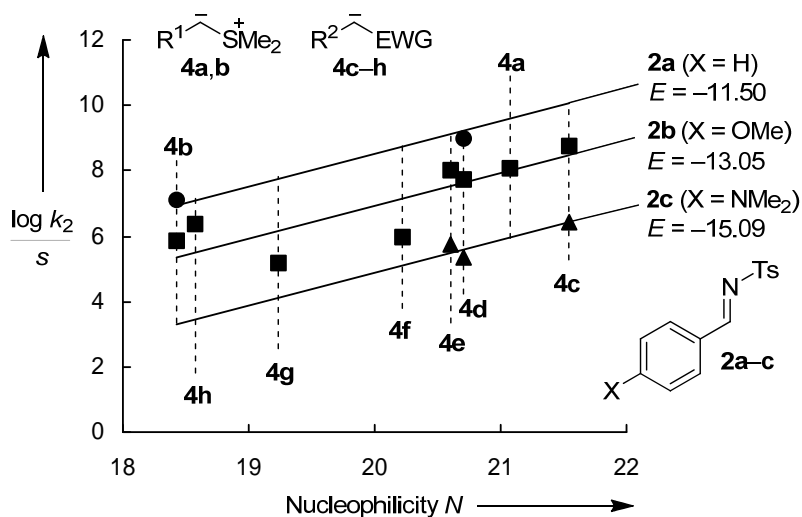
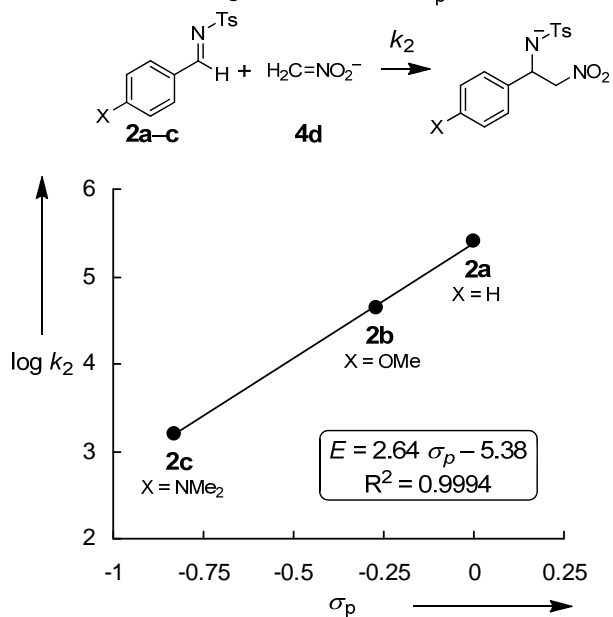


Figure 9: Correlation of the second-order rate constants ($\log k_2 / s$) for the reactions of the nucleophiles **4a–h** with the imines **2a–c** versus the nucleophilicity parameters N of **4a–h**. The slopes are fixed to one as required by $\log k_2 = s(N + E)$.

Correlation of $\log k_2$ for the Reactions of **2a–c** with **4d** against Hammett's σ_p [14]

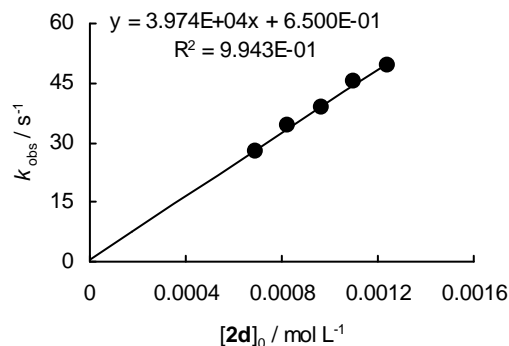


Reactions of the sulfur ylides **4a,b** with imine **2d****Table 31:** Kinetics of the reaction of **4a** with **2d** in DMSO at 20°C (stopped-flow UV-Vis spectrometer, $\lambda = 380$ nm).

No.	[4a] ₀ / mol L ⁻¹ *	[2d] ₀ / mol L ⁻¹	$k_{\text{obs}} / \text{s}^{-1}$
RAK 23.48-1	$\approx 6 \times 10^{-5}$	6.88×10^{-4}	2.75×10^1
RAK 23.48-2	$\approx 6 \times 10^{-5}$	8.26×10^{-4}	3.41×10^1
RAK 23.48-3	$\approx 6 \times 10^{-5}$	9.63×10^{-4}	3.86×10^1
RAK 23.48-4	$\approx 6 \times 10^{-5}$	1.10×10^{-3}	4.52×10^1
RAK 23.48-5	$\approx 6 \times 10^{-5}$	1.24×10^{-3}	4.93×10^1

$$k_2 = 3.97 \times 10^4 \text{ L mol}^{-1} \text{ s}^{-1}$$

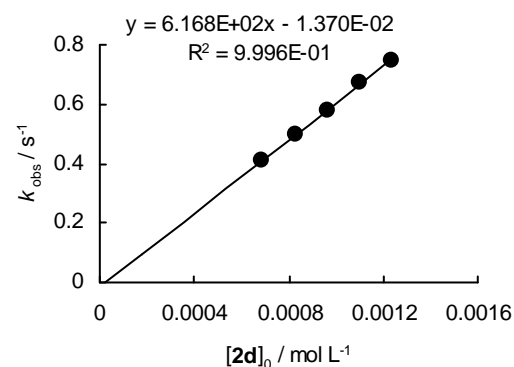
* Only approximate values are given for the initial concentration of the nucleophile (see general comments).

**Table 32:** Kinetics of the reaction of **4b** with **2d** in DMSO at 20°C (stopped-flow UV-Vis spectrometer, $\lambda = 520$ nm).

No.	[4b] ₀ / mol L ⁻¹ *	[2d] ₀ / mol L ⁻¹	$k_{\text{obs}} / \text{s}^{-1}$
RAK 23.49-1	$\approx 6 \times 10^{-5}$	6.88×10^{-4}	4.09×10^{-1}
RAK 23.49-2	$\approx 6 \times 10^{-5}$	8.26×10^{-4}	4.98×10^{-1}
RAK 23.49-3	$\approx 6 \times 10^{-5}$	9.63×10^{-4}	5.79×10^{-1}
RAK 23.49-4	$\approx 6 \times 10^{-5}$	1.10×10^{-3}	6.69×10^{-1}
RAK 23.49-5	$\approx 6 \times 10^{-5}$	1.24×10^{-3}	7.48×10^{-1}

$$k_2 = 6.17 \times 10^2 \text{ L mol}^{-1} \text{ s}^{-1}$$

* Only approximate values are given for the initial concentration of the nucleophile (see general comments).

Reactions of sulfur ylides **4a,b** with imine **2e****Table 33:** Kinetics of the reaction of **4a** with **2e** in DMSO at 20°C (stopped-flow UV-Vis spectrometer, $\lambda = 380$ nm).

No.	[4a] ₀ / mol L ⁻¹ *	[2e] ₀ / mol L ⁻¹	$k_{\text{obs}} / \text{s}^{-1}$
RAK 23.47-1	$\approx 6 \times 10^{-5}$	5.70×10^{-4}	2.40
RAK 23.47-2	$\approx 6 \times 10^{-5}$	8.55×10^{-4}	3.61
RAK 23.47-3	$\approx 6 \times 10^{-5}$	1.14×10^{-3}	4.91
RAK 23.47-4	$\approx 6 \times 10^{-5}$	1.42×10^{-3}	6.17
RAK 23.47-5	$\approx 6 \times 10^{-5}$	1.71×10^{-3}	7.47

$$k_2 = 4.46 \times 10^3 \text{ L mol}^{-1} \text{ s}^{-1}$$

* Only approximate values are given for the initial concentration of the nucleophile (see general comments).

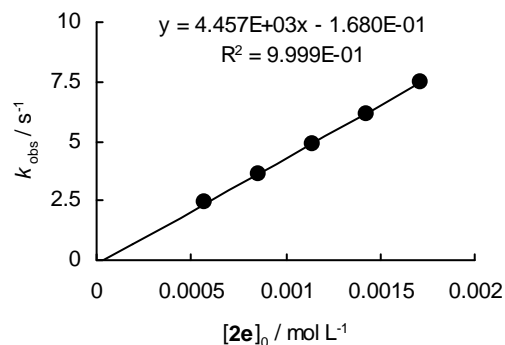
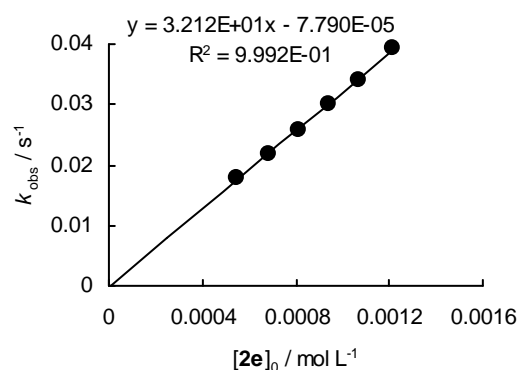


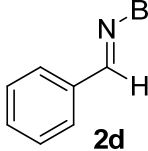
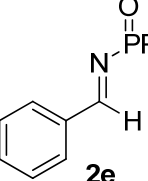
Table 34: Kinetics of the reaction of **4b** with **2e** in DMSO at 20°C (diode array UV-Vis spectrometer, $\lambda = 520$ nm).

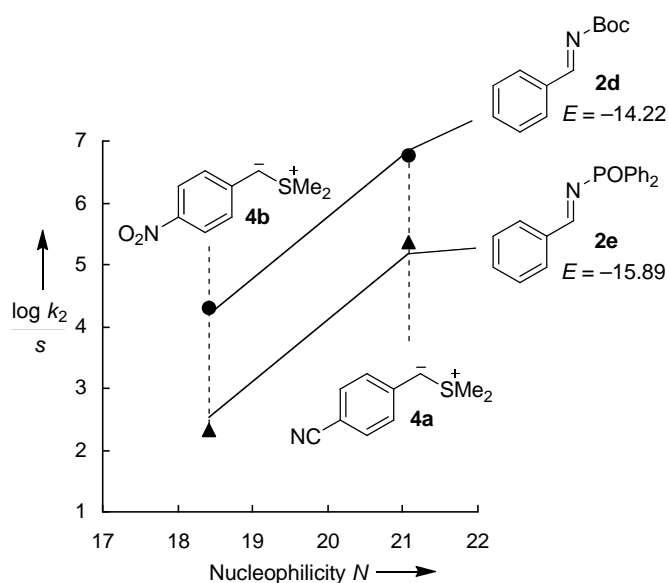
No.	[4b] ₀ / mol L ⁻¹ *	[2e] ₀ / mol L ⁻¹	<i>k</i> _{obs} / s ⁻¹
RAK 23.46-1	$\approx 5 \times 10^{-5}$	5.44×10^{-4}	1.77×10^{-2}
RAK 23.46-2	$\approx 6 \times 10^{-5}$	6.82×10^{-4}	2.17×10^{-2}
RAK 23.46-3	$\approx 6 \times 10^{-5}$	8.09×10^{-4}	2.57×10^{-2}
RAK 23.46-4	$\approx 6 \times 10^{-5}$	9.41×10^{-4}	3.00×10^{-2}
RAK 23.46-5	$\approx 6 \times 10^{-5}$	1.07×10^{-3}	3.41×10^{-2}
RAK 23.46-6	$\approx 6 \times 10^{-5}$	1.21×10^{-3}	3.92×10^{-2}

$k_2 = 3.21 \times 10^1 \text{ L mol}^{-1} \text{ s}^{-1}$

* Only approximate values are given for the initial concentration of the nucleophile (see general comments).

**Table 35:** Determination of the electrophilicity parameters *E* for **2d,e** (least-squares minimization of $\Delta^2 = \sum(\log k_2 - s(N + E))^2$ for the correlation of $\log k_2 / s$ of the reactions of **2d,e** with **4a,b** versus the nucleophilicity parameters *N* for **4a,b**).

Electrophile	Nucleophile (<i>N</i> , <i>s</i>)	<i>k</i> ₂ / L mol ⁻¹ s ⁻¹	Electrophilicity <i>E</i>
 2d	4a (21.07, 0.68)	3.97×10^4	<i>E</i> (2d) = -14.22
	4b (18.42, 0.65)	6.17×10^2	
 2e	4a (21.07, 0.68)	4.46×10^3	<i>E</i> (2e) = -15.89
	4b (18.42, 0.65)	3.21×10^1	

**Figure 10:** Correlation of the second-order rate constants ($\log k_2 / s$) for the reactions of the sulfur ylides **4a,b** with the imines **2d,e** versus the nucleophilicity parameters *N* of **4a,b**. The slopes are fixed to one as required by $\log k_2 = s(N + E)$.

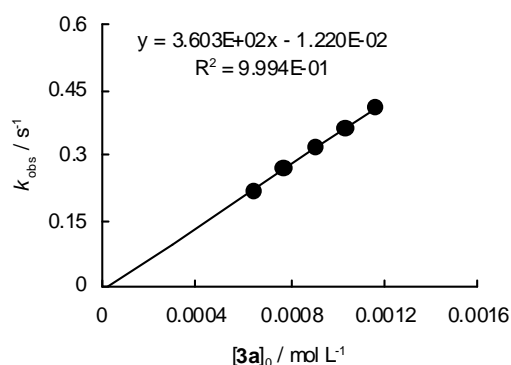
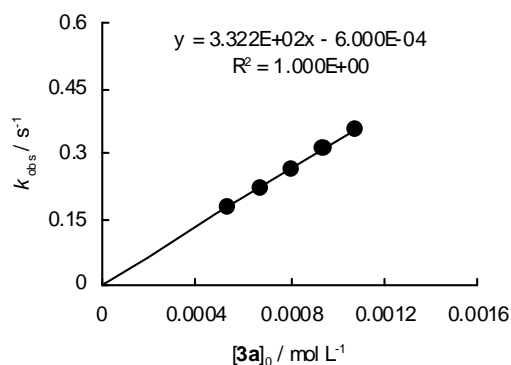
5.3.3 Reactions of the Sulfur Ylides 4a,b with the Enones 3a–f

Reactions of the sulfur ylides 4a,b with enone 3a

Table 36: Kinetics of the reaction of **4a** with **3a** in DMSO at 20°C (stopped-flow UV-Vis spectrometer, $\lambda = 400$ nm).

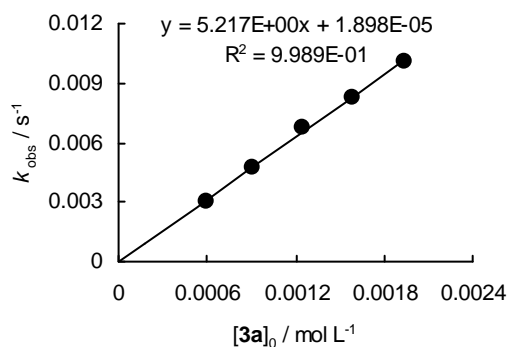
No.	[4a] ₀ / mol L ⁻¹ *	[3a] ₀ / mol L ⁻¹	$k_{\text{obs}}/ \text{s}^{-1}$
RAK 23.10-1	$\approx 5 \times 10^{-5}$	5.37×10^{-4}	1.78×10^{-1}
RAK 23.10-2	$\approx 5 \times 10^{-5}$	6.71×10^{-4}	2.22×10^{-1}
RAK 23.10-3	$\approx 5 \times 10^{-5}$	8.06×10^{-4}	2.67×10^{-1}
RAK 23.10-4	$\approx 5 \times 10^{-5}$	9.40×10^{-4}	3.12×10^{-1}
RAK 23.10-5	$\approx 5 \times 10^{-5}$	1.07×10^{-3}	3.56×10^{-1}
$k_2 = 3.32 \times 10^2 \text{ L mol}^{-1} \text{ s}^{-1}$			
RAK 23.10-2-1	$\approx 6 \times 10^{-5}$	6.47×10^{-4}	2.19×10^{-1}
RAK 23.10-2-2	$\approx 6 \times 10^{-5}$	7.76×10^{-4}	2.69×10^{-1}
RAK 23.10-2-3	$\approx 6 \times 10^{-5}$	9.05×10^{-4}	3.16×10^{-1}
RAK 23.10-2-4	$\approx 6 \times 10^{-5}$	1.03×10^{-3}	3.59×10^{-1}
RAK 23.10-2-5	$\approx 6 \times 10^{-5}$	1.16×10^{-3}	4.07×10^{-1}
$k_2 = 3.60 \times 10^2 \text{ L mol}^{-1} \text{ s}^{-1}$			
Average: $k_2 = 3.46 \times 10^2 \text{ L mol}^{-1} \text{ s}^{-1}$			

* Only approximate values are given for the initial concentration of the nucleophile (see general comments).

**Table 37:** Kinetics of the reaction of **4b** with **3a** in DMSO at 20°C (diode array UV-Vis spectrometer, $\lambda = 520$ nm).

No.	[4b] ₀ / mol L ⁻¹ *	[3a] ₀ / mol L ⁻¹	$k_{\text{obs}}/ \text{s}^{-1}$
RAK 23.6-1	$\approx 6 \times 10^{-5}$	5.99×10^{-4}	3.07×10^{-3}
RAK 23.6-2	$\approx 6 \times 10^{-5}$	9.11×10^{-4}	4.77×10^{-3}
RAK 23.6-3	$\approx 6 \times 10^{-5}$	1.25×10^{-3}	6.71×10^{-3}
RAK 23.6-4	$\approx 6 \times 10^{-5}$	1.58×10^{-3}	8.25×10^{-3}
RAK 23.6-5	$\approx 6 \times 10^{-5}$	1.94×10^{-3}	1.01×10^{-2}
$k_2 = 5.22 \text{ L mol}^{-1} \text{ s}^{-1}$			

* Only approximate values are given for the initial concentration of the nucleophile (see general comments).

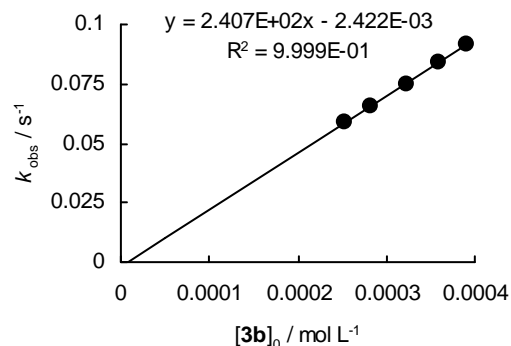


Reactions of the sulfur ylides **4a,b** with enone **3b****Table 38:** Kinetics of the reaction of **4a** with **3b** in DMSO at 20°C (diode array UV-Vis spectrometer, $\lambda = 400$ nm).

No.	[4a] ₀ / mol L ⁻¹ *	[3b] ₀ / mol L ⁻¹	$k_{\text{obs}} / \text{s}^{-1}$
RAK 23.11-5	$\approx 2 \times 10^{-5}$	2.53×10^{-4}	5.85×10^{-2}
RAK 23.11-2	$\approx 3 \times 10^{-5}$	2.82×10^{-4}	6.55×10^{-2}
RAK 23.11-3	$\approx 3 \times 10^{-5}$	3.23×10^{-4}	7.50×10^{-2}
RAK 23.11-1	$\approx 3 \times 10^{-5}$	3.60×10^{-4}	8.42×10^{-2}
RAK 23.11-4	$\approx 3 \times 10^{-5}$	3.90×10^{-4}	9.16×10^{-2}

$$k_2 = 2.41 \times 10^2 \text{ L mol}^{-1} \text{ s}^{-1}$$

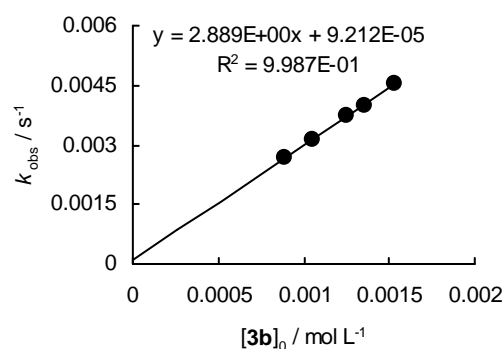
* Only approximate values are given for the initial concentration of the nucleophile (see general comments).

**Table 39:** Kinetics of the reaction of **4b** with **3b** in DMSO at 20°C (diode array UV-Vis spectrometer, $\lambda = 520$ nm).

No.	[4b] ₀ / mol L ⁻¹ *	[3b] ₀ / mol L ⁻¹	$k_{\text{obs}} / \text{s}^{-1}$
RAK 23.12-1	$\approx 4 \times 10^{-5}$	8.85×10^{-4}	2.65×10^{-3}
RAK 23.12-5	$\approx 8 \times 10^{-5}$	1.05×10^{-3}	3.12×10^{-3}
RAK 23.12-2	$\approx 5 \times 10^{-5}$	1.25×10^{-3}	3.74×10^{-3}
RAK 23.12-4	$\approx 8 \times 10^{-5}$	1.35×10^{-3}	3.97×10^{-3}
RAK 23.12-3	$\approx 8 \times 10^{-5}$	1.54×10^{-3}	4.53×10^{-3}

$$k_2 = 2.89 \text{ L mol}^{-1} \text{ s}^{-1}$$

* Only approximate values are given for the initial concentration of the nucleophile (see general comments).

Reaction of the sulfur ylide **4a** with enone **3c****Table 40:** Kinetics of the reaction of **4a** with **3c** in DMSO at 20°C (diode array UV-Vis spectrometer, $\lambda = 380$ nm).

No.	[4a] ₀ / mol L ⁻¹ *	[3c] ₀ / mol L ⁻¹	$k_{\text{obs}} / \text{s}^{-1}$
RAK 23.25-1	$\approx 4 \times 10^{-5}$	5.02×10^{-4}	1.81×10^{-2}
RAK 23.25-2	$\approx 5 \times 10^{-5}$	7.56×10^{-4}	2.60×10^{-2}
RAK 23.25-3	$\approx 5 \times 10^{-5}$	9.93×10^{-4}	3.44×10^{-2}
RAK 23.25-4	$\approx 5 \times 10^{-5}$	1.11×10^{-3}	3.83×10^{-2}
RAK 23.25-5	$\approx 5 \times 10^{-5}$	1.23×10^{-3}	4.28×10^{-2}

$$k_2 = 3.41 \times 10^4 \text{ L mol}^{-1} \text{ s}^{-1}$$

* Only approximate values are given for the initial concentration of the nucleophile (see general comments).

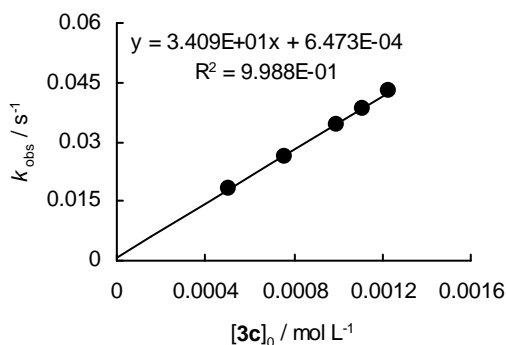
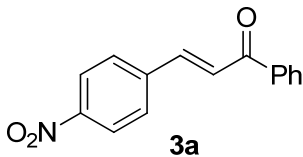
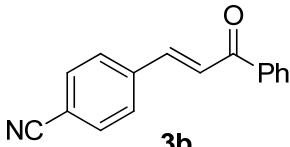
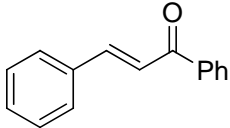


Table 41: Determination of the electrophilicity parameters E for **3a–c** (least-squares minimization of $\Delta^2 = \sum(\log k_2 - s(N+ E))^2$ for the correlation of $\log k_2 / s$ of the reactions of **3a,b** with **4a,b** versus the nucleophilicity parameters N for **4a,b**; Calculation of the electrophilicity parameter E for **3c** using the second-order rate constants for its reaction with sulfur ylide **4a** ($N = 21.07$, $s = 0.68$) and correlation equation $\log k_2 = s(N+ E)$).

Electrophile	Nucleophile (N, s)	$k_2 / \text{L mol}^{-1} \text{s}^{-1}$	Electrophilicity E
 3a	4a (21.07, 0.68)	3.46×10^2	$E(\mathbf{3a}) = -17.33$
	4b (18.42, 0.65)	5.22	
 3b	4a (21.07, 0.68)	2.41×10^2	$E(\mathbf{3b}) = -17.64$
	4b (18.42, 0.65)	2.89	
 3c	4a (21.07, 0.68)	3.41×10^1	$E(\mathbf{3c}) = -18.82$

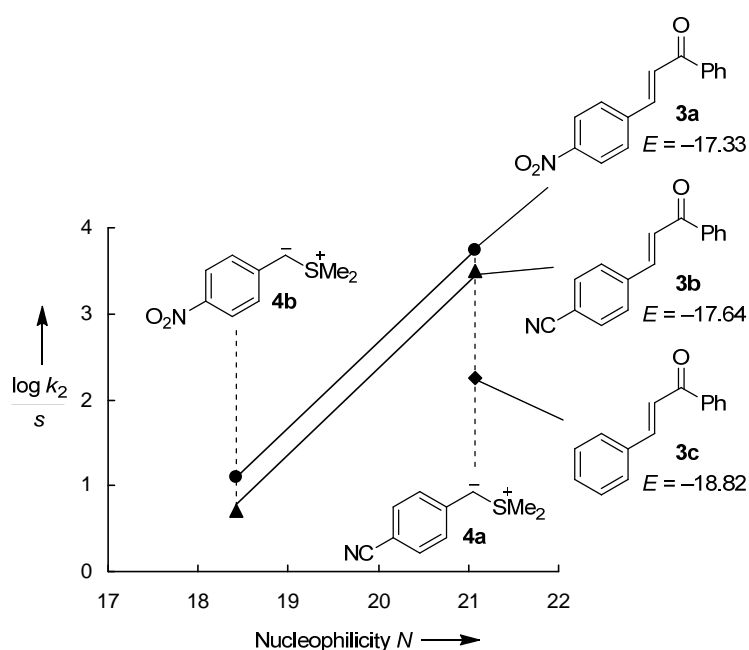
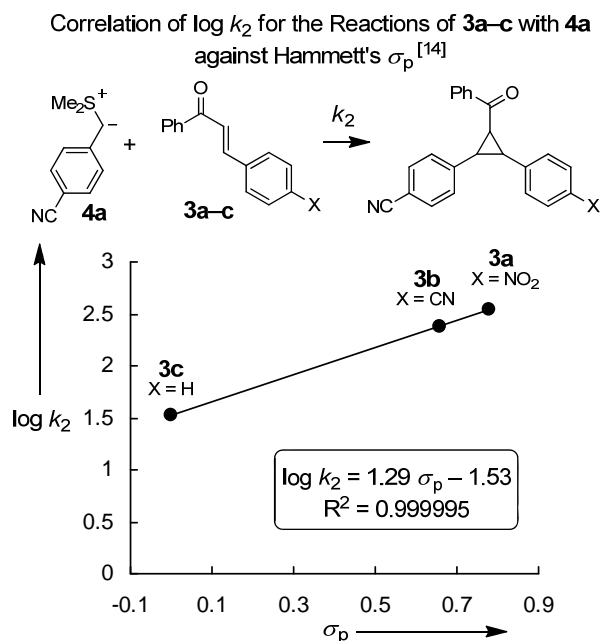


Figure 11: Correlation of the second-order rate constants ($\log k_2 / s$) for the reactions of the sulfur ylides **4a,b** with the enones **3a–c** versus the nucleophilicity parameters N of **4a,b**. The slopes are fixed to one as required by $\log k_2 = s(N+ E)$.



Reactions of the sulfur ylide **4a** with enones **3d–f**

Table 42: Kinetics of the reaction of **4a** with **3d** in DMSO at 20°C (diode array UV-Vis spectrometer, $\lambda = 380$ nm).

No.	$[\mathbf{4a}]_0 / \text{mol L}^{-1}$ *	$[\mathbf{3d}]_0 / \text{mol L}^{-1}$	$k_{\text{obs}} / \text{s}^{-1}$
RAK 23.54-1	$\approx 6 \times 10^{-5}$	5.69×10^{-4}	1.22×10^{-2}
RAK 23.54-2	$\approx 6 \times 10^{-5}$	7.21×10^{-4}	1.54×10^{-2}
RAK 23.54-3	$\approx 6 \times 10^{-5}$	8.80×10^{-4}	1.85×10^{-2}
RAK 23.54-4	$\approx 6 \times 10^{-5}$	1.03×10^{-3}	2.13×10^{-2}
RAK 23.54-5	$\approx 6 \times 10^{-5}$	1.18×10^{-3}	2.47×10^{-2}

$$k_2 = 2.02 \times 10^1 \text{ L mol}^{-1} \text{ s}^{-1}$$

* Only approximate values are given for the initial concentration of the nucleophile (see general comments).

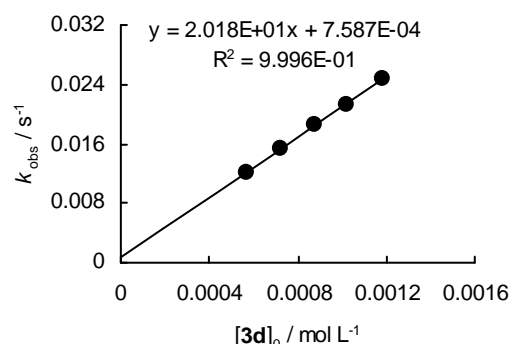


Table 43: Kinetics of the reaction of **4a** with **3e** in DMSO at 20°C (diode array UV-Vis spectrometer, $\lambda = 380$ nm).

No.	$[\mathbf{4a}]_0 / \text{mol L}^{-1}$ *	$[\mathbf{3e}]_0 / \text{mol L}^{-1}$	$k_{\text{obs}} / \text{s}^{-1}$
RAK 23.53-1	$\approx 5 \times 10^{-5}$	5.96×10^{-4}	1.25×10^{-2}
RAK 23.53-2	$\approx 6 \times 10^{-5}$	7.52×10^{-4}	1.57×10^{-2}
RAK 23.53-3	$\approx 6 \times 10^{-5}$	8.87×10^{-4}	1.84×10^{-2}
RAK 23.53-4	$\approx 6 \times 10^{-5}$	1.03×10^{-3}	2.11×10^{-2}
RAK 23.53-5	$\approx 6 \times 10^{-5}$	1.18×10^{-3}	2.41×10^{-2}

$$k_2 = 1.97 \times 10^1 \text{ L mol}^{-1} \text{ s}^{-1}$$

* Only approximate values are given for the initial concentration of the nucleophile (see general comments).

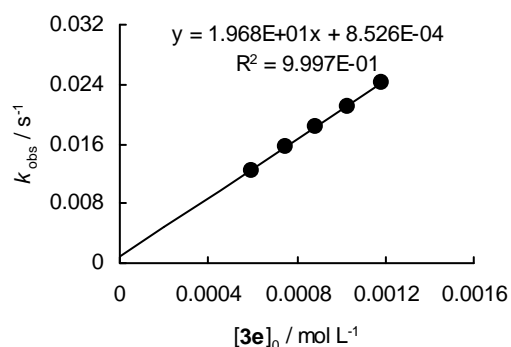
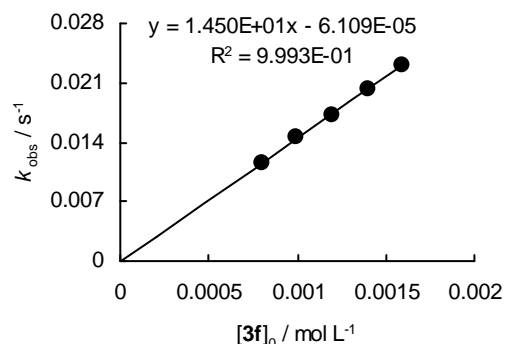


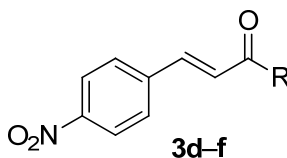
Table 44: Kinetics of the reaction of **4a** with **3f** in DMSO at 20°C (diode array UV-Vis spectrometer, $\lambda = 380$ nm).

No.	[4a] ₀ / mol L ⁻¹ *	[3f] ₀ / mol L ⁻¹	<i>k</i> _{obs} / s ⁻¹
RAK 23.15-2-1	≈ 4 × 10 ⁻⁵	8.01 × 10 ⁻⁴	1.15 × 10 ⁻²
RAK 23.15-2-2	≈ 5 × 10 ⁻⁵	9.92 × 10 ⁻⁴	1.45 × 10 ⁻²
RAK 23.15-2-3	≈ 6 × 10 ⁻⁵	1.20 × 10 ⁻³	1.72 × 10 ⁻²
RAK 23.15-2-4	≈ 6 × 10 ⁻⁵	1.40 × 10 ⁻³	2.03 × 10 ⁻²
RAK 23.15-2-5	≈ 6 × 10 ⁻⁵	1.59 × 10 ⁻³	2.31 × 10 ⁻²

$$k_2 = 1.45 \times 10^1 \text{ L mol}^{-1} \text{ s}^{-1}$$

* Only approximate values are given for the initial concentration of the nucleophile (see general comments).

**Table 45:** Calculation of the electrophilicity parameters *E* for **3d–f** using the second-order rate constants for their reactions with sulfur ylide **4a** ($N = 21.07$, $s = 0.68$) and correlation equation $\log k_2 = s(N + E)$.

Electrophile	<i>k</i> ₂ / L mol ⁻¹ s ⁻¹	Electrophilicity <i>E</i>
 3d (R = <i>t</i> Bu)	2.02 × 10 ¹	<i>E</i> (3d) = -19.15
3e (R = <i>i</i> Pr)	1.97 × 10 ¹	<i>E</i> (3e) = -19.17
3f (R = Me)	1.45 × 10 ¹	<i>E</i> (3f) = -19.36

6 References

- [1] (a) Mayr, H.; Patz, M. *Angew. Chem.* **1994**, *106*, 990-1010; *Angew. Chem. Int. Ed. Engl.* **1994**, *33*, 938-957. (b) Mayr, H.; Bug, T.; Gotta, M. F.; Hering, N.; Irrgang, B.; Janker, B.; Kempf, B.; Loos, R.; Ofial, A. R.; Remennikov, G.; Schimmel, H. *J. Am. Chem. Soc.* **2001**, *123*, 9500-9512. (c) Lucius, R.; Loos, R.; Mayr, H. *Angew. Chem.* **2002**, *114*, 97-102; *Angew. Chem. Int. Ed.* **2002**, *41*, 91-95. (d) Mayr, H.; Kempf, B.; Ofial, A. R. *Acc. Chem. Res.* **2003**, *36*, 66-77. (e) Mayr, H.; Ofial, A. R. *Pure Appl. Chem.* **2005**, *77*, 1807-1821. (f) Mayr, H.; Ofial, A. R. *J. Phys. Org. Chem.* **2008**, *21*, 584-595. (g) For a comprehensive database of nucleophilicity parameters *N* and *s* as well as electrophilicity parameters *E*, see <http://www.cup.lmu.de/oc/mayr/>.
- [2] (a) Lemek, T.; Mayr, H. *J. Org. Chem.* **2003**, *68*, 6880-6886. (b) Berger, S. T. A.; Seeliger, F. H.; Hofbauer, F.; Mayr, H. *Org. Biomol. Chem.* **2007**, *5*, 3020-3026. (c) Seeliger, F.; Berger, S. T. A.; Remennikov, G. Y.; Polborn, K.; Mayr, H. *J. Org. Chem.* **2007**, *72*, 9170-9180. (d) Kaumanns, O.; Lucius, R.; Mayr, H. *Chem. Eur. J.* **2008**, *14*, 9675-9682. (e) Kaumanns, O.; Mayr, H. *J. Org. Chem.* **2008**, *73*, 2738-2745. (f) Lakhdar, S.; Tokuyasu, T.; Mayr, H. *Angew. Chem.* **2008**, *120*, 8851-8854; *Angew. Chem. Int. Ed.* **2008**, *47*, 8723-8725.

- [3] (a) Yoshimine, M.; Hatch, M. J. *J. Am. Chem. Soc.* **1967**, *89*, 5831-5838. (b) Johnson, C. R.; Schroeck, C. W. *J. Am. Chem. Soc.* **1971**, *93*, 5303-5305. (c) Volatron, F.; Eisenstein, O. *J. Am. Chem. Soc.* **1987**, *109*, 1-14. (d) For the special case of a Corey-Chaykovsky reaction with oxathietane formation, see: Kawashima, T.; Ohno, F.; Okazaki, R.; Ikeda, H.; Inagaki, S. *J. Am. Chem. Soc.* **1996**, *118*, 12455-12456. (e) Aggarwal, V. K.; Calamai, S.; Ford, J. G. *J. Chem. Soc., Perkin Trans. 1* **1997**, 593-599. (f) Lindvall, M. K.; Koskinen, A. M. P. *J. Org. Chem.* **1999**, *64*, 4596-4606. (g) Myllymäki, V. T.; Lindvall, M. K.; Koskinen, A. M. P. *Tetrahedron* **2001**, *57*, 4629-4635. (h) Aggarwal, V. K.; Harvey, J. N.; Richardson, J. *J. Am. Chem. Soc.* **2002**, *124*, 5747-5756. (i) Silva, M. A.; Bellenie, B. R.; Goodman, J. M. *Org. Lett.* **2004**, *6*, 2559-2562. (j) Aggarwal, V. K.; Bi, J. *Beilstein J. Org. Chem.* **2005**, *1*, doi: 10.1186/1860-5397-1-4. (k) Aggarwal, V. K.; Hebach, C. *Org. Biomol. Chem.* **2005**, *3*, 1419-1427. (l) Aggarwal, V. K.; Charmant, J. P. H.; Fuentes, D.; Harvey, J. N.; Hynd, G.; Ohara, D.; Picoul, W.; Robiette, R.; Smith, C.; Vasse, J.-L.; Winn, C. L. *J. Am. Chem. Soc.* **2006**, *128*, 2105-2114. (m) Edwards, D. R.; Du, J.; Crudden, C. M. *Org. Lett.* **2007**, *9*, 2397-2400. (n) Edwards, D. R.; Montoya-Peleaz, P.; Crudden, C. M. *Org. Lett.* **2007**, *9*, 5481-5484.
- [4] (a) Aggarwal, V. K.; Charmant, J. P. H.; Ciampi, C.; Hornby, J. M.; O'Brien, C. J.; Hynd, G.; Parsons, R. *J. Chem. Soc., Perkin Trans. 1* **2001**, 3159-3166. (b) Yang, X.-F.; Zhang, M.-J.; Hou, X.-L.; Dai, L.-X. *J. Org. Chem.* **2002**, *67*, 8097-8103. (c) Robiette, R. *J. Org. Chem.* **2006**, *71*, 2726-2734. (d) Janardanan, D.; Sunoj, R. B. *Chem. Eur. J.* **2007**, *13*, 4805-4815. (e) Janardanan, D.; Sunoj, R. B. *J. Org. Chem.* **2008**, *73*, 8163-8174.
- [5] (a) Midura, W. H.; Krysiak, J. A.; Cypryk, M.; Mikolajczyk, M.; Wieczorek, M. W.; Filipczak, A. D. *Eur. J. Org. Chem.* **2005**, 653-662. (b) Aggarwal, V. K.; Grange, E. *Chem. Eur. J.* **2006**, *12*, 568-575. (c) Deng, X.-M.; Cai, P.; Ye, S.; Sun, X.-L.; Liao, W.-W.; Li, K.; Tang, Y.; Wu, Y.-D.; Dai, L.-X. *J. Am. Chem. Soc.* **2006**, *128*, 9730-9740. (d) Janardanan, D.; Sunoj, R. B. *J. Org. Chem.* **2007**, *72*, 331-341. (e) Riches, S. L.; Saha, C.; Filgueira, N. F.; Grange, E.; McGarrigle, E. M.; Aggarwal, V. K. *J. Am. Chem. Soc.* **2010**, *132*, 7626-7630.
- [6] (a) Lakhdar, S.; Appel, R.; Mayr, H. *Angew. Chem.* **2009**, *121*, 5134-5137; *Angew. Chem. Int. Ed.* **2009**, *48*, 5034-5037. (b) Appel, R.; Hartmann, N.; Mayr, H. *J. Am. Chem. Soc.* **2010**, *132*, 17894-17900.
- [7] Bug, T.; Lemek, T.; Mayr, H. *J. Org. Chem.* **2004**, *69*, 7565-7576.

- [8] Appel, R.; Mayr, H. *Chem. Eur. J.* **2010**, *16*, 8610-8614.
- [9] Appel, R.; Loos, R.; Mayr, H. *J. Am. Chem. Soc.* **2009**, *131*, 704-714.
- [10] (a) Aggarwal, V. K.; Ford, J. G.; Fonquerna, S.; Adams, H.; Jones, R. V. H.; Fieldhouse, R. *J. Am. Chem. Soc.* **1998**, *120*, 8328-8339. (b) Solladié-Cavallo, A.; Bouérat, L.; Roje, M. *Tetrahedron Lett.* **2000**, *41*, 7309-7312. (c) Aggarwal, V. K.; Alonso, E.; Bae, I.; Hynd, G.; Lydon, K. M.; Palmer, M. J.; Patel, M.; Porcelloni, M.; Richardson, J.; Stenson, R. A.; Studley, J. R.; Vasse, J.-L.; Winn, C. L. *J. Am. Chem. Soc.* **2003**, *125*, 10926-10940. (d) Phillips, D. J.; Graham, A. E. *Synlett* **2010**, 769-773.
- [11] Shen, Y.; Jiang, G.-F. *J. Chem. Res.* **2000**, 140-141.
- [12] Nickson, T. E. *J. Org. Chem.* **1988**, *53*, 3870-3872.
- [13] The observed second-order kinetics would also be compatible with an intermediate syn-betaine formation, if its retro-addition would be much slower than the time window of our kinetic measurements ($v_{\text{syn}} \ll v_{\text{anti}}$). The formation of a long-lived betaine intermediate **11** can be considered as rather unlikely, however, because it has been shown that oxy-anion species, e.g., simple alkoxides, have very high pK_{aH} values in DMSO (Olmstead, W. N.; Margolin, Z.; Bordwell, F. G. *J. Org. Chem.* **1980**, *45*, 3295-3299) and are, therefore, thermodynamically unstable species. The syn-betaine **11** must, therefore, be a short-lived intermediate which rapidly reverts to sulfur ylide and aldehyde as its cyclization has not been observed.
- [14] Hansch, C.; Leo, A.; Taft, R. W. *Chem. Rev.* **1991**, *91*, 165-195.
- [15] Rüchardt, C.; Panse, P.; Eichler, S. *Chem. Ber.* **1967**, *100*, 1144-1164.
- [16] For selected references on the mechanism of the Wittig reaction, see: (a) Maryanoff, B. E.; Reitz, A. B. *Chem. Rev.* **1989**, *89*, 863-927. (b) Yamataka, H.; Nagareda, K.; Ando, K.; Hanafusa, T. *J. Org. Chem.* **1992**, *57*, 2865-2869. (c) Vedejs, E.; Peterson, M. J. *Top. Stereochem.* **1994**, *21*, 1-157. (d) Vedejs, E.; Peterson, M. J. In *Advances in Carbanion Chemistry*; Snieckus, V., Ed.; JAI Press: London, 1996; Vol. 2; p 1-85. (e) Yamataka, H.; Nagase, S. *J. Am. Chem. Soc.* **1998**, *120*, 7530-7536. (f) Robiette, R.; Richardson, J.; Aggarwal, V. K.; Harvey, J. N. *J. Am. Chem. Soc.* **2005**, *127*, 13468-13469. (g) Robiette, R.; Richardson, J.; Aggarwal, V. K.; Harvey, J. N. *J. Am. Chem. Soc.* **2006**, *128*, 2394-2409.
- [17] The mechanism of the Horner-Wadsworth-Emmons reaction is closely related to that of the Wittig reaction, although it is still controversial if the oxaphosphetane formation occurs concerted or stepwise. For selected references, see: (a) Larsen, R. O.; Aksnes, G. *Phosphorus, Sulfur Silicon Relat. Elem.* **1983**, *15*, 219-228. (b) Larsen, R. O.; Aksnes,

- G. Phosphorus, Sulfur Silicon Relat. Elem.* **1983**, *15*, 229-237. (c) ref 15a. (d) Brandt, P.; Norrby, P. O.; Martin, I.; Rein, T. *J. Org. Chem.* **1998**, *63*, 1280-1289. (e) Ando, K. *J. Org. Chem.* **1999**, *64*, 6815-6821. (f) Motoyoshiya, J.; Kusaura, T.; Kokin, K.; Yokoya, S.-i.; Takaguchi, Y.; Narita, S.; Aoyama, H. *Tetrahedron* **2001**, *57*, 1715-1721.
- [18] For selected reviews, see: (a) Jones, G. In *Organic Reactions*; Wiley: New York, 1967; Vol. 15, pp 204-599. (b) Tietze, L. F.; Beifuss, U. In *Comprehensive Organic Synthesis*; Trost, B. M., Fleming, I., Heathcock, C. H., Eds.; Pergamon Press: Oxford, 1991; Vol. 2, pp 341-394. (c) Smith, M. B.; March, J. *March's Advanced Organic Chemistry: Reactions, Mechanisms, and Structure*; 6th ed.; Wiley: Hoboken, NJ, 2007; pp 1358-1363.
- [19] For selected reviews, see: (a) Rosini, G. In *Comprehensive Organic Synthesis*; Trost, B. M., Fleming, I., Heathcock, C. H., Eds.; Pergamon Press: Oxford, 1991; Vol. 2, pp 321-340. (b) Ono, N. *The Nitro Group in Organic Syntheses*; Wiley-VCH: New York, 2001; pp 30-69. (c) Luzzio, F. A. *Tetrahedron* **2001**, *57*, 915-945. (d) Palomo, C.; Oiarbide, M.; Laso, A. *Eur. J. Org. Chem.* **2007**, 2561-2574.
- [20] The observation that the non-catalyzed reaction of 2-methylindole with p-nitrobenzaldehyde occurs at 90°C in alcohols and water, but not in aprotic solvents as DMSO or DMF illustrates the increase of the electrophilicities of aldehydes in protic solvents: He, F.; Li, P.; Gu, Y.; Li, G. *Green Chem.* **2009**, *11*, 1767-1773.
- [21] For selected references, see: (a) Schleyer, P. v. R.; Jemmis, E. D.; Spitznagel, G. W. *J. Am. Chem. Soc.* **1985**, *107*, 6393-6394. (b) Richard, J. P.; Amyes, T. L.; Rice, D. J. *J. Am. Chem. Soc.* **1993**, *115*, 2523-2524. (c) Rakus, K.; Verevkin, S. P.; Peng, W.-H.; Beckhaus, H.-D.; Rüchardt, C. *Liebigs Ann.* **1995**, 2059-2067.
- [22] (a) Bunting, J. W.; Toth, A.; Heo, C. K. M.; Moors, R. G. *J. Am. Chem. Soc.* **1990**, *112*, 8878-8885. (b) Heo, C. K. M.; Bunting, J. W. *J. Org. Chem.* **1992**, *57*, 3570-3578.
- [23] (a) Labuschagne, A. J. H.; Malherbe, J. S.; Meyer, C. J.; Schneider, D. F. *J. Chem. Soc., Perkin Trans. 1* **1978**, 955-961. (b) Coppola, G. M.; Hardtmann, G. E. *J. Heterocycl. Chem.* **1979**, *16*, 1605-1610.
- [24] Waley, S. G. *J. Chem. Soc.* **1948**, 2008-2011.
- [25] Reichardt, C.; Harbusch-Görnert, E.; Schäfer, G. *Liebigs Ann. Chem.* **1988**, 839-844.
- [26] (a) Jennings, W. B.; Lovely, C. J. *Tetrahedron Lett.* **1988**, *29*, 3725-3728. (b) Jennings, W. B.; Lovely, C. J. *Tetrahedron* **1991**, *47*, 5561-5568.
- [27] Kanazawa, A. M.; Denis, J.-N.; Greene, A. E. *J. Org. Chem.* **1994**, *59*, 1238-1240.
- [28] Oudeyer, S.; Léonel, E.; Paugam, J. P.; Nédélec, J.-Y. *Synthesis* **2004**, 389-400.

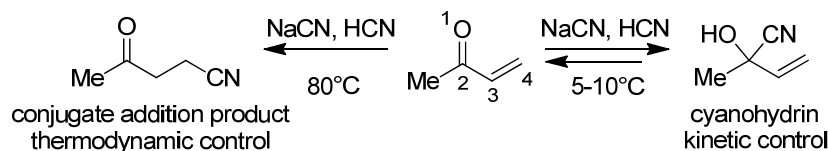
- [29] Gui, Y.; Shen, S.; Wang, H.-Y.; Li, Z.-Y.; Huang, Z.-Z. *Chem. Lett.* **2007**, *36*, 1436-1437.
- [30] (a) Qian, C.; Gao, F.; Chen, R. *Tetrahedron Lett.* **2001**, *42*, 4673-4675. (b) Gao, F.; Deng, M.; Qian, C. *Tetrahedron* **2005**, *61*, 12238-12243.

Chapter 8: Ambident Electrophilicity of a Cinnamaldehyde-Derived Imine

1 Introduction

In a series of investigations, it has been shown that the reactivity of typical ambident nucleophiles, e.g., SCN^- ,^[1] $\text{R}_2\text{C}=\text{NO}_2^-$,^[2] CN^- ,^[3] NO_2^- ,^[4] OCN^- ,^[5] and PhSO_2^- ,^[6] cannot be consistently rationalized by Pearson's principle of hard and soft acids and bases (HSAB)^[7] or by the related Klopman-Salem concept of charge- and frontier-orbital-controlled reactions.^[8] An alternative rationalization of the regioselectivity of ambident nucleophilic positions has been suggested. As illustrated by a quotation of Anslyn's and Dougherty's Modern Physical Organic Chemistry textbook, the HSAB- and Klopman-Salem concepts are also used for the explanation of the ambident electrophilicity of α,β -unsaturated carbonyl compounds: "(...) *Hard nucleophiles such as lithium reagents and Grignard reagents undergo preferential 1,2-addition, while softer nucleophiles such as amines, enolates, and thiolates undergo preferential 1,4-addition. (...) The harder nucleophiles are directed to the carbonyl carbon because their counter ions coordinate to the carbonyl oxygen as part of the mechanism of attack, and these nucleophiles are closely ion-paired, thereby delivering the nucleophile to the carbon. The softer nucleophiles tend to add to the site where the largest orbital character in the LUMO exists, which is the β -carbon.*"^[9] In contrast to these explanations, it was shown that the cyanide anion can react with methyl vinyl ketone both at the carbonyl group and at the conjugate position, where the kinetically favored attack in 2-position is reversible and the thermodynamically favored attack in 4-position is irreversible (Scheme 1).^[10]

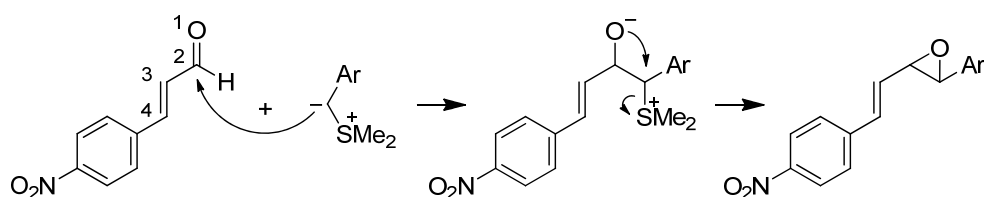
Scheme 1: Ambident Reaction of Cyanide with Methyl Vinyl Ketone.^[10]



A similar explanation was given for the modes of reactions of ambident cations derived from amides or esters in a review published by Hünig in 1964. The different structures of the isolated products under different conditions were explained by the result of the competition between a kinetically controlled but reversible reaction and a thermodynamically controlled reaction.^[11]

In our efforts to develop a comprehensive concept for the understanding of ambident reactivity in organic chemistry,^[12] we also set out for a systematic investigation of ambident electrophiles. As already shown in Scheme 1, α,β -unsaturated carbonyl compounds can be attacked by nucleophiles either at the 2-position or at the conjugate 4-position. We and other authors showed that aryl-stabilized sulfur ylides react with α,β -unsaturated aldehydes preferentially at the carbonyl group (2-position).^[13] In these cases, irreversible and rate-determining addition of the ylide to the carbonyl group is followed by a subsequent cyclization reaction to an epoxide, as shown exemplarily for the reaction of aryl-stabilized sulfur ylides with *p*-nitrocinnamaldehyde (Scheme 2).^[13e] In contrast to the reaction of cyanide with methyl vinyl ketone, the intramolecular cyclization to an epoxide prevents the reversion to the reactants, and, therefore, only the kinetically preferred addition to the carbonyl group is observed in reactions with aryl-stabilized sulfur ylides.

Scheme 2: Reactions of Aryl-Stabilized Sulfur Ylides with *p*-Nitrocinnamaldehyde.^[13e]



However, it was not possible to conveniently study the rates of the reactions of α,β -unsaturated aldehydes with other classes of nucleophiles than semi-stabilized sulfur ylides. For this reason, a different model compound for the investigation of ambident reactivities of α,β -unsaturated carbonyl compounds had to be employed. As *N*-tosyl-activated imines have been shown to react both with sulfur ylides and with carbanions,^[13e] we have systematically studied the rates of the reactions of imine **1** (Scheme 3) with the nucleophiles **2** (Table 1). The separate investigation of the reactivities of the two ambident electrophilic positions of imine **1** (i.e., 2- and 4-position) will be used to clarify, whether kinetic and thermodynamic control can also explain the regioselectivity of nucleophilic additions to imine **1**.

Scheme 3: Ambident Electrophilic Positions of Imine **1** (Ts = *p*-Methylbenzenesulfonyl).

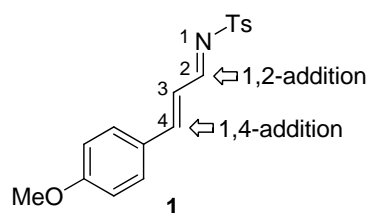
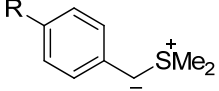
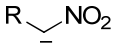
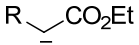
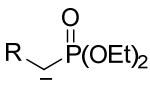
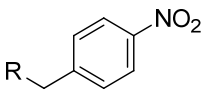
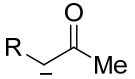


Table 1: Sulfur Ylide **2a**, Carbanions **2b–l**, and their Nucleophilicity Parameters N and s in DMSO at 20°C.

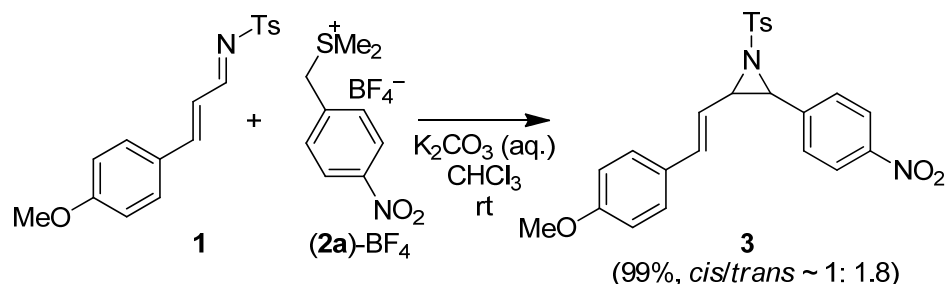
Nucleophile		R	$N (s)^a$
	2a	NO ₂	18.42 (0.65)
	2b	Me	21.54 (0.62)
	2c	H	20.71 (0.60)
	2d	S(O)Me	20.61 (0.64)
	2e	CO ₂ Et	20.22 (0.65)
	2f	CN	19.62 (0.67)
	2g	CO ₂ Et	19.23 (0.65)
	2h	CN	18.57 (0.66)
	2i	CN	19.67 (0.68)
	2j	SO ₂ Ph	18.50 (0.75)
	2k	CO ₂ Et	18.82 (0.69)
	2l	COMe	17.64 (0.73)

^a Nucleophilicity parameters N , s of **2a** were taken from ref 14, of **2b** from ref 15, of **2c** from ref 2, of **2d** from ref 16, of **2e,f,k,l** from ref 17, of **2g,h** from ref 18, of **2i** from ref 19, and of **2j** from ref 20.

2 Results

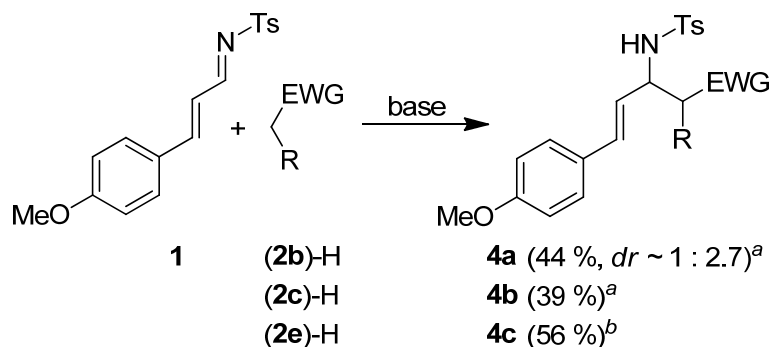
Product Analyses. In order to establish the course of the reactions, which have been studied kinetically, we have performed product studies of all combinations of the nucleophiles **2** with the imine **1**. In analogy to benzaldehyde-derived *N*-tosyl-activated imines,^[13e] the treatment of imine **1** with the aryl-stabilized sulfur ylide **2a** yields the aziridine **3** as a mixture of diastereomers (Scheme 4).

Scheme 4: Aziridination Reaction of Sulfur Ylide **2a** with Imine **1** (*cis/trans*-Ratio Corresponds to the Isolated Product).



The nitronate anions **2b,c** directly attack imine **1** at the imino group to form the addition products **4a** and **4b**, respectively (Scheme 5). Addition of the diethyl malonate anion (**2e**) at the 2-position of imine **1** to afford compound **4c** could only be achieved by working at low temperatures.

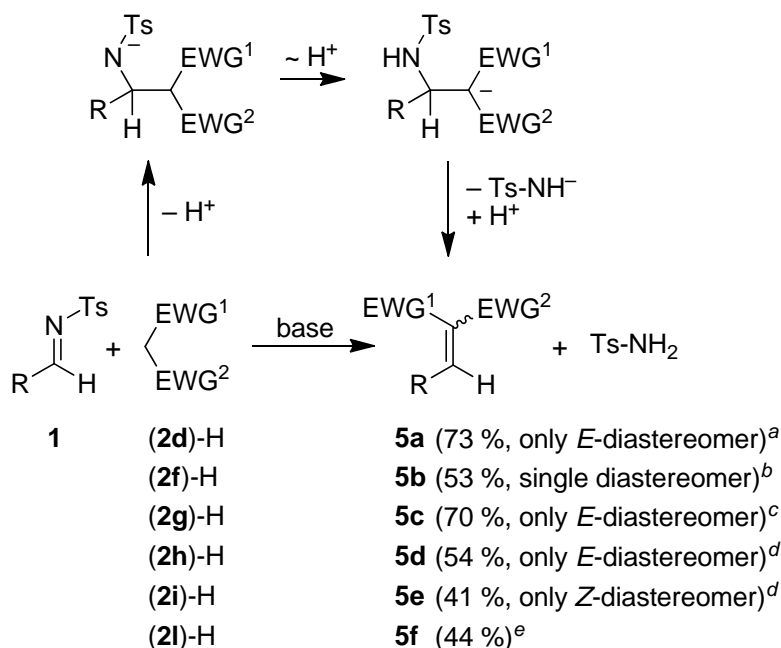
Scheme 5: Addition Reactions of the Carbanions **2b,c,e** at the Imino Group of Imine **1** (the *dr* Corresponds to the Isolated Product).



^a Et₃N (cat.), DMSO, rt. ^b KO^tBu, THF, < -70°C.

As shown in previous investigations,^[13e,21] *N*-tosyl-activated imines can undergo a Knoevenagel-type condensation reaction under loss of *p*-methylbenzenesulfonamide (Ts-NH₂), which was also observed when imine **1** was treated with the carbanions **2d,f-i,l** (Scheme 6).

Scheme 6: Condensation Reactions of the Carbanions **2d,f-i,l** at the Imino Group of Imine **1** and the Proposed Mechanism (R = (*E*)-*p*-MeO-C₆H₄-CH=CH-).

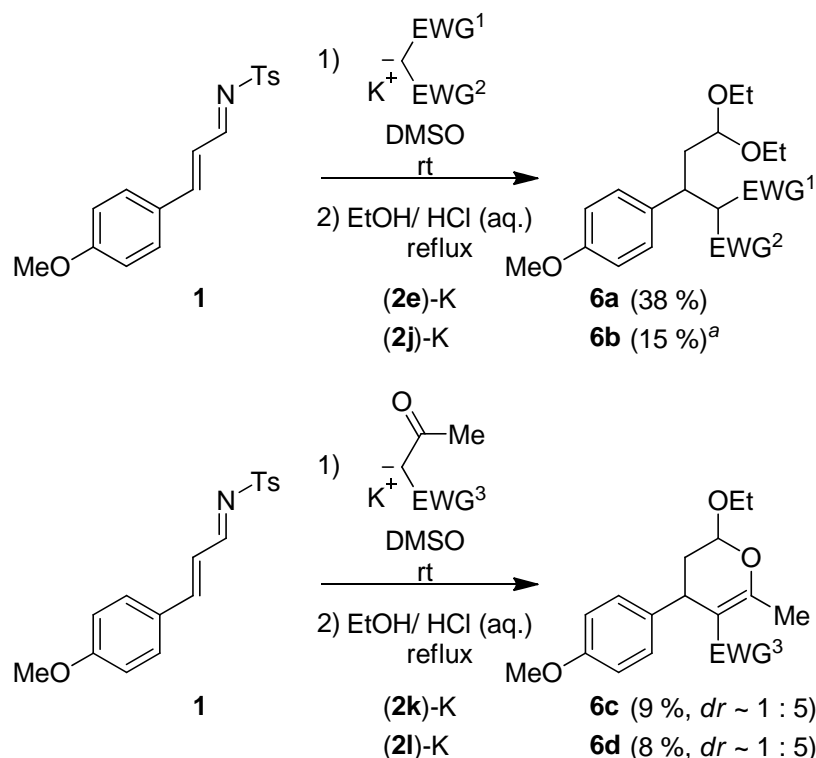


^a KO^tBu (cat.), Et₃N (cat.), DMSO, rt. ^b KO^tBu, THF, -20°C; Configuration (*E* or *Z*) was not be determined.

^c KO^tBu, THF, -40°C. ^d Et₃N (cat.), DMSO, rt. ^e KO^tBu, DMSO, rt.

While the diethyl malonate anion (**2e**) attacks imine **1** preferentially at the imino group at low temperatures (< -70°C), conjugate addition is preferred at room temperature (Scheme 7). The initially formed addition product between **2e** and **1** was subsequently hydrolyzed and immediately transferred to the acetal **6a**. The same reaction takes place when imine **1** was treated with the phenylsulfonyl-stabilized carbanion **2j**. In case of the methylcarbonyl-stabilized carbanions **2k,l** a cyclization reaction takes place before acetal formation and compounds **6c,d** could eventually be isolated. A proposed mechanism for the reactions in Scheme 7 (nucleophilic attack – hydrolysis – acetal formation – cyclization) is given in the Experimental Section.

Scheme 7: Addition Reactions of the Carbanions **2e,j** at the Conjugate Position of Imine **1** (*dr* Correspond to the Isolated Products).



^a Only major diastereomer isolated. *dr* could not be determined due to strongly superimposed NMR signals of diastereomers.

Kinetic Investigations. All kinetic investigations were performed in DMSO solution at 20°C. As reported earlier,^[14] the aryl-stabilized sulfur ylide **2a** is only persistent for a short time at room temperature and, therefore, was prepared by deprotonation of the corresponding C-H acid (**2a-H**)-BF₄ in dry THF at ≤ -50°C with 1.00-1.05 equiv of KO^{*t*}Bu. Small amounts of these solutions were dissolved in DMSO at room temperature directly before each kinetic experiment. Stock solutions of the carbanions **2b-I** were prepared by deprotonation of the corresponding CH acids (**2b-I**)-H with 1.00-1.05 equiv of KO^{*t*}Bu in DMSO. All kinetic investigations were monitored photometrically, either by following the disappearance of the colored imine **1**, the colored aryl-stabilized sulfur ylide **2a**, or the colored carbanions **2i,j** at or close to their absorption maxima. The kinetic investigations of the reactions of the carbanions **2b-h,k,l** with imine **1** (also prepared as stock solution in DMSO) were performed with a high excess of the nucleophiles over the electrophiles resulting in first-order kinetics. Vice versa, the first-order kinetics for the reactions of the aryl-stabilized ylide **2a** and the carbanions **2i,j** with imine **1** were realized by using at least 10 equiv of imine **1**. As the absolute concentration of the minor component is not crucial for the determination of the first-order

rate constants k_{obs} (eqs 1 and 2), we have thus circumvented the problem that the absolute concentration of the semi-stabilized ylide **2a** cannot precisely be determined due to its low stability.

From the exponential decays of the UV-Vis absorbances of imine **1** (Figure 1), the sulfur ylide **2a**, or the carbanions **2i,j**, the first-order rate constants k_{obs} were obtained. Plots of k_{obs} (s^{-1}) against the concentrations of the reaction partners used in excess were linear as required by the relations $k_{\text{obs}} = k_2[\text{Nu}]_0$ (eq 1, Figure 1) or $k_{\text{obs}} = k_2[\text{E}]_0$ (eq 2), respectively. Negligible intercepts for these plots were found for the reactions of imine **1** with sulfur ylide **2a**, the nitronates **2b,c**, the methylsulfinyl-stabilized carbanion **2d**, and the cyano-stabilized anion **2i** (when imine **1** was used in very high excess). For all other reactions, positive intercepts were found indicating equilibrium situations. However, the slopes of the plots of k_{obs} against $[\text{Nu}]_0$ or $[\text{E}]_0$ yielded the second-order rate constants k_2 of the corresponding reactions (Table 2, Figure 1).

$$-d[\text{E}]/dt = k_2 [\text{Nu}] [\text{E}] \quad \text{for } [\text{Nu}]_0 \gg [\text{E}]_0 \Rightarrow k_{\text{obs}} = k_2 [\text{Nu}]_0 \quad (1)$$

$$-d[\text{Nu}]/dt = k_2 [\text{Nu}] [\text{E}] \quad \text{for } [\text{E}]_0 \gg [\text{Nu}]_0 \Rightarrow k_{\text{obs}} = k_2 [\text{E}]_0 \quad (2)$$

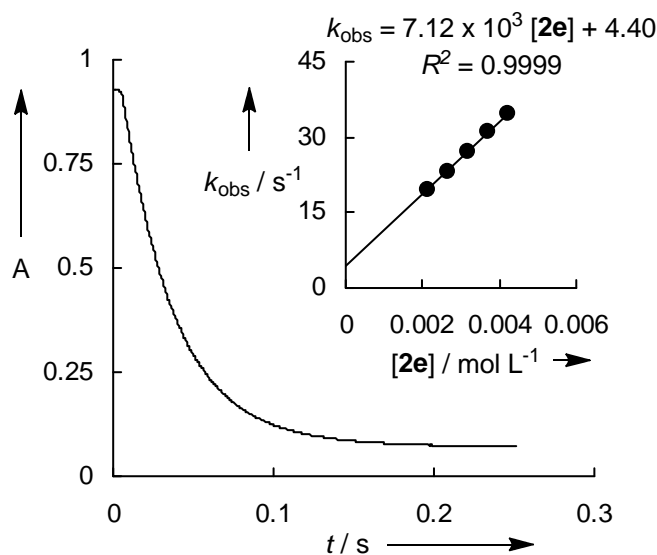


Figure 1: UV-Vis spectroscopic monitoring of the reaction of diethyl malonate anion (**2e**, $3.71 \times 10^{-3} \text{ mol L}^{-1}$) with the imine **1** ($2.60 \times 10^{-5} \text{ mol L}^{-1}$) at 358 nm in DMSO at 20°C. Insert: Determination of the second-order rate constant $k_2 = 7.12 \times 10^3 \text{ L mol}^{-1} \text{ s}^{-1}$ from the dependence of the first-order rate constant k_{obs} on the concentration of **2e**.

Figure 1 shows the mono-exponential decay of the absorbance of imine **1** after treatment with a high excess of diethyl malonate anion (**2e**). However, when a concentration of the carbanion

of less than 2 mmol L^{-1} was employed, a bis-exponential decay of the absorbance of the imine **1** was observed (Figure 2). These decays could be fitted by using GEPASI^[22] (i.e., a software package for modelling dynamics) and an appropriate kinetic model of two different additions of diethyl malonate anion (**2e**) to the imine **1**: one fast and reversible and one slow and irreversible addition.

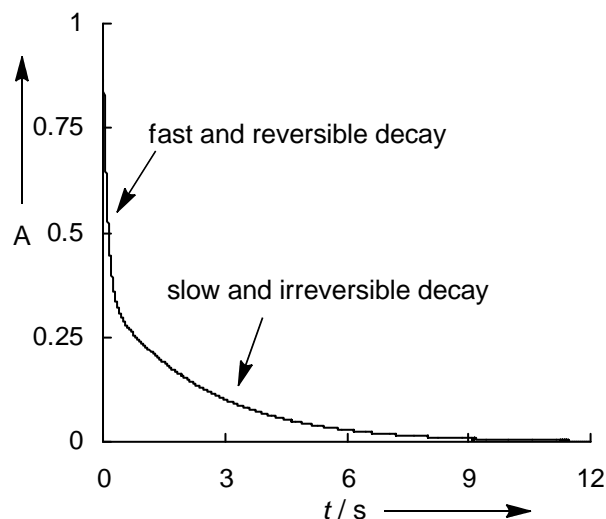


Figure 2: UV-Vis spectroscopic monitoring of the reaction of diethyl malonate anion (**2e**, $7.89 \times 10^{-4} \text{ mol L}^{-1}$) with the imine **1** ($2.38 \times 10^{-5} \text{ mol L}^{-1}$) at 358 nm in DMSO at 20°C.

A fast and slow decay of the absorption of the carbanion was also found during the reaction of *p*-nitrophenylacetonitrile anion (**2i**) with imine **1**. By using very high concentration of the imine ($> 3.5 \text{ mmol L}^{-1}$), the fast decay was observed exclusively. When smaller concentrations of the imine **1** were used ($< 1.5 \text{ mmol L}^{-1}$), the fast decay becomes less pronounced and a significantly slower decrease of the absorbance was observed. By using these different concentrations of imine **1**, it was possible to derive the second-order rate constants for the fast and the slow addition reaction independently.

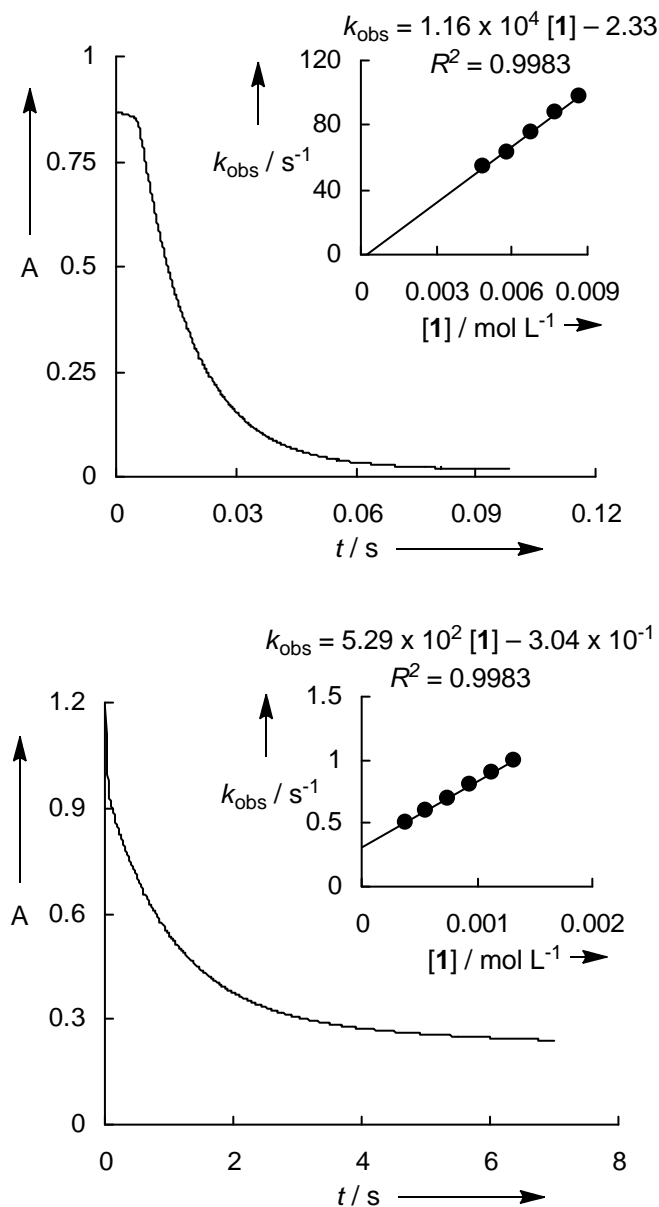


Figure 3: Fast and slow decays of the absorption of the *p*-nitrophenylacetonitrile anion (**2i**) during its reaction with imine **1** monitored at 530 nm (DMSO, 20°C). Inserts: Determination of the second-order rate constants $k_2 = 1.16 \times 10^4 \text{ L mol}^{-1} \text{ s}^{-1}$ and $k_2 = 5.29 \times 10^2 \text{ L mol}^{-1} \text{ s}^{-1}$ for the fast and slow addition of the carbanion **2i** to imine **1**.

In all the other reactions, it was only possible to study the rate constant of one type of addition of the carbanions **2** to imine **1** and Table 2 summarizes the obtained rate constants.

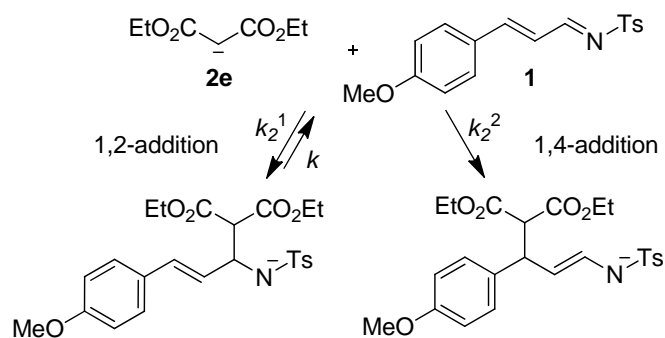
Table 2: Second-Order Rate Constants for the Reactions of Sulfur Ylide **2a** and the Carbanions **2b–l** with the Imine **1** in DMSO at 20°C.

Nucleophile	$k_2^1 / \text{M}^{-1} \text{s}^{-1}{}^a$	$k_2^2 / \text{M}^{-1} \text{s}^{-1}{}^b$	$k / \text{M}^{-1} \text{s}^{-1}{}^c$
2a	3.07×10^3	-	-
2b	1.63×10^5	-	-
2c	4.03×10^4	-	-
2d	1.46×10^5	-	-
2e	7.12×10^3	1.32×10^3	4.46
2f	-	6.08×10^2	-
2g	3.51×10^3	-	-
2h	2.00×10^4	-	-
2i	1.16×10^4	5.29×10^2	-
2j	-	1.79×10^2	-
2k	-	2.14×10^2	-
2l	-	9.22	-

^a Rate constant for the 1,2-addition reaction (see text for details). ^b Rate constant for the 1,4-addition reaction (see text for details). ^c Rate constant for the back reaction of reversible 1,2-addition (see text for details)

3 Discussion

Product analysis shows that the diethyl malonate anion (**2e**) attacks the imine **1** preferentially at the imino group at low temperatures, while conjugate addition is observed at room temperature. This finding can be interpreted by a fast but reversible addition of **2e** to the imino group, while a thermodynamically more favored but slower addition takes place at the 4-position (Scheme 8). At low temperatures, the faster addition at the 2-position becomes less reversible and the corresponding product can be isolated. On the contrary, the thermodynamically favored 1,4-addition product is formed at room temperature, when the 1,2-addition becomes reversible.

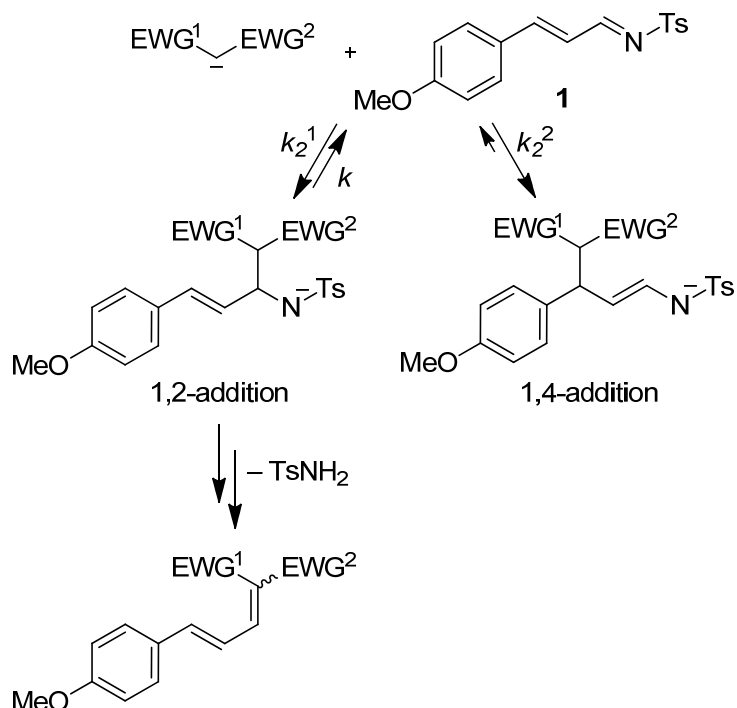
Scheme 8: Ambident Reaction of Diethyl Malonate Anion (**2e**) with the α,β -Unsaturated Imine **1**.

Therefore, we can conclude that the fast dynamics, which have been observed for the reactions of the nucleophiles **2** with imine **1** correspond to an attack at the imino group (k_2^1), while the slower dynamics reflect the conjugate addition (k_2^2). However, as shown in Table 2 and in Schemes 4-7, it was not possible to investigate both types of addition for every nucleophile-electrophile combination.

The nitronate anions **2b,c** are strong nucleophiles with high Lewis basicity and the attack at the 2-position of imine **1** is irreversible. A similar situation is found for sulfur ylide **2a**. Here, the attack at the imino group is irreversible, because it is followed by a fast cyclization reaction (i.e., aziridination, see Scheme 4). While the methylsulfinyl-stabilized carbanion **2d** was also found to react irreversibly at the 2-position of imine **1**, the addition of the phosphoryl-stabilized carbanions **2g,h** at the imino group are slightly reversible (indicated by incomplete consumption of the imine **1** during the kinetic experiments). The 1,2-addition of the carbanions **2f,i-l** to imine **1** become even more reversible and it was not possible anymore to determine the rate constants k_2^1 for all of these combinations (except for **2i**, when the imine **1** was used in very high excess, see Figure 3). In these cases, the rate constants for the 1,4-additions (k_2^2) could be determined instead.

Despite the high reversibility of the 1,2-additions and although 1,4-additions could be observed in the kinetic experiments of the carbanions **2e,f,i-l** with imine **1**, the corresponding 1,4-addition products could be only isolated from the reactions of **2e,j,k,l**. In the other cases, the subsequent, irreversible elimination of *p*-methylbenzenesulfonamide (Scheme 6) is shifting the equilibrium to the 1,2-addition product and as a consequence, only Knoevenagel-type condensation products can be isolated (Scheme 9). In analogous reactions with benzaldehyde-derived imines, the elimination of *p*-methylbenzenesulfonamide has been shown to proceed slowly.^[13e] We can, therefore, conclude that the initial attack of carbanions to imine **1** (1,2-addition and/or 1,4-addition) are observed within the time window of our kinetic experiments, but the slower subsequent elimination reaction can sometimes shift the equilibrium back to the 1,2-addition and only condensation products can be isolated. Therefore, the reversibility of the 1,2-addition as well as the tendency of the 1,2-addition product to eliminate *p*-methylbenzenesulfonamide decides if the 1,4-addition product of a certain carbanion-imine combination can be isolated.

Scheme 9: Irreversible Formation of Condensation Products During the Reaction of Carbanions with Imine **1** – A Subsequent Shift of the Kinetically Obtained Distribution of 1,2- and 1,4-Addition Products.



Correlation Analysis. In recent years, large efforts have been made for the construction of a most comprehensive nucleophilicity and electrophilicity scale. The basis for this quantification of polar organic reactivity is correlation equation 3, where $k_{20^\circ\text{C}}$ is the second-order rate constant in $\text{M}^{-1} \text{s}^{-1}$, s is a nucleophile-specific sensitivity parameter, N is a nucleophilicity parameter, and E is an electrophilicity parameter.^[14–20,23]

$$\log k_{20^\circ\text{C}} = s(N + E) \quad (3)$$

In order to determine the electrophilicity parameters E of imine **1** ($\log k_2$)/ s for the reactions of the nucleophiles **2** with the imine **1** versus the nucleophilicity parameters N of the nucleophiles **2** (Table 1) have been plotted in Figure 4, where two different correlation lines can be found (slopes are fixed to 1.0 as required by eq 3). While the upper correlation corresponds to the faster 1,2-addition reactions, the lower correlation corresponds to the slower 1,4-additions.

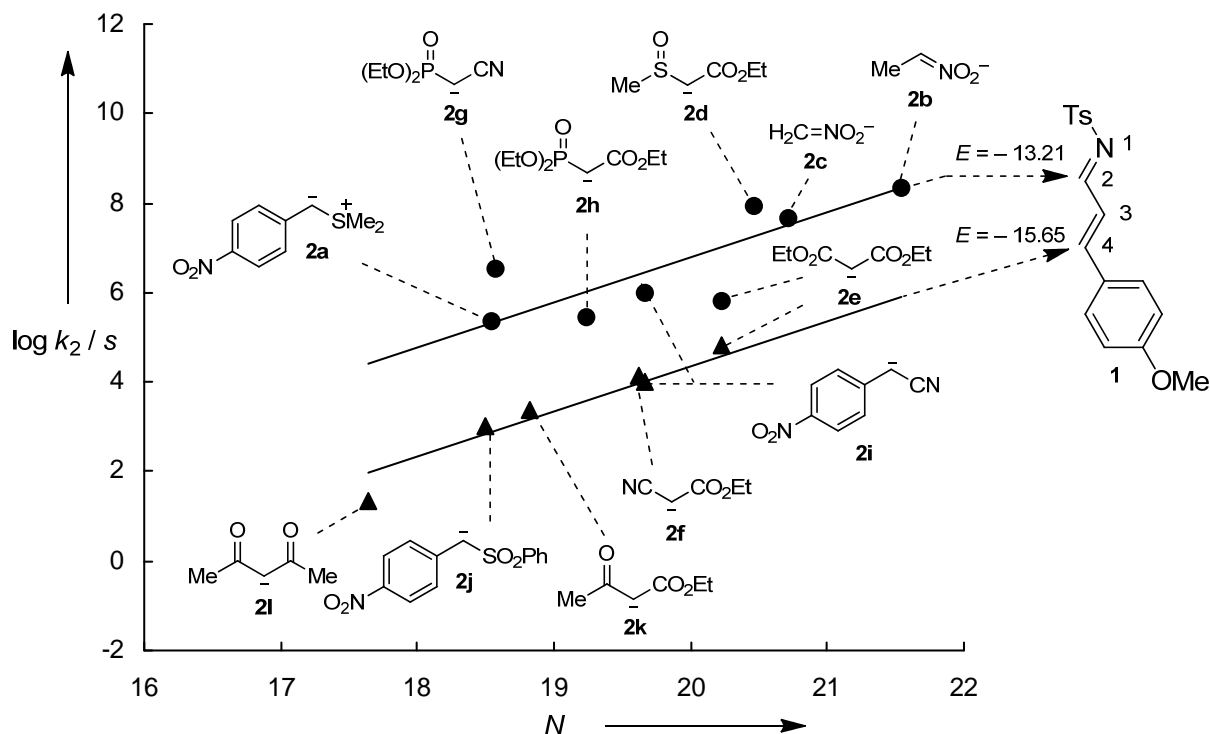


Figure 4: Correlation of $\log k_2 / s$ for the 1,2- and 1,4-additions of the nucleophiles **2** to imine **1** versus the nucleophilicity parameters N of the nucleophiles **2** in DMSO at 20°C. The slopes are fixed to one as required by eq 3.

As shown in Figure 4, the data points for the correlation line of 1,2-additions to imine **1** show a much larger scattering than that for the 1,4-addition reactions. As the nucleophilicity parameters for the carbanions **2b–l** were mainly derived from their reactions with quinone methides (i.e., Michael acceptors), a better correlation for the 1,4-addition reactions to imine **1** was expected. However, the correlation for the 1,2-addition shows a very similar pattern of scattering than it was previously found for the addition reactions of sulfur ylides and carbanions to benzaldehyde-derived *N*-tosyl-activated imines.^[13e] This finding is further illustrated in Figure 5, where a good correlation is found for the rates of the reactions of the nucleophiles **2a–e,g,h** with benzaldehyde-derived imine **7** and the rates for the attack of the nucleophiles **2a–e,g,h** at the 2-position of cinnamaldehyde-derived imine **1**.

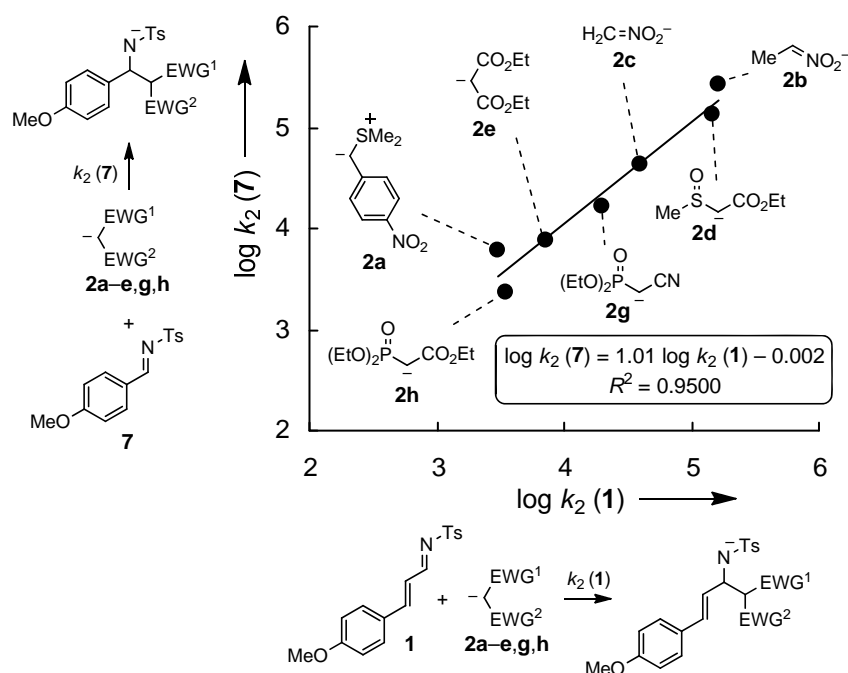


Figure 5: Correlation of the second-order rate constants for the reactions of the nucleophiles **2a–e,g,h** with benzaldehyde-derived imine **7** ($\log k_2(7)$) versus the second-order rate constants for the attack of the nucleophiles **2a–e,g,h** at the 2-position of cinnamaldehyde-derived imine **1** ($\log k_2(1)$).

Taking into account that all deviations from the correlation lines in Figure 4 are smaller than a factor of ten, we have calculated the electrophilicity parameters for the two ambident electrophilic positions of imine **1** by using least-squares minimization of $\Delta^2 = \sum(\log k_2 - s(N + E))^2$. The two ambident electrophilic positions of imine **1** differ approximately 2.5 orders of magnitude in electrophilic reactivity (Figure 6). While the conjugate position of imine **1** has a reactivity comparable to quinone methide **9**, the more reactive 2-position of imine **1** shows a reactivity comparable to benzylideneindandione **8**. Furthermore, the reactivity of the imino group of the cinnamaldehyde-derived imine **1** does not differ significantly from that of benzaldehyde-derived imine **7**.

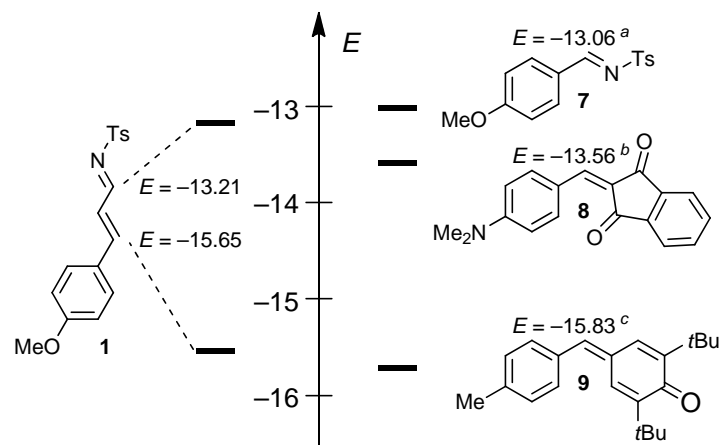


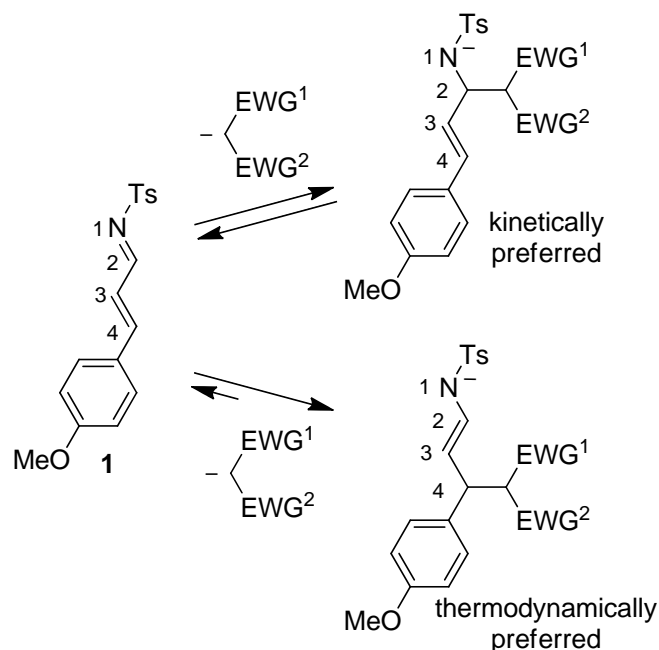
Figure 6: Comparison of the electrophilicity parameters E of the two ambident electrophilic positions of imine **1** with those of benzaldehyde-derived imine **7**, benzylideneindandione **8**, and quinone methide **9**. ^a Value taken from ref 13e. ^b Value taken from ref 24. ^c Value taken from ref 17.

4 Conclusion

The ambident reactivity of imine **1** (i.e., attack at 2- and 4-position) has been derived from reactions with sulfur ylide **2a** and the carbanions **2b–l**. It has been shown that attack at the 2-position is kinetically preferred over attack at the conjugate position, which yields the thermodynamically preferred products (Scheme 10). Consequently, nucleophiles which react irreversibly with the imino group (i.e., nucleophiles with high Lewis basicity or nucleophiles which undergo fast subsequent reactions) usually give 1,2-addition products. On the other hand, nucleophiles with low Lewis basicity will react reversibly with the imino group and eventually yield the thermodynamically more stable Michael adducts. As previously shown for ambident nucleophiles,^[12] smaller intrinsic barriers account for the kinetic preference of 1,2-additions.

Although it has so far not been possible to establish extensive kinetic investigations on the ambident electrophilicity of α,β -unsaturated aldehydes and ketones, the structural analogy with imine **1** as well as the experimental findings in Schemes 1 and 2 strongly suggest that kinetic and thermodynamic control also explain the ambident reactivity for α,β -unsaturated carbonyl compounds.

Scheme 10: Rationalization of the Ambident Electrophilic Reactivity of Imine **1** by Kinetic and Thermodynamic Control.



5 Experimental Section

5.1 General

Chemicals. The α,β -unsaturated imine **1** was prepared according to a literature procedure for benzaldehyde-derived imines^[25] and the ¹H-NMR signals were in agreement with those reported in the literature.^[26] The sulfonium tetrafluoroborate (**2a**-H)-BF₄ was prepared as reported earlier.^[14] 2-(Methylsulfinyl)acetate^[27] (**2d**-H) as well as 1-nitro-4-((phenylsulfonyl)methyl)benzene (**2j**-H) were prepared as reported in the literature.^[28] All other chemicals were purchased from commercial sources and (if necessary) purified by recrystallization or distillation prior to use.

Analytics. ¹H- and ¹³C-NMR spectra were recorded on Varian NMR-systems (300, 400, or 600 MHz) in CDCl₃ or DMSO-*d*₆ and the chemical shifts in ppm refer to TMS (δ_{H} 0.00, δ_{C} 0.00) in CDCl₃ or the solvent residual signal in DMSO-*d*₆ (δ_{H} 2.50, δ_{C} 39.43) as internal standard. The following abbreviations were used for chemical shift multiplicities: brs = broad singlet, s = singlet, d = doublet, t = triplet, q = quartet, m = multiplet. For reasons of simplicity, the ¹H-NMR signals of AA'BB'-spin systems of *p*-disubstituted aromatic rings were treated as doublets. NMR signal assignments were based on additional 2D-NMR experiments (e.g., COSY-, NOESY-, HSQC-, and HMBC experiments). Diastereomeric ratios (*dr*) were determined by ¹H-NMR. (HR-)MS was performed on a Finnigan MAT 95 (EI) or a

Thermo Finnigan LTQ FT (ESI) mass spectrometer. An Elementar Vario Micro Cube or an Elementar vario EL device was used for elemental analysis. Melting points were determined on a Büchi B-540 device and are not corrected.

Kinetics. The rates of all reactions were determined photometrically in dry DMSO (H₂O content < 50 ppm). The temperature was kept constant (20.0 ± 0.1°C) by using a circulating bath thermostat. All reactions have been performed under first-order conditions. The rates of slow reactions ($\tau_{1/2} > 15\text{-}20$ s) were determined by using a J&M TIDAS diode array spectrophotometer controlled by Labcontrol Spectacle software and connected to a Hellma 661.502-QX quartz Suprasil immersion probe (5 mm light path) via fiber optic cables and standard SMA connectors. For the evaluation of fast kinetics ($\tau_{1/2} < 15\text{-}20$ s) the stopped-flow spectrophotometer systems Hi-Tech SF-61DX2 or Applied Photophysics SX.18MV-R stopped-flow reaction analyser were used. First-order rate constants k_{obs} (s⁻¹) were obtained by fitting the single exponential $A_t = A_0 \exp(-k_{\text{obs}}t) + C$ (exponential decrease) to the observed time-dependent absorbance (averaged from at least 3 kinetic runs for each nucleophile concentration in case of stopped-flow method). Second-order rate constants k_2 (L mol⁻¹ s⁻¹) were derived from the slopes of the linear correlations of k_{obs} with the concentration of the reaction partner used in excess ($[\text{Nu}]_0$ or $[\text{E}]_0$). In case of the reaction of diethyl malonate anion (**2e**) with imine **1**, the kinetic traces at $[\mathbf{2e}] < 2$ mmol/L were fitted by using GEPASI^[22] (i.e., a software package for modelling dynamics).

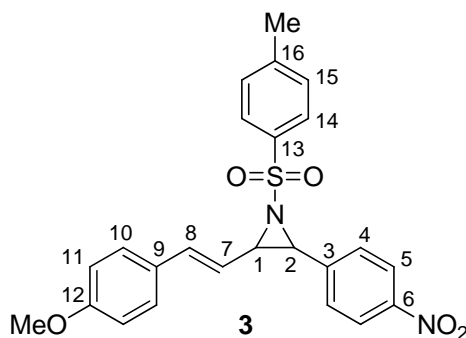
5.2 Product Analysis

5.2.1 Reactions of the Sulfur Ylide 2a and the Carbanions 2b–i,l with the 2-Position of Imine 1

Product study for the reaction of imine 1 with sulfur ylide 2a

(E)-2-(4-Methoxystyryl)-3-(4-nitrophenyl)-1-tosylaziridine (3). Saturated aqueous K_2CO_3 -solution (5 mL) was added to a vigorously stirred solution of sulfonium tetrafluoroborate (**2a-H**)- BF_4 (93.0 mg, 326 μ mol) and imine **1** (100 mg, 317 μ mol) in $CHCl_3$ (10 mL). The resulting biphasic mixture was vigorously stirred for 70 min. During this reaction further portions of (**2a-H**)- BF_4 (20 mg, 63.4 μ mol) were added after 30 and 60 min. The reaction was subsequently treated with water, the organic layer was separated and the aqueous phase additionally extracted by $CHCl_3$. The combined organic layers were washed with water and brine, dried over Na_2SO_4 and evaporated under reduced pressure. The aziridine **3** was obtained without further purification as yellow solid (142 mg, 315 μ mol, 99 %, *d.r.* ~ 1 : 1.8 *cis/trans*), which was subsequently characterized by 1H - and ^{13}C -NMR spectroscopy and MS. Signal assignments were based on additional COSY, HSQC and HMBC experiments.

RAP 69.4



1H -NMR ($CDCl_3$, 599 MHz): δ = 2.40* (s, 3 H, Ar-Me), 2.44# (s, 3 H, Ar-Me), 3.41* (dd, 1 H, J = 9.6, 3.9 Hz, 1-H), 3.75# (s, 3 H, OMe), 3.83* (s, 3 H, OMe), 3.84-3.87# (m, 1 H, 1-H), 4.17# (d, 1 H, J = 7.3 Hz, 2-H), 4.20* (d, 1 H, J = 3.9 Hz, 2-H), 5.24# (dd, 1 H, J = 15.8, 8.3 Hz, 7-H), 6.50* (dd, 1 H, J = 15.7, 9.7 Hz, 7-H), 6.70# (d, 1 H, J = 15.9 Hz, 8-H), 6.74-6.77 (m, 3 H, 8-H*, 11-H#), 6.88* (d, 2 H, J = 8.8 Hz, 11-H), 7.10# (d, 2 H, J = 8.7 Hz, 10-H), 7.27* (d, 2 H, J = 8.4 Hz, 15-H), 7.35-7.39 (m, 6 H, 10-H*, 4-H*, 15-H#), 7.45# (d, 2 H, J = 8.4 Hz, 4-H), 7.83* (d, 2 H, J = 8.3 Hz, 14-H), 7.91# (d, 2 H, J = 8.3 Hz, 14-H), 8.13-8.16 (m, 4 H, 5-H*, 5-H#). ^{13}C -NMR ($CDCl_3$, 151 MHz): δ = 21.6* (q, Ar-Me), 21.7# (q, Ar-Me), 45.7#

(d, C-2), 47.4* (d, C-2), 48.2[#] (d, C-1), 55.27[#] (q, OMe), 55.33* (q, OMe), 56.1* (d, C-1) 114.0[#] (d, C-11), 114.1* (d, C-11), 117.0[#] (d, C-7), 118.6* (d, C-7), 123.7[#] (s, C-5), 123.9* (d, C-5), 127.1* (d, C-4), 127.6* (d, C-14), 127.8[#], 127.9[#] (2d, C-10, C-14), 128.1* (d, C-10), 128.2[#] (s, C-9), 128.4* (s, C-9), 128.5[#] (d, C-4), 129.7* (d, C-15), 130.0[#] (d, C-15), 134.7 (s, C-13)[#], 136.4* (s, C-13), 137.1[#] (d, C-8), 137.9* (d, C-8), 140.3[#] (s, C-3), 142.6* (s, C-3), 144.7* (s, C-16), 1145.1[#] (s, C-16), 147.69[#] (s, C-6), 147.74* (s, C-6), 159.9[#] (s, C-12), 160.0* (s, C-12). HR-MS (ESI⁺) [M+H]⁺: calcd for [C₂₄H₂₃N₂O₅S]⁺: 451.1323; found 451.1321.

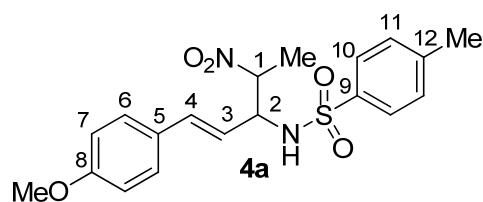
* signal can be assigned to *trans*-diastereomer

[#] signal can be assigned to *cis*-diastereomer

Product studies for the reaction of imine **1** with the carbanions **2b–i,l**

If not mentioned otherwise the reactions were performed according to *General procedure A*: The CH acids (**2b–i,l**)-H were dissolved with imine **1** in dry DMSO (2-3 mL). After the addition of a catalytic amount of base (Et₃N and/or KO^tBu), the reaction mixtures were stirred for an appropriate reaction time at rt. The reactions were subsequently quenched by the addition of water and brine, followed by the extraction with CH₂Cl₂. The combined organic layers were washed with water and brine, dried over Na₂SO₄ and evaporated under reduced pressure. The crude products were purified by column chromatography on silica gel (*n*-pentane/EtOAc) and subsequently characterized by ¹H- and ¹³C-NMR (if possible also ³¹P-NMR) spectroscopy and MS. Signal assignments were based on additional COSY, HSQC and HMBC experiments. If not mentioned otherwise, the diastereomeric ratios of the purified products did not differ significantly from those of the crude mixtures before column chromatography. Additional purifications by recrystallization from appropriate solvent mixtures were sometimes performed and are indicated in the corresponding section.

(E)-N-(1-(4-Methoxyphenyl)-4-nitropent-1-en-3-yl)-4-methylbenzenesulfonamide (4a) was obtained from nitroethane (**2b-H**, 60.0 mg, 799 μmol), the imine **1** (100 mg, 317 μmol), and Et₃N (5.8 mg, 57 μmol, 18 mol-%) after 2.5 h of reaction time as a yellow solid (72 mg, 0.18 mmol, 57 %, *d.r.* ~ 1 : 2.1) still containing impurities. Recrystallization from *n*-pentane/EtOAc yielded **4a** as yellow solid (54 mg, 0.14 mmol, 44 %, *d.r.* ~ 1 : 2.7).



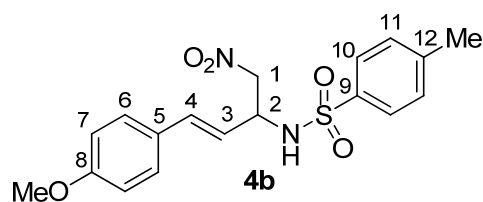
$^1\text{H-NMR}$ ($\text{DMSO-}d_6$, 400 MHz): $\delta = 1.40^*$ (d, 3 H, $J = 6.7$ Hz, Me), $1.44^\#$ (d, 3 H, $J = 6.7$ Hz, Me), 2.15^* (s, 3 H, Ar-Me), $2.21^\#$ (s, 3 H, Ar-Me), 3.73 (s, 6 H, OMe^* , $\text{OMe}^\#$, identical signals for both diastereomers), 4.20^* (ddd, 1 H, $J = 8.6, 8.6, 8.6$ Hz, 2-H), $4.27\text{--}4.33^\#$ (m, 1 H, 2-H), $4.67\text{--}4.80$ (m, 2 H, 1-H^* , $1\text{-H}^\#$), 5.46^* (dd, 1 H, $J = 15.9, 8.6$ Hz, 3-H), $5.62^\#$ (dd, 1 H, $J = 15.9, 7.8$ Hz, 3-H), $6.02^\#$ (d, 1 H, $J = 15.8$ Hz, 4-H), 6.09^* (d, 1 H, $J = 15.9$ Hz, 4-H), $6.80\text{--}6.84$ (m, 4 H, 7-H^* , $7\text{-H}^\#$), $6.97\text{--}7.02$ (m, 4 H, 6-H^* , $6\text{-H}^\#$), 7.20^* (d, 2 H, $J = 7.9$ Hz, 11-H), $7.25^\#$ (d, 2 H, $J = 7.9$ Hz, 11-H), 7.61^* (d, 2 H, $J = 8.3$ Hz, 10-H), $7.65^\#$ (d, 2 H, $J = 8.3$ Hz, 10-H), $8.09^\#$ (d, 1 H, $J = 9.2$ Hz, NH), 8.16^* (d, 1 H, $J = 9.3$ Hz, NH). $^{13}\text{C-NMR}$ ($d_6\text{-DMSO}$, 101 MHz): $\delta = 14.0^\#$ (q, Me), 15.6^* (q, Me), 20.67^* (q, Ar-Me), $20.71^\#$ (q, Ar-Me), 55.0 ($2 \times$ q, OMe^* , $\text{OMe}^\#$, identical signals for both diastereomers), $58.7^\#$ (d, C-2), 59.3^* (d, C-2), $85.3^\#$ (d, C-1), 85.5^* (d, C-1), 113.7^* (d, C-7), $113.8^\#$ (d, C-7), 119.9^* (d, C-3), $120.6^\#$ (d, C-3), 126.6 ($2 \times$ d, C-10 * , C-10 $^\#$, identical signals for both diastereomers), $127.47^\#$ (d, C-6), 127.50^* (d, C-6), $128.0^\#$ (s, C-5), 128.1^* (s, C-5), 129.2^* (d, C-11), $129.3^\#$ (d, C-11), $132.6^\#$ (d, C-4), 133.4^* (d, C-4), $138.0^\#$ (s, C-9), 138.1^* (s, C-9), 142.5^* (s, C-12), $142.6^\#$ (s, C-12), 158.97^* (s, C-8), $158.99^\#$ (s, C-8). MS (EI): m/e (%) = 390 (2) $[\text{M}]^+$, 316 (16), 315 (7), 314 (17), 161 (10), 160 (100), 159 (17), 155 (10), 145 (11), 133 (6), 117 (8), 91 (33), 90 (6), 77 (5), 65 (8). HR-MS (EI) $[\text{M}]^+$: calcd for $[\text{C}_{19}\text{H}_{22}\text{N}_2\text{O}_5\text{S}]^+$: 390.1244, found 390.1244.

* signal can be assigned to major diastereomer.

$^\#$ signal can be assigned to minor diastereomer.

(E)-N-(4-(4-Methoxyphenyl)-1-nitrobut-3-en-2-yl)-4-methylbenzenesulfonamide (4b) was obtained from nitromethane (**2c-H**, 100 mg, 1.64 mmol), the imine **1** (100 mg, 317 μmol), and Et_3N (6.3 mg, 62 μmol , 20 mol-%) after 2.5 h of reaction time as a orange solid (66 mg, 0.18 mmol, 57 %). Recrystallization from *n*-pentane/EtOAc yielded **4b** as a yellow solid (44 mg, 0.12 mmol, 39 %).

RAP 57.2

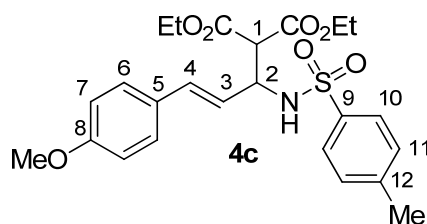


R_f (*n*-pentane/EtOAc 3:1, *v/v*): 0.22. Mp. (*n*-pentane/EtOAc): 145-147°C. $^1\text{H-NMR}$ (d_6 -DMSO- d_6 , 400 MHz): δ = 2.22 (s, 3 H, Ar-Me), 3.73 (s, 3 H, OMe), 4.46-4.58 (m, 2 H, 1-H, 2-H), 4.72 (dd, 1 H, J = 12.1, 5.0 Hz, 1-H), 5.60 (dd, 1 H, J = 16.0, 7.3 Hz, 3-H), 6.17 (d, 1 H, J = 15.9 Hz, 4-H), 6.84 (d, 2 H, J = 8.8 Hz, 7-H), 7.02 (d, 2 H, J = 8.8 Hz, 6-H), 7.26 (d, 2 H, J = 8.0 Hz, 11-H), 7.64 (d, 2 H, J = 8.3 Hz, 10-H), 8.22 (d, 1 H, J = 8.5 Hz, NH). $^{13}\text{C-NMR}$ (d_6 -DMSO, 101 MHz): δ = 20.8 (q, Ar-Me), 54.2 (q, C-2), 55.0 (q, OMe), 78.5 (t, C-1), 113.8 (d, C-7), 121.0 (d, C-3), 126.6 (d, C-10), 127.5 (d, C-6), 128.0 (s, C-5), 129.4 (d, C-11), 132.2 (d, C-4), 138.2 (s, C-9), 142.6 (s, C-12), 159.0 (s, C-8). MS (EI): m/e (%) = 376 (3) $[\text{M}]^+$, 314 (20), 174 (10), 171 (10), 161 (12), 160 (100), 159 (20), 155 (20), 145 (18), 117 (11), 91 (59), 65 (14), 44 (13). HR-MS (EI) $[\text{M}]^+$: calcd for $[\text{C}_{18}\text{H}_{20}\text{N}_2\text{O}_5\text{S}]^+$: 376.1088, found 376.1085.

(*E*)-Diethyl 2-(3-(4-methoxyphenyl)-1-(4-methylphenylsulfonamido)allyl)malonate (4c)

could not be obtained by *General Procedure A* because of the high reversibility of the addition of carbanion **2e** to the 2-position of imine **1**. Instead, the following procedure was used for the synthesis of **4c**: Diethyl malonate (**2e-H**, 73.0 mg, 456 μmol) and KO t Bu (51.0 mg, 455 μmol) were dissolved in 5 mL of dry THF at rt. The resulting suspension was cooled down to -80°C and the imine **1** (130 mg, 412 μmol , dissolved in 5 mL of dry THF) was added dropwise. After 4 h of stirring at a temperature below -70°C , the mixture was again cooled down to -80°C and treated first with concentrated acetic acid (0.1 mL) then with water. The crude mixture was extracted with CH_2Cl_2 and the combined organic layers were washed with water and brine, dried over Na_2SO_4 and evaporated under reduced pressure. The crude product was purified by precipitation from *n*-pentane/toluene and subsequent recrystallization from *n*-pentane/ Et_2O and yielded **4c** as colorless solid (110 mg, 231 μmol , 56%), which was characterized by ^1H - and ^{13}C -NMR spectroscopy and MS. Signal assignments were based on additional COSY, HSQC and HMBC experiments.

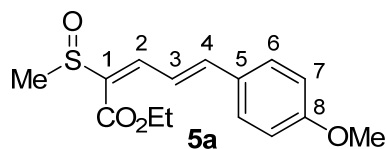
RAP 98.2



Mp. (*n*-pentane/Et₂O): 97-98°C. ¹H-NMR (DMSO-*d*₆, 400 MHz): δ = 1.07 (t, 3 H, J = 7.1 Hz, OCH₂CH₃), 1.18 (t, 3 H, J = 7.1 Hz, OCH₂CH₃), 2.16 (s, 3 H, Ar-Me), 3.60 (d, 1 H, J = 9.4 Hz, 1-H), 3.72 (s, 3 H, OMe), 3.97-4.15 (m, 4 H, OCH₂CH₃), 4.35 (ddd, 1 H, J = 9.0, 9.0, 9.0 Hz, 2-H), 5.54 (dd, 1 H, J = 15.9, 8.6 Hz, 3-H), 6.02 (d, 1 H, J = 15.9 Hz, 4-H), 6.81 (d, 2 H, J = 8.7 Hz, 7-H), 6.95 (d, 2 H, J = 8.7 Hz, 6-H), 7.20 (d, 2 H, J = 8.1 Hz, 11-H), 7.61 (d, 2 H, J = 8.2 Hz, 10-H), 7.95 (d, 1 H, J = 9.1 Hz, NH). ¹³C-NMR (d₆-DMSO, 101 MHz): δ = 13.7 (q, OCH₂CH₃), 13.8 (q, OCH₂CH₃), 20.7 (q, Ar-Me), 55.0 (q, OMe), 55.6 (d, C-2), 57.3 (d, C-1), 61.0 (t, OCH₂CH₃), 61.1 (t, OCH₂CH₃), 113.7 (d, C-7), 122.2 (d, C-3), 126.6 (d, C-10), 127.3 (d, C-6), 128.2 (s, C-5), 129.2 (d, C-11), 131.9 (d, C-4), 138.4 (s, C-9), 142.3 (s, C-12), 158.8 (s, C-8), 165.8 (s, CO), 165.9 (s, CO). MS (EI): m/e (%) = 475 (2) [M]⁺, 320 (20), 316 (21), 314 (25), 161 (12), 160 (100), 159 (20), 155 (10), 145 (11), 133 (27), 115 (40), 105 (17), 91 (31), 88 (11), 43 (13). HR-MS (EI) [M]⁺: calcd for [C₂₄H₂₉NO₇S]⁺: 475.1659, found 475.1651.

(2*E*,4*E*)-Ethyl 5-(4-methoxyphenyl)-2-(methylsulfinyl)penta-2,4-dienoate (5a) was obtained from ethyl 2-(methylsulfinyl)acetate (**2d-H**, 75.0 mg, 499 μ mol), the imine **1** (100 mg, 317 μ mol), Et₃N (5.6 mg, 55 μ mol, 17 mol-%) and KOtBu (5.6 mg, 49 μ mol, 15 mol-%) after 30 min of reaction time as a yellow oil (67 mg, 0.23 mmol, 73 %).

RAP 90.1

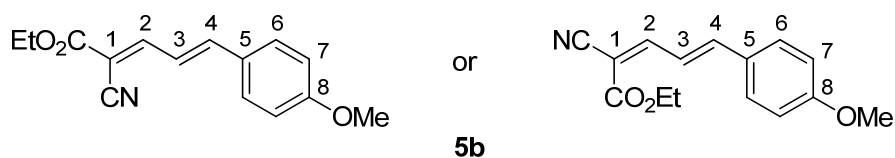


R_f (*n*-pentane/EtOAc 2:3, *v/v*): 0.32. ¹H-NMR (CDCl₃, 400 MHz): δ = 1.40 (t, 3 H, J = 7.1 Hz, OCH₂CH₃), 2.74 (s, 3 H, SOMe), 3.84 (s, 3 H, OMe), 4.27-4.42 (m, 2 H, OCH₂CH₃), 6.91 (d, 2 H, J = 8.8 Hz, 7-H), 7.09 (d, 1 H, J = 15.5 Hz, 4-H), 7.47-7.51 (m, 3 H, 2-H, 6-H), 7.91 (dd, 1 H, J = 15.5, 11.6 Hz, 3-H). ¹³C-NMR (CDCl₃, 101 MHz): δ = 14.3 (q, OCH₂CH₃), 42.1 (q, SOMe), 55.4 (q, OMe), 61.3 (t, OCH₂CH₃), 114.4 (d, C-7), 121.1 (d, C-3), 128.6 (s, C-5), 129.6 (d, C-6), 131.6 (s, C-1), 143.6 (d, C-2), 145.7 (d, C-4), 161.2 (s, C-8), 163.0 (s, CO). MS (EI): m/e (%) = 294 (38) [M]⁺, 279 (23), 231 (100), 230 (82), 185 (24), 158 (82),

145 (39), 115 (56). HR-MS (EI) $[M]^+$: calcd for $[C_{15}H_{18}O_4S]^+$: 294.0920, found 294.0923. HR-MS (ESI⁺) $[M+H]^+$: calcd for $[C_{15}H_{19}O_4S]^+$: 295.0999, found 295.1001. A NOE correlation between 2-H and SOMe indicates *E*-configuration of the CC double bond between C-1 and C-2.

(4*E*)-Ethyl 2-cyano-5-(4-methoxyphenyl)penta-2,4-dienoate (5b) was obtained by a different procedure as *General Procedure A*: Ethyl 2-cyanoacetate (**2f-H**, 60.0 mg, 530 μ mol) and KO^{*t*}Bu (60.0 mg, 535 μ mol) were dissolved in 5 mL of dry THF at rt. The resulting suspension was cooled down to -20°C and the imine **1** (150 mg, 476 μ mol, dissolved in 3 mL of dry THF) was added dropwise. The reaction mixture was stirred for 30 min and subsequently quenched by the addition of concentrated acetic acid (0.1 ml). The crude mixture was extracted with CH₂Cl₂ and the combined organic layers were washed with water and brine, dried over Na₂SO₄ and evaporated under reduced pressure. Purification by column chromatography on silica gel (*n*-pentane/EtOAc) yielded **5b** as a yellow solid (85 mg, 0.33 mmol, 69 %). Additional recrystallization from *n*-pentane/EtOAc yielded **5b** also as yellow solid (65 mg, 0.25 μ mol, 53 %), which was characterized by ¹H-, and ¹³C-NMR spectroscopy and MS. Signal assignments were based on additional COSY, HSQC and HMBC experiments.

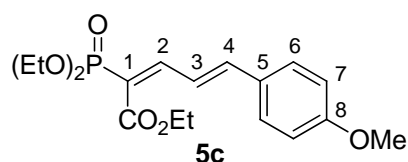
RAP 102.2



R_f (*n*-pentane/EtOAc 5:1, *v/v*): 0.39. Mp. (*n*-pentane/EtOAc): $>102^\circ\text{C}$ (decomp.). ¹H-NMR (CDCl₃, 599 MHz): δ = 1.37 (t, 3 H, J = 7.1 Hz, OCH₂CH₃), 3.86 (s, 3 H, OMe), 4.33 (q, 2 H, J = 7.1 Hz, OCH₂CH₃), 6.94 (d, 2 H, J = 8.8 Hz, 7-H), 7.15 (dd, 1 H, J = 15.2, 11.4 Hz, 3-H), 7.22 (d, 1 H, J = 15.3 Hz, 4-H), 7.55 (d, 2 H, J = 8.8 Hz, 6-H), 7.98 (d, 1 H, J = 11.4 Hz, 2-H). ¹³C-NMR (CDCl₃, 151 MHz): δ = 14.2 (q, OCH₂CH₃), 55.5 (q, OMe), 62.2 (t, OCH₂CH₃), 102.7 (s, C-1), 114.7 (d, C-7), 114.9 (s, CN), 121.0 (d, C-3), 127.6 (s, C-5), 130.4 (d, C-6), 148.8 (d, C-4), 155.9 (d, C-2), 162.3 (s, C-8), 162.7 (s, CO). MS (EI): m/e (%) = 258 (15), 257 (94) $[M]^+$, 228 (20), 212 (14), 185 (18), 184 (100), 183 (17), 169 (24), 145 (14), 141 (10), 140 (22). HR-MS (EI) $[M]^+$: calcd for $[C_{15}H_{15}NO_3]^+$: 257.1047, found 257.1047. An additional NOESY experiment did not give conclusive results, to determine the configuration of the CC double bond between C-1 and C-2.

(2E,4E)-Ethyl 2-(diethoxyphosphoryl)-5-(4-methoxyphenyl)penta-2,4-dienoate (5c) was obtained by a modification of *General Procedure A*: Ethyl 2-(diethoxyphosphoryl)acetate (**2g-H**, 100 mg, 446 μmol) and $\text{KO}t\text{Bu}$ (8.0 mg, 71 μmol , 16 mol-%) were dissolved in 3 mL of dry THF at rt. The resulting suspension was cooled down to -40°C and the imine **1** (170 mg, 539 μmol , dissolved in 3 mL of dry THF) was added dropwise. The reaction mixture was stirred for 30 min while it was slowly warmed to rt and subsequently quenched by the addition of water and brine. The crude product was purified by column chromatography on silica gel (*n*-pentane/EtOAc and $\text{CH}_2\text{Cl}_2/\text{MeOH}$) and yielded **5c** as a yellow oil (115 mg, 312 μmol , 70 %), which was subsequently characterized by ^1H -, ^{13}C -, and ^{31}P -NMR spectroscopy and MS. Signal assignments were based on additional COSY, HSQC and HMBC experiments.

RAP 79.5

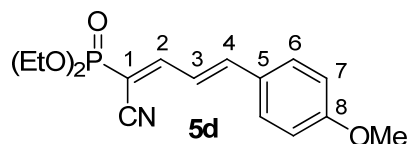


R_f ($\text{CH}_2\text{Cl}_2/\text{MeOH}$ 30:1, *v/v*): 0.15. ^1H -NMR (CDCl_3 , 300 MHz): δ = 1.32-1.40 (m, 9 H, $2 \times \text{POCH}_2\text{CH}_3$, $\text{CO}_2\text{CH}_2\text{CH}_3$), 3.83 (s, 3 H, OMe), 4.08-4.22 (m, 4 H, $2 \times \text{POCH}_2\text{CH}_3$), 4.33 (q, 2 H, $J = 7.1$ Hz, $\text{CO}_2\text{CH}_2\text{CH}_3$), 6.90 (d, 2 H, $J = 8.8$ Hz, 7-H), 7.04 (d, $J = 14.9$ Hz, 1 H, 4-H), 7.49 (d, 2 H, $J = 8.8$ Hz, 6-H), 7.67 (dd, 1 H, $J = 20.0, 11.1$ Hz, 2-H), 7.72-7.81 (m, 1 H, 3-H). ^{13}C -NMR (CDCl_3 , 75.5 MHz): δ = 14.3 (q, $\text{CO}_2\text{CH}_2\text{CH}_3$), 16.4 (q, d, $J_{\text{PC}} = 6.5$ Hz, POCH_2CH_3), 55.4 (q, OMe), 60.9 (t, $\text{CO}_2\text{CH}_2\text{CH}_3$), 62.3 (t, d, $J_{\text{PC}} = 5.5$ Hz, POCH_2CH_3), 114.4 (d, C-7), 117.9 (s, d, $J_{\text{PC}} = 187$ Hz, C-1), 122.3 (d, d, $J_{\text{PC}} = 19.3$ Hz, C-3), 128.4 (s, d, $J_{\text{PC}} = 1.6$ Hz, C-5), 129.8 (d, C-6), 146.6 (d, d, $J_{\text{PC}} = 1.2$ Hz, C-4), 156.3 (d, d, $J_{\text{PC}} = 7.7$ Hz, C-2), 161.3 (s, C-8), 165.0 (s, d, $J_{\text{PC}} = 13.8$ Hz, CO). ^{31}P -NMR (CDCl_3 , 81.0 MHz): δ = 17.6. MS (EI): *m/e* (%) = 368 (65) $[\text{M}]^+$, 339 (100), 323 (22), 322 (22), 311 (40), 283 (83), 265 (65), 230 (28), 185 (23), 158 (41), 145 (44), 115 (58). HR-MS (EI) $[\text{M}]^+$: calcd for $[\text{C}_{18}\text{H}_{25}\text{O}_6\text{P}]^+$: 368.1383, found 368.1379. The coupling constant $J_{\text{P-2-H}}$ of 20 Hz is consistent with an *E*-configuration of the CC double bond between C-1 and C-2.^[29]

Diethyl ((1E,3E)-1-cyano-4-(4-methoxyphenyl)buta-1,3-dien-1-yl)phosphonate (5d) was obtained from diethyl (cyanomethyl)phosphonate (**2h-H**, 74.0 mg, 418 μmol), the imine **1** (110 mg, 349 μmol), and Et_3N (6.7 mg, 66 μmol , 19 mol-%) after 1.5 h of reaction time as a

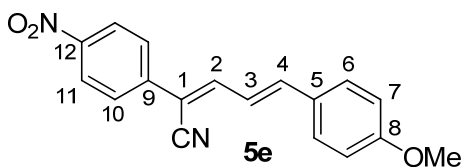
yellow oil (78 mg, 0.24 mmol, 69 %). Recrystallization from *i*-hexane yielded **5d** as a yellow solid (61 mg, 0.19 mmol, 54 %).

RAP 67.3



R_f (*n*-pentane/EtOAc 1:1, *v/v*): 0.18. Mp. (*i*-hexane): 82-83°C. $^1\text{H-NMR}$ (CDCl_3 , 300 MHz): δ = 1.39 (t, 6 H, J = 7.1 Hz, $2 \times \text{OCH}_2\text{CH}_3$), 3.86 (s, 3 H, OMe), 4.10-4.28 (m, 4 H, $2 \times \text{OCH}_2\text{CH}_3$), 6.93 (d, 2 H, J = 8.8 Hz, 7-H), 7.14-7.16 (m, 2 H, 3-H, 4-H), 7.53 (d, 2 H, J = 8.8 Hz, 6-H), 7.69-7.86 (m, 1 H, 2-H). $^{13}\text{C-NMR}$ (CDCl_3 , 75.5 MHz): δ = 16.3 (q, d, J_{PC} = 6.4 Hz, OCH_2CH_3), 55.5 (q, OMe), 63.3 (t, d, J_{PC} = 5.7 Hz, OCH_2CH_3), 98.8 (s, d, J_{PC} = 203 Hz, C-1), 114.6 (d, C-7), 115.0 (s, d, J_{PC} = 11.5 Hz, CN), 121.5 (d, d, J_{PC} = 18.4 Hz, C-3), 127.4 (s, d, J_{PC} = 1.5 Hz, C-5), 130.3 (d, C-6), 147.6 (d, C-4), 160.2 (d, d, J_{PC} = 7.2 Hz, C-2), 162.1 (s, C-8). $^{31}\text{P-NMR}$ (CDCl_3 , 81.0 MHz): δ = 12.4. MS (EI): m/e (%) = 321 (77) $[\text{M}]^+$, 265 (28), 264 (33), 185 (21), 184 (67), 183 (100), 169 (20), 140 (38), 111 (29). HR-MS (EI) $[\text{M}]^+$: calcd for $[\text{C}_{16}\text{H}_{20}\text{NO}_4\text{P}]^+$: 321.1124, found 321.1127.

(2Z,4E)-5-(4-Methoxyphenyl)-2-(4-nitrophenyl)penta-2,4-dienitrile (5e) was obtained from 2-(4-nitrophenyl)acetonitrile (**2i-H**, 60.0 mg, 370 μmol), the imine **1** (100 mg, 317 μmol), and Et_3N (4.4 mg, 43 μmol , 14 mol-%) after 20 min of reaction time as an orange solid (54 mg, 0.18 mmol, 57 %). Recrystallization from *n*-pentane/EtOAc yielded **5e** as an orange solid (41 mg, 0.13 mmol, 41 %).

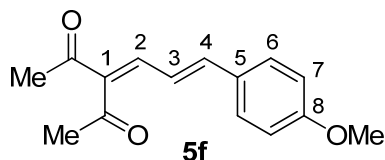


R_f (*n*-pentane/EtOAc 6:1, *v/v*): 0.24. Mp. (*n*-pentane/EtOAc): 164-166°C. $^1\text{H-NMR}$ (CDCl_3 , 599 MHz): δ = 3.86 (s, 3 H, OMe), 6.94 (d, 2 H, J = 8.7 Hz, 7-H), 7.11 (d, 1 H, J = 15.2 Hz, 4-H), 7.28 (dd, 1 H, J = 15.2, 11.2 Hz, 3-H, superimposed by CDCl_3 residual signal), 7.52-7.55 (m, 3 H, 2-H, 6-H), 7.75 (d, 2 H, J = 8.7 Hz, 10-H), 8.26 (d, 2 H, J = 8.7 Hz, 11-H). $^{13}\text{C-NMR}$ (CDCl_3 , 151 MHz): δ = 55.5 (q, OMe), 109.2 (s, C-1), 114.6 (d, C-7), 116.4 (s, CN), 122.6 (d, C-3), 124.4 (d, C-11), 125.9 (d, C-10), 128.1 (s, C-5), 129.7 (d, C-6), 139.7 (s, C-9), 144.3 (d, C-4), 145.5 (d, C-2), 147.4 (s, C-12), 161.6 (s, C-8). MS (EI): m/e (%) = 307 (25),

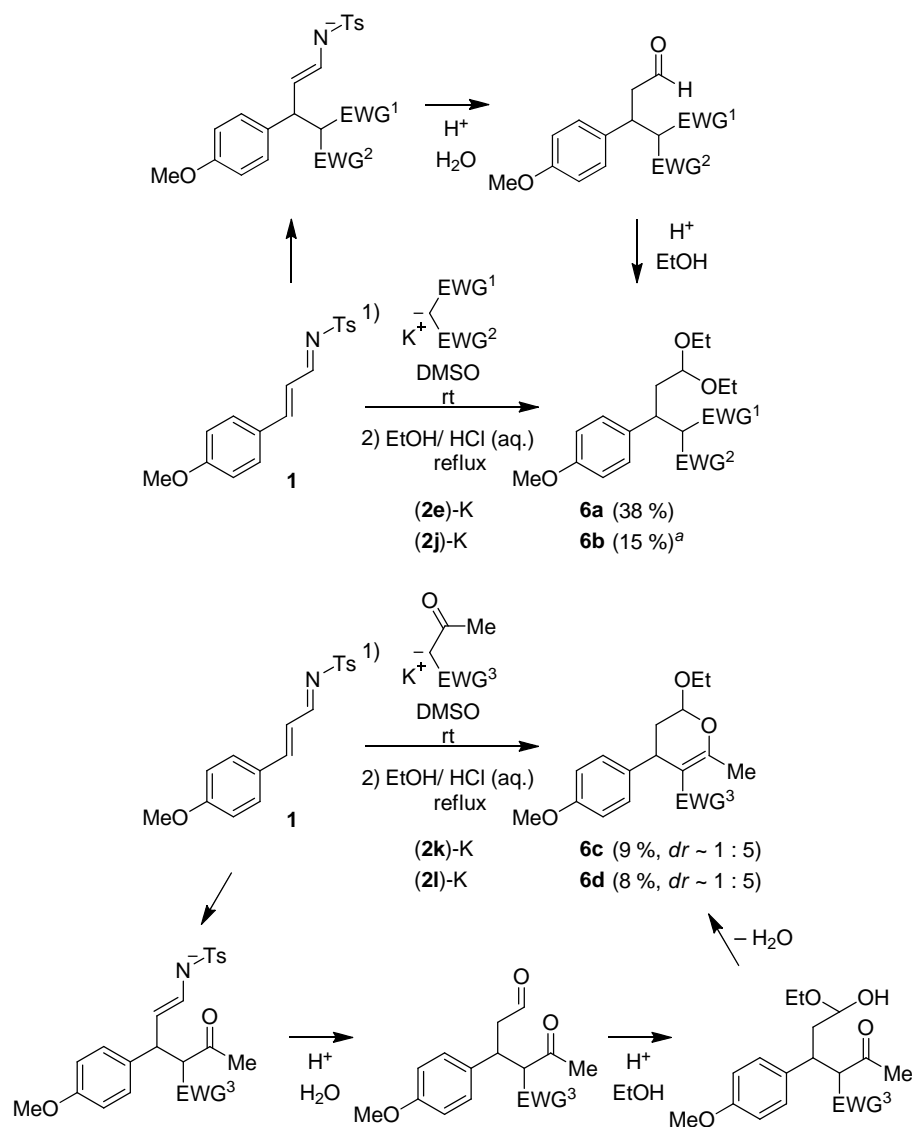
306 (100) $[M]^+$, 260 (5), 259 (9), 245 (5), 217 (8), 216 (9), 190 (7), 189 (8), 184 (15), 145 (11). HR-MS (EI) $[M]^+$: calcd for $[C_{18}H_{14}N_2O_3]^+$: 306.0999, found 306.1000. A NOE correlation between 10-H and 2-H indicates *Z*-configuration of the CC double bond between C-1 and C-2.

(E)-3-(3-(4-Methoxyphenyl)allylidene)pentane-2,4-dione (5f) was obtained by a different procedure as *General Procedure A*: Pentane-2,4-dione (**2I-H**, 50.0 mg, 499 μ mol) and *KOtBu* (37.3 mg, 332 μ mol) were dissolved in 3 mL of dry DMSO at rt and the imine **1** (100 mg, 317 μ mol, dissolved in 3 mL of dry DMSO) was added in one portion. The reaction mixture was stirred for 30 min and subsequently quenched by the addition of water and brine. The crude mixture was extracted with CH_2Cl_2 and the combined organic layers were washed with water and brine, dried over Na_2SO_4 and evaporated under reduced pressure. Purification by column chromatography on aluminum oxide (*n*-pentane/EtOAc) yielded **5f** as a yellow oil (45 mg, 0.18 mmol, 57 %). Recrystallization from *n*-pentane/ Et_2O yielded **5f** also as yellow solid (35 mg, 0.14 μ mol, 44 %), which was characterized by 1H -, and ^{13}C -NMR spectroscopy and MS. Signal assignments were based on additional COSY, HSQC and HMBC experiments.

RAP 95.1



R_f (*n*-pentane/EtOAc 5:1, *v/v*): 0.35. Mp. (*n*-pentane/ Et_2O): 111-112°C. 1H -NMR ($CDCl_3$, 400 MHz): δ = 2.40 (s, 3 H, COMe), 2.42 (s, 3 H, COMe), 3.84 (s, 3 H, OMe), 6.90 (d, 2 H, J = 8.9 Hz, 7-H), 7.02-7.03 (m, 2 H, 3-H, 4-H), 7.22 (dd, 1 H, J = 6.3, 4.5 Hz, 2-H), 7.46 (d, 2 H, J = 8.9 Hz, 6-H). ^{13}C -NMR ($CDCl_3$, 101 MHz): δ = 26.4 (q, COMe), 31.8 (q, COMe), 55.4 (q, OMe), 114.4 (d, C-7), 121.3 (d, C-3), 128.3 (s, C-5), 129.6 (d, C-6), 140.2 (s, C-1), 143.9 (d, C-2), 145.2 (d, C-4), 161.3 (s, C-8), 197.1 (s, CO), 203.2 (s, CO). MS (EI): *m/e* (%) = 245 (17), 244 (100) $[M]^+$, 243 (19), 229 (18), 201 (61), 187 (26), 145 (18), 115 (22), 43 (55). HR-MS (EI) $[M]^+$: calcd for $[C_{15}H_{16}O_3]^+$: 244.1094, found 244.1102.

5.2.2 Reactions of the Carbanions **2e,j,k,l** with the 4-Position of Imine **1**

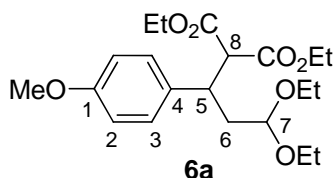
^a Only major diastereomer isolated. *dr* could not be determined due to strongly superimposed signals of diastereomers.

If not mentioned otherwise the reactions were performed according to *General procedure B*: Imine **1** (dissolved in 3 mL of dry DMSO) was added to a solution of the carbanions **(2e,k)-K**^[30] or a solution of the CH acids **(2j,l)-H** and KO^{*t*}Bu in dry DMSO (2-3 mL). After stirring for an appropriate reaction time at rt, the reactions were quenched by the addition of diluted aqueous acetic acid solution (1 %) followed by the extraction with CH₂Cl₂. The combined organic layers were washed with water and brine, dried over Na₂SO₄ and evaporated under reduced pressure. The residue was resolved in EtOH (20-30 mL), treated with 2 M HCl (2 mL), and stirred under reflux for 1 h. The resulting reaction mixture was subsequently extracted with CH₂Cl₂, the combined organic layers dried over Na₂SO₄ and evaporated under reduced pressure. The crude products were purified by column chromatography on silica gel

or aluminum oxide (*n*-pentane/EtOAc) and subsequently characterized by ^1H - and ^{13}C -NMR spectroscopy and MS. Signal assignments were based on additional COSY, HSQC and HMBC experiments. If not mentioned otherwise, the diastereomeric ratios of the purified products did not differ significantly from those of the crude mixtures before column chromatography. Additional purifications by recrystallization from appropriate solvent mixtures were sometimes performed and are indicated at this point.

Diethyl 2-(3,3-diethoxy-1-(4-methoxyphenyl)propyl)malonate (6a) was obtained from diethyl malonate potassium salt (**2e-K**, 68.0 mg, 328 μmol) and the imine **1** (100 mg, 317 μmol) after 5 min of reaction time as pale yellow oil (46 mg, 0.12 mmol, 38 %).

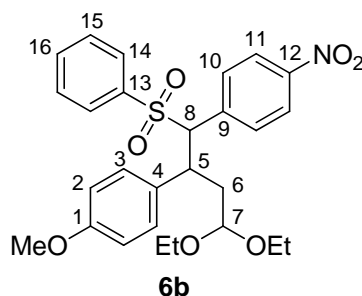
RAP 58.6



R_f (*n*-pentane/EtOAc 4:1, v/v): 0.47. ^1H -NMR (CDCl_3 , 599 MHz): δ = 0.98 (t, 3 H, J = 7.1 Hz, OCH_2CH_3), 1.08 (t, 3 H, J = 7.1 Hz, $\text{OCHH}'\text{CH}_3$), 1.20 (t, 3 H, J = 7.1 Hz, $\text{OCHH}'\text{CH}_3$), 1.28 (t, 3 H, J = 7.1 Hz, OCH_2CH_3), 1.84 (ddd, 1 H, J = 13.8, 11.4, 3.2 Hz, 6-H), 2.07 (ddd, 1 H, J = 13.6, 8.7, 3.6 Hz, 6-H), 3.28-3.33 (m, 1 H, $\text{OCHH}'\text{CH}_3$), 3.34-3.39 (m, 1 H, $\text{OCHH}'\text{CH}_3$), 3.45-3.51 (m, 2 H, $\text{OCHH}'\text{CH}_3$, 5-H), 3.59-3.65 (m, 2 H, $\text{OCHH}'\text{CH}_3$, 8-H), 3.77 (s, 3 H, OMe), 3.88-3.93 (m, 2 H, OCH_2CH_3), 4.09 (dd, 1 H, J = 8.7, 3.1 Hz, 7-H), 4.22 (q, 2 H, J = 7.2 Hz, OCH_2CH_3), 6.82 (d, 2 H, J = 8.7 Hz, 2-H), 7.15 (d, 2 H, J = 8.7 Hz, 3-H). ^{13}C -NMR (CDCl_3 , 151 MHz): δ = 13.8 (q, OCH_2CH_3), 14.1 (q, OCH_2CH_3), 15.2 (q, $\text{OCHH}'\text{CH}_3$), 15.3 (q, $\text{OCHH}'\text{CH}_3$), 37.6 (t, C-6), 40.9 (d, C-5), 55.2 (q, OCH_3), 58.7 (d, C-8), 59.7 (t, $\text{OCHH}'\text{CH}_3$), 61.1 (t, OCH_2CH_3), 61.4 (t, $\text{OCHH}'\text{CH}_3$), 61.5 (t, OCH_2CH_3), 100.4 (d, C-7), 113.8 (d, C-2), 129.4 (d, C-3), 132.2 (s, C-4), 158.5 (s, C-1), 167.8 (s, CO), 168.2 (s, CO). HR-MS (ESI $^-$) [$\text{M}-\text{H}$] $^-$: calcd for [$\text{C}_{21}\text{H}_{31}\text{O}_7$] $^-$: 395.2075, found 395.2070.

1-(4,4-Diethoxy-1-(4-nitrophenyl)-1-(phenylsulfonyl)butan-2-yl)-4-methoxybenzene (6b) was obtained from 1-nitro-4-((phenylsulfonyl)methyl)benzene (**2j-H**, 68.0 mg, 361 μmol), $\text{KO}t\text{Bu}$ (42.5 mg, 379 μmol), and the imine **1** (140 mg, 444 μmol) after 30 min of reaction time as colorless oil (54 mg) still containing impurities (*dr* could not be determined due to strongly superimposed signals of diastereomers). Recrystallization from *n*-pentane/EtOAc yielded **6b** as a colorless solid (28 mg, 55 μmol , 15 %, one diastereomer).

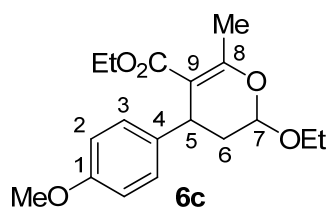
RAP 87.5



R_f (*n*-pentane/EtOAc 6:1, *v/v*): 0.08. Mp. (*n*-pentane/EtOAc): $> 83^\circ\text{C}$ (decomp.). $^1\text{H-NMR}$ (CDCl_3 , 400 MHz): $\delta = 1.04$ (t, 3 H, $J = 7.1$ Hz, $\text{OCHH}'\text{CH}_3$), 1.20 (t, 3 H, $J = 7.0$ Hz, $\text{OCHH}'\text{CH}_3$), 1.68 (ddd, 1 H, $J = 13.6, 12.6, 2.8$ Hz, 6-H), 2.10 (ddd, 1 H, $J = 13.5, 9.0, 3.2$ Hz, 6-H), 3.20-3.32 (m, 2 H, $2 \times \text{OCHH}'\text{CH}_3$), 3.37-3.34 (m, 1 H, $\text{OCHH}'\text{CH}_3$), 3.52-3.60 (m, 1 H, $\text{OCHH}'\text{CH}_3$), 3.77 (s, 3 H, OMe), 3.89-3.87 (m, 2 H, 5-H, 7-H), 4.42 (d, 1 H, $J = 8.0$ Hz, 8-H), 6.70 (d, 2 H, $J = 8.8$ Hz, 2-H), 6.92 (d, 2 H, $J = 8.7$ Hz, 3-H), 7.28-7.32 (m, 2 H, 15-H), 7.44-7.49 (m, 5 H, 10-H, 14-H, 16-H), 8.14 (d, 2 H, $J = 8.9$ Hz, 11-H). $^{13}\text{C-NMR}$ (CDCl_3 , 101 MHz): $\delta = 15.2$ (q, $\text{OCHH}'\text{CH}_3$), 15.3 (q, $\text{OCHH}'\text{CH}_3$), 36.8 (t, C-6), 41.4 (d, C-5), 55.2 (q, OCH_3), 60.9 (t, $\text{OCHH}'\text{CH}_3$), 61.8 (t, $\text{OCHH}'\text{CH}_3$), 75.9 (d, C-8), 100.3 (d, C-7), 114.0 (d, C-2), 123.6 (d, C-11), 128.2 (d, C-10), 128.8 (d, C-15), 129.4 (d, C-3), 131.0 (s, C-4), 131.4 (d, C-14), 133.3 (d, C-16), 139.0 (s, C-13), 139.4 (s, C-9), 148.0 (s, C-12), 158.8 (s, C-1). MS (EI): m/e (%) = 513 (1) $[\text{M}]^+$, 327 (8), 280 (15), 264 (5), 256 (6), 255 (12), 191 (5), 165 (16), 104 (5), 103 (100), 77 (5), 75 (22), 47 (18). HR-MS (EI) $[\text{M}]^+$: calcd for $[\text{C}_{27}\text{H}_{31}\text{NO}_7\text{S}]^+$: 513.1816, found 513.1815. HR-MS (ESI $^+$) $[\text{M}+\text{NH}_4]^+$: calcd for $[\text{C}_{27}\text{H}_{35}\text{N}_2\text{O}_7\text{S}]^+$: 531.2160, found 531.2166.

Ethyl 2-ethoxy-4-(4-methoxyphenyl)-6-methyl-3,4-dihydro-2H-pyran-5-carboxylate (6c) was obtained from ethyl 3-oxobutanoate potassium salt (**2k-K**, 70.0 mg, 416 μmol) and the imine **1** (110 mg, 349 μmol) after 5 min of reaction time as colorless oil (10 mg, 31 μmol , 9%, *d.r.* $\sim 5 : 1$). NMR signals are only given for the major diastereomer.

RAP 81.1

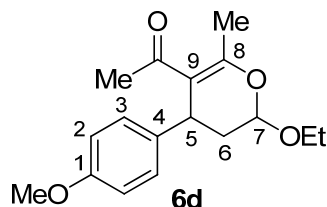


R_f (*n*-pentane/EtOAc 5:1, v/v): 0.64. ¹H-NMR (CDCl₃, 599 MHz): δ = 0.98 (t, 3 H, *J* = 7.1 Hz, OCH₂CH₃), 1.21 (t, 3 H, *J* = 7.1 Hz, OCHH'CH₃), 1.96 (ddd, 1 H, *J* = 13.3, 4.7, 2.5 Hz, 6-H), 2.03 (ddd, 1 H, *J* = 13.4, 8.0, 6.2 Hz, 6-H), 2.34 (d, 3 H, *J* = 1.4 Hz, Me), 3.51-3.57 (m, 1 H, OCHH'CH₃), 3.78 (s, 3 H, OMe), 3.91-4.00 (m, 4 H, 5-H, OCHH'CH₃, OCH₂CH₃), 4.85 (dd, 1 H, *J* = 8.0, 2.5 Hz, 7-H), 6.82 (d, 2 H, *J* = 8.7 Hz, 2-H), 7.08 (d, 2 H, *J* = 8.4 Hz, 3-H). ¹³C-NMR (CDCl₃, 151 MHz): δ = 14.0 (q, OCH₂CH₃), 15.2 (q, OCHH'CH₃), 16.9 (q, Me), 35.9 (t, C-6), 36.2 (d, C-5), 55.2 (q, OCH₃), 59.6 (t, OCH₂CH₃), 64.8 (t, OCHH'CH₃), 97.4 (d, C-7), 104.3 (s, C-9), 113.7 (d, C-2), 128.4 (d, C-3), 137.7 (s, C-4), 157.9 (s, C-1), 162.5 (s, C-8), 168.0 (s, CO). MS (EI): *m/e* (%) = 320 (35) [M]⁺, 302 (46), 275 (20), 274 (58), 273 (18), 248 (89), 247 (55), 245 (25), 233 (100), 231 (15), 228 (22), 217 (37), 203 (33), 201 (15), 191 (17), 174 (24), 161 (27), 134 (16), 43 (26). HR-MS (EI) [M]⁺: calcd for [C₁₈H₂₄O₅]⁺: 320.1618, found 320.1616.

1-(2-Ethoxy-4-(4-methoxyphenyl)-6-methyl-3,4-dihydro-2H-pyran-5-yl)ethanone (6d) was obtained by a slight modification of *General procedure B*: Imine **1** (150 mg, 476 μmol, dissolved in 3 mL of dry DMSO) was added to a solution of the CH acid (**2I**)-H (53.0 mg, 529 μmol) and KO^tBu (60.0 mg, 535 μmol) in dry DMSO (2-3 mL). After stirring for less than 1 min at rt, the reaction was quenched by the addition of diluted aqueous acetic acid solution (1 %) followed by the extraction with CH₂Cl₂. The combined organic layers were washed with water and brine, dried over Na₂SO₄ and evaporated under reduced pressure. The residue was resolved in EtOH (20-30 mL), treated with 2 M HCl (2 mL), and stirred under reflux for 1 h. The resulting reaction mixture was subsequently extracted with CH₂Cl₂, the combined organic layers dried over Na₂SO₄ and evaporated under reduced pressure. The residue was again resolved in EtOH (20 mL), treated with NaBH₄ (35 mg, 925 μmol), and stirred for 15 min at rt. This step was necessary to reduce *p*-methoxycinnamaldehyde (formed during the hydrolysis) to the corresponding alcohol, which could be more easily separated from the product by column chromatography. The reaction mixture was subsequently quenched with 0.5 M NH₄Cl solution and extracted with CH₂Cl₂. The combined organic layers were dried over Na₂SO₄ and evaporated under reduced pressure. Purification of the crude product by column chromatography on silica gel (*n*-pentane/EtOAc) yielded **6d** (11 mg, 38 μmol, 8 %, *dr* ~ 5 : 1) as colorless oil, which was subsequently characterized by ¹H- and ¹³C-NMR spectroscopy and MS. Signal assignments were based on additional COSY, HSQC and HMBC experiments. The diastereomeric ratio of the purified product did not differ

significantly from that of the crude mixtures before column chromatography. NMR signals are only given for the major diastereomer.

RAP 103.6



R_f (*n*-pentane/EtOAc 6:1, *v/v*): 0.41. $^1\text{H-NMR}$ (CDCl_3 , 599 MHz): δ = 1.21 (t, 3 H, J = 7.1 Hz, $\text{OCHH}'\text{CH}_3$), 1.95 (s, 3 H, COMe), 1.99 (ddd, 1 H, J = 13.2, 4.7, 2.5 Hz, 6-H), 2.07 (ddd, 1 H, J = 13.3, 8.1, 6.0 Hz, 6-H), 2.30 (d, 3 H, J = 1.3 Hz, Me), 3.50-3.56 (m, 1 H, $\text{OCHH}'\text{CH}_3$), 3.79 (s, 3 H, OMe), 3.91-3.98 (m, 2 H, 5-H, $\text{OCHH}'\text{CH}_3$), 4.81 (dd, 1 H, J = 8.1, 2.5 Hz, 7-H), 6.85 (d, 2 H, J = 8.8 Hz, 2-H), 7.09 (d, 2 H, J = 8.5 Hz, 3-H). $^{13}\text{C-NMR}$ (CDCl_3 , 151 MHz): δ = 15.2 (q, $\text{OCHH}'\text{CH}_3$), 20.6 (q, Me), 29.5 (q, COMe), 36.3 (t, C-6), 37.2 (d, C-5), 55.3 (q, OCH_3), 64.8 (t, $\text{OCHH}'\text{CH}_3$), 97.2 (d, C-7), 112.5 (s, C-9), 114.2 (d, C-2), 128.7 (d, C-3), 136.7 (s, C-4), 158.4 (s, C-1), 162.2 (s, C-8), 199.7 (s, CO). MS (EI): m/e (%) = 290 (30) $[\text{M}]^+$, 272 (72), 247 (52), 244 (69), 243 (99), 217 (35), 203 (97), 202 (33), 201 (52), 191 (31), 176 (35), 175 (49), 161 (88), 43 (100). HR-MS (EI) $[\text{M}]^+$: calcd for $[\text{C}_{17}\text{H}_{22}\text{O}_4]^+$: 290.1513, found 290.1507.

5.3 Kinetics

5.3.1 Reactions of the Sulfur Ylide 2a and the Carbanions 2b–e,g–i with the 2-Position of Imine 1

Table 3: Kinetics of the reaction of 2a with 1 in DMSO at 20°C (stopped-flow UV-Vis spectrometer, λ = 530 nm).

No.	$[\text{Nu}]_0 / \text{mol L}^{-1}$ *	$[\text{E}]_0 / \text{mol L}^{-1}$	$k_{\text{obs}} / \text{s}^{-1}$
RAK 23.41-1	$< 4 \times 10^{-5}$	4.43×10^{-4}	1.32
RAK 23.41-2	$< 4 \times 10^{-5}$	6.64×10^{-4}	2.01
RAK 23.41-3	$< 4 \times 10^{-5}$	8.85×10^{-4}	2.65
RAK 23.41-4	$< 4 \times 10^{-5}$	1.13×10^{-3}	3.35
RAK 23.41-5	$< 4 \times 10^{-5}$	1.33×10^{-3}	4.05

$$k_2 = 3.07 \times 10^3 \text{ L mol}^{-1} \text{ s}^{-1}$$

* Only approximate values are given for the initial concentration of the nucleophile (see general comments).

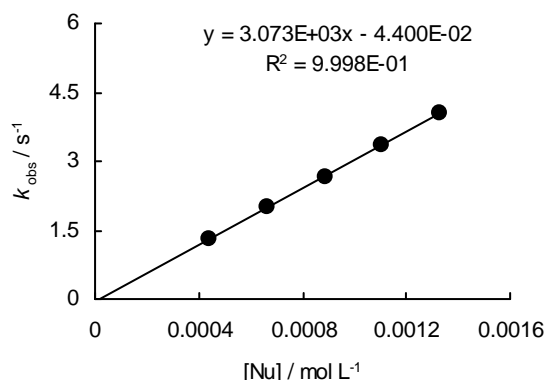
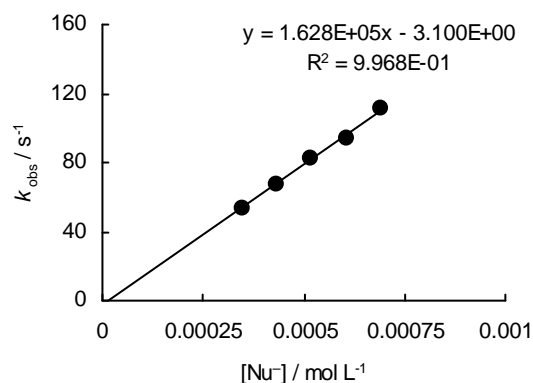
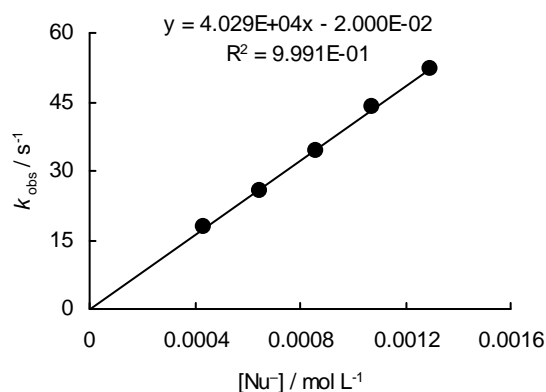


Table 4: Kinetics of the reaction of **2b** with **1** in DMSO at 20°C (stopped-flow UV-Vis spectrometer, $\lambda = 383$ nm).

No.	$[E]_0 / \text{mol L}^{-1}$	$[\text{Nu}^-]_0 / \text{mol L}^{-1}$	$k_{\text{obs}} / \text{s}^{-1}$
RAK 28.2-1	3.60×10^{-5}	3.46×10^{-4}	5.34×10^1
RAK 28.2-2	3.60×10^{-5}	4.33×10^{-4}	6.77×10^1
RAK 28.2-3	3.60×10^{-5}	5.20×10^{-4}	8.19×10^1
RAK 28.2-4	3.60×10^{-5}	6.06×10^{-4}	9.35×10^1
RAK 28.2-5	3.60×10^{-5}	6.93×10^{-4}	1.11×10^2
$k_2 = 1.63 \times 10^5 \text{ L mol}^{-1} \text{ s}^{-1}$			

**Table 5:** Kinetics of the reaction of **2c** with **1** in DMSO at 20°C (stopped-flow UV-Vis spectrometer, $\lambda = 383$ nm).

No.	$[E]_0 / \text{mol L}^{-1}$	$[\text{Nu}^-]_0 / \text{mol L}^{-1}$	$k_{\text{obs}} / \text{s}^{-1}$
RAK 28.1-1	3.60×10^{-5}	4.31×10^{-4}	1.78×10^1
RAK 28.1-2	3.60×10^{-5}	6.46×10^{-4}	2.55×10^1
RAK 28.1-3	3.60×10^{-5}	8.62×10^{-4}	3.44×10^1
RAK 28.1-4	3.60×10^{-5}	1.08×10^{-3}	4.37×10^1
RAK 28.1-5	3.60×10^{-5}	1.29×10^{-3}	5.21×10^1
$k_2 = 4.03 \times 10^4 \text{ L mol}^{-1} \text{ s}^{-1}$			

**Table 6:** Kinetics of the reaction of **2d** with **1** in DMSO at 20°C (stopped-flow UV-Vis spectrometer, $\lambda = 383$ nm).

No.	$[E]_0 / \text{mol L}^{-1}$	$[\text{Nu}^-]_0 / \text{mol L}^{-1}$	$k_{\text{obs}} / \text{s}^{-1}$
RAK 28.4-1	3.60×10^{-5}	4.43×10^{-4}	5.83×10^1
RAK 28.4-2	3.60×10^{-5}	6.64×10^{-4}	9.22×10^1
RAK 28.4-3	3.60×10^{-5}	8.85×10^{-4}	1.23×10^2
RAK 28.4-4	3.60×10^{-5}	1.11×10^{-3}	1.56×10^2
$k_2 = 1.46 \times 10^5 \text{ L mol}^{-1} \text{ s}^{-1}$			

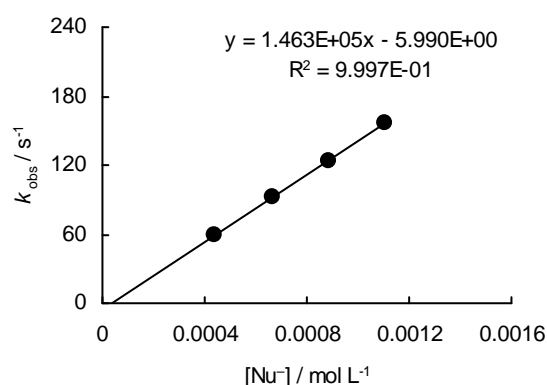
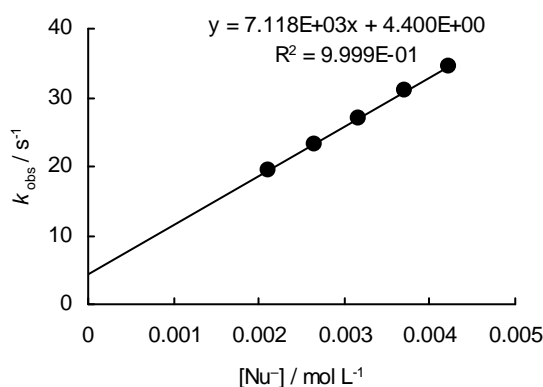


Table 7: Kinetics of the reaction of **2e** with **1** in DMSO at 20°C (addition of 1.17 equiv of 18-crown-6, stopped-flow UV-Vis spectrometer, $\lambda = 358$ nm).

No.	$[E]_0 / \text{mol L}^{-1}$	$[\text{Nu}^-]_0 / \text{mol L}^{-1}$	$[\text{18-crown-6}] / \text{mol L}^{-1}$	$k_{\text{obs}} / \text{s}^{-1}$
RAK 28.3-3-1	2.60×10^{-5}	2.12×10^{-3}	2.48×10^{-3}	1.95×10^1
RAK 28.3-3-2	2.60×10^{-5}	2.65×10^{-3}	3.10×10^{-3}	2.32×10^1
RAK 28.3-3-3	2.60×10^{-5}	3.18×10^{-3}	3.72×10^{-3}	2.70×10^1
RAK 28.3-3-4	2.60×10^{-5}	3.71×10^{-3}	4.34×10^{-3}	3.09×10^1
RAK 28.3-3-5	2.60×10^{-5}	4.24×10^{-3}	4.96×10^{-3}	3.45×10^1

$k_2 = 7.12 \times 10^3 \text{ L mol}^{-1} \text{ s}^{-1}$

**Table 8:** Kinetics of the reaction of **2g** with **1** in DMSO at 20°C (stopped-flow UV-Vis spectrometer, $\lambda = 358$ nm).

No.	$[E]_0 / \text{mol L}^{-1}$	$[\text{Nu}^-]_0 / \text{mol L}^{-1}$	$k_{\text{obs}} / \text{s}^{-1}$
RAK 28.6-1	2.38×10^{-5}	3.76×10^{-4}	1.79
RAK 28.6-2	2.38×10^{-5}	5.65×10^{-4}	2.44
RAK 28.6-3	2.38×10^{-5}	7.53×10^{-4}	3.11
RAK 28.6-4	2.38×10^{-5}	9.41×10^{-4}	3.77
RAK 28.6-5	2.38×10^{-5}	1.13×10^{-3}	4.43

$k_2 = 3.51 \times 10^3 \text{ L mol}^{-1} \text{ s}^{-1}$

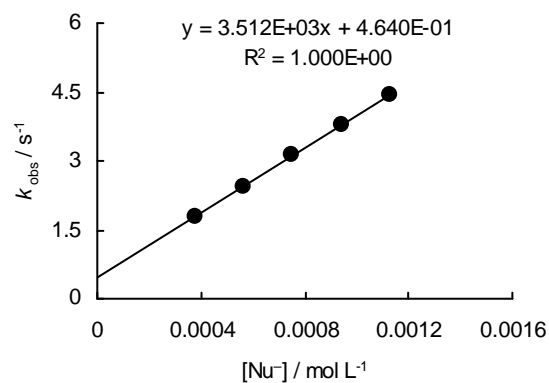
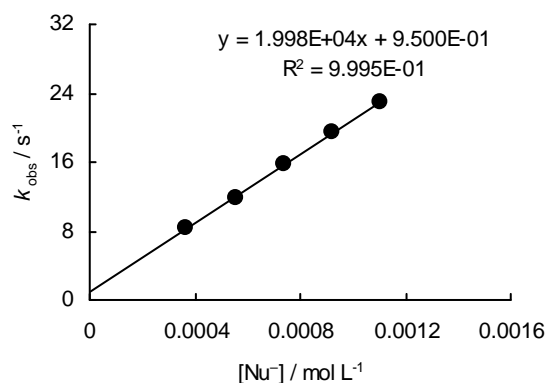
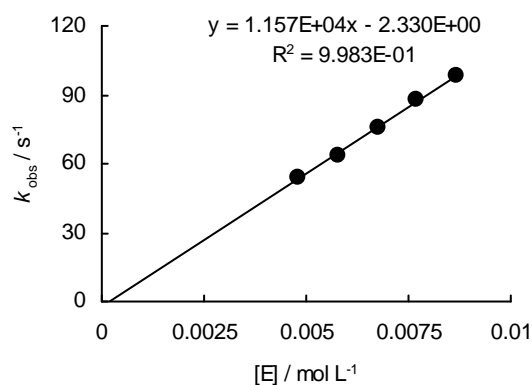


Table 9: Kinetics of the reaction of **2h** with **1** in DMSO at 20°C (stopped-flow UV-Vis spectrometer, $\lambda = 358$ nm).

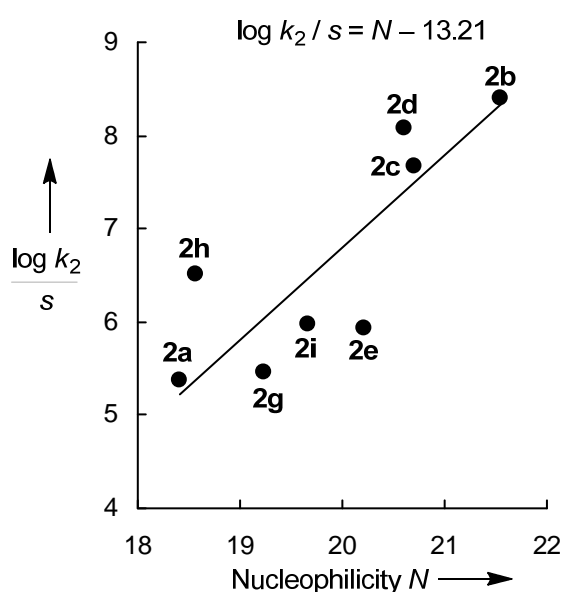
No.	$[E]_0 / \text{mol L}^{-1}$	$[\text{Nu}^-]_0 / \text{mol L}^{-1}$	$k_{\text{obs}} / \text{s}^{-1}$
RAK 28.5-1	2.38×10^{-5}	3.69×10^{-4}	8.39
RAK 28.5-2	2.38×10^{-5}	5.53×10^{-4}	1.18×10^1
RAK 28.5-3	2.38×10^{-5}	7.37×10^{-4}	1.58×10^1
RAK 28.5-4	2.38×10^{-5}	9.22×10^{-4}	1.94×10^1
RAK 28.5-5	2.38×10^{-5}	1.11×10^{-3}	2.30×10^1
$k_2 = 2.00 \times 10^4 \text{ L mol}^{-1} \text{ s}^{-1}$			

**Table 10:** Kinetics of the reaction of **2i** with **1** in DMSO at 20°C (stopped-flow UV-Vis spectrometer, $\lambda = 530$ nm).

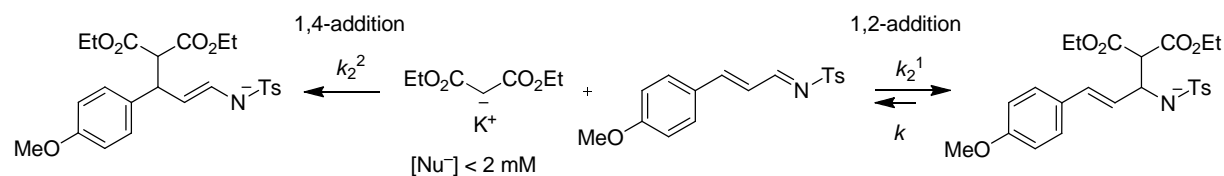
No.	$[\text{Nu}^-]_0 / \text{mol L}^{-1}$	$[E]_0 / \text{mol L}^{-1}$	$k_{\text{obs}} / \text{s}^{-1}$
RAK 28.15-2-4	3.44×10^{-5}	4.82×10^{-3}	5.42×10^1
RAK 28.15-2-5	3.44×10^{-5}	5.78×10^{-3}	6.36×10^1
RAK 28.15-2-6	3.44×10^{-5}	6.75×10^{-3}	7.53×10^1
RAK 28.15-2-7	3.44×10^{-5}	7.71×10^{-3}	8.75×10^1
RAK 28.15-2-8	3.44×10^{-5}	8.67×10^{-3}	9.80×10^1
$k_2 = 1.16 \times 10^4 \text{ L mol}^{-1} \text{ s}^{-1}$			

**Table 11:** Determination of the electrophilicity parameters E for the 2-position of **1** (least-squares minimization of $\Delta^2 = \sum (\log k_2 - s(N + E))^2$ for the correlation of $\log k_2 / s$ of the reactions of **1** with **2a–e,g–i** versus the nucleophilicity parameters N for **2a–e,g–i**)

Electrophile	Nucleophile (N, s)	$k_2 / \text{L mol}^{-1} \text{ s}^{-1}$	
 1	2a (18.42, 0.65)	3.07×10^3	
	2b (21.54, 0.62)	1.63×10^5	
	2c (20.71, 0.60)	4.03×10^4	
	2d (20.61, 0.64)	1.46×10^5	
	2e (20.22, 0.65)	7.12×10^3	
	2g (19.23, 0.65)	3.51×10^3	
	2h (18.57, 0.66)	2.00×10^4	
	2i (19.67, 0.68)	1.16×10^4	
	E (2-position) = -13.21		



5.3.2 Reactions of the Carbanions 2e,f,i-l with the 4-Position of Imine 1

Table 12: Kinetics of the reaction of **2e** with **1** in DMSO at 20°C (stopped-flow UV-Vis spectrometer, the bi-exponential decays have been fitted by GEPASI^[22] according to the kinetic model described below).

No.	[E] ₀ / mol L ⁻¹	[Nu ⁻] ₀ / mol L ⁻¹	<i>k</i> ₂ ¹ / L mol ⁻¹ s ⁻¹ ^c	<i>k</i> / s ⁻¹	<i>k</i> ₂ ² / L mol ⁻¹ s ⁻¹
RAK 28.3-1 ^a	3.60 × 10 ⁻⁵	3.89 × 10 ⁻⁴	(7.12 ± 0.03) × 10 ³	4.59 ± 0.02	(1.30 ± <0.01) × 10 ³
RAK 28.3-2 ^a	3.60 × 10 ⁻⁵	5.83 × 10 ⁻⁴	(7.12 ± 0.02) × 10 ³	4.48 ± 0.01	(1.35 ± <0.01) × 10 ³
RAK 28.3-3 ^a	3.60 × 10 ⁻⁵	7.78 × 10 ⁻⁴	(7.12 ± 0.02) × 10 ³	4.44 ± 0.01	(1.35 ± <0.01) × 10 ³
RAK 28.3-4 ^a	3.60 × 10 ⁻⁵	9.72 × 10 ⁻⁴	(7.12 ± 0.02) × 10 ³	4.58 ± 0.01	(1.32 ± <0.01) × 10 ³
RAK 28.3-5 ^a	3.60 × 10 ⁻⁵	1.17 × 10 ⁻³	(7.12 ± 0.02) × 10 ³	4.53 ± 0.01	(1.32 ± <0.01) × 10 ³
RAK 28.3-2-1 ^b	2.38 × 10 ⁻⁵	3.95 × 10 ⁻⁴	(7.12 ± 0.02) × 10 ³	4.40 ± 0.01	(1.36 ± <0.01) × 10 ³
RAK 28.3-2-1 ^b	2.38 × 10 ⁻⁵	5.92 × 10 ⁻⁴	(7.12 ± 0.02) × 10 ³	4.40 ± 0.01	(1.35 ± <0.01) × 10 ³
RAK 28.3-2-1 ^b	2.38 × 10 ⁻⁵	7.89 × 10 ⁻⁴	(7.12 ± 0.02) × 10 ³	4.37 ± 0.01	(1.32 ± <0.01) × 10 ³
RAK 28.3-2-1 ^b	2.38 × 10 ⁻⁵	9.86 × 10 ⁻⁴	(7.12 ± 0.02) × 10 ³	4.41 ± 0.01	(1.29 ± <0.01) × 10 ³
RAK 28.3-2-1 ^b	2.38 × 10 ⁻⁵	1.18 × 10 ⁻³	(7.12 ± 0.02) × 10 ³	4.38 ± 0.01	(1.27 ± <0.01) × 10 ³
Average			7.12 × 10³	4.46	1.32 × 10³

^a λ = 383 nm. ^b λ = 358 nm. ^c *k*₂¹ was kept constant (7.12 × 10³ L mol⁻¹ s⁻¹) during the fitting process because it was determined independently and more accurately by using very high concentrations of **2e** over imine **1** resulting in simple first-order kinetics with mono-exponential decays (see Table 7).

Table 13: Kinetics of the reaction of **2f** with **1** in DMSO at 20°C (stopped-flow UV-Vis spectrometer, λ = 358 nm).

No.	[E] ₀ / mol L ⁻¹	[Nu ⁻] ₀ / mol L ⁻¹	<i>k</i> _{obs} / s ⁻¹
RAK 28.7-1	2.53 × 10 ⁻⁵	4.50 × 10 ⁻⁴	4.38 × 10 ⁻¹
RAK 28.7-2-1	3.20 × 10 ⁻⁵	6.62 × 10 ⁻⁴	5.59 × 10 ⁻¹
RAK 28.7-2	2.53 × 10 ⁻⁵	6.75 × 10 ⁻⁴	5.94 × 10 ⁻¹
RAK 28.7-3	2.53 × 10 ⁻⁵	9.00 × 10 ⁻⁴	7.19 × 10 ⁻¹
RAK 28.7-2-2	3.20 × 10 ⁻⁵	9.93 × 10 ⁻⁴	7.74 × 10 ⁻¹
RAK 28.7-4	2.53 × 10 ⁻⁵	1.13 × 10 ⁻³	8.71 × 10 ⁻¹
RAK 28.7-2-3	3.20 × 10 ⁻⁵	1.32 × 10 ⁻³	9.85 × 10 ⁻¹
RAK 28.7-5	2.53 × 10 ⁻⁵	1.35 × 10 ⁻³	1.00
RAK 28.7-2-4	3.20 × 10 ⁻⁵	1.66 × 10 ⁻³	1.16
<i>k</i>₂ = 6.08 × 10² L mol⁻¹ s⁻¹			

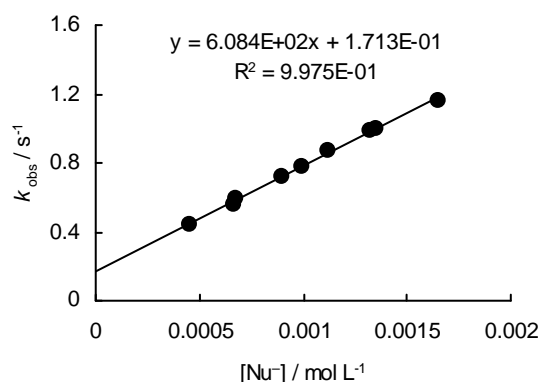
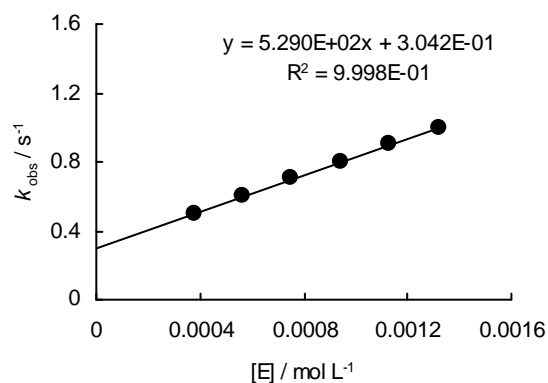
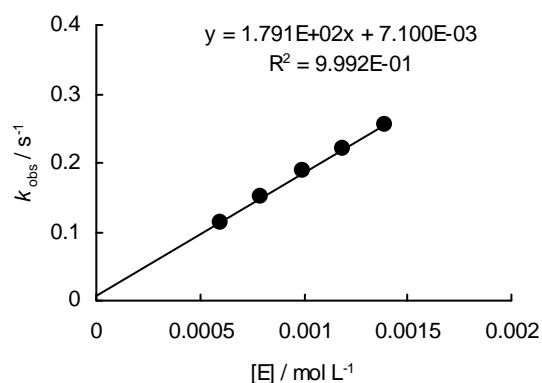


Table 14: Kinetics of the reaction of **2i** with **1** in DMSO at 20°C (stopped-flow UV-Vis spectrometer, $\lambda = 530$ nm).

No.	$[\text{Nu}^-]_0 / \text{mol L}^{-1}$	$[\text{E}]_0 / \text{mol L}^{-1}$	$k_{\text{obs}} / \text{s}^{-1}$
RAK 28.10-1	3.16×10^{-5}	3.77×10^{-4}	5.01×10^{-1}
RAK 28.10-2	3.16×10^{-5}	5.65×10^{-4}	6.07×10^{-1}
RAK 28.10-3	3.16×10^{-5}	7.53×10^{-4}	7.02×10^{-1}
RAK 28.10-4	3.16×10^{-5}	9.42×10^{-4}	8.00×10^{-1}
RAK 28.10-5	3.16×10^{-5}	1.13×10^{-3}	9.05×10^{-1}
RAK 28.10-6	3.16×10^{-5}	1.32×10^{-3}	1.00
$k_2 = 5.29 \times 10^2 \text{ L mol}^{-1} \text{ s}^{-1}$			

**Table 15:** Kinetics of the reaction of **2j** with **1** in DMSO at 20°C (stopped-flow UV-Vis spectrometer, $\lambda = 530$ nm).

No.	$[\text{Nu}^-]_0 / \text{mol L}^{-1}$	$[\text{E}]_0 / \text{mol L}^{-1}$	$k_{\text{obs}} / \text{s}^{-1}$
RAK 28.11-1	3.25×10^{-5}	5.95×10^{-4}	1.12×10^{-1}
RAK 28.11-2	3.25×10^{-5}	7.93×10^{-4}	1.50×10^{-1}
RAK 28.11-3	3.25×10^{-5}	9.91×10^{-4}	1.87×10^{-1}
RAK 28.11-4	3.25×10^{-5}	1.19×10^{-3}	2.19×10^{-1}
RAK 28.11-5	3.25×10^{-5}	1.39×10^{-3}	2.55×10^{-1}
$k_2 = 1.79 \times 10^2 \text{ L mol}^{-1} \text{ s}^{-1}$			

**Table 16:** Kinetics of the reaction of **2k** with **1** in DMSO at 20°C (stopped-flow UV-Vis spectrometer, $\lambda = 358$ nm).

No.	$[\text{E}]_0 / \text{mol L}^{-1}$	$[\text{Nu}^-]_0 / \text{mol L}^{-1}$	$k_{\text{obs}} / \text{s}^{-1}$
RAK 28.8-1	3.46×10^{-5}	4.71×10^{-4}	1.38×10^{-1}
RAK 28.8-2	3.46×10^{-5}	7.07×10^{-4}	1.85×10^{-1}
RAK 28.8-3	3.46×10^{-5}	9.42×10^{-4}	2.38×10^{-1}
RAK 28.8-4	3.46×10^{-5}	1.18×10^{-3}	2.90×10^{-1}
RAK 28.8-5	3.46×10^{-5}	1.41×10^{-3}	3.37×10^{-1}
$k_2 = 2.14 \times 10^2 \text{ L mol}^{-1} \text{ s}^{-1}$			

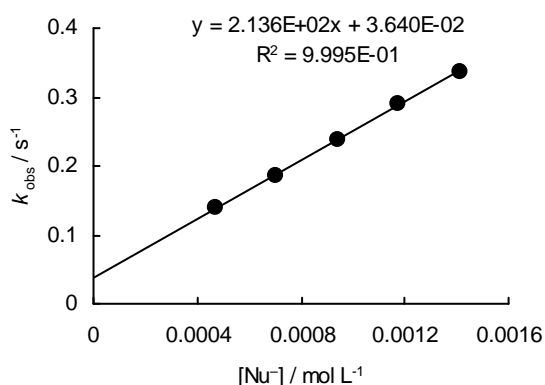
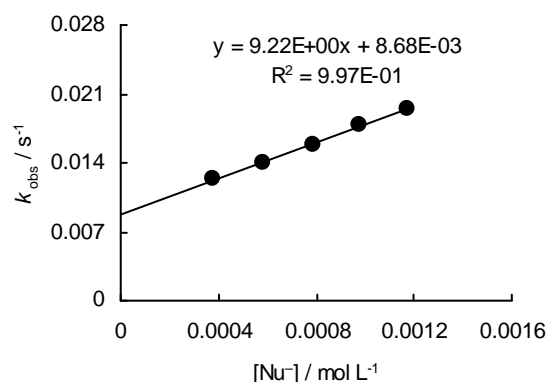
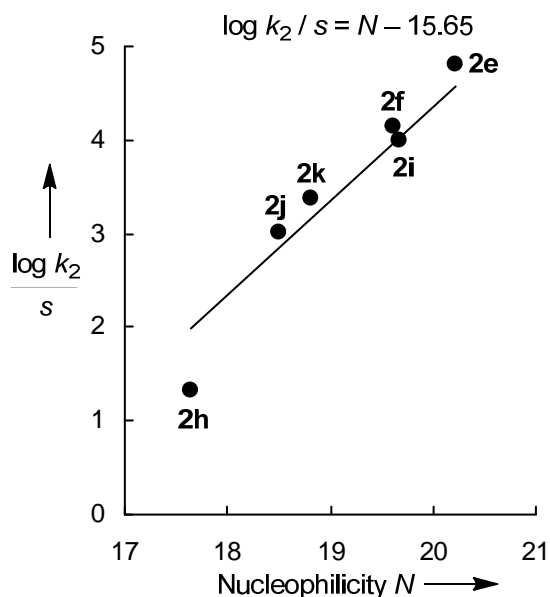


Table 17: Kinetics of the reaction of **2l** with **1** in DMSO at 20°C (diode array spectrometer, $\lambda = 358$ nm).

No.	$[E]_0 / \text{mol L}^{-1}$	$[\text{Nu}^-]_0 / \text{mol L}^{-1}$	$k_{\text{obs}} / \text{s}^{-1}$
RAK 28.9-1	3.64×10^{-5}	3.81×10^{-4}	1.23×10^{-2}
RAK 28.9-2	3.63×10^{-5}	5.82×10^{-4}	1.39×10^{-2}
RAK 28.9-3	3.63×10^{-5}	7.84×10^{-4}	1.58×10^{-2}
RAK 28.9-4	3.60×10^{-5}	9.78×10^{-4}	1.79×10^{-2}
RAK 28.9-5	3.57×10^{-5}	1.17×10^{-3}	1.94×10^{-2}
$k_2 = 9.22 \text{ L mol}^{-1} \text{ s}^{-1}$			

**Table 18:** Determination of the electrophilicity parameters E for the 4-position of **1** (least-squares minimization of $\Delta^2 = \sum(\log k_2 - s(N+ E))^2$ for the correlation of $\log k_2 / s$ of the reactions of **1** with **2e,f,i-l** versus the nucleophilicity parameters N for **2e,f,i-l**)

Electrophile	Nucleophile (N, s)	$k_2 / \text{L mol}^{-1} \text{ s}^{-1}$
<p style="text-align: center;">1</p>	2e (20.22, 0.65)	1.32×10^3
	2f (19.62, 0.67)	6.08×10^2
	2i (19.67, 0.68)	5.29×10^2
	2j (18.50, 0.75)	1.79×10^2
	2k (18.82, 0.69)	2.14×10^2
	2l (17.64, 0.73)	9.22
E (4-position) = -15.65		



6 References

- [1] Loos, R.; Kobayashi, S.; Mayr, H. *J. Am. Chem. Soc.* **2003**, *125*, 14126-14132.
- [2] Bug, T.; Lemek, T.; Mayr, H. *J. Org. Chem.* **2004**, *69*, 7565-7576.
- [3] Tishkov, A. A.; Mayr, H. *Angew. Chem.* **2005**, *117*, 145-148; *Angew. Chem. Int. Ed.* **2005**, *44*, 142-145.
- [4] Tishkov, A. A.; Schmidhammer, U.; Roth, S.; Riedle, E.; Mayr, H. *Angew. Chem.* **2005**, *117*, 4699-4703; *Angew. Chem. Int. Ed.* **2005**, *44*, 4623-4626.
- [5] Schaller, H. F.; Schmidhammer, U.; Riedle, E.; Mayr, H. *Chem. Eur. J.* **2008**, *14*, 3866-3868.
- [6] Baidya, M.; Kobayashi, S.; Mayr, H. *J. Am. Chem. Soc.* **2010**, *132*, 4796-4805.

- [7] (a) Pearson, R. G. *J. Am. Chem. Soc.* **1963**, *85*, 3533-3539. (b) Pearson, R. G. *Science* **1966**, *151*, 172-177. (c) Pearson, R. G.; Songstad, J. *J. Am. Chem. Soc.* **1967**, *89*, 1827-1836. (d) Pearson, R. G. *J. Chem. Educ.* **1968**, *45*, 581-587. (e) Pearson, R. G. *J. Chem. Educ.* **1968**, *45*, 643-648. (f) Pearson, R. G. *Chemical Hardness*; Wiley-VCH: Weinheim, Germany, 1997.
- [8] (a) Klopman, G. *J. Am. Chem. Soc.* **1968**, *90*, 223-234. (b) Salem, L. *J. Am. Chem. Soc.* **1968**, *90*, 543-552.
- [9] Anslyn, E. V.; Dougherty, D. A. *Modern Physical Organic Chemistry*; University Science Books, 2006; pp 567-568.
- [10] Clayden, J.; Greeves, N.; Warren, S.; Wothers, P. *Organic Chemistry*; Oxford University Press: New York, 2001; pp 234-235.
- [11] Hünig, S. *Angew. Chem.* **1964**, *76*, 400-412; *Angew. Chem. Int. Ed. Engl.* **1964**, *3*, 548-560.
- [12] a) Breugst, M.; Zipse, H.; Guthrie, J. P.; Mayr, H. *Angew. Chem.* **2010**, *122*, 5291-5295; *Angew. Chem. Int. Ed.* **2010**, *49*, 5165-5169. b) Mayr, H.; Breugst, M.; Ofial, A. R. *Angew. Chem.* **2010**, accepted.
- [13] (a) Aggarwal, V. K.; Ford, J. G.; Fonquerna, S.; Adams, H.; Jones, R. V. H.; Fieldhouse, R. *J. Am. Chem. Soc.* **1998**, *120*, 8328-8339. (b) Solladié-Cavallo, A.; Bouérat, L.; Roje, M. *Tetrahedron Lett.* **2000**, *41*, 7309-7312. (c) Aggarwal, V. K.; Alonso, E.; Bae, I.; Hynd, G.; Lydon, K. M.; Palmer, M. J.; Patel, M.; Porcelloni, M.; Richardson, J.; Stenson, R. A.; Studley, J. R.; Vasse, J.-L.; Winn, C. L. *J. Am. Chem. Soc.* **2003**, *125*, 10926-10940. (d) Phillips, D. J.; Graham, A. E. *Synlett* **2010**, 769-773. (e) See chapter 7 of this thesis.
- [14] Appel, R.; Hartmann, N.; Mayr, H. *J. Am. Chem. Soc.* **2010**, *132*, 17894-17900.
- [15] Lemek, T.; Mayr, H. *J. Org. Chem.* **2003**, *68*, 6880-6886.
- [16] Appel, R.; Mayr, H. *Chem. Eur. J.* **2010**, *16*, 8610-8614.
- [17] Lucius, R.; Loos, R.; Mayr, H. *Angew. Chem.* **2002**, *114*, 97-102; *Angew. Chem. Int. Ed.* **2002**, *41*, 91-95.
- [18] Appel, R.; Loos, R.; Mayr, H. *J. Am. Chem. Soc.* **2009**, *131*, 704-714.
- [19] Kaumanns, O.; Appel, R.; Lemek, T.; Seeliger, F.; Mayr, H. *J. Org. Chem.* **2009**, *74*, 75-81.
- [20] Seeliger, F.; Mayr, H. *Org. Biomol. Chem.* **2008**, *6*, 3052-3058.
- [21] Shen, Y.; Jiang, G.-F. *J. Chem. Res.* **2000**, 140-141.

- [22] (a) Mendes, P. *Comput. Applic. Biosci.* **1993**, *9*, 563-571. (b) Mendes, P. *Trends Biochem. Sci.* **1997**, *22*, 361-363. (c) Mendes, P.; Kell, D. B. *Bioinformatics* **1998**, *14*, 869-883. (d) For further information, see <http://www.gepasi.org/>.
- [23] (a) Mayr, H.; Patz, M. *Angew. Chem.* **1994**, *106*, 990-1010; *Angew. Chem. Int. Ed. Engl.* **1994**, *33*, 938-957. (b) Mayr, H.; Bug, T.; Gotta, M. F.; Hering, N.; Irrgang, B.; Janker, B.; Kempf, B.; Loos, R.; Ofial, A. R.; Remennikov, G.; Schimmel, H. *J. Am. Chem. Soc.* **2001**, *123*, 9500-9512. (c) Mayr, H.; Kempf, B.; Ofial, A. R. *Acc. Chem. Res.* **2003**, *36*, 66-77. (d) Mayr, H.; Ofial, A. R. *Pure Appl. Chem.* **2005**, *77*, 1807-1821. (e) Mayr, H.; Ofial, A. R. *J. Phys. Org. Chem.* **2008**, *21*, 584-595. (f) For a comprehensive database of nucleophilicity parameters N , s and electrophilicity parameters E , see <http://www.cup.lmu.de/oc/mayr/>.
- [24] Berger, S. T. A.; Seeliger, F. H.; Hofbauer, F.; Mayr, H. *Org. Biomol. Chem.* **2007**, *5*, 3020-3026.
- [25] Jennings, W. B.; Lovely, C. J. *Tetrahedron Lett.* **1988**, *29*, 3725-3728.
- [26] Yamada, K.-i.; Umeki, H.; Maekawa, M.; Yamamoto, Y.; Akindele, T.; Nakano, M.; Tomioka, K. *Tetrahedron* **2008**, *64*, 7258-7265.
- [27] (a) Labuschagne, A. J. H.; Malherbe, J. S.; Meyer, C. J.; Schneider, D. F. *J. Chem. Soc., Perkin Trans. 1* **1978**, 955-961. (b) Coppola, G. M.; Hardtmann, G. E. *J. Heterocycl. Chem.* **1979**, *16*, 1605-1610.
- [28] Scott, J. P.; Hammond, D. C.; Beck, E. M.; Brands, K. M. J.; Davies, A. J.; Dolling, U.-H.; Kennedy, D. J. *Tetrahedron Lett.* **2004**, *45*, 3345-3348.
- [29] Nickson, T. E. *J. Org. Chem.* **1988**, *53*, 3870-3872.
- [30] For the synthesis, see: Kaumanns, O.; Lucius, R.; Mayr, H. *Chem. Eur. J.* **2008**, *14*, 9675-9682.

Chapter 9: Nucleophilicities of the Anions of Arylacetonitriles and Arylpropionitriles in Dimethyl Sulfoxide

Oliver Kaumanns, Roland Appel, Tadeusz Lemek, Florian Seeliger, and Herbert Mayr
J. Org. Chem. **2009**, *74*, 75-81.

1 Introduction

The comparison of the nucleophilicities of different classes of compounds is of considerable importance for our understanding of organic reactivity. The most comprehensive nucleophilicity scale presently available is based on the reactions of benzhydrylium ions and structurally related quinone methides with different nucleophiles.^[1] With this method, we have been able to directly compare n -nucleophiles (amines, alcohols, and phosphanes), π -nucleophiles (alkenes, arenes, and organometallics), and σ -nucleophiles (hydride donors) with each other.^[1-4] Recently, we have investigated the reactivities of different carbanions^[5-10] including trifluoromethylsulfonyl-stabilized carbanions,^[6] phenylsulfonyl-stabilized carbanions,^[7] nitronates,^[8,9] as well as the bis(4-nitrophenyl)methyl anion^[10] and have demonstrated that their additions to benzhydryl cations and structurally related quinone methides can be described by eq 1, where E is an electrophile-specific parameter and N and s are nucleophile-specific parameters.

$$\log k_{20^\circ\text{C}} = s(N + E) \quad (1)$$

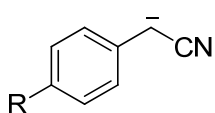
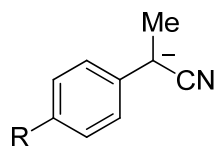
Vice versa, the second-order rate constants k_2 for the reactions of carbanions with Michael acceptors^[11-14] have been used to determine the electrophilicities of these electron-deficient π -systems.

Because UV-Vis spectroscopy is an efficient method to determine reaction rates, we have selected a set of colored benzhydrylium ions,^[2] quinone methides,^[4] and benzyldiene malonates^[14] as reference electrophiles for characterizing the reactivities of a large variety of nucleophiles. On the other hand, we do presently not yet have a comprehensive set of colored nucleophiles, which might be employed for the systematic investigation of the reactivities of electrophiles. So far, only colored carbanions of relatively low nucleophilicity ($N < 20$) have been characterized.^[5-10]

In view of the frequent use of cyano-substituted carbanions in organic synthesis, we have selected the carbanions **1a–c** and **2a–c** for systematic studies of the relationship between structure and nucleophilic reactivity of highly reactive carbanions.^[15]

Although the correlations between nucleophilicity (*N*) and basicity (pK_{aH}) of carbanions are not of high quality,^[6] the pK_{aH} values of the phenylacetonitrile anions (**1a–c**) and that of the phenylpropionitrile anion **2a** (Scheme 1) suggested that these carbanions have considerably higher reactivities than α -nitro- and α -trifluoromethylsulfonyl-stabilized benzyl anions.

Scheme 1: Phenylacetonitrile Anions **1a–c**, Phenylpropionitrile Anions **2a–c**, and their pK_{aH} Values in DMSO.

				
	R	pK_{aH}	R	pK_{aH}
1a	CF ₃	18.1 ^a	2a	H 23.0 ^b
1b	CN	16.0 ^b	2b	CN ^c
1c	NO ₂	12.3 ^b	2c	NO ₂ ^c

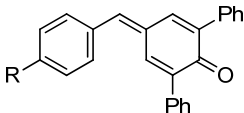
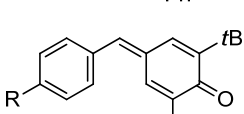
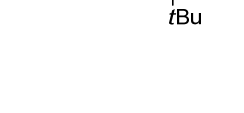
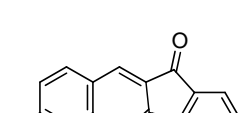
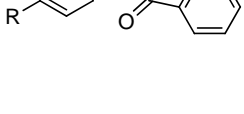
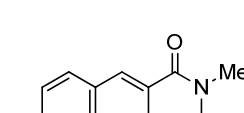
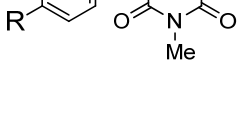
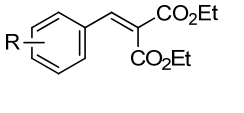


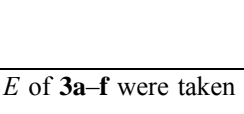
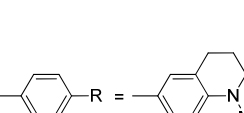


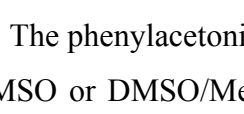
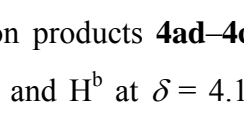


^a From ref 16a. ^b From ref 16b. ^c pK_{aH} values in DMSO not available.

Relative nucleophilicities of carbanions derived from α -substituted phenylacetonitriles **2** towards methyl iodide and other alkyl halides in liquid ammonia have previously been investigated by competition experiments.^[17]

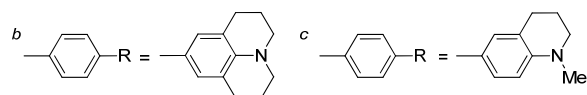
Recent studies of the oxidative nucleophilic substitution of hydrogen revealed that the phenylpropionitrile anion **2a** and its derivatives add to nitrobenzene and some nitrobenzene derivatives in liquid ammonia to form persistent σ^{H} -adducts, from which hydride was abstracted when treated subsequently with KMnO₄.^[18] When these σ^{H} -adducts were combined with dimethyldioxirane, replacement of the nitro group by hydroxyl took place prior to rearomatization, and the corresponding phenols were isolated as major products.^[19]

We will now report on the kinetics of the reactions of the phenylacetonitrile anions **1a–c** and the phenylpropionitrile anions **2a–c** with the electrophiles **3a–u** (Table 1) in DMSO at 20°C. The second-order rate constants k_2 will subsequently be used to derive the nucleophile-specific parameters *N* and *s* of the carbanions **1a–c** and **2a–c**.

Table 1. Michael Acceptors **3a–u** and their Electrophilicity Parameters E .

Electrophile	R	E^a
	3a OMe	-12.18
	3b NMe ₂	-13.39
	3c Me	-15.83
	3d OMe	-16.11
	3e NMe ₂	-17.29
	3f jul ^b	-17.90
	3g H	-10.11
	3h OMe	-11.32
	3i NMe ₂	-13.56
	3j jul ^b	-14.68
	3k OMe	-10.37
	3l NMe ₂	-12.76
	3m <i>p</i> -NO ₂	-17.67
	3n <i>p</i> -CN	-18.06
	3o <i>m</i> -Cl	-18.98
	3p H	-20.55
	3q <i>p</i> -Me	-21.11
	3r <i>p</i> -OMe	-21.47
	3s <i>p</i> -NMe ₂	-23.1
	3t thq ^c	-23.4
	3u jul ^b	-23.8

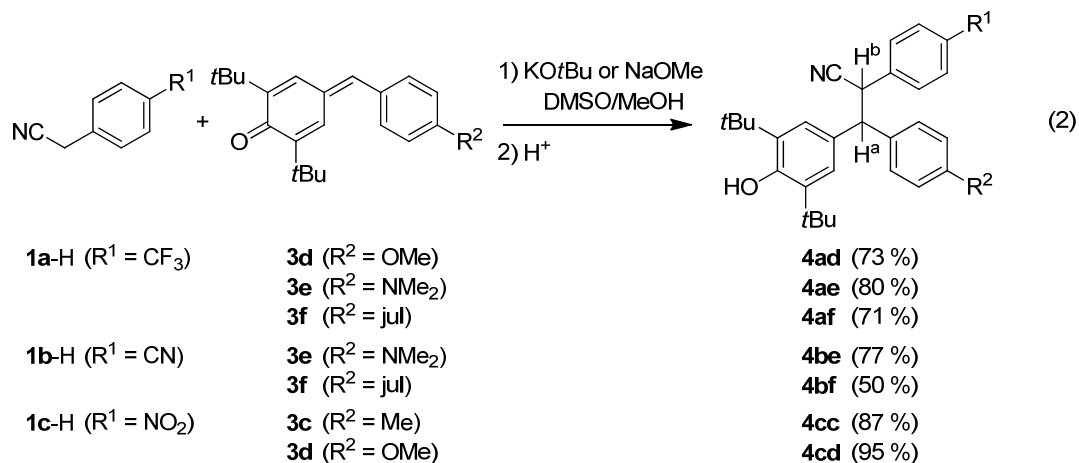
^a Electrophilicity parameters E of **3a–f** were taken from ref 4, of **3g–j** from ref 13, of **3k,l** from ref 12, and of **3m–u** from ref 14.



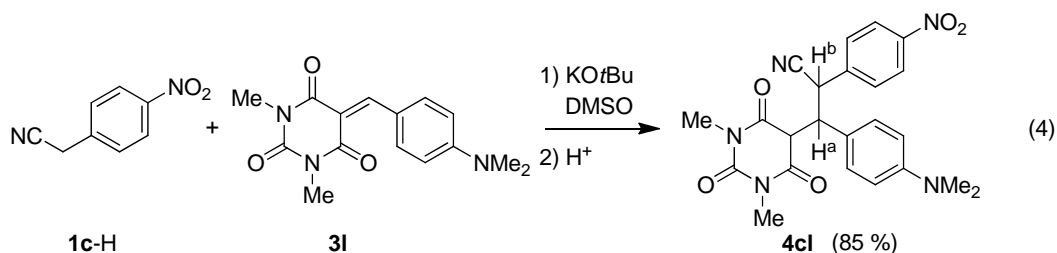
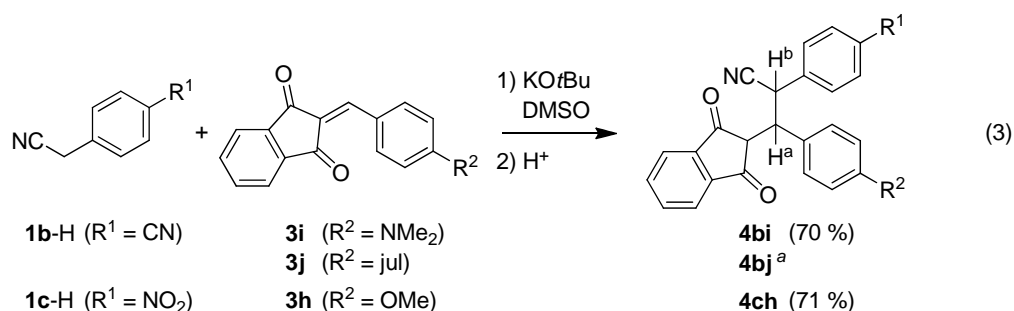
2 Results and Discussion

Product Studies. Products of representative combinations of nucleophiles with electrophiles have been characterized. The phenylacetonitrile anions **1a–c**, which were generated from (**1a–c**)-H with KO t Bu in DMSO or DMSO/MeOH mixtures, reacted with the quinone methides **3c–f** to give the addition products **4ad–4cd** (eq 2) in good yields. Their ¹H-NMR spectra showed doublets for H^a and H^b at $\delta = 4.11–4.54$ ppm and a signal for the hydroxy group.

Generally, two sets of signals in the $^1\text{H-NMR}$ spectra of the products **4** indicated the formation of almost equal amounts of two diastereomers.

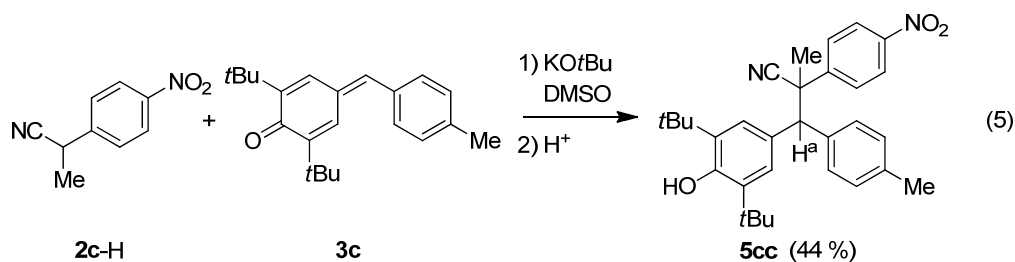


The reactions of carbanions **1b,c** with the benzylidene indandiones **3h–j** and of **1c** with the benzylidene barbituric acid **3l** showed the analogous formation of the addition products as a mixture of two diastereomers ($\approx 1:1$, eqs 3 and 4).

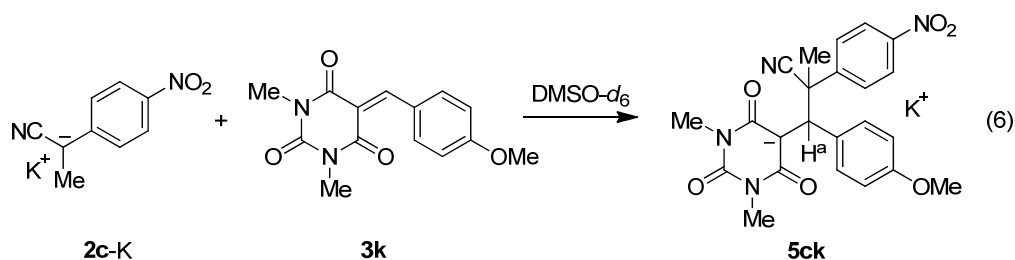


^a Product could not be isolated and was identified by $^1\text{H-NMR}$ of the crude mixture.

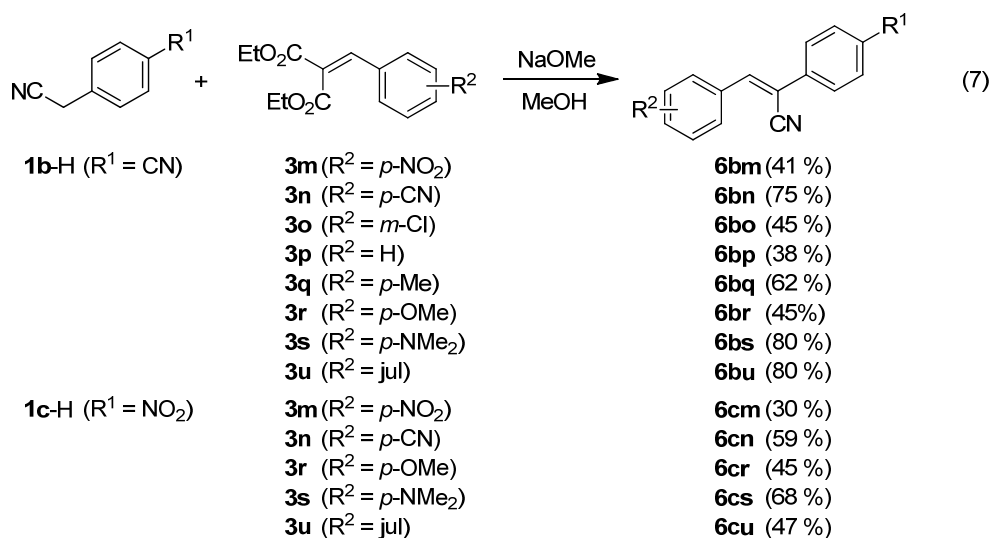
The reaction of the phenylpropionitrile anion **2c** with the quinone methide **3c** yielded **5cc** as a 1:1 pair of diastereomers, indicated by two singlets for H^a at $\delta = 3.95$ and 4.04 ppm, and for the hydroxy group at $\delta = 5.04$ and 5.20 ppm (eq 5).



The reaction of carbanion **2c** with **3k** was investigated by $^1\text{H-NMR}$ spectroscopy, which shows the formation of equal amounts of diastereomers of the anionic adduct **5ck** (eq 6).



In contrast, the reactions of the benzylidene malonates **3m–u** with the carbanions **1b,c** in methanol resulted in the formation of α -cyano stilbenes **6bm–6cu** via Michael addition, proton shift, and retro-Michael addition (eq 7). Compounds **6** were previously employed for the determination of H_R -acidity scales.^[20]



Kinetics. The rates of the reactions of the carbanions **1a–c** and **2b–c** with the electrophiles **3a–u** were determined photometrically under first-order conditions by using either the nucleophile or the electrophile in high excess as specified in Table 2.

Because of the large pK_a value of *t*BuOH in DMSO (29.4 or 32.2 from refs 21 and 22, respectively), all carbanions listed in Scheme 1 ($pK_{aH} < 23.0$) should be generated quantitatively when the corresponding CH acids were treated with one equiv of KO*t*Bu. Analogously, the deprotonation of (**1a–c**)-H and (**2a–c**)-H should also be quantitative with one equiv of the phosphazene base P₄-*t*Bu ($pK_{aH^+} = 30.2$).^[23] In order to verify the complete deprotonation of the CH acids (**1a–c**)-H, KO*t*Bu was added stepwise to solutions of (**1a–c**)-H and **2a**-H in DMSO. UV-Vis spectroscopy showed that in all cases, the limiting absorbances of the corresponding carbanions were achieved after the addition of one equivalent of KO*t*Bu, indicating quantitative deprotonation of these CH acids. While the absorbance of **1c** was persistent under these conditions, the absorbances of the carbanions **1a** and **1b** decreased slowly, when only one equiv of KO*t*Bu was added (see Figures 7–9 of the Experimental Section). Persistent absorbances of the carbanions **1a,b** could be observed, however, when they were generated from their conjugate acids (**1a,b**)-H with two equiv of KO*t*Bu. The unsubstituted phenylpropionitrile anion **2a**, which was also formed quantitatively with one equiv of KO*t*Bu or P₄-*t*Bu was not even persistent when generated with an excess (2–3 equiv) of base.

The kinetic experiments with the nitro-substituted carbanions **1c** and **2c** were unproblematic: Because of their stability, stock solutions of **1c**-K and **2c**-K were employed. On the other hand, solutions of the reactive carbanions **1a,b** and **2a,b** were generated immediately before the kinetic experiments by treatment of the corresponding CH acidic compounds with strong bases, and the kinetic investigations were restricted to reactions with active electrophiles, which proceeded faster than the decomposition of the carbanions.

For all reactions described in Table 2, first-order rate constants k_{obs} (s^{-1}) were obtained by least-squares fittings of the mono-exponential function $A_t = A_0 \exp(-k_{obs}t) + C$ to the time-dependent absorbances A of the minor components. Plots of k_{obs} versus the concentrations of the compounds used in excess were generally linear with negligible intercepts and the second-order rate constants k_2 ($L \text{ mol}^{-1} \text{ s}^{-1}$) as slopes (Figure 1, Table 2). Some exceptions are discussed below.

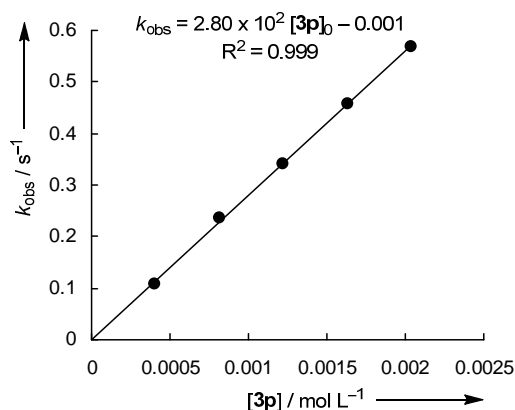


Figure 1: Determination of the second-order rate constant $k_2 = 2.80 \times 10^2 \text{ L mol}^{-1} \text{ s}^{-1}$ for the reaction of the *p*-cyanophenylacetonitrile anion (**1b**) with the Michael acceptor **3p** in DMSO at 20°C.

As mentioned above, we were not able to obtain persistent solutions of the carbanion **2a**. When its reactions with **3s** (used as the minor component) were followed photometrically, exponential decays of the electrophile (**3s**) absorbance were observed. Plots of k_{obs} vs the concentration of **2a** (calculated from $[\mathbf{2a-H}]$ assuming complete deprotonation) were linear, and the slopes, which equal the second-order rate constants k_2 , were almost identical (Table 2), independent of the quantity of the base (1.05 equiv of $\text{P}_4\text{-}t\text{Bu}$ or 1, 2, or 3 equiv of $\text{KO}t\text{Bu}$) used for the deprotonation of **2a**. However, significant negative intercepts of variable magnitude were observed in all cases, indicating fast and irreversible consumption of certain fractions of the carbanion **2a**. Similar observations, i.e., negative intercepts of variable magnitude and slopes, corresponding to second-order rate constants, which are almost independent of the nature and quantity of base used for the deprotonation of **2a-H**, were made for the analogous reactions of the carbanion **2a** with the electrophiles **3t,u**.

On the other hand, significant positive intercepts in plots of the first-order rate constants (k_{obs}) against the concentrations of the major component were observed for the reactions of the *p*-nitrophenylacetonitrile anion (**1c**) with the benzylidene malonates **3m** and **3n**. Positive intercepts are indicative of reversible reactions, and by theory, reflect the rate constants of the reverse reactions.^[24] However, as discussed above, the intercepts are also affected by side reactions that we refrain to employ the intercepts of these plots for calculating the rates of the reverse reactions and the equilibrium constants K .

As shown in Table 2, the addition of 18-crown-6 caused only insignificant changes of the second-order rate constants k_2 for the reactions of **1b** with **3j** and **3m** and of **1c** with **3c** and **3d**. These results confirm that ion-pairing is negligible in dilute DMSO solution, in accordance with literature reports^[25] and earlier findings of our group.^[6,8,26]

Table 2: Second-Order Rate Constants k_2 for the Reactions of the Phenylacetonitrile Anions **1a–c** and the Phenylpropionitrile Anions **2a–c** with the Michael Acceptors **3a–u** in DMSO at 20°C.

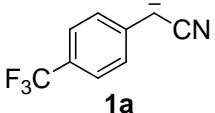
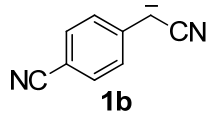
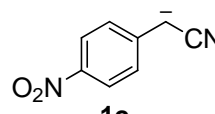
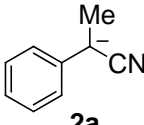
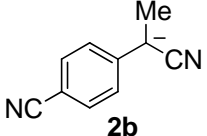
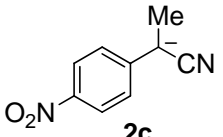
Nucleophile	Electrophile	λ / nm^a	$k_2 / \text{M}^{-1} \text{s}^{-1}^b$
 1a $N = 27.28; s = 0.50$	3d	3d / 440	4.04×10^5
	3e	3e / 486	8.24×10^4
	3f	3f / 521	5.45×10^4
 1b $N = 25.11; s = 0.54$	3e	3e / 486	1.10×10^4
	3f	3f / 521	6.59×10^3
	3i	3i / 490	1.61×10^6
	3j	3j / 523	3.94×10^5
	3j	3j / 523	4.09×10^{5c}
	3m	1b / 394	1.70×10^4
	3m	1b / 398	1.64×10^{4c}
	3m	1b / 398	$1.60 \times 10^{4c,d}$
	3m	1b / 398	$1.86 \times 10^{4c,e}$
	3n	1b / 394	8.87×10^3
	3o	1b / 397	2.81×10^3
	3p	1b / 397	2.80×10^2
	3q	1b / 394	1.54×10^2
	3r	1b / 394	6.50×10^1
 1c $N = 19.67; s = 0.68$	3a	3a / 400	1.29×10^{5c}
	3c	3c / 380	4.19×10^2
	3c	3c / 400	4.43×10^{2c}
	3d	3d / 400	3.43×10^2
	3d	3d / 400	3.26×10^{2c}
	3h	3h / 388	5.23×10^5
	3l	3l / 560	4.17×10^4
	3m	1c / 537	2.51×10^{1f}
3n	1c / 537	9.98^g	

Table 2: (Continued).

Nucleophile	Electrophile	λ / nm^a	$k_2 / \text{M}^{-1} \text{s}^{-1}^b$
 2a $N = 28.95; s = 0.58$	3f	3f / 524	$2.50 \times 10^6^g$
	3s	3s / 405	$3.05 \times 10^3^g$
	3s	3s / 410	$2.87 \times 10^3^g$
	3s	3s / 400	3.12×10^3
	3s	3s / 400	$3.09 \times 10^3^h$
	3s	3s / 400	$3.15 \times 10^3^i$
	3t	3t / 405	$1.86 \times 10^3^g$
	3t	3t / 405	$1.69 \times 10^3^h$
	3t	3t / 405	1.50×10^3
	3u	3u / 405	$9.90 \times 10^{-2}^g$
	3u	3u / 405	8.54×10^{-2}
	3u	3u / 405	$9.82 \times 10^{-2}^h$
	 2b $N = 25.35; s = 0.56$	3b	3b / 533
3e		3e / 488	$4.54 \times 10^4^j$
3e		3e / 488	3.20×10^4
3f		3f / 524	$2.51 \times 10^4^j$
3m		2b / 403	1.08×10^4
3m		2b / 403	1.15×10^4
3n		2b / 403	5.68×10^3
3o		2b / 403	2.44×10^3
3p		2b / 403	1.19×10^3
 2c $N = 19.61; s = 0.60$		3a	3a / 410
	3c	3c / 375	$2.04 \times 10^2^k$
	3d	2c / 590	$9.61 \times 10^1^k$
	3g	2c / 590	5.22×10^5
	3h	2c / 590	1.15×10^5
	3k	2c / 590	1.88×10^5
	3l	2c / 590	9.12×10^3

^a Minor component in the pseudo-first-order kinetics and monitored wavelength. ^b In the presence of 1 equiv KO^tBu. ^c In the presence of 18-crown-6. ^d In the presence of 3 equiv of **1b**-H. ^e Measurement at 25°C. ^f Reversible reactions (see text). ^g Deprotonation of **2a**-H with P₄-*t*Bu phosphazene base. ^h In the presence of 2 equiv of KO^tBu. ⁱ In the presence of 3 equiv of KO^tBu. ^j Deprotonation of **2b**-H with P₂-*t*Bu phosphazene base. ^k In the presence of **2c**-H.

Nucleophilicity of *tert*-Butoxide. As discussed above, persistent solutions of the more basic carbanions have only been obtained when more than 1 equiv of KO*t*Bu was used for the deprotonation of the corresponding CH acids. In order to elucidate the influence of excess KO*t*Bu on the kinetics, we have studied the reaction of **2b** with the quinone methide **3e** in the presence of variable excess of KO*t*Bu. As shown in Figure 2, the slope of the plot of k_{obs} vs [KO*t*Bu] was higher when [KO*t*Bu] > [2b-H] and from the different slopes in the range of [KO*t*Bu] < [2b-H] and [KO*t*Bu] > [2b-H] one can derive that KO*t*Bu is approximately two times more nucleophilic than **2b**. As a consequence, KO*t*Bu cannot be used in excess when nucleophiles with $N \leq 27$ are investigated. On the other hand, an excess of KO*t*Bu used for the deprotonation of **2a**-H will hardly affect the pseudo-first-order rate constant because **2a** reacts considerably faster than KO*t*Bu.

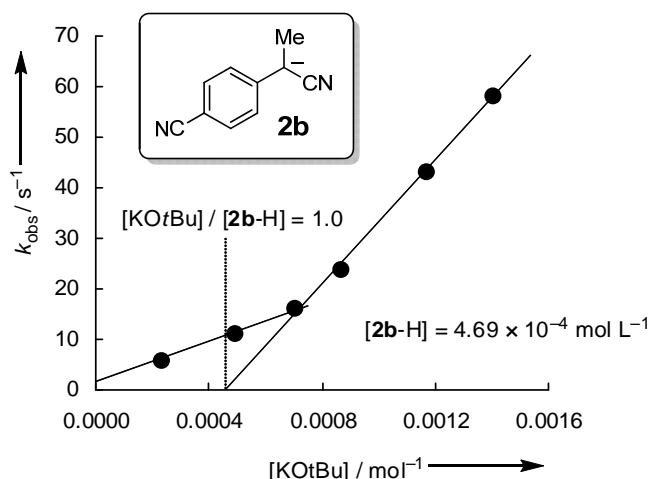


Figure 2. Plot of the observed first-order rate constants k_{obs} for the reactions of electrophile **3e** ($c_0 = 2.00 \times 10^{-5} \text{ mol L}^{-1}$) with the nucleophile **2b** against the concentration of KO*t*Bu used for the deprotonation of **2b**-H ($c_0 = 4.69 \times 10^{-4} \text{ mol L}^{-1}$) in DMSO at 20°C.

Correlation Analysis. In order to determine the nucleophile-specific parameters N and s for the phenylacetonitrile anions **1a**-**c** (Figure 3) and the phenylpropionitrile anions **2a**-**c** (Figure 4), the logarithmic second-order rate constants $\log k_2$ of their reactions with electrophiles **3a**-**u** were plotted against the electrophilicity parameters E of **3a**-**u**.

The linear correlations for the reactions of the phenylacetonitrile anions **1a**-**c** ($R^2 > 0.98$, Figure 3) allow us to determine the nucleophile-specific parameters N and s for these carbanions.

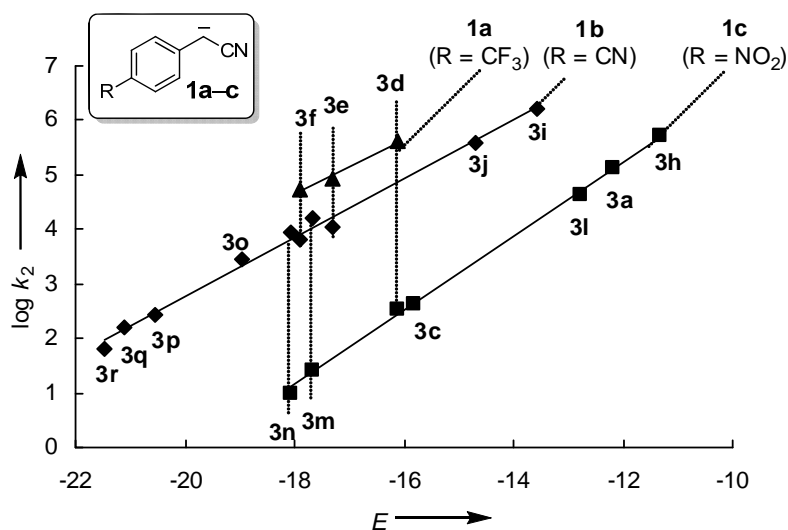


Figure 3: Plot of $\log k_2$ for the reactions of the nucleophiles **1a–c** with the electrophiles **3** in DMSO versus their electrophilicity parameters E .

The correlations for the reactions of the phenylpropionitrile anions **2a–c** ($R^2 \geq 0.95$, Figure 4) show larger deviations from linearity than those of the phenylacetonitrile anions **1a–c**. In particular, the reactions of the carbanion **2b** with benzylidenemalonate **3p**, as well as the reaction of carbanion **2c** with quinone methide **3a**, are two times faster than expected. On the other hand, the reactions of **2b** with the benzylidene malonates **3m,n** are approximately two times slower than expected. Taking into account that many different classes of Michael acceptors have been used as electrophiles, these deviations can be considered as rather small, and the correlation lines in Figure 4 were employed to determine the nucleophile-specific parameters N and s for the phenylpropionitriles **2a–c**.

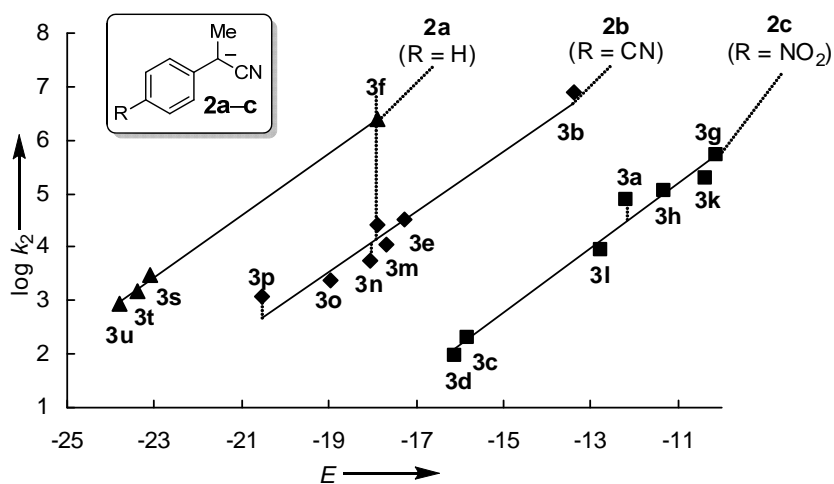


Figure 4: Plot of $\log k_2$ for the reactions of the nucleophiles **2a–c** with the electrophiles **3** in DMSO versus their electrophilicity parameters E .

As expected, electron-withdrawing groups at the *p*-position of the aromatic ring decrease the nucleophilicities *N* of the carbanions **1a–c** and **2a–c**. A comparison between the reactivities of the phenylacetonitrile anions **1a–c** and the phenylpropionitrile anions **2a–c** (Table 2 and Figure 5) shows that replacement of one hydrogen by a methyl group at the α -carbon of phenylacetonitrile anions does not significantly affect the nucleophilicities. The inductive effect of the methyl group and its steric demand obviously compensate each other resulting in similar reactivities of the analogously substituted carbanions **1b/2b** and **1c/2c**.

In order to determine reliable nucleophilicity or electrophilicity parameters, reaction partners should be employed, which differ by several orders of magnitude. The correlation lines for compounds **2a–c** fulfill this condition. However, it should be noted that the slopes of the correlation lines for compounds **2a** and **2b** are largely controlled by the reactions with the electrophiles **3f** and **3b**, respectively. The situation for compounds **1b,c** is much better because their *N* and *s* parameters can be derived from a balanced series of rate constants (Figure 3). Because the parameters *N* and *s* for carbanion **1a** have only been derived from three rate constants, which differ by less than one order of magnitude, the nucleophilicity parameters *N* and *s* for **1a** should be regarded with caution.

Figure 5 compares the colored α -acceptor-substituted benzyl anions whose nucleophilicity parameters *N* have so far been determined. They cover a reactivity range of almost 15 orders of magnitude. It is obvious that the phenylacetonitrile anions **1a–c** are much stronger nucleophiles than the analogously substituted α -trifluoromethylsulfonyl and α -nitro-substituted benzyl anions, whose reactivities have recently been determined.^[6,8] Because of the paucity of available data, Hammett-plots for the differently substituted phenylacetonitrile anions **1a–c** and phenylpropionitrile anions **2a–c** are not informative. Figure 5 reveals, however, that variation of the *p*-substituents in both series **1a–c** and **2a–c** have considerably larger effects on the nucleophilic reactivities than in the series of α -trifluoromethylsulfonyl and much more than in the series of α -nitro-substituted carbanions. Obviously, more negative charge is localized in the aromatic rings of carbanions **1a–c** and **2a–c** than in the corresponding α -triflate and α -nitro-substituted benzyl anions.

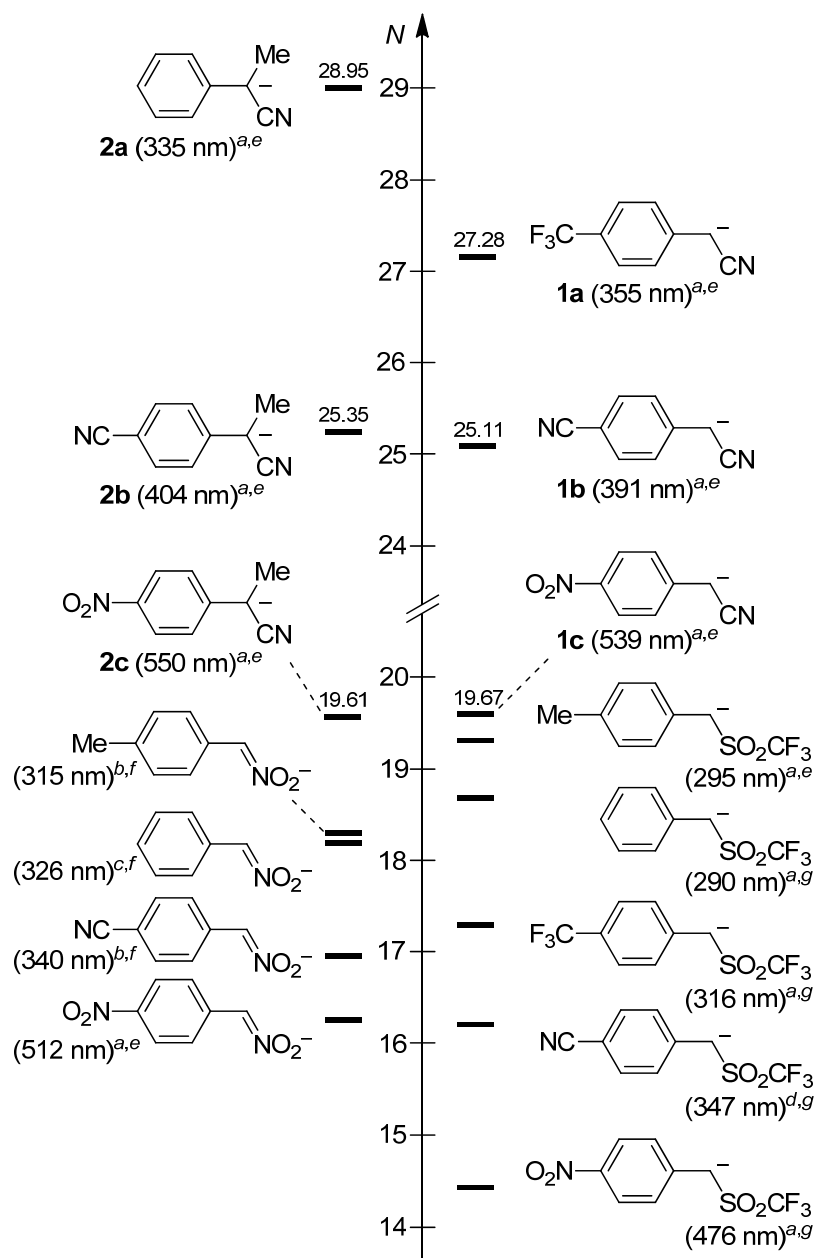


Figure 5: Comparison of the nucleophilicity parameters N of the phenylacetone anions **1a–c** and the phenylpropionitrile anions **2a–c** with those for α -nitro- and α -trifluoromethylsulfonyl-stabilized carbanions in DMSO. ^a λ_{\max} in DMSO. ^b λ_{\max} in MeOH. ^c λ_{\max} in DMSO/H₂O 10:90 (v/v). ^d λ_{\max} in DMSO/H₂O 30:70 (v/v). ^e Determined in this work. ^f See ref 9. ^g See ref 27.

pK_a values are generally considered to be a useful tool for estimating the nucleophilic reactivities of many compounds. We have already shown that this assumption only holds within groups of structurally closely related nucleophiles.^[6,28] For example, the correlation between nucleophilicities of primary and secondary amines versus their pK_{aH} values in water is very poor.^[28c] Figure 6 shows a moderate correlation between the nucleophilicity

parameters N of carbanions and the pK_a values of their conjugate CH acids (cf Scheme 1) in DMSO. It is obvious that the phenylacetonitrile anions **1a–c** and carbanion **2a** are considerably more nucleophilic than expected from the pK_a values of the corresponding CH acids,^[29] indicating the limitation of pK_a for predicting nucleophilic reactivities. In accordance with earlier reports,^[5,8,30] the positive deviations of the cyano-substituted carbanions are indicative of lower intrinsic barriers of their reactions.

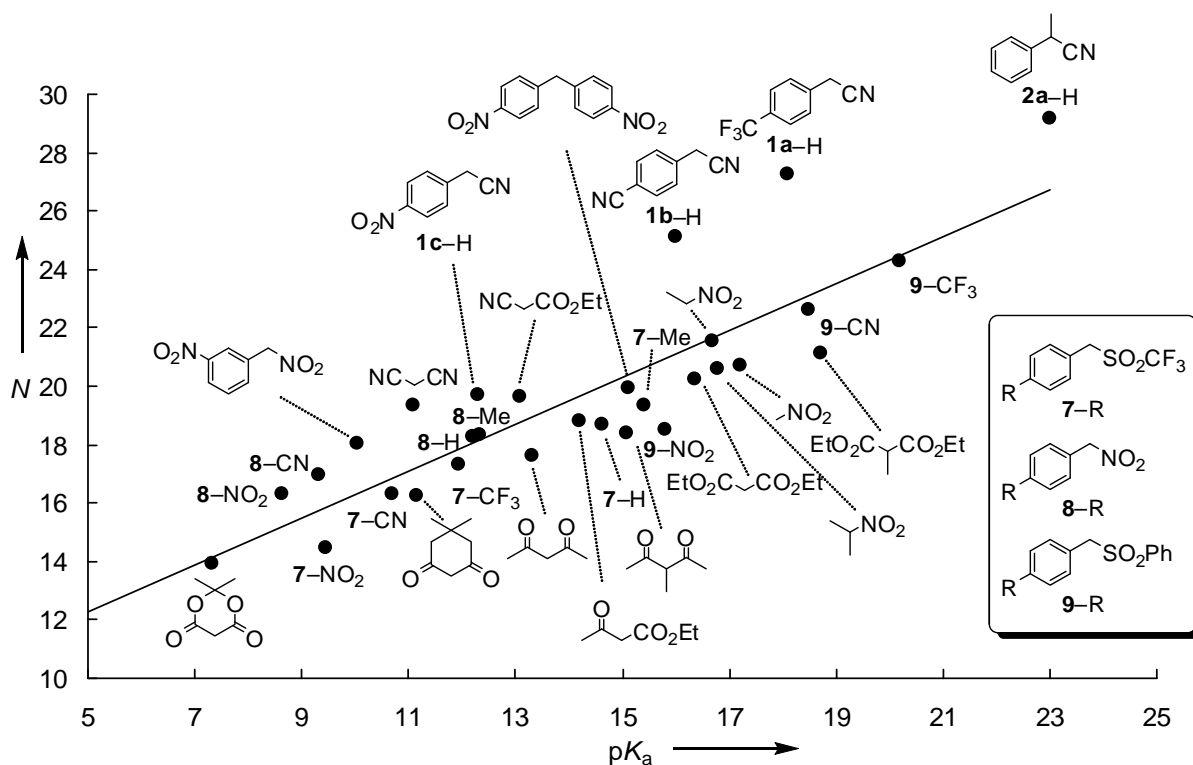


Figure 6: Correlation of the nucleophilicity parameters N of different carbanions versus the pK_a values of their corresponding CH acids in DMSO. Overall correlation: $N = 0.802 pK_a + 8.278$, $R^2 = 0.750$ (nucleophilicity parameters N and pK_a values used for this diagram are compiled in Table 3 of the Experimental Section).

3 Conclusion

α -Cyano-substituted benzyl anions are several orders of magnitude more nucleophilic than α - SO_2CF_3 - and α - NO_2 -substituted benzyl anions. The high reactivities of the cyano-substituted species **1a–c** and **2a–c** are only partially caused by their higher basicities (pK_{aH}). Lower intrinsic barriers for the reactions of these carbanions are indicated by positive deviations from the Brønsted plots and also contribute to their high nucleophilicities. Variation of the p -substituent in the aromatic ring has a considerably larger effect on the nucleophilicities of **1a–c** and **2a–c** than in the corresponding α - SO_2CF_3 - and α - NO_2 -substituted counterparts,

indicating a larger delocalization of the negative charge in the aromatic ring of carbanions **1a–c** and **2a–c**. As colored species of high nucleophilicities, these carbanions complement our series of reference nucleophiles, which can be employed for the photometric determination of electrophilic reactivities.

4 Experimental Section

In order to identify my contribution to this multiauthor publication, chapter 4.3, 4.4, and 4.5 of this Experimental Section consist exclusively of the experiments, which were performed by me.

4.1 General

Chemicals. Arylacetonitriles **1** are commercially available compounds and have been recrystallized from *n*-pentane/MeOH prior to use. Compounds (**2a–c**)-H have been prepared by methylation of the corresponding arylacetonitriles by using methyl iodide as described in the literature.^[31] Commercially available DMSO (content of H₂O < 50 ppm) was used without further purification. Stock solutions of KO^{*t*}Bu in DMSO were prepared under nitrogen atmosphere. All of the other chemicals were purchased from commercial sources and (if necessary) purified by recrystallization or distillation prior to use.

Analytcs. ¹H- and ¹³C-NMR spectra were recorded on Varian NMR-systems (300, 400, or 600 MHz) in CDCl₃ or DMSO-*d*₆ and the chemical shifts in ppm refer to the solvent residual signals as internal standard (δ_{H} 7.26 and δ_{C} 77.0 in CDCl₃; δ_{H} 2.50, δ_{C} 39.43 in DMSO-*d*₆). The following abbreviations were used for chemical shift multiplicities: brs = broad singlet, s = singlet, d = doublet, t = triplet, q = quartet, m = multiplet. For reasons of simplicity, the ¹H-NMR signals of AA'BB'-spin systems of *p*-disubstituted aromatic rings were treated as doublets. NMR signal assignments were based on additional 2D-NMR experiments (e.g., COSY-, HSQC-, and HMBC experiments). Diastereomeric ratios (*dr*) were determined by ¹H-NMR. (HR-)MS was performed on a Finnigan MAT 95 (EI) or a Thermo Finnigan LTQ FT (ESI) mass spectrometer. Melting points were determined on a Büchi B-540 device and are not corrected.

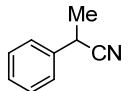
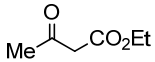
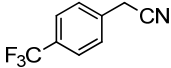
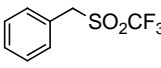
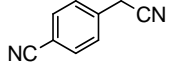
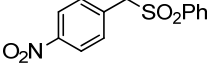
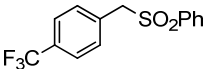
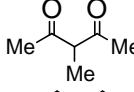
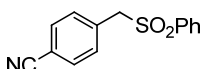
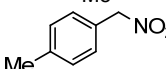

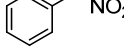
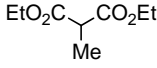
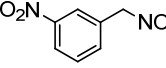
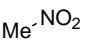
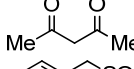
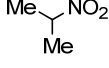
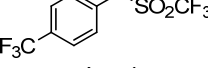
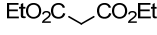
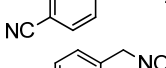
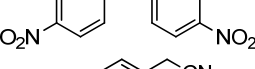
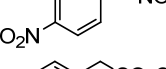
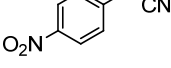
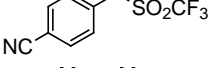
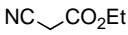
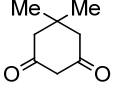
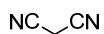
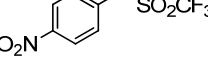
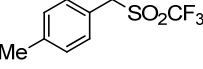
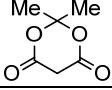
Kinetics. The general method for the determination of the rate constants is described in the experimental part of the chapter. The temperature of the solutions was kept constant (20 ± 0.1°C) during all kinetic experiments by using a circulating bath thermostat. All kinetic

investigations have been performed under first-order conditions as described above. Rate constants k_{obs} (s^{-1}) were obtained by fitting the single exponential function $A_t = A_0 \exp(-k_{\text{obs}}t) + C$ to the observed time-dependent absorbance of the minor component. Plotting k_{obs} against the concentrations of the nucleophiles resulted in linear correlations whose slopes correspond to the second-order rate constants k_2 ($\text{L mol}^{-1} \text{s}^{-1}$). For stopped-flow experiments with **1c** and **2c** two stock solutions were used: A solution of electrophiles **3a–u** in DMSO and a solution of the carbanions **1c** and **2c** in DMSO generated by deprotonation of the corresponding CH acid with KO t Bu, P $_2$ - t Bu, or P $_4$ - t Bu or, in case of **2c**, by dissolving the corresponding preformed potassium salt (**2c-K**). Due to their high reactivities and slow decomposition in DMSO solution, the carbanions **1a,b** and **2a,b** were generated by using a double-mixing mode of conventional stopped-flow instruments. In the first step, the CH acids (**1a,b**)-H and (**2a,b**)-H were mixed with the base to generate the corresponding carbanions directly in the sample cell. After a short remaining time of the carbanion solution in the mixing cell (age time), the electrophile solutions were added in a second step. Conditions different from those mentioned here, will be described explicitly in the corresponding tables.

For fast kinetic experiments ($\tau_{1/2} < 15$ s), standard stopped-flow UV-Vis spectrophotometer systems were used. Kinetics of slow reactions ($\tau_{1/2} > 15$ s) were determined by conventional UV-Vis spectroscopy using a diode array spectrophotometer, which was connected to an insertion probe via fibre optic cables.

4.2 Nucleophilicities of Different Carbanions and the Acidities of their Conjugate CH Acids in DMSO

Table 3: Nucleophilicities N for different types of carbanions and the pK_a values of their conjugate CH acids in DMSO.

Compound	N	pK_a	Compound	N	pK_a
	29.14	23.00 ^[Bor88]		18.82	14.20 ^[Bor81]
	27.29	18.10 ^[Bor86]		18.67	14.62 ^[Gou03]
	25.11	16.00 ^[Bor88]		18.50	15.80 ^[Bor88a]
	24.30	20.20 ^[Bor88a]		18.38	15.07 ^[Olm80]
	22.60	18.50 ^[Bor88a]		18.31	12.33 ^[Kee79]
	21.54	16.70 ^[Bor94]		18.29	12.20 ^[Bor94]
	21.13	18.70 ^[Bor88d]		18.06	10.04 ^[Kee79]
	20.71	17.20 ^[Olm80]		17.64	13.33 ^[Olm80]
	20.61	16.80 ^[Bor94]		17.33	11.95 ^[Gou03]
	20.22	16.37 ^[Olm80]		16.96	9.31 ^[Kee79]
	19.92	15.10 ^[Bor88b]		16.29	8.62 ^[Kee79]
	19.68	12.30 ^[Bor88]		16.28	10.70 ^[Bor88]
	19.62	13.10 ^[Bor88c]		16.27	11.16 ^[Olm80]
	19.36	11.10 ^[Bor89]		14.49	9.46 ^[Gou03]
	19.35	15.40 ^[Bor88]		13.91	7.33 ^[Am87]

[Arn87] Arnett, E. M.; Harrelson, J. A., Jr. *J. Am. Chem. Soc.* **1987**, *109*, 809-812.

[Bor81] Bordwell, F. G.; Fried, H. E. *J. Org. Chem.* **1981**, *46*, 4327-4331.

[Bor86] Bordwell, F. G.; Bausch, M. J. *J. Am. Chem. Soc.* **1986**, *108*, 1979-1985.

[Bor88] Bordwell, F. G.; Cheng, J. P.; Bausch, M. J.; Bares, J. E. *J. Phys. Org. Chem.* **1988**, *1*, 209-223.

[Bor88a] Bordwell, F. G.; Bausch, M. J.; Branca, J. C.; Harrelson, J. A., Jr. *J. Phys. Org. Chem.* **1988**, *1*, 225-239.

[Bor88b] Bordwell, F. G.; Algrim, D. J. *J. Am. Chem. Soc.* **1988**, *110*, 2964-2968.

- [Bor88c] Bordwell, F. G.; Branca, J. C.; Bares, J. E.; Filler, R. *J. Org. Chem.* **1988**, *53*, 780-782.
 [Bor88d] Bordwell, F. G. *Acc. Chem. Res.* **1988**, *21*, 456-463.
 [Bor89] Bordwell, F. G.; Harrelson, J. A., Jr.; Satish, A. V. *J. Org. Chem.* **1989**, *54*, 3101-3105.
 [Bor94] Bordwell, F. G.; Satish, A. V. *J. Am. Chem. Soc.* **1994**, *116*, 8885-8889.
 [Gou03] Goumont, R.; Kizilian, E.; Buncel, E.; Terrier, F. *Org. Biomol. Chem.* **2003**, *1*, 1741-1748.
 [Kee79] Keeffe, J. R.; Morey, J.; Palmer, C. A.; Lee, J. C. *J. Am. Chem. Soc.* **1979**, *101*, 1295-1297.
 [Olm80] Olmstead, W. N.; Bordwell, F. G. *J. Org. Chem.* **1980**, *45*, 3299-3305.

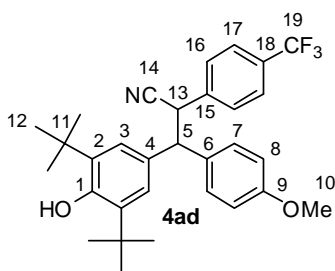
4.3 Product Studies

4.3.1 Syntheses of the Products **4** from the Reactions of the Nucleophiles **1a–c** with the Electrophiles **3c–f**

General Method. Compounds (**1a–c**)-H were mixed with 1.0-1.9 equiv of KO t Bu or NaOMe in dry methanol or in methanol/DMSO mixtures. After some minutes the electrophiles **3c–f** were added. The reaction mixtures were then stirred for 1 h at ambient temperature. Subsequently aqueous acetic acid solution (1 %) was added. The reaction mixture was then extracted with CH₂Cl₂. The combined organic layers were washed with H₂O and dried over Na₂SO₄. Evaporation of the solvent under reduced pressure yielded the crude products, which were purified by chromatography (SiO₂, *ihex*/EtOAc) and characterized by MS and NMR spectroscopy. Signal assignments are based on additional DEPT, COSY, gHMBC and gHSQC experiments. Diastereomeric ratios (*dr*) were determined on the basis of the integrals in the ¹H-NMR spectra.

3-(3,5-Di-*tert*-butyl-4-hydroxyphenyl)-3-(4-methoxyphenyl)-2-(4-(trifluoromethyl)phenyl)propionitrile (4ad). From **1a**-H (25.0 mg, 135 μmol), KO t Bu (22.8 mg, 203 μmol), and **3d** (82.0 mg, 253 μmol) in a 1:2 (v/v) MeOH/DMSO mixture (10.5 mL): 50.0 mg, (98.1 μmol, 73 %); colorless oil (*dr* ~ 1:1.4).

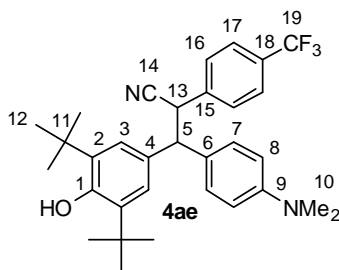
RAP 3.2



R_f (*i*hex/EtOAc 4:1) = 0.50. $^1\text{H-NMR}$ (CDCl_3 , 300 MHz): δ = 1.31, 1.36 (2s, 18 H, 12-H), 3.78, 3.81 (2s, 3 H, 10-H), 4.19, 4.20 (2d, 3J = 8.9 Hz, 3J = 7.3 Hz, 1 H, 5-H), 4.40 (d, 3J = 8.9 Hz, 0.58 H, 13-H), 4.54 (d, 3J = 7.3 Hz, 0.42 H, 13-H), 5.09, 5.15 (2s, 1 H, OH), 6.79-6.83 (m, 2 H, 3-H, 8-H), 6.88-6.91 (m, 2 H, 3-H, 8-H), 7.13-7.26 (m, 4 H, 7-H, 16-H), 7.49-7.52 ppm (m, 2 H, 17-H). $^{13}\text{C-NMR}$ (CDCl_3 , 75.5 MHz): δ = 30.10, 30.18 (2q, C-12), 34.26, 34.30 (2s, C-11), 43.58, 43.80 (2d, C-13), 55.23 (q, C-10, both diastereomers), 55.76, 56.24 (2d, C-5), 113.97, 114.08 (2d, C-8), 119.46, 119.67 (2s, C-14), 122.00 (s, C-18, signal for the other diastereomer superimposed), 124.67, 125.37 (2d, C-3), 125.44, 125.48 (2d, C-17), 128.69, 128.77, 128.96, 129.38 (4d, C-7, C-16), 130.23, 130.27 (2q, C-19), 130.28 (s, C-6, signal for the other diastereomer superimposed), 131.73, 132.44 (2s, C-4), 135.71, 135.93 (2s, C-2), 139.29 (s, C-15, signal for the other diastereomer superimposed), 152.82, 153.16 (2s, C-1), 158.58, 158.88 ppm (2s, C-9). HR-MS (ESI) $[\text{M-H}]^-$: calcd 508.2469; found 508.2461.

3-(3,5-Di-*tert*-butyl-4-hydroxyphenyl)-3-(4-(dimethylamino)phenyl)-2-(4-(trifluoromethyl)phenyl)propionitrile (4ae). From **1a-H** (30.0 mg, 162 μmol), $\text{KO}t\text{Bu}$ (27.0 mg, 241 μmol), and **3e** (82.0 mg, 243 μmol) in a 1:2 (v/v) MeOH/DMSO mixture (10.5 mL): 68.0 mg (130 μmol , 80 %); orange foam (*dr* ~ 1:1.4).

RAP 3.3

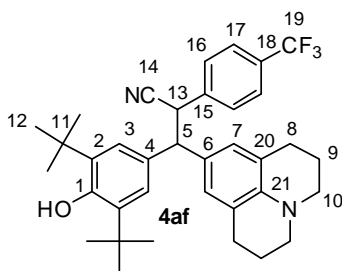


R_f (*i*hex/EtOAc 4:1) = 0.38. $^1\text{H-NMR}$ (CDCl_3 , 600 MHz): δ = 1.31, 1.37 (2s, 18 H, 12-H), 2.92, 2.95 (2s, 6 H, 10-H), 4.13-4.16 (m, 1 H, 5-H), 4.39 (d, 3J = 8.8 Hz, 0.58 H, 13-H), 4.54 (d, 3J = 7.3 Hz, 0.42 H, 13-H), 5.06, 5.12 (2s, 1 H, OH), 6.64, 6.71 (2d, $2 \times ^3J$ = 8.6 Hz, 2 H, 8-H), 6.82, 6.92 (2s, 2 H, 3-H), 7.12-7.26 (m, 4 H, 7-H, 16-H), 7.49-7.51 ppm (m, 2 H, 17-H). $^{13}\text{C-NMR}$ (CDCl_3 , 151 MHz): δ = 30.12, 30.20 (2q, C-12), 34.24, 34.28 (2s, C-11), 40.50 (q, C-10, both diastereomers), 43.76, 44.04 (2d, C-13), 55.84, 56.30 (2d, C-5), 112.52, 112.60 (2d, C-8), 119.67, 119.91 (2s, C-14), 122.94, 122.95 (2s, C-18), 124.67 (d, C-3), 125.31 (d, C-17, signals for the other diastereomer superimposed), 125.35 (d, C-3), 127.30, 128.02 (2s, C-6), 128.56, 128.70, 128.79, 128.95 (4d, C-7, C-16), 129.79 (s, C-4), 130.05, 130.10 (2q, C-

19), 130.77 (s, C-4), 135.55, 135.77 (2s, C-2), 139.57, 139.59 (2s, C-15), 149.54, 149.80 (2s, C-9), 152.66, 153.00 ppm (2s, C-1). HR-MS (ESI) $[M+H]^+$: calcd 523.2931; found 523.2914.

3-(3,5-Di-*tert*-butyl-4-hydroxyphenyl)-3-(1,2,3,5,6,7-hexahydropyrido[3,2,1-*ij*]quinolin-9-yl)-2-(4-(trifluoromethyl)phenyl)propionitrile (4af). From **1a-H** (30.0 mg, 162 μ mol), KO t Bu (27.0 mg, 241 μ mol), and **3f** (95.0 mg, 244 μ mol) in a 1:2 (v/v) MeOH/DMSO mixture (10.5 mL): 66.0 mg (115 μ mol, 71 %); red foam (*dr* ~ 1:1.8).

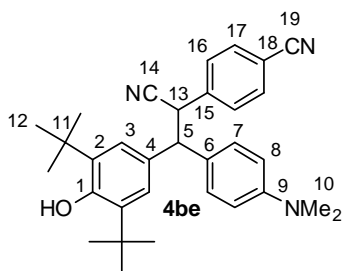
RAP 3.4



R_f (*i*hex/EtOAc 4:1) = 0.41. $^1\text{H-NMR}$ (CDCl_3 , 600 MHz): δ = 1.30, 1.37 (2s, 18 H, 12-H), 1.93-2.00 (m, 4 H, 9-H), 2.66-2.78 (m 4 H, 8-H), 3.10-3.14 (m, 4 H, 10-H), 3.98-4.01 (m, 1 H, 5-H), 4.31 (d, 3J = 9.7 Hz, 0.64 H, 13-H), 4.51 (d, 3J = 6.6 Hz, 0.35 H, 13-H), 5.03, 5.12 (2s, 1 H, OH), 6.71, 6.76 (2s, 2 H, 7-H), 6.77, 6.90 (2s, 2 H, 3-H), 7.12, 7.15 (2d, $2 \times ^3J$ = 8.0 Hz, 2 H, 16-H), 7.48, 7.51 ppm (2d, $2 \times ^3J_{7,48}$ = 8.1 Hz, 2 H, 17-H). $^{13}\text{C-NMR}$ (CDCl_3 , 151 MHz): δ = 22.04, 22.09 (2t, C-9), 27.68, 27.72 (2t, C-8) 30.08, 30.19 (2q, C-12), 34.20, 34.28 (2s, C-11), 43.96, 44.22 (2d, C-13), 49.91, 49.95 (2t, C-10), 55.11, 55.76 (2d, C-5), 119.73, 120.09 (2s, C-14), 121.50, 121.57 (2s, C-18), 122.94, 122.99 (2s, C-20), 124.69 (d, C-3), 125.18, 125.20 (2d, C-17), 125.52 (d, C-3), 126.35, 126.57 (2s, C-7), 126.67, 127.24 (2s, C-6), 128.66, 128.79 (2d, C-16), 129.58 (s, C-4), 129.96, 129.98 (2q, C-19), 130.71 (s, C-4), 135.40, 135.64 (2s, C-2), 139.78, 139.81 (2s, C-15), 141.92, 142.25 (2s, C-21), 152.57, 152.97 ppm (2s, C-1). HR-MS (ESI) $[M+H]^+$: calcd 575.3244; found 575.3229.

4-(1-Cyano-2-(3,5-di-*tert*-butyl-4-hydroxyphenyl)-2-(4-(dimethylamino)phenyl)ethyl)-benzonitrile (4be). From **1b-H** (25.0 mg, 176 μ mol), NaOMe (10.0 mg, 185 μ mol), and **3e** (59.0 mg, 175 μ mol) in MeOH (10 mL): 65.4 mg (136 μ mol, 77 %); red foam (*dr* ~ 1:1.2).

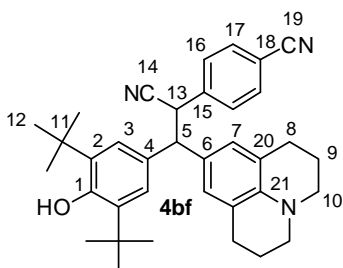
RAP 4.2



R_f (*i*hex/EtOAc 4:1) = 0.30. $^1\text{H-NMR}$ (CDCl_3 , 300 MHz): δ = 1.34, 1.39 (2s, 18 H, 12-H), 2.91, 2.94 (2s, 6 H, 10-H), 4.12-4.16 (m, 1 H, 5-H), 4.43 (d, 3J = 8.4 Hz, 0.57 H, 13-H), 4.51 (d, 3J = 7.9 Hz, 0.47 H, 13-H), 5.10, 5.14 (2s, 1 H, OH), 6.60-6.70 (m, 2 H, 8-H.), 6.89, 6.97 (2s, 2 H, 3-H), 7.05-7.20 (m, 4 H, 7-H, 16-H), 7.51-7.55 ppm (m, 2 H, 17-H). $^{13}\text{C-NMR}$ (CDCl_3 , 75.5 MHz): δ = 30.15, 30.22 (2q, C-12), 34.26, 34.29 (2s, C-11), 40.40, 40.41 (2q, C-10), 44.01, 44.19 (2d, C-13), 55.84, 56.10 (2d, C-5), 111.76, 111.77 (2s, C-18), 112.43, 112.48 (2d, C-8), 118.19, 118.25 (2s, C-19), 119.35, 119.48 (2s, C-14), 124.54, 125.08 (2d, C-3), 126.84, 127.56 (2s, C-6), 128.53, 128.97 (2d, C-7), 129.12, 129.16 (2d, C-16), 129.78, 130.64 (2s, C-4), 132.07, 132.12 (2d, C-17), 135.69, 135.90 (2s, C-2), 140.84, 140.86 (2s, C-15), 149.54, 149.80 (2d, C-9), 152.72, 153.03 ppm (2s, C-1). HR-MS (ESI) $[\text{M}+\text{H}]^+$: calcd 480.3009; found 480.2995.

4-(1-Cyano-2-(3,5-di-*tert*-butyl-4-hydroxyphenyl)-2-(1,2,3,5,6,7-hexahydropyrido[3,2,1-*ij*]quinolin-9-yl)ethylbenzonitrile (4bf). From **1b-H** (25.0 mg, 176 μmol), NaOMe (11.0 mg, 204 μmol), and **3f** (69.0 mg, 177 μmol) in MeOH (10 mL): 47.0 mg (88.4 μmol , 50 %); red foam (*dr* \sim 1:1.4).

RAP 4.4



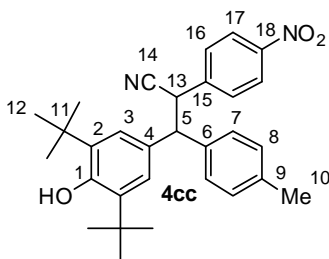
R_f (*i*hex/EtOAc 4:1) = 0.45. $^1\text{H-NMR}$ (CDCl_3 , 600 MHz): δ = 1.32, 1.37 (2s, 18 H, 12-H), 1.91-1.98 (m, 4 H, 9-H), 2.65-2.77 (m, 4 H, 8-H), 3.09-3.13 (m, 4 H, 10-H), 3.96-4.01 (m, 1 H, 5-H), 4.33 (d, 3J = 9.2 Hz, 0.59 H, 13-H), 4.48 (d, 3J = 6.9 Hz, 0.42 H, 13-H), 5.05, 5.12 (2s, 1 H, OH), 6.65, 6.71 (2s, 2 H, 7-H), 6.81, 6.93 (2s, 2 H, 3-H), 7.13, 7.16 (2d, $2 \times ^3J$ = 8.1 Hz, 2 H, 16-H), 7.51, 7.54 ppm (2d, $2 \times ^3J$ = 8.1 Hz, 2 H, 17-H). $^{13}\text{C-NMR}$ (CDCl_3 , 151 MHz): δ = 21.98, 22.03 (2t, C-9), 27.68, 27.72 (2t, C-8), 30.14, 30.23 (2q, C-12), 34.25, 34.30

(2s, C-11), 44.26, 44.41 (2d, C-13), 49.87, 49.91 (2t, C-10), 56.06, 56.57 (2d, C-5), 111.64, 111.68 (2s, C-18), 118.23, 118.30 (2s, C-19), 119.41, 119.67 (2s, C-14), 121.50, 121.54 (2s, C-20), 124.58, 125.30 (2d, C-3), 126.26 (s, C-6), 126.30, 126.57 (2d, C-7), 126.83 (s, C-6), 129.10, 129.20 (2d, C-16), 129.58, 130.59 (2s, C-4), 131.96, 132.04 (2d, C-17), 135.54, 135.77 (2s, C-2), 141.07, 141.10 (2s, C-15), 141.96, 142.30 (2s, C-21), 152.66, 153.02 ppm (2s, C-1). HR-MS (ESI) $[M+H]^+$: calcd 532.3322; found 532.3310.

3-(3,5-Di-*tert*-butyl-4-hydroxyphenyl)-2-(4-nitrophenyl)-3-*p*-tolylpropionitrile (4cc).

From **1c-H** (50.0 mg, 308 μ mol), NaOMe (18.3 mg, 339 μ mol), and **3c** (95.3 mg, 309 μ mol) in MeOH (10 mL): 126 mg (268 μ mol, 87 %); colorless foam (*dr* ~ 1:1.2).

RAP 1.7-2

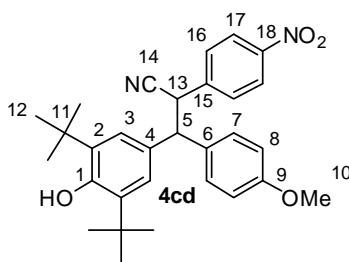


R_f (*i*hex/EtOAc 4:1) = 0.34. $^1\text{H-NMR}$ (CDCl_3 , 400 MHz): δ = 1.32, 1.38 (2s, 18 H, 12-H), 2.29, 3.34 (2s, 3 H, 10-H), 4.20-4.24 (m, 1 H, 5-H), 4.52 (d, $^3J = 8.7$ Hz, 0.52 H, 13-H), 4.59 (d, $^3J = 8.1$ Hz, 0.45 H, 13-H), 5.13, 5.18 (2s, 1 H, OH), 6.86, 6.98 (2s, 2 H, 3-H), 7.06-7.12 (m, 2 H, 7-H.), 7.14-7.21 (m, 2 H, 8-H.), 7.21-7.27 (m, 2 H, 16-H), 8.09-8.11 ppm (m, 2 H, 17-H.). $^{13}\text{C-NMR}$ (CDCl_3 , 101 MHz): δ = 20.98, 21.07 (2q, C-10), 30.11, 30.19 (2q, C-12), 34.27, 34.32 (2s, C-11), 43.46, 43.56 (2d, C-13), 55.19, 55.53 (2d, C-5), 119.12, 119.20 (2s, C-14), 123.58, 123.65 (2d, C-17), 124.57, 125.11 (2d, C-3), 127.68, 128.10 (2d, C-7), 129.22 (s, C-4), 129.29, 129.30 (2d, C-16), 129.41, 129.46 (2d, C-8), 129.89 (s, C-4), 135.84, 136.04 (2s, C-2), 136.19 (s, C-6), 136.85, 137.04 (2s, C-9), 137.34 (s, C-6), 142.40, 142.44 (2s, C-15), 147.42, 147.44 (2s, C-18), 152.95, 153.25 ppm (2s, C-1). HR-MS (ESI) $[M-H]^-$: calcd 469.2497; found 469.2490.

3-(3,5-Di-*tert*-butyl-4-hydroxyphenyl)-3-(4-methoxyphenyl)-2-(4-nitrophenyl)-

propionitrile (4cd). From **1c-H** (25.0 mg, 154 μ mol), NaOMe (8.3 mg, 0.15 mmol), and **3d** (50.0 mg, 154 μ mol) in MeOH (10 mL): 71.0 mg (146 μ mol, 95 %); yellow foam (*dr* ~ 1:1.2).

RAP 1.8



R_f (*i*hex/EtOAc 4:1) = 0.38. $^1\text{H-NMR}$ (CDCl_3 , 300 MHz): δ = 1.32, 1.38 (2s, 18 H, 12-H), 3.76, 3.80 (2s, 3 H, 10-H), 4.19-4.24 (m, 1 H, 5-H), 4.51 (d, $^3J = 8.4$ Hz, 0.50 H, 13-H), 4.57 (d, $^3J = 8.1$ Hz, 0.47 H, 13-H), 5.13, 5.17 (2s, 1 H, OH), 6.78-6.81 (m, 1 H, 8-H.), 6.85-6.89 (m, 2.20 H, 8-H, 3-H), 6.97 (s, 1 H, 3-H), 7.10-7.13 (m, 1 H, 7-H), 7.19-7.27 (m, 3 H, 7-H, 16-H) 8.07-8.11 ppm (m, 2 H, 17-H). $^{13}\text{C-NMR}$ (CDCl_3 , 75.5 MHz): δ = 30.15, 30.23 (2q, C-12), 34.32, 34.35 (2s, C-11), 43.64, 43.73 (2d, C-13), 55.22, 55.23 (2q, C-10), 55.82, 56.07 (2d, C-5), 114.07, 114.12 (2d, C-8), 119.13, 119.20 (2s, C-14), 123.61, 123.66 (2d, C-17), 124.55, 125.10 (2d, C-3), 128.95, 129.32, 129.43 (3d, C-7, C-16, peak for the other diastereomer superimposed), 129.35, 130.12 (s, C-4), 131.30, 132.00 (2s, C-6), 135.93, 136.12 (2s, C-2), 142.44, 142.47 (2s, C-15), 147.48, 147.50 (2s, C-18), 152.96, 153.26 (2s, C-1), 158.69, 158.99 ppm (2d, C-9). HR-MS (ESI) $[\text{M-H}]^-$: calcd 485.2446; found 485.2440.

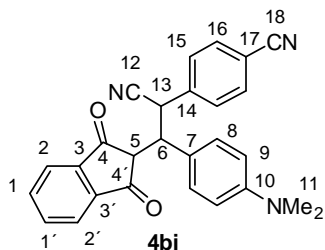
4.3.2 Syntheses of the Products 4 from the Reactions of the Nucleophiles 1b,c with the Electrophiles 3h-j

General Method. Compounds (**1b,c**)-H were mixed with KO t Bu in dry DMSO. After the addition of the electrophiles **3h-j** the reaction mixture was stirred for 1 h at ambient temperature. After the subsequent addition of water and concentrated aqueous HCl the products were isolated and purified as described separately for each reaction. The products were characterized by MS and NMR spectroscopy. Signal assignments are based on additional DEPT, COSY, gHMBC and gHSQC experiments.

4-(1-Cyano-2-(4-(dimethylamino)phenyl)-2-(1,3-dioxo-2,3-dihydro-1H-inden-2-yl)ethyl) benzonitrile (4bi). From **1b**-H (100 mg, 703 μmol), KO t Bu (95.0 mg, 847 μmol), and **3i** (195 mg, 703 μmol) in DMSO (6 mL). After the addition of water and hydrochloric acid, the resulting suspension was extracted with dichloromethane. The combined organic layers were washed with H $_2$ O and dried over MgSO $_4$. Evaporation of the solvent under reduced pressure

yielded the crude product, which was purified by chromatography (SiO₂, CHCl₃/MeOH): 206 mg (491 μmol, 70 %); yellow solid (*dr* ~ 1:1.9).

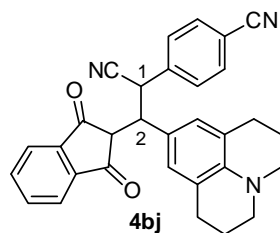
RAP 4.6-2



R_f (CHCl₃/MeOH 25:1) = 0.81. ¹H-NMR (CDCl₃, 300 MHz): δ = 2.75-2.83 (m, 6.41 H, 11-H, 5-H), 3.87 (dd, ³*J* = 12.1 Hz, ³*J* = 3.9 Hz, 1 H, 6-H, both diastereomers), 3.93 (d, ³*J* = 4.0 Hz, 0.35 H, 5-H), 5.01 (d, ³*J* = 11.8 Hz, 0.35 H, 13-H), 5.17 (d, ³*J* = 12.1 Hz, 0.65 H, 13-H), 6.26-6.30, 6.49-6.53 (2m, 2 H, 9-H), 6.71-6.75, 7.08-7.12 (2m, 2 H, 8-H), 7.24-7.27 (m, 0.92 H, 15-H), 7.47-7.50 (m, 0.70 H, 16-H), 7.69-7.87 (m, 6.10 H, 1-H, 1-H', s 2-H or 2-H', 15-H, 16-H), 7.96-7.99 ppm (m, 0.36 H, 2-H or 2-H'). ¹³C-NMR (CDCl₃, 75.5 MHz): δ = 39.98, 40.12 (2q, C-11), 40.20, 40.38 (2d, C-13), 48.69, 49.02 (2d, C-6), 53.65, 56.60 (2d, C-5), 111.96 (d, C-9), 112.10 (s, C-17), 112.37 (d, C-9), 112.93 (s, C-17), 117.97, 118.17 (2s, C-18), 119.15, 119.61 (s, C-12), 120.99, 122.71 (s, C-7), 122.97, 123.17, 123.34 (3d, C-2 und C-2', one signal superimposed), 129.16 (d, C-16), 129.27, 129.45 (2d, C-8), 129.79 (d, C-16), 132.38, 133.05 (2d, C-15), 135.69, 135.75, 135.80, 135.85 (4d, C-1 und C-1'), 139.84, 140.04 (2s, C-14), 142.34, 142.35, 142.46 (3s, C-3 und C-3', one signal superimposed), 149.72, 150.15 (2s, C-10), 197.66, 197.90, 199.69, 200.00 ppm (4s, C-4 and C-4'). HR-MS (ESI) [M+H]⁺: calcd 420.1707; found 420.1696.

4-(1-Cyano-2-(1,3-dioxo-2,3-dihydro-1*H*-inden-2-yl)-2-(1,2,3,5,6,7-hexahydropyrido [3,2,1-*ij*]quinolin)-9-yl)ethyl)benzonitrile (4bj). From **1b-H** (50.1 mg, 352 μmol), KO*t*Bu (43.4 mg, 387 μmol), and **3j** (117 mg, 355 μmol) in DMSO (10 mL). After the addition of water and conc. hydrochloric acid, the resulting suspension was extracted with ethyl acetate. The combined organic layers were washed with H₂O and dried over Na₂SO₄. Evaporation of the solvent under reduced pressure yielded the crude product. Attempts to purify the product by chromatography (SiO₂, *i*hex/EtOAc) failed because of partial decomposition. Nevertheless, the characteristic ¹H-NMR signals for 1-H and HR-MS gave evidence for the formation of **4bj**: red solid (*dr* ~ 1:1.3).

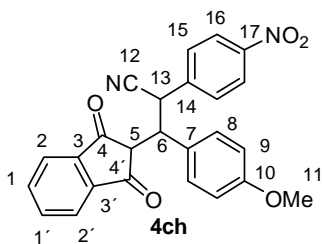
RAP 4.10



$^1\text{H-NMR}$ (CDCl_3 , 200 MHz): δ = 4.91 (d, 3J = 11.8 Hz, 0.43 H, 1-H), 5.07 ppm (d, 3J = 12.1 Hz, 0.58 H, 1-H). HR-MS (ESI) $[\text{M}+\text{H}]^+$: calcd 472.2020; found 472.2012.

3-(1,3-Dioxo-2,3-dihydro-1H-inden-2-yl)-3-(4-methoxyphenyl)-2-(4-nitrophenyl)propionitrile (4ch). From **1c-H** (50.0 mg, 308 μmol), KOtBu (41.5 mg, 370 μmol), and **3h** (81.5 mg, 308 μmol) in DMSO (6 mL). After the addition of water and conc. hydrochloric acid, a green solid precipitated which was isolated by filtration and washed with H_2O . The purified product precipitated from a chloroform/n-pentane mixture: 93.3 mg (219 μmol , 71 %); pale yellow solid ($dr \sim 1:1.9$).

RAP 1.12-2

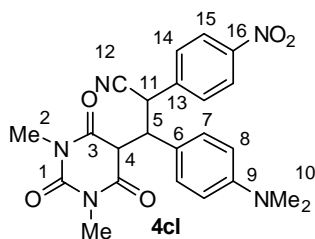


R_f (*i*hex/EtOAc 2:1) = 0.66. $^1\text{H-NMR}$ (CDCl_3 , 600 MHz): δ = 2.84 (d, 3J = 4.0 Hz, 0.62 H, 5-H), 3.59, 3.69 (2s, 3 H, 11-H), 3.92-3.98 (m, 1.35 H, 6-H, 5-H), 5.09 (d, 3J = 11.8 Hz, 0.35 H, 13-H), 5.25 (d, 3J = 12.0 Hz, 0.65 H, 13-H), 6.50-6.52, 6.72-6.74 (2m, 2 H, 9-H), 6.83-6.85, 7.18-7.20 (2m, 2 H, 8-H), 7.32-7.33 (m, 0.70 H, 15-H.), 7.70-7.88 (m, 4.90 H, 1-H, 1-H', 2-H oder 2-H', 15-H), 7.98 (d, 3J = 7.5 Hz, 0.36 H, 2-H oder 2-H') 8.05-8.07, 8.28-8.29 (2m, 2 H, 16-H). $^{13}\text{C-NMR}$ (CDCl_3 , 151 MHz): δ = 39.83, 39.89 (2d, C-13), 48.69, 49.03 (2d, C-6), 53.44 (d, C-5), 54.96, 55.09 (2q, C-11), 56.41 (d, C-5), 114.05, 114.33 (2d, C-9), 118.83, 119.26 (2s, C-12), 123.07, 123.23, 123.30, 123.39 (4d, C-2 und C-2'), 123.92, 124.54 (2d, C-16), 125.89, 127.40 (2s, C-7), 129.37 (d, C-15), 129.75, 129.90 (2d, C-8), 130.07 (d, C-15), 135.89, 135.96, 136.01, 136.07 (4d, C-1 und C-1'), 141.38, 141.51 (2s, C-14), 142.23, 142.24, 142.26, 142.35 (4s, C-3, C-3'), 147.62, 148.18 (2s, C-17), 159.10, 159.49 (2s, C-10), 197.38, 197.59, 199.39, 199.72 (4s, C-4, C-4'). HR-MS (ESI) $[\text{M}-\text{H}]^-$: calcd 425.1143; found 425.1149.

4.3.3 Synthesis of Product 4cl from the Reactions of the Nucleophiles 1c with the Electrophiles 3l

3-(1,3-Dimethyl-2,4,6-trioxohexahydropyrimidin-5-yl)-3-(4-(dimethylamino)phenyl)-2-(4-nitrophenyl)propionitrile (4cl). After mixing **1c-H** (30.0 mg, 185 μmol) with KO^tBu (25.0 mg, 223 μmol) in dry DMSO (5 mL) and subsequent addition of the electrophile **3l** (64.0 mg, 223 μmol), the reaction mixture was stirred for 1.5 h at ambient temperature. Subsequently water and concentrated hydrochloric acid were added. The resulting mixture was extracted with ethylacetate, and the combined organic layers were washed with H_2O and dried over Na_2SO_4 . Evaporation of the solvent under reduced pressure yielded the crude product, which was purified by chromatography (SiO_2 , $\text{CHCl}_3/\text{MeOH}$). The product was characterized by MS and NMR spectroscopy. Signal assignments are based on additional DEPT, COSY, gHMBC and gHSQC experiments: 71.0 mg (158 μmol , 85 %); orange solid (*dr* ~ 1:1).

RAP 1.11



R_f ($\text{CHCl}_3/\text{MeOH}$ 10:1): 0.17. $^1\text{H-NMR}$ (CDCl_3 , 600 MHz): δ = 2.85, 2.95 (2s, 6 H, 10-H), 3.06, 3.08 (2s, 3 H, 2-H), 3.13 (d, 3J = 3.1 Hz 0.52 H, 4-H), 3.14, 3.26 (2s, 3 H, 2-H), 3.96, 3.98 (2t, 3J = 3.1 Hz, 1 H, 5-H), 4.31 (d, 3J = 3.6 Hz, 0.50 H, 4-H), 4.93 (d, 3J = 12.1 Hz, 0.52 H, 11-H), 5.09 (d, 3J = 12.3 Hz, 0.52 H, 11-H), 6.37-6.40, 6.60-6.62 (2m, 2 H, 8-H), 6.64-6.70, 6.95-6.98 (2m, 2 H, 7-H), 7.33-7.35, 7.92-7.94 (2m, 2 H, 14-H), 8.04-8.06, 8.32-8.35 ppm (2m, 2 H, 15-H). $^{13}\text{C-NMR}$ (CDCl_3 , 151 MHz): δ = 28.20, 28.35 (2q, C-2), 28.47, 28.53 (2q, C-2), 39.48 (d, C-11), 39.94, 40.11 (2q, C-10), 40.18 (d, C-11), 49.45 (d, C-4), 52.31, 52.39 (2d, C-5), 53.01 (d, C-4), 111.93, 112.29 (2d, C-8), 118.45 (s, C-6), 118.70, 119.34 (2s, C-12), 120.20 (s, C-6), 123.90, 124.62 (2d, C-15), 128.16, 128.54 (2d, C-7), 129.48, 130.21 (2d, C-14), 141.28, 141.41 (2s, C-13), 147.58, 148.25 (2s, C-16), 150.35, 150.36 (2s, C-9), 150.59, 150.85 (2s, C-1), 166.93, 167.04, 167.19 ppm (3s, C-3, C-3', signal for the other diastereomer superimposed). HR-MS (ESI) $[\text{M}+\text{H}]^+$: calcd 450.1772; found 450.1758.

4.4 Deprotonation Experiments

General. The formation of the carbanions **1a–c** from their conjugate CH acids (**1a–c**)-H were recorded by using a diode array UV-Vis spectrometer. The temperature during all experiments was kept constant by using a circulating bath ($20.0 \pm 0.02^\circ\text{C}$). The CH acids (**1a–c**)-H were dissolved in DMSO (20-25 mL) and subsequently treated with various amounts of KO*t*Bu (dissolved in DMSO).

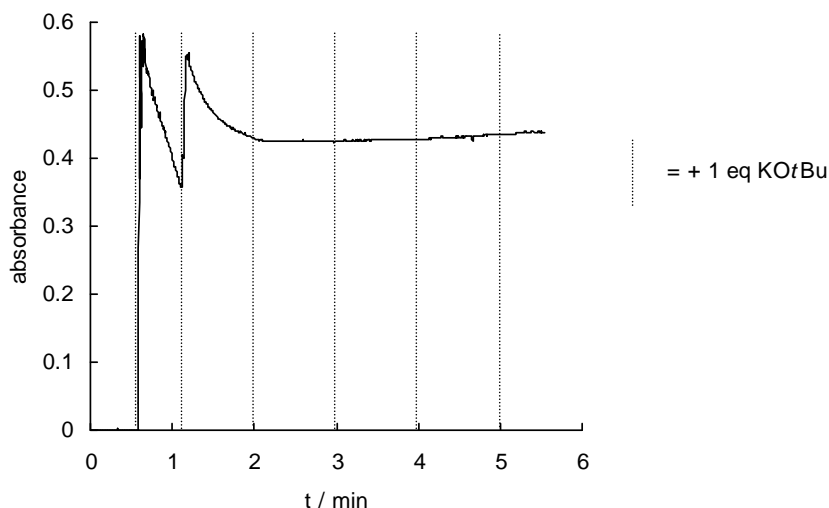


Figure 7: Deprotonation experiment with *p*-(trifluoromethyl)-phenyl-acetonitrile (**1a**-H, $n = 1.35 \times 10^{-6}$ mol) in DMSO at 20°C (deprotonated with KO*t*Bu, $\lambda = 360$ nm).

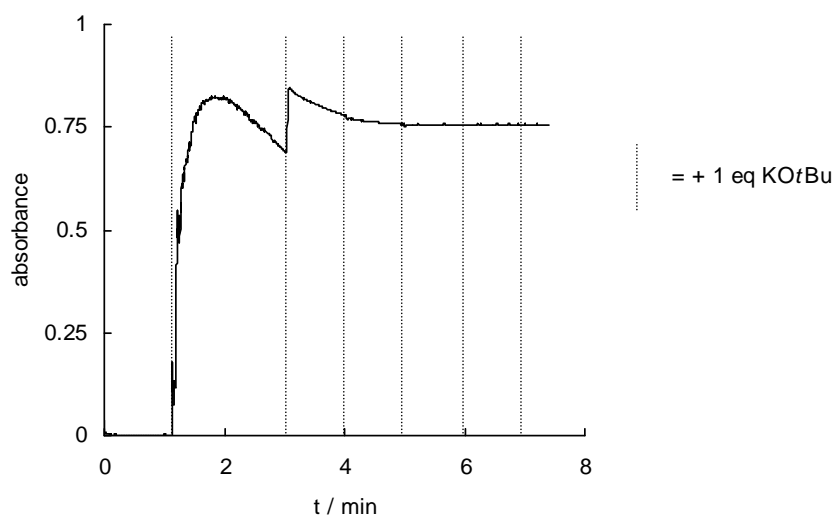


Figure 8: Deprotonation experiment with *p*-cyano-phenyl-acetonitrile (**1b**-H, $n = 1.31 \times 10^{-6}$ mol) in DMSO at 20°C (deprotonated with KO*t*Bu, $\lambda = 390$ nm).

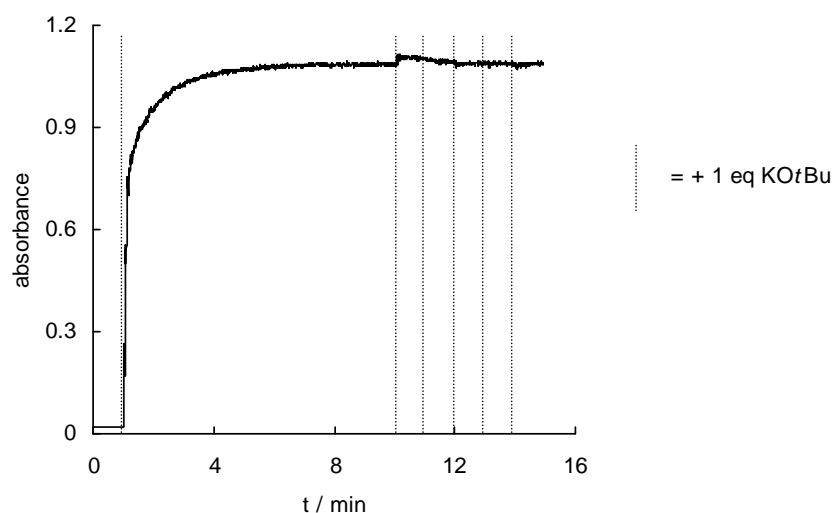


Figure 9: Deprotonation experiment with *p*-nitro-phenyl-acetonitrile (**1c-H**, $n = 1.52 \times 10^{-6}$ mol) in DMSO at 20°C (deprotonated with KOtBu, $\lambda = 540$ nm).

4.5 Kinetics

4.5.1 Kinetics for the Anion of (*p*-Trifluoromethyl-phenyl)acetonitrile (**1a**)

Table 4: Kinetics of the reaction of electrophile **3d** with the anion of (*p*-trifluoromethyl-phenyl)acetonitrile (**1a**) in DMSO at 20°C (deprotonated with 1.00 – 1.05 equiv KOtBu, stopped-flow UV-Vis spectrometer, $\lambda = 440$ nm).

Nr.	$[E]_0 / M$	$[Nu^-]_0 / M$	k_{obs} / s^{-1}
RAK 3.10-2	2.96×10^{-5}	3.59×10^{-4}	1.42×10^2
RAK 3.10-1	2.96×10^{-5}	4.06×10^{-4}	1.60×10^2
RAK 3.10-3	2.96×10^{-5}	4.54×10^{-4}	1.84×10^2
RAK 3.11-1	2.96×10^{-5}	4.95×10^{-4}	2.00×10^2
RAK 3.11-2	2.96×10^{-5}	5.54×10^{-4}	2.19×10^2
$k_2 = 4.04 \times 10^5 \text{ L mol}^{-1} \text{ s}^{-1}$			

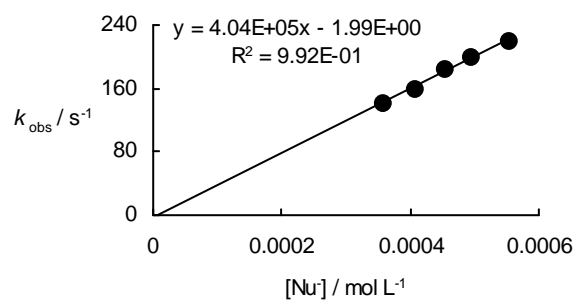


Table 5: Kinetics of the reaction of electrophile **3e** with the anion of (*p*-trifluoromethyl-phenyl)acetonitrile (**1a**) in DMSO at 20°C (deprotonated with 1.00-1.05 equiv KOtBu, stopped-flow UV-Vis spectrometer, $\lambda = 486$ nm).

Nr.	$[E]_0 / M$	$[Nu^-]_0 / M$	k_{obs} / s^{-1}
RAK 3.dma-1	1.26×10^{-5}	3.11×10^{-4}	2.72×10^1
RAK 3.dma-2	1.26×10^{-5}	4.04×10^{-4}	3.50×10^1
RAK 3.dma-3	1.26×10^{-5}	5.02×10^{-4}	3.98×10^1
RAK 3.dma-4	1.26×10^{-5}	6.37×10^{-4}	5.20×10^1
RAK 3.dma-5	1.26×10^{-5}	7.53×10^{-4}	6.06×10^1
RAK 3.dma-6	1.26×10^{-5}	1.01×10^{-3}	8.54×10^1
$k_2 = 8.24 \times 10^4 \text{ L mol}^{-1} \text{ s}^{-1}$			

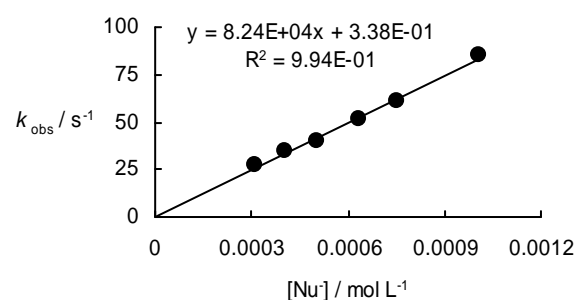
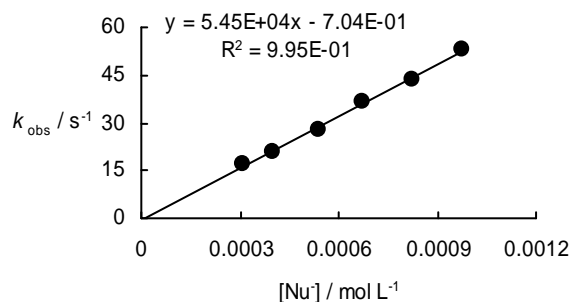


Table 6: Kinetics of the reaction of electrophile **3f** with the anion of (*p*-trifluoromethyl-phenyl)acetonitrile (**1a**) in DMSO at 20°C (deprotonated with 1.00-1.05 equiv KO^tBu, stopped-flow UV-Vis spectrometer, $\lambda = 521$ nm).

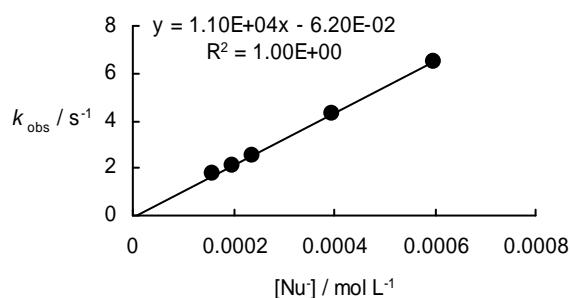
Nr.	[E] ₀ / M	[Nu ⁻] ₀ / M	<i>k</i> _{obs} / s ⁻¹
RAK 3.9-1	1.29×10^{-5}	3.11×10^{-4}	1.73×10^1
RAK 3.4-1	1.27×10^{-5}	4.03×10^{-4}	2.06×10^1
RAK 3.4-2	1.27×10^{-5}	5.38×10^{-4}	2.75×10^1
RAK 3.4-3	1.27×10^{-5}	6.72×10^{-4}	3.68×10^1
RAK 3.4-4	1.27×10^{-5}	8.22×10^{-4}	4.33×10^1
RAK 3.4-5	1.27×10^{-5}	9.77×10^{-4}	5.31×10^1
$k_2 = 5.45 \times 10^4$ L mol ⁻¹ s ⁻¹			



4.5.2 Kinetics for the Anion of (*p*-Cyano-phenyl)acetonitrile (**1b**)

Table 7: Kinetics of the reaction of electrophile **3e** with the anion of (*p*-cyano-phenyl)acetonitrile (**1b**) in DMSO at 20°C (deprotonated with 1.00-1.05 equiv KO^tBu, stopped-flow UV-Vis spectrometer, $\lambda = 486$ nm).

Nr.	[E] ₀ / M	[Nu ⁻] ₀ / M	<i>k</i> _{obs} / s ⁻¹
RAK 4.3Z-1	1.27×10^{-5}	1.59×10^{-4}	1.74
RAK 4.3Z-2	1.27×10^{-5}	1.98×10^{-4}	2.08
RAK 4.3Z-3	1.27×10^{-5}	2.38×10^{-4}	2.49
RAK 4.3Z-4	1.27×10^{-5}	3.96×10^{-4}	4.29
RAK 4.3Z-5	1.51×10^{-5}	5.98×10^{-4}	6.50
$k_2 = 1.10 \times 10^4$ L mol ⁻¹ s ⁻¹			

**Table 8:** Kinetics of the reaction of electrophile **3f** with the anion of (*p*-cyano-phenyl)acetonitrile (**1b**) in DMSO at 20°C (deprotonated with 1.00-1.05 equiv KO^tBu, stopped-flow UV-Vis spectrometer, $\lambda = 521$ nm).

Nr.	[E] ₀ / M	[Nu ⁻] ₀ / M	<i>k</i> _{obs} / s ⁻¹
RAK 4.1-1	1.03×10^{-5}	1.13×10^{-4}	7.27×10^{-1}
RAK 4.2-1	1.23×10^{-5}	1.33×10^{-4}	9.03×10^{-1}
RAK 4.1-6	1.03×10^{-5}	1.51×10^{-4}	9.35×10^{-1}
RAK 4.1-2	1.03×10^{-5}	1.88×10^{-4}	1.24
RAK 4.1-3	1.03×10^{-5}	2.64×10^{-4}	1.79
RAK 4.1-4	1.03×10^{-5}	3.39×10^{-4}	2.21
RAK 4.2-2	1.23×10^{-5}	4.43×10^{-4}	2.90
RAK 4.2-3	1.23×10^{-5}	5.40×10^{-4}	3.64
RAK 4.2-4	1.23×10^{-5}	7.76×10^{-4}	5.07
$k_2 = 6.59 \times 10^3$ L mol ⁻¹ s ⁻¹			

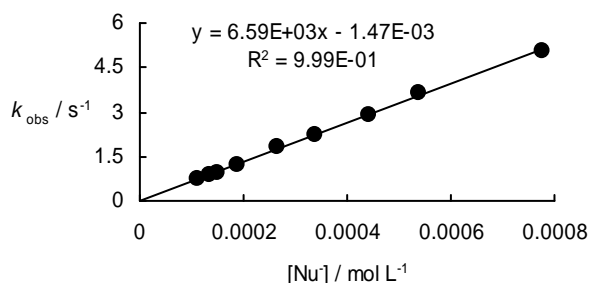
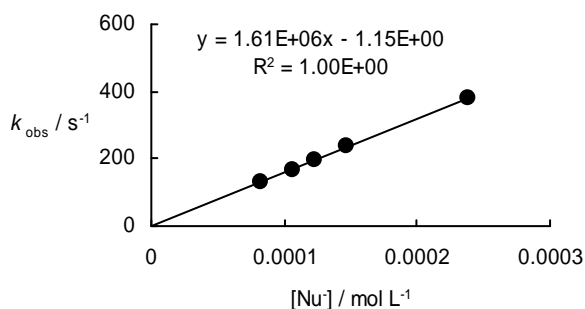
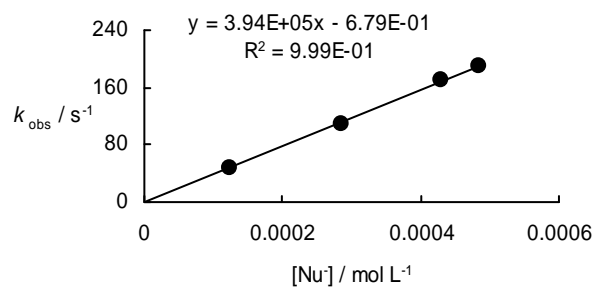


Table 9: Kinetics of the reaction of electrophile **3i** with the anion of (*p*-cyano-phenyl)acetonitrile (**1b**) in DMSO at 20°C (deprotonated with 1.00-1.05 equiv KO*t*Bu, stopped-flow UV-Vis spectrometer, $\lambda = 490$ nm).

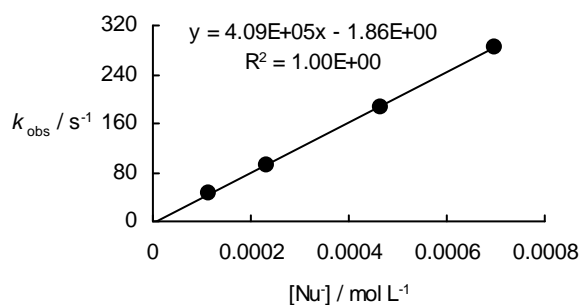
Nr.	[E] ₀ / M	[Nu ⁻] ₀ / M	<i>k</i> _{obs} / s ⁻¹
RAK 4.10-1	8.09×10^{-6}	8.18×10^{-5}	1.30×10^2
RAK 4.10-4	8.09×10^{-6}	1.06×10^{-4}	1.69×10^2
RAK 4.10-3	8.09×10^{-6}	1.23×10^{-4}	1.96×10^2
RAK 4.10-2	8.09×10^{-6}	1.47×10^{-4}	2.38×10^2
RAK 4.3-1	8.09×10^{-6}	2.38×10^{-4}	3.81×10^2
$k_2 = 1.61 \times 10^6 \text{ L mol}^{-1} \text{ s}^{-1}$			

**Table 10:** Kinetics of the reaction of electrophile **3j** with the anion of (*p*-cyano-phenyl)acetonitrile (**1b**) at 20°C (deprotonated with 1.00-1.05 equiv KO*t*Bu, stopped-flow UV-Vis spectrometer, $\lambda = 523$ nm).

Nr.	[E] ₀ / M	[Nu ⁻] ₀ / M	<i>k</i> _{obs} / s ⁻¹
RAK 4.5Z-1	8.50×10^{-6}	1.23×10^{-4}	4.88×10^1
RAK 4.5Z-2	8.21×10^{-6}	2.86×10^{-4}	1.10×10^2
RAK 4.5Z-3	8.21×10^{-6}	4.29×10^{-4}	1.70×10^2
RAK 4.5Z-4	8.21×10^{-6}	4.84×10^{-4}	1.90×10^2
$k_2 = 3.94 \times 10^5 \text{ L mol}^{-1} \text{ s}^{-1}$			

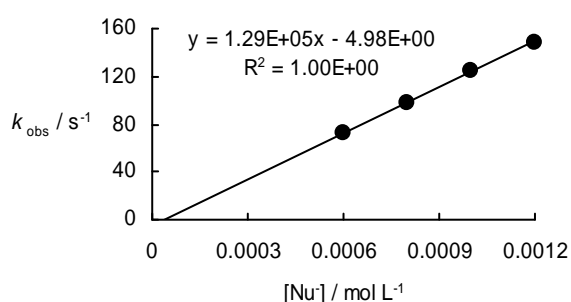
**Table 11:** Kinetics of the reaction of electrophile **3j** with the anion of (*p*-cyano-phenyl)acetonitrile (**1b**) in DMSO at 20°C in the presence of 18-crown-6 (deprotonated with 1.00-1.12 equiv KO*t*Bu, stopped-flow UV-Vis spectrometer, $\lambda = 523$ nm).

Nr.	[E] ₀ / M	[Nu ⁻] ₀ / M	[18-crown-6] / M	<i>k</i> _{obs} / s ⁻¹
RAK 4.11-1	8.96×10^{-6}	1.16×10^{-4}	-	4.63×10^1
RAK 4.11-2	8.96×10^{-6}	2.32×10^{-4}	1.27×10^{-3}	9.23×10^1
RAK 4.11-3	8.96×10^{-6}	4.64×10^{-4}	-	1.87×10^2
RAK 4.11-4	8.96×10^{-6}	6.96×10^{-4}	2.54×10^{-3}	2.83×10^2
$k_2 = 4.09 \times 10^5 \text{ L mol}^{-1} \text{ s}^{-1}$				



4.5.3 Kinetics for the Anion of (*p*-Nitro-phenyl)acetonitrile (**1c**)**Table 12:** Kinetics of the reaction of **3a** with the anion of (*p*-nitro-phenyl)acetonitrile (**1c**) in DMSO at 20°C in the presence of 18-crown-6 (deprotonated with 1.00-1.05 equiv KO^tBu, stopped-flow UV-Vis spectrometer, $\lambda = 400$ nm).

Nr.	[E] ₀ / M	[Nu ⁻] ₀ / M	[18-crown-6] / M	$k_{\text{obs}} / \text{s}^{-1}$
RAK 1.17-1	5.37×10^{-5}	5.99×10^{-4}	-	7.20×10^1
RAK 1.17-2	5.37×10^{-5}	7.98×10^{-4}	1.12×10^{-3}	9.74×10^1
RAK 1.17-3	5.37×10^{-5}	9.98×10^{-4}	-	1.24×10^2
RAK 1.17-4	5.37×10^{-5}	1.20×10^{-3}	1.60×10^{-3}	1.49×10^2
$k_2 = 1.29 \times 10^5 \text{ L mol}^{-1} \text{ s}^{-1}$				

**Table 13:** Kinetics of the reaction of electrophile **3c** with the anion of (*p*-nitro-phenyl)acetonitrile (**1c**) in DMSO at 20°C (deprotonated with 1.00-1.05 equiv KO^tBu, stopped-flow UV-Vis spectrometer, $\lambda = 380$ nm).

Nr.	[E] ₀ / M	[Nu ⁻] ₀ / M	$k_{\text{obs}} / \text{s}^{-1}$
RAK 1.8-1	6.03×10^{-5}	5.99×10^{-4}	2.63×10^{-1}
RAK 1.8-2	6.03×10^{-5}	7.50×10^{-4}	3.05×10^{-1}
RAK 1.8-3	6.03×10^{-5}	9.00×10^{-4}	3.95×10^{-1}
RAK 1.8-4	6.03×10^{-5}	1.01×10^{-3}	4.38×10^{-1}
RAK 1.8-5	6.03×10^{-5}	1.87×10^{-3}	7.90×10^{-1}
$k_2 = 4.19 \times 10^2 \text{ L mol}^{-1} \text{ s}^{-1}$			

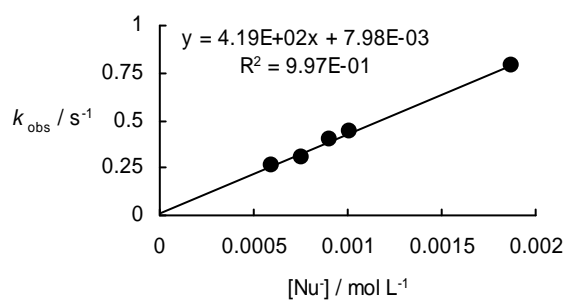
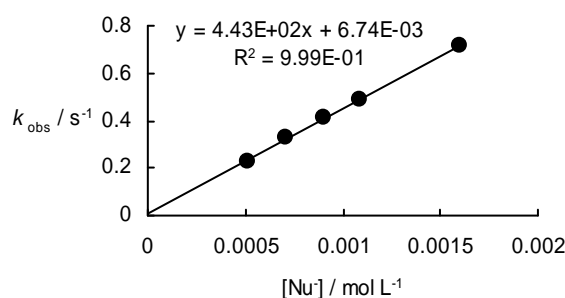
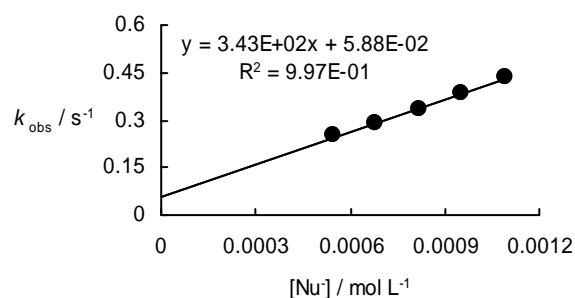


Table 14: Kinetics of the reaction of electrophile **3c** with the anion of (*p*-nitro-phenyl)acetonitrile (**1c**) in DMSO at 20°C in the presence of 18-crown-6 (deprotonated with 1.00-1.05 equiv KO*t*Bu, stopped-flow UV-Vis spectrometer, $\lambda = 400$ nm).

Nr.	$[E]_0 / M$	$[Nu^-]_0 / M$	$[18\text{-crown-6}] / M$	k_{obs} / s^{-1}
RAK 1.13-1	3.08×10^{-5}	5.13×10^{-4}	7.69×10^{-4}	2.27×10^{-1}
RAK 1.13-2	3.08×10^{-5}	7.06×10^{-4}	1.68×10^{-3}	3.25×10^{-1}
RAK 1.13-3	3.08×10^{-5}	8.98×10^{-4}	1.88×10^{-3}	4.10×10^{-1}
RAK 1.13-4	3.08×10^{-5}	1.09×10^{-3}	2.18×10^{-3}	4.89×10^{-1}
RAK 1.13-5	3.08×10^{-5}	1.60×10^{-3}	3.80×10^{-3}	7.14×10^{-1}
$k_2 = 4.43 \times 10^2 \text{ L mol}^{-1} \text{ s}^{-1}$				

**Table 15:** Kinetics of the reaction of electrophile **3d** with the anion of (*p*-nitro-phenyl)acetonitrile (**1c**) in DMSO at 20°C (deprotonated with 1.00-1.05 equiv KO*t*Bu, stopped-flow UV-Vis spectrometer, $\lambda = 400$ nm).

Nr.	$[E]_0 / M$	$[Nu^-]_0 / M$	k_{obs} / s^{-1}
RAK 1.7-1	5.03×10^{-5}	5.45×10^{-4}	2.51×10^{-1}
RAK 1.7-2	5.03×10^{-5}	6.82×10^{-4}	2.88×10^{-1}
RAK 1.7-3	5.03×10^{-5}	8.18×10^{-4}	3.35×10^{-1}
RAK 1.7-4	5.03×10^{-5}	9.54×10^{-4}	3.87×10^{-1}
RAK 1.7-5	5.03×10^{-5}	1.09×10^{-3}	4.35×10^{-1}
$k_2 = 3.43 \times 10^2 \text{ L mol}^{-1} \text{ s}^{-1}$			

**Table 16:** Kinetics of the reaction of electrophile **3d** with the anion of (*p*-nitro-phenyl)acetonitrile (**1c**) in DMSO at 20°C in the presence of 18-crown-6 (deprotonated with 1.00-1.05 equiv KO*t*Bu, stopped-flow UV-Vis spectrometer, $\lambda = 400$ nm).

Nr.	$[E]_0 / M$	$[Nu^-]_0 / M$	$[18\text{-crown-6}] / M$	k_{obs} / s^{-1}
RAK 1.16-1	4.33×10^{-5}	4.98×10^{-4}	-	2.32×10^{-1}
RAK 1.16-2	4.33×10^{-5}	6.09×10^{-4}	1.24×10^{-3}	2.68×10^{-1}
RAK 1.16-3	4.33×10^{-5}	7.93×10^{-4}	-	3.18×10^{-1}
RAK 1.16-4	4.33×10^{-5}	1.29×10^{-3}	1.31×10^{-3}	4.86×10^{-1}
RAK 1.16-5	4.33×10^{-5}	1.57×10^{-3}		5.85×10^{-1}
RAK 1.16-6	4.33×10^{-5}	1.75×10^{-3}	2.06×10^{-3}	6.35×10^{-1}
$k_2 = 3.26 \times 10^2 \text{ L mol}^{-1} \text{ s}^{-1}$				

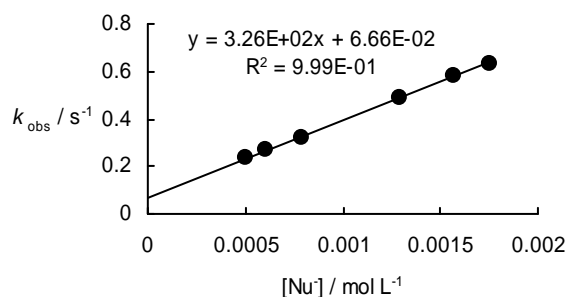


Table 17: Kinetics of the reaction of electrophile **3h** with the anion of (*p*-nitro-phenyl)acetonitrile (**1c**) in DMSO at 20°C (deprotonated with 1.00-1.05 equiv KO*t*Bu, stopped-flow UV-Vis spectrometer, $\lambda = 388$ nm).

Nr.	$[\text{E}]_0 / \text{M}$	$[\text{Nu}^-]_0 / \text{M}$	$k_{\text{obs}} / \text{s}^{-1}$
RAK 1.9-1	7.72×10^{-5}	7.77×10^{-4}	3.94×10^2
RAK 1.9-4	7.72×10^{-5}	9.33×10^{-4}	4.85×10^2
RAK 1.9-2	7.72×10^{-5}	1.04×10^{-3}	5.48×10^2
RAK 1.9-5	7.72×10^{-5}	1.14×10^{-3}	5.82×10^2
RAK 1.9-3	7.72×10^{-5}	1.30×10^{-3}	6.78×10^2
RAK 1.9-6	7.72×10^{-5}	1.40×10^{-3}	7.21×10^2
			$k_2 = 5.23 \times 10^5 \text{ L mol}^{-1} \text{ s}^{-1}$

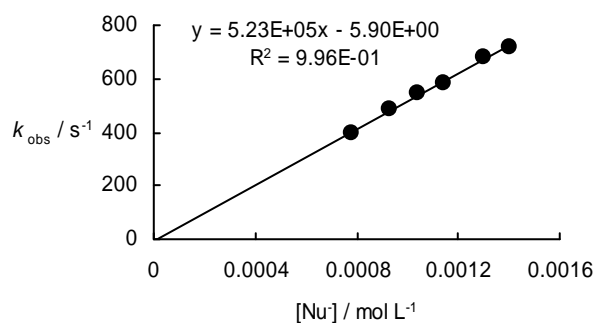
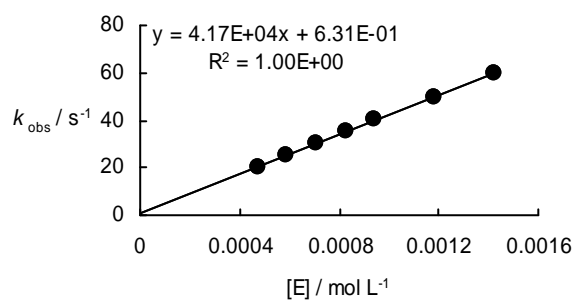


Table 18: Kinetics of the reaction of electrophile **3l** with the anion of (*p*-nitro-phenyl)acetonitrile (**1c**) in DMSO at 20°C (deprotonated with 1.00-1.05 equiv KO*t*Bu, stopped-flow UV-Vis spectrometer, $\lambda = 560$ nm).

Nr.	$[\text{E}]_0 / \text{M}$	$[\text{Nu}^-]_0 / \text{M}$	$k_{\text{obs}} / \text{s}^{-1}$
RAK 1.12-1	4.72×10^{-4}	4.63×10^{-5}	2.02×10^1
RAK 1.12-6	5.90×10^{-4}	4.63×10^{-5}	2.51×10^1
RAK 1.12-2	7.08×10^{-4}	4.63×10^{-5}	3.03×10^1
RAK 1.12-7	8.26×10^{-4}	4.63×10^{-5}	3.50×10^1
RAK 1.12-3	9.44×10^{-4}	4.63×10^{-5}	4.02×10^1
RAK 1.12-4	1.18×10^{-3}	4.63×10^{-5}	5.00×10^1
RAK 1.12-5	1.42×10^{-3}	4.63×10^{-5}	5.96×10^1
			$k_2 = 4.17 \times 10^4 \text{ L mol}^{-1} \text{ s}^{-1}$



5 References

- [1] (a) Mayr, H.; Kempf, B.; Ofial, A. R. *Acc. Chem. Res.* **2003**, *36*, 66-77. (b) Mayr, H.; Ofial, A. R. in *Carbocation Chemistry*; Olah, H. A., Prakash, G. K. S., eds.; Wiley: Hoboken (N. J.); **2004**, pp, 331-358. (c) Ofial, A. R.; Mayr, H. *Macromol. Symp.* **2004**, *215*, 353-367. (d) Mayr, H.; Ofial, A. R. *Pure Appl. Chem.* **2005**, *77*, 1807-1821. (e) Mayr, H.; Ofial, A. R. *J. Phys. Org. Chem.* **2008**, *21*, 584-595.
- [2] Mayr, H.; Bug, T.; Gotta, M. F.; Hering, N.; Irrgang, B.; Janker, B.; Kempf, B.; Loos, R.; Ofial, A. R.; Remennikov, G.; Schimmel, H. *J. Am. Chem. Soc.* **2001**, *123*, 9500-9512.
- [3] Mayr, H.; Patz, M. *Angew. Chem.* **1994**, *106*, 990-1010; *Angew. Chem. Int. Ed. Engl.* **1994**, *33*, 938-957.
- [4] Lucius, R.; Loos, R.; Mayr, H. *Angew. Chem.* **2002**, *114*, 97-102; *Angew. Chem. Int. Ed.* **2002**, *41*, 91-95.
- [5] Bug, T.; Mayr, H. *J. Am. Chem. Soc.* **2003**, *125*, 12980-12986.
- [6] Berger, S. T. A.; Ofial, A. R.; Mayr, H. *J. Am. Chem. Soc.* **2007**, *129*, 9753-9761.
- [7] Seeliger, F.; Mayr, H. *Org. Biomol. Chem.* **2008**, *6*, 3052-3058.
- [8] Bug, T.; Lemek, T.; Mayr, H. *J. Org. Chem.* **2004**, *69*, 7565-7576.
- [9] Phan, T. B.; Mayr, H. *Eur. J. Org. Chem.* **2006**, 2530-2537.
- [10] Berger, S. T. A.; Lemek, T.; Mayr, H. *ARKIVOC* **2008** (x), 37-53.
- [11] (a) Lemek, T.; Mayr, H. *J. Org. Chem.* **2003**, *68*, 6880-6886. (b) Kaumanns, O.; Mayr, H. *J. Org. Chem.* **2008**, *73*, 2738-2745.
- [12] Seeliger, F.; Berger, S. T. A.; Remennikov, G. Y.; Polborn, K.; Mayr, H. *J. Org. Chem.* **2007**, *72*, 9170-9180.
- [13] Berger, S. T. A.; Seeliger, F. H.; Hofbauer, F.; Mayr, H. *Org. Biomol. Chem.* **2007**, *5*, 3020-3026.
- [14] Kaumanns, O.; Lucius, R.; Mayr, H. *Chem. Eur. J.* **2008**, *14*, 9675-9682.
- [15] (a) Collier, S. J.; Langer, P. *Sci. Synth.* **2004**, *19*, 403-425. (b) Murahashi, S. I. *Sci. Synth.* **2004**, *19*, 345-402. (c) Fleming, F. F.; Zhang, Z. *Tetrahedron* **2005**, *61*, 747-789. (d) Fleming, F. F.; Wang, Q. *Chem. Rev.* **2003**, *103*, 2035-2077.
- [16] (a) Bordwell, F. G.; Bausch, M. J. *J. Am. Chem. Soc.* **1986**, *108*, 1979-1985. (b) Bordwell, F. G.; Cheng, J.-P.; Bausch, M. J.; Bares, J. E. *J. Phys. Org. Chem.* **1988**, *1*, 209-223.
- [17] Smith, H. A.; Bissell, R. L.; Kenyon, W. G.; MacClarence, J. W.; Hauser, C. R. *J. Org. Chem.* **1971**, *36*, 2132-2137.

- [18] (a) Makosza, M.; Stalinski, K.; Klepka, C. *Chem. Commun.* **1996**, 837-838. (b) Makosza, M.; Stalinski, K. *Chem. Eur. J.* **1997**, *3*, 2025-2031. (c) Makosza, M.; Stalinski, K. *Tetrahedron* **1998**, *54*, 8797-8810. (d) Makosza, M.; Stalinski, K. *Synthesis* **1998**, 1631-1634.
- [19] (a) Adam, W.; Makosza, M.; Zhao, C.-G.; Surowiec, M. *J. Org. Chem.* **2000**, *65*, 1099-1101. (b) Adam, W.; Makosza, M.; Stalinski, K.; Zhao, C.-G. *J. Org. Chem.* **1998**, *63*, 4390-4391.
- [20] Kroeger, D. J.; Stewart, R. *Can. J. Chem.* **1967**, *45*, 2163-2171.
- [21] Arnett, E. M.; Small, L. E. *J. Am. Chem. Soc.* **1977**, *99*, 808-816.
- [22] Olmstead, W. N.; Margolin, Z.; Bordwell, F. G. *J. Org. Chem.* **1980**, *45*, 3295-3299.
- [23] Schwesinger, R.; Schlemper, H.; Hasenfratz, C.; Willaredt, J.; Dambacher, T.; Breuer, T.; Ottaway, C.; Fletschinger, M.; Boele, J.; Fritz, H.; Putzas, D.; Rotter, H. W.; Bordwell, F. G.; Satish, A. V.; Ji, G. Z.; Peters, E. M.; Peters, K.; v. Schnering, H. G.; Walz, L. *Liebigs Ann.* **1996**, 1055-1081.
- [24] (a) *The Investigation of Organic Reactions and Their Mechanisms*; Maskill, H., ed.; Blackwell Publishing: Oxford, 2006. (b) Schmid, R.; Sapunov, V. N. *Non-Formal Kinetics*; VCH: Weinheim, 1982.
- [25] Binev, I. G.; Tsenov, J. A.; Velcheva, E. A.; Juchnovski, I. N. *J. Mol. Struct.* **1995**, *344*, 205-215.
- [26] Lucius, R.; Mayr, H. *Angew. Chem.* **2000**, *112*, 2086-2089; *Angew. Chem. Int. Ed.* **2000**, *39*, 1995-1997.
- [27] Goumont, R.; Kizilian, E.; Buncel, E.; Terrier, F. *Org. Biomol. Chem.* **2003**, *1*, 1741-1748.
- [28] (a) Nigst, T. A.; Westermaier, M.; Ofial, A. R.; Mayr, H. *Eur. J. Org. Chem.* **2008**, 2369-2374. (b) Brotzel, F.; Kempf, B.; Singer, T.; Zipse, H.; Mayr, H. *Chem. Eur. J.* **2007**, *13*, 336-345. (c) Brotzel, F.; Chu, Y. C.; Mayr, H. *J. Org. Chem.* **2007**, *72*, 3679-3688.
- [29] pK_a values for **2b** and **2c** have not been reported.
- [30] (a) Bernasconi, C. F.; Zitomer, J. L.; Fox, J. P.; Howard, K. A. *J. Org. Chem.* **1984**, *49*, 482-486. (b) Bernasconi, C. F. *Acc. Chem. Res.* **1987**, *20*, 301-308. (c) Bernasconi, C. F.; Wenzel, P. J. *J. Org. Chem.* **2003**, *68*, 6870-6879.
- [31] Bailey, W. F.; Jiang, X.-L.; McLeod, C. E. *J. Org. Chem.* **1995**, *60*, 7791-7795.
- [32] Bell, F.; Waring, D. H. *J. Chem. Soc.* **1948**, 1024-1026.

Chapter 10: Nucleophilic Reactivities of Alkali Cyclopentadienides (CpK, CpNa, CpLi)

1 Introduction

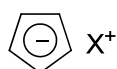
Organometallic compounds are versatile reagents, which have numerous applications in organic synthesis and often allow chemo- and stereoselective transformations.^[1] In many cases, qualitative trends about reactivities of organometallic compounds are known. However, the recent developments of highly functionalized organometallics with unprecedented functional group tolerance^[2] show the limited predictability of organometallic reactivities in particular cases.

In recent years, we have developed the most comprehensive nucleophilicity and electrophilicity scale presently available, which is based on the linear free-energy relationship of eq 1, where $k_{20^\circ\text{C}}$ is the second-order rate constant in $\text{M}^{-1} \text{s}^{-1}$, s is a nucleophile-specific sensitivity parameter, N is a nucleophilicity parameter, and E is an electrophilicity parameter.^[3]

$$\log k_{20^\circ\text{C}} = s(N + E) \quad (1)$$

By defining a series of structurally related benzhydrylium ions and Michael acceptors as reference electrophiles (some of them are depicted in Table 1), we have been able to characterize the nucleophilic reactivities of a large variety of (free) carbanions.^[4] On the other hand, we have also included allyl- and arylsilanes as well as stannes, i.e., organometallic compounds with less polar carbon-metal bonds, into our nucleophilicity scale.^[3b,c] We now set out to systematically investigate the influence of the metal counterion on the nucleophilic reactivities of carbanions, in order to provide a quantitative basis for the reactivities of organometallic species. For this reason, we have now studied the kinetics of the reactions of the alkali cyclopentadienides **1-K**, **1-Na**, and **1-Li** (Scheme 1) with the reference electrophiles **2a–e** (Table 1) in DMSO.

Scheme 1: Alkali Cyclopentadienides **1-K**, **1-Na**, and **1-Li**.



X = K (**1-K**), Na (**1-Na**), Li (**1-Li**)

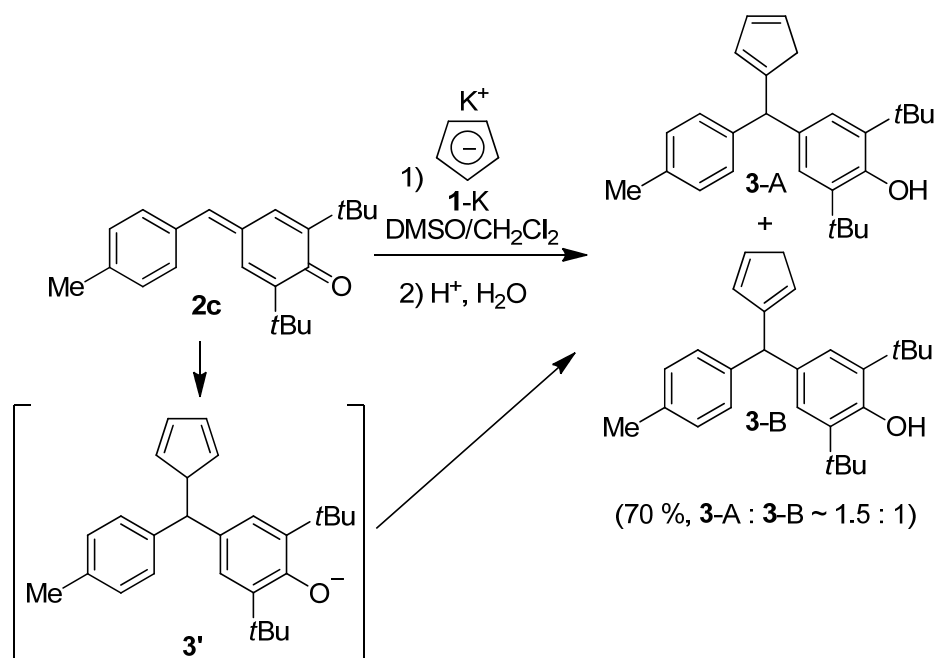
Table 1: Michael Acceptors **2a–e** and their Electrophilicity Parameters E .

Electrophile	E^a
2a	-13.84
2b	-14.68
2c (R = Me)	-15.83
2d (R = OMe)	-16.11
2e (R = NMe ₂)	-17.29

^aElectrophilicity parameters E of **2a** were taken from ref 5, of **2b** from ref 6, of **2c–e** from ref 4a.

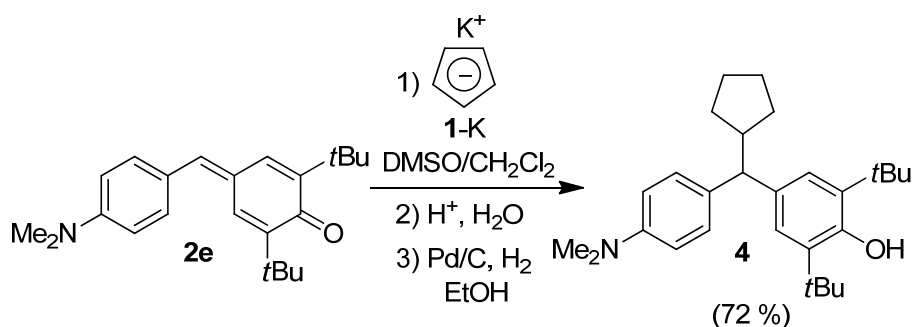
2 Results

Product Analysis. In order to elucidate the course of the reactions, which have been studied kinetically, we have performed representative product analyses for the reactions of **1-K** with the quinone methides **2c** and **2e**. As shown in Scheme 2, the reaction of cyclopentadienyl potassium (**1-K**) with **2c** yields the two regioisomers **3-A** and **3-B** as products. Obviously, the initially formed addition product **3'** is not stable and the compounds **3-A** and **3-B** are obtained either by subsequent [1,5]-sigmatropic hydrogen shifts^[7] or base-catalyzed isomerization.

Scheme 2: Reaction of Cyclopentadienide **1-K** with the Quinone Methide **2c**.

In the reaction of **1-K** with **2e**, we have circumvented the analysis of a mixture of regioisomers by subsequent hydrogenation of the crude products (Pd/C and H₂) yielding the cyclopentane derivative **4** (Scheme 3).

Scheme 3: Reaction of Cyclopentadienide **1-K** with Quinone Methide **2e** and Subsequent Hydrogenation.



Kinetic Investigations. All kinetic investigations were monitored photometrically by following the disappearance of the colored electrophiles **2** in the presence of more than 10 equiv of the nucleophiles **1** (first-order conditions). Stock solutions of the cyclopentadienides **1-K**, **1-Na**, and **1-Li** were freshly prepared in DMSO before the kinetic experiments. As the presence of 18-crown-6 did not affect the kinetics of **1-K** (see Experimental Section), one can conclude that the reactivity of the free cyclopentadienyl anion **1** was observed. From the exponential decays of the UV-Vis absorbances of the electrophiles **2**, the first-order rate constants k_{obs} were obtained. Plots of k_{obs} (s⁻¹) against the concentrations of the nucleophiles **1** were linear with negligible intercepts as required by eq 2 (Figure 1). The slopes of these correlations correspond to the second-order rate constants of the investigated reactions (Table 2).

$$-d[\mathbf{2}]/dt = k_2 [\mathbf{1}] [\mathbf{2}] \text{ for } [\mathbf{1}] \gg [\mathbf{2}] \Rightarrow k_{\text{obs}} = k_2 [\mathbf{1}] \quad (2)$$

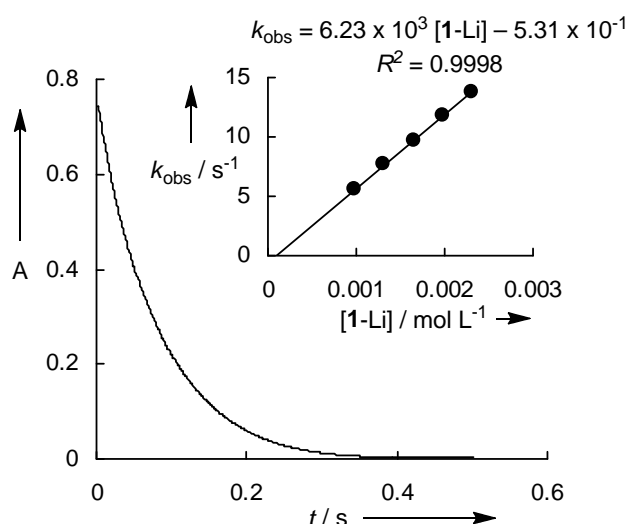
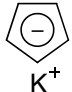
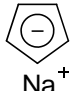
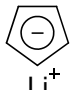


Figure 1: UV-Vis spectroscopic monitoring of the reaction of lithium cyclopentadienide (**1-Li**, $1.97 \times 10^{-3} \text{ mol L}^{-1}$) with the quinone methide **2d** ($2.55 \times 10^{-5} \text{ mol L}^{-1}$) at 393 nm in DMSO at 20°C . Insert: Determination of the second-order rate constant $k_2 = 6.23 \times 10^3 \text{ L mol}^{-1} \text{ s}^{-1}$ from the dependence of the first-order rate constant k_{obs} on the concentration of **1-Li**.

Table 2: Second-Order Rate Constants for the Reactions of the Alkali Cyclopentadienides **1-K**, **1-Na**, and **1-Li** with the Michael Acceptors **2** in DMSO at 20°C .

Nucleophiles N / s^a	Electrophile	$k_2 / \text{M}^{-1} \text{ s}^{-1}$
 K^+ 1-K 20.58 / 0.86	2a	5.07×10^5
	2b	1.69×10^5
	2c	1.21×10^4
	2d	6.39×10^3
	2e	6.74×10^2
 Na^+ 1-Na 20.64 / 0.85	2a	4.74×10^5
	2b	1.60×10^5
	2c	1.32×10^4
	2d	6.85×10^3
	2e	6.52×10^2
 Li^+ 1-Li 20.59 / 0.86	2a	4.86×10^5
	2b	1.64×10^5
	2c	1.28×10^4
	2d	6.23×10^3
	2e	6.49×10^2

^a Nucleophilicity parameters N and s derived by using equation 1; determination see below.

3 Discussion

As shown in Table 2, the second-order rate constants for the reactions of the investigated alkali cyclopentadienides (**1**)-K,Na,Li with the Michael acceptors **2** do not differ significantly. As a consequence, we can conclude that K^+ , Na^+ , and Li^+ do not affect the reactivity of the cyclopentadienyl anion under the employed conditions and all measured rate constants reflect the reactivity of the free anion. In order to include the cyclopentadienyl anion into our comprehensive nucleophilicity scale, we have plotted the obtained second-order rate constants for the reactions of (**1**)-K,Na,Li with the Michael acceptors **2** against their electrophilicity parameters. As shown exemplarily for **1**-K in Figure 2, these correlations are linear and, therefore, allow us to calculate the nucleophile-specific parameters N and s (Table 2) according to eq 1. The small deviations of the nucleophilicity parameters for the alkali cyclopentadienides **1**-K, **1**-Na, and **1**-Li lie within the experimental error and again illustrate that the nucleophilic reactivity of the cyclopentadienyl anion is not affected by the employed alkali counterions in DMSO at 20°C.

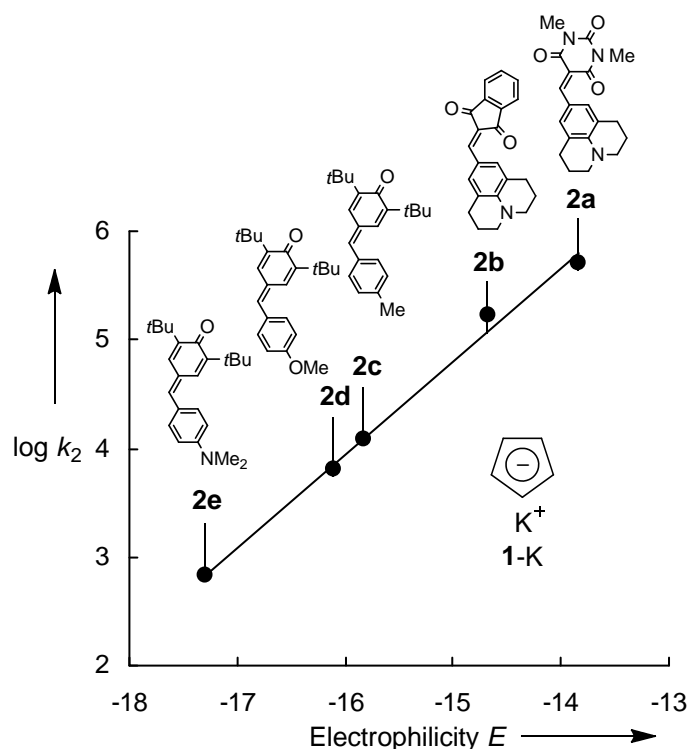


Figure 2: Plot of $\log k_2$ for the reactions of potassium cyclopentadienide (**1**-K) with the Michael acceptors **2a–e** at 20°C in DMSO versus their electrophilicity parameters E . For the sake of clarity, the correlation lines for **1**-Na and **1**-Li are not shown (see Experimental Section).

For carbanions with nucleophilicity parameters of $17 < N < 22$ in DMSO, we have usually found nucleophile-specific sensitivity parameters of $s \sim 0.6 - 0.7$.^[4] However, the nucleophile-specific sensitivity parameter of the cyclopentadienyl anion ($N = 20.58$) shows a significant higher value of $s = 0.86$ (Table 2). Consequently, the relative reactivities of the cyclopentadienyl anion **1** in comparison to carbanions with similar nucleophilicity N depend on the reactivity of the reaction partner and have therefore to be compared with respect to a certain electrophile (Figure 3).

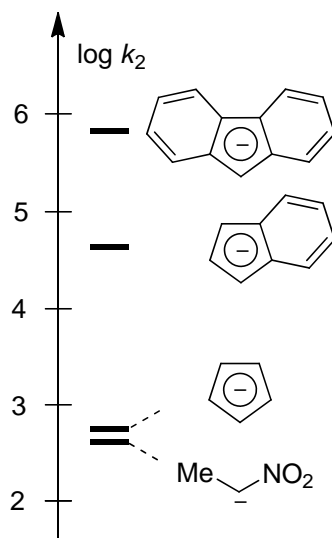


Figure 3: Comparison of the second-order rate constants for the reactions of different carbanions with the quinone methide **2e**. All values were taken for the corresponding potassium salts. Value for the cyclopentadienyl anion taken from Table 2, for the nitroethyl anion from ref 8a and for the indenyl- and fluorenyl anions from ref 8b.

Figure 3 compares the second-order rate constants for the reactions of the cyclopentadienyl anion and other carbanions^[8] with the quinone methide **2e**. The cyclopentadienyl anion shows a similar reactivity as the nitroethyl anion and is considerably less reactive than the fluorenyl- and indenyl anion. This finding can be rationalized by the better aromatic stabilization of the cyclopentadienyl anion in comparison to indenyl- and fluorenyl anions, which is reduced by benzoannulation.^[9] This trend can also be observed for the corresponding pK_{aH} values of these carbanions. The lowest basicity is found for the cyclopentadienyl anion ($pK_{aH} = 18.0$), followed by the indenyl anion ($pK_{aH} = 20.1$), and the fluorenyl anion ($pK_{aH} = 22.6$).^[9] The correlation of these pK_{aH} values with the corresponding second-order rate constants for the reactions of the cyclopentadienyl-, indenyl-, and fluorenyl anions with the quinone methide **2e** (Figure 4) shows that basicity can be a rough guideline for estimating the reactivity of

structurally closely related compounds. However, basicity and nucleophilicity show only poor correlations, when different classes of carbanions are compared.^[4b-e]

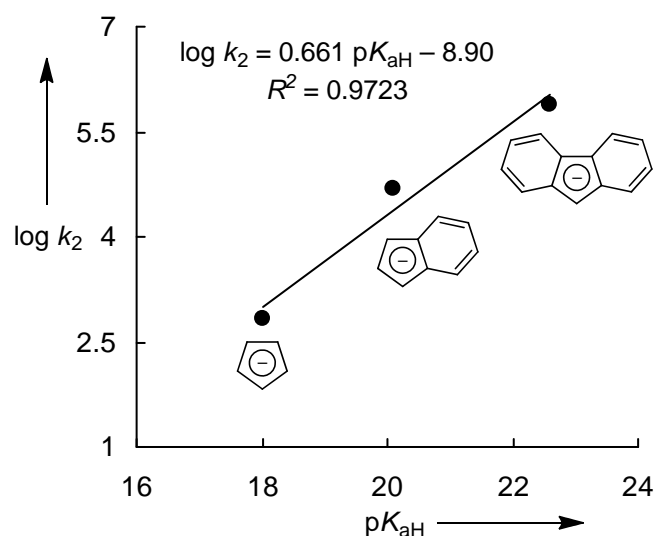


Figure 4: Comparison of the second-order rate constants for the reactions of cyclopentadienyl-, indenyl-, and fluorenyl anions with the quinone methide **2e**. All values taken for the corresponding potassium salts. Value for the cyclopentadienyl anion taken from Table 2 and for the indenyl- and fluorenyl anions from ref 8b.

4 Conclusion and Outlook

The reactions of the alkali cyclopentadienides (**1**)-K,Na,Li with the Michael acceptors **2** have been investigated kinetically in DMSO at 20°C. The obtained second-order rate constants could be correlated with the electrophilicity parameters E of the employed Michael acceptors **2** and the nucleophilicity parameters N and s of (**1**)-K,Na,Li could be obtained according to eq 1. Under the employed conditions (DMSO, 20°C, $[K^+]$, $[Na^+]$, or $[Li^+] < 2.5 \text{ mM L}^{-1}$), the alkali counterions did not significantly affect the nucleophilic reactivity of the free cyclopentadienyl anion.

In future experiments, the effect of different alkali counterions will be studied more detailed by performing the kinetic studies in the presence of extra amounts of alkali salts (e.g., $LiBF_4$), as previously reported for phosphoryl-stabilized carbanions.^[4e] Furthermore, the reactivities of carbanionic species with even less electropositive metal counterions (Figure 5) towards reference electrophiles will be investigated. The comparison of the reactivities of free carbanions with that of corresponding organometallic species will provide a quantitative expression for the influence of the counterion on the nucleophilic reactivity of a carbanion.

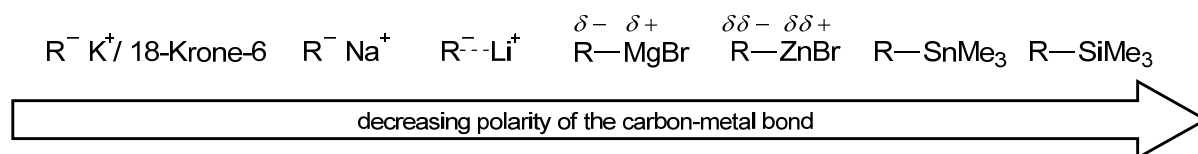


Figure 5: Varying the polarity of carbon-metal bonds by a successive change of the counterion.

5 Experimental Section

5.1 General

Chemicals. Potassium cyclopentadienide (**1**)-K,^[10] sodium cyclopentadienide (**1**)-Na,^[10] lithium cyclopentadienide (**1**)-Li,^[11] the benzylidenebarbituric acid **2a**^[5,12] and the benzylideneindandione **2b**^[6,13] were prepared according to literature procedures. The quinone methides **2c-e**^[8a,14] were prepared as described before. For the kinetic experiments, commercially available dimethyl sulfoxide (DMSO) with a content of H₂O < 50 ppm was used. All other chemicals were purchased from commercial sources and (if necessary) purified by recrystallization or distillation prior to use.

NMR spectroscopy. ¹H- and ¹³C-NMR spectra were recorded in CDCl₃ and the chemical shifts in ppm refer to CDCl₃ (δ_{H} 7.26, δ_{C} 77.0) as internal standard. The following abbreviations were used for chemical shift multiplicities: brs = broad singlet, s = singlet, d = doublet, t = triplet, q = quartet, m = multiplet. For reasons of simplicity, the ¹H-NMR signals of AA'BB'-spin systems of *p*-disubstituted aromatic rings were treated as doublets. NMR signal assignments were based on additional 2D-NMR experiments (e.g., DEPT-, COSY-, HSQC-, and HMBC experiments). Diastereomeric ratios (*dr*) were determined by ¹H-NMR.

Kinetics. The rates of all reactions were determined photometrically. The temperature was kept constant (20.0 ± 0.1°C) by using a circulating bath thermostat. For all kinetic experiments, freshly prepared stock solutions of the carbanions (**1**)-K,Na,Li and the Michael acceptors **2** were prepared in DMSO. In all cases, the carbanions (**1**)-K,Na,Li were employed with high excess over the electrophiles **2** resulting in first-order kinetics, which were evaluated by the stopped-flow spectrophotometer systems Hi-Tech SF-61DX2 or Applied Photophysics SX.18MV-R. First-order rate constants k_{obs} (s⁻¹) were obtained by fitting the single exponential $A_t = A_0 \exp(-k_{\text{obs}}t) + C$ (exponential decrease) to the observed time-dependent absorbance (averaged from at least 3 kinetic runs for each nucleophile concentration). Second-order rate constants k_2 (L mol⁻¹ s⁻¹) were derived from the slopes of

the linear correlations of k_{obs} (s^{-1}) with the concentration of the alkali cyclopentadienide used in excess ($[\text{1-K,Na,Li}]_0$).

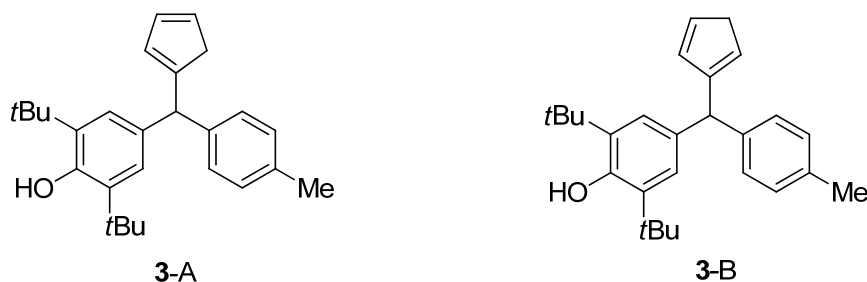
5.2 Product Analysis

Reaction of potassium cyclopentadienide (1-K) with quinone methide 2c

2,6-Di-*tert*-butyl-4-(cyclopenta-1,3-dien-1-yl(*p*-tolyl)methyl)phenol (3-A) and 2,6-di-*tert*-butyl-4-(cyclopenta-1,4-dien-1-yl(*p*-tolyl)methyl)phenol (3-B).

Potassium cyclopentadienide (1-K, 31.3 mg, 300 μmol) was dissolved in dry DMSO (5 mL). Subsequently, a solution of the quinone methide 2c (100 mg, 324 μmol , dissolved in 5 mL CH_2Cl_2) was added and the resulting reaction mixture was stirred for 2 min. The reaction was quenched by the addition of diluted aqueous HCl and extracted with CH_2Cl_2 . The combined organic layers were washed with water and brine, dried over Na_2SO_4 and evaporated under reduced pressure. The crude product was purified by column chromatography on silica gel (*n*-pentane/EtOAc) and a mixture of 3-A and 3-B was obtained as a pale yellow oil (80 mg, 0.21 mmol, 70 %, 3-A : 3-B ~ 1.5 : 1). NMR signal assignments were based on additional 2D-NMR experiments (COSY-, HSQC-, and HMBC experiments).

VM 18



$^1\text{H-NMR}$ (CDCl_3 , 300 MHz): $\delta = 1.40$ (s, 2×18 H, $t\text{Bu}^*$, $t\text{Bu}^\#$), 2.33 (s, 2×3 H, Me^* , $\text{Me}^\#$), 2.91-2.93 $^\#$ (m, 2 H, CH_2), 3.00-3.02 * (m, 2 H, CH_2), 5.02-5.05 (m, 4 H, CH^* , $\text{CH}^\#$, OH^* , $\text{OH}^\#$), 5.82-5.84 * (m, 1 H, $\text{CH}_{\text{olefin}}^*$), 5.99-6.00 $^\#$ (m, 1 H, $\text{CH}_{\text{olefin}}^\#$), 6.30-6.32 $^\#$ (m, 1 H, $\text{CH}_{\text{olefin}}^\#$), 6.38-6.43 (m, 3 H, $2 \times \text{CH}_{\text{olefin}}^*$, $\text{CH}_{\text{olefin}}^\#$), 6.98 (d, 4 H, $J = 4.3$ Hz, $\text{CH}_{\text{aryl}}^*$, $\text{CH}_{\text{aryl}}^\#$), 7.06-7.12 (m, 8 H, $\text{CH}_{\text{aryl}}^*$, $\text{CH}_{\text{aryl}}^\#$). $^{13}\text{C-NMR}$ (CDCl_3 , 75 MHz): $\delta = 21.02^\#$ (q, Me), 21.04 * (q, Me), 30.3 (q, $t\text{Bu}$, signals of the two isomers superimposed), 34.31 $^\#$ (s, $t\text{Bu}$), 34.32 * (s, $t\text{Bu}$), 41.0 * (t, CH_2), 43.2 $^\#$ (t, CH_2), 51.9 * (d, CH), 52.9 $^\#$ (d, CH), 125.3 $^\#$ (d, $\text{CH}_{\text{aryl}}^\#$), 125.5 * (d, $\text{CH}_{\text{aryl}}^*$), 128.57 (d), 128.60 (d), 128.7 (d), 128.80 (d), 128.82 (d), 129.6 (d), 131.6 $^\#$ (d, $\text{CH}_{\text{olefin}}^\#$), 132.0 $^\#$ (d, $\text{CH}_{\text{olefin}}^\#$), 133.3 * (d, $\text{CH}_{\text{olefin}}^*$), 133.8 * (s), 134.5 $^\#$ (s), 134.9 * (d, $\text{CH}_{\text{olefin}}^*$), 135.3 (s, two signals superimposed), 135.32 (s), 135.34 (s), 141.1 * (s), 141.8 $^\#$ (s), 150.0 * (s), 151.97 $^\#$ (s),

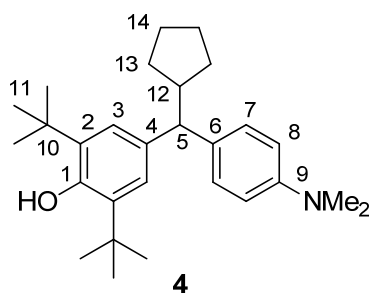
151.98^{*} (s), 152.64[#] (s). MS (EI): m/e (%) = 375 (31), 374 (100) [M]⁺, 360 (12), 359 (38), 318 (11), 317 (38), 310 (16), 309 (57), 269 (29), 261 (15), 219 (52), 169 (14), 154 (11), 57 (35). HR-MS (EI) [M]⁺: calcd for [C₂₇H₃₄O]⁺: 374.2605, found 374.2604.

* can be assigned to A-isomer

can be assigned to B-isomer

2,6-Di-*tert*-butyl-4-(cyclopentyl(4-(dimethylamino)phenyl)methyl)phenol (4) was synthesized according to a slight modification of the procedure for **3-A** and **3-B**: Potassium cyclopentadienide (**1-K**, 50.0 mg, 480 μmol) was dissolved in dry DMSO (2 mL). Subsequently, a solution of the quinone methide **2e** (160 mg, 474 μmol, dissolved in 3 mL of CH₂Cl₂) was added and the resulting reaction mixture was stirred for 2 min. The reaction was quenched by the addition of diluted aqueous HCl and extracted with CH₂Cl₂. The combined organic layers were washed with water and brine, dried over Na₂SO₄ and evaporated under reduced pressure. The remaining residue was dissolved in 15 mL of EtOH and Pd/C(10 %)-catalyst (10 mg) was added. After vigorous stirring for 15 h under H₂, the reaction mixture was filtrated over celite and evaporated under reduced pressure. Purification by column chromatography (*n*-pentane/EtOAc), yielded **4** as yellow solid (140 mg, 343 μmol, 72 %). NMR signal assignments were based on additional 2D-NMR experiments (COSY-, HSQC-, and HMBC experiments).

VM 20-2



R_f (*n*-pentane/EtOAc 10:1, *v/v*): 0.69. Mp. (*n*-pentane/EtOAc): 143-146°C. ¹H-NMR (CDCl₃, 600 MHz): δ = 1.10-1.14 (m, 2 H, 13-H), 1.40 (s, 18 H, 11-H), 1.49-1.53 (m, 2 H, 14-H), 1.58-1.63 (m, 4 H, 13-H, 14-H), 2.54-2.61 (m, 1 H, 12-H), 2.88 (s, 6 H, NMe₂), 3.35 (d, 1 H, *J* = 11.1 Hz, 5-H), 4.91 (s, 1 H, OH), 6.66 (d, 2 H, *J* = 8.7 Hz, 8-H), 7.04 (s, 2 H, 3-H), 7.15 (d, 2 H, *J* = 8.7 Hz, 7-H). ¹³C-NMR (CDCl₃, 150 MHz): δ = 25.42 (t, C-14), 25.45 (t, C-14), 30.4 (q, C-11), 32.3 (t, C-13), 32.4 (t, C-13), 34.3 (s, C-10), 40.8 (q, NMe₂), 45.3 (d, C-12),

57.6 (d, C-5), 112.8 (d, C-8), 124.2 (d, C-3), 128.4 (d, C-7), 135.1 (2s, C-2, C-6), 136.7 (s, C-4), 148.7 (s, C-9), 151.5 (s, C-1). MS (EI): m/e (%) = 407 (5) $[M]^+$, 339 (22), 338 (100). HR-MS (EI) $[M]^+$: calcd for $[C_{28}H_{41}NO]^+$: 407.3182, found 407.3190.

5.3 Kinetics

Reaction of 1-K with the electrophiles 2

Table 3: Kinetics of the reaction of 1-K with 2a in DMSO at 20°C (addition of 0-4.5 eq 18-crown-6, stopped-flow UV-Vis spectrometer, $\lambda = 520$ nm).

No.	$[E]_0 / \text{mol L}^{-1}$	$[\text{Nu}^-]_0 / \text{mol L}^{-1}$	[18-crown-6] / mol L^{-1}	$k_{\text{obs}} / \text{s}^{-1}$
VM 8-1	2.45×10^{-5}	2.53×10^{-4}	-	8.58×10^1
VM 8-2	2.45×10^{-5}	3.79×10^{-4}	1.70×10^{-3}	1.52×10^2
VM 8-3	2.45×10^{-5}	5.06×10^{-4}	-	2.14×10^2
VM 8-4	2.45×10^{-5}	6.32×10^{-4}	1.70×10^{-3}	2.81×10^2
VM 8-5	2.45×10^{-5}	7.59×10^{-4}	-	3.42×10^2

$k_2 = 5.07 \times 10^5 \text{ L mol}^{-1} \text{ s}^{-1}$

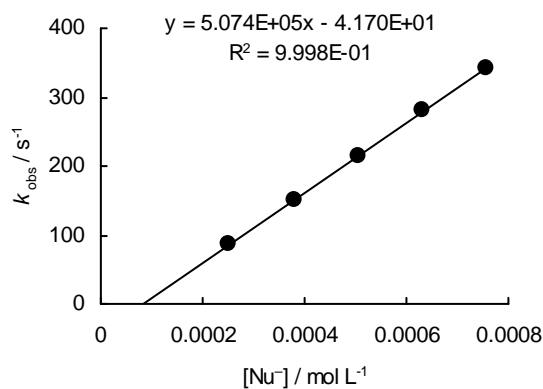
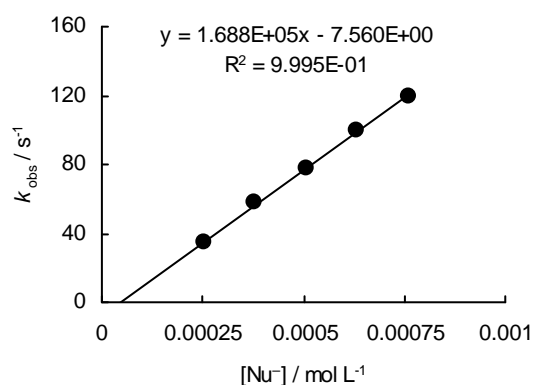


Table 4: Kinetics of the reaction of **1-K** with **2b** in DMSO at 20°C (addition of 0-2.7 eq 18-crown-6, stopped-flow UV-Vis spectrometer, $\lambda = 520$ nm).

No.	$[E]_0 / \text{mol L}^{-1}$	$[\text{Nu}^-]_0 / \text{mol L}^{-1}$	[18-crown-6] / mol L ⁻¹	$k_{\text{obs}} / \text{s}^{-1}$
VM 10-1	2.37×10^{-5}	2.53×10^{-4}	-	3.45×10^1
VM 10-2	2.37×10^{-5}	3.79×10^{-4}	8.48×10^{-4}	5.74×10^1
VM 10-3	2.37×10^{-5}	5.06×10^{-4}	-	7.73×10^1
VM 10-4	2.37×10^{-5}	6.32×10^{-4}	1.70×10^{-3}	9.98×10^1
VM 10-5	2.37×10^{-5}	7.59×10^{-4}	-	1.20×10^2

$k_2 = 1.69 \times 10^5 \text{ L mol}^{-1} \text{ s}^{-1}$

**Table 5:** Kinetics of the reaction of **1-K** with **2c** in DMSO at 20°C (addition of 0-1.2 eq 18-crown-6, stopped-flow UV-Vis spectrometer, $\lambda = 371$ nm).

No.	$[E]_0 / \text{mol L}^{-1}$	$[\text{Nu}^-]_0 / \text{mol L}^{-1}$	[18-crown-6] / mol L ⁻¹	$k_{\text{obs}} / \text{s}^{-1}$
VM 5-1	2.50×10^{-5}	7.21×10^{-4}	-	7.29
VM 5-2	2.50×10^{-5}	9.62×10^{-4}	8.53×10^{-4}	1.01×10^1
VM 5-3	2.50×10^{-5}	1.20×10^{-3}	-	1.30×10^1
VM 5-4	2.50×10^{-5}	1.44×10^{-3}	1.71×10^{-3}	1.59×10^1
VM 5-5	2.50×10^{-5}	1.68×10^{-4}	-	1.89×10^2

$k_2 = 1.21 \times 10^4 \text{ L mol}^{-1} \text{ s}^{-1}$

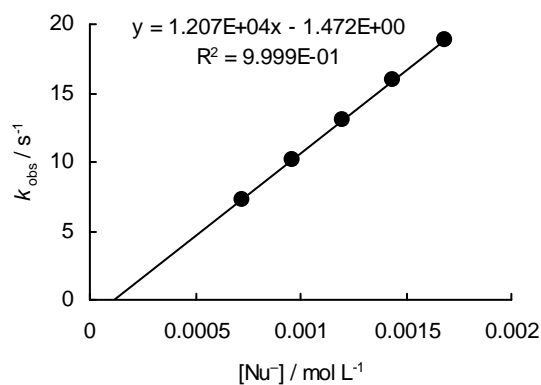
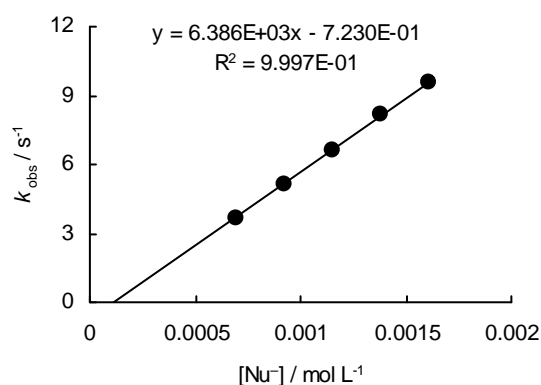


Table 6: Kinetics of the reaction of **1-K** with **2d** in DMSO at 20°C (addition of 0-1.4 eq 18-crown-6, stopped-flow UV-Vis spectrometer, $\lambda = 393$ nm).

No.	$[E]_0 / \text{mol L}^{-1}$	$[\text{Nu}^-]_0 / \text{mol L}^{-1}$	$[\text{18-crown-6}] / \text{mol L}^{-1}$	$k_{\text{obs}} / \text{s}^{-1}$
VM 4-1	2.54×10^{-5}	6.91×10^{-4}	-	3.68
VM 4-2	2.54×10^{-5}	9.21×10^{-4}	9.35×10^{-4}	5.15
VM 4-3	2.54×10^{-5}	1.15×10^{-3}	-	6.64
VM 4-4	2.54×10^{-5}	1.38×10^{-3}	1.87×10^{-3}	8.16
VM 4-5	2.54×10^{-5}	1.61×10^{-4}	-	9.53

$k_2 = 6.39 \times 10^3 \text{ L mol}^{-1} \text{ s}^{-1}$

**Table 7:** Kinetics of the reaction of **1-K** with **2e** in DMSO at 20°C (addition of 0-1.4 eq 18-crown-6, stopped-flow UV-Vis spectrometer, $\lambda = 486$ nm).

No.	$[E]_0 / \text{mol L}^{-1}$	$[\text{Nu}^-]_0 / \text{mol L}^{-1}$	$[\text{18-crown-6}] / \text{mol L}^{-1}$	$k_{\text{obs}} / \text{s}^{-1}$
VM 7-1	2.58×10^{-5}	6.91×10^{-4}	-	4.12×10^{-1}
VM 7-2	2.58×10^{-5}	9.21×10^{-4}	9.35×10^{-4}	5.57×10^{-1}
VM 7-3	2.58×10^{-5}	1.15×10^{-3}	-	7.18×10^{-1}
VM 7-4	2.58×10^{-5}	1.38×10^{-3}	1.87×10^{-3}	8.73×10^{-1}
VM 7-5	2.58×10^{-5}	1.61×10^{-4}	-	1.03

$k_2 = 6.74 \times 10^2 \text{ L mol}^{-1} \text{ s}^{-1}$

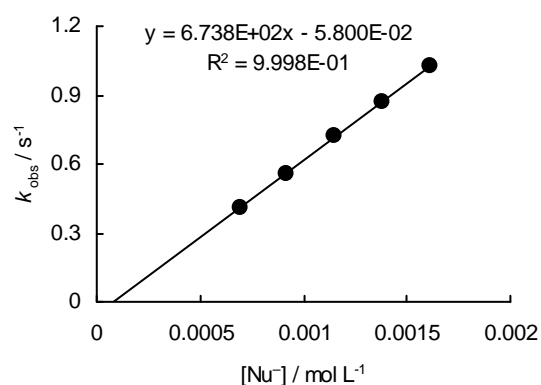

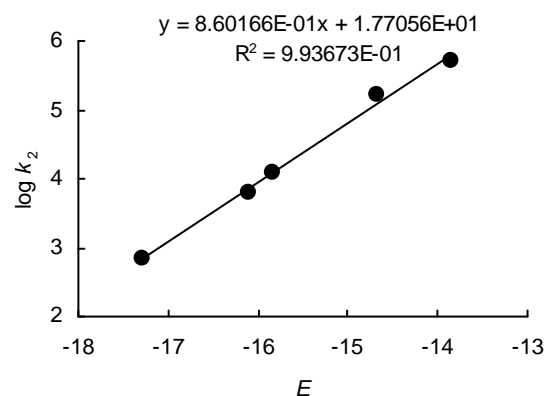


Table 8: Determination of the nucleophilicity parameters N , s for **1-K** (correlation of $\log k_2$ for the reactions of **1-K** with **2a–e** versus the electrophilicity parameters E for **2a–e**).

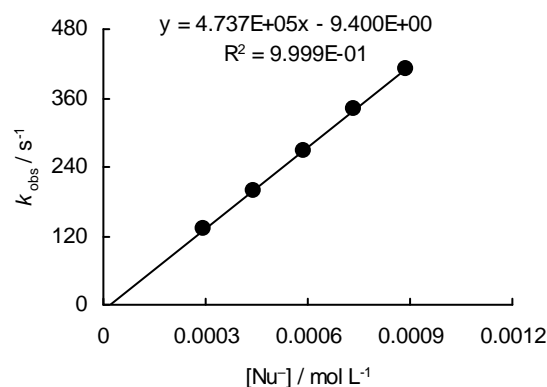
Nucleophile	Electrophile (E)	$k_2 / \text{L mol}^{-1} \text{s}^{-1}$
 K^+ 1-K	2a (-13.84)	5.07×10^5
	2b (-14.68)	1.69×10^5
	2c (-15.83)	1.21×10^4
	2d (-16.11)	6.39×10^3
	2e (-17.29)	6.74×10^2
		$N = 20.58, s = 0.86$



Reaction of **1-Na** with the electrophiles **2**

Table 9: Kinetics of the reaction of **1-Na** with **2a** in DMSO at 20°C (stopped-flow UV-Vis spectrometer, $\lambda = 520 \text{ nm}$).

No.	$[\text{E}]_0 / \text{mol L}^{-1}$	$[\text{Nu}^-]_0 / \text{mol L}^{-1}$	$k_{\text{obs}} / \text{s}^{-1}$
VM 26-1	2.53×10^{-5}	2.95×10^{-4}	1.31×10^2
VM 26-2	2.53×10^{-5}	4.43×10^{-4}	2.00×10^2
VM 26-3	2.53×10^{-5}	5.90×10^{-4}	2.69×10^2
VM 26-4	2.53×10^{-5}	7.38×10^{-4}	3.41×10^2
VM 26-5	2.53×10^{-5}	8.86×10^{-4}	4.10×10^2
			$k_2 = 4.74 \times 10^5 \text{ L mol}^{-1} \text{s}^{-1}$

**Table 10:** Kinetics of the reaction of **1-Na** with **2b** in DMSO at 20°C (stopped-flow UV-Vis spectrometer, $\lambda = 520 \text{ nm}$).

No.	$[\text{E}]_0 / \text{mol L}^{-1}$	$[\text{Nu}^-]_0 / \text{mol L}^{-1}$	$k_{\text{obs}} / \text{s}^{-1}$
VM 25-1	2.56×10^{-5}	3.30×10^{-4}	5.56×10^1
VM 25-2	2.56×10^{-5}	4.95×10^{-4}	8.13×10^1
VM 25-3	2.56×10^{-5}	6.60×10^{-4}	1.08×10^2
VM 25-4	2.56×10^{-5}	8.24×10^{-4}	1.33×10^2
VM 25-5	2.56×10^{-5}	9.89×10^{-4}	1.62×10^2
			$k_2 = 1.60 \times 10^5 \text{ L mol}^{-1} \text{s}^{-1}$

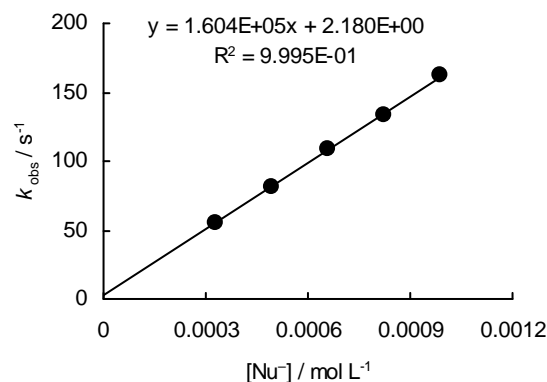
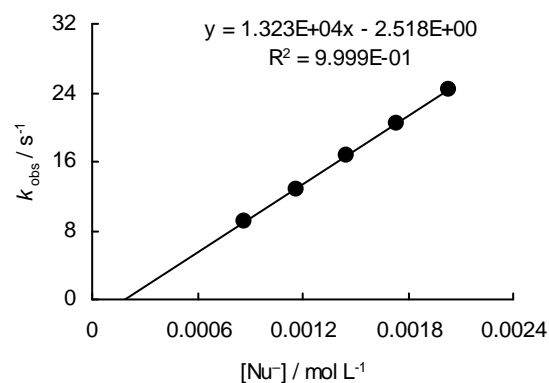
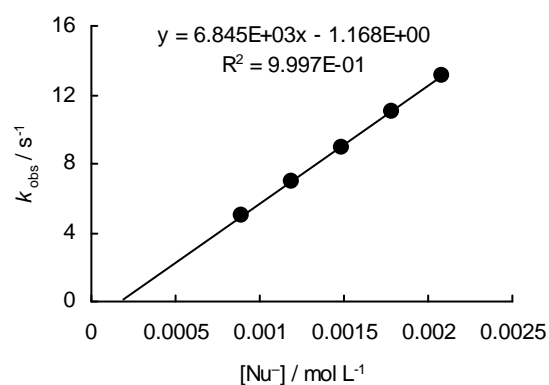


Table 11: Kinetics of the reaction of **1**-Na with **2c** in DMSO at 20°C (stopped-flow UV-Vis spectrometer, $\lambda = 371$ nm).

No.	$[E]_0 / \text{mol L}^{-1}$	$[\text{Nu}^-]_0 / \text{mol L}^{-1}$	$k_{\text{obs}} / \text{s}^{-1}$
VM 21-1	2.50×10^{-5}	8.70×10^{-4}	9.06
VM 21-2	2.50×10^{-5}	1.16×10^{-3}	1.28×10^1
VM 21-3	2.50×10^{-5}	1.45×10^{-3}	1.66×10^1
VM 21-4	2.50×10^{-5}	1.74×10^{-3}	2.05×10^1
VM 21-5	2.50×10^{-5}	2.03×10^{-3}	2.44×10^1
$k_2 = 1.32 \times 10^4 \text{ L mol}^{-1} \text{ s}^{-1}$			

**Table 12:** Kinetics of the reaction of **1**-Na with **2d** in DMSO at 20°C (stopped-flow UV-Vis spectrometer, $\lambda = 393$ nm).

No.	$[E]_0 / \text{mol L}^{-1}$	$[\text{Nu}^-]_0 / \text{mol L}^{-1}$	$k_{\text{obs}} / \text{s}^{-1}$
VM 24-1	2.50×10^{-5}	8.91×10^{-4}	4.99
VM 24-2	2.50×10^{-5}	1.19×10^{-3}	6.90
VM 24-3	2.50×10^{-5}	1.48×10^{-3}	8.97
VM 24-4	2.50×10^{-5}	1.78×10^{-3}	1.10×10^1
VM 24-5	2.50×10^{-5}	2.08×10^{-3}	1.31×10^2
$k_2 = 6.85 \times 10^3 \text{ L mol}^{-1} \text{ s}^{-1}$			

**Table 13:** Kinetics of the reaction of **1**-Na with **2e** in DMSO at 20°C (stopped-flow UV-Vis spectrometer, $\lambda = 486$ nm).

No.	$[E]_0 / \text{mol L}^{-1}$	$[\text{Nu}^-]_0 / \text{mol L}^{-1}$	$k_{\text{obs}} / \text{s}^{-1}$
VM 22-1	2.58×10^{-5}	8.70×10^{-4}	5.28×10^{-1}
VM 22-2	2.58×10^{-5}	1.16×10^{-3}	7.12×10^{-1}
VM 22-3	2.58×10^{-5}	1.45×10^{-3}	9.08×10^{-1}
VM 22-4	2.58×10^{-5}	1.74×10^{-3}	1.10
VM 22-5	2.58×10^{-5}	2.03×10^{-3}	1.28
$k_2 = 6.52 \times 10^2 \text{ L mol}^{-1} \text{ s}^{-1}$			

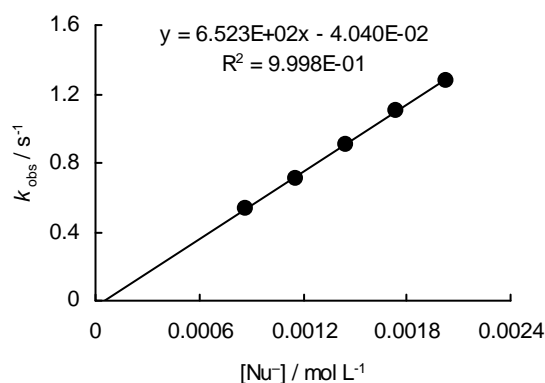

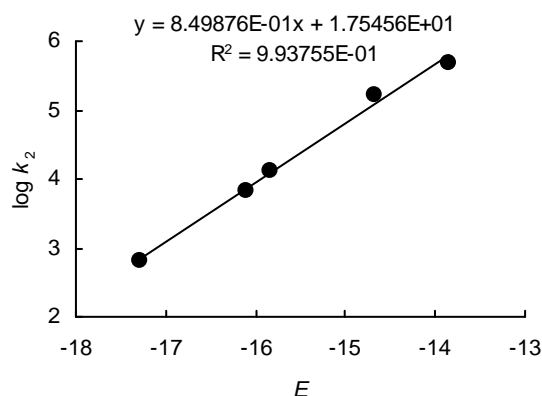


Table 14: Determination of the nucleophilicity parameters N , s for **1-Na** (correlation of $\log k_2$ for the reactions of **1-Na** with **2a–e** versus the electrophilicity parameters E for **2a–e**).

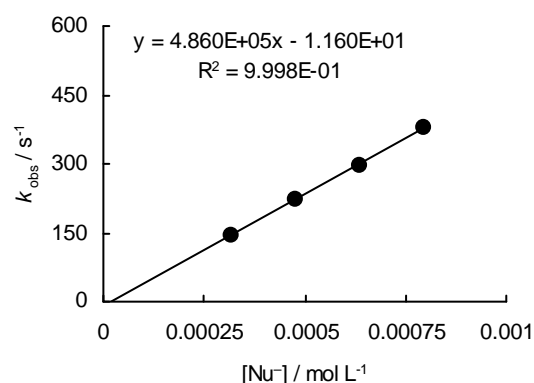
Nucleophile	Electrophile (E)	$k_2 / \text{L mol}^{-1} \text{s}^{-1}$
 Na^+ 1-Na	2a (-13.84)	4.74×10^5
	2b (-14.68)	1.60×10^5
	2c (-15.83)	1.32×10^4
	2d (-16.11)	6.85×10^3
	2e (-17.29)	6.52×10^2
$N = 20.64, s = 0.85$		



Reaction of **1-Li** with the electrophiles **2**

Table 15: Kinetics of the reaction of **1-Li** with **2a** in DMSO at 20°C (stopped-flow UV-Vis spectrometer, $\lambda = 520 \text{ nm}$).

No.	$[\text{E}]_0 / \text{mol L}^{-1}$	$[\text{Nu}^-]_0 / \text{mol L}^{-1}$	$k_{\text{obs}} / \text{s}^{-1}$
VM 16-1	2.51×10^{-5}	3.19×10^{-4}	1.43×10^2
VM 16-2	2.51×10^{-5}	4.79×10^{-4}	2.23×10^2
VM 16-3	2.51×10^{-5}	6.39×10^{-4}	2.97×10^2
VM 16-4	2.51×10^{-5}	7.98×10^{-4}	3.77×10^2
$k_2 = 4.86 \times 10^5 \text{ L mol}^{-1} \text{s}^{-1}$			

**Table 16:** Kinetics of the reaction of **1-Li** with **2b** in DMSO at 20°C (stopped-flow UV-Vis spectrometer, $\lambda = 520 \text{ nm}$).

No.	$[\text{E}]_0 / \text{mol L}^{-1}$	$[\text{Nu}^-]_0 / \text{mol L}^{-1}$	$k_{\text{obs}} / \text{s}^{-1}$
VM 15-1	2.56×10^{-5}	3.19×10^{-4}	5.20×10^1
VM 15-2	2.56×10^{-5}	4.79×10^{-4}	7.68×10^1
VM 15-3	2.56×10^{-5}	6.39×10^{-4}	1.04×10^2
VM 15-4	2.56×10^{-5}	7.98×10^{-4}	1.28×10^2
VM 15-5	2.56×10^{-5}	9.58×10^{-4}	1.58×10^2
$k_2 = 1.64 \times 10^5 \text{ L mol}^{-1} \text{s}^{-1}$			

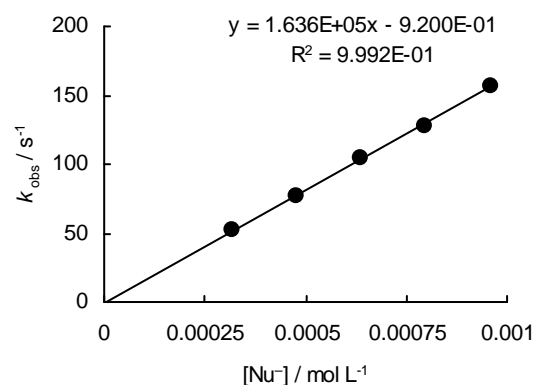
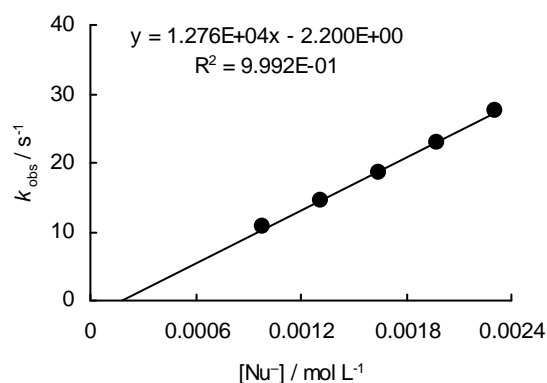
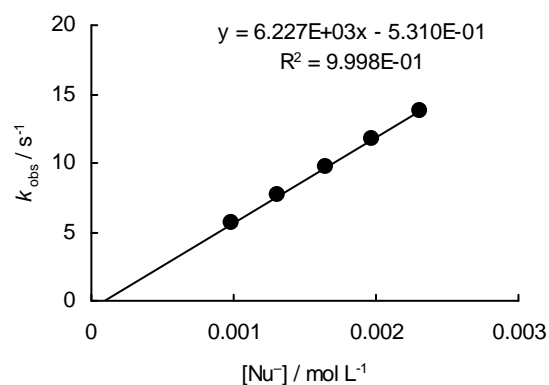


Table 17: Kinetics of the reaction of **1-Li** with **2c** in DMSO at 20°C (stopped-flow UV-Vis spectrometer, $\lambda = 371$ nm).

No.	$[E]_0 / \text{mol L}^{-1}$	$[\text{Nu}^-]_0 / \text{mol L}^{-1}$	$k_{\text{obs}} / \text{s}^{-1}$
VM 12-1	2.49×10^{-5}	9.87×10^{-4}	1.06×10^1
VM 12-2	2.49×10^{-5}	1.32×10^{-3}	1.45×10^1
VM 12-3	2.49×10^{-5}	1.65×10^{-3}	1.86×10^1
VM 12-4	2.49×10^{-5}	1.97×10^{-3}	2.29×10^1
VM 12-5	2.49×10^{-5}	2.30×10^{-3}	2.74×10^1
$k_2 = 1.28 \times 10^4 \text{ L mol}^{-1} \text{ s}^{-1}$			

**Table 18:** Kinetics of the reaction of **1-Li** with **2d** in DMSO at 20°C (stopped-flow UV-Vis spectrometer, $\lambda = 393$ nm).

No.	$[E]_0 / \text{mol L}^{-1}$	$[\text{Nu}^-]_0 / \text{mol L}^{-1}$	$k_{\text{obs}} / \text{s}^{-1}$
VM 11-1	2.55×10^{-5}	9.87×10^{-4}	5.60
VM 11-2	2.55×10^{-5}	1.32×10^{-3}	7.71
VM 11-3	2.55×10^{-5}	1.65×10^{-3}	9.66
VM 11-4	2.55×10^{-5}	1.97×10^{-3}	1.18×10^1
VM 11-5	2.55×10^{-5}	2.30×10^{-3}	1.38×10^1
$k_2 = 6.23 \times 10^3 \text{ L mol}^{-1} \text{ s}^{-1}$			

**Table 19:** Kinetics of the reaction of **1-Li** with **2e** in DMSO at 20°C (stopped-flow UV-Vis spectrometer, $\lambda = 486$ nm).

No.	$[E]_0 / \text{mol L}^{-1}$	$[\text{Nu}^-]_0 / \text{mol L}^{-1}$	$k_{\text{obs}} / \text{s}^{-1}$
VM 13-1	2.58×10^{-5}	9.85×10^{-4}	5.78×10^{-1}
VM 13-2	2.58×10^{-5}	1.31×10^{-3}	7.83×10^{-1}
VM 13-3	2.58×10^{-5}	1.64×10^{-3}	9.99×10^{-1}
VM 13-4	2.58×10^{-5}	1.97×10^{-3}	1.21
VM 13-5	2.58×10^{-5}	2.30×10^{-3}	1.43
$k_2 = 6.49 \times 10^2 \text{ L mol}^{-1} \text{ s}^{-1}$			

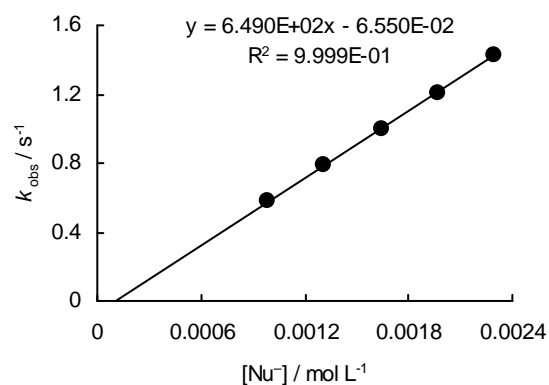
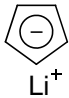
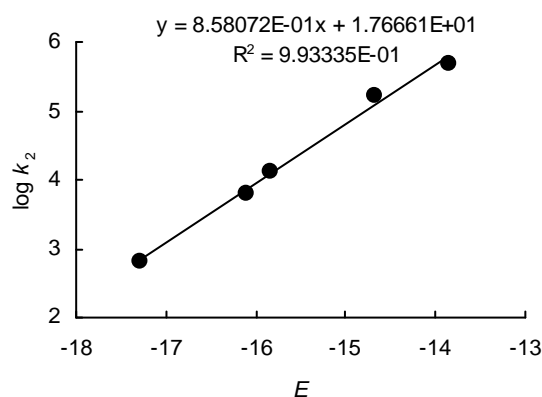


Table 20: Determination of the nucleophilicity parameters N , s for **1**-Li (correlation of $\log k_2$ for the reactions of **1**-Li with **2a–e** versus the electrophilicity parameters E for **2a–e**).

Nucleophile	Electrophile (E)	$k_2 / \text{L mol}^{-1} \text{s}^{-1}$
 1 -Li	2a (-13.84)	4.86×10^5
	2b (-14.68)	1.64×10^5
	2c (-15.83)	1.28×10^4
	2d (-16.11)	6.23×10^3
	2e (-17.29)	6.49×10^2
$N = 20.59, s = 0.86$		



6 References

- [1] For selected reviews, see: (a) Coldham, I. *J. Chem. Soc., Perkin Trans. I* **1998**, 1343-1364. (b) Knochel, P.; Hupe, E.; Dohle, W.; Lindsay, D. M.; Bonnet, V.; Quéguiner, G.; Boudier, A.; Kopp, F.; Demay, S.; Seidel, N.; Calaza, M. I.; Vu, V. A.; Sapountzis, I.; Bunlaksananusorn, T. *Pure Appl. Chem.* **2002**, *74*, 11-17. (c) Alberico, D.; Scott, M. E.; Lautens, M. *Chem. Rev.* **2007**, *107*, 174-238.
- [2] For selected recent examples of organometallic compounds with high functional group tolerance, see: (a) Krasovskiy, A.; Knochel, P. *Angew. Chem.* **2004**, *116*, 3396-3399. *Angew. Chem. Int. Ed.* **2004**, *43*, 3333-3336. (b) Ila, H.; Baron, O.; Wagner, A. J.; Knochel, P. *Chem. Commun.* **2006**, 583-593. (c) Metzger, A.; Schade, M. A.; Knochel, P. *Org. Lett.* **2008**, *10*, 1107-1110. (d) Rauhut, C. B.; Vu, V. A.; Fleming, F. F.; Knochel, P. *Org. Lett.* **2008**, *10*, 1187-1189. (e) Blümke, T. D.; Piller, F. M.; Knochel, P. *Chem. Commun.* **2010**, *46*, 4082-4084. (f) Metzger, A.; Bernhardt, S.; Manolikakes, G.; Knochel, P. *Angew. Chem.* **2010**, *122*, 4769-4773; *Angew. Chem. Int. Ed.* **2010**, *49*, 4665-4668.
- [3] (a) Mayr, H.; Patz, M. *Angew. Chem.* **1994**, *106*, 990-1010; *Angew. Chem. Int. Ed. Engl.* **1994**, *33*, 938-957. (b) Mayr, H.; Bug, T.; Gotta, M. F.; Hering, N.; Irrgang, B.; Janker, B.; Kempf, B.; Loos, R.; Ofial, A. R.; Remennikov, G.; Schimmel, H. *J. Am. Chem. Soc.* **2001**, *123*, 9500-9512. (c) Mayr, H.; Kempf, B.; Ofial, A. R. *Acc. Chem. Res.* **2003**, *36*, 66-77. (d) Mayr, H.; Ofial, A. R. *Pure Appl. Chem.* **2005**, *77*, 1807-1821. (e) Mayr, H.; Ofial, A. R. *J. Phys. Org. Chem.* **2008**, *21*, 584-595. (f) For a comprehensive database of nucleophilicity parameters N , s and electrophilicity parameters E , see <http://www.cup.lmu.de/oc/mayr/>.

- [4] (a) Lucius, R.; Loos, R.; Mayr, H. *Angew. Chem.* **2002**, *114*, 97-102; *Angew. Chem. Int. Ed.* **2002**, *41*, 91-95. (b) Bug, T.; Lemek, T.; Mayr, H. *J. Org. Chem.* **2004**, *69*, 7565-7576. (c) Berger, S. T. A.; Ofial, A. R.; Mayr, H. *J. Am. Chem. Soc.* **2007**, *129*, 9753-9761. (d) Kaumanns, O.; Appel, R.; Lemek, T.; Seeliger, F.; Mayr, H. *J. Org. Chem.* **2009**, *74*, 75-81. (e) Appel, R.; Loos, R.; Mayr, H. *J. Am. Chem. Soc.* **2009**, *131*, 704-714.
- [5] Seeliger, F.; Berger, S. T. A.; Remennikov, G. Y.; Polborn, K.; Mayr, H. *J. Org. Chem.* **2007**, *72*, 9170-9180.
- [6] Berger, S. T. A.; Seeliger, F. H.; Hofbauer, F.; Mayr, H. *Org. Biomol. Chem.* **2007**, *5*, 3020-3026.
- [7] (a) Roth, W. R. *Tetrahedron Lett.* **1964**, *5*, 1009-1013. (b) Replogle, K. S.; Carpenter, B. K. *J. Am. Chem. Soc.* **1984**, *106*, 5751-5753. (c) Kahn, S. D.; Hehre, W. J.; Rondan, N. G.; Houk, K. N. *J. Am. Chem. Soc.* **1985**, *107*, 8291-8292. (d) Bachrach, S. M. *J. Org. Chem.* **1993**, *58*, 5414-5421.
- [8] (a) Lucius, R.; Mayr, H. *Angew. Chem.* **2000**, *112*, 2086-2089; *Angew. Chem. Int. Ed.* **2000**, *39*, 1995-1997. (b) Corral, F., Ludwig-Maximilians-Universität München, Master Thesis, 2010.
- [9] Bordwell, F. G.; Drucker, G. E.; Fried, H. E. *J. Org. Chem.* **1981**, *46*, 632-635.
- [10] Panda, T. K.; Gamer, M. T.; Roesky, P. W. *Organometallics* **2003**, *22*, 877-878.
- [11] den Besten, R.; Harder, S.; Brandsma, L. *J. Organomet. Chem.* **1990**, *385*, 153-159.
- [12] Xu, Y.; Dolbier, W. R. *Tetrahedron* **1998**, *54*, 6319-6328.
- [13] Behera, R. K.; Nayak, A. *Indian J. Chem. B* **1976**, *14*, 223-224.
- [14] Evans, S.; Nesvadba, P.; Allenbach S. (Ciba-Geigy AG), EP-B 744392, **1996** [*Chem. Abstr.* **1997**, *126*, 46968v].

